0dB

20 15 10 6 321 0 1 2 3 4 5 6

15 10 6 321 0 1 2 3 4
−20dB
POWER LEVEL

DESIGNING

Audio Power
Amplifiers

BOB CORDELL

Designing Audio Power Amplifiers

About the Author

Bob Cordell is an electrical engineer who has been deeply involved in audio since his adventures with vacuum tube designs in his teen years. He is an equal-opportunity designer to this day, having built amplifiers with vacuum tubes, bipolar transistors, and MOSFETs. Bob is also a prolific designer of audio test equipment, including a high-performance THD analyzer and many purpose-built pieces of audio gear. He has published numerous articles and papers on power amplifier design and distortion measurement in the popular press and in the *Journal of the Audio Engineering Society*. In 1983 he published a power amplifier design combining vertical power MOSFETs with error correction, achieving unprecedented distortion levels of less than 0.001% at 20 kHz.

Bob is also an avid DIY loudspeaker builder, and has combined this endeavor with his electronic interests in the design of powered audiophile loudspeaker systems. He and his colleagues have presented audiophile listening and measurement workshops at the Rocky Mountain Audio Fest and the Home Entertainment Show.

As an electrical engineer, Bob has worked at Bell Laboratories and other telecommunications companies, where his work has included design of integrated circuits and fiber optic communications systems. He maintains an audiophile website at www.cordellaudio.com, where diverse material on audio electronics, loudspeakers, and instrumentation can be found.

Designing Audio Power Amplifiers

Bob Cordell

All trademarks are trademarks of their respective owners. Rather than put a trademark symbol after every occurrence of a trademarked name, we use names in an editorial fashion only, and to the benefit of the trademark owner, with no intention of infringement of the trademark. Where such designations appear in this book, they have been printed with initial caps.

McGraw-Hill eBooks are available at special quantity discounts to use as premiums and sales promotions, or for use in corporate training programs. To contact a representative please e-mail us at bulksales@mcgraw-hill.com.

Information contained in this work has been obtained by The McGraw-Hill Companies, Inc. ("McGraw-Hill") from sources believed to be reliable. However, neither McGraw-Hill nor its authors guarantee the accuracy or completeness of any information published herein, and neither McGraw-Hill nor its authors shall be responsible for any errors, omissions, or damages arising out of use of this information. This work is published with the understanding that McGraw-Hill and its authors are supplying information but are not attempting to render engineering or other professional services. If such services are required, the assistance of an appropriate professional should be sought.

TERMS OF USE

**This book is dedicated
to my dear wife Angela,
whose support and
encouragement made it all possible.**

This page intentionally left blank

Contents

Preface

There are several very good books on audio power amplifier design already out there, so you might ask why we need yet another book on power amplifier design. Hopefully this preface will answer that question. However, the short answer can be found in two observations. First, there have been many developments in audio power amplifier design since the release of most of the prior books. Second, there are some important topics that deserve more depth of coverage.

Designing Audio Power Amplifiers is written to address many advanced topics and important design subtleties. At the same time, however, it has enough introductory and tutorial coverage to allow designers relatively new to the field to absorb the material of the book without being overwhelmed. To this end, the book starts off at a relaxing pace that helps the reader develop an intuitive feel and understanding for amplifier design. Although this book covers advanced subjects, highly involved mathematics is kept to a minimum—much of that is left to the academics. Design choices and decisions are explained and analyzed.

This is not just a cookbook; it is intended to teach the reader how to think about power amplifier design and understand the many concepts and nuances, then analyze and synthesize the many possible variations of amplifier design.

I have divided the book into six parts. Part 1 introduces audio power amplifier design and includes the basics. This part is designed to be readable and friendly to those with less technical background while still providing a very sound footing for the more detailed design discussions that follow. In this part I show how a simple power amplifier design evolves in several steps to a modern architecture, describing how performance deficiencies are mitigated with circuit improvements at each step in the evolution. Even experienced designers may gain valuable insights here.

Part 2 delves into the design of advanced power amplifiers with state-of-the art performance. Crossover distortion, one of the most problematic distortions in power amplifiers, is covered in depth. Special attention is paid to dynamic crossover distortion, which is less well understood. This part also includes a detailed treatment of MOSFET power amplifiers, error correction techniques, advanced feedback compensation, ultra-low distortion drive circuits, and DC servos.

Part 3 covers those real-world design considerations that influence sound quality and reliability, including power supplies and grounding, short circuit and safe area protection, and amplifier behavior when driving difficult loads. Thermal design and thermal stability are given special attention. Electromagnetic interference ingress and egress via the input, output, and mains ports of the amplifier are also treated here.

SPICE simulation can be very important to power amplifier design, and its use is described in detail in Part 4. Even those with no SPICE experience will learn how to use this valuable tool, helped along by a tutorial chapter and ready-to-run amplifier simulations and transistor models available at www.cordellaudio.com. A full chapter describes how you can create your own accurate SPICE models for BJT and MOSFET transistors, many of which are poorly modeled by manufacturers. Numerous approaches to distortion measurement are also explained in Part 4. I've also described

some techniques for achieving the high sensitivity required to measure the low-distortion designs discussed in the book. Less well-known distortion measurements, such as TIM, PIM, and IIM, are also covered here. In the quest for meaningful correspondence between listening and measurement results, other non-traditional amplifier tests are also described.

Part 5, Topics in Amplifier Design, covers all of those other important matters that do not fit neatly into the other parts. Advanced designers as well as audiophiles will find many interesting topics in this part. Some of the controversies in audio, such as the use of negative feedback, are addressed here. For balance, the design of amplifiers without negative feedback is covered. Integrated circuit power amplifiers and drivers are also discussed.

Class D amplifiers are playing a more important role in audio amplification as every day passes. They have enjoyed vast improvements in performance over the last several years and can be expected to improve much further in the future. Four chapters in Part 6 cover this exciting technology.

Many of the following topics covered in *Designing Audio Power Amplifiers* should prove especially interesting to readers familiar with earlier texts:

- Ultra-low distortion input and voltage amplifier topologies
- Non-conventional feedback compensation techniques
- Lateral and vertical MOSFET power amplifiers
- Output stage error correction circuits
- Thermal stability analysis of BJT and MOSFET output stages
- Output transistors with temperature tracking diodes
- Integrated circuit amplifiers and drivers
- SPICE simulation and modeling for amplifier design
- Amplifier measurement instrumentation and techniques
- PC-based instrumentation for amplifier evaluation
- How amplifiers misbehave and why they sound different
- Sources of distortion in class D amplifiers
- PWM, sigma-delta, and direct digital class D amplifiers

No single text can cover all aspects of audio power amplifier design. It is my hope that an experienced designer or a hobbyist who seeks to learn more about audio amplifier design will find this book most helpful. I also hope that this text will provide a sound basis for those wishing to learn analog circuit design.

Bob Cordell

Acknowledgments

My Lord and Savior Jesus Christ has given me the peace and guidance that allowed me to complete this undertaking. My wife Angela was a constant source of encouragement and sacrificed enormous amounts of quality time in our relationship to allow me to focus my energy on this book. My mother inspired me with her autobiography. My father supported me in my audio and electronics activities beginning before my teen years, helping me to purchase electronic kits and showing me how to put them together.

Those many authors of other texts on audio who have gone before me have truly been an inspiration and have shown how good engineering can be applied to audio while making their writings understandable to those without a formal engineering background.

I owe a special debt of gratitude to Andy Connors for proofreading the book and helping me with numerous technical questions while providing insight and encouragement. I am also grateful to Jan Didden and Peter Smith for their generous support. Gene Pitts, past Editor of *Audio* magazine, was pivotal in enabling me to get my start in writing about audio. There are too many other friends and colleagues to list, but I wish especially to thank the members of the Audio Engineering Society and the DIYaudio Forum (www.diyaudio.com) for all that I have learned from them. The audiophile fraternity is alive and well.

Finally, I wish to thank the professional group at McGraw-Hill for turning my dream into reality.

This page intentionally left blank

Audio Power Amplifier Basics

Part 1 introduces audio power amplifier design and covers the basics. This part is written to be readable and friendly to those with less technical background while still providing a very sound footing for the more detailed design issues to follow. That footing includes discussions of transistor operation, important circuit building blocks, negative feedback, and the different amplifier classes. In Chapter 3 we show how a simple power amplifier design can be evolved in several steps to become a modern architecture with very good performance. At each step we describe how performance deficiencies are mitigated with circuit improvements. Part 1 closes with a chapter that summarizes in a succinct way the many issues that should be addressed in the power amplifier design process. This serves as a preamble for the more detailed chapters that follow in the later parts. Even experienced designers will gain valuable insights in Part 1.

This page intentionally left blank

Introduction

A udio power amplifier design is both an art and a science, in more ways than one. Solid-state power amplifiers have been around since the late 1960s, and yet new designs still proliferate. Questions about relating sonic performance to measured performance still abound. This is not just limited to the high end where audio mystique has a strong influence. While there is a tremendous amount of science to the design of audio power amplifiers, there are also many nuances that demand attention to detail. At times, it is difficult to separate the influence of experience from just plain art. There are also things we still do not understand fully, and this is where the art aspect of amplifier design flourishes.

This book is not meant to be a survey. Topologies of historical or narrow interest are ignored in favor of deeper coverage of important nuances in relevant contemporary designs. I have sought to touch on virtually every amplifier design subject, but some are treated in less depth when there is a better treatment elsewhere.

There are thousands of variations on amplifier architectures out there, and it would be impossible to study all of them. For that reason, there is a strong focus on deeply understanding the more popular architectures in a way that conveys enough understanding so that the reader can analyze and even conceive many variants, some of which may be very different from the ones covered here.

1.1 Organization of the Book

There is no right or wrong way to organize the enormous amount of material on power amplifier design. The approach taken here is to ramp up your confidence first, with emphasis on how to think about amplifier designs and analyze them. For this reason, some details and nuances are postponed to later parts of the book.

I begin with a very basic amplifier and show how it works and how to analyze it. I also discuss its shortcomings. The approach includes emphasis on examples and plugging in the numbers to evaluate design approaches and see how well they actually perform.

A strong attempt has been made in the early chapters to avoid distracting you with side trips along the way to understanding amplifier design. As you progress through the book, an adequate amount of just-in-time tutorial material is presented to aid the less experienced reader. This includes material on transistors and building block circuits that is written to be easily digestible. Nevertheless, even the experienced designer will find some welcome nuggets of detail here.

Power amplifier design is introduced by describing a very basic design. That design is analyzed and then followed through many stages of improvements. The explanation

of the reasons for and results of the improvements illustrates how to think about amplifier design and understand many of the trade-offs. Actual simulated distortion results are presented at each stage of the evolution of the design.

Once you are made comfortable with amplifier design and analysis, Part 2 delivers the meat of high-performance design and a much deeper understanding of performance-limiting factors and sources of distortion.

By the end of Part 2, you have gone deeply through the design of amplifiers that perform superbly on the lab bench. Alas, the real world is introduced in Part 3. There is indeed a large gap between a superlative laboratory amplifier and one that will perform that way and survive in the real world. Protection circuits, EMI filtering, power supplies, grounding, and many other things need to be taken into account, and that is the priority of Part 3.

Tools are very important to the successful design of power amplifiers, and these are covered in Part 4. Some tools are physical, like distortion analyzers, while others take the form of software, like the SPICE simulator. SPICE is most valuable in the design process before the amplifier is built, helping to evaluate and sort out the many possible combinations of circuit architectures from which to choose. SPICE can then be used in optimizing the selected design.

After the amplifier is built, it must be thoroughly evaluated for distortion and other behavior, and this is where different kinds of instrumentation and measurement techniques come into play. Here is where the rubber meets the road in terms of measuring an amplifier in ways that may have some correlation with how well it sounds. To some extent, amplifiers sound different because they misbehave differently. The ability to expose and sort out amplifier misbehavior is a key to making a fine-sounding amplifier.

Part 5 of the book is titled "Topics in Amplifier Design." Here a wide variety of subjects of keen interest are covered. For example, a book on audio power amplifier design would not be complete without discussion of the pros and cons of negative feedback; its pervasive use and sometimes controversial reputation demand it. Amplifier design myths and common misunderstandings are also discussed. Why amplifiers sound different and how that may correlate to measurable differences are also considered. This part of the book also covers other types of amplifiers, such as balanced amplifiers and amplifiers without negative feedback.

Part 6 covers class D amplifiers. Traditional amplifiers have served us well for many decades, and will continue to do so. However, class D amplifiers are the wave of the future. They are smaller and far more efficient. As a result, they generate less heat, making them ideal for multi-channel Home Theater receivers. Sound quality has historically been a problem for class D, but that has improved greatly in the last decade. Their design requires a somewhat different skill set. Part 6 will introduce you to these new design challenges.

1.2 The Role of the Power Amplifier

The power amplifier in an audio system converts the line-level signal to a large signal that can drive the loudspeaker. The line-level signal is typically on the order of 1 to 3 V RMS at maximum power and is not expected to supply much current to the power amplifier. A typical power amplifier will have an input impedance of greater than 10 kΩ. A 100-W power amplifier driving 8 Ω will need to produce about 28 V RMS at about 3.5 A RMS at full power with a sine wave. Thus, it is the job of the power amplifier to produce both relatively high voltage and high current. A very common range of power amplifier voltage gains is on the order of 20 to 30. One volt RMS into a power amplifier
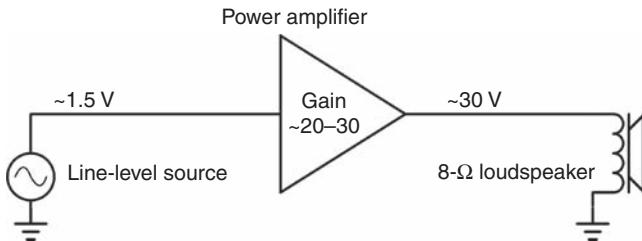
FIGURE 1.1   Power amplifier driving a load.

with a gain of 20 will produce 50 W into an 8-Ω load. Ideally, the power amplifier has very low output impedance so that it essentially acts like a voltage source driving the load. The power amplifier's role in the system is illustrated in Figure 1.1.

1.3   Basic Performance Specifications

The performance specifications listed by the manufacturer of an audio power amplifier range from a very sparse set to a fairly detailed list. The primary specifications include maximum power, frequency response, noise, and distortion.

Rated Output Power

Maximum output power is almost always quoted for a load of 8 Ω and is often quoted for a load of 4 Ω as well. A given voltage applied to a 4-Ω load will cause twice the amount of current to flow, and hence twice the amount of power to be delivered. Ideally, the output voltage of the power amplifier is independent of the load, both for small signals and large signals. This implies that the maximum power into a 4-Ω load would be twice that into an 8-Ω load. In practice, this is seldom the case, due to power supply sag and limitations on maximum available output current.

The correct terminology for power rating is *continuous average sine wave power*, as in *100-W continuous average sine wave power*. However, many often take the liberty of using the term *W RMS*. Although technically incorrect, this wording simply is referring to the fact that the power would have been measured by employing a sine wave whose RMS AC voltage was measured on a long-term basis. There are other ways of rating power that are sometimes used because they provide larger numbers for the marketing folks, but we will ignore them here. When you hear terms like *peak power* just realize that these are not the same as the more rigorous *continuous average power* rating.

Frequency Response

The frequency response of a power amplifier must extend over the full audio band from 20 Hz to 20 kHz within a reasonable tolerance. Modern amplifiers usually far exceed this range, with frequency response from 5 Hz to 200 kHz not the least bit uncommon. The frequency response for such an amplifier is illustrated with the solid curve in Figure 1.2. While the tolerance assigned to the frequency response of loudspeakers is often ± 3 dB, the tolerance associated with power amplifiers is usually + 0 dB, – 3 dB, or tighter. Specifying where an amplifier is down by 3 dB from the nominal 0 dB reference is the conventional way of specifying the bandwidth of a system. This is often referred to as the *3-dB bandwidth*.
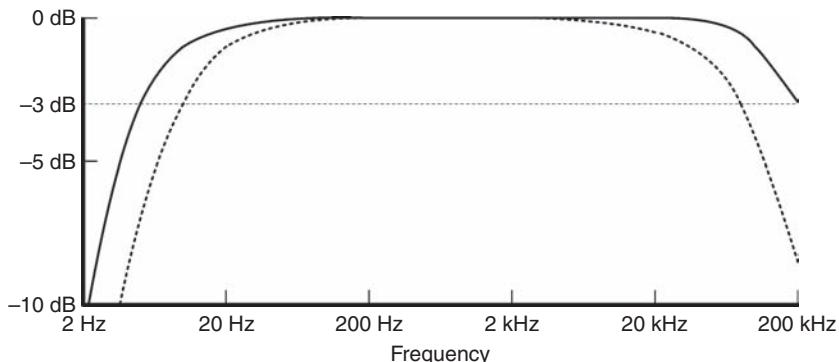
FIGURE 1.2 Amplifier frequency response.

The frequency response for a less capable amplifier is shown with the dashed curve in Figure 1.2. This amplifier has a 3-dB bandwidth from 10 Hz to 80 kHz. Its response is down 1 dB at 20 Hz and 0.5 dB at 20 kHz.

Noise

It is important that power amplifiers produce low noise, since the noise they make is always there, independent of the volume control setting and the listening level. This is particularly so when the amplifiers are used with high-efficiency loudspeakers. The noise is usually specified as being so many decibels down from either the maximum output power or with respect to 1 W. The former number will be larger by 20 dB for a 100-W amplifier, so it is often the one that manufacturers like to cite. The noise referenced to 1 W into 8 Ω (or, equivalently, 2.83 V RMS) is the one more often measured by reviewers.

The noise specification may be unweighted or weighted. Unweighted noise for an audio power amplifier will typically be specified over a full 20-kHz bandwidth (or more). Weighted noise specifications take into account the ear's sensitivity to noise in different parts of the frequency spectrum. The most common one used is *A weighting*, illustrated in Figure 1.3. Notice that the weighting curve is up about +1.2 dB at 2 kHz and down 3 dB at approximately 500 Hz and 10 kHz.
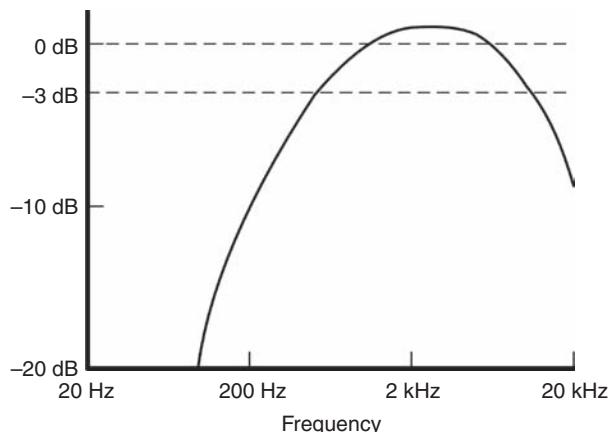
FIGURE 1.3 A weighting frequency response.

The A-weighted noise specification for an amplifier will usually be quite a bit better than the unweighted noise because the weighted measurement tends to attenuate noise contributions at higher frequencies and hum contributions at lower frequencies. A very good amplifier might have an unweighted signal to noise ratio (S/N) of 90 dB with respect to a 1-W output into 8 Ω, while that same amplifier might have an A-weighted S/N of 105 dB with respect to 1 W. A fair amplifier might sport 65 dB and 80 dB S/N figures, respectively. The A-weighted number will usually be 10–20 dB better than the unweighted number.

Distortion

The most common distortion specification is *total harmonic distortion* (THD). It will usually be specified at one or two frequencies or over a range of frequencies. It will be typically specified at a given power level with the amplifier driving a specified load impedance. A good 100-W amplifier might have a 1-kHz THD (referred to as *THD-1*) of 0.005% at 100 W into 8 Ω. That same amplifier might have a 20-kHz THD (*THD-20*) of 0.02% up to 100 W into 8 Ω. Although 1-kHz THD is at a frequency in the middle of the audible frequency range where hearing sensitivity is high, it is not very difficult to achieve low THD figures at 1 kHz. Good THD-20 performance is much more difficult to achieve and is generally a better indicator of amplifier performance.

In practice, the harmonic distortion specification will be described as *THD + N*, where the *N* refers to noise. This reflects the way in which THD is most often measured. When measuring THD-1, a 1-kHz *fundamental* sine wave is applied to the amplifier input. The 1-kHz fundamental appearing in the output signal is then notched out by a very sharp filter. Everything else, both distortion harmonics and noise, is measured, giving rise to the THD + N specification. At higher power testing levels, the true THD will often dominate the noise, but at lower power levels the measurement may often reflect the noise rather than the actual THD being measured. Graphs that show rising THD + N at lower power levels can be misleading. The rising level may actually be noise rather than distortion. This is because a fixed noise voltage becomes a larger percentage of the level of the fundamental as the fundamental decreases in amplitude at lower power levels. There are many other power amplifier distortion specifications, and these will be covered in detail in later chapters in this book.

The Federal Trade Commission (FTC) long ago tried to wrap things up in a single statement that would largely capture power, distortion, and bandwidth together [1]. It would read something like "100-W continuous average power from 20 Hz to 20 kHz with less than 0.02% total harmonic distortion." This was a reasonably comprehensive and honest way to describe the most basic capability of an amplifier. It is unfortunate that it has fallen into disuse by many manufacturers. Part of the reason was that it also required that the amplifier could be run at ⅓ rated power into 8 Ω for an extended period of time without overheating. Operating at ⅓ rated power is close to the point where most amplifiers dissipate the most heat, and it was expensive for many amplifier manufacturers to provide enough heat sinking to meet this requirement.

1.4   Additional Performance Specifications

There is almost no limit to the number of useful performance specifications for an audio power amplifier, but the following are a few that are a bit less basic and yet quite useful.
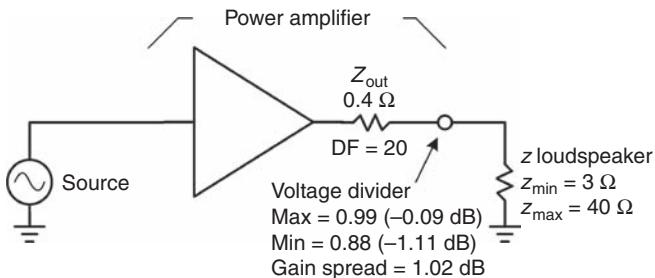
FIGURE 1.4   Amplifier output impedance.

Damping Factor

A flat frequency response is desirable to avoid tonal coloration, but a flat response may not always be obtained when the amplifier is driving a real-world loudspeaker load. The input impedance of real loudspeakers can vary dramatically as a function of frequency, while the output impedance of the power amplifier is nonzero. A voltage divider is thus formed by the amplifier output impedance and the loudspeaker input impedance, as illustrated in Figure 1.4. Here the amplifier is modeled with an ideal amplifier with zero output impedance in series with impedance Z_{out} that describes its actual output impedance. This is referred to as a Thévenin equivalent circuit.

This is where the *damping factor* (DF) comes into play. In spite of its important-sounding name, this is just a different way of expressing the output impedance of the amplifier. While amplifiers ideally act like voltage sources with zero output impedance, they all have finite output impedance. The term damping factor came from the fact that a loudspeaker is a mechanically resonant system; the low output impedance of an amplifier damps that resonance via the resistance of the loudspeaker's voice coil and *electromotive force*. An amplifier with higher output impedance will provide less damping of the loudspeaker cone motion because it adds to the total amount of resistance in the circuit.

Damping factor is defined as the ratio of 8 Ω to the actual output impedance of the amplifier. Thus, an amplifier with an output impedance of 0.2 Ω will have a DF of 40. Most vacuum tube amplifiers have a DF of less than 20, while many solid-state amplifiers have a DF in excess of 100. It is important to bear in mind that the DF is usually a function of frequency, often being larger at low frequencies. This is consistent with the need to dampen the cone motion of woofers, but ignores the influence of the DF on frequency response at higher frequencies. Many loudspeakers have a substantial peak or dip in their impedance at or near their crossover frequencies. This could result in coloration if the amplifier DF is low.

The effect of damping factor and output impedance on frequency response must not be underestimated in light of the large impedance variations seen in many contemporary loudspeakers. It is not unusual for a loudspeaker's impedance to dip as low as 3 Ω and rise as high as 40 Ω across the audio band. Consider this wildly varying load against the 0.4-Ω output impedance of a vacuum tube amplifier with a DF of 20. This will cause an audible peak-to-peak frequency response variation of ± 0.5 dB across the audio band.

Dynamic Headroom

Unlike a sine wave, music is impulsive and dynamic. Its power peaks are often many times its average power. This ratio is often referred to as the *crest factor*. *Dynamic headroom*

refers to the fact that an amplifier can usually put out a greater short-term burst of power than it can on a continuous basis. The primary cause of this is power supply sag which is a reflection of power supply regulation. The power supply voltages will initially remain high and near their no-load values for a brief period of time during heavy loading due to the energy storage of the large reservoir capacitors. Under long-term conditions, the voltage will sag and less maximum power will be available.

Consider an amplifier that clips at 100 W into 8 Ω on a continuous test basis. If this amplifier has a power supply with 10% regulation from no-load to full load (which is fairly good), the available power supply voltage will be about 10% higher during a short-term burst. This will result in a short-term power capability on the order of 120 W, since power goes as the square of voltage.

Dynamic headroom is a two-edged sword. It is good to have it because music tends to have an average power level much lower than the brief peak power levels it can demand (referring again to the crest factor). It is nice to have 20% to 40% more power available when it is needed for those brief peaks. On the other hand, a large amount of dynamic headroom is often symptomatic of an amplifier with a sloppy power supply.

Slew Rate

Slew rate is a measure of how fast the output voltage of the amplifier can change under large-signal conditions. It is specified in volts per microsecond. Slew rate is an indicator of how well an amplifier can respond to high-level transient program content. A less capable amplifier might have a slew rate of 5 V/μs, whereas a really high-performance amplifier might have a slew rate on the order of 50 to 300 V/μs. For a given type of program material, a higher-power amplifier needs to have a higher slew rate to do as well as a lower-power amplifier, since its voltage swings will be larger. A 100-W amplifier driving a loudspeaker whose efficiency is 85 dB will need to have 3.16 times the amount of slew rate capability as a 10-W amplifier driving a 95-dB speaker to the same sound pressure level.

As a point of reference, the maximum voltage rate of change of a 20-kHz sine wave is 0.125 V/μs per volt peak. This means that a 100-W amplifier that produces a level of 40-V peak at 20 kHz must have a slew rate of at least 5 V/μs. In practice a much larger value is desirable for low-distortion performance on high-frequency program content. Although technically imprecise, the rate of change of a signal is often referred to its slew rate for convenience.

The slew rate capability of audio power amplifiers received a lot more attention after the term *transient intermodulation distortion* (TIM) was coined and studied intensely during the 1970s and early 1980s [2,3,4]. This was largely another way of describing high-frequency distortion that resulted from slew rate deficiency. The TIM controversy will be discussed in greater detail in Chapter 24.

Output Current

Output current is another lesser-known amplifier specification that can have a strong influence on sonic quality. As we will see later, the complex reactive loudspeaker load presented to an amplifier can demand larger currents than the rated resistive load with which an amplifier is often tested. Add to this is the fact that many loudspeakers have impedances that dip well below their rated impedance, and we have a recipe for high current demands.

Minimum Load Impedance

Related to output current capability is the specification of minimum stable or safe output impedance that an amplifier can drive. Although there are many 4-Ω-rated loudspeakers out there (whose impedance often dips below 3 Ω), there are many amplifiers in AV receivers that are not able to properly drive a 4-Ω load. This is partly because cramming five or more amplifiers into one enclosure that can properly drive 4-Ω loads while being able to deliver over 100 W each into 8 Ω is quite difficult and surely more expensive. This is much less of a problem with stereo amplifiers, where heat removal for only two channels is necessary. However, even amplifiers that are rated to drive 4-Ω loads may at times find themselves with too little current drive capability to drive some contemporary loudspeakers. High-end loud-speakers are often designed with little regard for what it takes to drive them.

1.5   Output Voltage and Current

Here we will briefly touch on the reality of output voltage and current swing that an amplifier may have to deliver in practice. Table 1.1 shows the RMS value of the sine wave voltage, the peak voltage, the peak current, and the reserve current required for the popular 8-Ω resistive load as a function of power.

The reserve current listed below is simply a factor of three greater than the peak current required of a resistive load and represents the reality of driving difficult reactive loudspeaker loads with nonsinusoidal waveforms. In Chapter 18 we will see where this somewhat arbitrary factor of three comes from. The reserve current can be assumed to occur only in a brief time interval under fairly rare circumstances.

This data gives a glimpse of what is necessary for the amplifier to provide. Notice the very substantial voltage swings, and implied power supply voltages, required for a 400-W amplifier. The peak and reserve currents are also into the tens of amperes at 400 W. This is just the beginning of the story, however. Table 1.2 shows what the same amplifier would encounter when driving a 4-Ω load. Here we have assumed that the drive signal has remained the same and only the load impedance has dropped. We have also implicitly assumed that the amplifier has ideal power supply regulation, so all of the power numbers are doubled.

Given the nature of some of today's high-end loudspeakers, some have argued that really high-performance amplifiers should be rated for power delivery into 2 Ω (at least for short intervals). Indeed, the testing done in some amplifier technical reviews regularly subjects power amplifiers to a 2-Ω resistive load test. The figures for output current become almost bewildering under these conditions.

An important point here is that there are amplifiers sold every day that are rated at up to 400 W per channel into 8 Ω, and designers implement such amplifiers every day.

Power, W	V_{RMS}	V_{peak}	I_{peak}	$I_{reserve}$
50	20	28	3.5	10.5
100	28	40	5.0	15.0
200	40	56	7.0	21.0
400	57	80	10.0	30.0

TABLE 1.1   Voltage and Current into an 8-Ω Load

Power, W	V_{RMS}	V_{peak}	I_{peak}	$I_{reserve}$
100	20	28	7	21
200	28	40	10	30
400	40	56	14	42
800	57	80	20	60

TABLE 1.2   Voltage and Current into a 4-Ω Load

Power, W	V_{RMS}	V_{peak}	I_{peak}	$I_{reserve}$
200	20	28	14	42
400	28	40	20	60
800	40	56	28	84
1600	57	80	40	120

TABLE 1.3   Voltage and Current into a 2-Ω Load

The sobering point is that if at the same time the designer thinks in terms of his amplifier being 2-Ω compatible, the potential demanded burst current could on occasion be quite enormous. This is illustrated in Table 1.3.

1.6   Basic Amplifier Topology

Figure 1.5 shows a simplified three-stage audio power amplifier design. This is a direct descendant of the Lin topology introduced in the 1950s. Although other arrangements have appeared through the years, this one and its many derivatives account for the vast majority of power amplifier designs, and it will be the focus of most of this book.

Transistors Q1 and Q2 form the input differential pair. This arrangement is often called a *long-tailed pair* (*LTP*) because it is supplied with a so-called tail current from a very high-impedance circuit like the current source shown. We will often take the liberty of referring to the amplifier's *input stage* as the *IPS*. The input differential amplifier usually has a fairly low voltage gain, typically ranging from 1 to 15.

The IPS compares the applied input signal to a fraction of the output of the amplifier and provides the amount of signal necessary for the remainder of the amplifier to create the required output. This operation forms the essence of the negative feedback loop. The fraction of the output to which the input is compared is determined by the voltage divider consisting of R3 and R2. If the fraction is 1/20 and the forward gain of the amplifier is large, then very little difference need exist between the input and the fed back signal applied to the IPS in order to produce the required output voltage. The gain of the amplifier will then be very nearly 20. This is referred to as the *closed-loop gain* of the a*mplifier* (*CLG* or A_{cl}).

This simplified explanation of how negative feedback works is illustrated in Figure 1.6. The core of the amplifier that provides all of the *open-loop gain* (*OLG* or A_{ol}) is shown as a
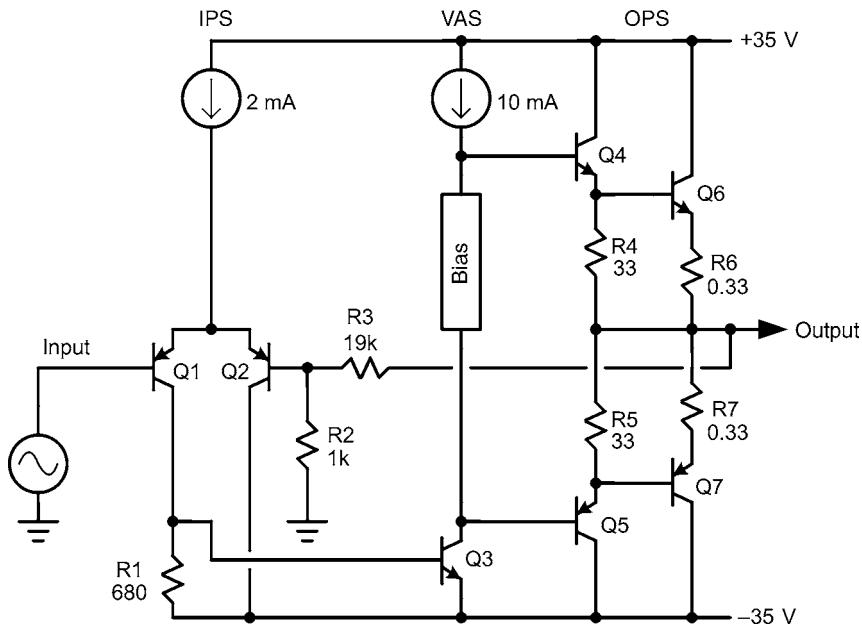
FIGURE 1.5   Simple three-stage power amplifier.
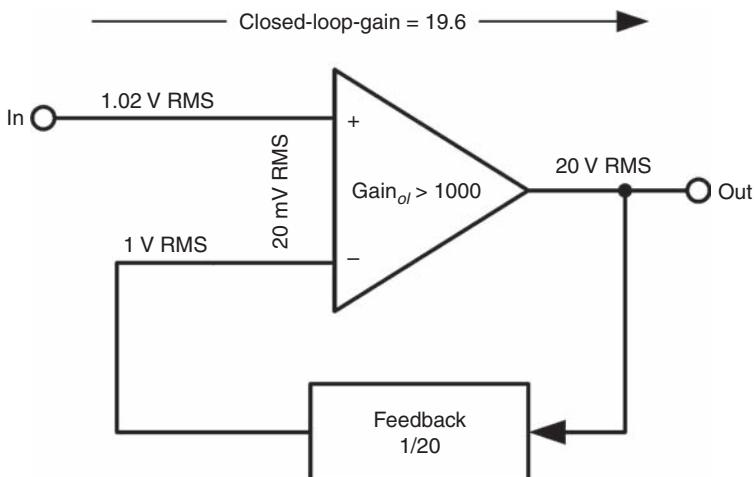
FIGURE 1.6   Negative feedback operation.

gain block symbol just like an operational amplifier. For purposes of illustration, it is shown with a gain of 1000. The feedback network is shown as a block that attenuates the signal being fed back by a factor of 20. Suppose the output of the amplifier is 20 V, the amount fed back will then be 1 V. The input across the differential inputs of the gain block will be 20 mV if the forward gain is 1000. The required input from the input terminal will then be 1.02 V. This simplified approach to looking at a feedback circuit is sometimes

referred to as *input-referred* feedback analysis because we start at the output and work our way back to the input to see what input would have been required to produce the assumed output. The closed-loop gain is thus 20/1.02 = 19.6. This is just 2% shy of what we would get if we assumed that the closed-loop gain were just the inverse of the attenuation in the feedback path.

Transistor Q3 in Figure 1.5 forms what is called the *voltage amplifier stage (VAS)*. It is a high-gain *common-emitter (CE)* stage that provides most of the voltage gain of the amplifier. Notice that it is loaded with a current source rather than a resistor so as to provide the highest possible gain. It is not unusual for the VAS to provide a voltage gain of 100 to 10,000. This means that the difference signal needed to drive the input stage does not need to be very large to drive the output to its required level. If the difference signal is close to zero, and 1/20 of the output is compared to the input, it follows that the output would be almost exactly 20 times the input.

The *output stage* (OPS) is composed of transistors Q4 through Q7. Its main job is to provide buffering in the form of current gain between the output of the VAS and the loudspeaker load. Most output stages have a voltage gain of approximately unity. The output stage here consists essentially of two pairs of *emitter followers* (EF), one for each polarity of the output swing. This is called a complementary push-pull output stage. Transistors Q4 and Q5 are referred to as the *drivers*, while Q6 and Q7 are the output devices.

The two-stage OPS, like this one, will typically provide a current gain between 500 and 10,000. This means that an 8-Ω load resistance will look like a load resistance between 4000 and 80,000 Ω to the output of the VAS. Other output stages, like so-called *triples*, can provide current gain of 100,000 to 1 million, greatly reducing the load on the VAS.

This OPS is the classic *class B* output stage used in most audio power amplifiers. The upper output transistor conducts on positive half-cycles of the signal when it is necessary to source current to the load. The bottom output transistor conducts on the negative half-cycle when it is necessary to sink current from the load. The signal thus follows a different path through the amplifier on different halves of the signal. This of course can lead to distortion

The box labeled *bias* provides a DC bias voltage that overcomes the turn-on base-emitter voltage drops (V_{be}) of the driver and output transistors. It also keeps them active with a small quiescent bias current even when no current is being delivered to the load. This bias circuit is usually referred to as the *bias spreader*. The output stage bias current creates a small region of overlapping conduction between the positive and negative output transistors. This smoothes the transition from the upper transistors to the lower transistors (and vice versa) when the output signal goes from positive to negative and the output stage goes from sourcing current to the load to sinking current from the load. We'll have much more to say about this crossover region and the distortion that it can create in Chapters 5 and 10. Because there is a small region of overlap where both transistors are conducting, this type of output stage is often referred to as a *class AB* output stage.

If the bias spreader is set to provide a very large output stage idle bias current, both the top and bottom output transistors will conduct on both half-cycles of the signal. One will be increasing its current as the other decreases its current, with the difference flowing into the load. In this case we have a so-called *class A* output stage. The fact that the signal is then always taking the same path to the output (consisting of two parallel paths) tends to result in less distortion because there is no crossover

from one half of the output stage to the other as the signal swings from positive to negative. The price paid is very high power dissipation as a result of the high output stage bias current.

Actual operation of the amplifier of Figure 1.5 is quite simple. The input differential amplifier compares the input voltage to a scaled-down version of the output voltage and acts to make them essentially the same. This action applies to both stabilization of the DC operating points and the processing of AC signals. In the quiescent state transistors Q1 and Q2 are conducting the same amount of current, in this case 1 mA each. The resulting voltage drop across R1 is just enough to turn on Q3 to conduct 10 mA, balancing the current supplied to its collector by the 10-mA current source.

Now suppose the output is more positive than it should be, the voltage at the base of PNP transistor Q1 will then be negative with respect to the scaled version of the output voltage at the base of Q2. A more negative voltage at the base of a PNP transistor causes it to conduct more current. Transistor Q1 will thus conduct more current and increase the voltage drop across R1. This will increase the voltage at the base of NPN transistor Q3. A more positive voltage at the base of an NPN transistor causes it to conduct more current. Transistor Q3 will thus turn on harder. This will cause an imbalance between Q3's collector current and the 10-mA current source. Q3's increased collector current will thus pull the voltage at its collector node more negative. This will drive the bases of the driver and output transistors more negative. Their emitters will follow this negative voltage change, causing the output of the amplifier to go more negative. The result will be that the initially assumed positive error in the output voltage will be corrected.

1.7   Summary

We've seen what an audio power amplifier can do, and the basic design described in qualitative terms. In the next chapter we'll learn a bit about bipolar transistors and the simple circuit building blocks that make up a power amplifier. Equipped with this knowledge, we will then analyze in some detail the workings of the basic power amplifier.

References

1. Federal Trade Commission (FTC), "Power Output Claims for Amplifiers Utilized in Home Entertainment Products", CFR 16, Part 432, 1974.
2. Otala, M, "Transient Distortion in Transistorized Audio Power Amplifiers," *IEEE Transactions on Audio and Electro-acoustics*, vol. AU-18, pp. 234–239, September, 1970.
3. Jung, W. G., M. L. Stephens, and C. C. Todd, "Slewing Induced Distortion and Its Effect on Audio Amplifier Performance–With Correlated Measurement Listening Results," AES preprint No. 1252 presented at the 57th AES Convention, Los Angeles, 1977.
4. Cordell, R. R., "Another View of TIM," *Audio,* February & March, 1980.

Power Amplifier Basics

I n this chapter we'll look at the design of a basic power amplifier in detail. Some information about transistors will first be discussed, followed by a simple analysis of the basic building block circuits that are inevitably used to build a complete amplifier circuit. This will provide a good foundation for the detailed analysis of the basic amplifier that follows. Chapter 3 will then take us on a tour of amplifier design, evolving and assessing a design as its performance is improved to a high level.

2.1   About Transistors

The *bipolar junction transistor (BJT)* is the primary building block of most audio power amplifiers. This section is not meant to be an exhaustive review of transistors, but rather presents enough knowledge for you to understand and analyze transistor amplifier circuits. More importantly, transistor behavior is discussed in the context of power amplifier design, with many relevant tips along the way.

Current Gain

If a small current is sourced into the base of an NPN transistor, a much larger current flows in the collector. The ratio of these two currents is the current gain, commonly called *beta* (β) or h_{fe}. Similarly, if one sinks a small current from the base of a PNP transistor, a much larger current flows in its collector.

The current gain for a typical small-signal transistor often lies between 50 and 200. For an output transistor, β typically lies between 20 and 100. Beta can vary quite a bit from transistor to transistor and is also a mild function of the transistor current and collector voltage.

Because transistor β can vary quite a bit, circuits are usually designed so that their operation does not depend heavily on the particular value of β for its transistors. Rather, the circuit is designed so that it operates well for a minimum value of β and better for very high β. Because β can sometimes be very high, it is usually bad practice to design a circuit that would misbehave if β became very high. The *transconductance* (*gm*) of the transistor is actually the more predictable and important design parameter (as long as β is high enough not to matter much). For those unfamiliar with the term, transconductance of a transistor is the change in collector current in response to a given change in base-emitter voltage, in units of siemens (S; amps per volt).

$$gm = \Delta I_c / \Delta V_{be}$$

The familiar collector current characteristics shown in Figure 2.1 illustrate the behavior of transistor current gain. This family of curves shows how the collector current
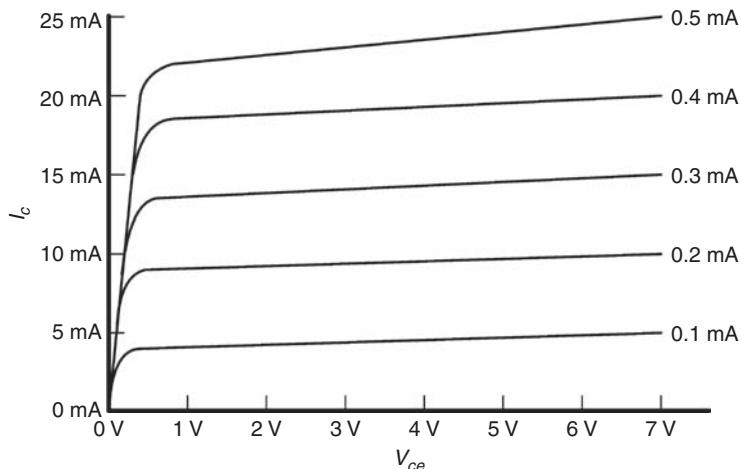
FIGURE 2.1 Transistor collector current characteristic.

increases as collector-emitter voltage (V_{ce}) increases, with base current as a parameter. The upward slope of each curve with increasing V_{ce} reveals the mild dependence of β on collector-emitter voltage. The spacing of the curves for different values of base current reveals the current gain. Notice that this spacing tends to increase as V_{ce} increases, once again revealing the dependence of current gain on V_{ce}. The spacing of the curves may be larger or smaller between different pairs of curves. This illustrates the dependence of current gain on collector current. The transistor shown has β of about 50.

Beta can be a strong function of current when current is high; it can decrease quickly with increases in current. This is referred to as *beta droop* and can be a source of distortion in power amplifiers. A typical power transistor may start with a β of 70 at a collector current of 1 A and have its β fall to 20 or less by the time I_c reaches 10 A. This is especially important when the amplifier is called on to drive low load impedances. This is sobering in light of the current requirements illustrated in Table 1.3.

Base-Emitter Voltage

The bipolar junction transistor requires a certain forward bias voltage at its base-emitter junction to begin to conduct collector current. This turn-on voltage is usually referred to as V_{be}. For silicon transistors, V_{be} is usually between 0.5 and 0.7 V. The actual value of V_{be} depends on the transistor device design and the amount of collector current (I_c).

The base-emitter voltage increases by about 60 mV for each decade of increase in collector current. This reflects the logarithmic relationship of V_{be} to collector current. For the popular 2N5551, for example, $V_{be} = 600$ mV at 100 μA and rises to 720 mV at 10 mA. This corresponds to a 120 mV increase for a two-decade (100:1) increase in collector current.

Tiny amounts of collector current actually begin to flow at quite low values of forward bias (V_{be}). Indeed, the collector current increases exponentially with V_{be}. That is why it looks like there is a fairly well-defined turn-on voltage when collector current is plotted against V_{be} on linear coordinates. It becomes a remarkably straight line when

the log of collector current is plotted against V_{be}. Some circuits, like multipliers, make great use of this logarithmic dependence of V_{be} on collector current.

Put another way, the collector current increases exponentially with base-emitter voltage, and we have the approximation

$$I_c = I_S e^{(V_{be}/V_T)}$$

where the voltage V_T is called the *thermal voltage*. Here V_T is about 26 mV at room temperature and is proportional to absolute temperature. This plays a role in the temperature dependence of V_{be}. However, the major cause of the temperature dependence of V_{be} is the strong increase with temperature of the *saturation current I_S*. This ultimately results in a negative temperature coefficient of V_{be} of about –2.2 mV/°C.

Expressing base-emitter voltage as a function of collector current, we have the analogous approximation

$$V_{be} = V_T \ln (I_c/I_S)$$

where $\ln (I_c/I_S)$ is the natural logarithm of the ratio I_c/I_S. The value of V_{be} here is the *intrinsic* base-emitter voltage, where any voltage drops across physical base resistance and emitter resistance are not included.

The base-emitter voltage for a given collector current typically decreases by about 2.2 mV for each degree Celsius increase in temperature. This means that when a transistor is biased with a fixed value of V_{be}, the collector current will increase as temperature increases. As collector current increases, so will the power dissipation and heating of the transistor; this will lead to further temperature increases and sometimes a vicious cycle called *thermal runaway*. This is essentially positive feedback in a local feedback system.

The V_{be} of power transistors will start out at a smaller voltage at a low collector current of about 100 mA, but may increase substantially to 1 V or more at current in the 1 to 10-A range. At currents below about 1 A, V_{be} typically follows the logarithmic rule, increasing by about 60 mV per decade of increase in collector current. As an example, V_{be} might increase from 550 mV at 150 mA to 630 mV at 1 A. Even this is more than 60 mV per decade.

Above about 1 A, V_{be} versus I_c for a power transistor often begins to behave linearly like a resistance. In the same example, V_{be} might increase to about 1.6 V at 1 A. This would correspond to effectively having a resistance of about 0.1 Ω in series with the emitter. The actual emitter resistance is not necessarily the physical origin of the increase in V_{be}. The voltage drop across the base resistance RB due to base current is often more significant. This voltage drop will be equal to $RB(I_c/\beta)$. The effective contribution to resistance as seen at the emitter by RB is thus RB/β. The base resistance divided by β is often the dominant source of this behavior.

Consider a power transistor operating at $I_c = 10$ A and having a base resistance of 4 Ω, an operating β of 50, and an emitter resistance of 20 mΩ. Base current will be 200 mA and voltage drop across the base resistance will be 0.8 V. Voltage drop across the emitter resistance will be 0.2 V. Adding the intrinsic V_{be} of perhaps 660 mV, the base-emitter voltage becomes 1.66 V. It is thus easy to see how rather high V_{be} can develop for power transistors at high operating currents.

The Gummel Plot

If the log of collector current is plotted as a function of V_{be}, the resulting diagram is very revealing. As mentioned above, it is ideally a straight line. The diagram becomes even
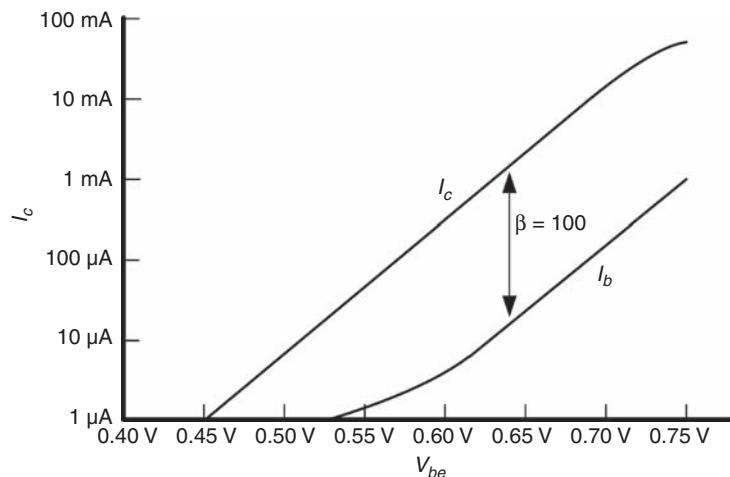
FIGURE 2.2 Transistor Gummel plot.

more useful and insightful if base current is plotted on the same axes. This is now called a *Gummel plot*. It sounds fancy, but that is all it is. The magic lies in what it reveals about the transistor. A Gummel plot is shown in Figure 2.2.

In practice, neither the collector current nor the base current plots are straight lines over the full range of V_{be}, and the bending illustrates various nonidealities in the transistor behavior. The vertical distance between the lines corresponds to the β of the transistor, and the change in distance shows how β changes as a function of V_{be} and, by extension, I_c. The curves in Figure 2.2 illustrate the typical loss in transistor current gain at both low and high current extremes.

Transconductance

While transistor current gain is an important parameter and largely the source of its amplifying ability, the transconductance of the transistor is perhaps the most important characteristic used by engineers when doing actual design. Transconductance, denoted as *gm*, is the ratio of the change in collector current to the change in base voltage.

The unit of measure of transconductance is the siemens (S), which corresponds to a current change of 1 A for a change of 1 V. This is the inverse of the measure of resistance, the ohm (it was once called the *mho, ohm* spelled backward). If the base-emitter voltage of a transistor is increased by 1 mV, and as a result the collector current increases by 40 μA, the transconductance of the transistor is 40 milliseimens (mS).

The transconductance of a bipolar transistor is governed by its collector current. This is a direct result of the exponential relationship of collector current to base-emitter voltage. The slope of that curve increases as I_c increases; this means that transconductance also increases. Transconductance is given simply as

$$gm = I_c/V_T$$

where V_T is the thermal voltage, typically 26 mV at room temperature. At a current of 1 mA, transconductance is 1 mA/26 mV = 0.038 S.

The inverse of *gm* is a resistance. Sometimes it is easier to visualize the behavior of a circuit by treating the transconductance of the transistor as if it were a built-in dynamic emitter resistance *re′*. This resistance is just the inverse of *gm*, so we have

$$re' = V_T/I_c = 0.026/I_c \qquad \text{(at room temperature)}$$

In the above case *re′* = 26 Ω at a collector current of 1 mA.

An important approximation that will be used frequently is that *re′* = 26 Ω/I_c where I_c is expressed in milliamperes. If a transistor is biased at 10 mA, *re′* will be about 2.6 Ω. The transistor will act as if a change in its base-emitter voltage is directly impressed across 2.6 Ω; this causes a corresponding change in its emitter current and very nearly the same change in its collector current. This forms the basis of the common-emitter (*CE*) amplifier.

It is important to recognize that *gm* = 1/*re′* is the *intrinsic* transconductance, ignoring the effects of base and emitter resistance. Actual transconductance will be reduced by emitter resistance (*RE*) and *RB*/β being added to *re′* to arrive at net transconductance. This is especially important in the case of power transistors.

Input Resistance

If a small change is made in the base-emitter voltage, how much change in base current will occur? This defines the effective input resistance of the transistor. The transconductance dictates that if the base-emitter voltage is changed by 1 mV, the collector current will change by about 40 μA if the transistor is biased at 1 mA. If the transistor has a β of 100, the base current will change by 0.38 μA. Note that the β here is the effective current gain of the transistor for small changes, which is more appropriately referred to as the *AC current gain* or *AC beta* ($β_{AC}$). The effective input resistance in this case is therefore about 1 mV/0.38 μA = 2.6 kΩ. The effective input resistance is just $β_{AC}$ times *re′*.

Early Effect

The Early effect manifests itself as finite output resistance at the collector of a transistor and is the result of the current gain of the transistor being a function of the collector-base voltage. The collector characteristic curves of Figure 2.1 show that the collector current at a given base current increases with increased collector voltage. This means that the current gain of the transistor is increasing with collector voltage. This also means that there is an equivalent output resistance in the collector circuit of the transistor.

The increase of collector current with increase in collector voltage is called the *Early effect*. If the straight portions of the collector current curves in Figure 2.1 are extrapolated to the left, back to the *X* axis, they will intersect the *X* axis at a negative voltage. The value of this voltage is called the *Early voltage (VA)*. The slope of these curves represents the output resistance *ro* of the device.

Typical values of *VA* for small-signal transistors lie between 20 and 200 V. A very common value of *VA* is 100 V, as for the 2N5551. The output resistance due to the Early effect decreases with increases in collector current. A typical value of this resistance for a small-signal transistor operating at 1 mA is on the order of 100 kΩ.

The Early effect is especially important because it acts as a resistance in parallel with the collector circuit of a transistor. This effectively makes the net load resistance on the collector smaller than the external load resistance in the circuit. As a result, the gain of a common-emitter stage decreases. Because the extra load resistance is a function of

collector voltage and current, it is a function of the signal and is therefore nonlinear and so causes distortion.

The Early effect can be modeled as a resistor ro connected from the collector to the emitter of an otherwise "perfect" transistor [1]. The value of ro is

$$ro = \frac{(VA + V_{ce})}{I_c}$$

For the 2N5551, with a VA of 100 and operating at $V_{ce} = 10$ V and $I_c = 10$ mA, ro comes out to be 11 kΩ. The value of ro is doubled as the collector voltage swings from very small voltages to a voltage equal to the Early voltage.

It is important to understand that this resistance is not, by itself, necessarily the output resistance of a transistor stage, since it is not connected from collector to ground. It is connected from collector to emitter. Any resistance or impedance in the emitter circuit will significantly increase the effective output resistance caused by ro.

The Early effect is especially important in the VAS of an audio power amplifier. In that location the device is subjected to very large collector voltage swings and the impedance at the collector node is quite high due to the usual current source loading and good buffering of the output load from this node.

A 2N5551 VAS transistor biased at 10 mA and having no emitter degeneration will have an output resistance on the order of 14 kΩ at a collector-emitter voltage of 35 V. This would correspond to a signal output voltage of 0 V in an arrangement with ± 35 V power supplies. The same transistor with 10:1 emitter degeneration will have an output resistance of about 135 kΩ.

At a collector-emitter voltage of only 5 V (corresponding to a −30-V output swing) that transistor will have a reduced output resistance of 105 kΩ. At a collector-emitter voltage of 65 V (corresponding to a +30-V output swing), that transistor will have an output resistance of about 165 kΩ. These changes in output resistance as a result of signal voltage imply a change in gain and thus second harmonic distortion.

Because the Early effect manifests itself as a change in the β of the transistor as a function of collector voltage, and because a higher-β transistor will require less base current, it can be argued that a given amount of Early effect has less influence in some circuits if the β of the transistor is high. A transistor whose β varies from 50 to 100 due to the Early effect and collector voltage swing will have more effect on circuit performance in many cases than a transistor whose β varies from 100 to 200 over the same collector voltage swing. The variation in base current will be less in the latter than in the former. For this reason, the product of β and VA is an important *figure of merit* (FOM) for transistors. In the case of the 2N5551, with a current gain of 100 and an Early voltage VA of 100 V, this FOM is 10,000 V. The FOM for bipolar transistors often lies in the range of 5000 to 50,000 V.

$$\text{Early effect FOM} = β * VA$$

Junction Capacitance

All BJTs have base-emitter capacitance (C_{be}) and collector-base capacitance (C_{cb}). This limits the high-frequency response, but also can introduce distortion because these junction capacitances are a function of voltage.

The base, emitter, and collector regions of a transistor can be thought of as plates of a capacitor separated by nonconducting regions. The base is separated from the emitter

by the base-emitter junction, and it is separated from the collector by the base-collector junction. Each of these junctions has capacitance, whether it is forward biased or reverse biased. Indeed, these junctions store charge, and that is a characteristic of capacitance.

A reverse-biased junction has a so-called *depletion region*. The depletion region can be thought of roughly as the spacing of the plates of the capacitor. With greater reverse bias of the junction, the depletion region becomes larger. The spacing of the capacitor plates is then larger, and the capacitance decreases. The junction capacitance is thus a function of the voltage across the junction, decreasing as the reverse bias increases.

This behavior is mainly of interest for the collector-base capacitance C_{cb}, since in normal operation the collector-base junction is reverse biased while the base-emitter junction is forward biased. It will be shown that the effective capacitance of the forward-biased base-emitter junction is quite high.

The variance of semiconductor junction capacitance with reverse voltage is taken to good use in *varactor diodes,* where circuits are electronically tuned by varying the reverse bias on the varactor diode. In audio amplifiers, the effect is an undesired one, since capacitance varying with signal voltage represents nonlinearity. It is obviously undesirable for the bandwidth or high-frequency gain of an amplifier stage to be varying as a function of the signal voltage.

The collector-base capacitance of the popular 2N5551 small-signal NPN transistor ranges from a typical value of 5 pF at 0 V reverse bias (V_{cb}) down to 1 pF at 100 V. For what it's worth, its base-emitter capacitance ranges from 17 pF at 0.1-V reverse bias to 10 pF at 5 V reverse bias. Remember, however, that this junction is usually forward biased in normal operation. The junction capacitances of a typical power transistor are often about two orders of magnitude larger than those of a small-signal transistor.

Speed and f_T

The AC current gain of a transistor falls off at higher frequencies in part due to the need for the input current to charge and discharge the relatively large capacitance of the forward-biased base-emitter junction.

The most important speed characteristic for a BJT is its f_T, or *transition frequency*. This is the frequency where the AC current gain β_{AC} falls to approximately unity. For small-signal transistors used in audio amplifiers, f_T will usually be on the order of 50 to 300 MHz. A transistor with a low-frequency β_{AC} of 100 and an f_T of 100 MHz will have its β_{AC} begin to fall off (be down 3 dB) at about 1 MHz. This frequency is referred to as f_β.

The effective value of the base-emitter capacitance of a conducting BJT can be shown to be approximately

$$C_{be} = gm/\omega_T$$

where ω_T is the radian frequency equal to $2\pi f_T$ and gm is the transconductance.

Because $gm = I_c/V_T$, one can also state that

$$C_{be} = I_c/(V_T * \omega_T)$$

This capacitance is often referred to as C_π for its use in the so-called hybrid pi model. Because transconductance increases with collector current, so does C_{be}. For a transistor with a 100 MHz f_T and operating at 1 mA, the effective base-emitter capacitance will be about 61 pF.

Power transistors usually have a much lower value of f_T, often in the range of 1 to 8 MHz for conventional power devices. The effective base-emitter capacitance for a power transistor can be surprisingly large. Consider a power transistor whose f_T is 2 MHz. Assume it is operating at $I_c = 1$ A. Its transconductance will be $I_c/V_T = 1.0/0.026 = 38.5$ S. Its ω_T will be 12.6 Mrad/s. Its C_{be} will be

$$C_{be} = gm/\omega_T = 3.1\ \mu F$$

Needless to say, this is a real eye-opener!

This explains why it can be difficult to turn off a power transistor quickly. Suppose the current gain of the power transistor is 50, making the base current 20 mA. If that base-current drive is removed and the transistor is allowed to turn off, the V_{be} will change at a rate of

$$I_b/C_\pi = 0.02/3.1 \times 10^{-6} = 6.4\ mV/\mu s$$

Recall that a 60 mV change in V_{be} will change the collector current by a factor of about 10. This means that it will take about 9 μs for the collector current to fall from 1 to 0.1 A. This illustrates why it is important to actively pull current out of the base to turn off a transistor quickly. This estimate was only an approximation because it was assumed that C_π was constant during the discharge period. It was not, since I_c was decreasing. However, the base current, which was the discharge current in this case, was also decreasing during the discharge period. The decreasing C_π and the decreasing base current largely cancel each other's effects, so the original approximation was not too bad.

In a real circuit there will usually be some means of pulling current out of the base, even if it is just a resistor from base to emitter. This will help turn off the transistor more quickly.

In order to decrease the collector current of the transistor from 1 to 0.1 A, C_π must be discharged by 60 mV. Recognizing that the capacitance will decrease as the collector current is brought down, the capacitance can be approximated by using an average value of one-half, or about 1.5 μF. Assume high transistor β so that the base current that normally must flow to keep the transistor turned on can be ignored. If a constant base discharge current of 30 mA is employed, the time it takes to ramp down the collector current by a decade can be estimated as follows:

$$T = C * V/I = 3.0\ \mu s$$

This is still quite a long time if the amplifier is trying to rapidly change the output current as a result of a large high-frequency signal transient. Here the average rate of change of collector current is about 0.3 A/μs. To put this in perspective, assume an amplifier is driving 40-V peak into a 4-Ω load at 20 kHz. The voltage rate of change is 5 V/μs and the current rate of change must be 1.25 A/μs.

Unfortunately, just as BJTs experience beta droop at higher currents, so they also suffer from f_T *droop* at higher currents. A good conventional power transistor might start off with f_T of 6 MHz at 1 A, be down in f_T by 20% at 3 A, and be all the way down to 2 MHz at 10 A. At the same time, BJTs also suffer f_T droop at lower collector-emitter voltages while operating at high currents. This compounds the problem when an output stage is at a high-amplitude portion of a high-frequency waveform and delivering high current into the load. Under these conditions, V_{ce} might be as little as 5 V or less and device current might be several amperes.
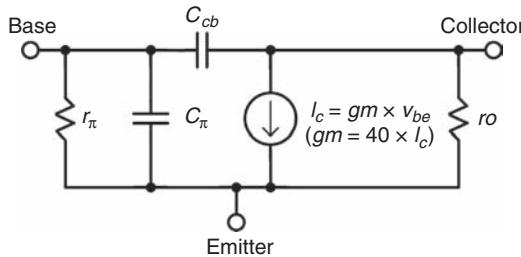
FIGURE 2.3 Hybrid pi model.

So-called *ring emitter transistors* (*RETs*) and similar advanced BJT power transistor designs can have f_T in the 20- to 80-MHz range. However, they also suffer from f_T droop at high currents. A typical RET might start out with an f_T of 40 MHz at 1 A and maintain it quite well to 3 A, then have it crash to 4 MHz or less at 10 A. The RET devices also lose f_T at low current. At 100 mA, where they may be biased in a class AB output stage, the same RET may have f_T of only 20 MHz.

The Hybrid Pi Model

Those more familiar with transistors will recognize that much of what has been discussed above is the makeup of the hybrid pi small-signal model of the transistor, shown in Figure 2.3. The fundamental active element of the transistor is a voltage-controlled current source, namely a *transconductance*. Everything else in the model is essentially a passive *parasitic* component. AC current gain is taken into account by the base-emitter resistance r_π. The Early effect is taken into account by ro. Collector-base capacitance is shown as C_{cb}. Current gain roll-off with frequency (as defined by f_T) is modeled by C_π. The values of these elements are as described above. This is a small-signal model; element values will change with the operating point of the transistor.

The Ideal Transistor

Operational amplifier circuits are often designed by assuming an ideal op amp, at least initially. In the same way a transistor circuit can be designed by assuming an "ideal" transistor. This is like starting with the hybrid pi model stripped of all of its passive parasitic elements. The ideal transistor is just a lump of transconductance. As needed, relevant impairments, such as finite β, can be added to the ideal transistor. This usually depends on what aspect of performance is important at the time.

The ideal transistor has infinite current gain, infinite input impedance, and infinite output resistance. It acts as if it applies all of the small-signal base voltage to the emitter through an internal intrinsic emitter resistance *re'*.

Safe Operating Area

The *safe operating area* (*SOA*) for a transistor describes the safe combinations of voltage and current for the device. This area will be bounded on the *X* axis by the maximum operating voltage and on the *Y* axis by the maximum operating current. The SOA is also bounded by a line that defines the maximum power dissipation of the device. Such a plot is shown for a power transistor in Figure 2.4, where voltage and current are plotted on log scales and the power dissipation limiting line becomes the outermost straight line.
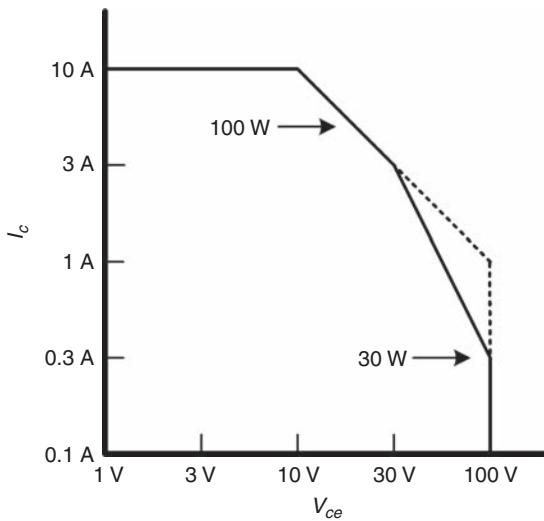
Figure 2.4 Safe operating area.

Unfortunately, power transistors are not just limited in their safe current-handling capability by their power dissipation. At higher voltages they are more seriously limited by a phenomenon called *secondary breakdown*. This is illustrated by the more steeply sloped inner line in Figure 2.4.

Although there are many different ways to specify SOA, perhaps the single most indicative number for audio power amplifier design is the amount of current the transistor can safely sustain for at least 1 second at some high collector-emitter voltage such as 100 V. In the absence of secondary breakdown, a 150-W power transistor could sustain a current of 1.5 A at 100 V. In reality, this number may only be 0.5 A, corresponding to only 50 W of dissipation. Secondary breakdown causes the sustainable power dissipation at high voltages to be less than that at low voltages.

Secondary breakdown results from localized hot spots in the transistor. At higher voltages the depletion region of the collector-base junction has become larger and the effective base region has become thinner. Recall that the collector current of a transistor increases as the junction temperature increases if the base-emitter voltage is held constant. A localized increase in the power transistor's base-emitter junction temperature will cause that area to hog more of the total collector current. This causes the local area to become hotter, conduct even more current, and still become hotter; this leads to a localized thermal runaway.

SOA is very important in the design of audio amplifier output stages because the SOA can be exceeded, especially when the amplifier is driving a reactive load. This can lead to the destruction of the output transistors unless there are safe area protection circuits in place. There will be a much deeper examination of power transistor SOA in Chapter 15, including discussion of the higher value of SOA that a transistor can withstand for shorter periods of time.

JFETs and MOSFETs

So far nothing has been said about JFET and MOSFET transistors. These will be discussed in Chapters 7 and 11 where their use in power amplifiers is covered. The short

version is that they are really not much different than BJTs in many of the characteristics that have been discussed. Their gate draws essentially no DC current in normal opera-tion, as they are voltage-controlled devices. Just think of them as transistors with infinite current gain and about 1/10 the transconductance of BJTs, and you will not be far off. This is a major simplification, but it is extremely useful for small-signal analysis. In real-ity, a FET is a square-law device, while the current in a BJT follows an exponential law.

2.2   Circuit Building Blocks

An audio power amplifier is composed of just a few important circuit building blocks put together in many different combinations. Once each of those building blocks can be under-stood and analyzed, it is not difficult to do an approximate analysis by inspection of a complete power amplifier. Knowledge of how these building blocks perform and bring performance value to the table permits the designer to analyze and synthesize circuits.

Common-Emitter Stage

The common-emitter (*CE*) amplifier is possibly the most important circuit building block, as it provides basic voltage gain. Assume that the transistor's emitter is at ground and that a bias current has been established in the transistor. If a small voltage signal is applied to the base of the transistor, the collector current will vary in accordance with the base voltage. If a load resistance R_L is provided in the collector circuit, that resistance will convert the varying collector current to a voltage. A voltage-in, voltage-out ampli-fier is the result, and it likely has quite a bit of voltage gain. A simple common emitter amplifier is shown in Figure 2.5a.

The voltage gain will be approximately equal to the collector load resistance times the transconductance *gm*. Recall that the intrinsic emitter resistance $re' = 1/gm$. Thus, more conveniently, assuming the ideal transistor with intrinsic emitter resistance re', the gain is simply R_L/re'.

Consider a transistor biased at 1 mA with a load resistance of 5000 Ω and a supply voltage of 10 V, as shown in Figure 2.5a. The intrinsic emitter resistance re' will be about 26 Ω. The gain will be approximately 5000/26 = 192.
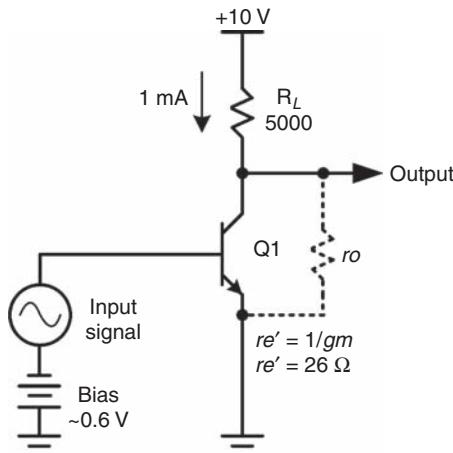
Figure 2.5a   Common-emitter amplifier.

This is quite a large value. However, any loading by other circuits that are driven by the output has been ignored. Such loading will reduce the gain.

The Early effect has also been ignored. It effectively places another resistance *ro* in parallel with the 5-kΩ load resistance. This is illustrated by the dashed resistor drawn in the figure. As mentioned earlier, *ro* for a 2N5551 operating at 1 mA and relatively low collector-emitter voltages will be on the order of 100 kΩ, so the error introduced by ignoring the Early effect here will be about 5%.

Because *re′* is a function of collector current, the gain will vary with signal swing and the gain stage will suffer from some distortion. The gain will be smaller as the current swings low and the output voltage swings high. The gain will be larger as the current swings high and the output voltage swings low. This results in second harmonic distortion.

If the input signal swings positive so that the collector current increases to 1.5 mA and the collector voltage falls to 2.5 V, *re′* will be about 17.3 Ω and the incremental gain will be 5000/17.3 = 289. If the input signal swings negative so that the collector current falls to 0.5 mA and the collector voltage rises to 7.5 V, then *re′* will rise to about 52 Ω and incremental gain will fall to 5000/52 = 96. The incremental gain of this stage has thus changed by over a factor of 3 when the output signal has swung 5 V peak-to-peak. This represents a high level of distortion.

If external emitter resistance is added as shown in Figure 2.5b, then the gain will simply be the ratio of R_L to the total emitter circuit resistance consisting of *re′* and the external emitter resistance R_e. Since the external emitter resistance does not change with the signal, the overall gain is stabilized and is more linear. This is called *emitter degeneration*. It is a form of local negative feedback.

The CE stage in Figure 2.5b is essentially the same as that in 2.5a but with a 234-Ω emitter resistor added. This corresponds to 10:1 emitter degeneration because the total effective resistance in the emitter circuit has been increased by a factor of 10 from 26 to 260 Ω. The nominal gain has also been reduced by a factor of 10 to a value of approximately 5000/260 = 19.2.
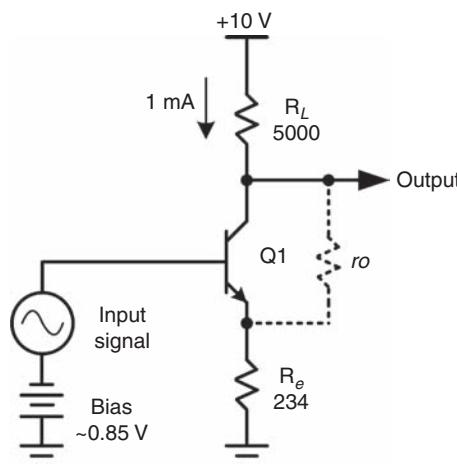
FIGURE 2.5b   CE stage with emitter degeneration.

Consider once again what happens to the gain when the input signal swings positive and negative to cause a 5-V peak-to-peak output swing. If the input signal swings positive so that the collector current increases to 1.5 mA and the collector voltage falls to 2.5 V, total emitter circuit resistance R_e will become 17 + 234 = 251 Ω, and the incremental gain will rise to 5000/251 = 19.9.

If the input signal swings negative so that the collector current falls to 0.5 mA and the collector voltage rises to 7.5 V, then R_e will rise to about 234 + 52 = 287 Ω and incremental gain will fall to 5000/287 = 17.4. The incremental gain of this stage has now swung over a factor of 1.14:1, or only 14%, when the output signal has swung 5 V peak to peak. This is indeed a much lower level of distortion than occurred in the undegenerated circuit of Figure 2.5a. This illustrates the effect of local negative feedback without resort to any negative feedback theory.

We thus have, for the CE stage, the approximation

$$\text{Gain} = R_L / (re' + R_e)$$

where R_L is the net collector load resistance and R_e is the external emitter resistance. The emitter degeneration factor is defined as $(re' + R_e)/re'$. In this case that factor is 10.

Emitter degeneration also mitigates nonlinearity caused by the Early effect in the CE stage. As shown by the dotted resistance *ro* in Figure 2.5b, most of the signal current flowing in *ro* is returned to the collector by way of being injected into the emitter. If 100% of the signal current in *ro* were returned to the collector, the presence of *ro* would have no effect on the output resistance of the stage. In reality, some of the signal current in *ro* is lost by flowing in the external emitter resistor R_e instead of through emitter resistance *re'* (some is also lost due to the finite current gain of the transistor). The fraction of current lost depends on the ratio of *re'* to R_e, which in turn is a reflection of the amount of the emitter degeneration. As a rough approximation, the output resistance due to the Early effect for a degenerated CE stage is

$$R_{out} \sim ro * \text{degeneration factor}$$

If *ro* is 100 kΩ and 10:1 emitter degeneration is used as in Fig. 2.5b, then the output resistance of the CE stage due to the Early effect will be on the order of 1 MΩ. Bear in mind that this is just a convenient approximation. In practice, the output resistance of the stage cannot exceed approximately *ro* times the current gain of the transistor. It has been assumed that the CE stage here is driven with a voltage source. If it is driven by a source with significant impedance, the output resistance of the degenerated CE stage will decrease somewhat from the values predicted above. That reduction will occur because of the changes in base current that result from the Early effect.

Bandwidth of the Common-Emitter Stage and Miller Effect

The high-frequency response of a CE stage will be limited if it must drive any load capacitance. This is no different than when a source resistance drives a shunt capacitance, forming a first-order low-pass filter. A pole is formed at the frequency where the source resistance and reactance of the shunt capacitance are the same; this causes the frequency response to be down 3 dB at that frequency. The reactance of a capacitor is equal to $1/(2\pi f C) = 0.159/(f C)$. The –3 dB frequency f_3 will then be 0.159/(RC).

In Figure 2.5a the output impedance of the CE stage is approximately that of the 5-kΩ collector load resistance. Suppose the stage is driving a load capacitance of 100 pF.

The bandwidth will be dictated by the low-pass filter formed by the output impedance of the stage and the load capacitance. A pole will be formed at

$$f_3 = 1/(2\pi R_L C_L) = 0.159/(5 \text{ k}\Omega * 100 \text{ pF}) = 318 \text{ kHz}$$

As an approximation, the collector-base capacitance should also be considered part of C_L. The bandwidth of a CE stage is often further limited by the collector-base capacitance of the transistor when the CE stage is fed from a source with significant impedance. The source must supply current to charge and discharge the collector-base capacitance through the large voltage excursion that exists between the collector and the base. This phenomenon is called the *Miller effect*.

Suppose the collector-base capacitance is 5 pF and assume that the CE stage is being fed from a 5-kΩ source impedance R_S. Recall that the voltage gain G of the circuit in Figure 2.5a was approximately 192. This means that the voltage across C_{cb} is 193 times as large as the input signal (bearing in mind that the input signal is out of phase with the output signal, adding to the difference). This means that the current flowing through C_{cb} is 193 times as large as the current that would flow through it if it were connected from the base to ground instead of base to collector. The input circuit thus sees an effective input capacitance C_{in} that is $1 + G$ times that of the collector-base capacitance. This phenomenon is referred to as *Miller multiplication* of the capacitance. In this case the effective value of C_{in} would be 965 pF.

The base-collector capacitance effectively forms a shunt feedback circuit that ultimately controls the gain of the stage at higher frequencies where the reactance of the capacitor becomes small. As frequency increases, a higher proportion of the input signal current must flow to the collector-base capacitance as opposed to the small fixed amount of signal current required to flow into the base of the transistor. If essentially all of the input signal current flowed through the collector-base capacitance, the gain of the stage would simply be the ratio of the capacitive reactance of C_{cb} to the source resistance

$$G = \frac{X_{Ccb}}{R_S} = \frac{1}{(2\pi f C_{cb})(R_S)} = \frac{0.159}{(f C_{cb} R_S)}$$

This represents a value of gain that declines at 6 dB per octave as frequency increases. This decline will begin at a frequency where the gain calculated here is equal to the low-frequency gain of the stage. The Miller effect is often used to advantage in providing the high-frequency roll-off needed to stabilize a negative feedback loop. This is referred to as *Miller compensation*.

Differential Amplifier

The differential amplifier is illustrated in Figure 2.6. It is much like a pair of common emitter amplifiers tied together at the emitters and biased with a common current. This current is called the *tail current*. The arrangement is often referred to as a *long-tailed pair* (*LTP*).

The differential amplifier routes its tail current to the two collectors of Q1 and Q2 in accordance with the voltage differential across the bases of Q1 and Q2. If the base voltages are equal, then equal currents will flow in the collectors of Q1 and Q2. If the base of Q1 is more positive than that of Q2, more of the tail current will flow in the collector of Q1 and less will flow in the collector of Q2. This will result in a larger voltage drop across the collector load resistor R_{L1} and a smaller voltage drop across load resistor R_{L2}.
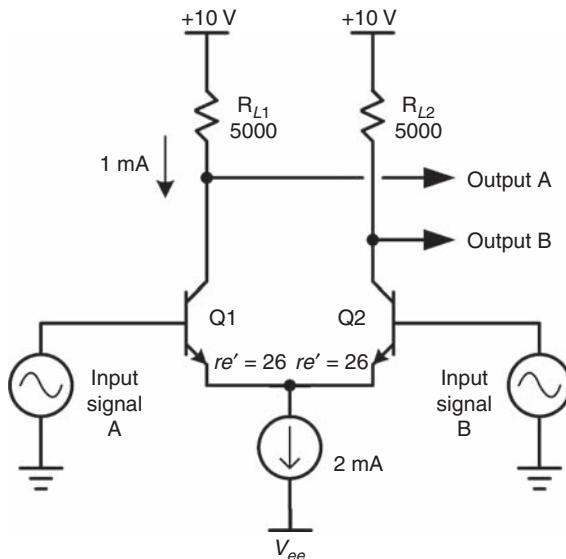
FIGURE 2.6 Differential amplifier.

Output A is thus inverted with respect to Input A, while Output B is noninverted with respect to Input A.

Visualize the intrinsic emitter resistance re' present in each emitter leg of Q1 and Q2. Recall that the value of re' is approximately 26 Ω divided by the transistor operating current in milliamperes. With 1 mA flowing nominally through each of Q1 and Q2, each can be seen as having an emitter resistance re' of 26 Ω. Note that since $gm = 1/re'$ is dependent on the instantaneous transistor current, the values of gm and re' are somewhat signal dependent, and indeed this represents a nonlinearity that gives rise to distortion.

Having visualized the ideal transistor with emitter resistance re', one can now assume that the idealized internal emitter of each device moves exactly with the base of the transistor, but with a fixed DC voltage offset equal to V_{be}. Now look what happens if the base of Q1 is 5.2 mV more positive than the base of Q2. The total emitter resistance separating these two voltage points is 52 Ω, so a current of 5.2 mV/52 Ω = 0.1 mA will flow from the emitter of Q1 to the emitter of Q2. This means that the collector current of Q1 will be 100 μA more than nominal, and the collector current of Q2 will be 100 μA less than nominal. The collector currents of Q1 and Q2 are thus 1.1 mA and 0.9 mA, respectively, since they must sum to the tail current of 2.0 mA (assuming very high β for the transistors).

This 100-μA increase in the collector current of Q1 will result in a change of 500 mV at Output A, due to the collector load resistance of 5000 Ω. A 5.2-mV input change at the base of Q1 has thus caused a 500-mV change at the collector of Q1, so the stage gain to Output A in this case is approximately 500/5.2 = 96.2. More significantly, the stage gain defined this way is just equal numerically to the load resistance of 5000 Ω divided by the total emitter resistance $re' = 52$ Ω across the emitters.

Had additional external emitter degeneration resistors been included in series with each emitter, their value would have been added into this calculation. For example, if 48-Ω emitter degeneration resistors were employed, the gain would then become 5000/ (52 + 48 + 48 + 52) = 5000/200 = 25. This approach to estimating stage gain is a very

important back-of-the-envelope concept in amplifier design. In a typical amplifier design, one will often start with these approximations and then knowingly account for some of the deviations from the ideal. This will be evident in the numerous design analyses to follow.

It was pointed out earlier that the change in transconductance of the transistor as a function of signal current can be a source of distortion. Consider the situation where a negative input signal at the base of Q1 causes Q1 to conduct 0.5 mA and Q2 to conduct 1.5 mA. The emitter resistance re' of Q1 is now $26/0.5 = 52\ \Omega$. The emitter resistance re' of Q2 is now $26/1.5 = 17.3\ \Omega$. The total emitter resistance from emitter to emitter has now risen from 52 Ω in the case above to 69.3 Ω. This results in a reduced gain of $5000/69.3 = 72.15$. This represents a reduction in gain by a factor of 0.75, or about 25%. This is an important origin of distortion in the LTP. The presumed signal swing that caused the imbalance of collector currents between Q1 and Q2 resulted in a substantial decrease in the incremental gain of the stage. More often than not, distortion is indeed the result of a change in incremental gain as a function of instantaneous signal amplitude.

The gain of an LTP is typically highest in its balanced state and decreases as the signal goes positive or negative away from the balance point. This symmetrical behavior is in contrast to the asymmetrical behavior of the common-emitter stage, where the gain increases with signal swing in one direction and decreases with signal swing in the other direction. To first order, the symmetrical distortion here is third harmonic distortion, while that of the CE stage is predominantly second harmonic distortion.

Notice that the differential input voltage needed to cause the above imbalance in the LTP is only on the order of 25 mV. This means that it is fairly easy to overload an LTP that does not incorporate emitter degeneration. This is of great importance in the design of most power amplifiers that employ an LTP input stage.

Suppose the LTP is pushed to 90% of its output capability. In this case Q1 would be conducting 0.1 mA and Q2 would be conducting 1.9 mA. The two values of re' will be 260 Ω and 14 Ω, for a total of 274 Ω. The gain of the stage is now reduced to $5000/274 = 18.25$. The nominal gain of this un-degenerated LTP was about 96.2. The incremental gain under these large signal conditions is down by about 80%, implying gross distortion.

As in the case of the CE stage, adding emitter degeneration to the LTP will substantially reduce its distortion while also reducing its gain. In summary we have the approximation

$$\text{Gain} = \frac{R_{L1}}{2(r_e' + R_e)}$$

where R_{L1} is a single-ended collector load resistance and R_e is the value of external emitter degeneration resistance in each emitter of the differential pair. This gain is for the case where only a single-ended output is taken from the collector of Q1. If a differential output is taken from across the collectors of Q1 and Q2, the gain will be doubled. For convenience, the total emitter-to-emitter resistance in an LTP, including the intrinsic re' resistances, will be called R_{LTP}. In the example above,

$$R_{LTP} = 2(re' + R_e)$$

Emitter Follower

The emitter follower (*EF*) is essentially a unity voltage gain amplifier that provides current gain. It is most often used as a buffer stage, permitting the high impedance output of a CE or LTP stage to drive a heavier load.
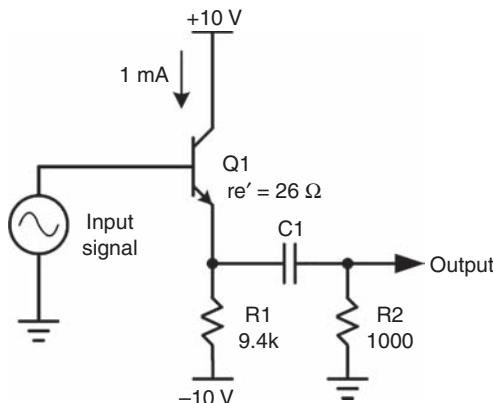
FIGURE 2.7 Emitter follower.

The emitter follower is illustrated in Figure 2.7. It is also called a common collector (*CC*) stage because the collector is connected to an AC ground. The output pull-down resistor R1 establishes a fairly constant operating collector current in Q1. For illustration, a load resistor R2 is being driven through a coupling capacitor. For AC signals, the net load resistance R_L at the emitter of Q1 is the parallel combination of R1 and R2. If *re'* of Q1 is small compared to R_L, virtually all of the signal voltage applied to the base of Q1 will appear at the emitter, and the voltage gain of the emitter follower will be nearly unity.

The signal current in the emitter will be equal to V_{out}/R_L, while the signal current in the base of Q1 will be this amount divided by the β of the transistor. It is immediately apparent that the input impedance seen looking into the base of Q1 is equal to the impedance of the load multiplied by the current gain of Q1. This is the most important function of the emitter follower.

As mentioned above, the voltage gain of the emitter follower is nearly unity. Suppose R1 is 9.4 kΩ and the transistor bias current is 1 mA. The intrinsic emitter resistance *re'* will then be about 26 Ω. Suppose R2 is 1 kΩ, making net R_L equal to 904 Ω. The voltage gain of the emitter follower is then approximately

$$G = R_L/(R_L + re') = 0.97$$

At larger voltage swings the instantaneous collector current of Q1 will change with signal, causing a change in *re'*. This will result in a change in incremental gain that corresponds to distortion. Suppose the signal current in the emitter is 0.9 mA peak in each direction, resulting in an output voltage of about 814 mV peak. At the negative peak swing, emitter current is only 0.1 mA and *re'* has risen to 260 Ω. Incremental gain is down to about 0.78. At the positive peak swing the emitter current is 1.9 mA and *re'* has fallen to 13.7 Ω; this results in a voltage gain of 0.985.

Voltage gain has thus changed by about 21% over the voltage swing excursion; this causes considerable second harmonic distortion. One solution to this is to reduce R1 so that a greater amount of bias current flows, making *re'* a smaller part of the gain equation. This of course also reduces net R_L somewhat. A better solution is to replace R1 with a constant current source.

The transformation of low-value load impedance to much higher input impedance by the emitter follower is a function of the current gain of the transistor. The β is

a function of frequency, as dictated by the f_T of the transistor. This means, for example, that a resistive load will be transformed to impedance at the input of the emitter follower that eventually begins to decrease with frequency as β_{AC} decreases with frequency. A transistor with a nominal β of 100 and f_T of 100 MHz will have an f_β of 1 MHz. The AC β of the transistor will begin to drop at 1 MHz. The decreasing input impedance of the emitter follower thus looks capacitive in nature, and the phase of the input current will lead the phase of the voltage by an amount approaching 90 degrees.

The impedance transformation works both ways. Suppose we have an emitter follower that is driven by a source impedance of 1 kΩ. The low-frequency output impedance of the EF will then be approximately 1 kΩ divided by β, or about 10 Ω (ignoring re'). However, the output impedance will begin to rise above 1 MHz where β begins to fall. Impedance that increases with frequency is inductive. Thus, Z_{out} of an emitter follower tends to be inductive at high frequencies.

Now consider an emitter follower that is loaded by a capacitance. This can lead to instability, as we will see. The load impedance presented by the capacitance falls with increasing frequency. The amount by which this load impedance is multiplied by β_{AC} also falls with frequencies above 1 MHz. This means that the input impedance of the emitter follower is ultimately falling with the square of frequency. It also means that the current in the load, already leading the voltage by 90 degrees, will be further transformed by another 90 degrees by the falling transistor current gain with frequency. This means that the input current of the emitter follower will lead the voltage by an amount approaching 180 degrees. When current is 180 degrees out of phase with voltage, this corresponds to a *negative resistance*. This can lead to instability, since the input impedance of this emitter follower is a frequency-dependent negative resistance under these conditions. This explains why placing a resistance in series with the base of an emitter follower will sometimes stabilize it; the positive resistance adds to the negative resistance by an amount that is sufficient to make the net resistance positive.

There is one more aspect of emitter follower behavior that pertains largely to its use in the output stage of a power amplifier. It was implied above that if an emitter follower was driven from a very low impedance source that its output impedance would simply be re' of its transistor. This is not quite the whole story. Transistors have finite base resistance. The output impedance of an emitter follower will actually be the value of re' plus the value of the base resistance divided by β of the transistor. This can be significant in an output stage. Consider a power transistor operating at 100 mA. Its re' will be about 0.26 Ω. Suppose that transistor has a base resistance of 5 Ω and a current gain of 50. The value of the transformed base resistance will be 0.1 Ω. This is not insignificant compared to the value of re' and must be taken into account in some aspects of design. This can also be said for the emitter resistance of the power transistor, which may range from 0.01 to 0.1 Ω.

The simplicity of the emitter follower, combined with its great ability to buffer a load, accounts for it being the most common type of circuit used for the output stage of power amplifiers. An emitter follower will often be used to drive a second emitter follower to achieve even larger amounts of current gain and buffering. This arrangement is sometimes called a *Darlington connection*. Such a pair of transistors, each with a current gain of 50, can increase the impedance seen driving a load by a factor of 2500. Such an output stage driving an 8-Ω load would present an input impedance of 20,000 Ω.
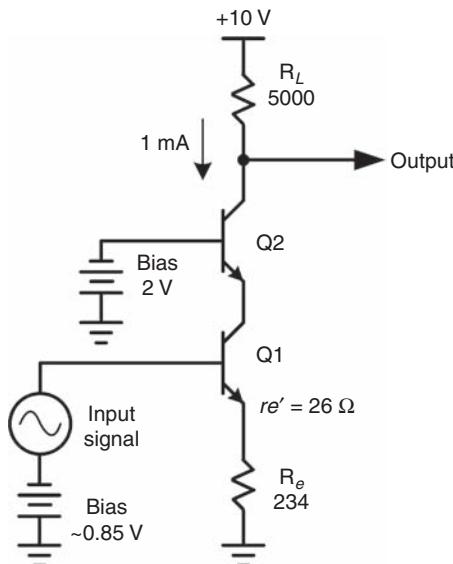
FIGURE 2.8 Cascode.

Cascode

A cascode stage is implemented by Q2 in Figure 2.8. The cascode stage is also called a *common base* stage because the base of its transistor is connected to AC ground. Here the cascode is being driven at its emitter by a CE stage comprising Q1. The most important function of a cascode stage is to provide isolation. It provides near-unity current gain, but can provide very substantial voltage gain. In some ways it is like the dual of an emitter follower.

A key benefit of the cascode stage is that it largely keeps the collector of the driving CE stage at a constant potential. It thus isolates the collector of the CE stage from the large swing of the output signal. This eliminates most of the effect of the collector-base capacitance of Q2, resulting in wider bandwidth due to suppression of the Miller effect. Similarly, it mitigates distortion caused by the nonlinear collector-base junction capacitance of the CE stage, since very little voltage swing now appears across the collector-base junction to modulate its capacitance.

The cascode connection also avoids most of the Early effect in the CE stage by nearly eliminating signal swing at its collector. A small amount of Early effect remains, however, because the signal swing at the base of the CE stage modulates the collector-base voltage slightly.

If the current gain of the cascode transistor is 100, then 99% of the signal current entering the emitter will flow in the collector. The input-output current gain is thus 0.99. This current transfer factor from emitter to collector is sometimes referred to as the *alpha* of the transistor.

The Early effect resistance *ro* still exists in the cascode transistor. It is represented as a resistance *ro* connected from collector to emitter. Suppose *ro* is only 10 kΩ. Is the output impedance of the collector of the cascode 10 kΩ? No, it is not.

Recall that 99% of the signal current entering the emitter of the cascode re-appears at the collector. This means that 99% of the current flowing in *ro* also returns to the

collector. Only the lost 1% of the current in *ro* results in a change in the net collector current at the collector terminal. This means that the net effect of *ro* on the collector output impedance in the cascode is roughly like that of a 1-MΩ resistor to ground. This is why the output impedance of cascode stages is so high even though Early effect still is present in the cascode transistor.

$$R_{out} = \beta * ro$$

$$ro = \frac{VA + V_{ce}}{I_c}$$

$$ro \approx VA / I_c \quad \text{at low } V_{ce}$$

$$R_{out} = \beta * VA / I_c$$

Notice that the product of β and *VA* is the Early effect figure of merit mentioned previously. The output resistance of a cascode is thus the FOM divided by the collector current.

$$R_{out} = FOM / I_c$$

Current Mirror
Figure 2.9a depicts a very useful circuit called a current mirror. If a given amount of current is sourced into Q1, that same amount of current will be sunk by Q2, assuming that the emitter degeneration resistors R1 and R2 are equal, that the transistor V_{be} drops are the same, and that losses through base currents can be ignored. The values of R1 and R2 will often be selected to drop about 100 mV to ensure decent matching in the face of unmatched transistor V_{be} drops, but this is not critical.
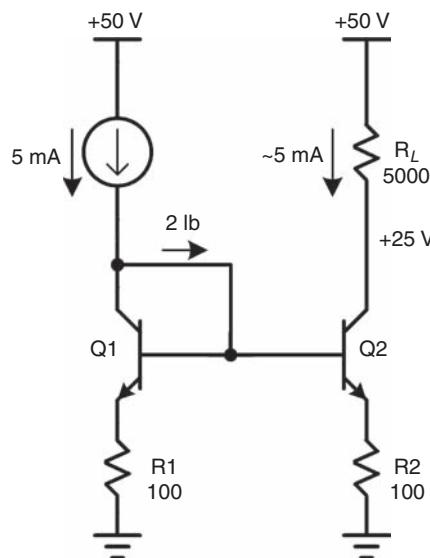
FIGURE 2.9a   Simple current mirror.
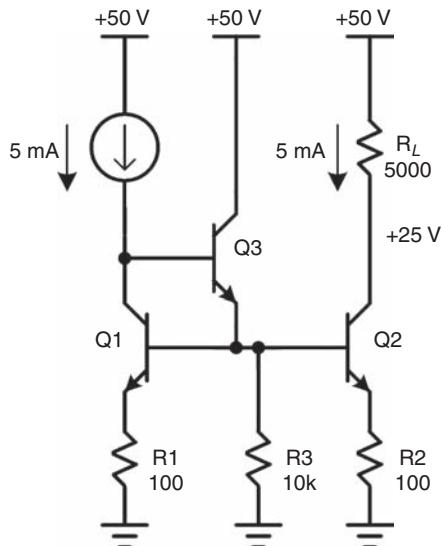
Improved current mirror.

If R1 and R2 are made different, a larger or smaller multiple if the input current can be made to flow in the collector of Q2. In practice, the base currents of Q1 and Q2 cause a small error in the output current with respect to the input current. In the example above, if transistor β is 100, the base current I_b of each transistor will be 50 μA, causing a total error of 100 μA, or 2% in the output current.

Figure 2.9b shows a variation of the current mirror that minimizes errors due to the finite current gain of the transistors. Here emitter follower Q3, often called a *helper* transistor, provides current gain to minimize that error. Resistor R3 assures that a small minimum amount of current flows in Q3 even if the current gains of Q1 and Q2 are very high. Note that the input node of the current mirror now sits one V_{be} higher above the supply rail than in Figure 2.9a.

Many other variations of current mirrors exist, such as the *Wilson* current mirror shown in Figure 2.9c. The Wilson current mirror includes transistors Q1, Q2, and Q3. Input current is applied to the base of Q3 and is largely balanced by current flowing in the collector of Q1. Input current that flows into the base of output transistor Q3 will turn Q3 on, with its emitter current flowing through Q2 and R2. Q1 and Q2 form a conventional current mirror. The emitter current of Q3 is mirrored and pulled from the source of input current by Q1.

Any difference between the current of Q1 and the input current is available to drive the base of Q3. If the input current exceeds the mirrored emitter current of Q3, the base voltage of Q3 will increase, causing the emitter current of Q3 to increase and self-correct the situation with feedback action. The equilibrium condition can be seen to be when the input current and the output current are the same, providing an overall 1:1 current mirror function.

Notice that in normal operation all three of the transistors operate at essentially the same current, namely the supplied input current. Ignoring the Early effect, all of the base currents will be the same if the betas are matched. Assume that each base current
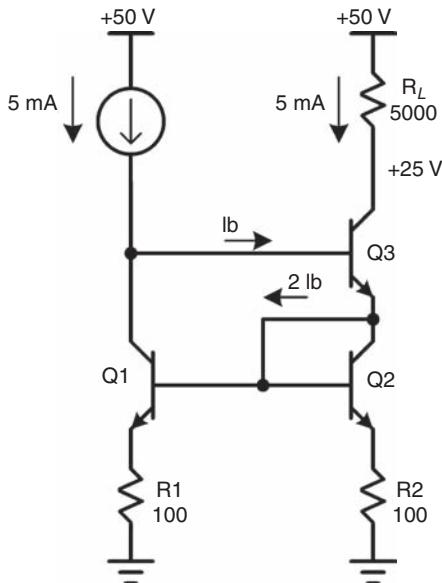
is I_b and that the collector current in Q1 is equal to I. It can be quickly seen that the input current must then be $I + I_b$ and that the emitter current of Q3 must be $I + 2I_b$. It is then evident that the collector current of Q3, which is the output current, will be $I + I_b$, which is the same as the input current. This illustrates the precision of the input-output relationship when the transistors are matched.

Transistor Q3 acts much like a cascode, and this helps the Wilson current mirror to achieve high output impedance. Transistors Q1 and Q2 operate at a low collector voltage, while output transistor Q3 will normally operate at a higher collector voltage. Thus, the Early effect will cause the base current of Q3 to be smaller, and this will result in a slightly higher voltage-dependent output current. This is reflected in the output resistance of the Wilson current mirror.

Current Sources

Current sources are used in many different ways in a power amplifier, and there are many different ways to make a current source. The distinguishing feature of a current source is that it is an element through which a current flows wherein that current is independent of the voltage across that element. The current source in the tail of the differential pair is a good example of its use.

Most current sources are based on the observation that if a known voltage is impressed across a resistor, a known current will flow. A simple current source is shown in Figure 2.10a. The voltage divider composed of R2 and R3 places 2.7 V at the base of Q1. After a V_{be} drop of 0.7 V, about 2 V is impressed across emitter resistor R1. If R1 is a 400-Ω resistor, 5 mA will flow in R1 and very nearly 5 mA will flow in the collector of Q1. The collector current of Q1 will be largely independent of the voltage at the collector of Q1, so the circuit behaves as a decent current source. The load resistance R_L is just shown for purposes of illustration. The output impedance of the current source itself (not including the shunting effect of R_L) will be determined largely by the Early effect in
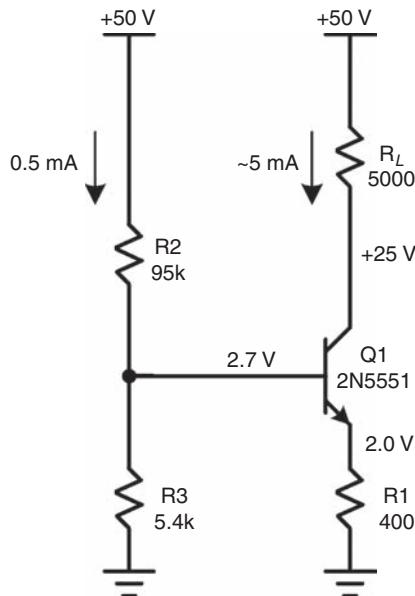
Figure 2.10a   Simple current source.

the same way as for the CE stage. The output impedance for this current source is found by SPICE simulation to be about 290 kΩ.

In Figure 2.10b, R3 is replaced with a pair of silicon diodes. Here one diode drop is impressed across R1 to generate the desired current. The circuit employs 1N4148 diodes biased with the same 0.5 mA used in the voltage divider in the first example. Together
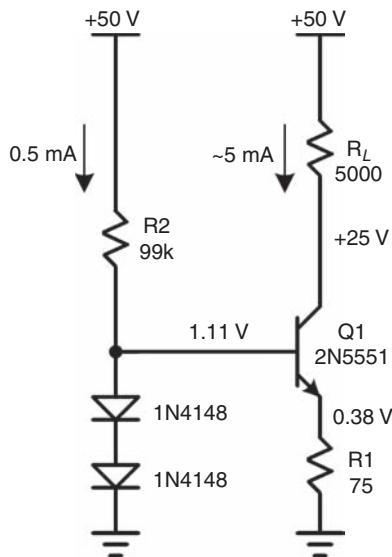
Figure 2.10b   Current source using diodes.
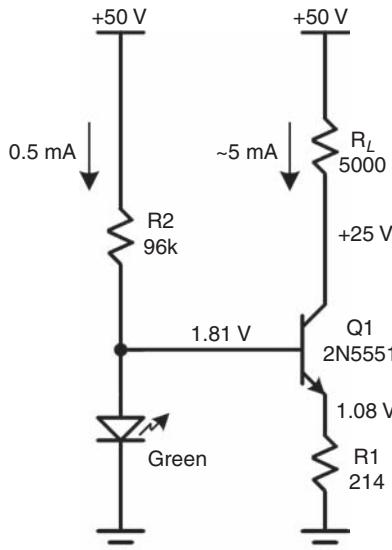
FIGURE 2.10c Current source using LED.

they drop only about 1.1 V, and about 0.38 V is impressed across the 75-Ω resistor R1. The output impedance of this current source is approximately 300 kΩ, about the same as the one above.

Turning to Figure 2.10c, R3 is replaced instead with a Green LED, providing a convenient voltage reference of about 1.8 V, putting about 1.1 V across R1. Once again, 0.5 mA is used to bias the LED. The output impedance of this current source is about 750 kΩ. It is higher than in the design of Figure 2.10b because there is effectively more emitter degeneration for Q1 with the larger value of R1.

R3 is replaced with a 6.2-V *Zener* diode in Figure 2.10d. This puts about 5.5 V across R1. The output impedance of this current source is about 2 MΩ, quite a bit higher than the earlier arrangements due to the larger emitter degeneration for Q1. The price paid here is that the base of the transistor is fully 6.2 V above the supply rail, reducing head-room in some applications.

In Figure 2.10e, a current mirror fed from a known supply voltage is used to imple-ment a current source. Here a 1:1 current mirror is used and 5 mA is supplied from the known power rail. The output impedance of this current source is about 230 kΩ. Only 0.25 V is dropped across R1 (corresponding to 10:1 emitter degeneration), and the base is only 1 V above the rail.

Figure 2.10f illustrates a clever two-transistor feedback circuit that is used to force one V_{be} of voltage drop across R1. It does so by using transistor Q2 to effectively regu-late the current of Q1. If the current of Q1 is too large, Q2 will be turned on harder and pull down on the base of Q1, adjusting its current downward appropriately. As in Fig-ure 2.10a through 2.10d, a 0.5-mA current is supplied to bias the current source. This current flows through Q2. The output impedance of this current source is an impressive 3 MΩ. This circuit achieves higher output impedance than the Zener-based version and yet only requires the base of Q1 to be 1.4 V above the power rail. This circuit can also be used to place an overcurrent limit on a CE transistor stage implemented with Q1.
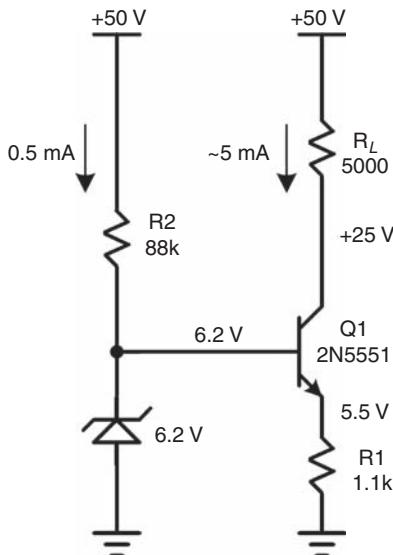
Figure 2.10d   Current source using Zener diode.
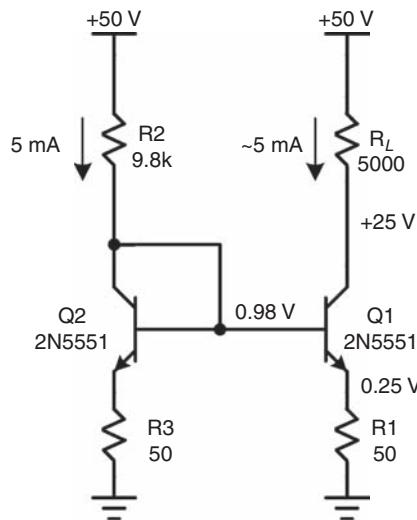
Figure 2.10e   Current mirror current source.

This circuit will work satisfactorily even if less than 0.5 mA (one-tenth of the output current) is supplied as bias for Q2, but then the output impedance will fall to a lower value and the "quality" of the current source will suffer somewhat. This happens because at lower collector current, Q2 has less transconductance and its feedback control of the current variations in Q1 as a result of the Early effect is less strong. If the bias current is reduced to 0.1 mA, for example, the output impedance falls to about 1 MΩ.
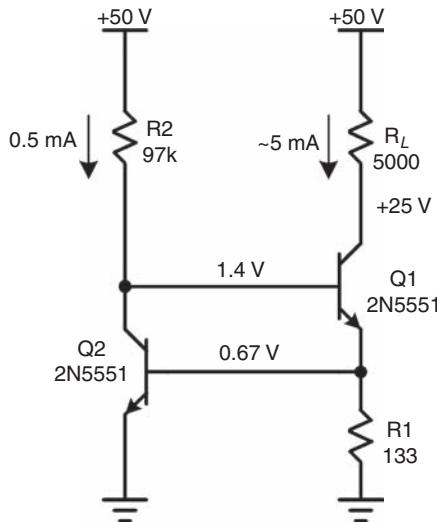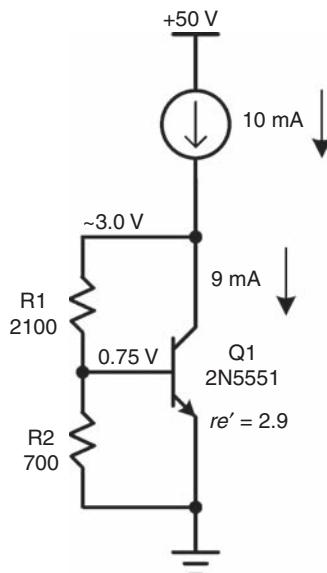
FIGURE 2.10f   Feedback current source.

V_{be} Multiplier

Figure 2.11 shows what is called a V_{be} *multiplier*. This circuit is used when a voltage drop equal to some multiple of V_{be} drops is needed. This circuit is most often used as the bias spreader for power amplifier output stages, partly because its voltage is conveniently adjustable.

FIGURE 2.11 V_{be} multiplier.

In the circuit shown, the V_{be} of Q1 is multiplied by a factor of approximately 4. Notice that the voltage divider formed by R1 and R2 places about one-fourth of the collector voltage at the base of Q1. Thus, in equilibrium, when the voltage at the collector is at four V_{be}, one V_{be} will be at the base, just enough to turn on Q1 by the amount necessary to carry the current supplied. This is simply a shunt feedback circuit. In this arrangement, about 1 mA flows through the resistive divider while about 9 mA flows through Q1.

When the V_{be} multiplier is used as a bias spreader, R2 will be made adjustable with a trim pot. As R2 is made smaller the amount of bias voltage is increased. Notice that if for some reason R2 fails open, the voltage across the V_{be} multiplier falls to about one V_{be}, failing in the safe direction.

In practice the V_{be} multiplication ratio will be a bit greater than 4 due to the base current required by Q1 as a result of its finite current gain. The extra drop caused across R1 by the base current will slightly increase the collector voltage at equilibrium, making the apparent multiplier factor slightly larger than 4.

The impedance of the V_{be} multiplier is about 4 re' for Q1. At 9 mA, re' is 2.9 Ω, so ideally the impedance of the multiplier would be about 11.6 Ω. In practice, SPICE simulation shows it to be about 25 Ω. This larger value is mainly a result of the finite current gain of Q1.

The impedance of the V_{be} multiplier rises at high frequencies. This is a result of the fact that the impedance is established by a negative feedback process. The amount of feedback decreases at high frequencies and the impedance-reducing effect is lessened. The impedance of the V_{be} multiplier in Figure 2.11 is up by 3 dB at about 2.3 MHz and doubles for every octave increase in frequency from there. It is thus inductive. For this reason, the V_{be} multiplier is often shunted by a capacitor of 0.1 to 10 μF. A shunt capacitance of as little as 0.1 μF eliminates the increase in impedance at high frequencies.

2.3   Amplifier Design Analysis

Here we apply the understanding of transistors and circuit building blocks to analyze the basic power amplifier. Having accomplished this, we will be well armed to explore, evolve, and analyze the amplifier design steps that will be taken to achieve high performance in the next chapter.

Figure 2.12 is a schematic of a basic 50-W power amplifier that includes the three stages that appear in most solid-state power amplifiers.

- Differential input stage (IPS) comprising Q1–Q3
- Voltage Amplification Stage (VAS) comprising Q4, Q6, and Q7
- Output stage (OPS) comprising Q8–Q11

The design also includes a bias spreader implemented with Q5 connected as a V_{be} multiplier. Some details like coupling capacitors, input networks, and output networks have been left out for simplicity.

The amplifier of Figure 2.12 will be described in simple terms, so that those who are less familiar with circuit design will quickly come to understand its behavior. Those who are already familiar with these concepts can relax and skim through this section.
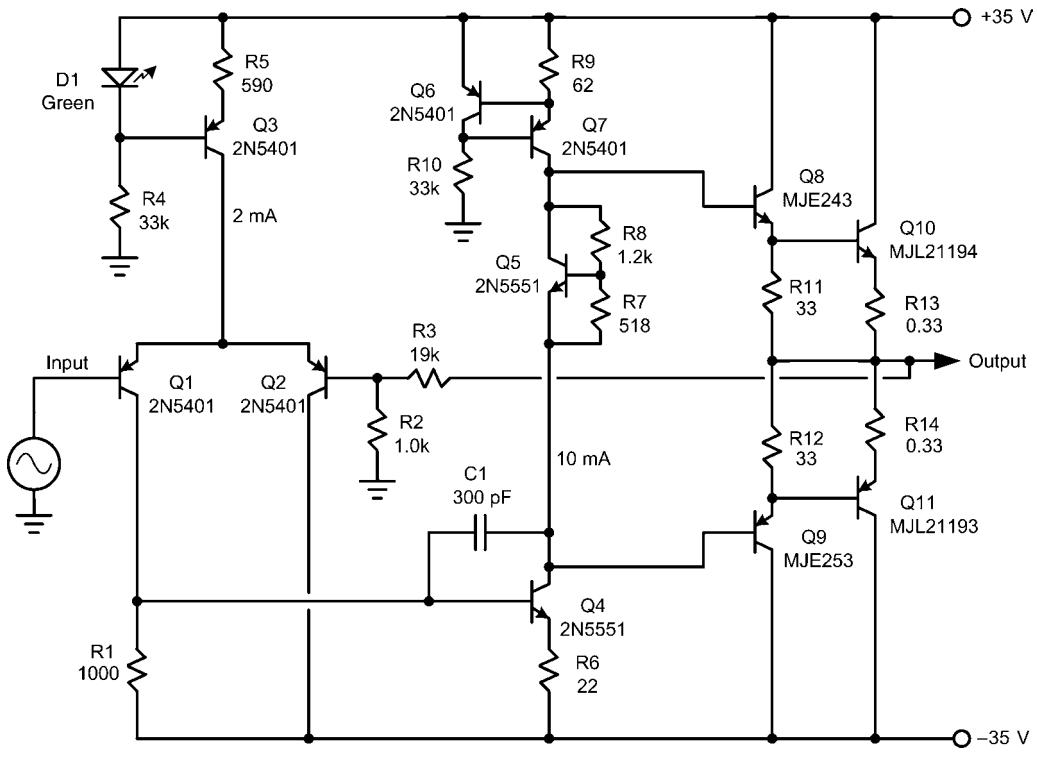
FIGURE 2.12 A basic 50-W power amplifier.

Basic Operation

This simple design is a more detailed version of the basic amplifier design illustrated in Figure 1.5. As shown, it is a DC-coupled design, so that even DC changes at the input will be amplified and presented at the output.

Input Stage

The input signal is applied to the input differential pair at the base of Q1. A fraction of the output signal is coupled via the negative feedback path to the other differential input at the base of Q2. Transistor Q3 implements a 2-mA current source that provides tail current to the differential pair. This input arrangement is often called a *Long-Tailed Pair (LTP)*.

Feedback resistors R2 and R3 implement a voltage divider that feeds back 1/20 of the output signal to the input stage. The forward path gain of the amplifier in the absence of negative feedback is called the *open-loop gain* (A_{ol}). If the open-loop gain is large, then the error signal across the bases of Q1 and Q2 need only be very small to produce the desired output. If the signals at the bases of Q1 and Q2 are nearly equal, then the output of the amplifier must be 20 times that of the input, resulting in a *closed-loop gain* (A_{cl}) of 20. This is just a very simplified explanation of the negative feedback process.
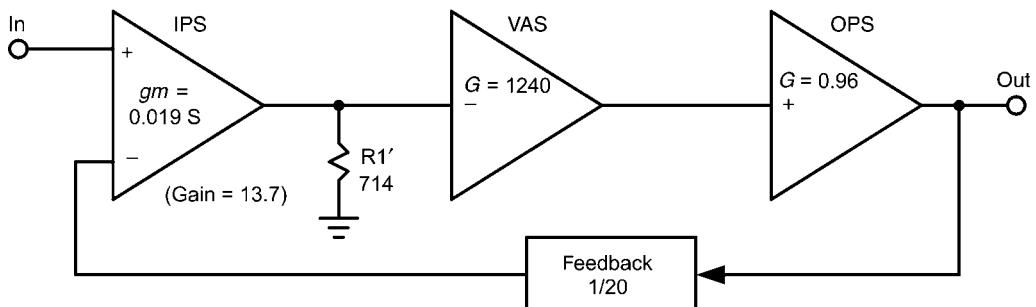
FIGURE 2.13 Amplifier gain at low frequencies.

The approximate low-frequency gain of the input stage is the ratio of the net collector load resistance divided by the total emitter-to-emitter resistance R_{LTP} (which includes the intrinsic emitter resistance re' of Q1 and Q2). With each transistor biased at 1 mA, the intrinsic emitter resistance re' is about 26 Ω each, so the total emitter-to-emitter resistance is 52 Ω. If we assume that the β of the following VAS transistor Q4 is infinity, the net IPS collector load resistance is just that of R1. The DC gain of the IPS is then 1000/52 = 19. In practice the finite β of Q4 reduces this to about 13.7 if we assume that the β of Q4 is 100.

$$\text{IPS gain} \approx 13.7$$

The amplifier at low frequencies is illustrated in Figure 2.13 where the input stage is shown as a block of transconductance with $gm = 1/52\ \Omega = 0.019$ S. The R1′ load of 714 Ω on the IPS is just the parallel combination of R1 and the estimated input impedance of the VAS.

The VAS

The VAS is formed by common-emitter transistor Q4 loaded by the 10-mA current source formed by Q6 and Q7. Recall from the discussion of current sources above that Q6 forces one V_{be} (here about 620 mV) across 62-Ω resistor R9; this produces the desired current flow.

Emitter degeneration has been applied to Q4 in the form of R6. At 10 mA, re' of Q4 is about 2.6 Ω. The 22-Ω resistance of R6 therefore increases the total effective emitter circuit resistance to about 25 Ω, or by a factor of nearly 10. This corresponds to 10:1 emitter degeneration. The emitter degeneration makes the VAS stage more linear in its operation.

If the β of Q4 is assumed to be 100, the input impedance of the VAS will be about 100 ∗ 25 Ω = 2500 Ω. This impedance is in parallel with R1, making the actual load on the first stage approximately 714 Ω. The voltage gain of the input stage is therefore close to 13.7. The loading of Q4 thus plays a substantial role in determining the first-stage gain. It would play a far greater role if Q4 were not degenerated by R6. In that case the impedance seen looking into the base of Q4 would be only about 260 Ω (β = 100 times $re' = 2.6$ Ω).

The low-frequency gain of the VAS will be set by the ratio of its collector load impedance to its total effective emitter resistance of about 25 Ω. The VAS collector load

impedance in this simple design is dominated by the loading of the output stage, since the output impedance of the current source is quite high.

The output stage is a complementary Darlington arrangement, buffering the loudspeaker load impedance as seen by the VAS collector circuit. The amount of buffering depends on the current gain of the driver and output transistors. Throughout these discussions it will be assumed that small-signal transistors have current gain of 100 and power transistors have current gain of 50. If the driver and output transistor current gains are assumed to be 100 and 50 respectively, the buffering factor will be the product of these, or about 5000. If the load impedance at the output is assumed to be 8 Ω, this will appear as a load impedance of 40,000 Ω to the VAS collector circuit. The gain of the VAS is thus on the order of 40,000/25 = 1600.

In the discussion on the Early effect in Section 2.1 it was shown that a common-emitter stage like the VAS used here (10-mA bias, 10:1 emitter degeneration) has an intrinsic output impedance of about 135 kΩ. Recall that the output resistance ro for a transistor is

$$ro = \frac{VA + V_{ce}}{I_c}$$

and that R_{out} for a common-emitter stage with degeneration is approximated by

$$R_{out} = ro * \text{degeneration factor}$$

The Early voltage for the 2N5551 is about 100 V. At a collector current of 10 mA and a V_{ce} of 35 V, ro for the 2N5551 will be about 13.5 kΩ. With 10:1 degeneration, R_{out} of the CE stage will be about 135 kΩ, or about 3.4 times that of the load imposed by the output stage.

The net collector load impedance is the parallel combination of the 135-kΩ Early effect resistance and the 40-kΩ effective external load resistance, or 31 kΩ. The output resistance of the current source has been ignored because it is much higher. The estimated voltage gain of the VAS equal to 31 kΩ/25 = 1240.

$$\text{VAS gain} \approx 1240$$

This VAS voltage gain of 1240 is shown in Figure 2.13.

Open-Loop Gain

If the voltage gain of the output stage is approximately unity, the forward gain of the amplifier (without considering negative feedback) is the product of the input stage gain and the VAS gain, or about 13.7 * 1240 ≈ 17,000. Recall that we refer to this as the open-loop gain A_{ol}. In reality the gain of the output stage is about 0.96 when driving an 8-Ω load, so the open-loop gain is a bit less.

$$\text{Open-loop gain} \approx 16,300$$

Because the feedback network attenuates the signal by a factor of 20, the gain around the feedback loop, or loop gain, is about 816. This corresponds to about 58 dB of negative feedback (*NFB*) at low frequencies.

$$\text{Loop gain} \approx 816$$

$$\text{NFB} \approx 20 \log(816) \approx 58 \text{ dB}$$

If the amplifier is producing 20 V at its output, the error signal across the bases of Q1 and Q2 needs only to be 20/16,300 = 1.2 mV. Earlier it was asserted that the closed-loop gain would be approximately 20 on the basis of the feedback network attenuating the output by a factor of 20 and the required differential input to the amplifier being small. Because the input only needs to be 1.2 mV (compared to the input signal level of 1 V), it is apparent that this is a very good approximation.

Miller Feedback Compensation

Capacitor C1 is the so-called Miller compensation capacitor C_M. It plays a critical role in stabilizing the global negative feedback loop around the amplifier. It does this by rolling off the high-frequency gain of the amplifier so that the gain around the feedback loop falls below unity before enough phase lag builds up to cause instability. This will be discussed in much more detail in Chapter 4.

The effect of Miller compensation capacitor C1 on the open-loop gain is illustrated in Figure 2.14. Here the topology of the amplifier has effectively transitioned from that of Figure 2.13 to that of Figure 2.14 as the analysis has gone from low frequencies to high frequencies. In Figure 2.14 the combined gain of the input stage and the VAS is equal to the product of the transconductance of the IPS and the impedance of C1. At high frequencies the gain is dominated by C1 rather than by R1'.

The capacitor controls the high-frequency AC gain of the VAS by forming a shunt feedback loop around the VAS transistor. At higher frequencies, virtually all of the signal current from the LTP input stage flows through C1. This creates a voltage drop across C1 that becomes the output voltage of the VAS. At this point the VAS is acting like a so-called Miller integrator, where the output voltage is the integral of the input current.

While at low frequencies the gain of the combined input stage and VAS is set by the product of the individual voltage gains of those two stages, at higher frequencies that combined gain is set by the ratio of the impedance of C1 to the total emitter resistance ($1/gm$) in the LTP. That is because the signal current from the input stage is inversely proportional to the total LTP emitter resistance R_{LTP}. Since the impedance of C1 is inversely related to frequency, the gain set by it will decrease at 6 dB per octave as frequency increases. The frequency at which the AC gain based on this calculation becomes
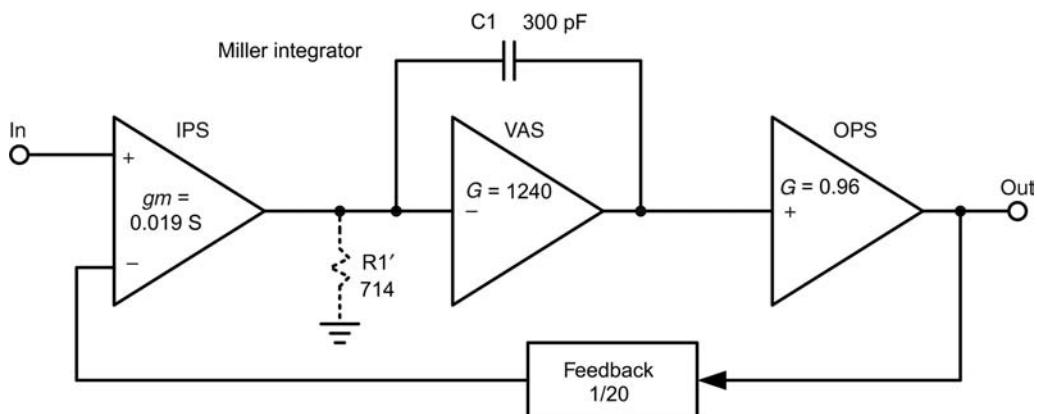
FIGURE 2.14 Amplifier gain at high frequencies.

smaller than the DC gain is where the roll-off of the amplifier's open-loop frequency response begins.

Assume for the moment an operating frequency of 20 kHz. At this frequency the reactance of C1 is $1/(2\pi * 20\text{ kHz} * 300\text{ pF}) = 26,500\ \Omega$. If all of the signal current provided by the LTP passes through C1, then the gain of the combined input and VAS stage at this frequency is $26,500/52 = 510$. This is considerably less than the low-frequency open-loop gain of 17,000. This means that the capacitor is dominating the gain at this frequency. This further supports the validity of the assumption that essentially all signal current from the LTP flows through the capacitor at this frequency.

The frequency where the gain around the negative feedback loop becomes unity is called the *gain crossover frequency f_c*, or simply the *unity-gain frequency*. This is illustrated by Figure 2.15, which is called a *Bode plot*. It shows the various gains of the amplifier in an idealized form with straight lines.

The open-loop gain starts out at 84 dB at low frequencies and begins to fall off at 20 dB per decade starting at about 613 Hz. This frequency corresponds to the open-loop bandwidth and is the frequency where the behavior of the amplifier transitions from that of Figure 2.13 to that of Figure 2.14.

The closed-loop gain of 20, corresponding to 26 dB, is shown as the horizontal dotted line. Where it intersects the falling open-loop gain line is the *gain crossover frequency*. This also corresponds approximately to the actual closed-loop bandwidth of the amplifier. Here, that crossing occurs at 500 kHz. The distance between the closed-loop gain line and the open-loop gain curve represents the amount of negative feedback, often called *loop gain* because it is the gain around the feedback loop.

The gain crossover frequency f_c is chosen to be low enough to assure adequate feedback loop stability. There is a trade-off between stability and distortion here. Making the gain crossover frequency higher results in more negative feedback at high frequencies
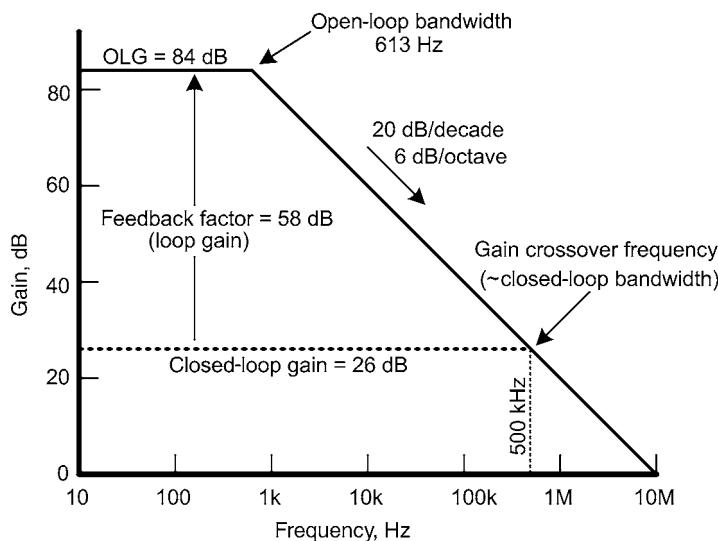
Figure 2.15   Bode plot of the amplifier.

and less high-frequency distortion. Making the gain crossover frequency too high jeopardizes loop stability. For this amplifier f_c has been chosen to be 500 kHz as a reasonable compromise between distortion reduction and stability.

The high-frequency open-loop gain of this simple amplifier is the ratio of Miller capacitor reactance to IPS total emitter resistance R_{LTP}. The closed-loop gain A_{cl} is the same as the attenuation ratio in the feedback path. The Miller capacitance needed to establish a gain crossover frequency f_c is then simply

$$C_{Miller} = 1/(2\pi f_c * R_{LTP} * A_{cl})$$
$$= 0.159/(500 \text{ kHz} * 52 \text{ } \Omega * 20) = 306 \text{ pF}$$

If instead we define C_{Miller} in terms of the transconductance of the IPS, gm_{LTP}, we have

$$C_{Miller} = gm_{LTP}/(2\pi f_c * A_{cl})$$

This shows clearly that increasing the gm of the LTP requires a corresponding increase in C_{Miller} to maintain the same f_c.

The gain crossover frequency for most audio power amplifiers usually lies between 200 kHz and 2 MHz. If the open-loop gain falls off at 6 dB per octave (as it does with simple Miller compensation), this corresponds to 20 dB per decade. It can then be seen that an amplifier with a gain crossover frequency of 200 kHz will have about 20 dB of negative feedback at 20 kHz. An amplifier with a 2-MHz gain crossover frequency will have about 40 dB of negative feedback at 20 kHz.

The Output Stage

The output stage is a class AB complementary Darlington arrangement consisting of emitter follower drivers Q8 and Q9 followed by output devices Q10 and Q11. Emitter resistors R11 and R12 set the idle current of the drivers at about 20 mA. The output stage emitter resistors R13 and R14 provide thermal bias stability and also play a role in controlling crossover distortion. These resistors will also be referred to as R_E. The output stage provides a voltage gain of slightly less than unity. Its main role is to buffer the output of the VAS with a large current gain. If driver transistor betas are assumed to be 100 and output transistor betas are assumed to be 50, the combined current gain of the output stage is 5000. When driving the 8-Ω output load as shown, the load impedance seen by the VAS looking into the output stage will be about 40,000 Ω.

On positive half-cycles of the signal, Q8 and Q10 conduct current and transport the signal to the output node by sourcing current into the load. On negative half-cycles, Q9 and Q11 conduct current and transport the signal to the output node by sinking current from the load. When there is no signal, a small idle bias current of approximately 100 mA flows from the top NPN output transistor through the bottom PNP output transistor. A key observation is that the signal takes a different path through the output stage on positive and negative half-cycles. If the voltage or current gains of the top and bottom parts of the output stage are different, distortion will result. Moreover, the "splice point" where the signal current passes through zero and crosses from one path to the other can be tricky, and this can lead to so-called crossover distortion.

The voltage gain of the output stage is determined by the voltage divider formed by the output stage emitter follower output impedance and the loudspeaker load impedance. The output impedance of each half of the output stage is approximately equal to re' plus R_E. This is illustrated in Figure 2.16.
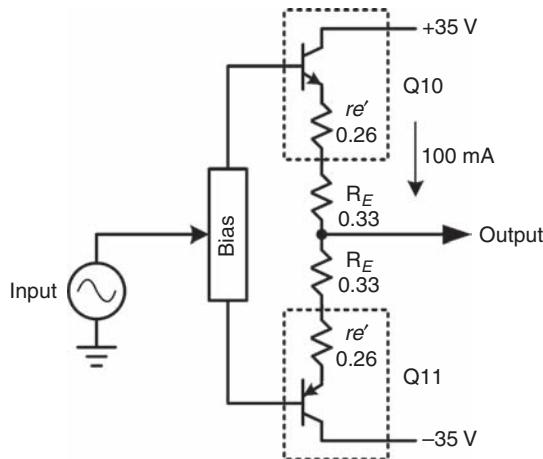
FIGURE 2.16 Push-pull output stage.

Since the two halves of the output stage act in parallel when they are both active at idle and under small-signal conditions, the net output impedance will be about half that of each side.

$$Z_{out(small\ signal)} \approx (re'_{idle} + R_E)/2$$

If the output stage is biased at 100 mA, then re' of each output transistor will be about 0.26 Ω. The summed resistance for each side will then be $0.26 + 0.33 = 0.59$ Ω. Both output halves being in parallel will then result in an output impedance of about 0.3 Ω. Because voltage gain is being calculated, these figures assume that the output stage is being driven by a voltage source. If the load impedance is 8 Ω, then the voltage gain of the output stage will be $8/(8 + 0.3) = 0.96$, as shown in Figures. 2.13 and 2.14. If instead the load impedance is 4 Ω, the gain of the output stage will fall to 0.93. The voltage divider action governing the output stage gain is illustrated in Figure 2.17.

Bear in mind that the small-signal gain of the output stage has been calculated at its quiescent bias current. The value of re' for each of the output transistors will change as transistor currents increase or decrease, giving rise to complex changes in the output stage gain. Moreover, at larger signal swings only one half of the output stage is active. This means that the output impedance under those conditions will be approximately
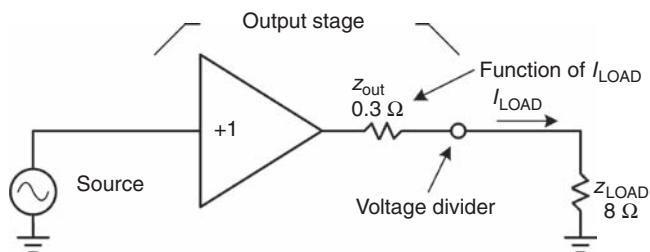
FIGURE 2.17 Amplifier output stage gain.

$re' + R_E$ rather than half that amount. These changes in incremental output stage gain as a function of output signal current cause what is called *static crossover distortion*.

$$Z_{out(large\,signal)} \approx re'_{high\,current} + R_E \approx R_E$$

At high current, re' becomes very small. At 1 A, re' is just 0.026 Ω, much smaller than a typical value of R_E. At 10 A, re' is theoretically just 0.0026 Ω. That is why $Z_{out(large\,signal)} \approx R_E$. If R_E is chosen so that

$$R_E = re'_{idle}$$

then

$$Z_{out(large\,signal)} \approx Z_{out(small\,signal)} \approx R_E$$

and crossover distortion is minimized by making the large-signal and small-signal output stage gains approximately equal [2]. This is only a compromise solution and does not eliminate static crossover distortion because the equality does not hold at intermediate values of output current as the signal passes through the crossover region. This variation in output stage gain as a function of output current is illustrated in Figure 2.18.

Output Stage Bias Current

The idle bias current of the output stage plays a critical role in controlling crossover distortion. It is important that the right amount of bias current flows through the output stage, from top to bottom, when the output is not delivering any current to the load. Notice that together the two driver and two output transistors require at least four V_{be} voltage drops from the base of Q8 to the base of Q9 to begin to turn on. Any additional drop across the output emitter resistors will increase the needed bias spreading voltage.
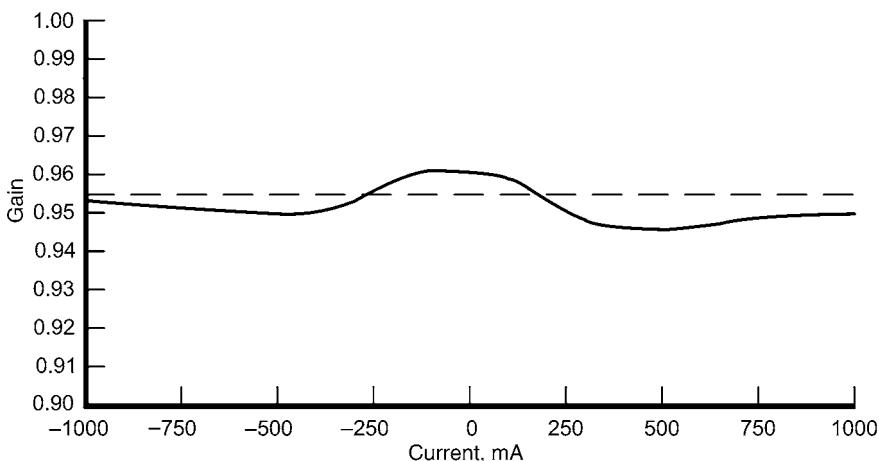
Figure 2.18 Output stage gain versus output current.

The optimum class AB idle bias for a conventional output stage like this is that amount of current that produces a voltage drop of approximately 26 mV across each of the output emitter resistors [2]. Recall that

$$re' = V_T/I_c = 26 \text{ mV}/I_c$$

Then

$$I_c = 26 \text{ mV}/re' = 26 \text{ mV}/R_E$$

and

$$V_{RE} = I_c * R_E = 26 \text{ mV}$$

This amount of bias current makes re' of the output transistor equal to the resistance of its associated emitter resistor. With 0.33-Ω emitter resistors, this corresponds to about 79 mA. In the example design here I have chosen to overbias the output stage slightly to a current of 100 mA. This means that small-signal gain will be slightly larger than large-signal gain in this case. This is evident in Figure 2.18.

There is a caveat to the assertion that the optimum bias point occurs when 26 mV is dropped across each output emitter resistor. Recall from Section 2.1 that the actual output impedance of an emitter follower is slightly greater than re'. The additional resistance results from physical base and emitter resistances inside the transistor. This additional resistive component acts as an extension of the external emitter resistor R_E. This means that the optimum voltage drop across the external emitter resistor will be somewhat less than 26 mV.

The required bias voltage for the output stage is developed across the bias spreader comprising a V_{be} multiplier built around Q5. In practice R7 is adjusted to set the output stage bias current to the desired value.

The objective of the bias spreader design is temperature stability of the bias point of the output stage. The temperature coefficient of the voltage produced by the V_{be} multiplier should match approximately that of the base-emitter junction voltages of the driver and output transistors. Since the V_{be} of a transistor decreases by about 2.2 mV/°C, it is important for thermal bias stability that these junction drops track one another reasonably. The output transistors will usually heat up the most. Because they are mounted on a heat sink, Q5 should also be mounted on the heat sink so that it is exposed to the same approximate temperature. This approach is only an approximation, because the drivers are often not mounted on the heat sink and because the temperature of the heat sink changes more slowly in time than that of the power transistor junctions.

Performance Limitations of the Simple Amplifier

The basic amplifier of Figure 2.12 has a decent low-frequency open-loop gain of about 16,300, or about 84 dB. With a closed-loop gain of 20 (26 dB) it has a feedback factor of about 816, corresponding to about 58 dB of negative feedback. However, its open-loop gain has not been made very linear and it is very vulnerable to β variations with signal in the output stage.

The feedback compensation was set to obtain a moderate negative feedback gain crossover frequency f_c of 500 kHz. This will typically result in a closed-loop 3-dB bandwidth of about 500 kHz. Selection of $f_c = 500$ kHz is what governed the choice of C1 at 300 pF. With $f_c = 500$ kHz and the assumed 6 dB per octave roll-off, the amount of negative

feedback at 20 kHz is about 500 kHz/20 kHz = 25, corresponding to 28 dB. This means that there will be less distortion correction at 20 kHz than at low frequencies.

Notice that the input stage can never deliver more than ±1 mA with respect to its nominal bias point. If all of this 1-mA swing goes into charging or discharging C1, the maximum voltage rate of change across C1 will be 1 mA/300 pF = 3.3 V/μs. This is very inadequate for virtually any power amplifier and will likely result in high frequency distortion often referred to as *slewing-induced distortion (SID)* or *transient intermodulation distortion (TIM)* [3, 4, 5]. Even with a demanded voltage rate of change well below the slew rate limit of 3.3 V/μs, the un-degenerated input differential stage will become nonlinear and produce high-frequency distortion.

These limitations will all be addressed in the next chapter as the design is evolved to a high-performance architecture.

References

1. Massobrio, Giuseppe, and Paolo Antognetti, *Semiconductor Device Modeling with SPICE,* 2d ed., New York, McGraw-Hill, 1993.
2. Oliver, B. M., "Distortion in Complementary Pair Class B Amplifiers," *Hewlett Packard Journal*, pp. 11–16, February, 1971.
3. Otala, M., "Transient Distortion in Transistorized Audio Power Amplifiers," *IEEE Transactions on Audio and Electro-acoustics*, Vol. AU-18, pp. 234–239, September, 1970.
4. Jung, W.G., M. L. Stephens, and C.C. Todd, "Slewing Induced Distortion and Its Effect on Audio Amplifier Performance–With Correlated Measurement Listening Results," AES preprint No. 1252 presented at the 57th AES Convention, Los Angeles, May, 1977.
5. Cordell, R. R., "Another View of TIM," *Audio*, February & March, 1980.

This page intentionally left blank

Power Amplifier Design Evolution

I n this chapter I begin by describing and analyzing a simple power amplifier and then progress through various improvements to it. The rationale for the performance-improving changes is described at each step of the way. The amplifier does not include all of the usual circuit details needed in a real amplifier, such as input AC coupling and filtering, output stage protection circuits, and output stage networks. Nevertheless, it serves to illustrate the design choices and process in evolving a design to a high performance level.

3.1   The Basic Power Amplifier

Figure 3.1 is the simple 50-W amplifier analyzed in the last chapter. It has many performance limitations as a result of its simple design.

The performance of the amplifier was evaluated by simulating it with a version of the SPICE program called *LTspice* [1, 2]. This free program is very useful for audio electronics design and its use is described in detail in Chapter 19. Of special interest is its ability to perform distortion analysis. Because simulations do not always capture or model all of the distortion mechanisms that can exist in the real world, results can sometimes be a bit optimistic. Nevertheless, they do provide valuable comparisons among different circuit design arrangements.

The 50-W amplifier was simulated under various conditions to evaluate its Total Harmonic Distortion (THD). Performance of the first version of the amplifier is shown in Chart 3.1 below. THD results are presented at 1 kHz and 20 kHz at 50 W when driving an 8-Ω load. This corresponds to a peak output voltage of 28 V. For comparison, results are also shown for the same voltage output with a no-load condition. Distortion at slightly reduced output voltages when the amplifier drives a 4-Ω load and a 2-Ω load are also shown, exposing the effects of heavier loading. Those voltages correspond to power levels of 90 W at 4 Ω and 145 W at 2 Ω.

For reference, the 1-kHz clipping points for this amplifier into 8, 4, and 2 Ω are 62 W, 110 W, and 178 W, respectively. Note that a real amplifier incorporating only a single pair of output transistors would be unable to safely produce 178 W into a 2-Ω load.

The first thing to notice is the fairly low amount of distortion at 1 kHz (THD-1) of about 0.01% when driving no load. This rises by almost a factor of 5 when driving an 8-Ω load, reflecting the loading on the output stage. The higher peak currents required
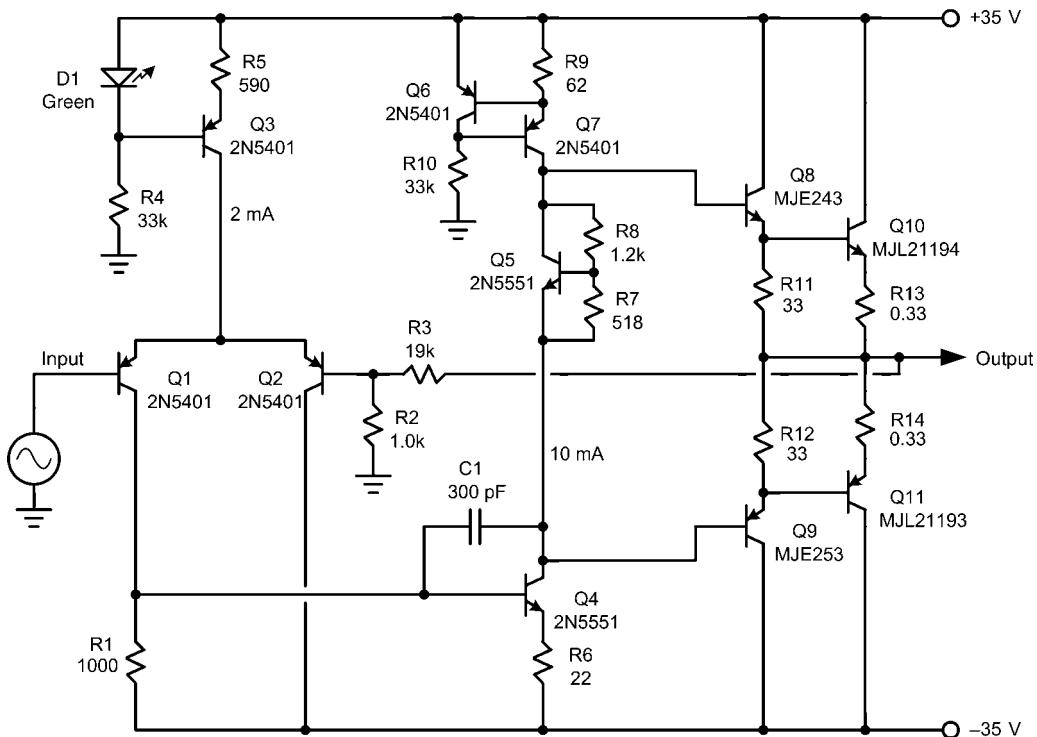
FIGURE 3.1   A basic 50-W power amplifier.
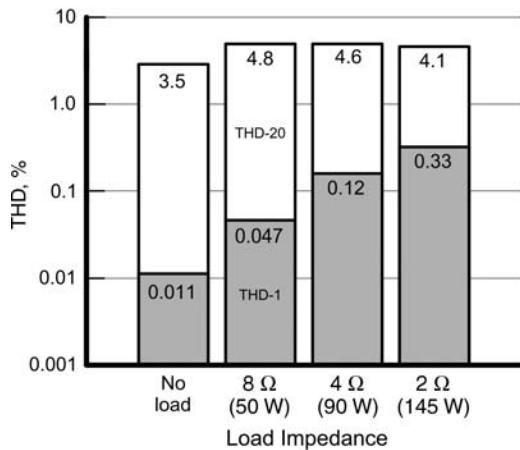
CHART 3.1   THD for amplifier of Figure 3.1.

to drive the 4-Ω and 2-Ω loads are reflected in even higher amounts of distortion. At a drive level of 17 V RMS into a 2-Ω load, the peak current is 12 A. At this current level the output transistors are suffering considerable beta droop, contributing significantly to the distortion.

It is very revealing to evaluate distortion under conditions ranging from no-load to a heavy load. This helps isolate the distortion contributions of the output stage from those of the remainder of the amplifier.

At 20 kHz distortion is very high, even under a no-load condition. This is a direct reflection of the inadequate slew rate of the amplifier. Recall from Chapter 2 that the estimated slew rate of this amplifier is 3.3 V/μs. A 28-V peak sine wave at 20 kHz has a maximum rate of change of 3.5 V/μs. This means that at 20 kHz this amplifier is just into slew rate limiting when it is attempting to deliver 50 W. The THD-20 results are in the range of 4%.

3.2 Adding Input Stage Degeneration

There are several different ways in which to evolve this amplifier and improve it. There is nothing sacred about the order in which the improvements are made. Here I have chosen to make the first improvement by adding emitter degeneration to the input stage LTP to improve the slew rate and reduce high-frequency distortion.

The design of Figure 3.2 differs from that of Figure 3.1 by the addition of emitter degeneration resistors R15 and R16 and by reducing C1 from 300 pF to 30 pF. The pair of 234-Ω emitter degeneration resistors implements 10:1 degeneration of the input differential pair by increasing the total emitter-to-emitter resistance R_{LTP} from 52 Ω to 520 Ω. This reduces its transconductance by a factor of 10. In order to keep the negative
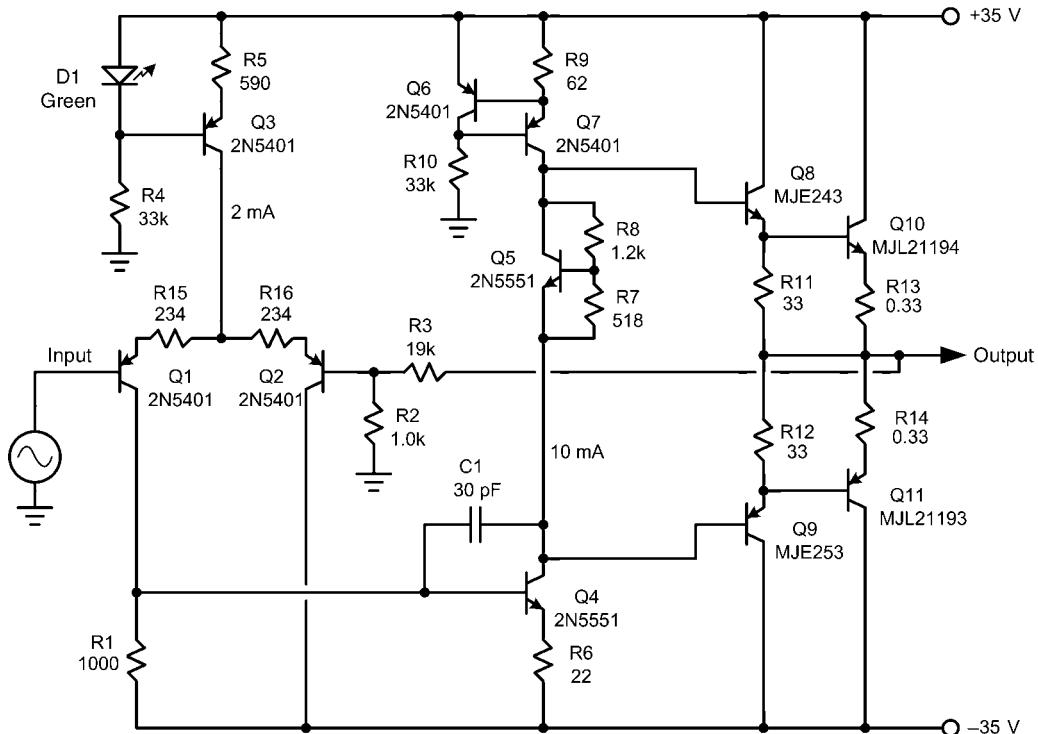
FIGURE 3.2 Input stage emitter degeneration.

feedback gain crossover frequency f_c at the same 500 kHz for equivalent stability, C1 must be reduced by that same 10:1 factor.

Recall the relationship described in Chapter 2 for Miller compensation.

$$C_{Miller} = 1/(2\pi f_c * R_{LTP} * A_{cl})$$

A_{cl} is the closed-loop gain, R_{LTP} is the total emitter-to-emitter LTP resistance including re', and f_c is the desired gain crossover frequency for the negative feedback loop.

$$C1 = C_{Miller} = 0.159/(500 \text{ kHz} * 520 \text{ } \Omega * 20) = 30.6 \text{ pF}$$

By this calculation C1 must be reduced to about 30 pF. Notice that the same maximum ± 1 mA is still available from the input stage to charge and discharge C1. This now results in an achievable slew rate of 1 mA/30 pF = 33 V/μs. This is a much more respectable value of slew rate for an audio power amplifier. At the same time, the input stage has been made significantly more linear by the addition of the emitter degeneration. This leads to lower input stage distortion under virtually all signal conditions.

Figure 3.3 shows the transfer function of the input stage before and after the introduction of emitter degeneration. The relative output current at the collector of Q1 is plotted as a function of differential input voltage applied between the base of Q1 and the base of Q2. The great improvement in linearity with degeneration is notable. The very small range of input voltage over which the un-degenerated pair is linear is quite obvious. Differential input signals greater than about 40 mV will produce gross distortion in the un-degenerated pair, while differential inputs of 400 mV are producing just barely perceptible bending at the edge of the range in the degenerated pair.

Figure 3.4 illustrates the behavior of the two cases by plotting differential stage gain as a function of relative output current. As in Figure 3.3, these plots assume that the collector load at Q1 is only the 1-kΩ resistor R1. Two things are immediately apparent. First, the gain at the quiescent point has been reduced by the expected factor of 10 when degeneration is introduced. Secondly, the gain in the un-degenerated case is a strong
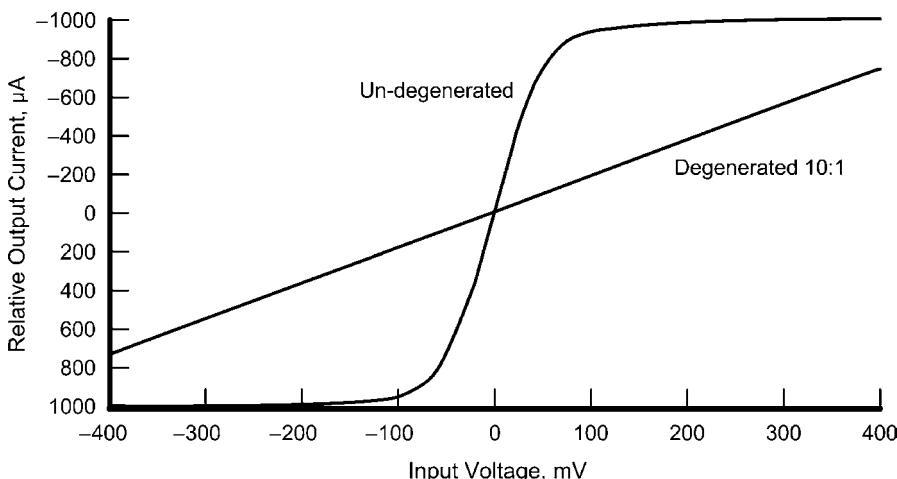
FIGURE 3.3   Differential stage current versus input voltage.
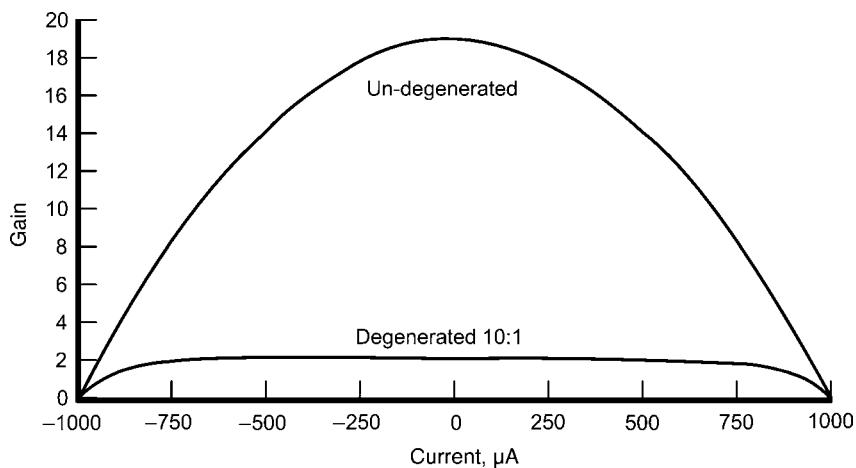
FIGURE 3.4 Differential stage gain versus output current.

function of the output current. This was also apparent in Figure 3.3 when one recognizes that the gain of the stage corresponds to the slope of the transfer function curve. At an output current of only half its maximum value, the gain in the un-degenerated case has fallen from 19 to 14.

The Bode plot in Figure 3.5 illustrates how the gain variation with signal in the un-degenerated input stage also affects dynamically the frequency responses in the amplifier. The shaded region shows the variation in open-loop gain as the output current from the input stage varies from its quiescent point to half its maximum signal value. Because the closed-loop bandwidth is changing with signal, the in-band phase response of the amplifier will also change with the signal. This phenomenon has been termed *phase intermodulation (PIM) distortion* [3, 4], and will be discussed in more detail in Chapter 22.
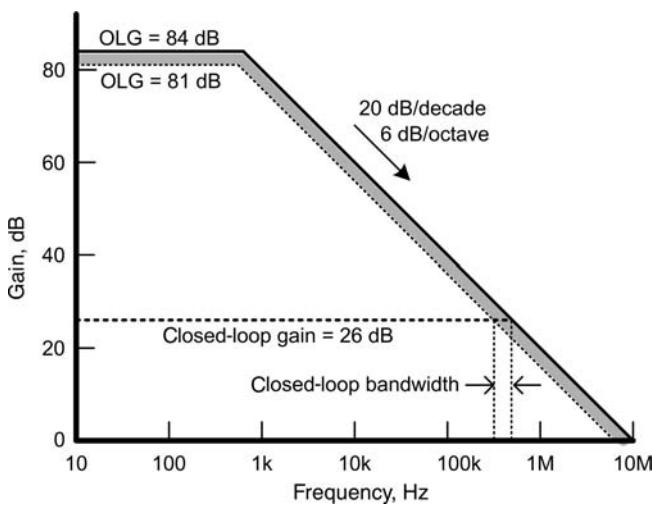
FIGURE 3.5 Modulation of frequency response.

There is a price to be paid for employing emitter degeneration in the input stage. The DC gain of the input stage was previously 13.7; it is now only 1.37. This combined with the VAS-OPS gain of about 1200 yields an open-loop gain of about 1644 and a loop gain of about 82.

$$\text{IPS gain} \approx 1.4$$

$$\text{NFB} \approx 38 \text{ dB}$$

The reduced IPS gain means that the amplifier's low-frequency open-loop gain and negative feedback factor have been reduced by a factor of 10 (20 dB). The amplifier now has only 38 dB of negative feedback available at low frequencies. This reduces the ability of the negative feedback to reduce distortion caused by the VAS and the OPS. Feedback at 20 kHz is still about the same, approximately 28 dB. This change in the open-loop frequency response of the amplifier is illustrated in Figure 3.6. The important thing to notice is that the high-frequency gain behavior above the open-loop bandwidth frequency remains unchanged because the value of the Miller compensation capacitor was changed to account for the reduced input stage gain.

Notice that a side effect of the reduced open-loop gain at low frequencies is an increase in the open-loop bandwidth frequency from 613 to 6130 Hz. Some have been misled in the past to conclude that higher open-loop bandwidth is required for higher slew rate and lower *Transient Intermodulation Distortion* (TIM) [5]. As will be shown later, this view is wrong; high open-loop bandwidth is not required for low TIM [6]. It is merely coincidental here that the open-loop bandwidth increased as a consequence of the reduced input stage gain.

Another price to be paid is noise. While the introduction of emitter degeneration into the input stage will cause a modest noise increase in the LTP itself, the bigger issue is the fact that the near-unity gain of the input stage allows the noise of the VAS to play a nearly equal role, degrading overall amplifier noise performance. Chapter 7 will present a closer look at noise sources in power amplifiers and will discuss how to minimize them. Suffice it to say that voltage gain in the IPS substantially reduces the noise contribution of the VAS.
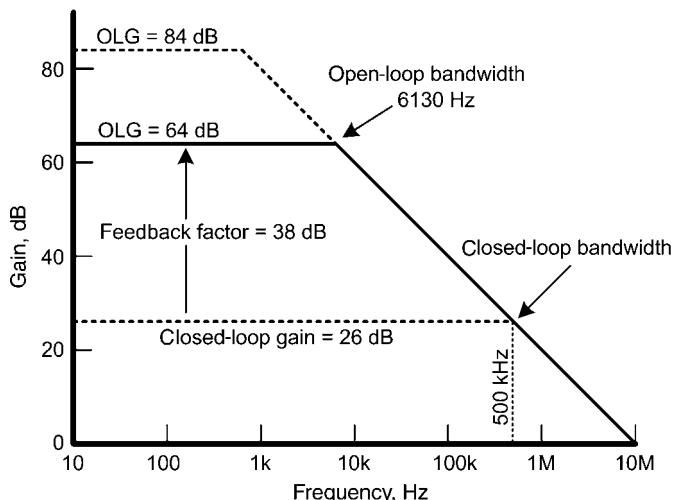
FIGURE 3.6 Reduced open-loop gain with degeneration.
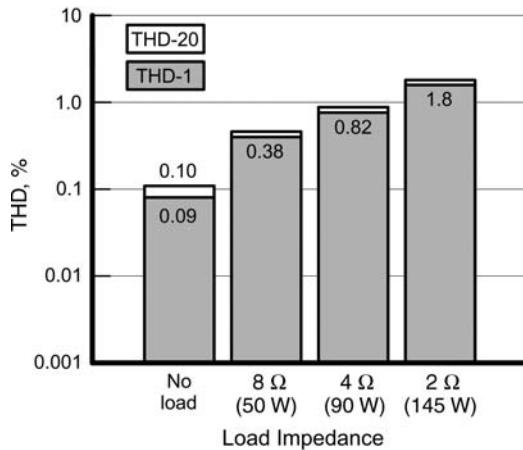
CHART 3.2 THD for amplifier of Figure 3.2.

Shown below in Chart 3.2 is the corresponding distortion performance of the amplifier of Figure 3.2.

There is a dramatic improvement in the high-frequency performance of the amplifier with this very simple and inexpensive change to the input stage. Notice especially the reduction in distortion at 20 kHz when there is no load. In this situation, the distortion caused by the output stage is minimized because it is not being called on to drive a load. The no-load condition exposes the distortion contribution of the input stage and VAS more clearly. The reduced distortion at 20 kHz is a direct result of the greatly increased slew rate capability of the amplifier and the improved linearity of the input stage as a result of the introduction of the emitter degeneration.

Unfortunately, the distortion at 1 kHz has worsened under all loading conditions. This is a direct result of the reduction in negative feedback that has occurred because of the emitter degeneration introduced into the input stage.

It is interesting to observe that the distortion at 20 kHz is not much different from the distortion at 1 kHz. This is not always what we would expect. As can be seen in Figure 3.6, there is still more global negative feedback present at 1 kHz than at 20 kHz. This would normally lead one to expect lower distortion at 1 kHz.

The reason for this seemingly anomalous behavior is that the dominant source of distortion in this version of the amplifier is the VAS. At low frequencies the VAS does indeed have more negative feedback surrounding it via the normal global negative feedback loop. However, at higher frequencies the loss of global negative feedback around the VAS is replaced by greater local negative feedback introduced by the Miller compensation capacitor. The two effects largely cancel, leaving the distortion caused by the VAS about the same at low and high frequencies.

3.3 Adding a Darlington VAS

The next logical evolution is to try and get back some of that open-loop gain that was lost by the introduction of the input stage emitter degeneration. This can be accomplished by adding an emitter follower in front of the VAS transistor to provide some
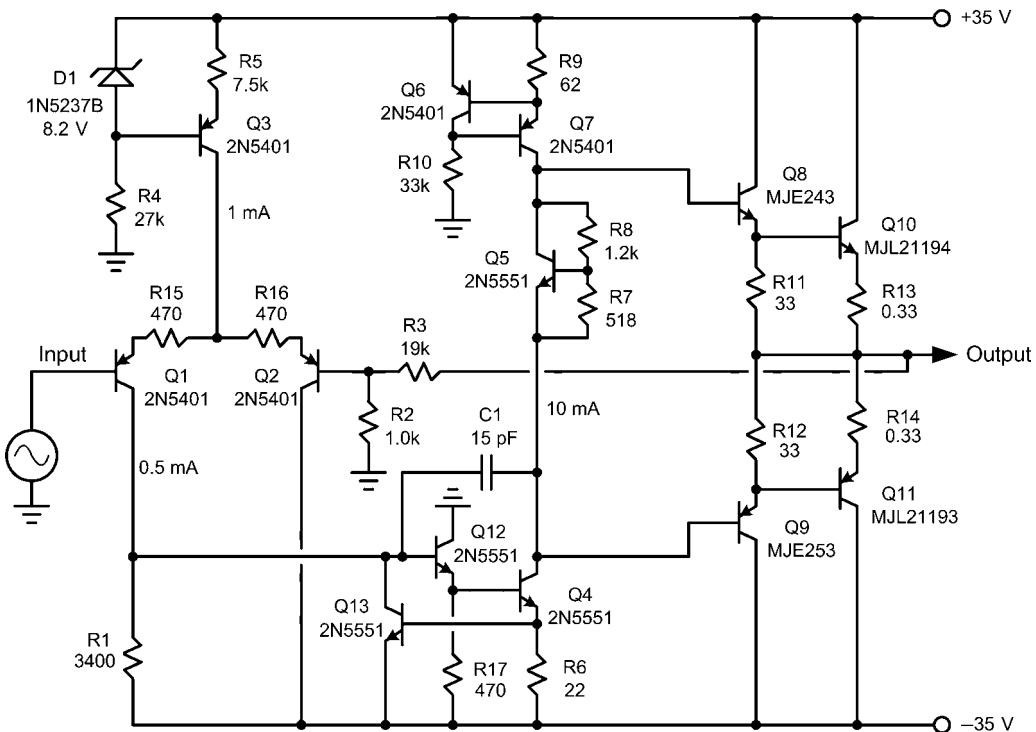
FIGURE 3.7 Amplifier with Darlington VAS added.

current gain. This is shown in the design of Figure 3.7, where Q12 has been added to buffer the input of the VAS. This is often referred to as a *Darlington* VAS, although in the strict sense the transistor connection would only be a Darlington if the collector of Q12 were connected to the collector of Q4. There is a good reason to connect Q12's collector to ground that will be discussed shortly.

The inclusion of Q12 increases the input impedance of the new VAS to about 40 kΩ, assuming a beta of 100 for Q12. Also note that this 40-kΩ input impedance is largely determined by the choice of the 470-Ω emitter resistor R17, which provides a healthy 2 mA of turn-off current to the base of Q4. This is needed to sustain a high slew rate in the face of the collector-base capacitance of Q4. If Q4 has a C_{cb} of 5 pF, this turn-off current will sustain a slew rate of about 2 mA/5 pF = 400 V/μs, far more than what is needed.

I have also chosen to reduce the bias current in the LTP by a factor of 2 to reduce input noise current contributions. Keeping the same 10:1 degree of emitter degeneration raises the required value of R15 and R16 by a factor of 2 to 470 Ω. This halves the input stage transconductance and halves the capacitance value needed for compensating capacitor C1 to 15 pF. Since the available charging current was halved and the amount of capacitance was halved, the achievable slew rate remains the same at 33 V/μs. Notice that the 1-mA tail current source formed by Q3 is now implemented with an

8.2-V Zener diode; this results in a higher current source output impedance and better power supply rejection.

The inclusion of Q12 also raises the node voltage at the output of the LTP to about 1.7 V above the negative rail. This calls for the use of a larger LTP load resistor R1. With R1 now at 3.4 kΩ, the input stage load resistance is about 3.1 kΩ and IPS voltage gain is back up to about 3.0. Combined with the VAS-OPS gain of 1200, the open-loop gain becomes 3600 and the loop gain becomes 180, corresponding to about 45 dB. This approximate 7-dB increase in negative feedback as compared to the design of Figure 3.2 will tend to reduce low-frequency distortion by nearly 7 dB.

$$\text{IPS gain} \approx 3.0$$

$$\text{NFB} \approx 45 \text{ dB}$$

Transistor Q13 has also been added to limit the maximum current of Q4 if the amplifier clips on negative-going signals. Under such clipping conditions, Q1 will conduct the full 1 mA of LTP tail current and will attempt to raise the node voltage at the base of Q12 to almost 3.4 V above the negative rail, severely overloading the VAS. Current limiter transistor Q13 turns on only if the emitter current of Q4 exceeds about 27 mA. This protection is desirable because the addition of the Darlington transistor Q12 made substantial overdrive of Q4 possible. In many cases the current source loading the VAS will limit the current of Q4 to about 10 mA; however, this will not be the case in the event of an output short circuit. It will also not be the case with some safe area protection circuits that shunt the VAS output node to the output node when they protect. Even in a normal clipping scenario, Q12 will attempt to deliver high current to the emitter of Q4 through Q4's base-emitter junction, and Q13 will limit this current by limiting the total emitter current of Q4 to about 27 mA.

Another important improvement has taken place with the introduction of the Darlington VAS. Prior to the use of the Q12 buffer, the collector-base capacitance of Q4 was effectively in parallel with the Miller compensation capacitor C1 in the earlier design. Unfortunately, the collector-base junction capacitance of a transistor is nonlinear, going from a high value when collector-base voltage is low, to a smaller value when V_{cb} is high. The resulting change in net compensation capacitance with signal causes the high-frequency gain of the amplifier to change with signal, corresponding to a source of high-frequency nonlinear distortion. The isolation afforded by buffer Q12 suppresses this effect.

Chart 3.3 lists the corresponding distortion performance of the amplifier of Figure 3.7. Note the significant improvement in performance at both low and high frequencies provided by this very inexpensive addition of two small-signal transistors Q12 and Q13. Both low- and high-frequency distortion when driving an 8-Ω load have decreased by a factor of about 2. This correlates with the approximate 2:1 increase in input stage gain. The no-load distortion at 20 kHz has been significantly reduced from 0.1% to 0.028%. The 1-kHz distortion has also been improved by a factor of over 3. These improvements are a result of the increase in low-frequency feedback factor. Distortion is still quite high with 4-Ω and 2-Ω loads, however. This is a reflection of the output stage struggling to drive the low-value load impedances.

It is still the case that THD-1 and THD-20 are about the same at all load impedances. This is a reflection of the fact that VAS distortion is still dominating performance.
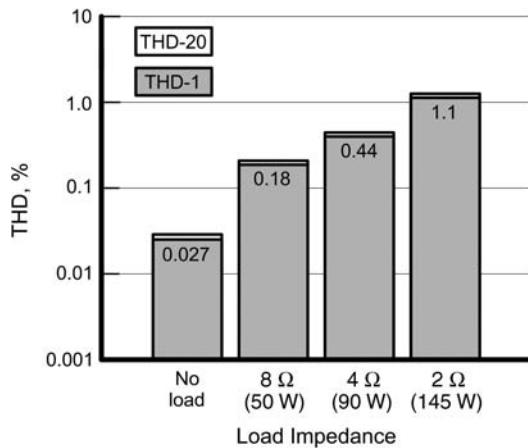
CHART 3.3 THD for the amplifier of Figure 3.7.

3.4 Input Stage Current Mirror Load

The voltage gain of the input stage has been limited by the load impedance at its output collector in the designs that have been discussed to this point. This impedance is governed by load resistor R1 in parallel with the input impedance of the VAS. The introduction of the Darlington VAS greatly reduced the loading due to the latter, but only reduced the influence of the collector-load resistance by a factor of about 3. The single-ended use of just one of the output collector signals from the LTP is also wasteful of gain.

Figure 3.8 shows the addition of a current mirror to serve as the load for the input stage. The current mirror is composed of Q14 and Q15 along with their associated emitter degeneration resistors. An added benefit of the current mirror is that it forces the collector currents of input transistors Q1 and Q2 to be essentially the same. In the earlier designs the balance of the collector currents of Q1 and Q2 depended on the proper relationship among numerous parameters, such as the tail current in relation to R1 and the voltage at the input to the VAS. Differential amplifier input stages produce lowest distortion only when they are well balanced. Even a fairly small amount of imbalance in an LTP can cause the creation of second harmonic distortion.

The gain of the input stage has now increased by a large amount because its transconductance has doubled and because its output load impedance is now just the input impedance of the Darlington VAS, which is on the order of 40 kΩ. The gain of the input stage is now approximately 80. When combined with the VAS-OPS gain of 1200, the open-loop gain becomes about 96,000, corresponding to nearly 100 dB. Loop gain will be 26 dB below that, or about 74 dB.

$$\text{IPS gain} \approx 2 * (40 \text{ k}\Omega / 1 \text{ k}\Omega) = 80$$

$$\text{NFB} \approx 74 \text{ dB}$$

The open-loop gain and amount of negative feedback are greater by a factor of over 27 as compared to the case in Figure 3.7. The total open-loop gain of this version of the amplifier is illustrated in Figure 3.9.
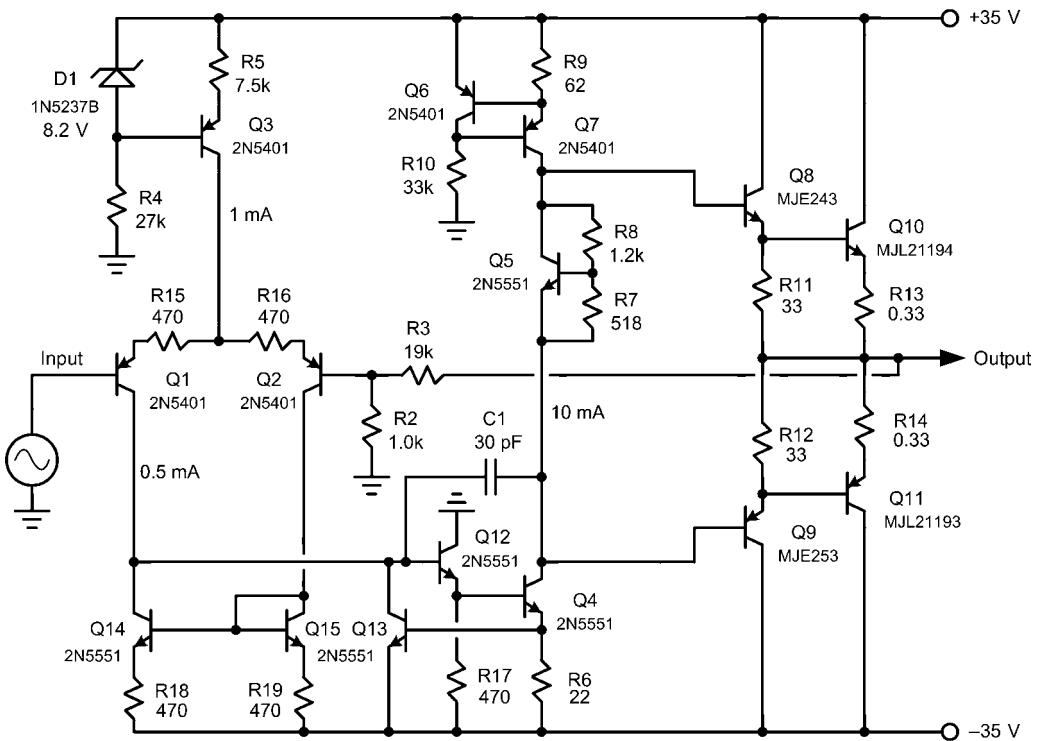
FIGURE 3.8 Input stage with current mirror load.
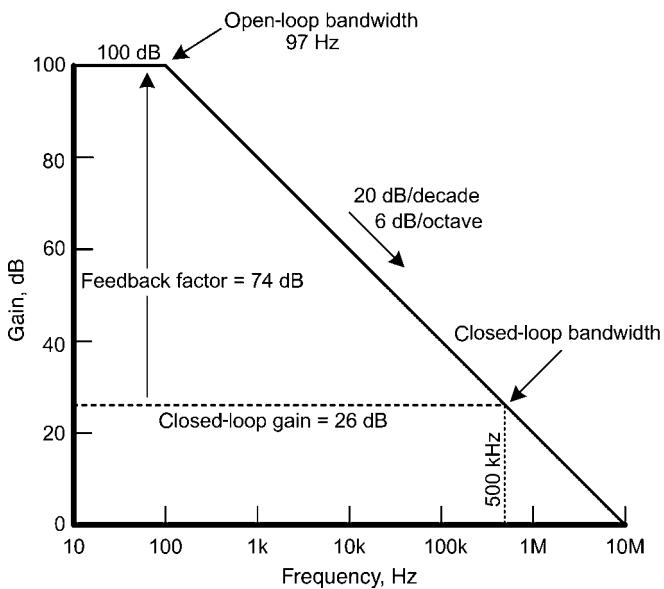
FIGURE 3.9 Performance with IPS current mirror load.
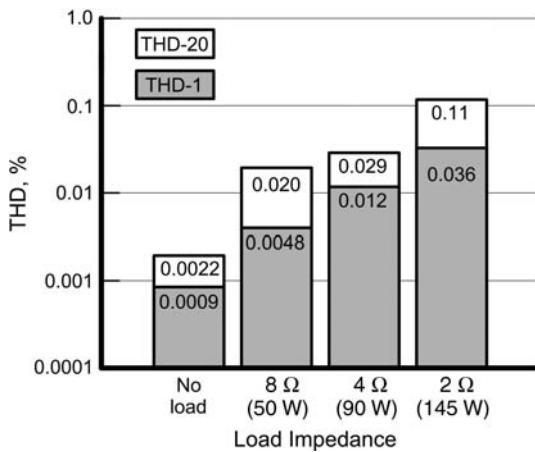
CHART 3.4   THD of amplifier of Figure 3.8.

The use of both signal currents from the collectors of the LTP effectively doubles the transconductance of the LTP. This means that C1 must be doubled to 30 pF in order to maintain the negative feedback gain crossover frequency at about 500 kHz.

As an aside, it should be mentioned that the current mirror chosen here is a very simple one. A slightly more complex current mirror arrangement could be employed to maintain the collector voltages of both Q14 and Q15 at more nearly the same value, further improving symmetry and performance. One of the other current mirrors described in Chapter 2 would help accomplish this. The current mirror of Figure 2.9b would be a good choice.

Chart 3.4 lists the corresponding distortion performance of the amplifier of Figure 3.8.

Note the very significant improvement in performance at both low and high frequencies provided by this very inexpensive addition of the current mirror load. No-load THD-1 has been reduced by a factor of 30, and no-load THD-20 has been reduced by a factor of 13. These reductions in distortion are attributable to two things. First, the input stage does not have to work as hard to drive the VAS to produce a given output level. Second, there is now a far greater amount of negative feedback. Notice that the input stage gain has been increased by a factor of 27 and that this is similar to the factor by which THD-1 was reduced.

Especially notable is the very low amount of THD-20 under no-load conditions. This suggests that the IPS-VAS combination is capable of very good performance even out to high frequencies. It now becomes much clearer how the output stage is limiting both low-frequency and high-frequency performance as the load becomes heavier.

3.5   The Output Triple

With this section the design evolution begins in earnest to improve the output stage. The performance comparisons thus far have shown that performance degrades as the amplifier goes from a no-load condition to a heavy-load condition. This is almost always a sign of distortion that originates in the output stage or in the way the output stage loads the VAS.

The use of two stages of emitter follower current gain in the output stage is simply not sufficient for driving lower-impedance loads with the highest quality. To the extent possible, it is very desirable to isolate the high impedance output of the VAS from the loudspeaker load.

Figure 3.10 shows the use of an output stage that is a triple emitter follower, often just called a *Triple*. This output stage was popularized by Bart Locanthi, and is also known as the *Locanthi T circuit* [7, 8]. The extra emitter follower stage provides an additional amount of buffering for the VAS stage in the form of higher current gain by a factor of about 100.

Transistors Q16 and Q17 act as pre-driver emitter followers that provide the extra current gain and buffering. This increases the input impedance of the output stage to a typical value of about 4 MΩ when an 8-Ω load is being driven. With the Triple, the total current gain in the output stage is on the order of 500,000. The extra buffering is especially effective in mitigating the effects of beta droop at high currents in the output transistors.

The VAS gain was previously estimated to be governed by an output stage load resistance of 40 kΩ in parallel with a 135-kΩ Early effect output resistance of the VAS transistor, for a net load of 31 kΩ. The ratio of 31 kΩ to the effective VAS emitter resistance provided the VAS voltage gain figure of 1240. When combined with an output stage gain of about 0.96 when driving an 8-Ω load, the VAS-OPS gain became about 1200.
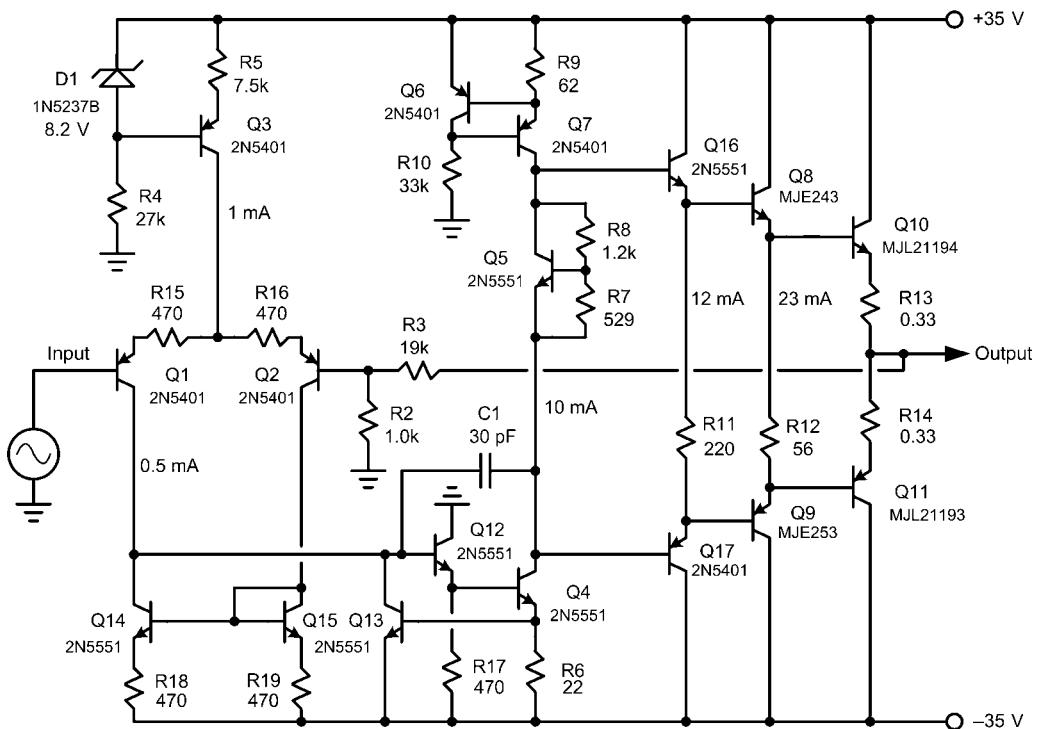
FIGURE 3.10   Output stage with Triple emitter follower.

The 40-kΩ output stage load resistance has now become 4 MΩ with the introduction of the Triple, for a net VAS load resistance on the order of 130 kΩ. With the effective emitter resistance in the VAS at about 25 Ω, the VAS gain now becomes 130 kΩ/25 = 5200. This is an increase of about 12 dB in VAS gain.

$$\text{IPS gain} \approx 80$$

$$\text{VAS gain} \approx 5200$$

$$\text{OPS gain} \approx 0.96$$

$$\text{Open-loop gain} \approx 400{,}000 \ (112 \text{ dB})$$

$$\text{Feedback factor} \approx 20{,}000 \ (86 \text{ dB})$$

The frequency responses of the amplifier employing the Triple output stage are shown in the Bode plot of Figure 3.11. It is important to notice that although the amount of open-loop gain and negative feedback have increased substantially, the high-frequency portion of the frequency responses remains the same, including the gain crossover frequency and closed-loop bandwidth. This is again due to the fact that the Miller compensation capacitor is controlling the gain at high frequencies. In this context, that means all frequencies above 25 Hz. The gain at low frequencies is actually poorly controlled because it depends heavily on the β of many transistors and on the Early effect. For this reason, the estimated value of low-frequency gain of 112 dB is indeed a very rough estimate. What is important is that the number is large, even if it is uncertain.

A second benefit of the Locanthi T output stage architecture is the way in which the bias current in the predriver and driver stages is established. In each case a single resistor
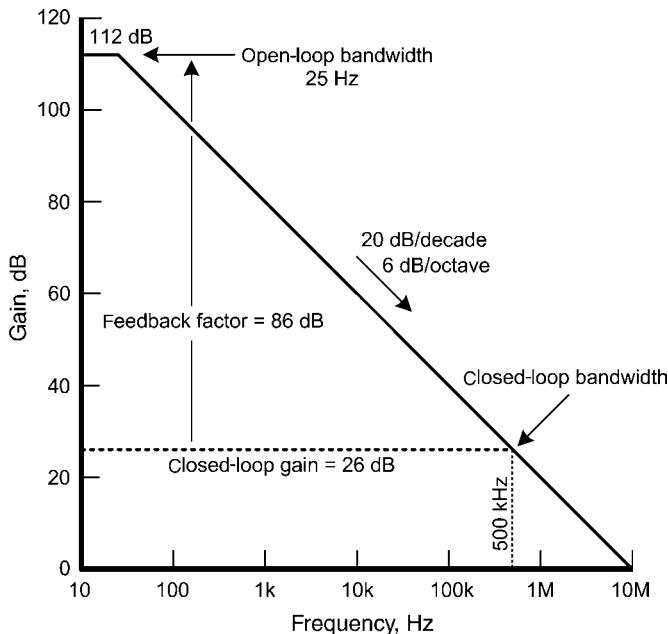
FIGURE 3.11   Performance with output Triple.

is connected from emitter to emitter of the respective stage. This can be seen in the way that R11 and R12 are connected. This gives the output stage its T-like appearance. More importantly, this connection of the bias resistors causes the predriver and driver emitter follower stages to stay turned on throughout the signal swing. They are operating in class A. In the earlier designs, where the bias resistors were connected to the output rail, the driver transistors turned off for one-half of the signal cycle, just like the output transistors.

As with many of the other improvements made in the evolution of this amplifier, this improvement has been made with the addition of only two inexpensive small-signal transistors, Q16 and Q17. Yet another advantage of the Triple is that the VAS no longer needs to drive the larger transistors that are usually required to supply the fairly high base currents of the output transistors. This often means that the smaller predriver transistors will load the high-impedance VAS output node with less nonlinear collector-base junction capacitance.

Chart 3.5 lists the corresponding distortion performance of the amplifier of Figure 3.10.

Note the very significant improvement in performance at low frequencies provided by this very inexpensive addition of two small-signal transistors. As expected, this improvement is especially notable when driving the 2-Ω load, where THD-1 has been reduced by a factor of 14 as compared to the same design using only a Darlington output stage.

The improvement at 20 kHz is less dramatic, ranging from a reduction factor of 2.5 when driving an 8-Ω load down to a factor of 1.5 when driving a 2-Ω load. This suggests that at high frequencies the performance is being limited largely by output stage crossover distortion. In Chapter 10 it will be shown how such crossover distortion can be reduced.

Note that while the introduction of the Triple increased the amount of negative feedback at very low frequencies by about 12 dB, a comparison of Figures 3.9 and 3.11 reveals that it did not increase the amount of global negative feedback at either 1 kHz or 20 kHz. The reductions in distortion occurred as a result of the Triple making the VAS-OPS combination more linear.
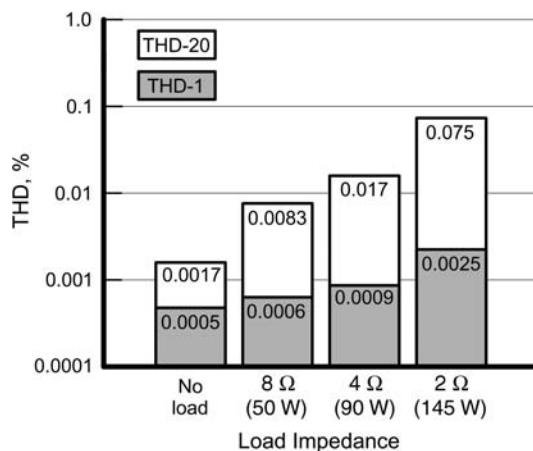
CHART 3.5   THD for amplifier of Figure 3.10.

3.6 Cascoded VAS

It was shown in the earlier discussion on the Early effect that the transistor has a very finite output resistance characteristic as a result of the current gain of the transistor increasing as the collector voltage increases. Since the current gain of the device is changing with signal, this is a nonlinear effect.

The load impedance presented by the output stage is now much larger due to the use of the Triple, so the intrinsic output impedance of the VAS matters much more. Recall that the estimated Early effect output resistance of the VAS is about 135 kΩ, while the Triple output stage presents a load of about 4 MΩ when it is driving an 8-Ω load. Indeed, the addition of the VAS cascode would not have made much sense until the Triple output stage was introduced into the design.

Figure 3.12 illustrates the addition of a cascode transistor Q18 to the VAS. The base of Q18 is held at a fixed potential of about 2.5 V above the negative supply rail by the combination of D2 (a Green LED) and D3 (a conventional silicon diode). This biasing arrangement provides VAS transistor Q4 with enough operating collector voltage without seriously compromising the negative voltage swing capability of the VAS.

The addition of the cascode increases the output impedance of the VAS to several MΩ. As a consequence, the very low-frequency open-loop gain of the circuit is further
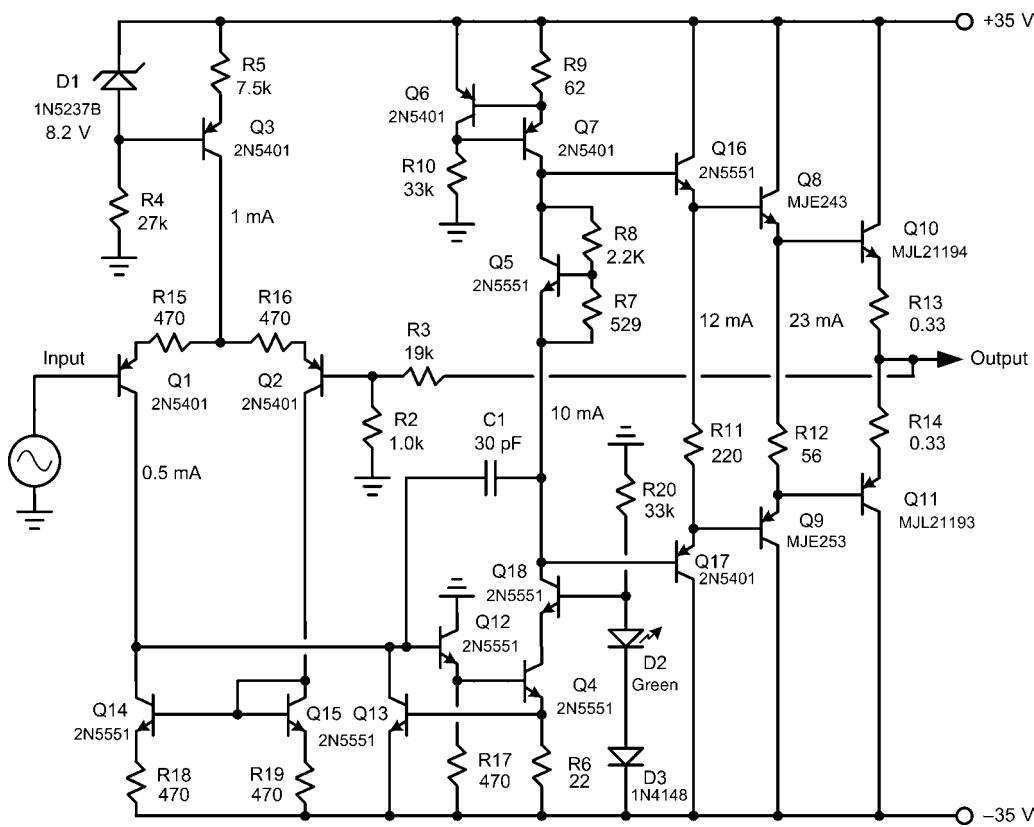
FIGURE 3.12 Amplifier with cascoded VAS.
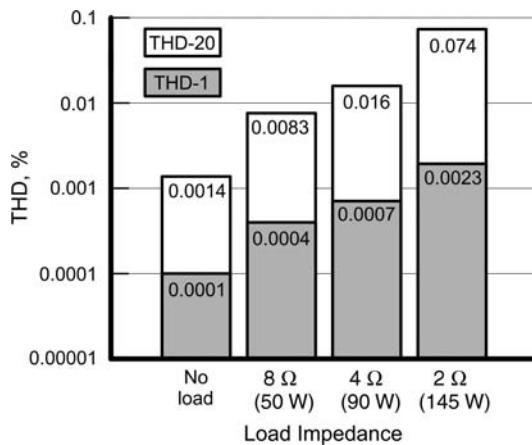
CHART 3.6 THD for amplifier of Figure 3.12.

increased at frequencies below 25 Hz. Increased open-loop gain and negative feedback in this very low-frequency region make little difference in the performance of the amplifier.

The high-frequency open-loop gain is largely determined by the Miller compensation, so it is essentially unchanged. It is once again important to point out that the amount of open-loop gain at both 1 kHz and 20 kHz has not been changed by the addition of the cascode, since the open-loop gain even at 1 kHz is being fully controlled by the Miller compensation capacitor. The amount of global negative feedback at both 1 kHz and 20 kHz is essentially the same in this design with the VAS cascode and the previous design without the VAS cascode.

The biggest benefit of the cascode is the reduction in open-loop nonlinearity and distortion in the VAS due to the near-elimination of the Early effect. Chart 3.6 lists the corresponding distortion performance of the amplifier of Figure 3.12. The distortion scale has been shifted down by a factor of 10 compared to the previous chart. The minimum distortion on the vertical scale is now 0.00001%.

Note the further improvement in performance at low frequencies under no-load conditions. THD-1 has decreased by a factor of about 5. However, only a small improvement in THD-20 under no-load conditions has occurred. This is because the Early effect contribution to distortion is less dominant at higher frequencies. Virtually no performance improvement is seen under any conditions under the heavily loaded 2-Ω condition. Less performance improvement is seen under loaded conditions because the distortion is being dominated by output stage crossover distortion.

3.7 Paralleling Output Transistors

The power amplifier that has been evolved to this point has been rated at only 50 W when driving an 8-Ω load. This has served well the purpose of comparisons during design evolution, but it has been noted earlier that this design would not really be able to support (at full power) the 2-Ω load conditions for which it has been simulated. At the same time, it is true that this design is scalable to higher power levels by simply increasing the power supply rail voltages.

Amplifiers operating at high power levels require more power dissipation capability in the output stage than one transistor can provide, but this is only part of the story. First, the current gain of typical power transistors begins to fall off fairly rapidly at collector currents beyond a certain point. This is commonly referred to as *beta droop*. This causes distortion and may impose unreasonable current demands on the driver transistors. If the safe operating area of the driver transistors is exceeded, destruction may result. At the rated power of 145 W into a 2-Ω load, the peak output current is 12 A. At a collector current of 12 A, the current gain of the MJL21193 has drooped to about 12, meaning that the driver transistor would have to supply about 1 A. The MJE243 has a safe operating area of only 12 V at a current of 1 A, even at room temperature.

Secondly, the paralleling of output transistors allows one to achieve lower output impedance for a given amount of thermal stability. The output transistor emitter resistors R_E play an important role here. If R_E is kept the same and each of the output pairs is biased at the same idle current, thermal stability will be the same and output impedance will be halved due to the paralleling action. When the output impedance is halved, any percentage variation in output impedance will have half the effect on output stage gain. This then reduces crossover distortion. Of course, the amplifier now dissipates twice as much power under the idle condition.

The amplifier of Figure 3.13 employs an output stage that uses two pairs of output devices to drive the load. The remainder of the amplifier is identical to that of Figure 3.12. At a given load current, each transistor in this arrangement only needs to supply half
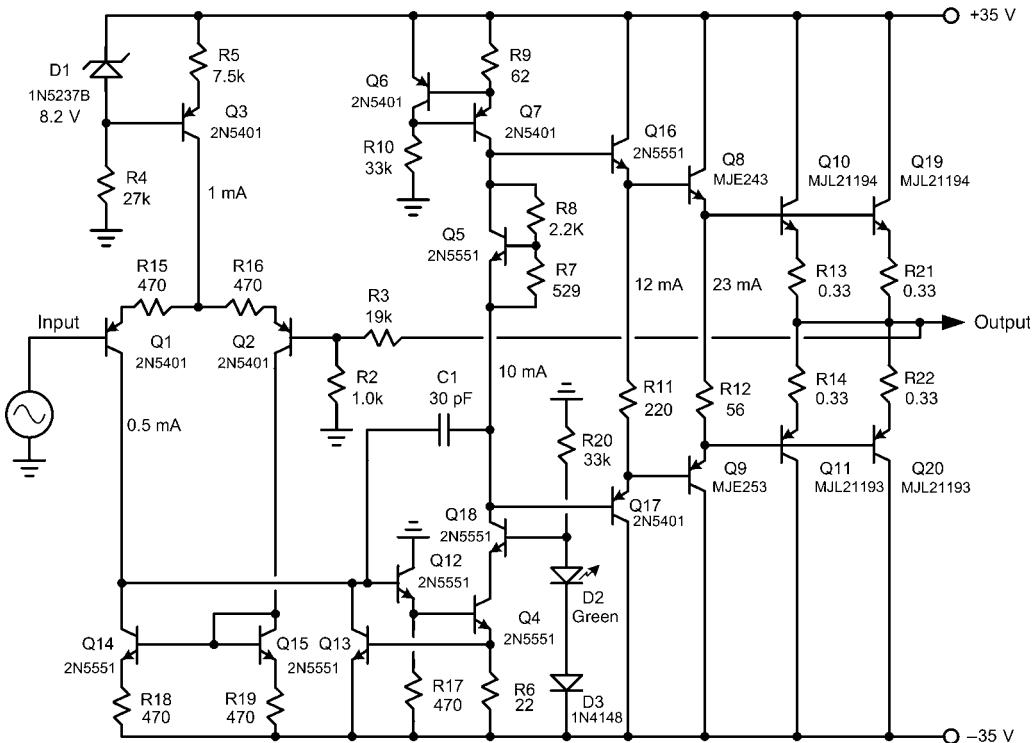
FIGURE 3.13   Amplifier with double output stage.
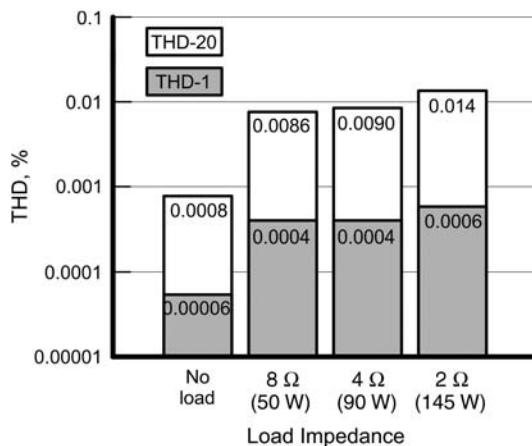
CHART 3.7   THD for amplifier of Figure 3.13.

the current that the output transistor had to supply in the previous arrangements. This significantly reduces the deleterious effects of beta droop. Chart 3.7 lists the corresponding distortion performance of the amplifier of Figure 3.13.

As expected, the most dramatic improvement is seen when the amplifier is driving the 2-Ω load. Here the THD-1 falls from 0.0023% to 0.0006% with the introduction of the paralleled output stage. More importantly, THD-20 falls by a factor of more than 5 from 0.074% to 0.014%. This demonstrates the distortion-reducing value of employing paralleled output devices.

As mentioned above, the output impedance is halved if it is assumed that the output stage was driven with a voltage source, since two pairs of emitter resistors are now effectively in parallel driving the load. Moreover, the total amount of idle bias current has been doubled without overbiasing the output stage. The doubling of idle current means that the class A region of operation of the output stage has been quadrupled in terms of watts of output power where the transition from class A to class B operation occurs. In the earlier design, with an idle bias of 100 mA, this transition occurred at a peak output current of 200 mA, corresponding to 0.16 W when driving an 8-Ω load. This design, with an idle bias of 200 mA, remains in class A up to an output power of 0.64 W when driving an 8-Ω load.

These improvements have been made without compromising the thermal stability of the output stage because the values of R_E for each output transistor have remained the same. This will be explained in much greater detail in a later chapter that deals with thermal stability. However, the temperature rise of the heat sink under idle conditions will be larger because the idle power dissipation of the output transistors has increased from approximately 7 W to 14 W. To put this in perspective, note that output stage dissipation will be about 55 W when the amplifier is driving a 4-Ω load at 1/3 power (30 W). If the heat sink temperature is allowed to rise by 35°C under these conditions, the heat sink must be designed to have a thermal resistance of about 0.6°C per watt. With such a heat sink, the 7-W increase in idle dissipation will cause a rise in heat sink temperature of only 4°C under idle conditions.

3.8   Higher-Power Amplifiers

Thus far the evolution of a 50-W power amplifier has been illustrated. Keeping the discussion to a fairly low-power design has simplified some things and allowed a level playing field to be maintained throughout the evolution of the design. We now take a look at what happens as the power capability of the design is increased.

Here the amplifier design is evolved to one rated at 200 W when driving an 8-Ω load, with correspondingly higher powers when driving loads of 4 Ω and 2 Ω. Such an amplifier requires higher power supply rail voltages to accommodate the 56.6-V peak output swing required for 200 W with an 8-Ω load. Here ± 64-V rails have been specified.

The amplifier of Figure 3.14 employs an output stage that uses four pairs of output devices to drive the load. This is done in order to support the higher peak current that will occur. This also provides the necessary higher output stage safe operating area (SOA) and power dissipation capability. When driving its rated 580 W into a 2-Ω load, peak output current will be 24 A, or 6 A for each of the four output devices.

Some other changes have been made to accommodate the higher supply voltage and the higher power dissipation that will result. The VAS cascode and current source transistors have been replaced by the 2SC3503/2SA1381 pair. These devices are rated at 300 V and are provided in a TO-126 package that can dissipate more power than the TO-92 package of the 2N5551/2N5401 pair used in the earlier examples. These devices also feature a fairly high f_T of 150 MHz and a very high Early voltage of over 500 V. These devices have also been used as the predrivers in the output Triple. The VAS transistors in this example each dissipate 640 mW, while the predriver transistors each dissipate 1 W.
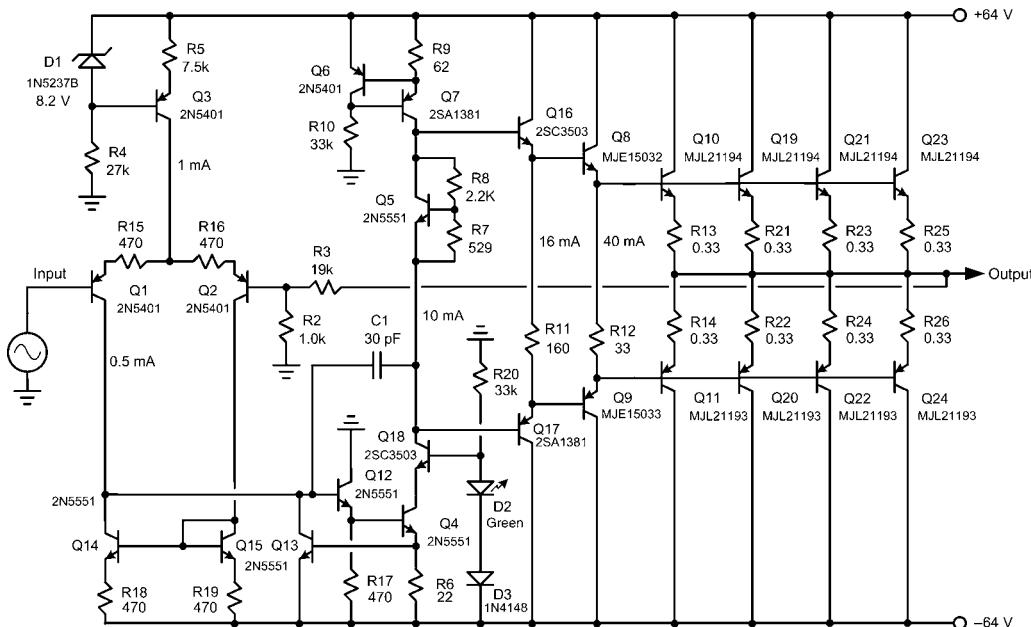
Figure 3.14   High-power version of the amplifier.
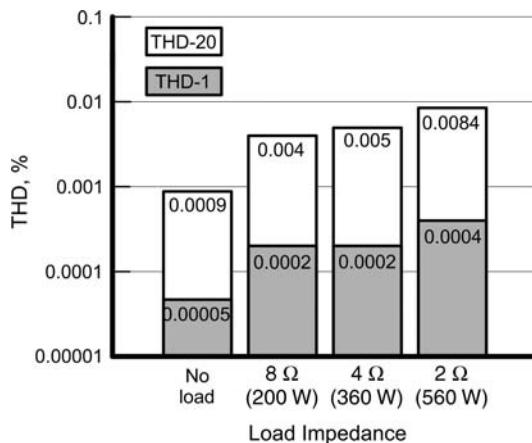
CHART 3.8 THD for amplifier of Figure 3.14.

The MJE243 and MJE253 drivers have also been replaced by the MJE15032 and MJE15033 transistors. This change provides the higher driver SOA and power dissipation capability needed for the higher-power amplifier. These devices are provided in a TO-220 package and are rated at 250 V. They will dissipate up to 28 W when used with a heat sink to limit the case temperature to no more than 80°C. The bias current in the drivers has been nearly doubled from 23 mA to 40 mA to provide more turn-off current for the larger output stage. As a result, the driver transistors now dissipate about 2.6 W each. Each output transistor is still biased at 100 mA, so in this design each one dissipates about 6.4 W. The complete output stage thus dissipates about 51 W at idle.

Sometimes the kind of quality low-noise transistors that would be preferred for use in the input stage are not able to withstand high rail voltages. While this is not a serious problem for 50-W to 100-W amplifiers, it does become an issue for larger power amplifiers with higher rail voltages, sometimes in the 60- to 100-V range. This problem is a special concern when JFET devices are used in the input stage. Although not used in this example, a common solution to this problem is to cascode the input stage so that the collector or drain voltages of the LTP may reside at a lower voltage like 15 V.

Chart 3.8 lists the corresponding distortion performance of the amplifier of Figure 3.14. Although it is operating at quadruple the power levels of the amplifier of Figure 3.13, distortion levels are quite comparable and in some cases even smaller. Notably, THD-20 has fallen from 0.014% to 0.0084%. This is a further reflection of reduced crossover distortion resulting from the doubled-size and halved-output impedance of the output stage.

3.9 Crossover Distortion

Crossover distortion has been mentioned many times during this evolution of the amplifier design, but amplifier performance has always been compared on the basis of full-rated power into the different load impedances. Before leaving the discussion on amplifier evolution, it is instructive to show the effect of crossover distortion.

It is generally understood that crossover distortion becomes worse at high frequencies and when lower-impedance loads are being driven. THD-20 is a better indicator of
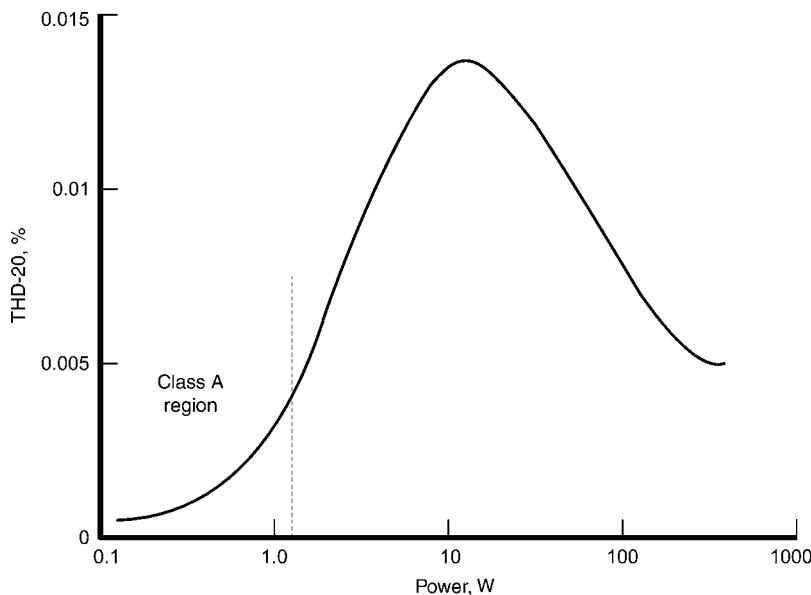
FIGURE 3.15 THD-20 versus power into 4-Ω load.

crossover distortion because there is less negative feedback available at 20 kHz and its harmonic frequencies to reduce distortion. THD-20 also captures both static and dynamic (switching) crossover distortion.

Crossover distortion characteristically becomes worse at lower power levels. Figure 3.15 shows THD-20 as a function of power when the amplifier of Figure 3.14 is driving a 4-Ω load. The graph illustrates how crossover distortion peaks at a relatively low power. Here the crossover distortion manifests itself as a peak in THD-20 at a power level of 11 W for an amplifier that is rated at 360 W into this 4-Ω load.

Full power distortion thus does not tell the whole story. Here THD-20 peaks at 0.014% when THD-20 at maximum power is only 0.0084%. Crossover distortion in this example results in THD-20 that is greater by a factor of 1.7.

Figure 3.15 also illustrates where the transition occurs from class A operation to class B operation for this amplifier when driving the 4-Ω load. With an idle bias current of 400 mA in the output stage, this amplifier can drive about 800 mA into the load before either the top or bottom power transistors go into cutoff. This 800 mA of peak current into a 4-Ω load corresponds to 1.28 W.

It was mentioned earlier in this chapter that the output stage of this amplifier design was not fully optimized for low crossover distortion. The per-transistor operating current of 100 mA represents an approximate 26% overbiasing compared to the theoretical optimum that places a voltage drop of 26 mV across the emitter resistors [9]. The choice of 0.33-Ω emitter resistors is also not optimal. Smaller emitter resistors and correspondingly higher bias currents would reduce crossover distortion by further reducing output stage output impedance. However, this would be at the expense of some thermal stability. Much more will be said about crossover distortion in Chapter 10.
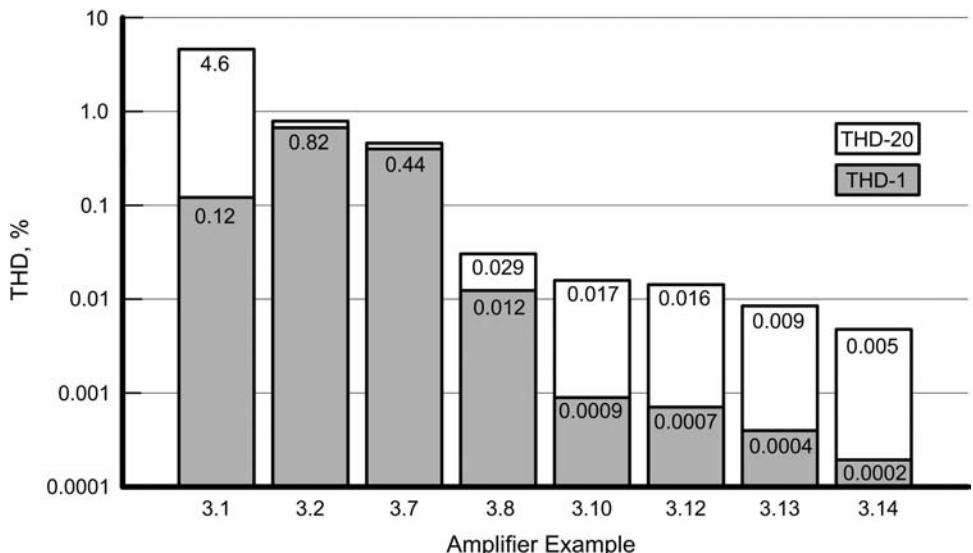
CHART 3.9 Performance comparison of the amplifiers. All driving 90 W into 4 Ω except 3.14 driving 360 W into 4Ω.

3.10   Performance Summary

Chart 3.9 shows a summary of distortion performance for all the example amplifiers discussed in this chapter. In all cases the load being driven is 4 Ω and each amplifier is being driven at the maximum power level that was used in the individual discussions. This power level was 90 W for all cases except the high-power amplifier of Figure 3.14, where the power level was 360 W. THD-1 decreased by a factor of 600 from beginning to end, while THD-20 decreased by a factor of 900 from beginning to end.

3.11   Completing an Amplifier

The amplifier versions described have been deliberately simplified in some ways. Before leaving this chapter, I will discuss a couple of necessary additions to these amplifier cores to make them at least somewhat complete.

Much of this added circuitry is illustrated in Figure 3.16, where the core amplifier is merely shown as a block of open-loop gain. Feedback network resistors R2 and R3 that were included in the core amplifier designs above are shown here for clarity.

Input Network

Resistor R_{in} and capacitor C_{in} form a first-order input low-pass filter that keeps out unwanted radio frequencies. This filter is often designed to limit the bandwidth of the complete amplifier to a frequency that is somewhat less than the actual closed-loop bandwidth of the amplifier proper. A typical 3-dB frequency for the input filter might be 270 kHz, as shown in Figure 3.16 with $R_{in} = 2.2$ kΩ and $C_{in} = 270$ pF. Resistor R_g keeps the input terminal from floating at DC.
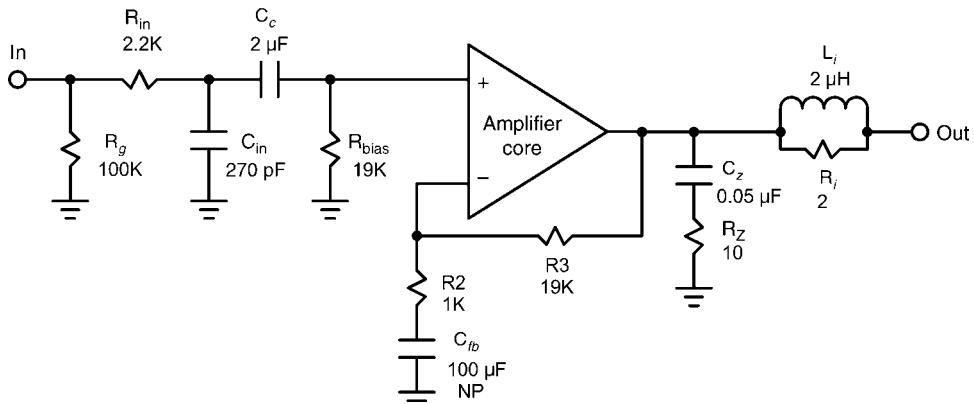
FIGURE 3.16 A more complete amplifier.

Coupling capacitor C_c blocks any DC that might be present from the source, while R_{bias} provides a return path for the input bias current of the amplifier's input stage. This keeps the noninverting input node of the amplifier near 0 V. Notice that if Q1 in the amplifier is biased at 0.5 mA and it has a beta of 100, its base current will be approximately 0.005 mA. This will cause a voltage drop of 95 mV across R_{bias}. The value of R_{bias} will often be set to equal that of R3 so that voltage drops across these two resistors balance out any DC offset. In this case, R_{bias} would be set to 19 kΩ. The capacitance of C_c against R_{bias} forms a high-pass filter whose 3-dB frequency we wish to keep below 5 Hz so as not to introduce significant frequency response roll-off at 20 Hz. Here a 2 µF capacitor provides a lower 3-dB frequency of 4 Hz. This capacitor should be of very high quality, and performance would be even better if it were 5 µF. However, there is a cost and size issue here. Later we will see that some other trade-offs can be made.

Feedback AC Decoupling Network

The core amplifiers illustrated thus far have been DC coupled. They have the same gain of 20 at DC as AC signals. This means that any offset at the input of the amplifier will be amplified 20 times. In the case where there is an input R_{bias} whose voltage drop is not fully compensated, that voltage will be amplified by a factor of 20. A 10-mV offset will become a 200-mV offset at the output, for example. This is excessive. For this reason capacitor C_{fb} is placed in series with feedback network resistor R2. This causes the gain of the amplifier to become unity at DC, greatly reducing the creation of output offset voltage.

Of course, C_{fb} in combination with R2 forms a high-pass filter that will decrease amplifier gain at low frequencies. Once again, we desire that the 3-dB frequency of this filter be at a very low frequency of 5 Hz or less. Because C_{fb} is working against a smaller resistor, it will have to be a significantly larger value than was used for C_c. Because R2 at 1 kΩ is 19 times smaller than R_{bias} at 19 kΩ, the value of C_{fb} will have to be 19 times as large to achieve comparable performance. This comes out to 38 µF. In practice, a 100-µF nonpolarized electrolytic capacitor would typically be used for C_{fb}. Once again, capacitor quality comes into play with few easy solutions here. The quality of this capacitor is every bit as important as that of coupling capacitor C_c. We will later see some discussion of alternatives to the use of this capacitor in Chapter 8 where DC servos are discussed.

Output Network

Most solid-state power amplifiers include an output network to keep them from becoming unstable under unusual load conditions. The emitter follower output stage itself can sometimes become unstable at high frequencies under a no-load condition. This problem is avoided by inclusion of the shunt *Zobel* network consisting of R_z and C_z. This network assures that at very high frequencies the output stage is never loaded by less than the load provided by R_z. Typical values for R_z and C_z are 10 Ω and 0.05 µF, respectively.

Capacitive loads can destabilize an emitter follower stage. For this reason, most amplifiers incorporate a parallel R-L isolating network in series with the output of the amplifier. At very high frequencies the impedance of the inductor becomes large; this leaves the series resistance of the resistor to isolate any load capacitance from the emitter follower output stage. Typical values of L_i and R_i might be 2 µH and 2 Ω, respectively. The series output impedance of this network reduces damping factor at high frequencies and can cause a reduction in high-frequency response. The impedance of a 2-µH inductor at 20 kHz is about 0.25 Ω. This corresponds to a damping factor of 32 even if the output impedance of the amplifier proper is zero. When a 4-Ω load is being driven, this will cause a frequency response droop at 20 kHz of about 0.06 dB. Much more will be said about these output networks in a later chapter.

Power Supply Decoupling

A single pair of positive and negative power supply rails has been used to power all of the circuits in the amplifiers that have been described. This was done for simplicity. In a practical amplifier the IPS and VAS circuits will usually have an R-C filter inserted in the power supply rail to filter their supply. This provides them with a much cleaner power supply rail than the high-current portion of the rail that supplies the output stage. The high-current portion of the rail usually has considerable ripple and noise on it.

3.12   Summary

We've seen how the basic power amplifier topology can be evolved with straightforward steps into a design with fairly high performance. The main purpose of this chapter has been to show the thinking that goes into such an evolution. Although the result achieved here is quite good, this is just the beginning of high-performance design. There are many more nuances and topologies to be considered in the following chapters. Other approaches include JFET input stages, complementary push-pull VAS designs, MOSFET output stages, and many more variations and improvements. Moreover, the designs evolved here did not address many real-world issues like protection circuits, power supplies, and many other such matters.

References

1. L.W. Nagel and D.O. Pederson, "Simulation program with Integrated Circuit Emphasis," *Proc. Sixteenth Midwest Symposium on Circuit Theory*, Waterloo, Canada, April 12, 1973; available as Memorandum No. ERL-M382, Electronics Research Laboratory, University of California, Berkeley.
2. LTspice™, developed and distributed by Linear Technology Corporation. See www .linear.com.

3. Otala, M., "Conversion of Amplitude Nonlinearities to Phase Nonlinearities in Feedback Audio Amplifiers," *Proceedings of IEEE International Conference on Acoustics, Speech and Signal Processing,* pp. 498–499, Denver, CO, 1980.

4. Cordell, R. R., "Phase Intermodulation Distortion–Instrumentation and Measurements," *Journal of the Audio Engineering Society*, vol. 31, March 1983.

5. Otala, M, "Transient Distortion in Transistorized Audio Power Amplifiers," *IEEE Transactions on Audio and Electro-acoustics*, vol. AU-18, pp. 234–239, September, 1970.

6. Cordell, R. R., "Another View of TIM," *Audio,* February & March, 1980.

7. Locanthi, B., "Operational Amplifier Circuit for Hi-Fi," *Electronics World,* pp. 39–41, January 1967.

8. Locanthi, B., "An Ultra-low Distortion Direct-current Amplifier," *Journal of the Audio Engineering Society*, vol. 15, no. 3, pp. 290–294, July 1967.

9. Oliver, B.M., "Distortion in Complementary Pair Class B Amplifiers," *Hewlett Packard Journal*, pp. 11–16, February 1971.

Negative Feedback, Compensation, and Slew Rate

In Chapters 1 and 3 the basic concepts of negative feedback were discussed briefly so that the basic amplifier design concepts could be understood. Negative feedback is fundamental to the vast majority of audio power amplifiers and its optimal use requires more understanding. Much of that will be provided in this chapter.

4.1 How Negative Feedback Works

Negative feedback was invented in 1927 by Harold Black to reduce distortions and better control gain and frequency response in telephone amplifiers [1]. Figure 4.1 shows a simplified block diagram of a negative feedback amplifier. The basic amplifier has a forward gain A_{ol}. This is called the *open-loop gain* because it is the gain that the overall amplifier would have from input to output if there were no negative feedback.

A portion of the output is fed back to the input with a negative polarity. The fraction governing how much of the output is fed back is referred to as *beta* (β). The negative feedback *loop gain* is the product of A_{ol} and β. The overall gain of the closed-loop amplifier is called the *closed-loop gain* and is designated as A_{cl}. The action of the negative feedback opposes the input signal and makes the closed-loop gain smaller than the open-loop gain, often by a large factor.

The output of the subtractor at the input of the amplifier is called the *error signal*. It is the difference between the input signal v_{in} and the divided-down replica of the output signal. The error signal, when multiplied by the open-loop gain of the amplifier, becomes the output signal. As the gain A_{ol} becomes large, it can be seen that the error signal will necessarily become small, meaning that the output signal will become close to the value $v_{in}/β$. If A_{ol} is very large and β is 0.05, it is easy to see that the closed-loop gain A_{cl} will approach 20. The important thing to notice here is that the closed-loop gain in this case has been determined by β and not by the open-loop gain A_{ol}. Since β is usually set by passive components like resistors, the closed-loop gain has been stabilized by the use of negative feedback. Because distortion can often be viewed as a signal-dependent variation in amplifier gain, it can be seen that the application of negative feedback also reduces distortion.
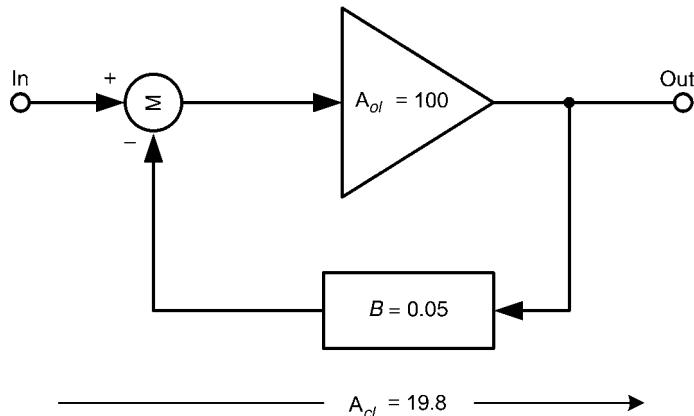
FIGURE 4.1   Block diagram of a negative feedback amplifier.

The closed-loop gain for finite values of open-loop gain is shown in Eq. 4.1. As an example, if A_{ol} is 100 and β is 0.05, then the product $A_{ol}\beta = 5$ and the closed-loop gain (A_{cl}) will be equal to $100/(1 + 5) = 100/6 = 16.7$. This is slightly less than the closed loop gain of 20 that would result for an infinite value of A_{ol}. If A_{ol} were 2000, A_{cl} would be $2000/(1 + 100) = 2000/101 = 19.8$. Here we see that if $A_{ol}\beta = 100$, the error in gain from the ideal value is about 1%. The product $A_{ol}\beta$ is called the *loop gain* because it is the gain around the feedback loop. The net gain around the feedback loop is a negative number when the negative sign at the input subtractor is taken into account.

$$A_{cl} = A_{ol}/(1 + A_{ol}\, \beta) \tag{4.1}$$

Notice that if the sign of $A_{ol}\beta$ is negative for some reason, the closed-loop gain will become greater than the open-loop gain. The closed-loop gain will ultimately go to infinity, and oscillation will result if the product $A_{ol}\beta$ reaches –1. The potential for positive feedback effects is of central importance to feedback compensation and stability.

Negative feedback is said to have a phase of 180 degrees, corresponding to a net inversion as the signal circles the loop. Positive feedback has a phase of 0 degrees, which is the same as 360 degrees.

4.2   Input-Referred Feedback Analysis

A useful way to look at the action of negative feedback is to view the circuit from the input, essentially answering the question, " What input is required to produce a given output?" Viewing negative feedback this way essentially breaks the loop. We will find later that viewing distortion in an *input-referred* way can also be helpful and lend insight.

In the example above with $A_{ol} = 100$ and $\beta = 0.05$, assume that there is 1.0 V at the output of the amplifier. The amount of signal fed back will be 0.05 V. The error signal driving the forward gain path will need to be 0.01 V to drive the forward amplifier. An additional 0.05 V must be supplied by the input signal to overcome the voltage being fed back. The input must therefore be 0.06 V. This corresponds to a gain of 16.7 as calculated above in Eq. 4.1.

Suppose that $\beta = -0.009$. This corresponds to positive feedback, which reinforces the input signal in driving the forward amplifier. With an output of 1.0 V, the feedback would be -0.009 V. The drive required for the forward amplifier to produce 1.0 V is only 0.01 V, of which 0.009 V will be supplied by the positive feedback. The required input is then only 0.001 V. The closed-loop gain has been enhanced to 1000 by the presence of the positive feedback. If β were -0.01, the product $A_{ol}\beta$ would be -1 and the denominator in Eq. 4.1 would go to 0, implying infinite gain and oscillation.

4.3   Feedback Compensation and Stability

Negative feedback must remain negative in order to do its job. Indeed, if for some reason the feedback produced by the loop becomes positive, instability or oscillation may result. As we have seen above, simple negative feedback relies on a 180-degree phase inversion located somewhere in the loop. High-frequency *roll-off* within the loop can add additional lagging phase shift that will cause the loop phase to be larger than 180 degrees. These excess phase shifts are usually frequency dependent.

At the 3-dB frequency f_p of a pole, the additional lagging phase shift is 45 degrees. At very high frequencies a pole will contribute 90 degrees of phase shift. If a system has multiple poles this added phase shift may reach 180 degrees at some high frequency. The total phase shift around the loop will then equal 360 degrees, and there will be positive feedback. If the gain around the loop at this frequency is still greater than unity, oscillation will occur.

Poles and Zeros

The concepts of *poles* and *zeros* are fairly simple, and yet central to the understanding of feedback compensation. Ordinary circuits that create high-frequency and low-frequency roll-offs contain poles and zeros, respectively (or some combination of them). Poles introduce lagging phase shift (negative), and zeros introduce leading phase shift (positive).

Figure 4.2 illustrates three simple circuits. The first one implements a simple pole, with a 3-dB roll-off at the pole frequency $f_p = 1/2\pi R1C1$. This is just a simple first-order
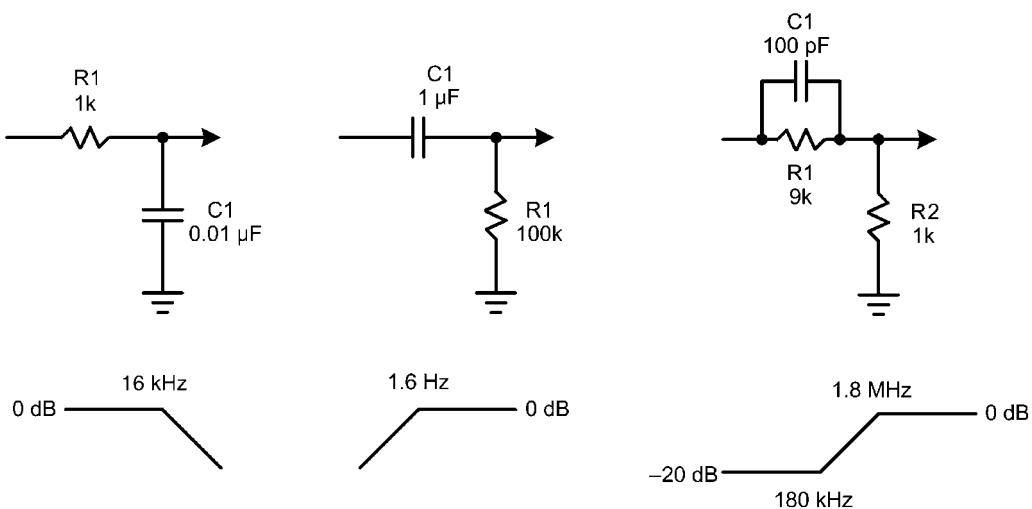
Figure 4.2   R-C circuits implementing poles and zeros.

low-pass filter. The second circuit implements a zero at $f_z = 0$ Hz, causing the gain to rise as frequency increases, resulting in a high-pass filter. The gain can't get any larger than unity, so there is a pole to level off the frequency response at the frequency $f_p = 1/2\pi R1C1$.

The third circuit implements a *pole-zero pair,* with a resulting frequency response that begins at a lower value and increases to unity at higher frequencies. In this case the zero is not at 0 Hz, but rather at a finite frequency $f_z = 1/2\pi R1C1$. Once again, the gain cannot get any larger than unity, so there is a pole at a higher frequency $f_p = 1/2\pi R_p C1$, where R_p is the resistance of the parallel combination of R1 and R2.

Figure 4.2 also shows *Bode plots* of the three circuits. The first circuit forms a low-pass filter. Its frequency response falls at frequencies above the pole frequency f_p at a rate of 6 dB per octave or 20 dB per decade. The phase lag (negative values of phase) increases to –45 degrees at the pole frequency and eventually increases to 90 degrees at high frequencies.

The second circuit forms a high-pass filter. Its frequency response is unity at high frequencies and falls to –3 dB at the frequency of the pole. At this frequency the phase shift is leading at +45 degrees. As frequency goes lower, its response falls off at 6 dB per octave and the phase lead eventually increases to +90 degrees.

The third circuit has a rising slope in frequency response beginning at f_z and continuing until f_p. Its gain is equal to $R2/(R1 + R2)$ at low frequencies and rises to unity at high frequencies. This circuit creates a leading phase shift that is at its maximum at the geometric mean of the pole and zero frequencies. At very high and very low frequencies its phase shift approaches to 0 degrees.

Figure 4.3 shows the actual gain and phase for a pole at normalized frequencies f/f_p extending far away from the pole. This can be very useful in estimating the impact of multiple additional poles. It illustrates the way that the phase contribution of a pole asymptotes to –90 degrees at frequencies far above the pole, while the attenuation from the pole continues to increase. The phase lag for a pole is about 23 degrees from its asymptotic value one octave on either side of the pole frequency.

Phase and Gain Margin

If the accumulation of lagging phase shift causes negative feedback to become positive feedback at some frequencies, instability can result. The nominal phase shift around a simple negative feedback loop is 180 degrees as a result of the inversion. Additional
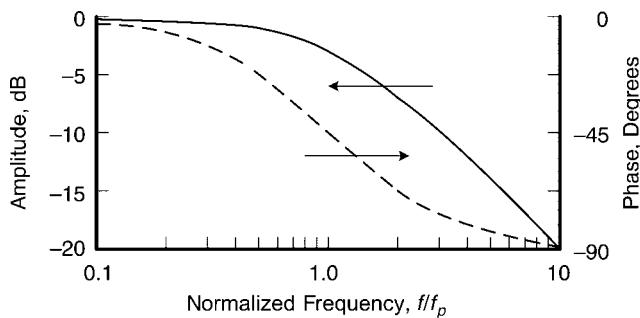
FIGURE 4.3 Gain and phase for a pole at frequencies far from the pole frequency.

lagging phase shift will be introduced by high-frequency roll-offs created by feedback compensation networks and unwanted poles in the circuit. If the total phase shift in the loop reaches 360 degrees at the point where the magnitude of the loop gain is unity, oscillation will result. Central to stability analysis in the frequency domain are the concepts of *phase margin* and *gain margin*. They describe how much margin a circuit has against instability.

The concept of phase margin describes how close we are to 360 degrees of phase shift at the point in frequency where the loop gain has fallen to unity. This frequency is often referred to as the gain crossover frequency f_c. If the phase shift accumulates to a value greater than 360 degrees at a higher frequency than this where there is less than unity gain, oscillation will not result.

Gain margin refers to how much margin we have against the gain becoming unity at a frequency where the loop phase shift has accumulated to a total of 360 degrees. This is of particular concern because component tolerances can cause a nominal design to have higher gain under some conditions.

Figure 4.4 illustrates the concepts of phase margin and gain margin. The Y axis on the left is loop gain in dB. The Y axis on the right is lagging phase shift in the product $A_{ol}\beta$. When this lagging phase reaches 180 degrees, oscillation may result. The X axis is frequency.

The amplifier has a gain crossover frequency of 1 MHz. This is where the loop gain has fallen to 0 dB. Loop gain rises 6 dB per octave as frequency is reduced, reaching about 40 dB at 10 kHz. Lagging phase shift at low frequencies is 90 degrees. Two poles in the open-loop response are located at 2 MHz. Each contributes 22.5 degrees at 1 MHz, so total lagging phase shift at 1 MHz is 135 degrees. This corresponds to a phase margin of 45 degrees. Loop gain is down to –10 dB at 2 MHz where loop phase shift is 180 degrees. Gain margin is thus 10 dB.

Stability against oscillation is not the only reason why adequate phase and gain margin is needed. Amplifiers with inadequate phase or gain margin usually have poor transient response and undesirable peaking in their frequency response.
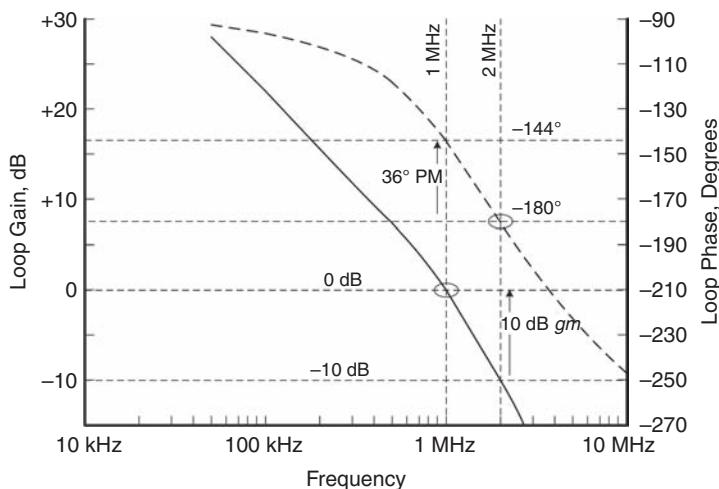
FIGURE 4.4   Plot showing phase margin and gain margin.

Gain and Phase Variation

Component tolerances are not the only contributors to gain and phase variation. Changes in the operating points of active elements like transistors can cause gain and phase changes. One example is the change in collector-base capacitance of a transistor with signal voltage. Another example is change in transistor speed with operating current. Changes in the impedance of the load connected to the amplifier can also affect loop gain and phase.

4.4   Feedback Compensation Principles

The simplest way to compensate a negative feedback loop is to roll-off the loop gain at a frequency low enough that the lagging phase shift accumulated in the loop is well less than 180 degrees at the frequency where loop gain has fallen below unity. This approach recognizes that as frequency increases in a real amplifier, more extraneous poles come into play to create extra lagging phase shift.

Dominant Pole Compensation

Dominant pole compensation is the basis for most compensation approaches. The strategy is to reduce loop gain with frequency while accumulating as little lagging phase beyond 90 degrees as possible. The key to achieving this is that a single pole continues to attenuate with frequency while its contribution to lagging phase shift is limited to 90 degrees. For this reason a feedback circuit with a single pole in its loop can never become unstable.

In real circuits there will be many poles, but if the roll-off behavior is strongly dominated by a single pole, the stability criteria will be more straightforward to meet. The effects of all other poles can then be lumped together as so-called excess phase. In this case, at the frequency where the gain around the loop has fallen to 0 dB, the phase lag of the dominant pole will be 90 degrees. This means that there is an additional 90 degrees to play with before hitting instability. You might allocate 40 degrees for excess phase from all other sources and keep the remaining 50 degrees in your pocket as phase margin. You then choose the maximum gain crossover frequency f_c as the frequency where the total amount of excess phase does not exceed 40 degrees.

Excess Phase

Excess phase is usually thought of as additional lagging phase shift that would not have been expected based on the amount of high-frequency amplitude roll-off. A pure delay is a very good example of excess phase. If a signal runs through 10 ft of coaxial cable, it will encounter very little loss, but it will experience a time delay due to the speed of light in the cable. This will be on the order of 1.5 ns per foot. At 67 MHz, this would correspond to about 36 degrees of phase lag.

More often, excess phase is not truly time delay, but rather the accumulation of phase shift from many high-frequency poles, sometimes called *parasitic poles*. Even together, these poles may not create much attenuation, but the amount of phase shift they create can accumulate to an amount sufficient to reduce phase margin in a negative feedback circuit. Excess phase in the amplifier output stage is an important contributor. It results from multiple far-out poles due in part to base resistance and AC β roll-off of the driver and output transistors. Output stage excess phase can vary significantly with load and current/voltage conditions.

Excess phase can also originate at the feedback input to the LTP input stage. The resistance of the feedback network can form a pole against the input capacitance of the LTP. This input capacitance can be a combination of base-emitter capacitance due to finite f_T and the base-collector capacitance of the transistor. This latter capacitance can be multiplied by the Miller effect if the input stage has voltage gain to its collector.

Lag Compensation

Lag compensation is perhaps the simplest form of frequency compensation, but is sometimes not the best. It simply involves the introduction of a low-frequency pole by placing a shunt capacitor from the output of the VAS to ground. Unfortunately, there is also a pole in the base circuit of the VAS at a low enough frequency to add a large amount of excess phase. This will often force you to set the gain crossover frequency fairly low. You may have two poles running together over a significant frequency range before the loop gain falls to 0 dB.

The pole at the base of the VAS can be canceled by introducing a zero into the lag compensation circuit at the same frequency. This simply involves adding a resistor in series with the lag compensation shunt capacitor, forming a pole-zero pair. Figure 4.5 illustrates an amplifier with lag compensation where the pole at the base of the VAS has been canceled by a zero in the lag compensation network at the VAS collector. The gain crossover frequency f_c for this amplifier is set at 500 kHz. Capacitor C1 has been added to create a stable pole at 500 kHz at the base of Q3. Lag compensation capacitor C2 has
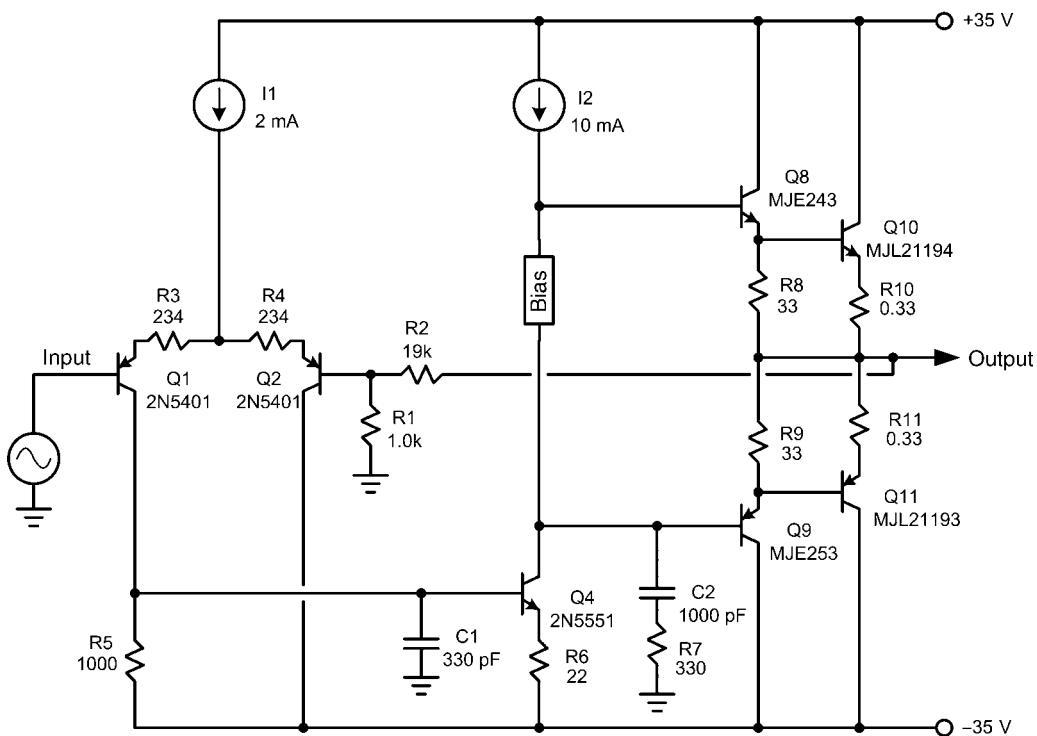
FIGURE 4.5   An amplifier where lag compensation is employed.

been set to establish f_c at 500 kHz. R7 is put in series with C2 to create a zero at 500 kHz. In this amplifier the pole-zero compensation has been set at the same frequency as f_c, but this will not always be the case.

The use of lag compensation can reduce the amount of slew rate that might be otherwise available in the amplifier, all else remaining equal. The slew rate of this amplifier is about 10 V/μs in the positive direction, established by I2 and C2. It is much higher in the negative direction.

Miller Compensation

Miller compensation uses local feedback to roll-off the high-frequency response of the amplifier. The gain that is "thrown away" acts to linearize the VAS with shunt feedback. The same amplifier as in Figure 4.5 is shown with Miller compensation in Figure 4.6. Capacitor C1 is the so-called Miller compensation capacitor C_M. It stabilizes the global negative feedback loop by rolling off the high-frequency gain of the amplifier so that the gain around the feedback loop falls below unity before enough phase lag builds up to cause instability. At high frequencies the combined gain of the input stage and the VAS is equal to the product of the transconductance of the IPS and the impedance of C1. At high frequencies the gain is dominated by C1 rather than by R5 and/or R6. Since the impedance of C1 is inversely related to frequency, the gain set by it will decrease at 6 dB per octave as frequency increases. The transconductance *gm* is just the inverse of the total LTP emitter resistance R_{LTP}.
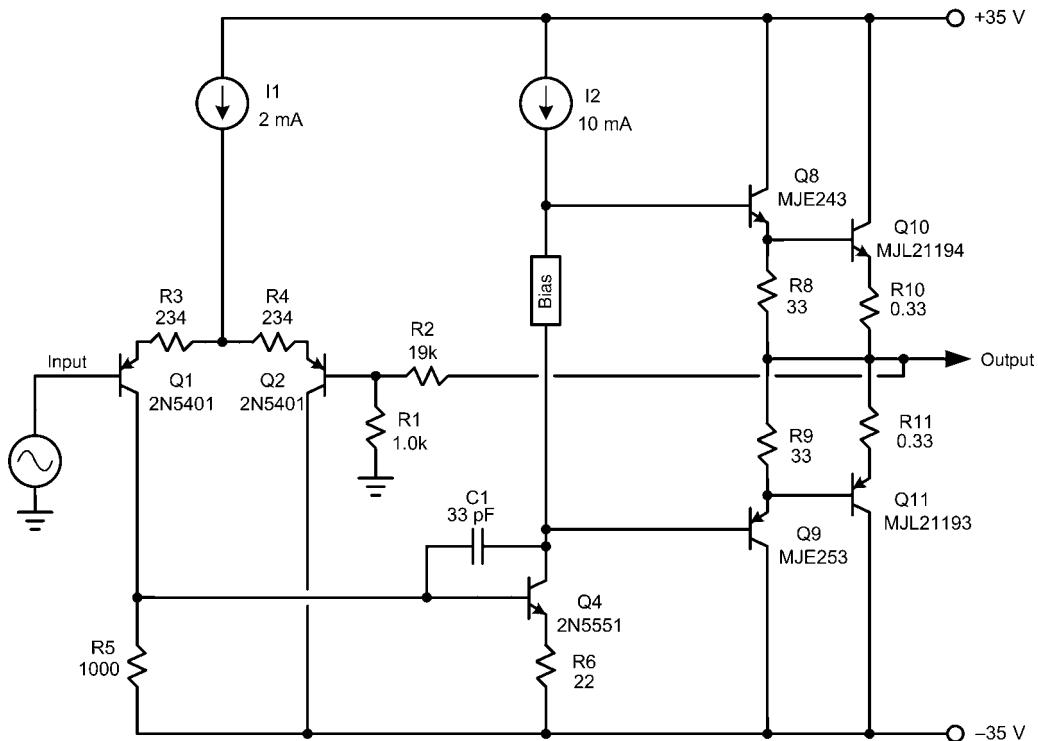
FIGURE 4.6 A Miller-compensated amplifier.

The capacitor controls the high-frequency AC gain of the VAS by forming a shunt feedback loop around the VAS transistor. At higher frequencies, virtually all of the signal current from the LTP input stage flows through C1. This creates a voltage drop across C1 that equates to the output voltage of the VAS. At this point the VAS is acting like a so-called *Miller integrator*, where the output voltage is the integral of the input current.

While at low frequencies the gain of the combined input stage and VAS is set by the product of the individual voltage gains of those two stages, at higher frequencies that combined gain is set by the ratio of the impedance of C1 to R_{LTP}. The frequency at which the gain set by R_{LTP} and C1 becomes smaller than the DC gain is where the roll-off of the amplifier's open-loop frequency response begins. R_{LTP} for this design is about 480 Ω.

Assume for the moment an operating frequency of 20 kHz. At this frequency the reactance of C1 is $1/(2\pi * 20 \text{ kHz} * 33 \text{ pF}) = 24{,}000$ Ω. If all of the signal current provided by the LTP passes through the capacitor, then the gain of the combined input and VAS stage at this frequency is $24{,}000/480 = 500$. This is considerably less than the low-frequency forward gain of the amplifier. This means that the capacitor is dominating the gain at this frequency. Falling at 6 dB per octave, A_{ol} will become 26 dB at 500 kHz. Since A_{cl} is also 26 dB, the gain crossover frequency occurs at 500 kHz.

The peak signal current that the LTP can deliver to C1 is about 1 mA in either direction. This puts the amplifier slew rate at a symmetrical 30 V/μs, superior to the amplifier with lag compensation.

An optional resistor can be placed in series with C1 to create a zero that can be used to cancel a pole elsewhere in the circuit or cancel some excess phase. A 2.4-kΩ resistor placed in series with C1 will create a zero at 2 MHz, two octaves above the gain crossover frequency.

4.5   Evaluating Loop Gain

In order to meet the stability target, the gain around the feedback loop must be estimated. There are a number of ways to do this, both in simulation and with laboratory measurements.

Breaking the Loop

The most obvious way to estimate or evaluate the loop gain is to break the loop. A stimulus signal is applied at the input side of the loop. The frequency and phase response is then measured at the output side of the loop. Means must be used to maintain proper biasing and DC levels in the amplifier when this is done. This is not always practical in the real world where very large amounts of gain may be involved.

There is also a caveat: The loading of the output side of the break will often not be identical after the loop is broken, and this will cause some error. If the source on the output side of the break is of very low impedance compared to the load seen looking into the input side of the break, the error will be quite small. This will often be the case in a power amplifier where the loop is broken at the input to the feedback network.

In SPICE simulations the loop can be kept closed at DC by connecting an extremely large inductor across the break. It is possible to employ a 1 GH inductor. The source signal is then applied to the feedback network through an AC coupling capacitor. The low-frequency corner of this coupling capacitor against the input resistance of the feedback network will determine how low in frequency the results of this method will be accurate. The loop gain is then inferred by viewing the signal at the output of the amplifier. This is illustrated in Figure 4.7.
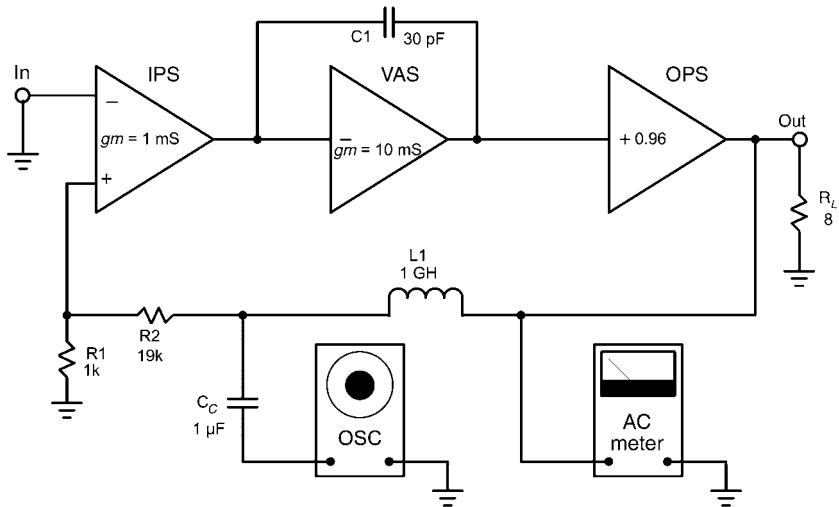
FIGURE 4.7   Breaking the loop with a large inductor.

In the laboratory, the loop can be kept closed at DC by connecting a noninverting auxiliary DC servo circuit from the output of the amplifier to the feedback input of the IPS (see Chapter 8 on DC servos). The low-level test signal from the signal generator can then be applied to the input of the feedback network. This technique is illustrated in Figure 4.8. Caution should be observed here in light of the very high
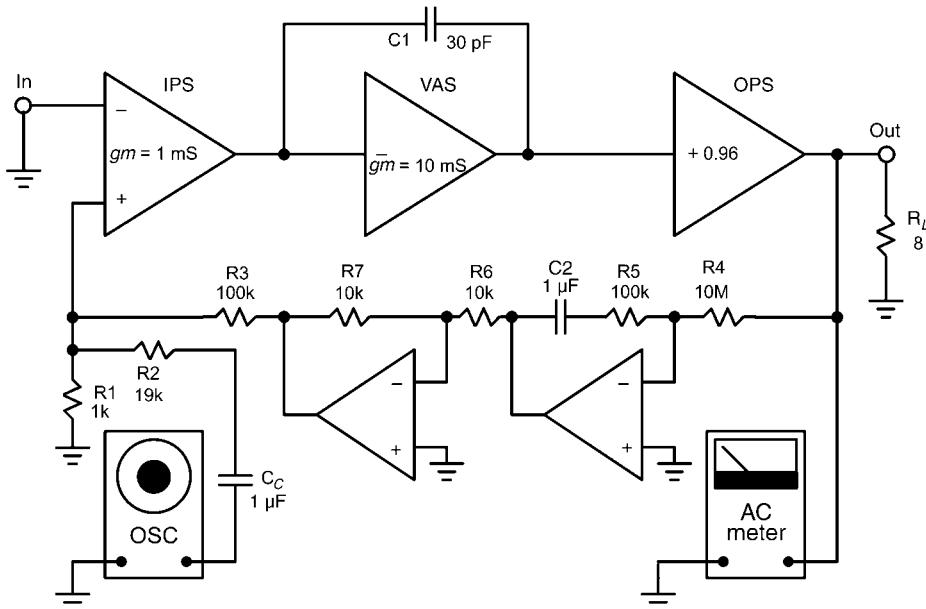
FIGURE 4.8   Breaking the loop using a servo for DC loop closure.

gain that may be encountered from the signal generator to the output of the amplifier. The accuracy of measurement is limited at low frequencies by the feedback through the DC servo. For example, in this arrangement, it will limit open-loop gain readings to about 76 dB at 10 Hz. R5 places a zero in the integrator at 16 Hz to prevent low-frequency instability in the event that the open-loop bandwidth of the amplifier is less than about 10 Hz.

Exposing Open-Loop Gain

Exposing the forward gain A_{ol} by setting closed-loop gain very high is an accurate way to estimate the high-frequency open-loop gain roll-off and phase shift. The forward gain is *exposed* by increasing the closed-loop gain by a factor of 100. This decreases the loop gain by a sufficient amount over the frequency range of interest that feedback effects do not affect the gain from input to output at these frequencies. The technique will not be accurate at low frequencies where the open-loop gain would be greater than 100 times the nominal closed-loop gain. This approach will not take into account the gain and phase characteristics of the feedback network. This includes the pole at the input of the IPS and any lead compensation.

Simulation

SPICE simulation of the power amplifier can be very valuable in assessing loop gain and stability because internal nodes can be viewed, impractical component values can be used, and functions of probed voltages and currents can be calculated and plotted, such as the ratio of amplifier output voltage to forward path input error voltage. Time domain performance can also be evaluated with transient simulations to observe square-wave behavior, for example.

4.6 Evaluating Stability

One of the most important aspects of feedback amplifier design is assessing its stability. Although it is true that one can design for stability, it still must be assessed in simulation and/or in the actual prototype circuit. Obviously, what can be seen and evaluated is different in simulation than in the real circuit. Each has advantages where the other may be a bit blind. A proper assessment of stability in the real world using the real circuit is a must, but for those who can simulate, it is also desirable and beneficial to assess stability in simulation.

Feedback stability can often be inferred from viewing the closed-loop frequency response and looking for peaking. It is especially important in these tests to bypass any input low-pass filters in the amplifier. Peaking of the closed-loop response by more than about 1 dB just prior to final roll-off is a danger sign. However, apparent flatness of the closed-loop frequency response is not always sufficient evidence of adequate stability. Transient response must always be checked as well; this is best done with a transient simulation using a square-wave source.

Instability can be either local or in the global feedback loop. Local instability can originate from a local feedback loop or from local circuit instability such as an emitter follower driving a capacitive load. Such local instabilities can often occur in output stages.
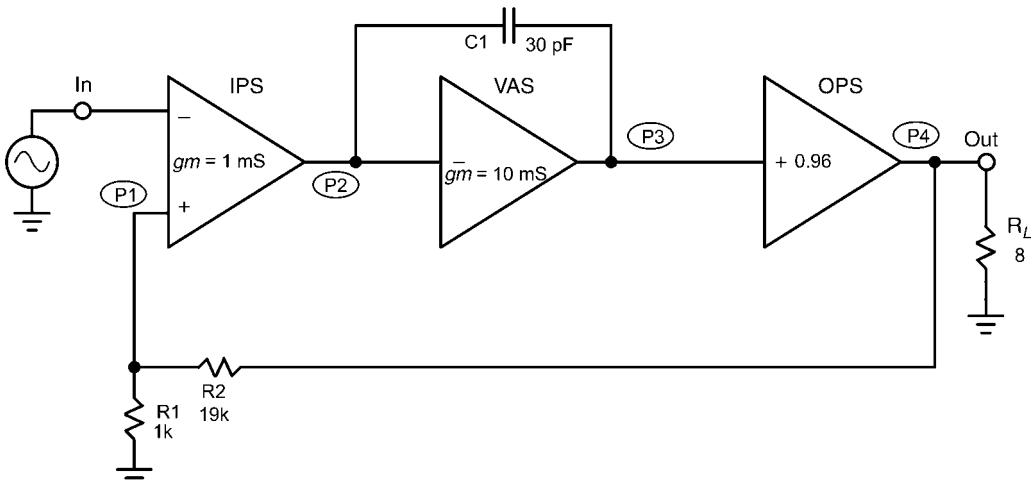
Probing points for stability evaluation.

Probing Internal Nodes in Simulation

In assessing stability with AC simulations, it is important to look for evidence of peaking (or sometimes sharp dips) at nodes internal to the circuit. Figure 4.9 shows a block diagram of a simplified power amplifier with some suggested probing points. The feedback input P1 of the IPS should represent a unity-gain follower amplifier stage with respect to the amplifier input signal. Probe this point and look for overshoot, ringing, and peaking. This may show behavior that is masked at the output of the amplifier by high-frequency roll-offs. If this is done in a real amplifier, the IPS feedback input should be probed with a high-impedance low-capacitance probe. This test should be done with no amplifier input filters in place.

Stability of local loops can be assessed with an AC simulation in a relatively noninvasive way by injecting an AC current at a chosen node and observing the resulting signal voltage. This procedure reveals the impedance of the node as a function of frequency. At frequencies where there is instability, the impedance will rise markedly. In simulation, the current injection is often conveniently carried out with a voltage source in series with a 10-MΩ resistor. The probing locations shown in Figure 4.9 are examples of where this technique can be applied in simulation. If the stability probe is placed at the input node P2 of a Miller-compensated VAS, the results may uncover a local instability. The same can be said for probing at P3. Such local oscillations can be in the 20- to 200-MHz range, and can easily be overlooked.

Figure 4.10 is a plot of square-wave overshoot (left) and frequency response peaking (right) as a function of phase margin on the X axis from 90 degrees down to 0 degrees. This data was obtained by simulating an amplifier with a dominant pole and four parasitic poles at a high frequency above the gain crossover frequency. As the frequency of the parasitic poles was reduced, the phase margin, square-wave overshoot and frequency response peaking were recorded and plotted. These numbers will not be accurate for all amplifier designs and roll-off profiles, but are helpfully representative.
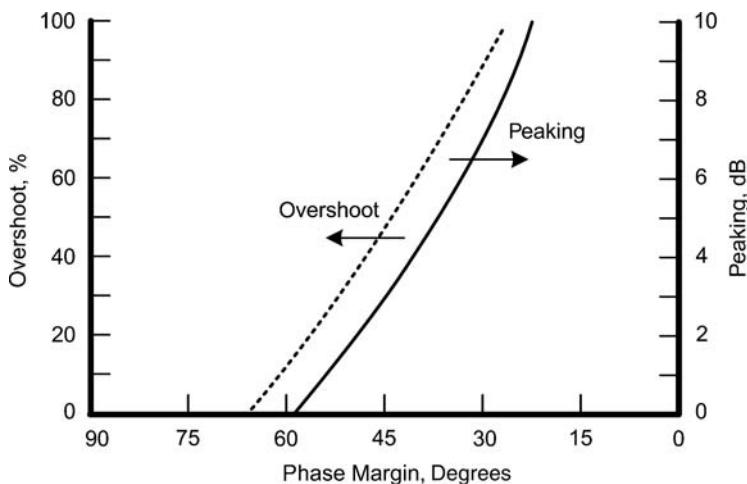
FIGURE 4.10 (a) Square-wave overshoot. (b) Frequency response peaking as a function of phase margin.

Checking Gain Margin

Power amplifiers should have at least 6 dB of gain margin. Gain margin can be checked by reducing the closed-loop gain by 6 dB. In a power amplifier with a gain of 20, this would mean reducing the feedback resistor to change the gain to 10. If the amplifier has adequate gain margin, it should still be stable under these conditions.

Checking Phase Margin

Power amplifiers should have at least 45 degrees of phase margin. Phase margin adequacy can be checked by adding a pole in the feedback loop at the estimated gain crossover frequency f_c. This pole will add 45 degrees of lagging phase shift to the loop. It will also introduce 3 dB of loss in loop gain, which must be made up by decreasing closed-loop gain by 3 dB. If the amplifier has adequate phase margin, it should still be stable under these conditions. The pole can be added with a low-impedance lag network placed between the amplifier output and the feedback resistor. A 100-Ω series resistor and a 3300-pF shunt capacitor will create a pole at about 500 kHz.

Recommendations

For stability in general (both local and global), do not trust only one type of stability assessment, especially in the simulation world where multiple approaches are practical and can be tried without great effort. At the breadboard level, don't assume that there is adequate stability just because the circuit does not oscillate. Carefully evaluate frequency response and square-wave response.

Operate the circuit with lighter compensation to assess margin against instability. This can be accomplished by reducing the value of the Miller compensation capacitor by perhaps a factor of 2. Operate the circuit under large-signal conditions, recognizing that transistor parameters change with operating point and that instability at operating points other than quiescent can appear. Operate power amplifiers into difficult and diverse loads to see if instability can be provoked.

4.7   Compensation Loop Stability

The loop formed by the Miller compensation capacitor is itself a feedback loop and must also obey the rules for stability. This is often a very tight, wideband loop and will not need compensation for stability. Connecting the Miller capacitor from the collector to the base of a simple one-transistor VAS is a good example. If more complexity is added to the compensation loop, stability of this loop may have to be evaluated carefully. For example, the use of a cascoded Darlington VAS places three transistors in the compensation loop, all capable of contributing to excess phase (see the amplifier in Figure 3.12). If the Miller capacitor is connected to the output of a predriver emitter follower instead of to the VAS collector node, a further opportunity for instability is introduced. This will be touched on again in Chapter 9 where more complex compensation approaches are discussed.

Figure 4.11 illustrates an amplifier segment where all of these additions to a feedback compensation loop have been made. These latter arrangements make the feedback compensation loop less "local" and in some cases can make it less stable by allowing the introduction of excess phase shift by the added stages. Notice also that the connection of C1 to the output of the predrivers leaves the VAS collector node as a high-impedance point, without even the benefit of loading normally provided by C1. This VAS is driven by an IPS loaded with a current mirror. Figure 4.12 shows the simulation result of a stability probe placed at the collector of the VAS in this circuit. The stability probe injected 1 µA RMS into the node through a 1-MΩ resistor and the voltage on the node was monitored. Notice the fairly large peak at about 90 MHz.
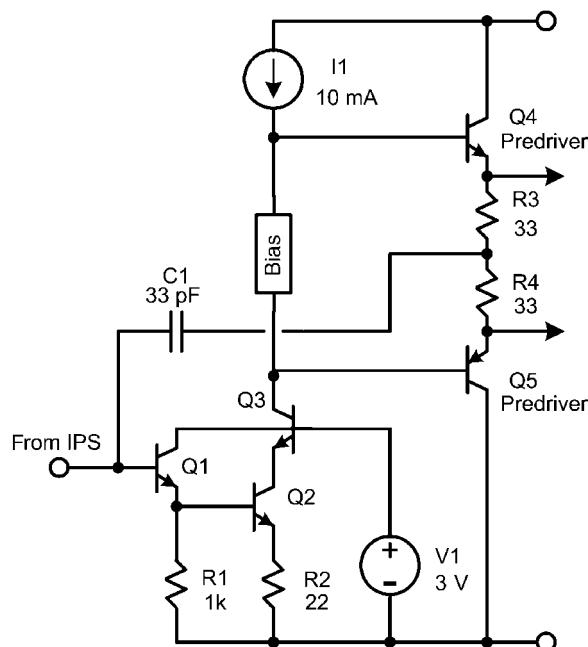
FIGURE 4.11   Example of a "longer" Miller compensation loop.
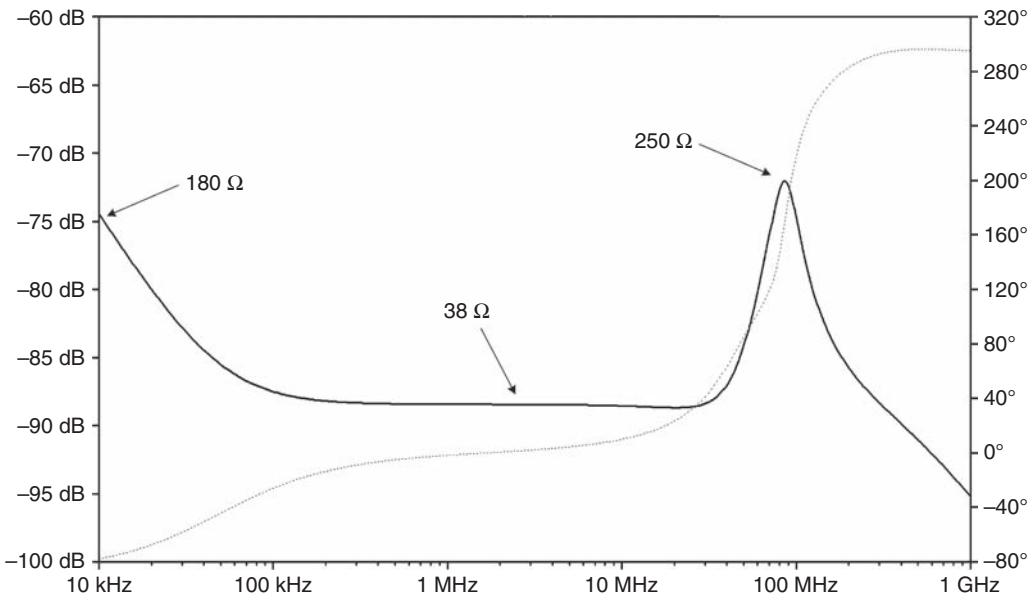
FIGURE 4.12   Stability probe result at the collector of the VAS.

4.8   Slew Rate

The maximum rate of voltage change that an amplifier can achieve is usually referred to as the *slew rate*. It is often expressed in volts per microsecond. Slew rate in an amplifier is usually limited by the ability of a particular circuit to charge a capacitance at a given rate. Indeed, for a circuit that can supply a current I_{max} to a node with capacitance C on it, the slew rate is simply I_{max}/C. If a maximum current of 1 mA is available for charging 100 pF, the slew rate will be limited to 10 V/μs.

We saw in Chapter 3 that negative feedback compensation can place a limitation on slew rate. It is important to point out that negative feedback compensation is not the only thing that limits slew rate, but in many cases it is the first one to come into play.

Figure 4.13 shows an amplifier with traditional Miller feedback compensation. The values shown are similar to those in the simple amplifier depicted in Figure 4.6. Closed-loop gain is 20 and f_c = 500 kHz. Capacitor C_M forms a local feedback loop around the VAS that turns the VAS into an integrator. This means that the VAS will have a straight 6 dB per octave roll-off over a very large frequency range, from very low frequencies to frequencies above the gain crossover frequency. Once C_M is determined and we know the maximum peak signal current output of the input stage I_{max}, the slew rate is SR = I_{max}/C_M.

Calculating the Required Miller Capacitance

The required Miller compensation capacitance is calculated to yield the desired unity-gain crossover frequency f_c. This calculation depends on the transconductance of the
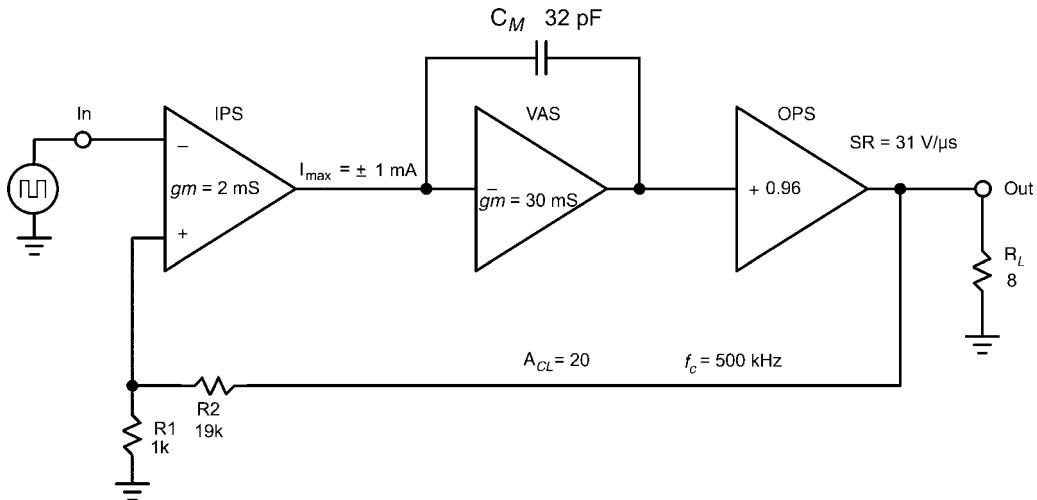
Figure 4.13 Traditional Miller feedback compensation.

input stage and the chosen closed-loop gain for the amplifier. C_M is chosen so that $A_{ol} = A_{cl}$ at f_c. If transconductance of the input stage is gm, then

$$A_{ol} = \frac{gm}{2\pi C_M f_c} \tag{4.2}$$

Setting $A_{ol} = A_{cl}$, we have

$$C_M = \frac{gm}{2\pi A_{cl} f_c} \tag{4.3}$$

For $gm = 2$ mS, $A_{cl} = 20$, and $f_c = 500$ kHz, we have $C_M = 32$ pF.

Slew Rate
The slew rate of the amplifier is simply SR = I_{max}/C_M. Substituting Eq. 4.3 for C_M and doing some rearrangement, we have

$$\text{SR} = 2\pi A_{cl} f_c \left(\frac{I_{max}}{gm} \right) \tag{4.4}$$

Notice that I_{max}/gm is a key parameter of the input stage that determines achievable slew rate. It has the units of volts. For Eq. 4.4, when $I_{max} = 1$ mA and $gm = 2$ mS, $I_{max}/gm = 0.52$ V. Interestingly, $gm = I_c/V_T$ for a BJT and $gm = I_{tail}/2V_T$ for an un-degenerated differential pair. We thus have $I_{max}/gm = V_T = 52$ mV for an un-degenerated differential pair.

The LTP of Figures 4.6 and 4.13 is degenerated by a factor of $R_{\mathrm{LTP}}/2re'$, or $F_{\mathrm{D}} = 2(220 + 26)/52 = 490\ \Omega/52\ \Omega = 9.46$. This means that the transconductance or gain is 9.46 times smaller than it would be without degeneration by emitter resistors. We have

$$F_{\mathrm{D}} = \frac{R_{\mathrm{LTP}}}{2re'} \tag{4.5}$$

$$\frac{I_{\mathrm{max}}}{gm} = 2V_{\mathrm{T}}F_{\mathrm{D}} \tag{4.6}$$

$$\mathrm{SR} = 4\pi\, A_{\mathrm{cl}} f_{\mathrm{c}} V_{\mathrm{T}} F_{\mathrm{D}} \tag{4.7}$$

Traditional Miller feedback compensation is suboptimal in regard to slew rate and high-frequency linearity. The reason for this is that Miller compensation establishes a fixed relationship among input stage transconductance, input stage tail current, closed-loop gain, closed-loop bandwidth, and slew rate. This relationship is such that, for a given closed-loop gain and closed-loop bandwidth, slew rate can only be increased by adding degeneration to the input stage. This corresponds to the degeneration factor F_{D} in Eq. 4.7. This explains why amplifiers with un-degenerated BJT LTPs have such poor slew rate. For these stages I_{max}/gm is only 52 mV. This number is typically 10 times larger for an un-degenerated JFET differential pair. This is why many designers do not degenerate JFET input stages. In Chapter 9 we'll discuss a compensation technique that breaks the relationships of Eqs. 4.4 and 4.7.

References

1. Black, Harold, U.S. patent 2,102,671, issued 1937.

This page intentionally left blank

Amplifier Classes, Output Stages, and Efficiency

The output stage of a power amplifier has perhaps the greatest influence on performance and cost. It is also challenged by its interface to the real world, where difficult loads, high voltages, and high currents may exist. The output stage must also operate at high power levels, often at elevated temperatures. Indeed, there is often a trade-off between heat generation and sound quality. The class A output stage is perhaps the best example of this.

This chapter serves as an overview and introduction to output stages. Detailed design and nuances will be covered in Chapter 10. BJT output stages will be discussed here, while MOSFET output stages will be discussed in Chapter 11. Many of the principles and technical challenges are the same for MOSFET power amplifiers.

Several important issues involving output stages and different topologies and classes will be discussed. This chapter will begin with a review of the popular class AB emitter follower (EF) output stage and the basics of crossover distortion. The latter will be discussed in much greater detail in Chapter 10. The Complementary Feedback Pair (CFP) output stage is an alternative to the EF output stage, and its merits and shortcomings will be considered. Output stage efficiency and power dissipation will be covered, as well as output stages that operate more efficiently.

5.1 Class A, AB, and B Operation

The output transistors in a push-pull class A power amplifier remain in conduction throughout the entire cycle of the audio signal, always contributing transconductance to the output stage signal path. In contrast, the output transistors in a class B design remain on for only one-half of the signal cycle. When the output stage is sourcing current to the load, the top transistor is on. When the output stage is sinking current from the load, the bottom transistor is on. There is thus an abrupt transition from the top transistor to the bottom transistor as the output current goes through zero.

The formal definition of classes A and B is in terms of the so-called conduction angle. The conduction angle for class A is 360 degrees (meaning all of the cycle), while that for class B is 180 degrees. More accurately, the definition should really be the angle over which the transistor contributes transconductance to the output stage and signal current to the output. This precludes many so-called nonswitching amplifiers from

being called class A. Such amplifiers include bias arrangements that prevent the power transistor from completely turning off when it otherwise would.

Most power amplifiers are designed to have some overlap of conduction between the top and bottom output transistors. This smooths out the crossover region as the output current goes through zero. For small output signal currents, the output transistors are in the overlap zone and the output stage effectively operates in class A. These amplifiers are called *class AB amplifiers* because they possess some of the characteristics and advantages of both class A amplifiers and class B amplifiers. Most push-pull vacuum tube amplifiers operate in class AB mode. Class AB output stages have a conduction angle that is greater than 180 degrees, although sometimes only slightly so.

There is some semantic controversy in the definition of class B and class AB output stages. This arises partly because transistors do not turn on and off abruptly, so the definition of 180-degree conduction is fuzzy. There is a grey region between class B and class AB. I view class B as an amplifier that is underbiased. I also say that a class AB output stage has transitioned into its class B region when it exits its class A region.

I will use the term *class AB* to describe the optimally biased output stage, as it has important historical origins in push-pull vacuum tube amplifiers. Optimally biased class AB output stages can have a very substantial quiescent current when multiple output pairs and low-value emitter resistors are used. They have a class A region that extends to double the value of the output stage quiescent bias current.

5.2   The Complementary Emitter Follower Output Stage

The complementary emitter follower is the workhorse for the majority of power amplifiers that employ BJT output stages. Figure 5.1 shows simplified views of the Darlington and *Triple* emitter follower (EF) output stages. In each case the bias spreader is split to show how it would be driven from a voltage source. In a real amplifier the bias spreader (usually a V_{be} multiplier) is driven from a pair of VAS transistor collectors.

The output stage in Figure 5.1a is a class AB complementary Darlington arrangement comprising emitter follower drivers Q1 and Q2 followed by output devices Q3 and Q4. Emitter resistors R1 and R2 set the idle current of the drivers at about 50 mA. The output stage emitter resistors R3 and R4 provide thermal bias stability and also play a role in controlling crossover distortion. The output stage provides a voltage gain of slightly less than unity. Its main role is to buffer the output of the VAS with a large current gain. If driver transistor beta (β) is assumed to be 100 and output transistor β is assumed to be 50, the combined current gain of the output stage is 5000. When driving an 8-Ω load, the impedance seen by the VAS looking into the output stage will be about 40 kΩ.

The triple emitter follower (Triple) shown in Figure 5.1b provides much higher current gain and better buffering of the VAS. This output stage was popularized by Bart Locanthi, and is also known as the *Locanthi T circuit* [1, 2]. If the added predriver transistors Q5 and Q6 have betas of 100, the current gain of this output stage will be approximately 500,000, and when driving an 8-Ω load, the VAS will see a very light load of about 4 MΩ. The predriver and driver stages operate in class A in the Locanthi T circuit.

Returning to the Darlington output stage of Figure 5.1a, Q1 and Q3 conduct on positive half-cycles and transport the signal to the output node by sourcing current into the load. On negative half-cycles, Q2 and Q4 conduct current and transport the signal
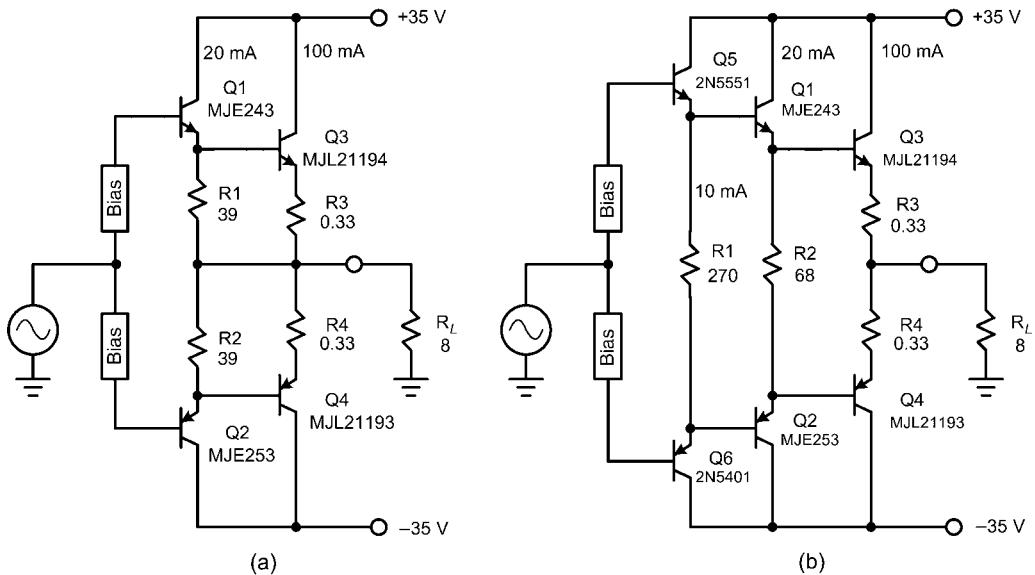
FIGURE 5.1 (a) Darlington and (b) Triple class AB output stages.

to the output node by sinking current from the load. When there is no signal, a small idle bias current of approximately 100 mA flows from the top NPN output transistor through the bottom PNP output transistor. A key observation is that the signal takes a different path through the output stage on positive and negative half-cycles. If the voltage or current gain of the top and bottom parts of the output stage is different, distortion will result. Moreover, the *splice point* where the signal current passes through zero and crosses from one path to the other is usually nonlinear, and this leads to so-called crossover distortion.

Output Stage Voltage Gain

The voltage gain of the output stage is determined by the voltage divider formed by the output stage emitter follower output impedance and the loudspeaker load impedance. The output impedance of each half of the output stage is the sum of the output transistor's re' and R_E. This is illustrated in Figure 5.2.

Since the two halves of the output stage act in parallel when they are both active at idle and under small-signal conditions, the net output impedance will be about half that of each side.

$$Z_{out(small\ signal)} \approx (re'_{quiescent} + R_E)/2 \tag{5.1}$$

If the output stage is biased at 100 mA, then re' of each output transistor will be about 0.26 Ω. The summed resistance for each side will then be $0.26 + 0.33 = 0.59$ Ω. Both output halves being in parallel will then result in a net output impedance of about 0.3 Ω. Because voltage gain is being calculated, these figures assume that the output stage is being driven by a voltage source. If the load impedance is 8 Ω, the voltage gain of the output stage will be $8/(8 + 0.3) = 0.96$. If instead the load impedance is 4 Ω, the gain of
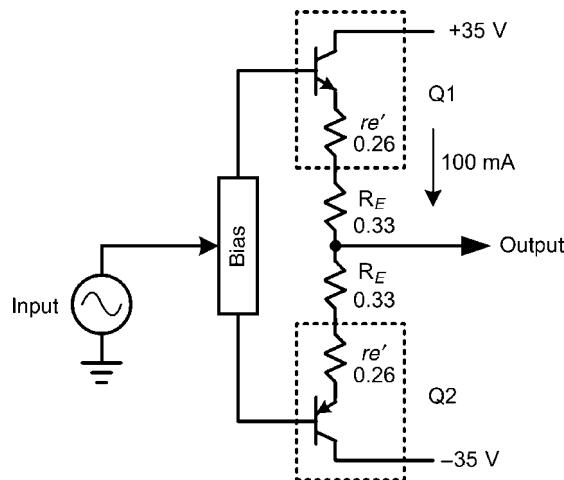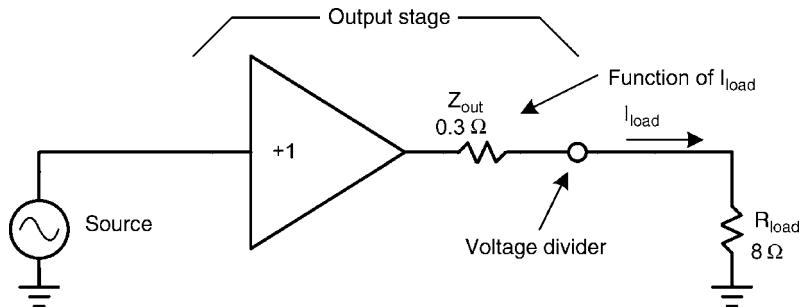
FIGURE 5.3 Amplifier output stage gain.

the output stage will fall to 0.93. The voltage divider action governing the output stage gain is illustrated in Figure 5.3.

Bear in mind that the small-signal gain of the output stage has been calculated at its quiescent bias current. The value of re' for each of the output transistors will change as transistor currents increase or decrease, giving rise to complex changes in the output stage gain. Moreover, for larger signal current swings, only half of the output stage is active. The output impedance under those conditions will be approximately $re' + R_E$ rather than half of that amount. These changes in incremental output stage gain as a function of output signal current cause what is called *static crossover distortion*.

$$Z_{out(large\ signal)} \approx re'_{high\ current} + R_E \approx R_E \qquad (5.2)$$

At high current, re' becomes very small. At $I_c = 1$ A, re' is just 0.026 Ω, much smaller than a typical value of R_E. At 10 A, re' is theoretically just 0.0026 Ω. That is why for large signals $Z_{out} \approx R_E$.

The Optimal Class AB Bias Condition

If R_E is chosen so that

$$R_E = re'_{quiescent} \tag{5.3}$$

then

$$Z_{out(large\ signal)} \approx Z_{out(small\ signal)} \approx R_E \tag{5.4}$$

and crossover distortion is minimized. Oliver showed this mathematically in Ref. 3.

We have

$$re'_{quiescent} = V_T/I_q \tag{5.5}$$

$$R_E = V_T/I_q \tag{5.6}$$

$$V_q = V_{RE\_quiescent} = R_E I_q = V_T \tag{5.7}$$

The voltage V_q is the voltage that appears across each emitter resistor when the condition in Eq. 5.3 is met and the class AB output stage is optimally biased. The optimal quiescent bias current $I_q = V_T/R_E$. Here that number is 79 mA.

When Oliver's condition is met, the output impedance at idle of each half of the output stage is $re' + R_E = 2R_E$, so the parallel combination is once again equal to R_E. Thus, the nominal output impedance of the output stage when voltage driven is R_E for an optimally biased class AB stage. Satisfying the Oliver condition is about the best one can do to minimize crossover variation in net output impedance of the stage. All of this is valid for ideal BJTs. Real-world BJTs have some intrinsic ohmic emitter resistance that must be counted as part of R_E. It often results largely from base resistance RB divided by β of the transistor. If intrinsic $RB = 3\ \Omega$ and $\beta = 100$, this added resistance will be 0.03 Ω. This will reduce slightly V_q when the stage is optimally biased.

Equalizing the large-signal and small-signal output stage gains is only a compromise solution and does not eliminate static crossover distortion because the equality does not hold at intermediate values of output current as the signal passes through the crossover region. This variation in output stage gain as a function of output current is illustrated in Figure 5.4. This data corresponds to the simple amplifier of Figure 5.2 with a quiescent bias current of 100 mA and employing 0.33-Ω emitter resistors. The MJL21193/21194 output pair was used for the simulation. The theoretical optimum bias current for this arrangement is 79 mA (placing 26 mV across each R_E), so this represents a very slightly overbiased condition. As a result the output stage gain is slightly higher in the crossover region, evidencing slight *gm* doubling [4]. The slight asymmetry on the left and right sides of the plot result from differences in the NPN and PNP output transistors.

Output Stage Bias Current

The quiescent bias current I_q of the output stage plays a critical role in controlling crossover distortion. It is important that the right amount of bias current flows through the output stage, from top to bottom, when the output stage is not delivering any current to the load. Notice that together the two driver and two output transistors require at least four V_{be} voltage drops from the base of Q1 to the base of Q2 to begin to turn on.
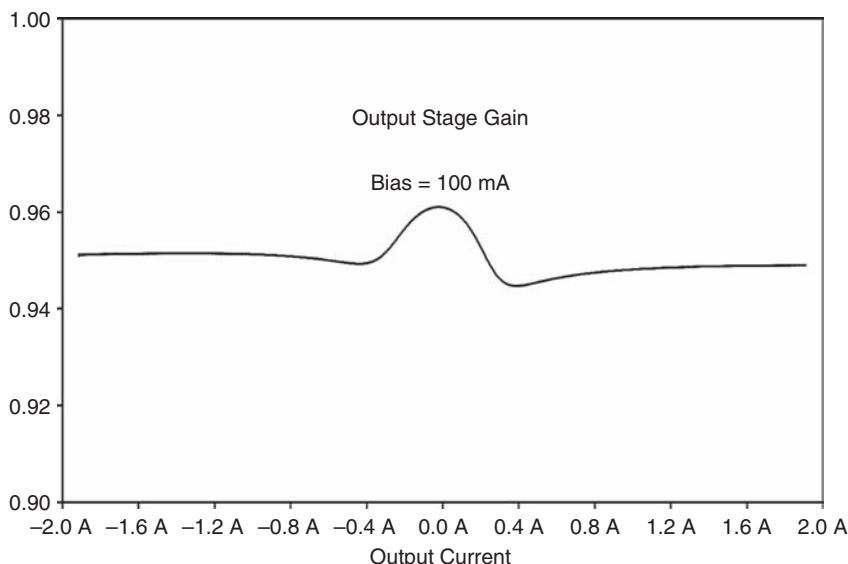
FIGURE 5.4 Output stage gain versus output current.

Any additional drop across the output emitter resistors will increase the required bias-spreading voltage.

The required bias voltage for the output stage is developed across the bias spreader, which is usually a V_{be} multiplier. The objective of the bias spreader design is temperature stability of the output stage quiescent current. The temperature coefficient of the voltage produced by the V_{be} multiplier should match that of the base-emitter junction voltages of the driver and output transistors. Since the V_{be} of a transistor decreases 2.2 mV/°C, it is important for thermal bias stability that these junction drops track one another. The output transistors will usually heat up the most. Because they are mounted on a heat sink, the V_{be} multiplier transistor is often mounted on the heat sink so that it is exposed to the same approximate temperature. This approach is only an approximation, because the drivers are often not mounted on the heat sink and the temperature of the heat sink changes more slowly than that of the power transistor junctions.

gm Doubling

If the output stage is strongly overbiased, well beyond Oliver's criterion, the intrinsic emitter resistance *re'* of the BJT is very low, even under quiescent conditions. The net output impedance of the stage at idle will then be closer to $R_E/2$. The output stage transconductance *gm* is just the inverse of its output impedance. The quiescent *gm* of the output stage is doubled in the limiting case of very high bias. However, the output impedance at extremes of output current, when only one output transistor is contributing transconductance, is still equal to R_E. Thus, *gm* has doubled in the crossover region with respect to *gm* outside the crossover region. This gives rise to the term *gm doubling* [4]. The *gm*-doubling phenomenon is illustrated in Figure 5.5, where the quiescent bias of the output stage has been increased to 300 mA. All other conditions remain the same as in Figure 5.4.
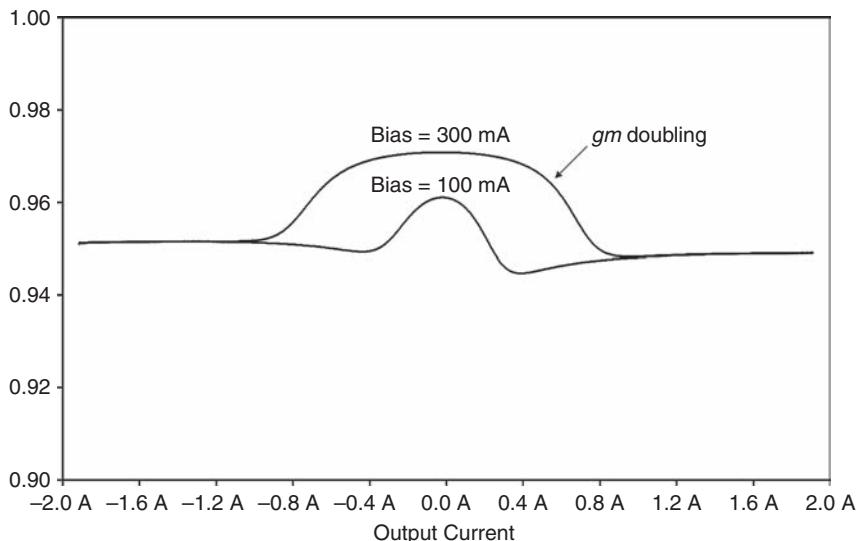
FIGURE 5.5   The *gm*-doubling effect in an overbiased class AB output stage.

These observations all assume that the output stage is effectively being driven in voltage mode. This will always be the case when the output impedance of the VAS is significantly lower than the impedance seen looking into the output stage. This will certainly be the case with a Triple output stage and a VAS whose output impedance is quite low due to the shunt feedback of Miller compensation. An output stage that is effectively current driven will not suffer *gm* doubling because it is not operating in a transconductance mode but rather in a current gain mode. Distortion will then be governed by beta mismatch of the NPN and PNP transistors. Pick your poison.

The Small Class A Region of Many Amplifiers

The class A region of many class AB power amplifiers is remarkably small. This gives rise to crossover distortion at very low signal levels. Consider an amplifier with 0.33-Ω emitter resistors. With 26 mV across each R_E, the bias current will be 79 mA. The peak current output at the edge of the class A region will be twice this amount, or 158 mA. With a 4-Ω load, this will correspond to 0.63V peak, for a power level of 50 mW.

If the quiescent bias is set well above the optimum described by Oliver, there will be a large conduction overlap region and a correspondingly large class A region. This will lead to lower distortion at small power levels, but result in *gm*-doubling distortion when signal amplitudes are sufficient to cause the output stage to exit the class A region.

5.3   Output Stage Efficiency

Even apart from the electric bill, output stage efficiency is very important because any input power that is not converted to output power is converted to heat. This directly affects the cost of the amplifier because increased heat production requires more expensive heat sinks.

Heat versus Sound Quality

Minimizing heat dissipation is where any designer will have some difficult decisions to make. There are some unavoidable trade-offs to be made between heat and sound quality. This does not mean that one must choose class A or even heavily overbiased class AB, but such trade-offs with sound quality will exist.

The heat trade-off is especially so with respect to quiescent power dissipation in each output stage. For a 100-W amplifier, quiescent dissipation can range from about 10 W for a mediocre BJT output stage to over 30 W for an excellent BJT output stage to perhaps 45 W for a high performance MOSFET output stage.

Power dissipation at 1/3 power or 1/8 power into the load must also be considered. The 1974 FTC rule on power output claims for amplifiers required an amplifier to sustain 1/3 rated power into an 8-Ω load for one hour without overheating [5]. Some designers do not adhere to this part of the rule. However, doing so tends to produce an amplifier that is more reliable in practice. Some designs will instead sustain 1/8 power into the load for one hour.

Estimating Power Dissipation

The most important thing to recognize is that power dissipation equals input power less output power. Most power dissipation in an amplifier is in the output stage transistors. It results from the product of output transistor V_{ce} and I_c, where V_{ce} is the power supply rail voltage less the output voltage V_{out}. Consider an ideal 100-W amplifier driving an 8-Ω resistive load. The power supply rails are 40 V, and at a full output swing of 40 V the output current will be 5 A.

At small V_{out}, V_{ce} is nearly 40 V, but the collector current is quite low, so there is relatively little power dissipation. At medium output voltages like 20 V, both voltage and current are moderate, so instantaneous power dissipation is fairly high (in this case about 40 W). At high output voltages, like 38 V, the collector current is high (in this case nearly 5 A), but V_{ce} is low, so dissipation is low. These relationships hold for a resistive load, but are altered for a reactive load.

Average power dissipation for a sinusoidal signal will behave in a similar way. Power dissipation of a class AB output stage will be small at low power levels and will increase with output power up to about 1/3 maximum output power. At higher output power levels the dissipation will actually decrease a bit because the voltage across the output transistors will tend to be smaller when they are conducting the greatest current (at the peaks of the sine wave). When operated at 1/3 power, dissipation for an ideal amplifier is equal to about 40% of its clipping power. This number is closer to 46% for a real-world amplifier. When operated at full power, a real-world amplifier will dissipate about 37% of its clipping power; the ideal amplifier will dissipate about 26%. These figures do not include power dissipation in the drivers or any other part of the power amplifier preceding the output stage.

Interestingly, the power dissipation for a class A amplifier tends to decrease with increases in output power. This is so because the input power is constant while the output power is increasing; this leaves less power to dissipate.

Estimating the Input Power

Consider a 100-W, 8-Ω BJT design that uses a single pair of idealized output transistors with 0.5-Ω emitter resistors. The output of this idealized design can swing all the way to the 40-V rails. This is often the model used to estimate output stage power dissipation as a function of output power, ignoring many realities. This example also illustrates how
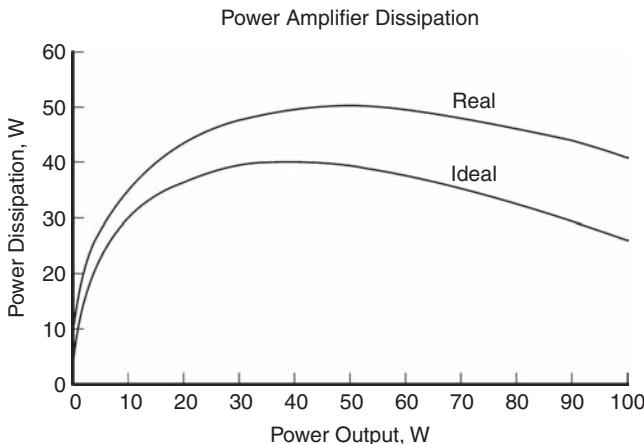
FIGURE 5.6 Power dissipation as a function of output power.

low the quiescent bias current can be in such a class AB output stage. There were in fact many BJT output stages designed with 0.5-Ω emitter resistors. The optimum idle bias current in this design is only 52 mA, resulting in a quiescent power dissipation of 4 W.

At full power into an 8-Ω load, the output voltage is 40-V peak and the output current is 5-A peak. The current drawn from each supply rail is a half-wave rectified waveform with a peak current of 5 A. The average of a half-sine is about 63% and the duty cycle is 50%, so the average rail current is $0.5 * 0.63 * 5 \, \text{A} = 1.58 \, \text{A}$. Average input for two 40-V rails is then 126 W. With 100-W output, the power dissipation is 26 W. The same calculation at 1/3 power of 33 W results in an average rail current of 0.91 A and an input power of 73 W, leaving a power dissipation of 40 W.

An Example

A 100-W/8-Ω power amplifier was simulated to illustrate the power dissipation of a real amplifier design as compared with one whose dissipation is estimated with ideal output transistors and output voltage swings that extend to the rails. The amplifier employed an output Triple with ± 48-V rails and two output pairs with 0.33-Ω emitter resistors.

Figure 5.6 is a plot of amplifier power dissipation as a function of output power for the 100-W design when it is driving an 8-Ω resistive load. Only the power dissipation for the output stage is shown. The second curve represents an idealized 100-W amplifier with 40-V rails.

5.4 Complementary Feedback Pair Output Stages

The emitter follower output stage is simple and straightforward, but there also exist common emitter-based output stages. In some situations, for example, they may be able to swing closer to the power supply rail. A complementary feedback pair is illustrated in Figure 5.7a. This circuit, called a *CFP*, can be used in small signal and power stages as well. It consists of an NPN transistor feeding a PNP transistor in a tight feedback loop. In many ways it acts like an NPN transistor with some improved properties. The CFP in Figure 5.7a is configured as an emitter follower. It has a current gain that is the product of the β of the two transistors, so it shares the buffering capability of the Darlington connection. However, because of the local feedback, it has low output impedance.
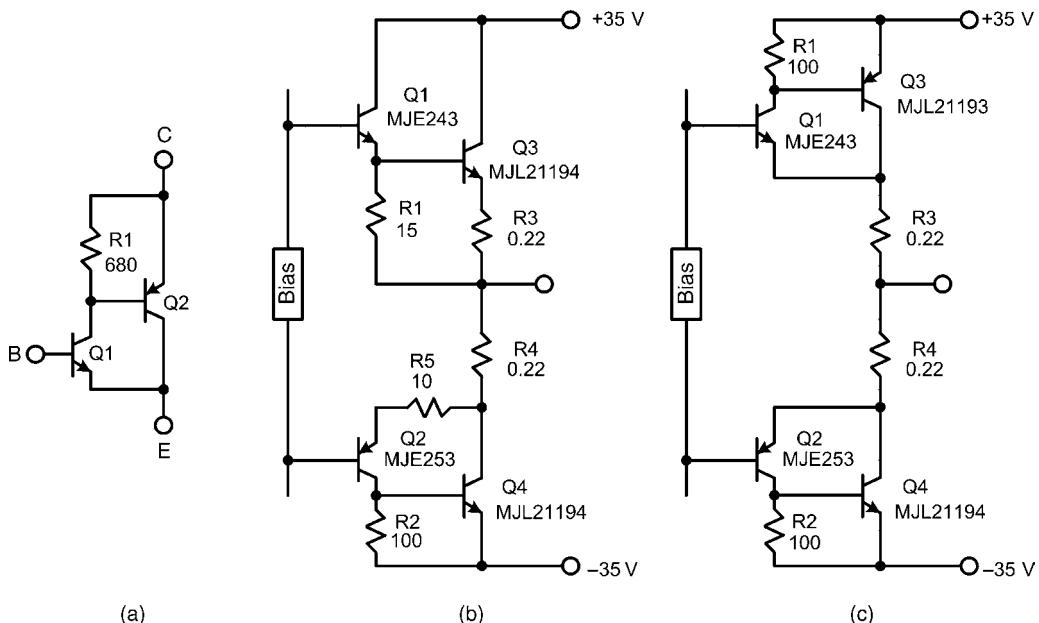
FIGURE 5.7   (a) Complementary feedback pair (CFP). (b) Quasi-complementary output stage. (c) CFP output stage.

The Quasi-complementary Output Stage

During the 1960s and early 1970s there were few, if any, good silicon PNP power transistors, so the complementary output stages that we take for granted nowadays were not common. In order to make an output stage with the properties of a complementary push-pull output stage, an NPN power transistor was configured with a PNP driver in a CFP arrangement that emulated a PNP power transistor. This was the basis of the quasi-complementary output stage illustrated in Figure 5.7b. This output stage suffered from its fundamental asymmetry. Different mechanisms govern the dynamic output impedance of the top and bottom parts of the stage, and the Oliver criterion for minimizing crossover distortion is virtually impossible to apply. The quasi-complementary output stage is only mentioned here for historical purposes, and by way of introduction of the use of the CFP in modern true complementary output stages.

The CFP Output Stage

A *Complementary Feedback Pair (CFP)* output stage is shown in Figure 5.7c. Here both output devices are operated in the common-emitter (CE) mode rather than as emitter followers. Some designers advocate the CFP output stage because it has a high degree of local feedback that linearizes each half of the output stage [4]. This results in very low output impedance for each half of the output stage and thus, presumably, reduced crossover distortion. Each of the upper and lower CFP stages acts like a super emitter follower with extremely high transconductance. Assuming that emitter resistors (R_E) are still used between each stage and the output node, the output impedance will be very low and largely dominated by the R_E value.

Biasing and Thermal Stability

Bias stability in the CFP output stage will tend to be better than that in an emitter follower output stage. This is because the bias in the CFP is mainly dependent on the driver transistor, which is subject to less heating. The bias current is less influenced by the changing power dissipation of the output transistor, allowing bias to be set with greater precision and stability. For this reason it is possible to obtain adequate bias stability with smaller values of R_E in the CFP arrangement than would be permitted in the emitter follower arrangement. The use of smaller R_E can lead to a reduced amount of crossover distortion because the net output impedance of the output stage is smaller, so dynamic variations in it will have less effect on incremental gain.

Optimum Class AB Bias Point and *gm* Doubling

The output impedance of the CFP is much lower than that of the emitter follower as a result of the local feedback. This means that the output transistor's *re'* is no longer a major determinant of the output impedance of each half. The output impedance is much more fully determined by the emitter resistor R_E. This makes it more difficult to avoid *gm* doubling and the crossover distortion that it brings.

The optimum quiescent voltage V_q across each emitter resistor in an EF output stage is ideally 26 mV. This makes the product of *gm* and R_E equal to unity, in accordance with Oliver [3]. The optimum V_q across the analogous R_E output resistor in the CFP output stage is on the order of 3.1 to 7.2 mV, depending on where R_E falls in the range of 0.47 Ω to 0.1 Ω [4]. This corresponds to output transistor bias currents on the order of 15 mA to 31 mA. This is a direct result of the higher *gm* of the CFP stages for a given operating current. The output transistors are thus operating in a starved mode in order to get the net stage transconductance down to a point where *gm* doubling will not be too bad. Indeed, when there are multiple devices in parallel, each has only a fraction of this current. The f_T of the output transistors is quite low under these conditions.

The greater bias precision and stability of the CFP provides little net value because it is really needed to keep crossover distortion down because crossover distortion in the CFP output stage is more sensitive to the bias setting. The high transconductance of each half of the output stage causes the crossover region for the CFP to be much narrower and more abrupt. This implies higher-order crossover distortion products.

Although the claim may be true that as a single stage the CFP is more linear than a double EF, this does not hold for a class AB stage consisting of a complementary CFP pair due to the *gm* doubling that will occur under most realistic conditions.

High-Frequency Stability

The second major concern is one of high-frequency stability. The CFP can be notoriously difficult to stabilize under all conditions. This is because of the larger amount of local feedback resulting from the feedback loop in the CFP. Its loop gain is a function of the load impedance and of the β, f_T, and C_{cb} of the output transistors. These stages may also be more vulnerable to destabilizing influences like capacitive loads. Some sort of local feedback compensation network is often needed with the CFP.

Turn-Off Issues in CFP Output Stages

The conventional CFP output stage has no problem turning on, as the driver transistor can pull quite a bit of current from the base in the turn-on direction. The CFP does,

however, suffer from limited ability to turn off quickly. Turn-off current is supplied by R1 and R2 in Figure 5.7c, where only 7 mA of turn-off current is available. The voltage across these resistors can never be more than the V_{be} of the output transistor. This is in contrast to the emitter follower output stage where current flowing in the opposite half of the output stage provides an increased voltage drop across the driver emitter resistor in the Locanthi T circuit [1]. There are few options for improvement of turn-off in the CFP output stage. For example, the *speed-up* capacitor sometimes used in emitter follower output stages cannot be used. As a result, the CFP is often shower to switch off and may be more prone to high-frequency switching distortion and common mode conduction (*shoot-through*).

The driver transistors in the CFP output stage do not operate in class A. This is a further disadvantage for this arrangement.

Miller Effect in the CFP Output Stage

The collector-base capacitance in the CE-operated output devices creates a Miller effect in the CFP. The small-signal effect is to reduce CFP bandwidth and to partially compensate its feedback loop. The large-signal effect is to cause high-frequency distortion due to the nonlinearity of C_{cb} of the output transistor. Moreover, there is also the large-signal action of the Miller effect that opposes turn-off. Consider the case where total C_{cb} is 500 pF and the output voltage slew rate is 50 V/μs. This current will be 25 mA, more than what is often run through the base-emitter resistor.

CFP Triples

As with simple Darlington output stages, the conventional two-transistor CFP does not have adequate current gain to enable the really high performance achievable by lightening the load on the VAS. As with emitter follower Triples, there are CFP Triples. Although there are many ways to incorporate three transistors into a CFP, the safest and most straightforward is to simply precede the CFP with an emitter follower predriver. It adds two V_{be} to the required amount of bias spread and does not change any of the stability or transconductance characteristics of the CFP.

CFP Degeneration

The CFP output stages described thus far do not include emitter degeneration in the driver or output transistors. This is partially responsible for the high transconductance of the CFP. Modest emitter degeneration in each transistor can reduce CFP loop gain and provide smaller transconductance for a given amount of bias current. A typical design would employ a 100-Ω resistor in the emitter of the driver and a resistor of the same value as R_E in the emitter of the output transistor. The use of paralleled output transistors requires emitter degeneration of the CFP output transistors anyway.

5.5 Stacked Output Stages

Some output stages are designed with two transistors in series to share the voltage swing required to produce the output signal. This reduces the maximum rated voltage requirement for the power transistors, but more importantly it increases the available *Safe Operating Area (SOA)*. This is especially significant because safe area in bipolar transistors often decreases rapidly at higher voltage due to second breakdown effects.

However, modern transistors have higher voltage ratings and are less prone to second breakdown. As a result, the use of stacked output stages is much less common than it used to be.

Figure 5.8 illustrates a simple stacked output stage design where two Locanthi Triples are stacked atop one another. A popular example of the stacked output stage is the Double Barreled Amplifier by Marshall Leach (also referred to as the *Leach Superamp*) [6]. The inner transistors drive the load in a conventional fashion, while the outer transistors provide a signal voltage to the collectors of the inner transistors. The outer stage of the stacked arrangement is driven in a bootstrapped arrangement with a signal derived from the output. The bootstrap signal is divided in half by R5 and R7 on the top half so that inner and outer parts of the output stage divide the voltage swing equally.

R5 is shown connected to the rail, where garbage will unnecessarily get into the circuit and appear at the collectors of the inner devices. For this reason, R-C filters should be placed in the rail lines to R5 and R6. For simplicity, the stage is shown with only one output pair. Most stacked designs will be high-power amplifiers, so that two or more pairs will be used.

Stacked output stages suffer some loss of headroom as a result of two power transistors being connected in series. For this reason, they are slightly less efficient. The
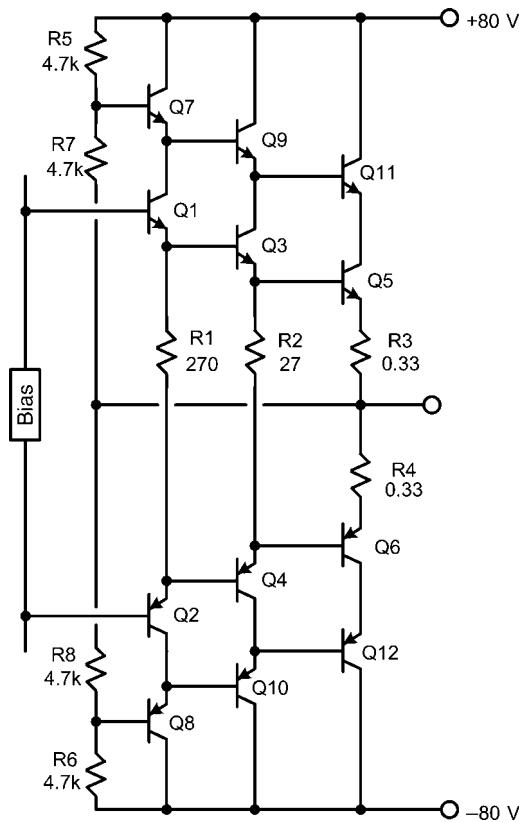
FIGURE 5.8 Stacked output stage design.

outer transistors in the stack shield the more important inner transistors from garbage on the power rail and also reduce the Early effect.

Cascode Output Stage

If the upper stage in the NPN stack is fed with the full audio signal, V_{ce} of the bottom output transistors will be constant (at a few volts) and a cascode output stage will result. This architecture has been discussed by Nelson Pass [7]. The upper stage can be fed in a feed-forward arrangement from the VAS or a bootstrapped arrangement from the output node. The arrangement places nearly the full SOA burden on the outer power transistors, but allows the power transistors that actually drive the load to operate in a constant V_{ce} mode. This eliminates the Early effect and improves the PSRR of the output stage. Similarly, any effect due to nonlinear base-collector capacitance of the output transistors will be greatly reduced. The inner transistors driving the load can also be faster power transistors because they are not subject to large voltage and SOA requirements.

The cascode output stage keeps the main output devices cooler by exposing them to a relatively small, constant V_{ce}. Power dissipation swings with program material are thus smaller, leading to smaller output stage dynamic thermal effects (a form of so-called *memory distortion*).

Soft Rail Regulation

If instead the upper transistors in the stack are fed with no signal but with only a filtered version of the rail voltage, this becomes an output stage that is fed from a quasi-regulated supply voltage. The filtered rail tracks the available rail voltage and does not dissipate as much power as a conventional fixed-voltage-regulated output stage. This is what I refer to as *soft rail regulation*. It is little more than feeding the output stage through a pass transistor that is configured as a capacitance multiplier.

The advantage of this scheme is that the output transistor is shielded from the noise and ripple on the high-current main rail power supply. This imparts a very high effective PSRR to the output stage. It also prevents the nasty pass-through of power supply ripple to the amplifier output when the amplifier clips. As with other stacked output stages, some operating headroom and operating efficiency are lost. The pass transistor can also function as a fast electronic circuit breaker if appropriate control circuitry is included.

5.6   Classes G and H

The quest for higher efficiency has led to the development of other types of output stages, the better-known variants being *class G* and *class H*. The class G and class H output stage configurations are designed to reduce output stage power dissipation by effectively changing the rail voltage applied to a conventional class AB output stage as a function of the instantaneous program amplitude. These amplifiers are popular in professional audio applications where the sonic penalties sometimes associated with these designs are not such a big problem.

Conflicting Terminology

In class G, the rail voltage is elevated in a linear way to a higher voltage once the program peak output level requires it. Class H is very much like class G, but the power

supply for the output stage is switched abruptly to higher levels when the signal waveform exceeds a certain threshold.

The U.S. and Japanese naming conventions for these classes is sometimes reversed, as explained in Ref. 8. The remainder of this section will focus on class G, in accordance with the *Anglo-Japanese* class nomenclature, where the supply voltages to the output stage are increased in a linear fashion when required.

Class G Operation

Figure 5.9 illustrates how the rail voltages change as a function of the signal for a class G amplifier. At low power levels the output stage operates from a fixed intermediate rail voltage supplied through *commutating diodes*. As the signal increases and the headroom for the output stage becomes small, the rail is lifted by a set of power transistors above in a fashion that is linear with the signal so as to provide a constant amount of headroom as the signal increases further. The upper power transistor is connected to the high-voltage rail. In a sense, the bottom output stage transistor is transformed into a cascoded output stage for the higher signal levels, since under these high-level conditions its collector is moving with the signal.

Figure 5.10 shows a simplified schematic of a Class G output stage. This design is very similar to the stacked output stage of Figure 5.8, except that R7 and R8 have been replaced by bypassed Zener diodes D5 and D6 to provide a full bootstrapped signal swing to the outer Triples. Diodes D1 and D2 are the commutating diodes. They supply the rail current from the low-voltage power supply when the signal swing is small. When the signal swing becomes large enough to reduce the V_{ce} of Q5 or Q6 to a small value, outer transistors Q11 and Q12 lift the rail, maintaining a fixed minimum V_{ce} across Q5 and Q6.

The breakdown voltage of D5 and D6 establishes the minimum V_{ce} that Q5 and Q6 will see. The relevant voltage is between the collector of Q5 and the output node and must be set to take into account the voltage drop across the emitter resistors under high-current conditions. At the same time, the Zener breakdown voltage must not be so large that the base of Q7 is driven beyond the high-voltage rail. A typical value for the Zener
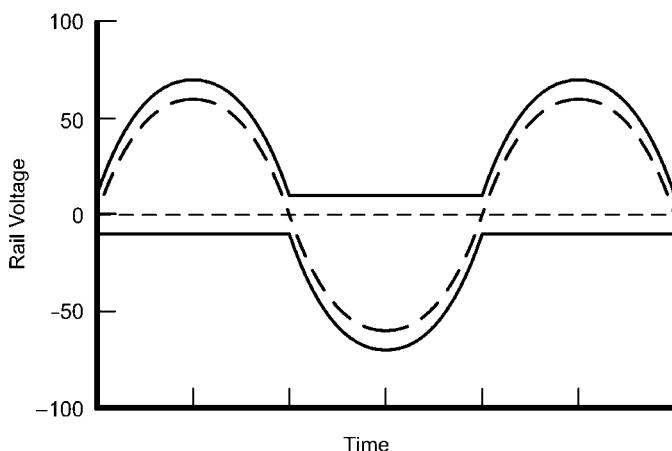
FIGURE 5.9   Rail voltage is a function of the signal in a class G output stage.
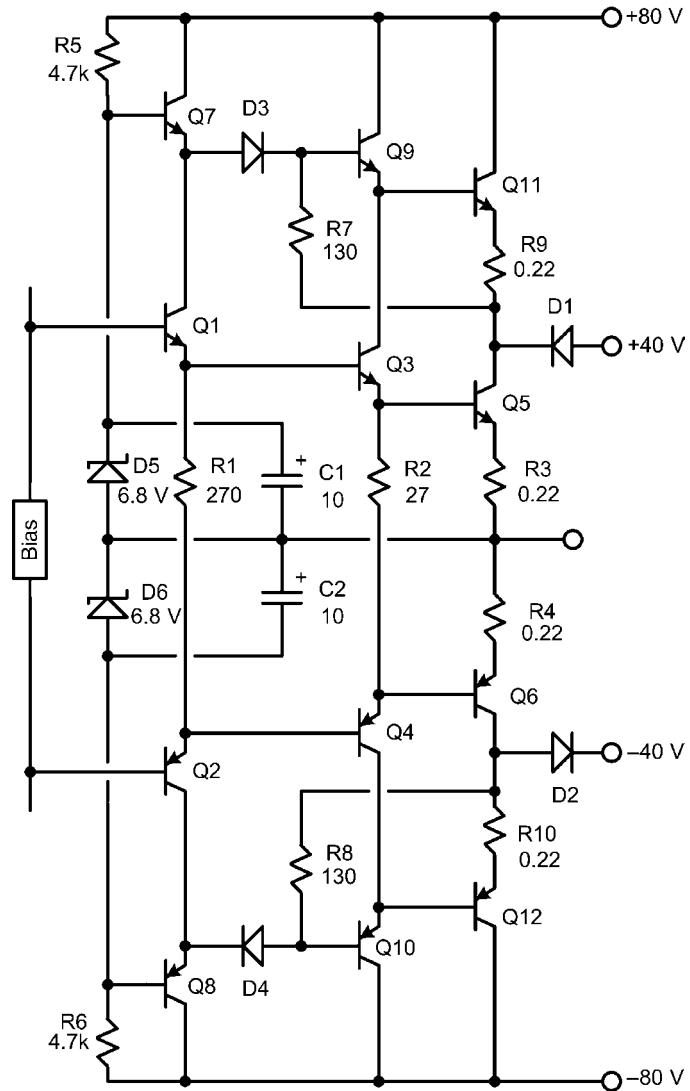
FIGURE 5.10 Class G output stage design.

voltage might be 6.8 V. The amplifier output therefore must never be driven to within less than 6.8 V of the rail. If necessary, Baker clamps can be used to prevent this from happening.

Driver isolation diodes D3 and D4 prevent excessive reverse base-emitter voltage from being applied to drivers Q9 and Q10 when the output signal swings negative with respect to the low-voltage rail. R7 and R8 establish the forward bias current of these diodes when they are on at about 10 mA. R7 and R8 also provide turn-off current to Q9 and Q10.
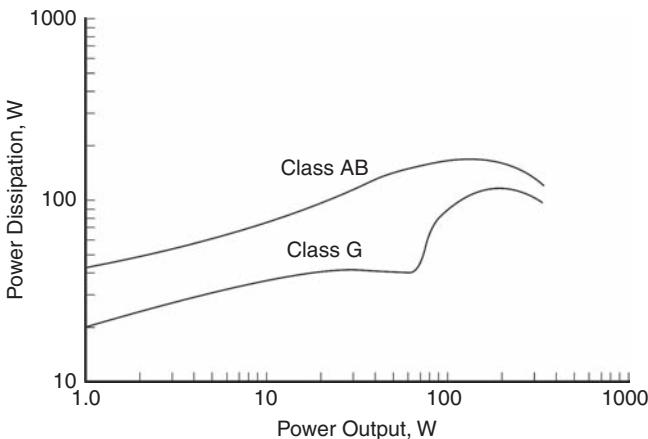
Figure 5.11 Class G power dissipation as a function of output power.

A feed-forward approach to driving Q7 and Q8 can also be used. In that case Zener diodes D5 and D6 are instead placed in the VAS collector path on either side of the bias spreader to provide offset voltages to the bases of Q7 and Q8. This approach takes away from available VAS headroom, so boosted VAS rails are recommended.

Class G Efficiency

Figure 5.11 is a plot of power dissipation as a function of output power for a 250-W class G output stage. The power dissipation for a comparable class AB design is also plotted.

Choice of Intermediate Rail Voltage

The choice of the intermediate rail voltage determines the signal amplitude at which the amplifier transitions its current draw from the low-voltage supply to the high-voltage supply. As such, it affects the power dissipation profile of the amplifier as a function of the signal level. If sine wave signals were the governing criteria, one might adjust the low-voltage rail so that the two peaks in power dissipation had the same maximum power dissipation. However, real program material has a higher crest factor than sine waves; this means that it spends relatively less time at high amplitudes. This argues for choosing a lower intermediate rail voltage to reduce power dissipation for conditions of small signal amplitude.

Headroom Considerations

Class G requires additional rail voltage headroom because of the presence of the outer stage and the need for headroom for the inner stage. This decreases the value-added contributed by class G for lower-power amplifiers. Class G may also benefit from boosted driver rails that allow the outer transistors to swing closer to the rails while maintaining adequate headroom for the VAS.

Rail Commutation Diode Speed

Turn-off time of the rail commutation diodes is a problem that creates a performance challenge for Class G amplifiers. The commutation diode provides the intermediate rail voltage to the output transistor under low-swing conditions. When a signal peak occurs, the high-rail output transistor pulls the collector node of the main output transistor to a higher voltage, following the signal as its amplitude increases. This action turns off the commutating diode at a fairly high rate of change of current and voltage. Prior to this switching action, the commutation diode will have been conducting fairly high current. Diodes cannot instantly stop conducting current.

As a result, the commutation diode will resist the change in its voltage to the reverse direction. The turn-off current for the commutation diode must be supplied from the high-side transistor. This can cause a significant current spike and possibly a voltage spike at a time when the main output transistor is operating at low V_{ce} where its ability to provide power supply rejection is minimal.

When the commutation diode lets go as the signal goes more positive, the high-side transistor has been conducting this extra diode current and still wants to conduct the higher current. It will create a positive voltage glitch at the collector of the main output transistor as it tries to put this extra current into the collector of the output transistor. It may in theory have no other place to go than into the output load. For this reason, reverse recovery time of the commutation diodes is very important.

Fast Recovery Epitaxial Diodes (FRED) are a good solution because they have minimal charge storage and fast reverse switching times. These silicon diodes are available in voltage and current ratings that are adequate for high-power class G amplifiers. The Vishay HEXFRED® devices are especially well suited to this application [9].

The Transition to Cascode Operation

By now it should be apparent that the class G output stage is just another type of stacked output stage that operates in two modes. For smaller signals, it operates as a conventional class AB output stage powered with the intermediate rail voltage. At higher signal levels, when the commutation diode is turned off, the output stage acts like a cascode as described in Section 5.6. As observed by Self [4], Early effect is present in the former case but not in the latter case. This means that transistor current gain will vary with the signal in the former case but not in the latter case. If changes in current gain alter the effective load impedance seen by the VAS, distortion will result. Similarly, if current gain variations alter the voltage gain of the output stage, distortion will also result. For this reason it is important to design the class G output stage so that beta variations have a minimal effect on its circuit behavior. Use of the Triple-based class G output stage discussed above is very effective to this end.

Safe Operating Area

The stacked nature of the class G output stage reduces the maximum required SOA on the output transistors as compared to a straight class AB design. This happens because the inner transistors are never subjected to a V_{ce} greater than the intermediate rail voltage plus the main rail voltage. The outer transistors are never subjected to V_{ce} greater than the difference between the main rail voltage and the intermediate rail voltage.

5.7 Class D

No chapter on output stages would be complete without discussion of class D amplifiers, whose popularity and performance increase daily. An entire book could be written on class D, not to mention a chapter. Here we touch on it very briefly for completeness, but defer any meaningful discussion to Chapters 28-31.

Class D amplifiers are popular as a result of the never-ending quest for efficiency. They rely on the fact that an on-off switch (a MOSFET transistor) cannot dissipate any power if it has no voltage across it or if it has no current passing through it. The simple class D output stage uses high-speed solid-state switches to connect the positive and negative supply rails to the output node alternately, with different duty cycles, such that the average value applied to the output is the desired value corresponding to the signal. This is referred to as pulse width modulation (PWM). The alternation between positive and negative connection of the supply rails to the output node is at a high frequency well above the audio band.

When the output signal is to have large positive amplitude, the positive supply rail is connected to the output most of the time (i.e., with a high duty cycle). When the average output signal should be zero, the pulse widths of the positive and negative connections of the rails to the output node will be equal, corresponding to a 50% duty cycle.

The way in which the input signal is converted into a PWM representation and the way in which the output switches are driven is where most of the complexity and innovation lie. Approaches range from simple analog techniques to sophisticated high-speed DSP-based techniques, some of which rely on Sigma-*Delta* techniques borrowed from the land of A/D and D/A converters.

Achieving low distortion and high sound quality is a special challenge for class D amplifiers, but great progress has been made. One example of such a challenge is the poor power supply rejection inherent in the simple class D approach. If the power supply rail is connected to the output node through a switch, it is easy to see that there will be very little power supply rejection in the circuit.

References

1. Locanthi, B. N., "Operational Amplifier Circuit for Hi-Fi," *Electronics World*, pp. 39–41, January 1967.
2. Locanthi, B. N., "An Ultra-low Distortion Direct-current Amplifier," *Journal of the Audio Engineering Society,* vol. 15, no. 3, pp. 290–294, July 1967.
3. Oliver, B. M. "Distortion in Complementary Pair Class B Amplifiers," *Hewlett Packard Journal,* pp. 11–16, February 1971.
4. Self, D., *Audio Power Amplifier Design Handbook*, 5th ed., Focal Press, 2009.
5. Federal Trade Commission (FTC), "Power Output Claims for Amplifiers Utilized in Home Entertainment Products," *CFR* 16, part 432, 1974.
6. Leach, W. Marshall, Jr., "Double Barreled Amplifier," *Audio*, vol. 64, no. 4, pp. 36–51, April 1980.
7. Pass, Nelson "Cascode Amplifier Design," Pass Labs, www.passdiy.com.
8. Duncan, B., *High Performance Audio Power Amplifiers*, Newnes, 1996.
9. HFA25PB60 HEXFRED®, Ultrafast Soft Recovery 25A diode, Vishay, www.vishay.com.

This page intentionally left blank

Summary of Amplifier Design Considerations

T his chapter is intended to summarize the numerous considerations that should be addressed in designing a power amplifier. Now that basic power amplifier design principles have been covered, it is a good time to go over this before getting into deeper design considerations. This will also help put into perspective those later discussions. All of these topics will be covered in much greater detail in later chapters.

6.1 Power and Loads

This may seem obvious, but one first needs to decide what the rated power of the amplifier should be and into how low an impedance load it will be operated, taking into account the fact that rated power will usually be a function of the load impedance. Nominal power is usually stated into 8 Ω, but what power will be needed into 4 Ω or even 2 Ω? An ideal amplifier doubles its power as the load is halved. How close to this ideal should this amplifier come? Will this amplifier need to be able to operate continuously into a load impedance of 4 Ω or even 2 Ω? What are the expectations for testing? Will the amplifier be expected to operate at 1/3 power with both channels driven into a 2-Ω load for an extended period?

Worst-Case Loads

Loudspeakers are anything but a resistive load. What will the criteria be for the worst-case load? What minimum impedance will be designed for? What phase angle of the load impedance will be tolerated? How much direct load capacitance will be allowed without stability problems?

Peak Output Current

High-output-current capability is often associated with good-sounding amplifiers. At minimum, it is good insurance against the unpredictability of difficult speaker loads that are driven by unusual program material. It is not difficult to concoct scenarios where the peak load current into a reactive load can be twice that into a resistive load of the same impedance. An amplifier rated at 100 W into an 8-Ω load will attempt to produce peak currents of 40 V/2 Ω = 20 A into a resistive 2-Ω load. Double this and you get 40 A for a nominal 100-W amplifier. The numbers get ugly fast.

Slew Rate

The required slew rate for an amplifier can sometimes be a point of controversy, but some minimum guidelines can put things into perspective and prove useful. Much of it amounts to how much margin is desired against the maximum slew rate likely to occur in program material. To be generous, assume it is that of a full-power sinusoid at 20 kHz. A decent margin to add on top of that is to require the amplifier to have sufficient slew rate to support a full-power sinusoid at 50 kHz.

The required slew rate for a sinusoid at 20 kHz is 0.125 V/µs per peak volt of output. This means that a 100-W amplifier producing 40 V peak requires a minimum slew rate capability of 5 V/µs. Adding the margin for full-power capability at 50 kHz raises this number to 12.5 V/µs. Required slew rate tends to increase as the square root of power, so a corresponding 400-W amplifier would require a minimum slew rate capability of 25 V/µs. In reality, for very high quality reproduction, substantially higher slew rate capabilities are desirable and not difficult to achieve. Unfortunately, high slew rate alone does not guarantee low values of high-frequency distortion.

6.2   Sizing the Power Supply

The power supply design will have the greatest influence on achievable output power, on both a short-term basis and a long-term basis. All unregulated power supplies sag under a heavy load. A stiffer power supply sags by a smaller amount. The amount by which a power supply sags under a given load is referred to as its regulation.

When the amplifier is operating under a no-load condition, the power supply must only deliver the bias currents, perhaps on the order of 100 to 200 mA per channel for a modest-sized power amplifier. When the amplifier is delivering full power into an 8-Ω load, the power supply will have to deliver considerably more current, in the order of amperes. Still more current will have to be delivered when a 4- or 2-Ω load is being driven to rated power.

Average Power Supply Current

A 100-W amplifier driving a resistive 8-Ω load will put out 40 V peak at a current of 5 A peak. The average current drawn from each rail will be about 63% of the peak for half of the cycle for a class AB output stage. This comes to about 1.6 A average per rail. Note that with 45-V rails this corresponds to input power of 144 W and thus an output stage power dissipation of 44 W.

Average power supply current will increase as the square root of rated power and the inverse of the load resistance. The 100-W amplifier (with a perfect power supply that does not sag) will produce 400 W into a 2-Ω load, and its average power supply rail current will be 6.4 A. Input power will be 576 W, and power dissipation will be 176 W.

Sizing the Power Transformer

Power transformers are usually rated in Volt-Amperes (VA) delivered as AC into a resistive load with a given degree of sag (regulation) from no-load to full-load. It is not always easy to correlate this to the amount of current that can be delivered as DC by a capacitor-input rectifier into a load with a given amount of regulation.

One of the biggest issues in sizing the power transformer is the desired degree of stiffness of the resulting power supply. Some designers will prefer a power supply with

higher compliance (less regulation), resulting in greater dynamic headroom. The legendary Phase Linear 700 is a good example of this philosophy. In more recent times, it appears that designers of very high-quality amplifiers prefer a stiff power supply, eschewing dynamic headroom for greater output current capability and greater ability to handle smaller load impedances. Stiffer power supplies may produce better sound quality as a result of less program-dependent rail voltage variations.

Sizing the Reservoir Capacitors

Large reservoir capacitors are always a good thing, but they are expensive. There is no objective way to state the required size, but a look at power supply ripple as a function of reservoir capacitance and output current can provide useful perspective.

The 100-W/8-Ω amplifier driving 400 W into a 2-Ω load will consume an average rail current of 6.4 A. A gross approximation of the peak-to-peak ripple voltage is arrived at by assuming that the rail voltage decays over one-half cycle (8.3 ms) in the amount of $V = I * T/C$. If the 100-W amplifier has reservoir capacitors of only 10,000 µF, then the ripple under these conditions (6.4-A average load current) becomes 5.3 V peak to peak. It is easy to see why some better power amplifiers have 100,000 µF of reservoir capacitance on each rail.

A 400-W/8-Ω amplifier driving 1600 W into a 2-Ω load will consume average DC current of 12.8 A. If ripple is to be limited to 1 V peak to peak, then the reservoir capacitance must be on the order of $C = I * T/V = 106,000$ µF.

6.3   Sizing the Output Stage

The output stage must be able to handle the maximum anticipated power supply rail voltages that will occur under no-load conditions with high mains voltage conditions. It is easy for a designer to reason that a 100-W/8-Ω amplifier requires 45-V rails and thus the output stage will see no more than 90 V. This is far, far from safe. In addition to the usual safety margins, one must take into account power supply regulation (the rails will rise under no-load conditions) and high mains voltages. With 20% regulation and 130-V mains, the rail voltages may rise to over 60 V if the nominal mains voltage is 120 V.

Even more importantly, the amount of available safe operating area in the output stage must be adequate to handle the most difficult load conditions anticipated, taking into account the kind of output stage protection to be employed. This will influence the number of output pairs needed. More aggressive protection circuits will allow the use of a smaller output stage, but will likely interfere with audio performance under some conditions. How rarely do we want the protection circuit to have to engage? Will we employ a V-I protection circuit at all?

Number of Output Pairs

The required number of output pairs depends on power dissipation, needed safe operating area, and desired maximum output current. Even if the latter two considerations are ignored for now, a conservative look at power dissipation can lend some insight.

The 100-W/8-Ω amplifier driving 400 W into a 2-Ω load will dissipate 176 W in its output stage. Let's arbitrarily argue that the output stage should be sized to withstand this full-power dissipation indefinitely for purposes of full-power bench testing into a 2-Ω load. Let's further assume that the heat sink temperature is allowed to reach 70°C under these conditions and that junction temperature must not exceed 150°C. There is

thus an 80°C rise allowed to the junctions for 176 W. This amounts to a net thermal resistance from heat sink to junction of 0.45°C/W spread out over the total number of output transistors including their heat sink insulators.

Consider two output pairs comprising four transistors. This means that each transistor is allowed 1.8°C/W from junction to heat sink. Assume the insulators have a thermal resistance of 0.5°C/W. This means that the junction-to-case thermal resistance of each transistor must be no greater than 1.3°C/W. This corresponds to a transistor with a power dissipation rating of about 96 W. Thus two output pairs are adequate for this output stage power dissipation criteria. For simplicity, assume that the required number of output pairs increases in proportion to the rated amplifier power.

For 150-W output transistors, the amplifier could possibly go to 150 W/8 Ω under these dissipation criteria. A rule-of-thumb thus emerges: divide the rated power by 75 and round up to the next integer. This is the minimum number of output pairs recommended to satisfy this thermal criterion. A 400-W amplifier would thus require six pairs of output devices.

It is important to remember that this rule of thumb does not take into account SOA requirements and possible output current requirements. It also does not take into account operating at 1/3 power into a 2-Ω load, where output stage dissipation will be higher. Power transistors are not as expensive as they used to be, so it is easier to be generous in this regard. A greater number of output transistors relaxes thermal concerns, improves thermal stability, and makes the amplifier performance less vulnerable to beta droop effects.

6.4 Sizing the Heat Sink

Getting rid of the heat in a power amplifier is one of the most important design considerations and it can be a large factor in the cost of the amplifier. The size of the heat sink will largely be determined by the nominal power rating of the amplifier in combination with the lowest anticipated load impedance. How long the amplifier will have to be able to run safely into that load will also influence the required size of the heat sink. A key point here is that the maximum power dissipation for a typical class AB output stage occurs at an output power that is approximately 1/3 rated power. It is important to note that other types of output stages, such as class A, class G, and class H, may have very different heat sinking requirements.

A Simple Guideline

A fairly conservative approach to estimating the required heat sink thermal resistance can be arrived at by assuming that the heat sink temperature shall not exceed 60°C when the amplifier is operated at 1/3 power into an 8-Ω load. The highest temperature of an object that you can touch without excessive pain is about 60°C. The FTC metric of 1/3 power into an 8-Ω load for 1 hour may seem conservative, but remember that things get worse rapidly when the amplifier is called on to deliver its power into the many loudspeakers that exhibit much lower impedances than 8 Ω [1].

A 100-W/8-Ω amplifier will dissipate about 50 W in its output stage at 1/3 rated power when driving an 8-Ω load. If the ambient temperature is 25°C, then a rise of 35°C will be allowed. This translates to a required heat sink thermal resistance of 0.7°C/W. Amplifiers with higher power ratings will require a correspondingly smaller thermal resistance to ambient.

Amplifiers designed to handle today's often highly compressed program material at high levels while driving low-impedance speaker loads should be designed with significantly lower heat sink thermal resistance, especially if they are expected to operate in hot environments.

6.5   Protecting the Amplifier and Loudspeaker

One of the tougher practical design considerations for a power amplifier is protection. There are two major aspects here. The first, and most important, is that the amplifier should not fail in such a way that it will destroy the expensive loudspeakers to which it is connected. The second is that the amplifier should not self-destruct when driving a difficult load at high power levels or when it is subjected to a short circuit at the output. Finally, it is desirable that when the protection circuits engage, they do so in a way that is benign and that causes as little damage to the audio signal as possible. Some protection circuits can create high-amplitude spikes which are very audible and can even damage tweeters.

Loudspeaker Protection

It is very important to protect loudspeakers from high DC voltages at the output of the amplifier. An output stage that fails will often do so by shorting the output of the amplifier to one of the rails. Speaker fuses are often used, but they can be unreliable and introduce low-frequency distortion. Active circuits that sense a DC level at the output of the amplifier can be used to open a loudspeaker relay or disable the power supply to the output stage. An alternative is to *crowbar* the output of the amplifier to ground with a TRIAC that is fired when DC is sensed.

Short Circuit Protection

This is the most fundamental form of protection for the amplifier itself. With a rugged output stage, a loudspeaker fuse or rail fuses or circuit breakers may be sufficient. How long it takes them to act is the key here. Current limiting and active amplifier shut down circuits can also play an important role in protecting the amplifier against short circuits.

Safe Area Protection

SOA protection is much more sophisticated than short circuit protection or current limiting. Its purpose is specifically to protect the output transistors from unsafe combinations of voltage and current that may cause the output transistors to fail. Safe area protection is often associated with V-I combinations that occur when complex load impedances are being driven. Safe area protection, often synonymous with V-I limiting, has a dubious reputation for interfering with sound quality, and some designers dispense with it. If the output stage is made big enough, V-I limiting can sometimes be avoided without incurring undue risk to the output transistors.

6.6   Power and Ground Distribution

The schematic may not tell all when it comes to power and ground distribution. Even well-designed amplifiers can sound bad if they are implemented with poor power and ground distribution. The key here is to understand the nature of all the current flows in

the power and ground circuits of the amplifier, and to recognize that no wires have zero impedance. Moreover, current flowing in any wire will create a magnetic field that may induce noise or distortion into neighboring circuits.

When Ground Is Not Ground

Ground is whatever single reference point you pick it to be. Ground is not ground when current flows from the point being considered to the reference point. This reality is simply due to the finite impedance present in any wire or piece of interconnect. The best recommendation is to follow the currents and to understand the nature of those currents.

The well-known star grounding approach seeks to keep the currents of one circuit from flowing through the ground line of another circuit. In such a case, a small-signal reference ground will have very little current flowing in it and will remain at pretty much the same potential as the reference ground. Life is not that simple, and most power amplifier ground topologies are only an approximation to star grounding at best. A key point to understand is that most of the currents that are important to avoid are AC currents. Bypass capacitors can often destroy the integrity of a star ground arrangement by providing another (unintended) path through which these AC currents can flow.

Ground Loops

Unintended ground loops can make great antennas. They don't just pick up and introduce hum. They can serve as an entryway for EMI. They can also serve to pick up and distribute voltages resulting from nonlinear magnetic fields in the amplifier. These include magnetic fields associated with power supply rectification and signal currents.

Nonlinear Power Supply Currents

The class AB output stage creates nasty half-wave-rectified nonlinear currents of large amplitude in the power rails. These currents can cause unwanted nonlinear voltage drops in power lines and grounds through which they are allowed to flow. They can also create AC magnetic fields that induce nonlinear voltages into nearby circuits [2].

Current Flows Through the Shortest Path

Make this reality work for you rather than against you. Manage impedances and topology so as to force currents to circulate locally when possible.

6.7   Other Considerations

There is a myriad of additional design choices and implementation considerations that come into play in the design of an amplifier. Some could be classified as feature choices, whereas others could be classified as performance targets.

Output Stage Bias and Thermal Stability

Special attention needs to be paid to how the output stage bias will be set and how its variation over environmental and program conditions will be minimized. This will help minimize crossover distortion. At the same time, it is very important that the output

stage never be allowed to enter a condition of thermal runaway. There can be conditions where the output stage can run away before the heat sink even knows what happened.

Output Node Catch Diodes

The output node of the amplifier must never be allowed to go beyond the power supply rails by more than a diode drop. Such high-voltage excursions can occur as the result of an inductive speaker load whose current has suddenly been interrupted or limited. Such inductive kicks can damage output transistors, speaker relay contacts, and tweeters. For this reason, silicon diodes are wired in a reverse-biased manner from the output node to each of the power supply rails. They will conduct if the output voltage attempts to go beyond the rail voltage. For amplifiers that incorporate speaker relays, it is best to include such catch diodes on both sides of the relay.

Protection of Speaker Relay Contacts

Speaker relay contacts can be more vulnerable to damage than one might think, often as a result of arcing when they open. Such damage can result in pitted contacts that will impair the sound quality. The output catch diodes mentioned above can help by avoiding voltages greater than the rail voltage from appearing across the contacts. This by itself may not be fully sufficient. Sometimes an R-C snubber network across the contacts can help avoid arcing as well.

Physical Design and Layout

One should always be aware of the surroundings of the path of a sensitive signal or of an inductive component. For example, input and feedback lines should be kept away from the power supply and the main rail lines to the output stage. If the amplifier uses an output coil, that coil should not be near ferrous material or low-level circuits.

The Feedback Path

The negative feedback should be tapped from the output after the high-side and low-side currents of the class AB output stage have been merged where the emitter resistors are joined. The signal should remain a high-level, low-impedance signal until it reaches the physical location of the input stage. In other words, most of the feedback network should reside in close proximity to the input stage. This reduces the effect of any corrupting influences on its way from the output to the input stage.

References

1. Federal Trade Commission (FTC), "Power Output Claims for Amplifiers Utilized in Home Entertainment Products," *CFR 16*, Part. 432, 1974.
2. Cherry, E. M., "A New Distortion Mechanism in Class B Amplifiers", *J. Audio Eng. Soc.*, vol. 29, no. 5, May 1981.

This page intentionally left blank

Advanced Power Amplifier Design Techniques

P art 2 delves deeply into the design of advanced power amplifiers with state-of-the-art performance. Advanced input, VAS, and output stages are discussed in depth, as are DC servos for DC offset control. A complete chapter is devoted to advanced forms of negative feedback compensation that can provide high slew rate and low distortion without compromising stability. A detailed discussion of noise sources is also included in Chapter 7 where input and VAS circuits are covered. Crossover distortion, one of the most problematic distortions in power amplifiers, is studied in depth in Chapter 10. Both static and dynamic crossover distortions are covered. Part 2 also includes a detailed treatment of MOSFET output stages and error correction techniques. Part 2 closes with a discussion of other sources of distortion that are less well known.

This page intentionally left blank

Input and VAS Circuits

The amplifier that was evolved in Chapter 3 served as a good platform for amplifier design understanding, but it did not include significant sophistication of the input stage (IPS) and voltage amplifier stage (VAS) circuits. Rather, it started with the most basic IPS-VAS and evolved it in a linear way to achieve much-improved performance. Although the end result was quite good, there are many ways to skin a cat and achieve further improved performance. Moreover, the analysis of the IPS-VAS was fairly superficial, for example, there was little discussion of noise.

7.1 Single-Ended IPS-VAS

The single-ended IPS-VAS was discussed at length in Chapter 3 where a basic amplifier was evolved to a high-performance amplifier. Most of the evolution in the design took place in the IPS-VAS. It is referred to as single ended because the VAS is single ended with a current source load. Later in this chapter we will focus on designs that include a push-pull VAS for improved performance.

The IPS-VAS shown in Figure 7.1 is unlike the simple IPS-VAS that was used as a starting point in Chapter 3. It is provided with ±45-V rails that correspond to an amplifier capable of delivering about 100 W into an 8-Ω load. This IPS-VAS includes emitter degeneration and is arranged with output stage predrivers and drivers as if a Triple EF was being used for the output stage. The output stage is not present, and the feedback is taken from a center tap on the driver emitter bias resistor. This allows distortion of the IPS-VAS to be evaluated in the absence of the distortion of an output stage.

The pair of 234-Ω emitter degeneration resistors implements 10:1 degeneration of the input differential pair by increasing the total emitter-to-emitter resistance R_{LTP} from 52 Ω to 520 Ω. This reduces its transconductance by a factor of 10.

Recall the relationship described in Chapter 2 for Miller compensation:

$$C_{\text{Miller}} = 1/(2\pi f_c R_{\text{LTP}} A_{cl})$$

where A_{cl} is the closed-loop gain, R_{LTP} is the total emitter-to-emitter LTP resistance including re', and f_c is the desired gain crossover frequency for the negative feedback loop. Setting f_c to 500 kHz and closed-loop gain to 20, we have

$$C1 = C_{\text{Miller}} = 0.159/(500 \text{ kHz} * 520 \text{ Ω} * 20) = 30.6 \text{ pF}$$

By this calculation $C1$ must be about 30 pF.

Notice that ±1 mA is available from the input stage to charge and discharge $C1$. This results in an achievable slew rate of 1 mA/30 pF = 33 V/μs. This is a respectable value of slew rate for an audio power amplifier of modest power level.
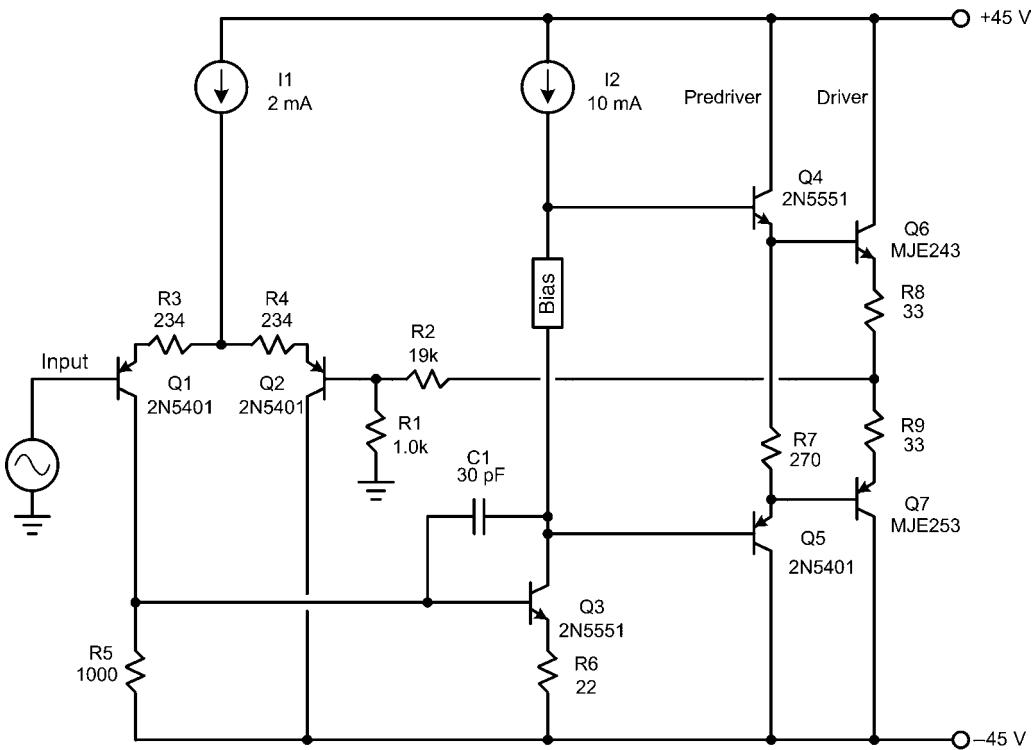
FIGURE 7.1   A simple single-ended IPS-VAS.

Improved Single-Ended IPS-VAS

The IPS-VAS shown in Figure 7.2 is very much like the last one shown in Chapter 3 that was evolved to a high-performance level. The major improvements made to that design included a current mirror load on the IPS and a Darlington-cascode VAS with current limiting. This combination of improvements greatly increased the open-loop gain while virtually eliminating the Early effect in the VAS.

Figure 7.3 plots 20-kHz THD as a function of output level for the IPS-VAS circuits of Figures 7.1 and 7.2. One can see the great improvement in performance achieved by merely adding a few small-signal transistors to the circuit. Bear in mind that this distortion does not include output stage distortion. Isolating the IPS-VAS distortion is the best way to compare different designs of this portion of an amplifier.

Shortcomings of the Single-Ended IPS-VAS

The single-ended IPS-VAS is asymmetrical. With a 10-mA quiescent current, the single-ended VAS can never source more than 10 mA to the output stage. However, it can sink an amount of current that is limited only by whatever current limiting is built into the VAS. The transconductance of the single VAS transistor varies in accordance with the amplitude and polarity of the output current. When the VAS is sourcing high current to the output stage, the VAS transistor is operating at a low collector current, and its transconductance is correspondingly low. When the VAS is sinking high current from the output
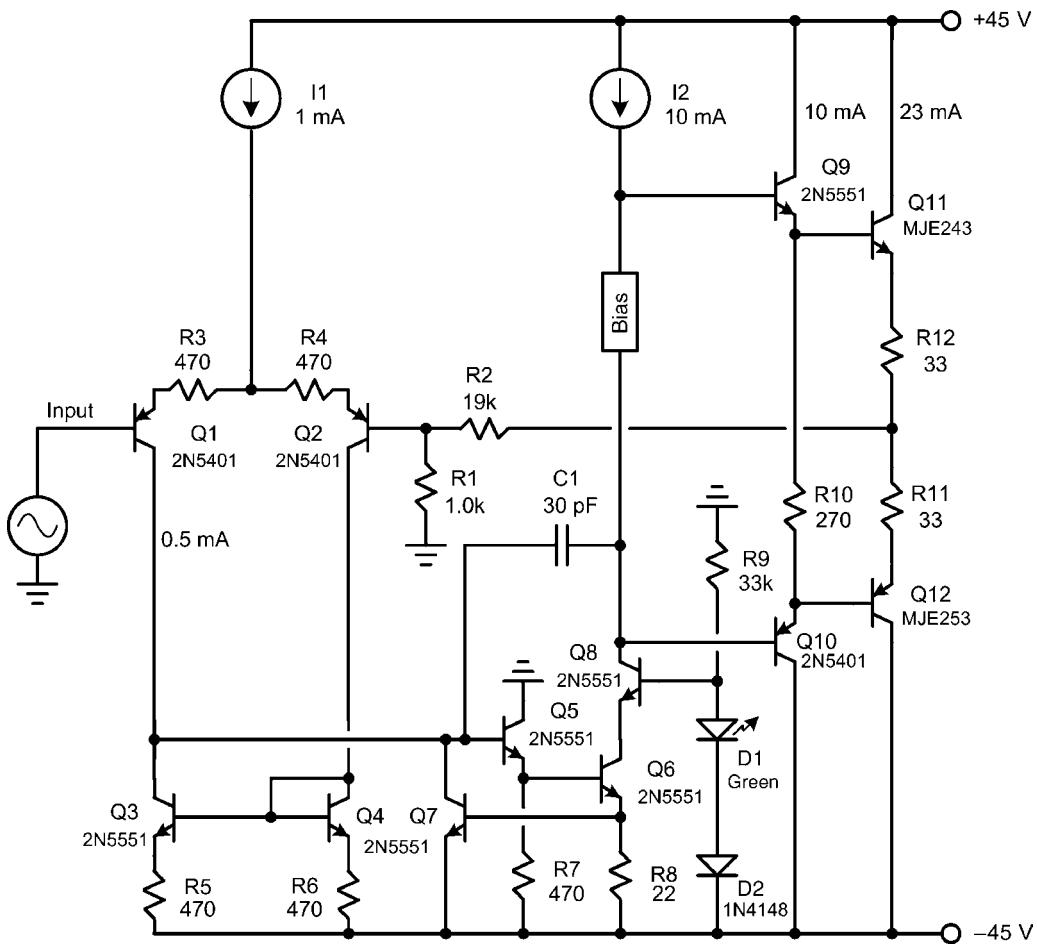
FIGURE 7.2   An improved single-ended IPS-VAS.

stage, the VAS transistor is operating at high current and has high transconductance. Such signal-dependent changes in transconductance lead to open-loop gain variations that are dependent on the signal in such a way as to cause second harmonic distortion. The degeneration of the VAS mitigates this problem but does not eliminate it.

A VAS design in which the Early effect can play a significant role will suffer second harmonic distortion from the Early effect as well, since the current gain and output impedance of the VAS will depend on the output signal voltage.

Perhaps the single biggest improvement that can be made to the VAS is to make it push-pull, replacing the current source load with a second common emitter VAS transistor that is driven with a signal of polarity opposite to that driving the first VAS transistor. This makes the VAS symmetrical, providing equal sourcing and sinking current capabilities and canceling most effects that create second harmonic distortion. The transconductance of the VAS is doubled because it becomes the sum of the transconductances of the positive and negative VAS transistors. When one transistor's *gm* is
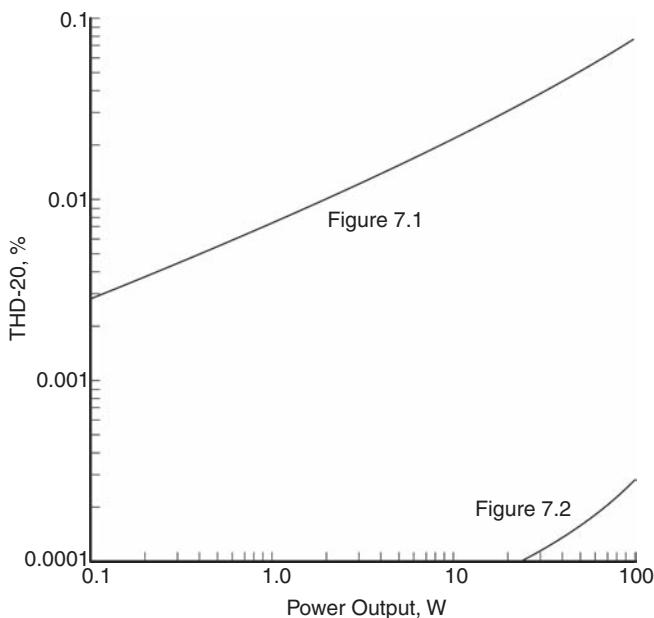
FIGURE 7.3 THD-20 as a function of output power for the VAS circuits of Figures 7.1 and 7.2.

high, the *gm* of the other one is low. For a given quiescent current, the maximum available VAS output drive current is doubled.

Most of the IPS-VAS variations that will be seen in this chapter simply reflect different approaches to delivering the necessary drive signal to the added complementary VAS transistor.

Opportunities for Further Improvement

Many variations on the IPS and VAS are possible. Some provide improved symmetry and performance, while others bring functional features like Baker clamps to control clipping behavior. Others simply represent alternative approaches to the IPS-VAS that some believe sound better or are more immune to things like EMI ingress.

Input Stage Stress

Input stage distortion cannot be ignored. Some IPS-VAS architectures will increase or decrease the susceptibility of the amplifier to distortion that originates in the IPS. Perhaps the most well known effect is high-frequency distortion caused by increased error signal input amplitude at high frequencies. This distortion is associated with *transient intermodulation distortion* (TIM) and *slewing-induced distortion* (SID) [1, 2, 3, 4]. Input stage distortion is reduced, but not eliminated, by input stage degeneration.

The size of the error signal presented to the input stage is a measure of input stage stress that results in input stage distortion. For a given output signal amplitude, the input stage stress is inversely proportional to the open-loop gain for a sinusoidal signal. In a typical amplifier design with dominant pole compensation, the open-loop gain is smaller at high frequencies (like 20 kHz), leading to greater input stage stress. At low

frequencies, the open-loop gain is substantially higher, leading to substantially reduced input stage stress. Amplifiers with wide open-loop bandwidth have the same open-loop gain at low and high audio frequencies and thus place just as much stress on the input stage at low frequencies as they do at high frequencies.

Amplifiers with low amounts of negative feedback (and thus low open-loop gain) across the audio band subject the input stage to correspondingly greater input stage stress. Amplifiers with no global negative feedback have open-loop gain simply equal to the amplifier gain; this means that the full amplitude of the line level input signal is applied to the input stage, creating the greatest stress and demanding the design of an input stage that is very linear up to high input signal levels. This requires an input stage with very high dynamic range.

There is one caveat to the above observations. The error signal applied to the input stage in amplifiers with high open-loop gain at low frequencies is essentially a differentiated version of the input signal. If the amplifier is driven with a square wave, the peak error signal under some conditions can approach the peak-to-peak value of the input signal, implying an error signal swing that could in theory be twice as large as the case where open-loop gain was uniform across the bandwidth to which the square wave is limited.

7.2   JFET Input Stages

A popular alternative to the BJT input differential pair is the JFET input pair. This choice has advantages and disadvantages. Many believe that the sound is better while others believe that its superior resistance to input EMI is important. JFETs usually have increased input referred voltage noise, but in power amplifier applications this is not a serious issue due to the line-level signal voltages involved. Moreover, JFETs have virtually no input current noise. When a BJT-LTP is degenerated to the same transconductance as a JFET (to help slew rate, for example), the noise contributed by the emitter degeneration resistors will often increase the input voltage noise of the BJT stage to be similar to that of the JFET stage.

In the strictest sense, the *gm* of a JFET-LTP is not as linear as that of a BJT-LTP degenerated to the same low value of transconductance. However, the cutoff characteristic of a BJT pair is much sharper. Figure 7.4 shows a comparison of the differential pair transfer characteristic for BJT and JFET input pairs that have the same small-signal transconductance. For the JFET differential pair, the device is the Linear Systems LS844 operating with a tail current of 2 mA and with *gm* of about 2.0 mS for each transistor. The BJT-LTP operates at a tail current of 1 mA and is degenerated by a factor of 10 with 470-Ω emitter resistors to bring its transconductance down to the same 2 mS. Both LTPs are loaded with a current mirror.

Figure 7.5 shows THD-1 as a function of signal level for the same two input stages. The bottom two traces show the sum of fifth- and seventh-order harmonics for these stages, giving an idea of the relative levels of the less benign higher-order harmonics.

The JFET has the advantage of extremely high input impedance and essentially no input bias current, but sometimes its higher input offset voltage detracts from the advantage of no input bias current. Because JFETs do not need a relatively low-value return resistor for bias, they simplify the DC offset design of the input stage, even when DC servos are employed. The ability to employ large-value return resistors results in an amplifier that can have inherently higher input impedance and employ a much smaller input coupling capacitor.
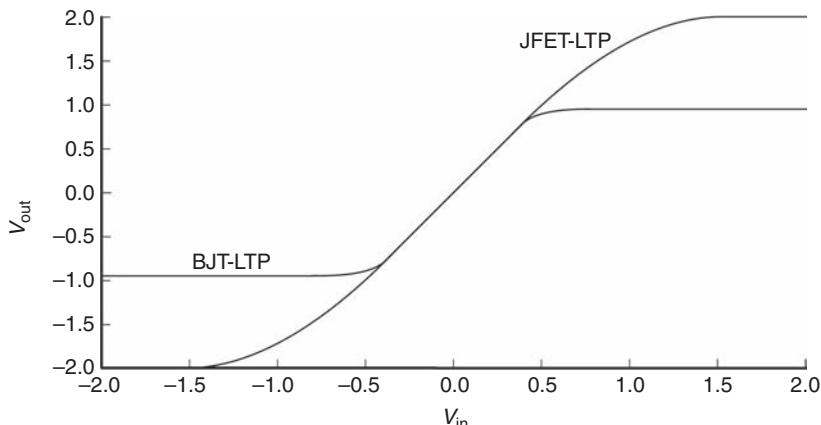
FIGURE 7.4   Transfer characteristics for BJT and JFET differential pairs with the same transconductance.
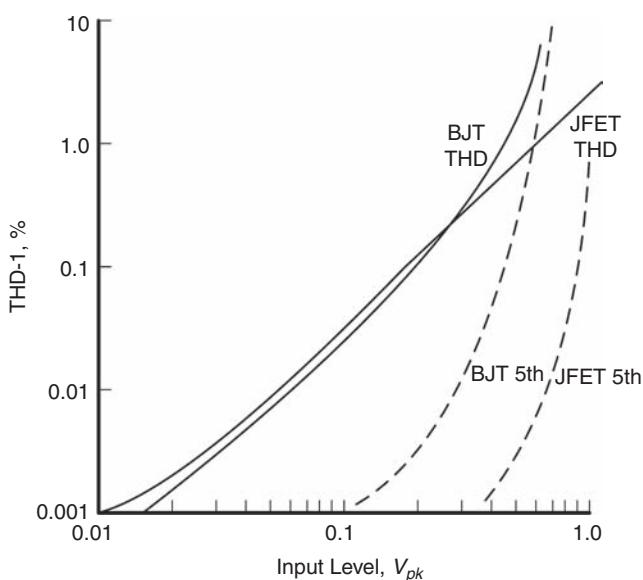
FIGURE 7.5   THD-1 for the input stages of Figure 7.4.

JFET Transistors

JFETs operate on a different principle than BJTs. Picture a bar of n-type doped silicon connected from source to drain. This bar will act like a resistor. Now add a pn junction somewhere along the length of this bar by adding a region with p-type doping. This is the gate. As the p-type gate is reverse biased, a *depletion region* will be formed, and this will begin to pinch off the region of conductivity in the n-type bar. This reduces current flow. This is called a *depletion-mode* device. The JFET is nominally on, and its degree of

conductance will decrease as reverse bias on its gate is increased until the channel is completely pinched off.

The reverse gate voltage where pinch-off occurs is referred to as the *threshold voltage V_t*. The threshold voltage is often on the order of –.5V to –4V for most small-signal N-channel JFETs. Note that control of a JFET is opposite to the way a BJT is controlled. The BJT is normally off and the JFET is normally on. The BJT is turned on by application of a forward bias to the base-emitter junction, while the JFET is turned off by application of a reverse bias to its gate-source junction.

The reverse voltage that exists between the drain and the gate can also act to pinch off the channel. At V_{dg} greater than V_t, the channel will be pinched in such a way that the drain current becomes self-limiting. In this region the JFET no longer acts like a resistor, but rather like a voltage-controlled current source. These two operating regions are referred to as the *linear region* and the *saturation region*, respectively. JFET amplifier stages usually operate in the saturation region.

JFET I_d versus V_{gs} Behavior

Figure 7.6a shows how drain current changes as a function of gate voltage in the saturation region; Figure 7.6b illustrates how transconductance changes as a function of drain current in the same region. The device is one-half of a Linear Systems LS844 dual JFET. Threshold voltage for this device is nominally about –1.8 V.

The JFET I-V characteristic (I_d versus V_{gs}) obeys a square law, rather than the exponential law applicable to BJTs. The simple relationship below is valid for $V_{ds} > V_T$ and does not take into account the influence of V_{ds} that is responsible for output resistance of the device.

$$I_d = \beta(V_{gs} - V_t)^2 \tag{7.1}$$

The equation is valid only for positive values of $V_{gs} - V_t$. The factor β governs the transconductance of the device. When $V_{gs} = V_t$, the $V_{gs} - V_t$ term is zero and no current flows. When $V_{gs} = 0$ V, the term is equal to V_t^2 and maximum current flows.

The maximum current that flows when $V_{gs} = 0$ V and $V_{ds} >> V_t$ is referred to as I_{DSS}, a key JFET parameter usually specified on data sheets. Under these conditions the channel is at the edge of pinch off and the current is largely self-limiting. In this case it is the reverse bias of the gate junction with respect to the drain that is pinching off the channel. The parameter β is the transconductance coefficient and is related to I_{DSS} and V_t. The value of I_{DSS} for the LS844 is about 3.1 mA, and the value of β is about 0.9 mA/V^2.

$$\beta = I_{DSS}/V_t^2 \tag{7.2}$$

The parameter β can also be expressed in mS/V; this means that if *gm* is plotted as a function of V_{gs}, a straight line will result. With some manipulation of Eq. 7.1, it can be seen that the transconductance of the JFET is proportional to the square root of the drain current.

$$gm = 2\sqrt{\beta I_d} \tag{7.3}$$

This is different from the behavior of a BJT, where *gm* is proportional to collector current. Transconductance for a JFET at a given operating current is smaller than that of a BJT by a factor of 10 or more in many cases. The transconductance for the LS844 at
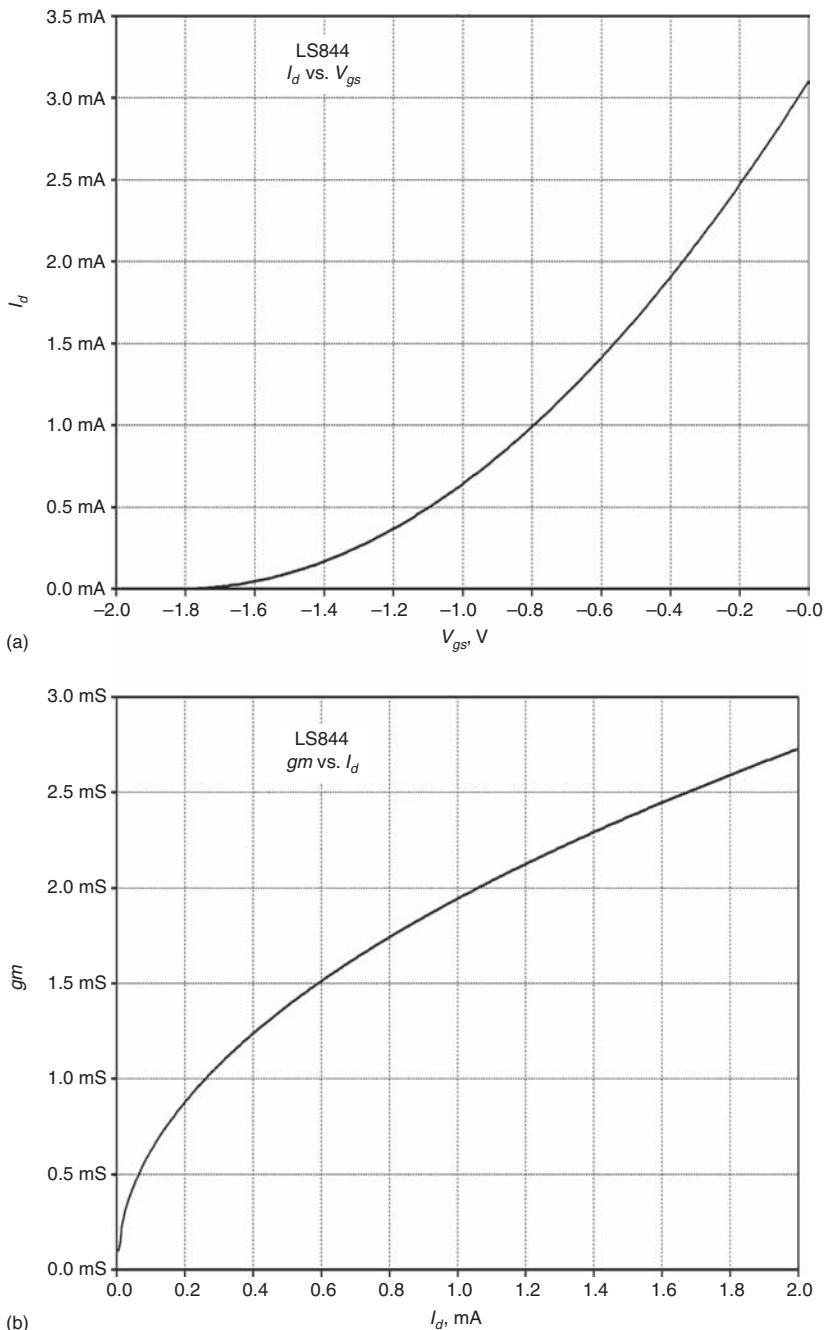
Figure 7.6 (a) JFET drain current as a function of gate voltage. (b) Transconductance as a function of drain current.

I_d = 1 mA is about 2 mS. The *gm* of a BJT at I_c = 1 mA is about 40 mS, greater by a factor of 20. The larger LSK389 has V_t = −0.54 V, I_{DSS} = 8.4 mA, and *gm* of 11.3 mS at 1 mA.

The JFET turn-on characteristic is much less abrupt that that of a BJT. Absent degeneration of a BJT, the input voltage range over which the JFET is reasonably linear is much greater than that of a BJT. The collector current of the BJT increases by a factor of about 2 for every increase of 18 mV in V_{be}. Between 0.75 mA and 1.5 mA, V_{gs} of an LS844 changes by about 370 mV.

JFET RFI Immunity

When operating in the quiescent state, the gate-source junction of the JFET is typically reverse biased by a volt or two. In contrast, the base-emitter junction of the BJT is forward biased by about 600 mV. This means that the latter is more prone to rectification effects at its base-emitter junction, making the un-degenerated BJT far more prone to RFI pickup, demodulation, and intermodulation. A degenerated BJT is less prone to this effect because it has a higher signal overload voltage as a result of the emitter degeneration.

Voltage Ratings

JFETs often do not have as high a voltage rating as BJTs, and this sometimes requires that JFET input stages be cascoded. The LSK389, for example, has maximum V_{ds} of only 40 V. Most of the voltage drop required in an IPS can be accommodated by the addition of BJT cascode transistors. Figure 7.7 illustrates a JFET-IPS that can handle the rail voltages encountered in a typical power amplifier. Each LS844 JFET is operated at a drain current of 1 mA, and its drain is loaded by a BJT cascode whose bases are biased at +15 V.
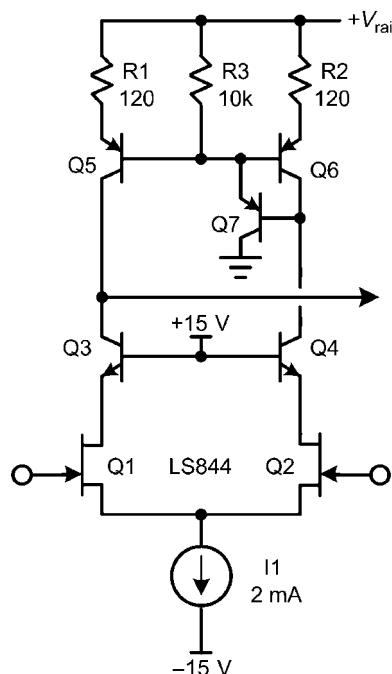
Figure 7.7 A cascoded JFET input stage.

The JFETs employed are the Linear Systems monolithic dual-matched LS844 devices. These devices are matched to within ±5 mV and have typical input-referred noise of 3 nv/$\sqrt{\text{Hz}}$. The 2-mA tail current for the JFETs is required to bring their transconductance up to that of the degenerated BJTs in Figure 7.2. This means that the Miller compensation capacitor can remain of the same value. Note, however, that slew rate will be doubled as a result of the doubled tail current for the JFETs.

JFET Input Pairs and Matching

The threshold voltages among discrete JFETs can be quite different, so it is virtually mandatory to employ monolithic dual-matched pair devices. While discrete P-channel JFETs are readily available, dual-matched pairs like the Toshiba 2SK389/2SJ09 are scarce and largely no longer in production. That is why the IPS-VAS of Figure 7.7 is upside down from the BJT version of Figure 7.2. N-channel matched JFET pairs are better performing and much more readily available.

Some IPS-VAS circuits use a full-complementary IPS-VAS with two pairs of JFET-LTPs, one N-channel, and one P-channel. The scarcity of P-channel matched pairs makes this kind of IPS difficult to build in practice. It is also true that the P-channel matched pairs, when available, may not be well matched to the N-channel complements for transconductance at a given operating current.

7.3   Complementary IPS and Push-Pull VAS

The VAS designs illustrated in Chapter 3 were all of a single-ended drive nature, where the large voltage swing at the output of the VAS was developed by a common-emitter stage loaded by a constant current source. In those examples, the maximum amount of pull-up current on the VAS output node was limited to the value of the current source, which in turn was equal to the idle current of the VAS. The pull-down current would not be limited in the same way. The collector current of the VAS transistor would be smaller when the output node was being pulled up and larger when the output node was being pulled down. This in turn meant that the transconductance of the VAS transistor would be different under these two conditions. This asymmetrical structure and behavior of the VAS can lead to second harmonic distortion and other performance impairments.

The push-pull VAS addresses these limitations by employing active common-emitter VAS transistors of each polarity, one pulling up and one pulling down. Such a symmetrical architecture has many advantages. Twice the peak drive current is available for a given VAS quiescent current and the symmetry suppresses the creation of second harmonic distortion.

The key challenge with the push-pull VAS is how to drive the two common-emitter VAS transistors, one referenced to the positive rail and the other referenced to the negative rail. In the approaches described in this section, two input pairs are employed, one a PNP-LTP and one an NPN-LTP. P-channel and N-channel JFET-LTPs can be used also. The PNP-LTP provides drive to the NPN-VAS transistor on the bottom while the NPN-LTP drives the PNP-VAS transistor on the top. A simplified version of an IPS-VAS using this approach is illustrated in Figure 7.8.

Each LTP is powered by its own tail current source. Twin Miller compensation capacitors are employed; one feeds back to the input of each polarity of VAS transistor. Many amplifiers have been designed with arrangements like this one. It is an elegant
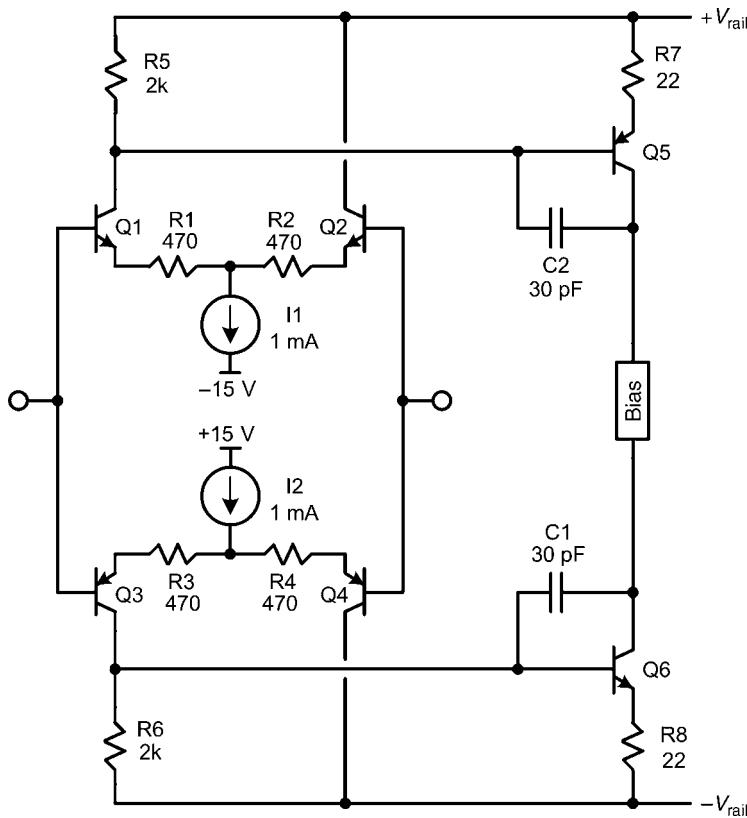
FIGURE 7.8   Complementary IPS-VAS circuit.

way to drive a push-pull VAS and, if nothing else, has appealing symmetry on the schematic. Many of the usual IPS-VAS improvements can be applied to the arrangement of Figure 7.8, such as Darlington-connected VAS transistors.

Complementary IPS with Current Mirrors

We saw in Chapter 3 the great improvement that resulted from employing current mirror loads on the IPS-LTP. Such an approach is illustrated in Figure 7.9. Here there is a current mirror on top driving the PNP-VAS transistor and another current mirror on the bottom driving the NPN-VAS transistor. Both current mirrors enable the input stage to provide high gain, especially given that both of the VAS transistors employ a Darlington connection. Look at the circuit and see if you can calculate the VAS quiescent current from the components and currents shown. You can't. That is the problem with this circuit. The VAS quiescent current is indeterminate. This is not a practical and reliable circuit. Some means must be introduced to establish some reliability with the VAS bias current. Such a means will cause the output voltage of the current mirror to be at a defined level when the LTP is in balance.

One approach to solving this problem is illustrated in Figure 7.10. First notice that each current mirror has had a *helper transistor* added to it (Q13, Q14). This is little more than an emitter follower that supplies the base current for the current mirror transistors,
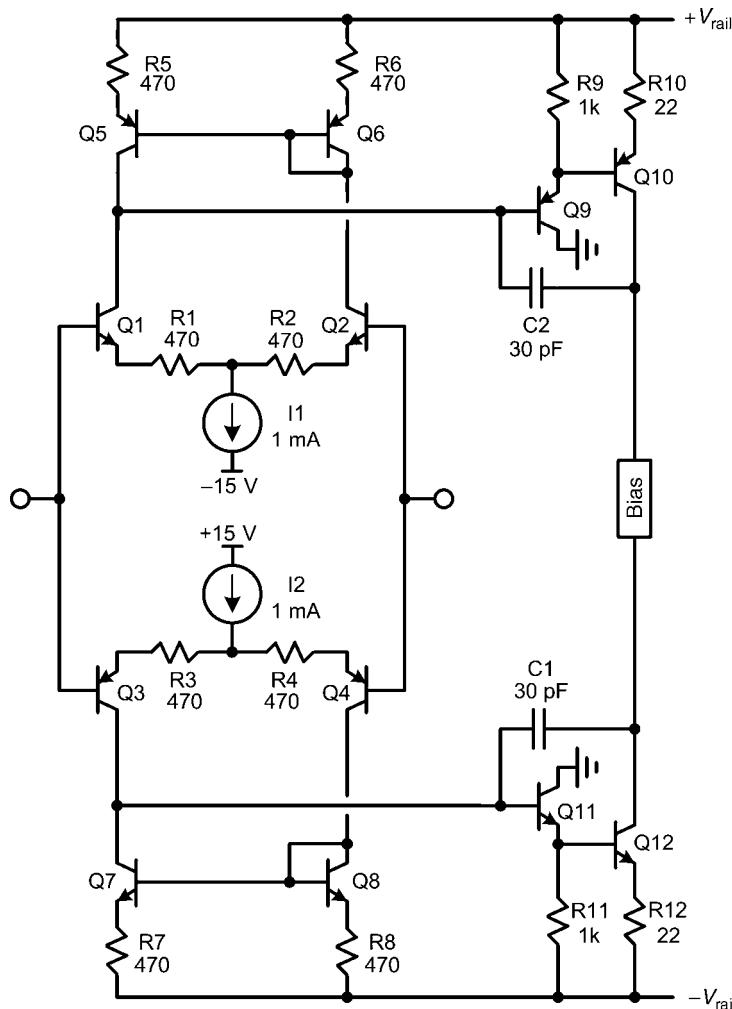
FIGURE 7.9 Complementary differential input stage with current mirror loads suffers quiescent bias instability.

rather than having it drained from the incoming current. This improves DC balance of the current mirror and greatly decreases the influence of transistor beta on its operation.

Notice also that the helper transistor separates the voltage at the current mirror input (collector of Q6) by one additional V_{be} from the rail. This puts that voltage $2V_{be}$ plus the drop across R6 away from the rail. This happens to be the same voltage drop from the rail as exists at the input to the Darlington VAS transistor if V_{be} drops are the same and amount of degeneration voltage drop is the same.

Resistor R14 connected across the collectors of Q1 and Q2 accomplishes the remainder of solving the problem. When the LTP is in balance, no current flows through R14; the voltage on both sides is the same. The voltage at the emitter of the VAS transistor then becomes approximately the same as the voltages at the emitters of the current mirror transistors, which are set by the LTP tail current. It is easily seen that the quiescent current of the VAS is now established so that it depends directly on the tail current in the LTPs.
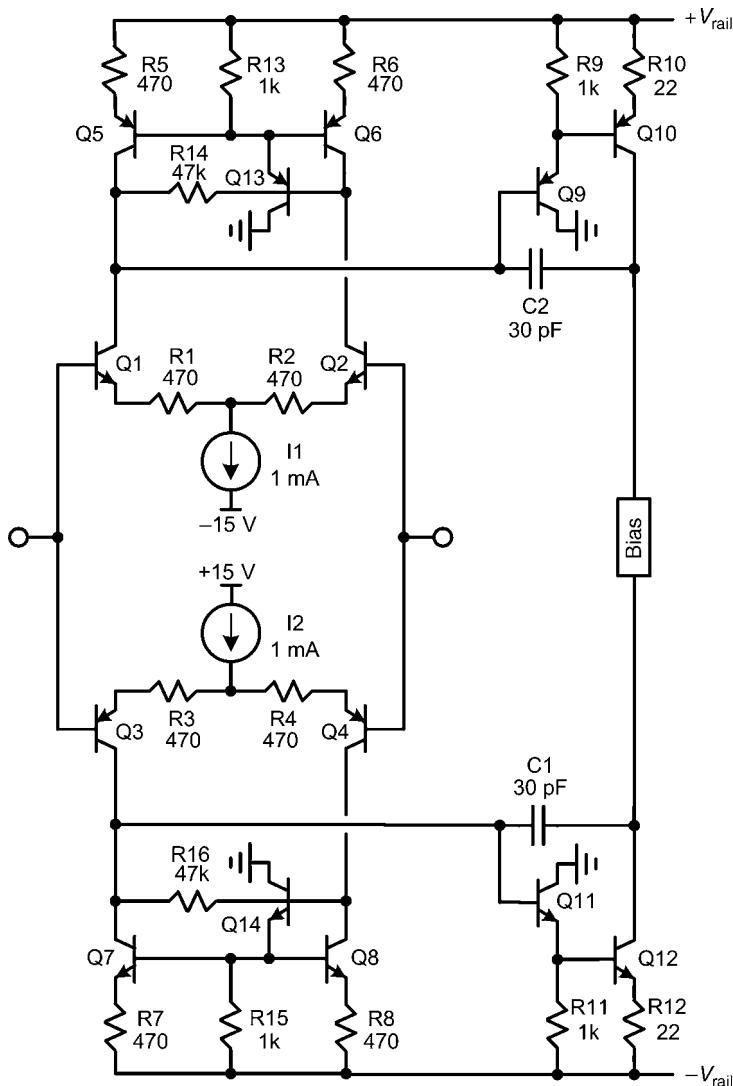
Figure 7.10 Complementary differential input stage with stabilized current mirror loads.

The price being paid here is a slight reduction in the gain of the input stage. It is differentially loaded by R14 instead with very high indeterminate impedance set by transistor betas. The effective load resistance is half the value of R14, since the current flowing through R14 is recirculated through the current mirror to further oppose voltage change at the output of the current mirror. The value of the differential shunt resistor can be quite high if well-balanced circuitry is used with precision resistors.

This circuit is sensitive to differences in the tail currents for the NPN and PNP LTPs. It can be seen that any such difference will attempt to set a different quiescent current for the top and bottom halves of the VAS. This cannot be, so an input offset voltage will be created for the overall stage that forces the top and bottom VAS transistors to operate at the same current.

Complementary IPS with JFETs

Many fine amplifiers have been made with the complementary IPS using JFETs, as illustrated in Figure 7.11. All of the same approaches and caveats apply. The JFET-LTPs are cascoded to keep the drain voltages of the JFETs at suitable levels.

There are two concerns that apply with complementary JFET input stages. First and foremost, P-channel dual-matched JFETs are very difficult to find. Few, if any, are still in production as of this writing. Secondly, the transconductance of the P-channel pair does not match that of the N-channel pair at the same operating current without painstaking selection of devices.

Complementary IPS circuits do not perform well if the transconductances of the top and bottom halves are not well matched; each half will have different gain, and the top and bottom parts of the VAS will tend to fight each other. This results in second harmonic distortion. This is especially so if twin Miller compensation capacitors are used as shown. Each compensation capacitor creates a shunt feedback loop that makes the
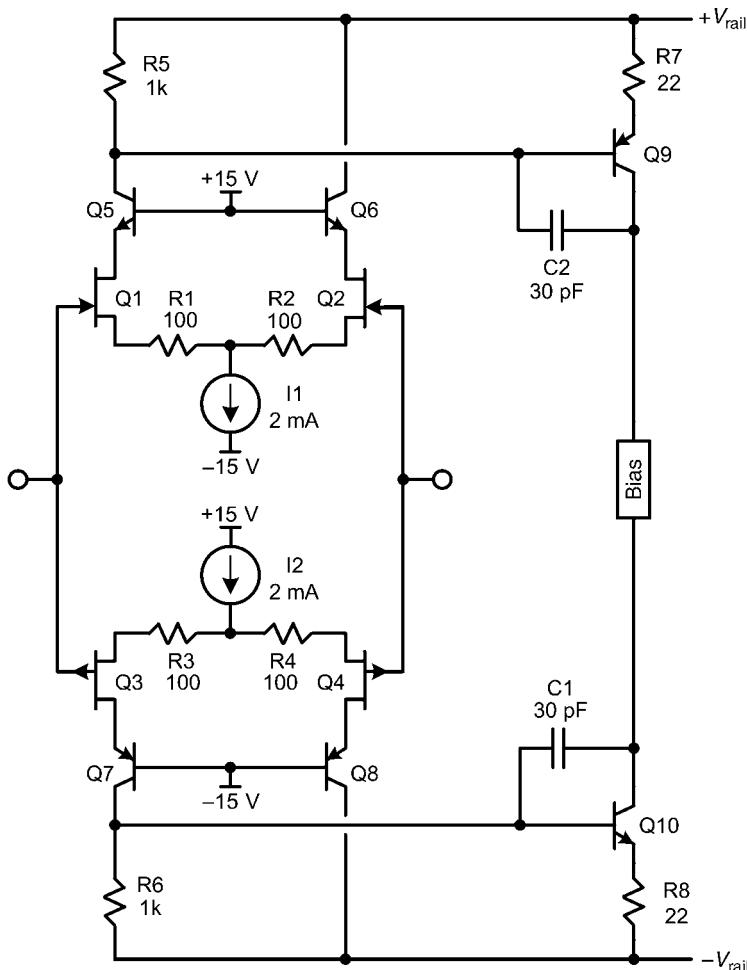
Figure 7.11   Complementary differential input stage with JFETs.

output impedance of its half of the VAS low. Two low-impedance sources connected in parallel (the top and bottom halves of the VAS) will fight each other unless each one is trying to put out the exact same voltage as the other one. If the transconductances of the top and bottom LTPs are not the same, this condition will not be satisfied. Optional emitter degeneration resistor pairs R1-R2 and R3-R4 can be set to different values in order to better equalize the transconductances of the top and bottom LTPs.

Floating Complementary JFET-IPS

An elegant complementary JFET-IPS popularized by John Curl floats the complementary differential pairs. An arrangement like this is shown in Figure 7.12. This design takes advantage of the depletion mode biasing of the JFETs to create what is effectively a floating common current source for the N-channel and P-channel LTPs. The sum of the V_{gs} voltages of the top and bottom JFET pairs at the chosen operating current is forced to
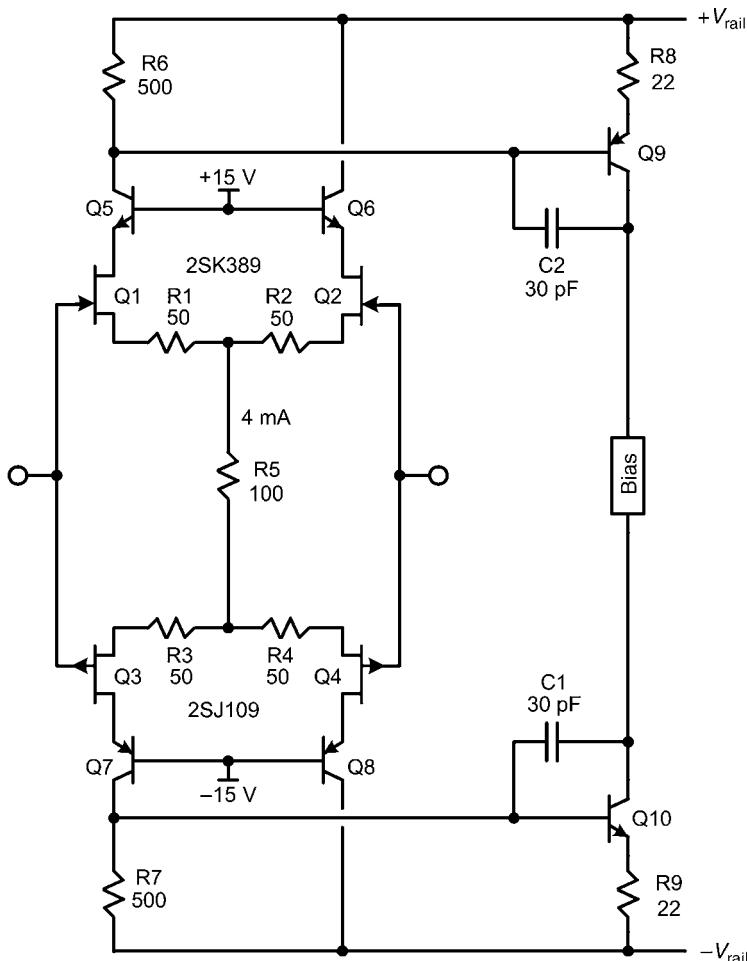
FIGURE 7.12   Complementary differential input stage with floating JFETs.

appear across bias resistor R5 connecting the two pairs, thus establishing the tail currents, which will be equal. Optional source degeneration resistor pairs R1-R2 and R3-R4 can be used to help equalize top and bottom LTP transconductances. The resistances of any degeneration resistors must be taken into account in choosing the value of R5.

The tail current in this design will depend directly on the threshold voltages of the JFET pairs, so some selection or adjustment of R5 may be necessary to arrive at the desired tail current.

Complementary IPS with Unipolar JFETs

The relative unavailability of P-channel dual-matched JFETs makes it tempting to pursue an input stage which uses only N-channel JFETs but which still is able to create output signal currents that face both upward and downward.

This is made possible by the circuit shown in Figure 7.13. The N-channel JFETs (Q1, Q2) still act as a differential pair in the upward direction, but their source currents are *harvested* with a pair of PNP cascode transistors in their source circuit (Q3, Q4). The collector currents of these cascode transistors flow downward to a current mirror to drive the NPN-VAS transistor. Resistors R1 and R2 provide the degeneration. If one assumes that the base line connecting Q3 and Q4 floats, it is easy to see that the differential input voltage creates a current that flows through the loop created by Q1, R1, Q3, Q4, R2, and Q2.

The key to making this arrangement work is to get the right bias currents to flow without interfering with common mode rejection. This involves properly generating the voltage at the interconnected bases of Q3 and Q4. This voltage must float with the common mode input voltage and be offset downward by the proper amount to establish the desired bias current. Transistors Q5 and Q6 perform this function.

Q5 and Q6 are emitter followers whose output is summed by R3 and R4 to form a replica of the common-mode voltage. This replica is applied to the bases of Q3 and Q4. Current source I1 provides the necessary pull-down bias current for the emitter followers. Notice that the V_{be} drops of Q3 and Q5 cancel each other, as do those of Q4 and Q6. As a result, the voltage drop across R1 and R3 are equal if all V_{be} drops are equal. Likewise, the voltage drop across R2 is the same as that across R4. The DC voltage drops across R1 and R2 set the bias current, and the drop across R3 and R4 is controlled by current source I1. If R3 and R4 equal R1 and R2, then the bias current flowing in Q1 will be equal to one-half I1. Current I1 is the "tail current" of the arrangement.

The arrangement is completed with upper cascode transistors Q7 and Q8. Current mirrors at the top and bottom (Q9, Q10, Q11 and Q12, Q13, Q14) provide the loading. R11 and R12 provide differential loading on the current mirror outputs to provide VAS quiescent current stability.

7.4   Unipolar Input Stage and Push-Pull VAS

The relative scarcity of complementary JFET pairs also makes it desirable to have designs that require only a conventional LTP of one polarity (usually N-channel JFET) while still being able to drive a push-pull VAS. The key to achieving this is how to *turn around* the signal drive for the opposite side of the VAS. Tom Holman's *APT-1* power amplifier is a good example of this design approach (wherein NPN BJT devices were used) [5].

Figure 7.14 shows such an approach where a current mirror (Q5, Q6) is used to generate the drive signal for the NPN-VAS transistor. The signal current from one side of
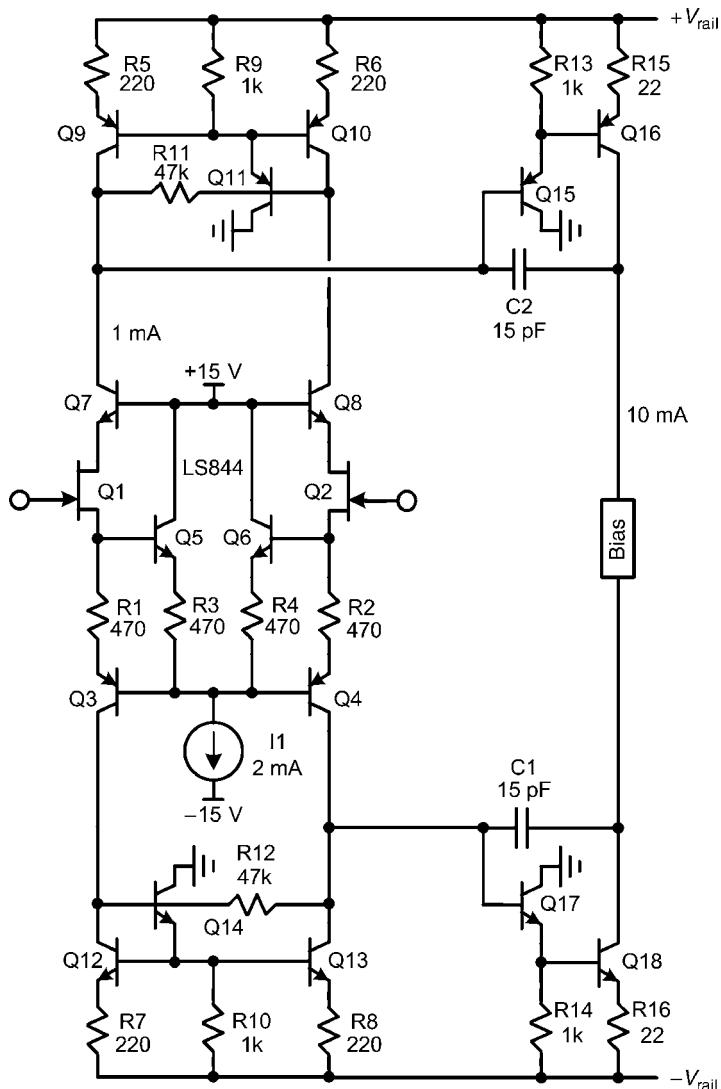
Figure 7.13   Complementary IPS with N-channel JFETs.

the LTP output is reflected down to the negative rail where it is used to drive the NPN-VAS transistor. A cascode transistor is placed in the path of the reflected current so as to reduce quiescent voltage on Q6. This architecture does not appear to lend itself well to the use of LTP current mirror loads in the way that they were employed in some earlier arrangements.

Differential Pair VAS with Current Mirror

A slightly different approach is illustrated in Figure 7.15. Here the PNP VAS is actually a differential pair. It is fed from an IPS with a current mirror load, so high gain and good
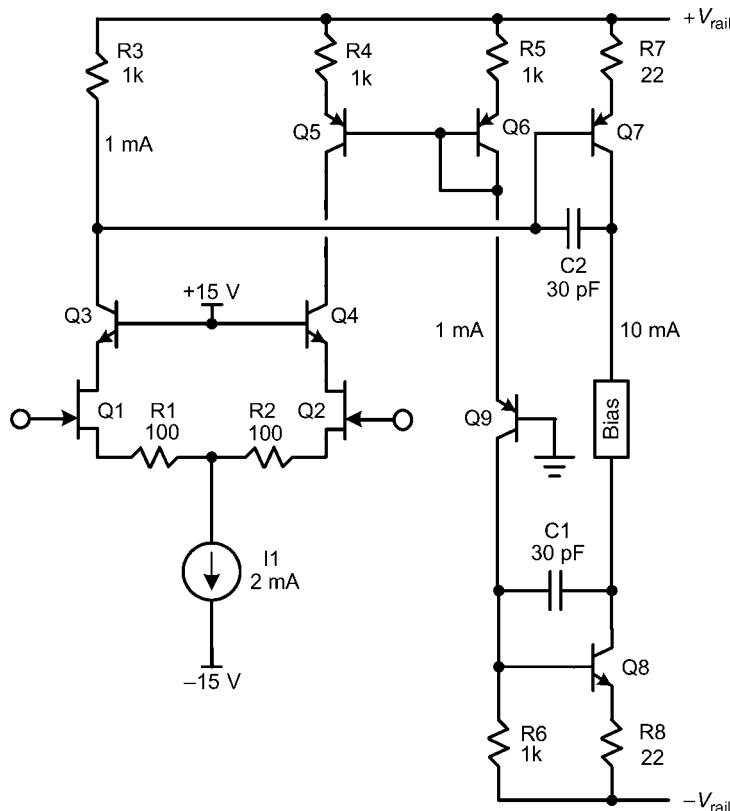
Figure 7.14 N-channel input stage with complementary VAS.

DC balance is achieved in the IPS. The VAS LTP is fed from both outputs of the IPS, but because of the current mirror arrangement only the IPS output from Q3 has significant voltage movement. The IPS output from Q4 acts as a voltage reference for the other input of the VAS LTP. Diodes D1 and D2 prevent the current mirror transistors from saturating when the amplifier clips. The PNP VAS LTP (Q10, Q11) is preceded by NPN emitter followers Q8 and Q9. Their V_{be} drops cancel those of the LTP transistors. The LTP is powered by twin current sources and its gain is set by R8 connected between the emitters of Q10 and Q11. The twin current source arrangement helps conserve voltage headroom because the VAS bias current does not flow through the emitter degeneration resistance.

The bottom half of the VAS is formed by a current mirror (Q13, Q14, Q15). A cascode (Q12) is situated in the path of the current from Q10 to the current mirror to share the voltage drop that spans both supply rails. Conventional Miller compensation is provided by C1 connected from the collector of Q11 to the base of Q9. A further advantage of this design is that the VAS is naturally current limited; it can never sink or source more than the total amount of its LTP tail current.

IPS with Differential Current Mirror Load

A more advanced form of unipolar IPS-VAS front end is shown in Figure 7.16. This arrangement was used in Ref. 6. The key advantage of this circuit is that it allows the
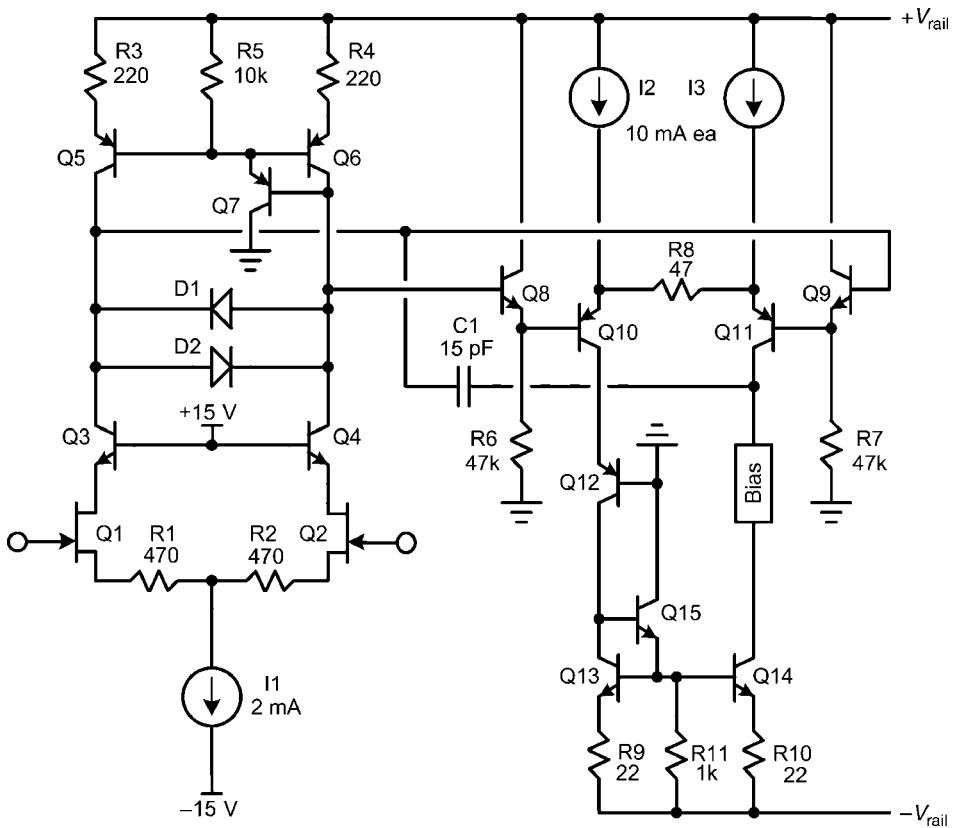
FIGURE 7.15   Differential pair VAS with current mirror load.

use of a balanced current mirror structure to load the input stage. The differential current mirror exhibits very high impedance in the differential mode, but rather low impedance in the common mode. It thus provides some additional common-mode rejection. The primary elements of the differential current mirror are current sources Q5 and Q6. Emitter followers Q7 and Q8 jointly act as the current mirror helper transistors, creating and feeding back a common mode voltage to control current sources Q5 and Q6. The emitter followers also buffer the differential signal before application to the VAS LTP.

The differential current mirror establishes a well-defined common-mode voltage level to be applied to the VAS LTP. This, combined with the differential drive of the LTP, allows the use of a simple resistor tail for Q9 and Q10. The VAS in Figure 7.16 also employs cascodes Q11 and Q12, suppressing the Early effect and allowing the use of fast, low-voltage transistors for Q9 and Q10. The bias voltage provided for the cascodes is also used to power emitter followers Q7 and Q8, again allowing the use of fast, low-voltage transistors. A similar approach is used for the cascoded current mirror Q14-Q17.

Diodes D1 and D2 clamp the IPS differential output voltage to prevent saturation of Q5 and Q6 when the amplifier clips. This IPS-VAS is best used with *Miller input compensation* (MIC) as implemented by C1 and R18. MIC will be described in Chapter 9. The series R-C network across the IPS collectors (C2 and R5) provides some lag-lead frequency compensation for the high-impedance intermediate nodes between the IPS and
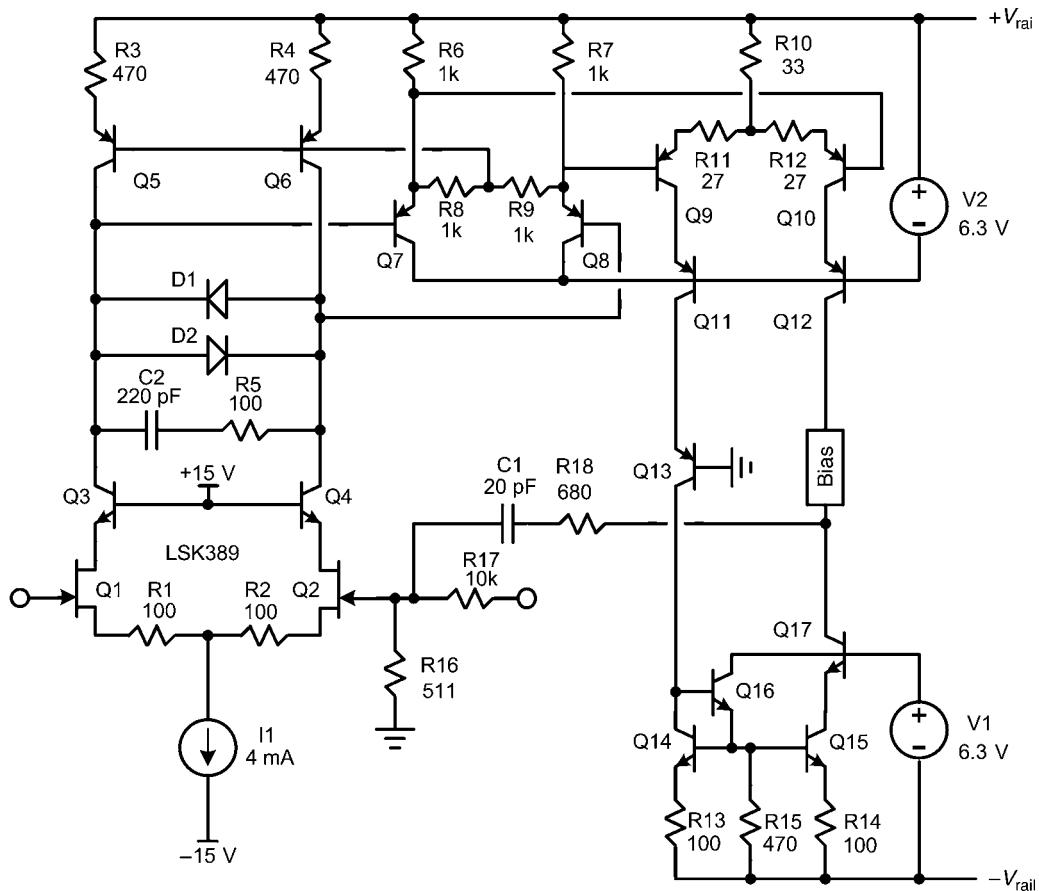
Figure 7.16   Input stage with differential current mirror load.

VAS. This compensates the local MIC feedback loop. In some MIC implementations an additional series R-C network is required from the VAS output to ground.

7.5   Input Common Mode Distortion

In the customary noninverting amplifier configuration the full line-level input signal is applied to the input stage as a common mode signal. This can create distortion in a number of ways. Since this distortion makes itself apparent as an effective input-referred differential signal at the input stage, negative feedback cannot reduce it.

One source of common-mode distortion can originate in the tail current source. A cascoded current source can reduce this contributor. Another problem can arise from the Early effect in the LTP transistors. At high frequencies the nonlinear collector-base capacitance of the LTP transistors can also introduce common-mode distortion, especially if the impedances of the networks driving the LTP are not very low. An IPS with a single-ended output and not loaded by a current mirror is more vulnerable to common-mode distortion. In some cases JFETs may be more susceptible to common-mode distortion than BJT devices.
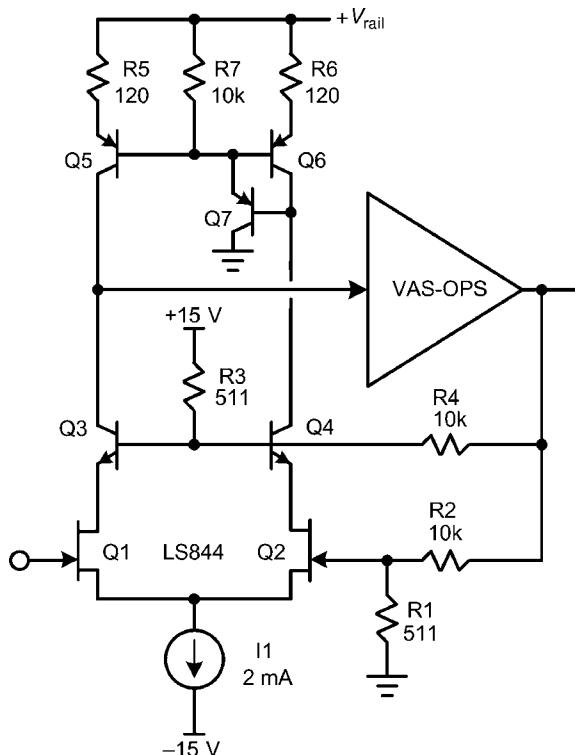
FIGURE 7.17   N-channel input stage with driven cascode.

Input common-mode distortion can be reduced with a *driven cascode*. Figure 7.17 shows how an input stage cascode can be driven with a replica of the common-mode signal, making the collector-base voltage of the LTP transistors constant, independent of signal. The replica is formed by passing the amplifier output signal through a second feedback network formed by R3 and R4. Other approaches to generating the common-mode signal for driving the cascode are also possible. For example, the tail signal of the LTP can be buffered and level shifted as needed.

7.6 Early Effect

As discussed in Chapters 2 and 3, the current gain of a transistor is mildly dependent on the collector voltage. This leads to a finite output resistance in a common-emitter stage, and unfortunately this resistance is nonlinear. It was shown that the use of a cascode VAS greatly reduces this effect, but does not eliminate it completely. The usual cascode fixes the potential at the collector of the common-emitter stage, so that signal voltage at the base still modulates V_{bc}.

There is also the Early effect at the input to the driver or predriver transistors of the output stage. This is because the base-collector voltage of the driver transistor is modulated by the signal, and thus its beta is influenced via its Early effect. The bias current flowing through the driver, even if constant, will result in a changing base current for

the driver. The shunt feedback provided by the usual Miller compensation will reduce the output impedance of the VAS, and this will also reduce the influence of the Early effect.

7.7   Baker Clamps

When amplifiers are overdriven, they will clip. How cleanly they clip can have an effect on the sonic performance of the amplifier. How often amplifiers clip depends on many factors, not the least of which include loudspeaker efficiency and the crest factor of the program material being played. In some cases, amplifiers may clip more often than we think. When they do, it is important that they clip cleanly.

In the VAS circuits we have seen thus far, if the amplifier is driven to clipping, the VAS transistor will almost certainly go into saturation. This occurs when the collector voltage goes so low that the base-collector junction becomes forward-biased. Transistors tend to be slow to come out of saturation, and this can lead to a phenomenon called *sticking*.

A Baker clamp is a diode-based circuit that prevents the signal excursion from going far enough to allow the protected transistors to saturate. A Baker clamp can be as simple as a diode connected to a fixed voltage reference. Baker clamps and related circuitry to control amplifier behavior in the real world are discussed in Chapter 17.

7.8   Amplifier Noise

This section is not intended to be a thorough coverage of noise, but rather to introduce a basic understanding of it. Although the noise characteristics of a power amplifier are not as critical as those of a preamp, it is still important to achieve low noise because there is no volume control in the power amplifier to reduce noise from the input stage under normal listening conditions. This is particularly so when the amplifiers are used with high-efficiency loudspeakers. Here we will explore the way in which noise is governed by the circuits and discuss ways to minimize it.

Power amplifier noise is usually specified as being so many dB down from either the maximum output power or with respect to 1 W. The former number will be larger by 20 dB for a 100-W amplifier, so it is often the one that manufacturers like to cite. The noise referenced to 1 W into 8 Ω (or, equivalently 2.83 V RMS) is the one more often measured by reviewers.

The noise specification may be unweighted or weighted. Unweighted noise for an audio power amplifier will typically be specified over a full 20-kHz bandwidth (or more). Weighted noise specifications take into account the ear's sensitivity to noise in different parts of the frequency spectrum. The most common one used is *A weighting*, illustrated in Figure 7.18. Notice that the weighting curve is up about +1.2 dB at 2 kHz, whereas it is down 3 dB at approximately 500 Hz and 10 kHz.

Noise Power

The noise arising from different sources is usually assumed to be uncorrelated. For this reason, it adds on a power basis. This means that noise voltage adds up on an RMS basis as the square root of the sum of the squares of the various sources. Two noise sources each 10 μV RMS will add to 14.1 μV RMS. Two noise sources, one 10 μV and the other 3 μV will sum to $\sqrt{(100+9)} = \sqrt{(109)} = 10.44$ μV. This shows how a larger noise source will tend to dominate over a smaller noise source.

Noise Bandwidth

Most noise sources have a flat noise spectral density, meaning that there is the same amount of noise power in each hertz of frequency spectrum. This means that total noise power in a measurement is proportional to the bandwidth of the measurement being made. This gives rise to the concept of noise bandwidth.

A perfect brick-wall filter would have a noise bandwidth equal to its signal bandwidth. Because real filters roll-off gradually, the noise bandwidth is slightly different than the 3-dB bandwidth of a filter (often slightly more). A 12.7-kHz single-pole LPF has an *equivalent noise bandwidth* (ENBW) of 20 kHz. Conversely, the ENBW of a 20-kHz first-order LPF is 31.4 kHz. The ENBW of a single-pole roll-off is equal to 1.57 times the pole frequency. The ENBW of the *A-weighting* function is 13.5 kHz.

Noise Voltage Density

White noise has equal noise power in each hertz of bandwidth. If the number of hertz is doubled, the noise power will double, but the noise voltage will increase by only 3 dB or a factor of $\sqrt{2}$. Thus noise voltage increases as the square root of noise bandwidth, and noise voltage is expressed in nanovolts per root hertz ($nV/\sqrt{Hz}$). There are $141\sqrt{Hz}$ in a 20-kHz bandwidth. A $100\text{-}nV/\sqrt{Hz}$ noise source will produce 14.1 µV RMS in a 20-kHz measurement bandwidth.

As an aside, so-called pink noise has the same noise power in each octave of bandwidth. Pink noise is usually employed in certain test measurements. Pink noise is created by passing white noise through a low-pass filter having a 3 dB per octave roll-off slope.

Relating Input Noise Density to Signal-to-Noise Ratio

Most of the noise in an amplifier is usually contributed by the input stage or other early stages. For this reason, the noise of an amplifier is often referred back to the input. Input-referred noise is calculated by measuring the output noise and dividing it by the gain of the amplifier. A good op amp might have input-referred noise of $2\,nV/\sqrt{Hz}$.

If an amplifier has $10\,nV/\sqrt{Hz}$ of input-referred noise, what is its *signal-to-noise ratio* (SNR)? Assume that the SNR is in an unweighted 20-kHz bandwidth and that it is referred to 2.83 V RMS out. Also assume that the amplifier has a voltage gain of 20. The output noise voltage will be $10\,nV/\sqrt{Hz} * 141\sqrt{Hz} * 20 = 28.2\,\mu V$. This is 100,000 times smaller than 2.83 V, so the SNR is 100 dB.

Now consider a wideband unweighted noise measurement of the same amplifier. Assume the amplifier has a closed-loop bandwidth of 500 kHz with a single-pole roll-off. The ENBW will be 785 kHz ($886\sqrt{Hz}$), and the output noise will be 177 µV RMS. The SNR will be 16,000, corresponding to about 84 dB.

A-Weighted Noise Specifications

The frequency response of the A-weighting curve is shown in Figure 7.18. It weights the noise in accordance with the human ear's perception of noise loudness.

The A-weighted noise specification for an amplifier will usually be quite a bit better than the unweighted noise because the A-weighted measurement tends to attenuate noise contributions at higher frequencies and hum contributions at lower frequencies. A very good amplifier might have an unweighted signal-to-noise ratio of –90 dB with respect to 1 W into 8 Ω, while that same amplifier might have an A-weighted
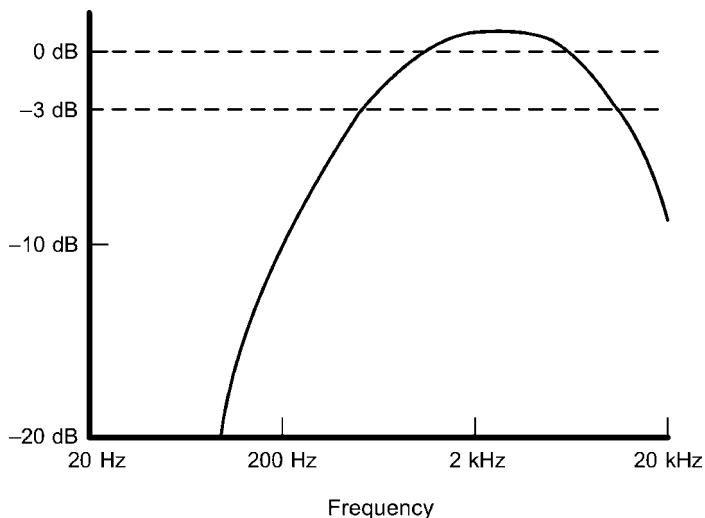
FIGURE 7.18   A-weighting frequency response.

SNR of 105 dB with respect to 1 W. A fair amplifier might sport 65-dB and 80-dB SNR figures, respectively. The A-weighted number will sometimes be 10-20 dB better than the unweighted number.

VAS Noise

The input stage is not the only source of noise in an amplifier, even though it often dominates. Later stages create noise, and their input-referred noise can be referred back to the input of the amplifier by the voltage gain that precedes them. For example, a VAS with input noise of $30\,\mathrm{nV}/\sqrt{\mathrm{Hz}}$ will contribute an amplifier input-referred noise component of $10\,\mathrm{nV}/\sqrt{\mathrm{Hz}}$ if the voltage gain of the input stage is 3. The message here is that VAS noise cannot be ignored, and may even dominate the noise in some amplifier designs. This can happen because the VAS is not usually designed for low noise and input stage gain is sometimes quite small.

Power Supply Noise

The power supply rails in any amplifier are often corrupted by numerous sources of noise. These may include random noise and other noises like power supply ripple and EMI and program-dependent noise from the output stage. The power supply noise can get into the signal path as a result of the signal circuit's limited *power supply rejection ratio* (PSRR).

There are two important ways to control power supply noise. The first is to do a better job filtering the power supply rails. This is especially effective for power supply rails that provide power to low-level circuits. The second is to employ circuit topologies that have inherently high PSRR. The ability of a circuit to reject power supply noise usually decreases as the frequency of the noise increases. In other words, PSRR degrades at high frequencies. Fortunately, it is often possible to do a more effective job of filtering the power supply rails at higher frequencies.

Resistor Noise

All resistors have noise. This is referred to as *Johnson noise* or *thermal noise*. It is the most basic source of noise in electronic circuits. It is most often modeled as a noise voltage source in series with the resistor. The noise power in a resistor is dependent on temperature.

$$P_n = 4kTB \text{ W} = 1.66 \times 10^{-20} \text{ W/Hz} \tag{7.4}$$

where k = Boltzman's constant = 1.38×10^{-23} J/°K
T = temperature in °K = 300°K @ 27°C
B = bandwidth in hertz

The open-circuit RMS noise voltage across a resistor of value R is simply

$$e_n = \sqrt{4kTRB} \tag{7.5}$$

$$e_n = 0.129 \text{ nV}/\sqrt{\text{Hz}} \text{ per } \sqrt{\Omega} \tag{7.6}$$

Noise voltage for a resistor thus increases as the square root of both bandwidth and resistance. A convenient reference is the noise voltage of a 1-kΩ resistor:

$$1 \text{ k}\Omega => 4.1 \text{ nV}/\sqrt{\text{Hz}}$$

From this the noise voltage of any resistance in any noise bandwidth can be estimated.

Shot Noise

Bipolar transistors generate a different kind of noise. This noise is related to current flow and the discreteness of current. This is called *shot noise* and is associated with the current flows in the collector and the base of the transistor. The collector shot noise current is usually referred back to the base as an equivalent input noise voltage in series with the base. It is referred back to the base as a voltage by dividing it by the transconductance of the transistor. Once again, the resulting input-referred noise is usually measured in nanovolts per root hertz.

The shot noise current is usually stated in picoamperes per root hertz ($pA/\sqrt{\text{Hz}}$) and has the RMS value of

$$I_{\text{shot}} = \sqrt{2qI_{dc}B} \tag{7.7}$$

$$I_{\text{shot}} = 0.57 \text{ pA}/\sqrt{\text{Hz}}/\sqrt{\mu\text{A}} \tag{7.8}$$

where $q = 1.6 \times 10^{-19}$ Coulombs per electron.
B = bandwidth in hertz

It is easily seen that shot noise current increases as the square root of bandwidth and as the square root of current. An 1-mA collector current flow will have a shot noise component of $18 \text{ pA}/\sqrt{\text{Hz}}$.

$$1 \text{ mA} => 18 \text{ pA}/\sqrt{\text{Hz}}$$

The transconductance of a BJT operating at 1 mA is 38.5 <u>mS</u>. Dividing the shot noise current by *gm* we have input-referred noise $e_n = 0.47\text{nV}/\sqrt{\text{Hz}}$. From Equation 7.6 we can see that this is the voltage noise of a 13-Ω resistor.

At the same time, notice that *re'* for this transistor is 26 Ω. The noise voltage for a 26-Ω resistor is $0.66\,\text{nV}/\sqrt{\text{Hz}}$. The input-referred voltage noise of a transistor is equal to the Johnson noise of a resistor of half the value of *re'*. This is a very handy relationship.

BJT Input Noise Current

The base current of a transistor also has a shot noise component measured in units of $\text{pA}/\sqrt{\text{Hz}}$. Recall that

$$I_{\text{shot}} = 0.57\,\text{pA}/\sqrt{\text{Hz}}/\sqrt{\mu\text{A}} \qquad (7.8)$$

Consider a BJT biased at 1 mA and with a beta of 100. Base current will be 10 μA. This corresponds to $3.16\sqrt{\mu\text{A}}$. Input noise current will be $1.8\,\text{pA}/\sqrt{\text{Hz}}$. Put another way, base shot noise is collector shot noise divided by $\sqrt{\beta}$.

If the base circuit includes source resistance, the base shot noise current will develop an equivalent noise voltage across that resistance. If the source impedance driving that transistor's base is 1 kΩ, then the input noise voltage due to input noise current will be $1.8\,\text{nV}/\sqrt{\text{Hz}}$.

Noise of a Degenerated LTP

Consider an LTP input stage biased with a tail current of 1 mA and degenerated with 470-Ω emitter resistors. Assume that the stage is fed from a voltage source. The noise contributions of the transistors and degeneration resistors will each be increased by a factor of $\sqrt{2}$ because there are two of each in series.

The resistor noise of each emitter resistor is $2.9\,\text{nV}/\sqrt{\text{Hz}}$. The collector shot noise current of each transistor will be $12.7\,\text{pA}/\sqrt{\text{Hz}}$. Transistor *gm* is 19.3 mS. Input-referred base-emitter noise is $0.66\,\text{nV}/\sqrt{\text{Hz}}$. Input-referred voltage noise of each half of the LTP is thus $3.0\,\text{nV}/\sqrt{\text{Hz}}$, with the degeneration resistor noise strongly dominating. Input voltage noise for the stage is 3 dB higher, at $4.2\,\text{nV}/\sqrt{\text{Hz}}$.

Now assume that the stage is fed from a 1-kΩ source. Resistor noise is $4.1\,\text{nV}/\sqrt{\text{Hz}}$. Assume that transistor beta is 100. Base current is 5 μA. Input noise current is $1.3\,\text{pA}/\sqrt{\text{Hz}}$. Input noise voltage due to input noise current is $1.3\,\text{nV}/\sqrt{\text{Hz}}$. Total input noise voltage across the input impedance is thus $4.3\,\text{nV}/\sqrt{\text{Hz}}$.

Total input noise for the arrangement is the power sum of $4.2\,\text{nV}/\sqrt{\text{Hz}}$ and $4.3\,\text{nV}/\sqrt{\text{Hz}}$, which is $6.0\,\text{nV}/\sqrt{\text{Hz}}$.

JFET Noise

JFET noise results primarily from *thermal channel noise*. That noise is modeled as an equivalent input resistor r_n whose resistance is equal to approximately $0.6/gm$ [7]. If we model the effect of *gm* as *rs'* (analogous to *re'* for a BJT), we have $r_n = 0.6rs'$. This is remarkably similar to the equivalent voltage noise source for a BJT, which is the voltage noise of a resistor whose value is *re'*/2. The noise of a BJT goes down as the square root of I_c because *gm* is proportional to I_c, and *re'* goes down linearly as well. However, the *gm* of a JFET increases as the square root of I_d. As a result, JFET input voltage noise goes down as the 1/4 power of I_d. The factor 0.6 is approximate, and SPICE modeling of the LS844 suggests that the number is closer to 0.67.

At $I_d = 0.5$ mA, *gm* for the LS844 is about 1 mS, corresponding to a resistance *rs'* of 1 kΩ. Multiplying by the factor 0.67, we have an equivalent resistance r_n of 670 Ω, which has a noise voltage of $3.4\,\text{nV}/\sqrt{\text{Hz}}$.

Noise Simulation

With an understanding of the basics of noise and the cause-effect relationships, noise analysis is best handled by SPICE simulations. In this approach, the noise contribution of every element can be evaluated by clicking on the circuit element. The base-current noise in a simulation will show up as a component of the voltage noise in the resistors that make up the source impedance to the base node.

References

1. Otala, M., "Transient Distortion in Transistorized Audio Power Amplifiers," *IEEE Transactions on Audio and Electro-acoustics*, vol. AU-18, pp. 234–239, September 1970.
2. Leach, W. M., "Transient IM Distortion in Power Amplifiers," *Audio,* vol. 59, no. 2, pp. 34–41, February 1975.
3. Jung, W. G., Stephens, M. L., and Todd, C. C. "Slewing Induced Distortion and Its Effect on Audio Amplifier Performance–With Correlated Measurement Listening Results," AES preprint No. 1252, presented at the 57th AES Convention, Los Angeles, May 1977.
4. Cordell, R. R., "Another View of TIM," *Audio*, pp. 38–49 February, & pp. 39–42 March, 1980; available at www.cordellaudio.com.
5. "The Apt 1 Power Amplifier Owner's Manual," Apt Corporation, 1979.
6. Cordell, R. R., "A MOSFET Power Amplifier with Error Correction," *Journal of the Audio Engineering Society,* vol. 32, no. 1, pp. 2–17, January 1984; available at www.cordellaudio.com.
7. Haslett, J. W., and Trofimenkoff, F. N. "Thermal Noise in Field-effect Devices," *Proceedings of the ROC. IEE,* vol. 116, no. 11, pp. 1863–1868, November 1969.

This page intentionally left blank

DC Servos

Virtually all of the discussion on power amplifiers thus far has ignored the reality of AC coupling and DC offset. The primary focus of this chapter is *DC servos*. They make up a separate global feedback loop that acts at DC to control amplifier output offset. However, it is also important to understand the origins and potential magnitudes of DC offsets in amplifiers of conventional design. Some approaches to reducing offsets in conventional designs are also discussed, and some of them are relevant to designs incorporating DC servos.

Figure 8.1 shows a simple amplifier with the usual DC blocking arrangements. The VAS and output stage are shown as an amplifier symbol. Coupling capacitor C1 blocks any DC from the source. Input return resistor R1 biases the LTP input node at about 0 V. With a 20-kΩ input return resistor, a 5-μF coupling capacitor is required to push the input cutoff frequency below 2 Hz. This capacitor should be of very high quality.

The negative feedback network includes a 20-kΩ feedback resistor (R3) and a 1.05-kΩ feedback shunt resistor (R2). These resistors set the closed-loop gain at 20. The network also includes an electrolytic capacitor (C2) in the shunt leg that allows the DC gain of the amplifier to fall to unity at DC. This prevents LTP input voltage offsets from being multiplied by the closed-loop gain of the amplifier.

The electrolytic capacitor introduces a second low-frequency roll-off with a time constant approximately equal to R2 ∗ C2. The value of C2 must be 100 μF to push this second roll-off frequency to below 2 Hz. This is why the capacitor usually must be an electrolytic type, preferably nonpolarized. The back-to-back diodes across the electrolytic prevent it from being subjected to excessive voltages in the event that the output of the amplifier becomes stuck to one rail or is otherwise driven to a large voltage for a significant period of time. A 100-W sinusoid at 2 Hz would attempt to place about 1.4 V peak across C2. Under these conditions the diodes would become forward-biased and cause distortion. Sometimes the diodes are left out for this reason. In other cases two diodes are put in series or two Zener diodes are used.

The electrolytic capacitor is problematic because it is in the signal path. Electrolytic capacitors can be notoriously nonlinear and will cause distortion. Any signal voltage appearing across the electrolytic will be distorted. At minimum, capacitance is nonlinear with voltage across the capacitor and ESR is nonlinear with current through the capacitor. Distortion from the capacitor rises at lower frequencies as a larger signal voltage appears across the capacitor. A very high-quality nonpolarized electrolytic should be used for C2. Some designers bypass C2 with a quality film capacitor. This can improve the sound, but the higher impedance of the film capacitor over much of the audio band limits its effectiveness in reducing distortion from C2.
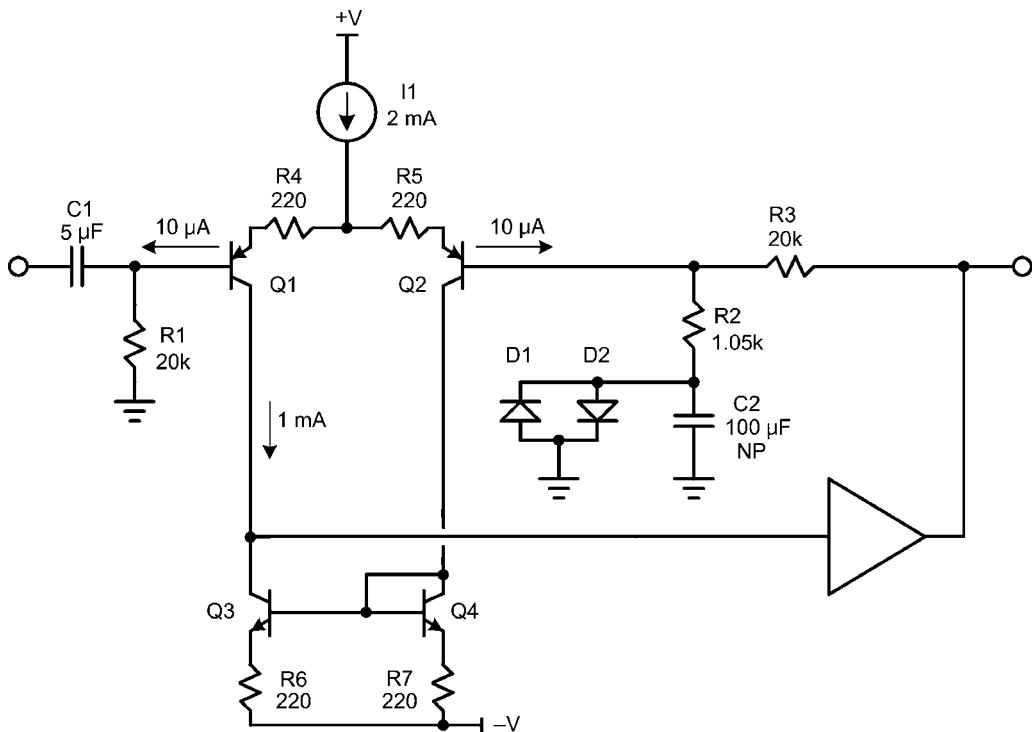
Figure 8.1 Conventional amplifier DC block arrangement.

An alternative to the electrolytic capacitor is a large film capacitor in combination with higher circuit impedances in the feedback network. If R2 is set to 5 kΩ and R3 is set to 95 kΩ, then a 22-μF film capacitor will yield a low-frequency corner below 2 Hz. This is a costly and bulky solution. The high impedance in the feedback network invites noise and DC offset impairments.

We will see that the single biggest reason for employing a DC servo is the elimination of the electrolytic capacitor. The DC servo is a smaller and less expensive solution that provides much higher sound quality and performance.

8.1 Origins and Consequences of DC Offset

Input offset voltage of the LTP can be less than 1 mV for dual monolithic BJTs or can be more than 20 mV for unmatched discrete BJTs. A JFET-LTP implemented with dual monolithic JFETs can be had with input offset voltages less than 10 mV without great difficulty. As long as these input voltage offsets are not multiplied by a DC closed-loop gain greater than unity, satisfactory amplifier output offsets are achievable. Amplifier DC offsets greater than about 50 mV should be avoided.

Input Bias Current

Input offset voltage of the differential pair is not the only source of DC offset in the amplifier. A more serious problem with DC offset occurs in amplifiers with BJT input stages as a result of base current. Importantly, JFET input stages do not suffer this problem.

The PNP-LTP transistors in Figure 8.1 are each biased at 1 mA. If transistor beta is 100, base current will be 10 μA. The base current on the input side of the LTP flows through input return resistor R1, resulting in a small positive voltage at the base of Q1. If the base current is 10 μA, the base of Q1 will be at +0.2 V.

Assume that the betas of the LTP transistors are the same, so that 10 μA also flows from Q2 through feedback resistor R3. If the feedback resistor is of the same value as the input return resistor, 0.2 V will be dropped across it as well. In this case the output voltage of the amplifier will be zero, as desired (assuming no input offset voltage in the LTP). DC offset due to base current will largely be canceled if the betas of the transistors in the LTP are reasonably matched. If the betas of the LTP transistors are mismatched by 10%, then a net offset of 20 mV will occur. Once again, this is acceptable if it is only multiplied by unity at the amplifier output. Many amplifiers are designed with this approach.

If the amplifier design has R1 and R3 at substantially different values, offset from input bias current can become serious. This could happen if the designer wished to have amplifier input impedance larger than 20 kΩ (which would also allow C1 to be smaller) without compromising noise by increasing the impedance of the feedback network. This is illustrated in simplified form in Figure 8.2. Here the entire forward path of the amplifier is abstracted by an amplifier symbol with the understanding that the input stage is a PNP-LTP that sources about 10 μA from each of its input terminals. The diodes are also removed for clarity. A 50-kΩ input return resistor combined with a 20-kΩ feedback resistor will result in a net offset of about 300 mV. This would be completely unacceptable.

A similar problem arises if a DC coupled low impedance feedback network is employed, as in the case when a DC servo is being used. In this case, if R1 is set to 50 kΩ and the electrolytic capacitor is removed, an input offset of +500 mV will result at the base of Q1. This large offset will have to be opposed and canceled by the DC servo.

Conflicting Impedance Requirements

In amplifiers with AC coupling at the input, the input impedance to ground is simply that of the return resistor R1. This resistor sets the input impedance of the amplifier and
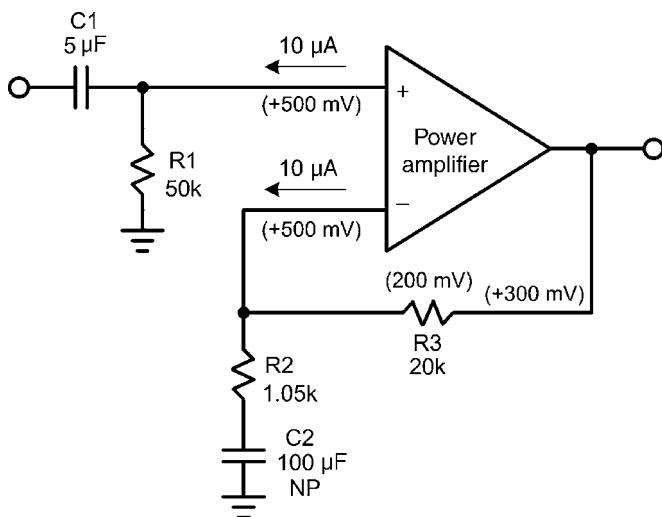
FIGURE 8.2 Conventional amplifier DC bias arrangement with higher input impedance and worse DC offset performance.

also sets the size of the coupling capacitor required to achieve a given low-frequency cutoff. For these reasons, it is desirable for this resistor to be a large value, perhaps on the order of 50 kΩ.

Unfortunately, for reasons of noise and distortion, the feedback resistor R3 should be of a lower resistance value than a value like 50 kΩ. Bear in mind that the AC impedance feeding the LTP on the input side is quite low because the input coupling capacitor acts like a short circuit at audio frequencies. Ideally, the AC impedance on the feedback network side should also be low in order to minimize noise. There is thus a conflict between the DC and AC requirements at the input stage. It is also notable that when the feedback network impedance is reduced, the value of the electrolytic capacitor in the feedback shunt path must be increased accordingly.

Bypassed Equalizing Resistor

Some designers have sought to mitigate the impedance conflict by using a slightly different arrangement on the feedback side, as shown in Figure 8.3a. R4 is added in series with the input of the LTP and bypassed. The sum of R3 and R4 is made equal to that of R1, returning DC balance to the arrangement. Here the feedback network can be of arbitrarily low impedance, subject to power dissipation in the network and to the needed size of C2. Bypass capacitor C3 has very little signal current flowing in it because of the high impedance seen looking into the LTP, so this capacitor need not be as large a value as the coupling capacitor used on the input side.

DC-Coupled Feedback Network

Figure 8.3b shows a similar arrangement where the feedback network is DC-coupled and C2 is eliminated. Here R4 is a resistor of nearly equal value to return resistor R1. The combination of R4 and the resistance of the feedback network allows the same amount of positive voltage offset as does R1, canceling amplifier offset in the same way as the arrangement of Figure 8.3a.

This arrangement reduces some of the input offset concerns without resort to an electrolytic capacitor. However, the DC gain of the amplifier is now equal to the
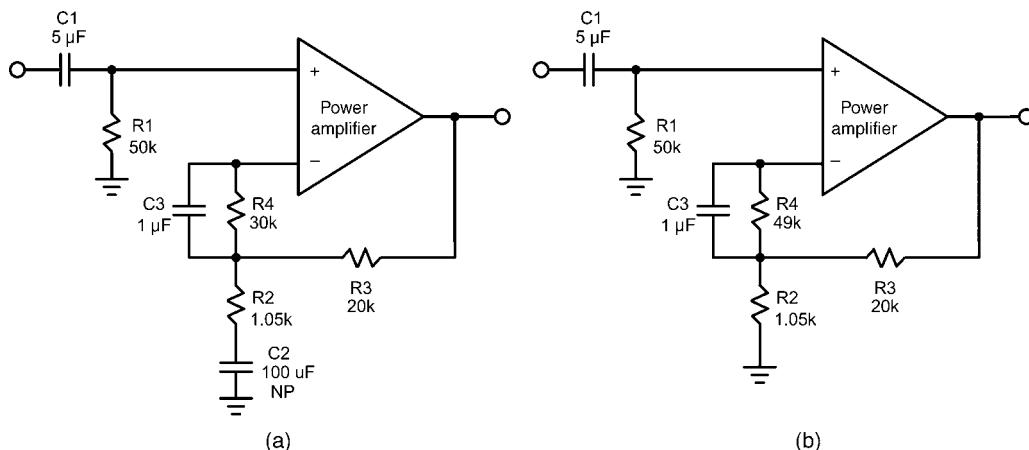
FIGURE 8.3   (a) Amplifier with bypassed equalizing resistor. (b) Amplifier with DC-coupled feedback network.
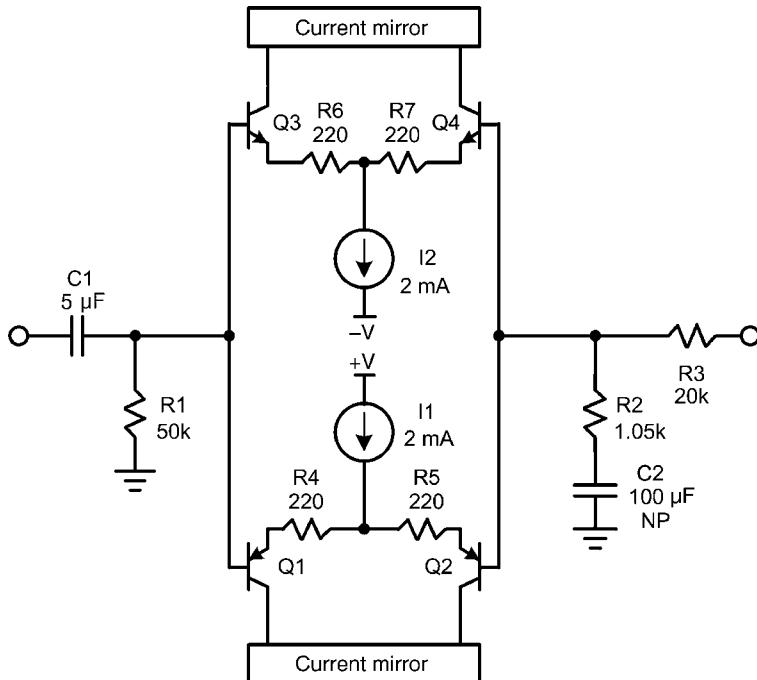
FIGURE 8.4   The complementary input differential pair.

closed-loop gain, so a big part of the advantage of having an electrolytic in the conventional arrangement is lost (due to input voltage offset). This approach can be used in combination with a DC servo to reduce the amount of correction that must be supplied by the DC servo.

Complementary Input Stages

Many amplifiers with BJT input stages employ the popular complementary differential input stage architecture shown in Figure 8.4. This approach reduces the input bias current problem because the base current flowing in the PNP transistors is of opposite sign to that of the NPN pair, resulting in some cancellation. This reduces the offset problem to the extent that the betas of the PNP and NPN input pairs are well matched. However, if betas are not matched between the NPN and PNP pairs, there may be as much as a 2:1 difference in beta, reducing the advantage gained by this arrangement to a factor of only 2 compared to a unipolar input stage.

If the NPN and PNP betas are matched to within 10%, this architecture will reduce the offset problem by a factor of 10 as compared to the situation where only a single NPN differential pair is used. Matching incurs extra cost, however. If the net input bias current is 1 µA in Figure 8.4, then output offset will be a tolerable 30 mV.

DC Trim Pots

Regardless of which of the approaches described above is used, many amplifiers end up using a DC trimmer potentiometer to achieve low output offset. This adds cost, and

its effectiveness is sometimes temperature dependent as a result of transistor beta temperature dependence. The correction current can be injected on either side of the input through a large-value resistor.

JFET Input Stages

Although JFET input stages typically start off with greater input voltage offset than BJT stages (assuming both are dual matched pairs), it should be very apparent by now that their absence of input bias current makes them superior in terms of overall amplifier DC offset. They free the designer from trying to balance the DC resistances on the input and feedback sides of the input stage.

8.2   DC Servo Basics

The concept of a DC servo is quite simple. The average DC level at the output is extracted by a low-pass filter, amplified and fed back to the feedback side of the input stage. This drives the output DC value to zero or a very small value. This permits the use of a low-impedance DC-coupled feedback network while retaining high amplifier input impedance. In practice, an integrator is almost always used to provide both the low-pass filtering function and the gain. This is illustrated in Figure 8.5 where the input pair of the amplifier is implemented with JFETs. Without the DC servo, output offset would be 200 mV with a JFET offset of 10 mV.

The amplifier output is applied to a conventional inverting integrator followed by a unity-gain inverter to provide the proper feedback polarity. The integrator input
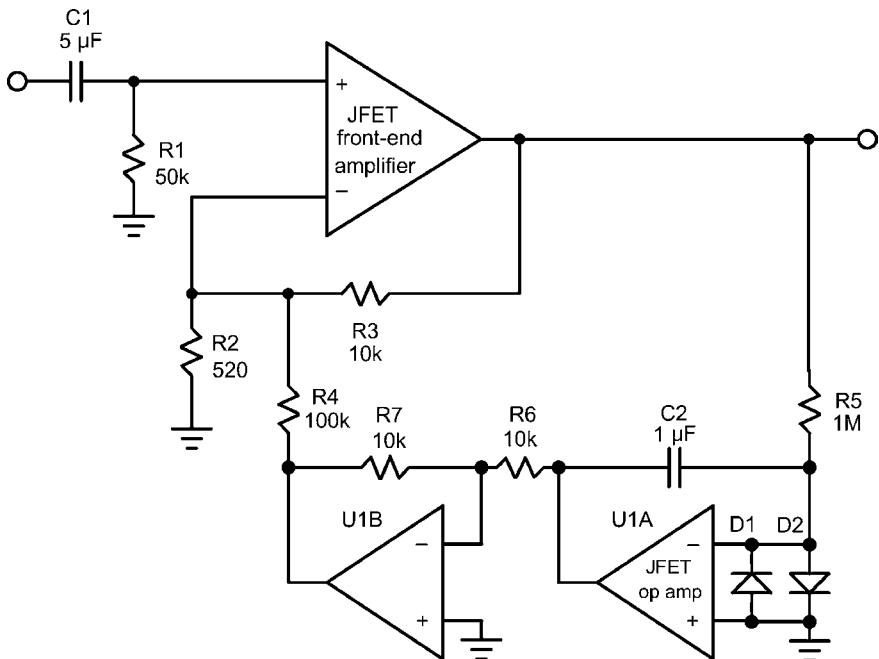
FIGURE 8.5   A power amplifier with a simple DC servo using an inverting integrator.

resistor R5 is chosen to be 1 MΩ, while the integrator capacitor C2 is set to 1 µF. The integrator is usually implemented with a JFET op amp to avoid integrator offsets created by input bias current. The integrator inputs are protected from excessive input voltages by diodes D1 and D2. The servo output from the inverter is applied to the feedback input of the amplifier input stage. This effectively creates an auxiliary feedback loop that is active at DC and very low frequencies.

If there exists a small positive average DC value at the amplifier output, integrator capacitor C2 will charge by the current sourced to it through R5, driving the output of the integrator negative. The output of the inverter will go positive and source current to the feedback input to drive the feedback input positive. This in turn will drive the output of the amplifier negative. The very high DC gain of the integrator forces the output of the amplifier to essentially zero. In practice, it forces the output voltage to equal the input offset voltage of the integrator op amp in the absence of input bias current. This will typically be less than ±10 mV for a JFET op amp.

On paper the complexity of the amplifier is higher, but cost and space for the same quality is lower. The only major components are a dual op amp and a film integrating capacitor. The output of the servo drives the amplifier's feedback input node through a fairly high-value resistor (R4) because it needs only to inject enough correction current to overcome the maximum anticipated input-referred offset error. The large resistor tends to reduce the ability of the servo and its op amp to adversely impact sound quality via noise or distortion in the servo. As discussed below, caution is required to avoid setting R4 too high.

The servo provides increased negative feedback as frequency goes lower. As such it does indeed introduce a high-pass filter function into the audio path, but so did the simple electrolytic in the feedback return leg. With the DC servo, however, you have now removed an evil 100-µF electrolytic that would have been bad for the sound even if bypassed by a smaller film capacitor.

DC Servo Architectures

Figure 8.6 shows a noninverting integrator that requires only one op amp. It is like a single op-amp differential amplifier but with the feedback and shunt resistors replaced with capacitors to make it into an integrator. It requires two capacitors, and this is a disadvantage.

I prefer DC servos that employ a dual op amp and only require a single integrating capacitor, perhaps on the order of 1 µF. It is quite economical to employ a high-quality 1-µF film capacitor. Dual op amps that are of high quality are also relatively inexpensive.

Setting the Low-Frequency Corner

Now let's set the LF 3-dB point for the overall amplifier to 1 Hz, excluding the high-pass filter formed by the input coupling capacitor. This means that the gain around the servo loop will fall to unity at 1 Hz. This also means that the amount of feedback provided through the servo circuit equals that provided through the feedback network at 1 Hz.

Assume that the feedback network consists of a series 10-kΩ feedback resistor with a 520-Ω shunt resistor, setting the amplifier closed-loop gain at 20. The attenuation of the feedback network is 20:1. The servo circuit should provide this same amount of attenuation at 1 Hz. Set the integrator resistor to 160 kΩ and the integrator capacitor to 1 µF. This makes the gain of the integrator unity at 1 Hz. Make the inverter gain unity. Set the servo signal injection resistor to 10 kΩ. This combination of component values
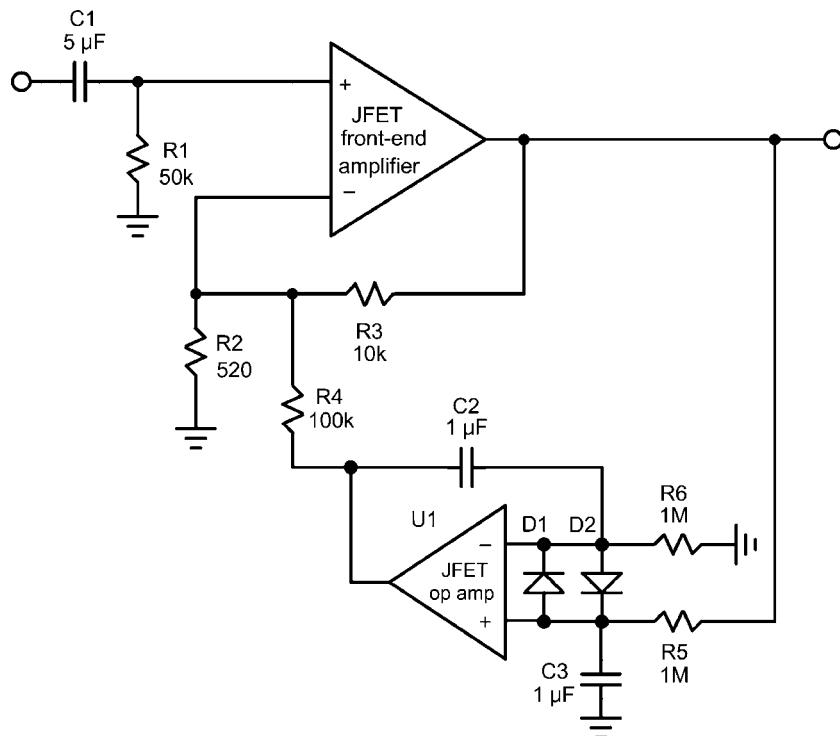
FIGURE 8.6 A DC servo implemented with a noninverting integrator requiring only one op amp but two integrator capacitors.

makes the servo feedback signal equal to the main feedback signal at 1 Hz. The gain of the servo to the output of the inverter is only 0.1 at 10 Hz. This means that a 40-V-peak, 10-Hz test signal at the output of the amplifier will produce 4-V peak at the output of the servo op amps. They will have adequate margin against clipping if they are powered from ±15-V supplies.

Amount of Offset to Be Corrected

If a DC servo is used with a low-impedance DC-coupled feedback network, then the DC servo must correct the full amount of offset created by input bias current flowing in the input return resistor. In the case above where a single NPN differential pair is used with transistors biased at 1 mA and an input return resistance of 50 kΩ, the DC servo must be able to create a full 0.5 V of compensating offset on the feedback side of the LTP. This assumes that beta of the input transistors is 100.

This amount of compensating offset is substantial. This offset needs to be taken into account in determining how much correction range the servo will need to be able to apply. In the example cited above, if the op amp can provide ±14 V, the servo will be able to accommodate ±0.7 V of input offset. Other DC servo designs that employ a larger servo injection resistance (sometimes for good reason) may not be able to satisfy the ±0.5-V requirement. Here, there is an advantage in using JFETs for the LTP because the input offset due to base current is eliminated.

An interesting trick shown in Figure 8.3b is to add a DC balancing resistor between the feedback shunt resistor and the input of the BJT input stage. The value of this resistor is chosen to be that of the return resistor less the DC resistance of the feedback network. The added resistance will equalize the offset due to input bias current. This resistor can be bypassed with a 1-µF film capacitor, since signal current flow in it is very small. This will reduce the required DC servo control range when BJT input stages are used.

Servo Control Range

My philosophy in applying a DC servo is that it should do as little as possible to the amplifier circuit, and its effect should be as subtle as possible. The DC servo is there to eliminate the *natural* offset of the amplifier that would exist if a capacitor in the feedback return leg were not used. The servo should not be more powerful than is necessary to do this job with some margin. This philosophy argues for the use of a servo injection resistor with the highest value that is consistent with meeting all servo performance requirements.

Servo Clipping

The signal voltage at the output of the DC servo will increase as frequency decreases. If the amplifier is subjected to full-power subsonic signals during testing, it is possible that the output of the DC servo will clip. For this reason, the gain of the DC servo at low frequencies must be kept in mind. If that gain is set too high so as to allow a larger value of injection resistor, then the clipping point might be reached at uncomfortably high frequencies. The tendency to clip is also governed by the chosen low-frequency cutoff frequency for which the servo is designed. Servos designed to yield a higher cutoff frequency will tend to clip at a higher frequency. A good rule of thumb is that the servo should never clip at a frequency higher than 10 Hz when the amplifier is operating at full power.

The DC servo described above having a 1-Hz bandwidth will produce a peak signal swing of 4-V peak when the amplifier is producing 40-V peak at 10 Hz (corresponding to 100 W/8 Ω). A 400-W/8-Ω amplifier will only produce an 8-V peak output from the servo at 10 Hz, indicating that this servo design is adequate for such an amplifier, but there is a caveat.

Servo Headroom

If the servo op amp can produce ±14 V, it will be able to counteract ±700 mV of offset at the input. If a BJT input stage is being used with 10-µA input bias current flowing through a 50-kΩ return resistor, offset at the input is –500 mV. The servo can handle this, but it will exhibit a constant output voltage of –10 V under quiescent conditions. This asymmetry will eat into the clipping headroom of the servo on low-frequency signals, leaving only 4 V on the negative side. This is an important consideration in the design of the servo.

The JFET Advantage

While some prefer JFET input pairs for reasons of sound quality and EMI resistance, there is another reason that makes them attractive. The JFET input stage does not suffer from DC offset caused by input bias current, and that makes the job of the DC servo much easier.

If an amplifier is to have reasonably high input impedance, its input return resistor must be large (at least 20 kΩ). BJT input bias current flowing through this resistor will cause a far larger offset than the input voltage offset of the input pair or of input-referred offset from the VAS stage. If a JFET input stage is used instead, there is no DC offset from input

bias current, and the servo need only compensate for the 5-15 mV of offset of the JFET pair. The bottom line here is that the servo must typically work much harder when used in a typical DC servo arrangement with BJT input pairs as opposed to JFET input pairs.

8.3   The Servo Is in the Signal Path

The DC servo in Figure 8.5 is in the feedback path with modest gain at low frequencies. As such, the DC servo is in the signal path of the amplifier, and its performance can affect sound quality. The fact that it is injecting a signal at the input stage gives it opportunity to inject noise and distortion into the signal path. This can influence the quality of the audio signal, but is still better than having an electrolytic in the signal path.

For this reason, audio-grade op amps should be used for the DC servo's integrator and inverter. Pay attention to the noise and class B crossover distortion created by the op amp and consider pulling its output down to force its output stage to operate in class A. Design the servo as if it were part of a quality IC-based preamp. Provide a good clean power supply to the op amp and use a quality integrating capacitor (e.g., polypropylene film). The capacitor can be of slightly lower quality than those in the main signal path of the amplifier only because its output is attenuated before being applied to the input circuit.

Servo Op Amp Distortion and Noise

If the output of the servo is attenuated by 100:1 before application to the amplifier input and the amplifier has a closed-loop gain of 20, then the attenuation of the servo output to the output of the amplifier is only 5:1, or 14 dB.

There is thus flat gain (albeit usually less than unity) from the output of the servo to the output of the amplifier. This will depend on the ratio of the amplifier feedback resistor to the servo injection resistor. In some designs, this gain can be near unity. Given the fact that the output of the servo will be reproducing a strongly low-pass-filtered version of the output signal at some amplitude, it is possible for the servo op amp to create distortion that will make its way to the output of the amplifier. Indeed, if the servo op amp's output is hovering around zero, it could be experiencing some crossover distortion from the class B output stage of the op amp. This can be minimized by using a pull-down resistor on the output of the op amp to force its output stage into class A operation.

Noise created by the integrator and inverter op amps will be transported to the amplifier output with the gain mentioned above. The noise will also be influenced by the size of the integrator input resistor and the size of the integrator capacitor. Using a large input resistor, like 1 MΩ, allows the use of a much smaller integrator capacitor, sometimes as small as 0.1 μF. This takes up less space and is less expensive to obtain in a high-quality capacitor. The price paid is increased servo noise. This noise increases at low frequencies, however, so its sonic effect is limited. It can be thought of as being akin to 1/f noise. If high impedances are used in the integrator, it is especially important to employ a JFET op amp for the integrator for two reasons. First, input base current of a bipolar op amp will create an undesirable DC offset voltage across the integrator input resistor. Second, the input noise current of a BJT op amp will cause significant noise with such a high-impedance source. The JFET op amp should be a low-noise design.

Beware of well-intentioned efforts to reduce servo noise and distortion. Some can result in instability, some can result in frequency response anomalies, and some can result in servo clipping. The very best way to reduce injected servo noise and distortion is to use high-quality parts and audio design practices in the servo.
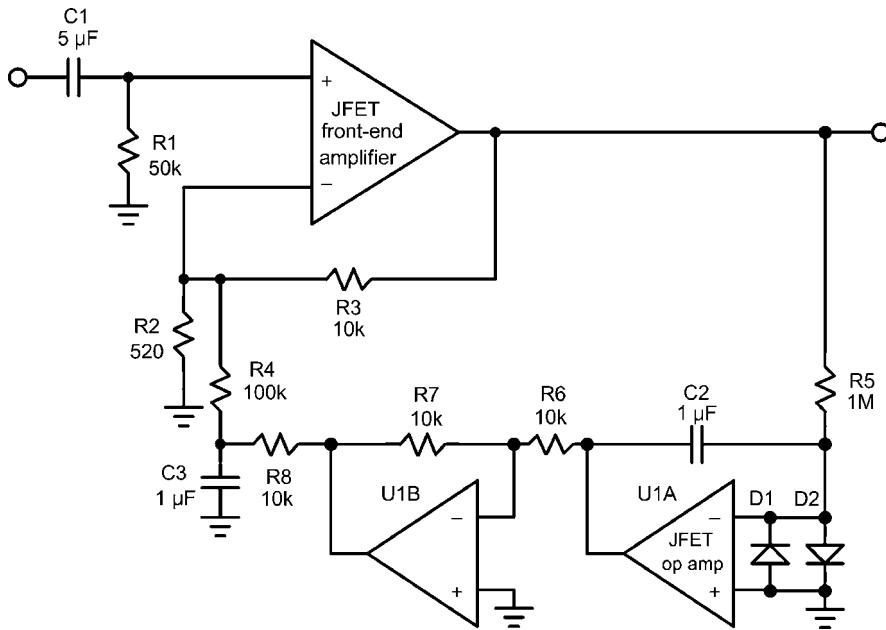
FIGURE 8.7   DC servo with additional low-pass filter.

Adding a Second Pole

The integrator in the DC servo may not be a perfect integrator at all frequencies. This can lead to some high-frequency program material or interference sneaking through the integrator. This leakage can be reduced by adding a passive low-pass filter at the output of the servo, as shown in Figure 8.7. This can be done by splitting the servo injection resistor and taking a capacitor from the junction to ground. This is implemented by R8 and C3, placing a pole at about 16 Hz. The idea is to further keep noise and distortion from the servo op amp out of the signal path. The DC servo of Figure 8.7 presumes the use of a JFET input stage in the amplifier and JFET op amps for the DC servo.

However, this technique can have subtle effects on the low-frequency response if it is not implemented with care. This is because the frequency-dependent impedance seen looking back into the servo injection network acts as though it is in parallel with the main negative feedback network shunt resistor to ground (R2). The low-frequency response step created in the design of Figure 8.7 is only 0.005 dB. The added capacitor is also somewhat in the effective signal path, so its quality matters.

A different approach is shown in Figure 8.8. It can be implemented in the case of a servo with an inverting integrator followed by an inverter, as in Figure 8.5. Some capacitance can be put across the inverter's feedback resistor, giving the inverter a low-pass response. Here the second pole is implemented by C3 working against R7, producing a pole at 16 Hz. This approach still leaves the door open a crack for noise and high-frequency sneak-through from the inverter, however.

Adding a second pole to a feedback loop usually invites instability or frequency response peaking if it is not done carefully. Figure 8.9 shows the frequency response of a poorly designed servo. In order to avoid this, the added pole should be well above the
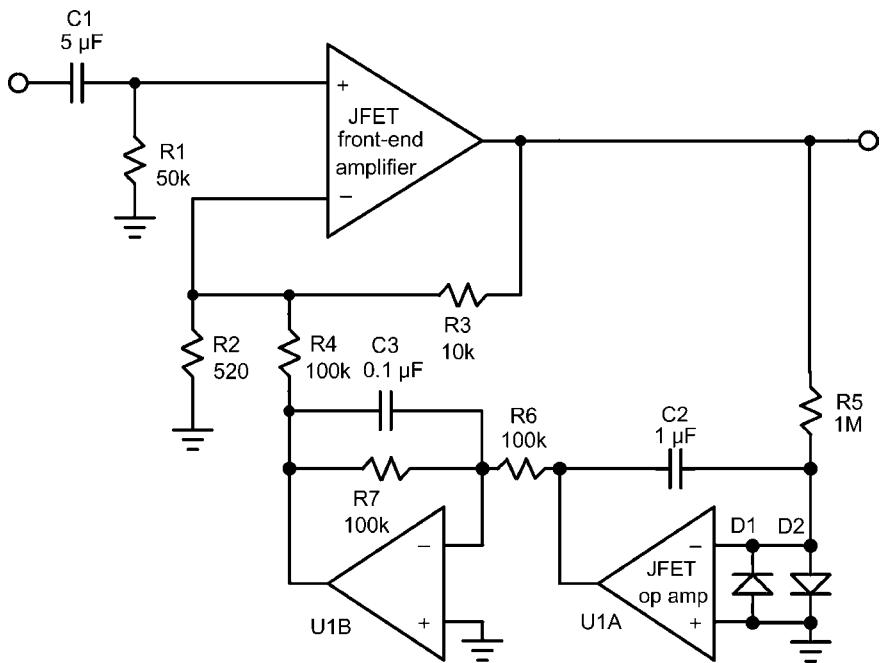
FIGURE 8.8   DC servo with LPF implemented with a capacitor around the inverter.
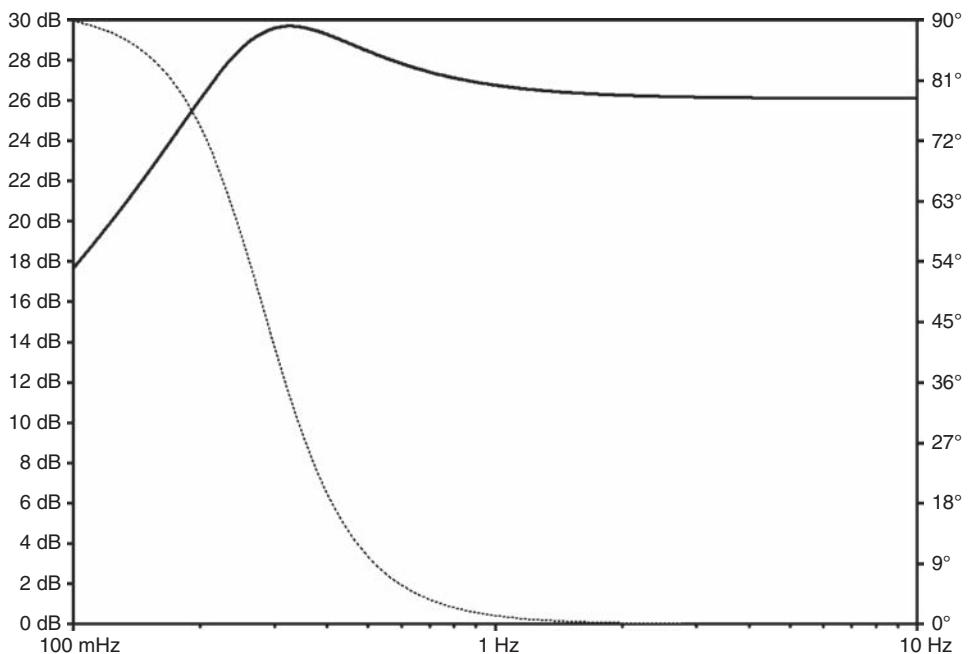
FIGURE 8.9   Frequency response of a poorly designed DC servo.

servo bandwidth frequency, perhaps by a decade. This constraint is easily satisfied in both of the designs above where the servo bandwidth is only 0.016 Hz.

8.4   DC Offset Detection and Protection

The servo's integrator output provides a convenient monitoring point for the DC health of the amplifier. If DC persists at a certain voltage level over a certain period of time, the servo integrator will build up a large voltage to try to counteract the DC offset. This voltage can be fed to a window detector to open the speaker relay or otherwise engage protection circuits. The window detector can be constructed from two comparators, each fed an appropriate threshold voltage. If there is a known typical servo offset due to the use of a BJT input pair, then the servo output should be offset before application to a symmetrical window detector, or the window edges will have to be made asymmetrical. There will be some error in this approach, since the BJT base currents that cause the offset may be different for each amplifier and are temperature dependent. Once again, JFETs are at an advantage, but keep in mind that a JFET offset of 10 mV will create 2 V of servo output offset uncertainty in the design shown having a 100-kΩ servo injection resistor. The difficult trade-off of servo injection resistor size, relative to the feedback resistor, is once again highlighted.

8.5   DC Servo Example

The amplifier shown in Figure 8.10 has a closed loop gain equal to 20, set with a 10-kΩ feedback resistor and a 520-Ω feedback shunt. The DC servo uses an inverting servo integrator with a 1-MΩ series resistor and a 1-µF capacitor. The integrator will have a gain of 0.16 at 1 Hz.
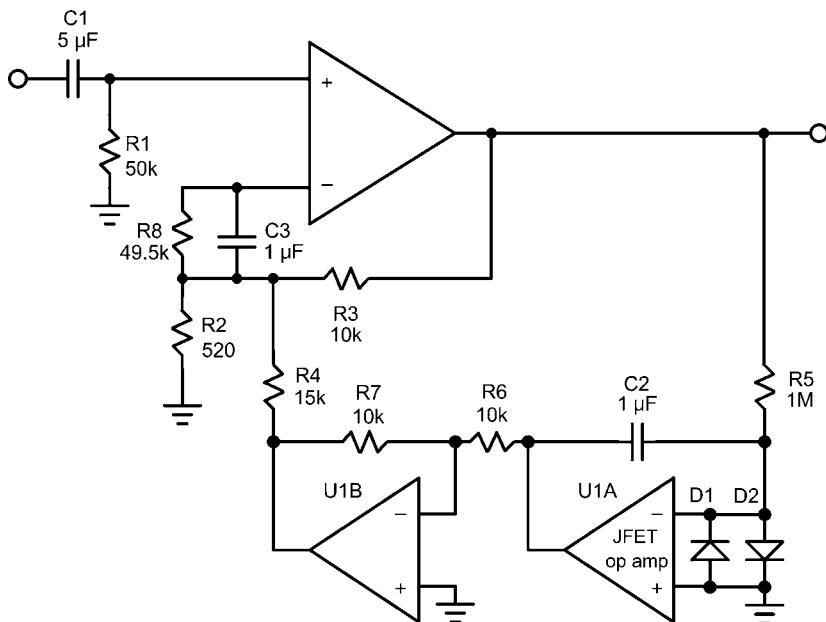
FIGURE 8.10   Example power amplifier with a DC servo.

Assume a unity-gain servo inverter at the output of the integrator. A 15-kΩ servo injection resistor connects the servo inverter to the inverting input of the power amplifier, providing a servo attenuation factor of about 30:1. The servo loop gain at 1 Hz will be the integrator gain times the ratio of R3 to R4. This equals 0.11. This means that the low-frequency cutoff created by the servo is at about 0.11 Hz (the servo-based LF cutoff is simply the frequency where the servo loop gain falls to unity).

We have an LF cutoff frequency of only 0.11 Hz, not simply because we wanted to really go low, but because the numbers will work out nicely, especially in terms of servo signal-handling ability. Bear in mind that the overall amplifier low-frequency cut-off will still be largely determined by the input coupling capacitor.

With a 30:1 servo attenuation factor and op amps capable of ±14 V, servo correction range is only ±470 mV. The BJT input stage requiring 10 µA combined with a 50-kΩ return resistor requires more than that. Moreover, at that point all of the servo's dynamic range for handling AC feedback signals at low frequencies is used up. This servo requires the use of high-β BJTs or JFETs at the input. The optional DC balance network consisting of R8 and C3 can be added to reduce the effects of BJT input offset current.

Assume that this is a 100-W amplifier with a 40-V peak output. Let the DC protection be triggered when the servo output reaches a threshold of 6 V. If the servo needs to correct a fairly large input offset of 100 mV, the servo output only goes to about 3 V, well within its safe range. The servo can handle nearly 200 mV offset before triggering DC protection and is still not even close to the output limits of the integrator op amp. However, LF signal swings have yet to be taken into account.

With a full-power (40-V peak) 10-Hz sinusoid produced by the amplifier, the sinusoidal output of the servo integrator will only be about 0.6-V peak. It will be 10 times this if the input signal is at 1 Hz and will just trigger the DC protection (in the absence of offset correction). If the amplifier fails shorted to a rail and produces 40 V of DC, the servo integrator output will rise to the 6-V protection trigger point within 0.25 second.

If we want to reduce servo influence at the expense of offset that can be handled, we can simply increase the servo injection resistance from 15 to 50 kΩ. This will reduce by 10 dB the opportunity for servo noise and distortion to get into the signal path. This will also reduce the LF cutoff to 0.03 Hz. As long as the amplifier design and architecture does not cause a turn-on settling issue that must be corrected, there is probably no problem with this lower LF cutoff frequency. The peak voltage at the output of the integrator will increase by nearly a factor of 3 for a given amount of offset correction. This may increase the chances of triggering DC protection circuits. This approach is best suited to a JFET input LTP so that base current offsets are absent.

If for some reason we want to go to a higher LF cutoff frequency, we must increase servo loop gain. We can do this by reducing the 15-kΩ servo injection resistance at the expense of greater opportunity for servo garbage to get into the signal path. Alternatively, we can achieve the same result by increasing the integrator gain. Changing to a 0.1-µF integrator capacitor will increase the integrator gain by a factor of 10 and bring the LF cutoff up to 1 Hz. Unfortunately, the servo is now more easily overloaded by large low-frequency signals at the amplifier output. A full-amplitude 10-Hz signal at the output of the amplifier will now cause triggering of the DC protection. This is just a design decision and it may be OK. Many audiophiles would not want a high-level signal at 10 Hz to drive their loudspeakers anyway.

There are many possible variations to this kind of servo, but this is a good illustration of typical operation and trade-offs.

8.6   Eliminating the Input Coupling Capacitor

A system signal path often contains more coupling capacitors than necessary. There will usually be one at the output of the preamplifier, and yet another one at the input of the power amplifier. If the power amplifier has a DC servo, the input coupling capacitor of the amplifier can be bypassed, knowing that the output of the preamp is probably at or very close to zero. This is no more risky than using a DC-coupled power amplifier. Any small DC offset present at the input of the amplifier will be handled by the DC servo. In this case, an overall improvement in low-frequency transient response will have been had by the use of a servo. Removal of the input coupling capacitor is strictly a choice in regard to managing risk. Many DC-coupled power amplifiers have the option of switching in a blocking capacitor at the input. This is a good idea that can be applied in the general case if one uses a servo in the power amplifier.

8.7   DC Servo Design Issues and Nuances

It is easy even for experienced designers to fall into a trap when it comes to servo design. Just because the servo may not need to do much correction in some designs, do not make the mistake of making the servo strength too small. If you do, the integrator gain will be necessarily higher, all else remaining equal, and the servo will be vulnerable to clipping on large subsonic signals.

Servo Start-Up Transients

The servo will often be designed to have a very low-frequency cutoff. This reflects the fact that it should act largely as a long-term automatic screwdriver adjustment. The integrator capacitor will start out at zero on power-up, so initially there will be no servo correction. This means that the power-on transient will include the uncorrected offset of the amplifier, which will often be dominated by the offset induced by base current in the case of a BJT input stage. A power-on delay implemented with a speaker relay will eliminate this.

Low-Frequency Testing of Amplifiers Employing Servos

Full-power testing of power amplifiers at frequencies well below 20 Hz may cause problems with servo clipping or with servo-based DC protection. This is because the servo is merely an integrator fed with the output signal of the amplifier. The integrator gain increases as frequency decreases. Consider an amplifier producing 45 V peak at its output. At a frequency where the integrator gain has risen to 1/3, the signal at the output of the integrator will be 15 V peak, enough to clip the integrator op amp.

Simulation

It is wise to conduct a SPICE simulation of all DC servo designs to verify behavior. This is especially the case when verifying the LF amplifier corner and any frequency response peaking that might occur. This can be done with an AC simulation.

The issue of unbalanced LTP return resistances and resulting need for correcting servo action can be evaluated with a DC simulation. Static offset at the output of the servo should always be evaluated.

This page intentionally left blank

CHAPTER **9**

Advanced Forms of
Feedback Compensation

The conventional Miller compensation described in Chapter 4 is by far the most widely used form of frequency compensation for amplifiers employing negative feedback. It is simple and reliable. However, as we will see here, there are alternatives to, and variants of, Miller compensation that can provide substantial performance improvements. This chapter takes up where Chapter 4 left off.

The following are some of the reasons for choosing advanced forms of compensation:

- Improved slew rate
- Greater amounts of in-band negative feedback
- Increased negative feedback at high frequencies
- Addition of local feedback around the output stage
- Inclusion of the input stage in local feedback loops

Miller compensation sets a strict relationship that limits slew rate in accordance with closed-loop gain, input stage transconductance, and gain crossover frequency. Some forms of advanced compensation allow this limitation to be avoided. A greater amount of in-band negative feedback reduces in-band IM products, even if it does not reduce the amount of higher-harmonic high-frequency out-of-band distortion. Some advanced compensation techniques provide greater in-band feedback without a corresponding increase in high-frequency feedback that might compromise stability.

Increased feedback at high audio frequencies like 20 kHz is very desirable because some circuits create more distortion at high frequencies, like crossover distortion. Compensation techniques that permit greater negative feedback at 20 kHz without requiring a higher gain crossover frequency are valuable. The output stage is a major contributor to distortion, and some advanced compensation techniques permit the introduction of additional local negative feedback around the output stage to reduce its distortion. The input stage is a source of distortion in many amplifiers, yet global negative feedback is not fully effective in reducing some forms of input stage distortion, such as common-mode distortion. Some advanced compensation techniques enclose the input stage in a local feedback loop to increase its dynamic range and reduce this problem.

171

9.1   Understanding Stability Issues

The general concepts of feedback stability were addressed in Chapter 4, and we will review them only briefly here. The main point to take away is that the gain and phase response of the feedback loop must be tailored in such a way that adequate gain margin and phase margin are achieved under all conditions.

The most significant influence on stability is the choice of the gain crossover frequency. If it is chosen too high, the accumulation of *excess phase* with increasing frequency will reduce phase margin to the point where instability is likely. If it is chosen too low, slew rate will be reduced and high-frequency distortion will be increased due to less feedback at frequencies like 20 kHz.

The open-loop gain and phase will often be a function of signal voltage and current. For example, f_T droop in the output transistors can reduce phase margin under conditions of high current. For this reason it is important that the feedback compensation be sufficiently conservative that adequate phase margin is preserved under signal swing conditions.

The load placed on an amplifier can have a profound influence on stability because it affects the open-loop gain and phase of the amplifier. Even though the open-loop output impedance is generally thought to be small at high frequencies, declining transistor AC beta at high frequencies can cause it to increase. Heavier loads in general tend to exacerbate the creation of excess phase in the output stage. This is especially so for capacitive loads whose impedance becomes small at high frequencies.

Some feedback compensation schemes are stable only for a range of open-loop gain and phase characteristics, and even become unstable if open-loop gain decreases. These arrangements are referred to as having conditional stability. If an amplifier breaks into oscillation when it is turned off, this is an example of conditional stability.

Finally, some advanced feedback compensation schemes involve feedback loops themselves that may extend over more than one stage in the open-loop amplifier. The stability of these local compensation loops must also be assured. These loops often involve much higher gain crossover frequencies. The conventional Miller compensation scheme involves a shunt feedback loop of very wide bandwidth, but it is usually very stable because it only encircles one or two transistors.

Dominant Pole Compensation

Most conventional feedback amplifiers depend on frequency compensation in which a single-pole roll-off dominates the gain and phase characteristics of the loop gain. If there is really only one pole in the loop, the phase shift around the loop at high frequencies will be 90 degrees up to extremely high frequencies. This means that the phase margin will be 90 degrees and that the gain margin will be an unlimited number of decibels. As explained in Chapter 4, the nondominant poles at higher frequencies ultimately contribute excess phase that increases with frequency, detracting from phase margin and leading to instability if the gain crossover frequency is set too high.

9.2   Miller Compensation

Miller compensation is the most common form of dominant pole compensation employed in audio amplifiers. It is named in connection with the Miller Effect and Miller Integrators. As explained in Chapter 4, Miller compensation is implemented by

(Miller integrator)

C1   30 pF

In

IPS

−

$gm =$
2 mS

+

VAS

−

$gm =$
40 mS

OPS

+ 0.96

Out
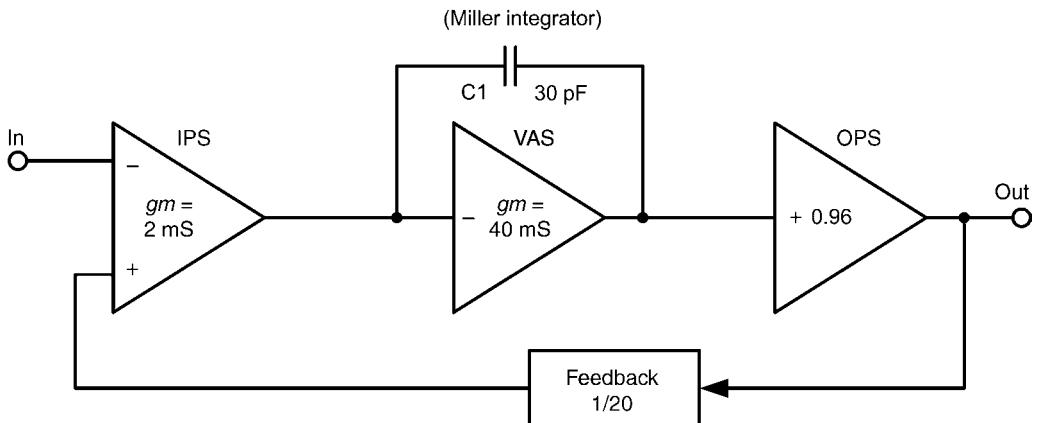
Feedback
1/20

FIGURE 9.1   A Miller-compensated amplifier.

a negative feedback process and, as a result, enjoys inherent advantages. In particular, it makes use of all of the gain for distortion reduction. The shunt feedback process in Miller compensation increases local feedback around the VAS as it decreases global feedback with increasing frequency. This acts to further linearize the VAS at high frequencies. Shunt feedback by its nature decreases the output impedance of an amplifier stage. This means that the output impedance of the Miller-compensated VAS decreases with frequency, making the VAS gain and phase more immune to loading effects from the output stage.

Figure 9.1 shows an amplifier with Miller compensation. Throughout this chapter the IPS will be assumed to be an LTP that is simply characterized by a transconductance of 2 mS. In the arrangement of Figure 9.1, all of the signal current produced by the LTP will be assumed to flow into C1. The VAS will be assumed to be a common-emitter stage characterized by a transconductance of 40 mS. The OPS will be assumed to be an emitter follower with nearly unity-voltage gain and high-current gain. The VAS in such a design is essentially a Miller integrator that is characterized by a 6 dB per octave roll-off over a very wide range of frequencies. If the loop gain is 0 dB at the 500-kHz gain crossover frequency, it will be 40 dB at 5 kHz and 60 dB at 500 Hz, assuming that there is enough DC gain in the real circuit to support this amount of loop gain.

As explained in Chapter 2, the value of C1 in combination with the IPS transconductance determines the open-loop gain as a function of frequency. The open-loop gain is simply $gm * X_{C1}$, where X_{C1} is the impedance of C1 at a given frequency. The gain crossover frequency f_c is determined by the open-loop gain A_{ol} and the closed-loop gain A_{cl}. The frequency where A_{ol} falls equal to A_{cl} is the gain crossover frequency. These relationships are illustrated by the Bode plot in Figure 9.2. It follows that the value of C1 to set f_c is

$$C1 = gm / (2\pi * A_{cl} * f_c) \tag{9.1}$$

The circuit of Figure 9.1 is designed to have $f_c = 500$ kHz, making the required value for C1 equal to 30 pF.
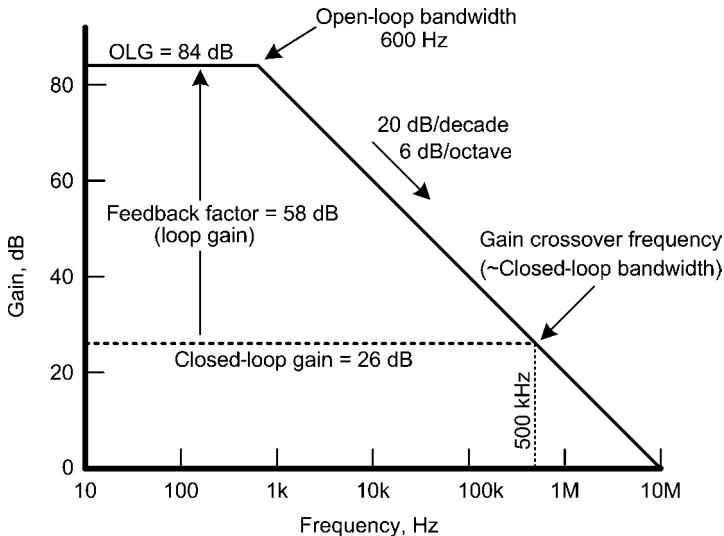
FIGURE 9.2 Bode diagram for the amplifier of Figure 9.1.

Pole-Splitting

The output of the IPS is a high-impedance point. The output of the VAS is also a high-impedance point. In the absence of Miller compensation shunt feedback, both of these nodes can form poles. Both of those poles can lie at a similar frequency. Such a two-pole situation in the open-loop amplifier will greatly jeopardize stability because both poles will contribute nearly 90 degrees of lagging phase shift at frequencies well above the pole frequencies but probably below the gain crossover frequency.

The shunt feedback provided by the Miller compensation causes what is called *pole-splitting* to occur. Of the two poles that would have been present without Miller feedback, one pole is moved far down in frequency and the other pole is moved far up in frequency. This is why the process is called *pole-splitting*; the frequencies of the poles are split to become far away from each other. The pole that is pushed to a high frequency is usually pushed to a frequency that lies well above the gain crossover frequency. The result is an amplifier stage characterized by a 6 dB per octave roll-off that begins at a very low frequency and continues over many decades to a very high frequency, without the lagging phase contribution exceeding 90 degrees.

Limitation on Slew Rate

As explained in Chapter 4, conventional Miller compensation places a limit on slew rate (SR) that is closely bound to the gain crossover frequency and the closed-loop gain of the amplifier. The equation for slew rate is

$$SR = 2\pi f_c A_{cl} I_{max}/gm \qquad (9.2)$$

The term I_{max}/gm is the ratio of the maximum output current of the IPS to the transconductance of the IPS. Once closed-loop gain and gain crossover frequency are

chosen, slew rate is determined by the ratio I_{max}/gm. This number is 52 mV for an un-degenerated BJT differential pair. The number is about 10 times larger for an LTP that has 10:1 emitter degeneration. This is why it is so important to incorporate emitter degeneration into BJT input stages. The number is also about 10 times larger for an un-degenerated JFET differential pair.

An amplifier with $f_c = 500$ kHz and $A_{cl} = 20$ will have a slew rate of only 3.3 V/μs with an un-degenerated BJT-LTP. If the LTP is degenerated by a factor of 10, slew rate will rise to a usable 33 V/μs.

Some of the advanced compensation schemes to be discussed in this chapter break that relationship, allowing higher slew rate to be achieved without requiring higher gain crossover frequencies or excessive amounts of IPS degeneration.

Distortion Reduction as a Free Side Benefit

Feedback compensation involves throwing open-loop gain away at high frequencies. It would be nice if this *thrown-away* gain could be put to good use. This is exactly what Miller compensation does. It exchanges high-frequency global feedback for high-frequency local feedback. Miller compensation reduces high-frequency open-loop gain through the use of local feedback that increases with frequency. This local shunt feedback serves to reduce distortion in the VAS. Virtually all of the advanced forms of compensation to be discussed here operate in the same way, linearizing the VAS while reducing gain as frequency increases.

VAS Output Impedance

The output impedance of the VAS is reduced by the effect of the shunt feedback, making the VAS less affected by nonlinearities of the output stage load. The VAS output impedance is estimated by injecting a small voltage at the output node of the VAS and calculating how much change in VAS current will result. This current will be related to the voltage attenuation ratio of the Miller feedback and the transconductance of the VAS stage.

Consider an amplifier with a Darlington VAS operated at 10 mA and having 10:1 emitter degeneration. Its effective emitter resistance will be approximately 26 Ω and its gm will be about 38 mS. Assume that $C_M = 15$ pF and that there is a 3.4-kΩ resistor shunting the input to the VAS. At 1 kHz the impedance of C_M is about 10.6 MΩ. The Miller feedback attenuation ratio will be approximately 3.4 kΩ/10.6 MΩ = 0.00032.

A 1-V change forced on the VAS collector will thus result in a 0.32-mV change at the input to the VAS, creating a 12-μA change as a result of the 38-mS transconductance. The VAS output impedance is thus 1V/12 μA = 83 kΩ. This value assumes that there are no other effects causing the output impedance to be lower, such as the Early effect or output stage loading. The estimated output impedance will decrease with frequency as the impedance of C_M decreases with frequency. At 20 kHz the VAS output impedance is about 4 kΩ.

Now assume that the Darlington VAS is driven from an LTP with a current mirror load, as shown in Figure 9.3. The impedance at the input of the VAS will be much higher, on the order of 40 kΩ. At 1 kHz and with a $C_M = 30$ pF and $X_{CM} = 5.3$ MΩ, the Miller feedback attenuation factor will be 40 kΩ/5.3 MΩ = 0.0075 and the VAS output impedance will be $Z_{out} = 1/(0.0075 * 38$ mS$) = 3.5$ kΩ. This is a remarkable and important reduction from the example above. At 20 kHz the impedance of C_M is about 265 kΩ and
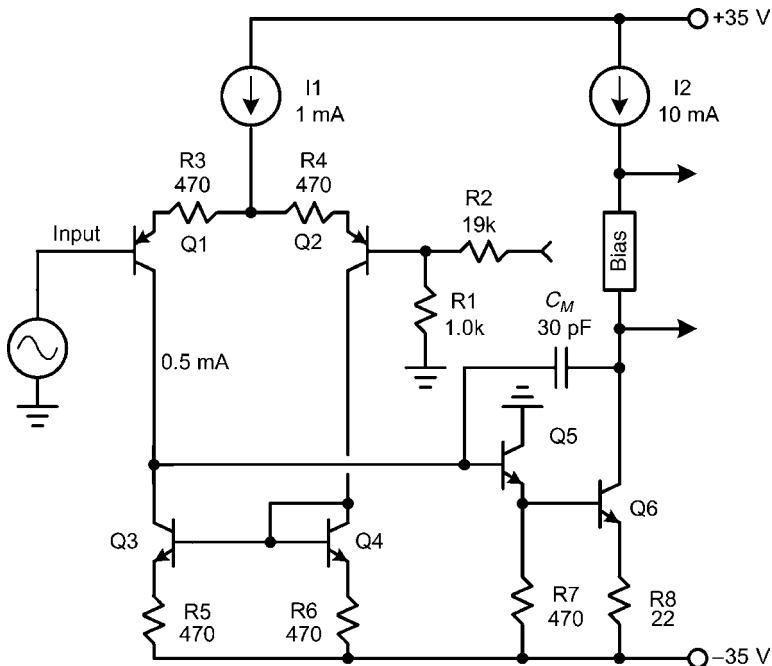
FIGURE 9.3   Simple IPS-VAS arrangement with a current mirror LTP load.

the impedance ratio of the divider elements is about 0.15. VAS output impedance will be on the order of 175 Ω.

At very high frequencies, where C_M begins to look like a short, the VAS output impedance will begin to level off as close to 26 Ω, which is $1/gm$ of the VAS. In these estimates the capacitance at the input node of the VAS is assumed to be small compared to C_M. Capacitance to ground at that node will tend to increase VAS output impedance because it will form a capacitance voltage divider with C_M for the shunt feedback.

The Feed-Forward Zero

At very high frequencies where C_M is essentially a short circuit it can be seen that the VAS is no longer inverting and that the voltage gain of the VAS is $gm1/gm2$ (noninverting), where $gm1$ is the transconductance of the IPS and $gm2$ is the transconductance of the VAS. This means that there is a *right-half-plane* zero in the transfer function of the VAS created by feed-forward of current from the IPS through C_M. This zero can reduce phase margin of the global feedback loop. It can be eliminated by placing a resistance R2 in series with C_M whose value is equal to or greater than $1/gm2$. The zero is located at the frequency where the reactance of C_M equals $1/gm2$. In the case of $C_M = 30$ pF and $gm2 = 38$ mS, the zero is at about 200 MHz and is of little concern.

Inserting a Zero to Cancel or Mitigate a Pole

Increasing the resistance in series with the Miller capacitance creates an ordinary zero that can cancel other parasitic poles in the circuit. If this zero is placed well above f_c at a frequency where the first parasitic pole is thought to be located, phase margin can be

improved. If the first parasitic pole is thought to lie at 5 MHz and $C_M = 30$ pF, a value for R2 of 1 kΩ might be appropriate. Caution must be exercised with this technique to avoid compromising gain margin.

Power Supply Rejection

The Miller compensation capacitor straddles the power supply rail and ground. Power supply noise thus creates noise current through C_M, resulting in injection of noise into the signal path. This is a potential disadvantage of conventional Miller compensation and calls for extra care in keeping the power supply to the IPS-VAS quiet. In some alternative compensation approaches both ends of the compensation capacitor are referenced to signal ground, removing this potential source of power supply noise ingress.

Buffered Miller Feedback Pick-Off Point

In some cases it is advantageous to tap the Miller feedback from the predriver or driver instead from the collector of the VAS. This reduces the load of the compensating capacitor on the VAS and (for what it is worth) includes the predriver in the local feedback loop formed by the Miller compensation. Although it may seem of limited benefit for conventional Miller compensation, it can be more valuable for other compensation schemes that will be discussed.

A key issue with buffered compensation loop pick-off is its effect on pole-splitting and compensation loop stability. The compensation loop now encloses more circuitry and the VAS high-impedance collector circuit is not directly part of that loop and is allowed to have very high impedance. It is tempting to argue that the buffered and unbuffered schemes must behave identically because the buffer has unity gain, so that the signal picked off is essentially identical in both cases. However, the loading of the VAS collector node is not the same, allowing the gain of the loop so formed to be much higher, especially at very high frequencies. As discussed in Chapter 4, the stability of the compensation loop itself must always be considered.

If the VAS high-impedance node is loaded with a replica of what it would have seen, it can be argued that the behaviors may be the same. What is the net benefit, then? One can argue that the replica load need not be as heavy as the load that the actual compensation network would have placed on it; it only needs to be heavy enough to adequately limit the high-frequency loop gain of the compensation loop.

Indeed, one could even argue that the light replica load could be brought back to the input of the VAS, so that at very high frequencies the architecture would devolve to that of a conventional Miller compensation approach.

9.3   Two-Pole Compensation

Bode showed that optimal compensation might be had with a 9-dB per octave roll-off (30 dB per decade) instead of a 6 dB per octave roll-off (20 dB per decade). In this case, the phase margin would still be a respectable 45 degree and yet the steeper roll-off would permit much higher gain in the audio band for a given gain crossover frequency. Consider an amplifier with a 2-MHz gain crossover. There are two decades between 20 kHz and 2 MHz. With a conventional 20 dB per decade loop-gain roll-off, the amplifier will have 40 dB of negative feedback at 20 kHz. With a 30 dB per decade roll-off, the amplifier enjoys fully 60 dB of negative feedback at 20 kHz. This implies potentially 10 times less distortion at 20 kHz.

Two-pole compensation (TPC) can be thought of as a very simple and crude approximation to the steeper 9 dB per octave roll-off proposed by Bode. A second pole is put in the dominant pole roll-off characteristic at a low frequency f_1. The pole is canceled by a zero placed at a higher frequency f_2 (usually well below the gain crossover frequency). For example, in the amplifier with a 500 kHz gain crossover frequency, one might insert this 12 dB per octave roll-off segment below 80 kHz. The roll-off characteristic in this region will roll-off more steeply at 12 dB per octave, lending an extra 12 dB of roll-off between 20 kHz and 80 kHz. The amount of loop gain available at 20 kHz will thus be increased by 12 dB.

Figure 9.4 illustrates an amplifier with a two-pole compensation network. The compensation is essentially like Miller compensation, but the compensation capacitor is split. The junction of C1 and C2 is returned to ground through resistor R1. To first order, the series combination of C1 and C2 will be the same as the value of C1 in conventional Miller compensation to arrive at the same f_c. Resistor R1 increases the VAS gain at frequencies at least an octave below f_c by introducing attenuation into the shunt feedback path. This network can sometimes create additional loading on the VAS that might not be desired, and this is an example of where the compensation feedback might instead be tapped off from the predriver emitter follower. Bear in mind that C1 and C2 need not have the same value, and in fact in some designs C2 might be significantly larger than C1.

There are many approaches to picking C1, C2, and R1. I recommend doing it using SPICE simulation of the amplifier, starting with C1 = C2 = 2 * C_M of a conventional Miller compensation scheme. This keeps the gain crossover frequency f_c about the same. Then add R1, starting with a high value that has little effect. Decrease R1 until closed-loop gain peaking of about 1 dB is evident. This gets you in the ballpark. Check the loop-gain characteristic, phase margin, and square-wave overshoot. Experiment with component values from there. This is definitely a process of iteration.

Figure 9.5 shows the loop gain for the amplifier of Figure 9.4 with the curve labeled *TPC*. Loop gain for conventional Miller compensation is also shown for comparison.
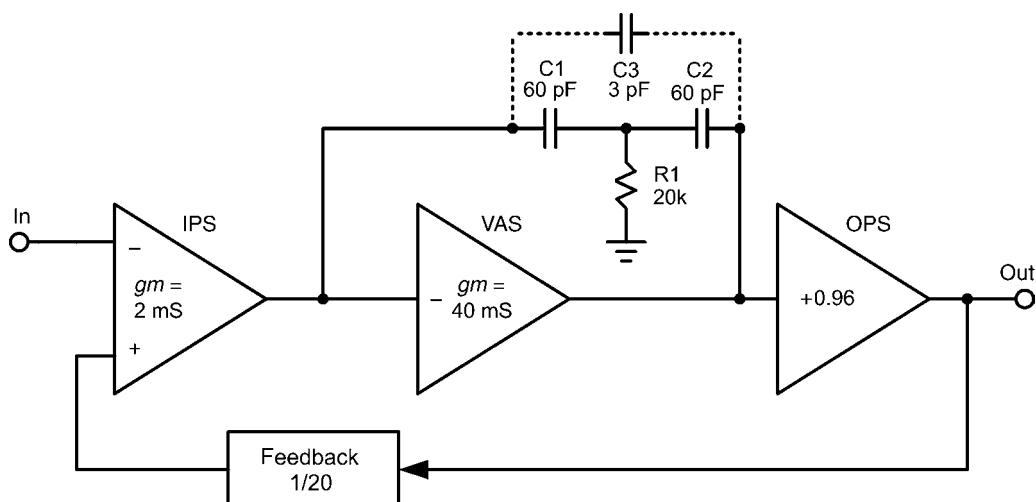
FIGURE 9.4 An amplifier with two-pole compensation.
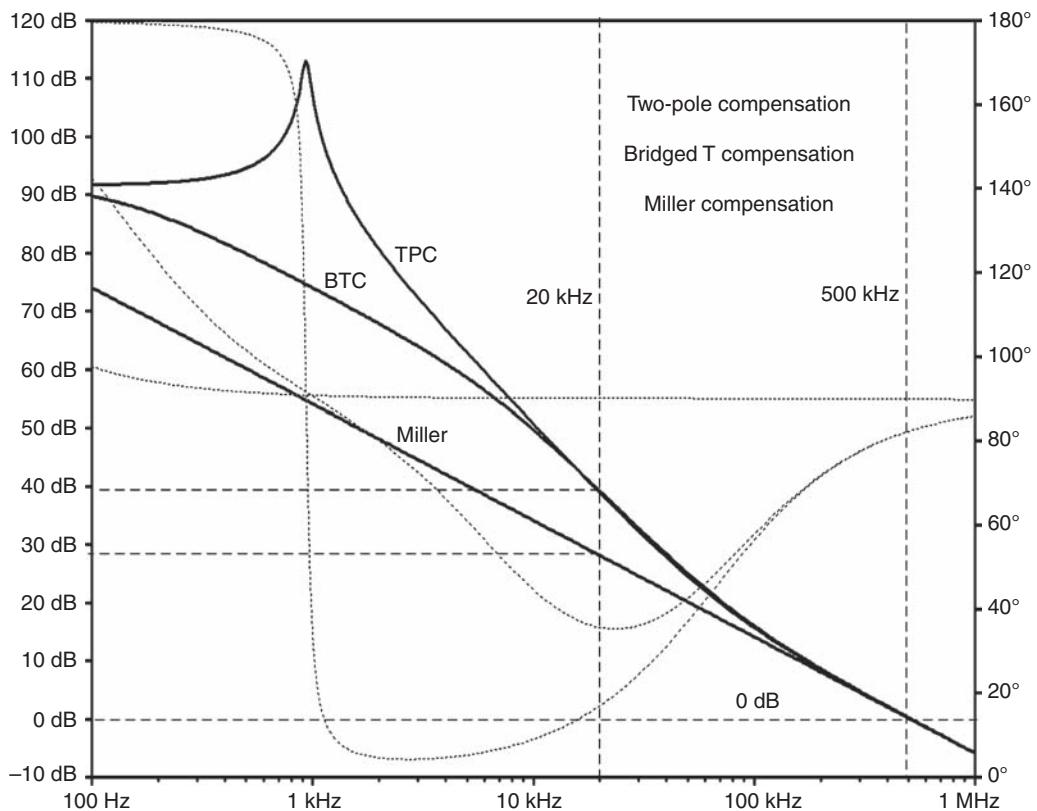
Figure 9.5 Loop gain plots for amplifiers with two-pole compensation and bridged T compensation.

Almost 12 dB of additional loop gain is available at 20 kHz. A further increase in loop gain is achieved at frequencies below 20 kHz. However, notice the large peak in loop gain just above 1 kHz. This happens with conventional TPC as a result of the steep slope in the local compensation feedback loop caused by the series combination of C1 and C2. Such an anomaly in the open-loop gain of the amplifier in the middle of the audio band is undesirable.

The addition of C3 to the circuit of Figure 9.4 eliminates this anomaly by limiting the increase in compensated VAS gain to about 20 dB. It does so by bridging the combination of C1 and C2. Notice that C3, with a value of 3 pF, is smaller than the series combination of C1 and C2 by a factor of 10; this is why the gain step is limited to about 20 dB. I call this *bridged T compensation* (BTC). The loop gain curve labeled BTC in Figure 9.5 shows none of the gain peaking anomaly associated with conventional two-pole compensation.

Conditional Stability

The open-loop phase of conventional Miller compensated amplifiers is a constant 90 degrees (absent excess phase). The open-loop phase of a TPC design dips more negative

at frequencies between the added zero and pole. As long as the loop gain is well above unity where this phase dip occurs, there is little degradation of stability. However, if for some reason the forward gain is substantially reduced so that the gain crossover falls to the frequency of maximum dip, then the phase margin at the lower gain crossover frequency could be much smaller. One example of such an open-loop gain reduction occurs when power is turned off and the circuits become starved as rail voltages decline.

For this, one can define a positive gain margin as the amount of loop gain at the frequency of the maximum amount of phase dip. Similarly, one can define a TPC phase margin as the amount of phase margin existing at that same frequency. This can be defined as the conditional stability gain and phase margin.

Frequency Response Peaking and Overshoot

It is fundamental to TPC that there will be at least some very slight closed-loop frequency response peaking at high frequencies above the audio band. There will also be some corresponding square-wave overshoot. In general, more aggressive TPC will cause greater frequency response peaking. TPC based on the suggested values above will yield a frequency response peak of about 0.8 dB at 125 kHz and square-wave overshoot of about 15% in an amplifier with no excess phase. The usual input low-pass filtering in the amplifier will reduce these effects.

9.4   Miller Input Compensation

Some amplifiers incorporate what is called *input compensation,* as illustrated in Figure 9.6. This is usually in the form of dominant pole shunt lag compensation placed across the input of the IPS. This form of compensation has the advantage that it does not suffer the bond between slew rate and gain crossover frequency that conventional Miller compensation introduces. Unfortunately, it can have detrimental effects on input-referred noise and input impedances. It also does not provide the benefit of pole-splitting. Notice that this approach allows there to be poles at fairly low frequencies at both the input and output of the VAS. R3 can be used to insert a zero that will cancel one of those poles. Other measures may have to be taken to push the remaining pole to a high enough frequency. This kind of input compensation is not recommended for audio amplifiers.
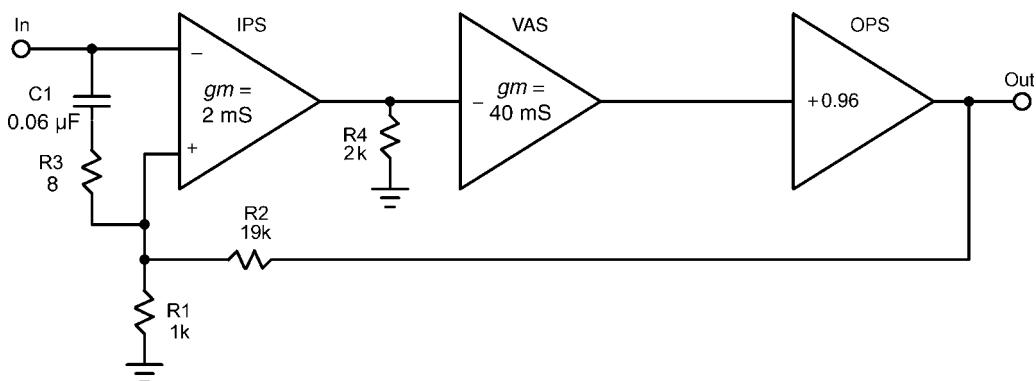
Figure 9.6   Amplifier with input compensation.
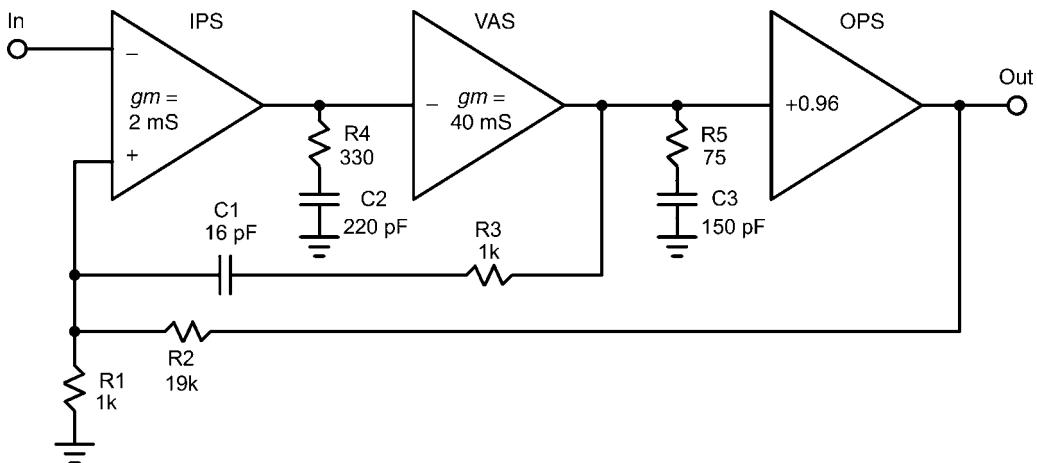
FIGURE 9.7 Amplifier with Miller input compensation.

Combining the Best of Input and Miller Compensation

Miller input compensation (MIC) implements input compensation by means of negative feedback to the input stage [1]. It provides many advantages analogous to those that Miller compensation provides over simple shunt lag compensation. Figure 9.7 illustrates an amplifier with Miller input compensation. Instead of routing the compensation capacitor back to the input of the VAS, it is routed all the way back to the input of the IPS. This encloses the input stage in the wideband compensation loop, reducing its distortion and increasing its dynamic range. For this reason, it breaks the relationship between gain crossover frequency and slew rate. The 50-W amplifier in Ref. 1 achieved a slew rate of 300 V/µs using this compensation technique. The gain crossover frequency f_c in this scheme is the frequency where $X_{C1} = R2$. This frequency is set to 500 kHz in Figure 9.7.

Compensating the Compensation Loop

The Miller compensation loop in Figure 9.7 spans several stages. These stages are implemented with fairly fast small-signal transistors, so the gain crossover frequency of the compensation loop can be made fairly high, perhaps on the order of 10–20 MHz. Nevertheless, that loop itself must be compensated. There still exists the high-impedance intermediate node at the input of the VAS where a pole can contribute instability to the local loop (which is not so local anymore). For this reason the series R-C network consisting of C2 and R4 is added at this intermediate node. In some designs a second series R-C network (C3, R5) is added shunting the output node of the VAS. This reduces the proportion of current at high frequencies that can pass through C1 to the IPS input node, reducing loop gain of the compensation loop. Compensating this loop can be difficult and requires a good deal of experimentation and simulation.

Notice that R3 places a zero in the open-loop roll-off at a frequency above f_c that can cancel some excess phase in the output stage. However, it also transforms the compensation loop to a flat-gain amplifier at higher frequencies. That gain will be (R1 + R3)/R1.

9.5   Transitional Miller Compensation

Cherry proposed a form of Miller compensation that included the amplifier output stage in the local feedback loop formed by Miller compensation. This was done by connecting one end of the Miller capacitor to the output of the output stage instead of to the output of the VAS, as shown in Figure 9.8. This can be called *inclusive Miller compensation* (IMC). The idea was to extend the distortion-reducing benefit of the Miller compensation loop to the output stage. Unfortunately, the output stage is often the largest source of excess phase shift in an amplifier, and this connection often leads to unacceptable risk of instability.

Baxandall proposed a compromise approach that was later dubbed *transitional Miller compensation* (TMC) by Stuart [2].

Figure 9.9 shows an amplifier that employs TMC. Its topology resembles that of TPC, with a pair of series-connected compensation capacitors and a resistor at their junction. However, the resistor is connected to the output node instead of to ground. At
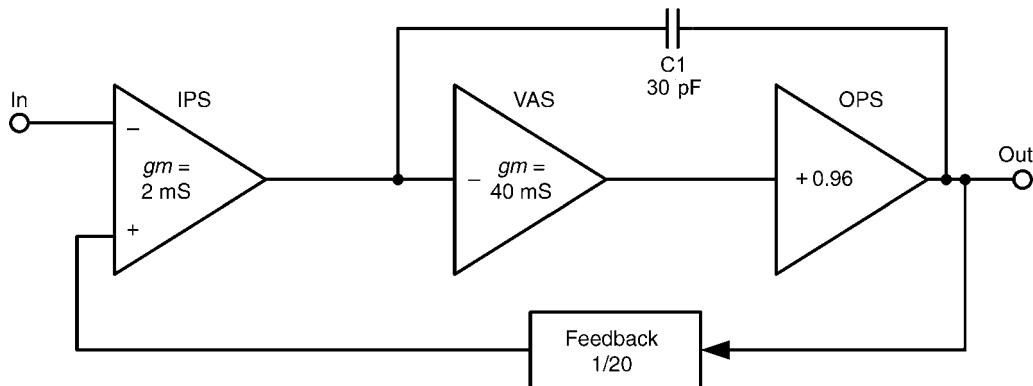
FIGURE 9.8   Amplifier with inclusive Miller compensation.
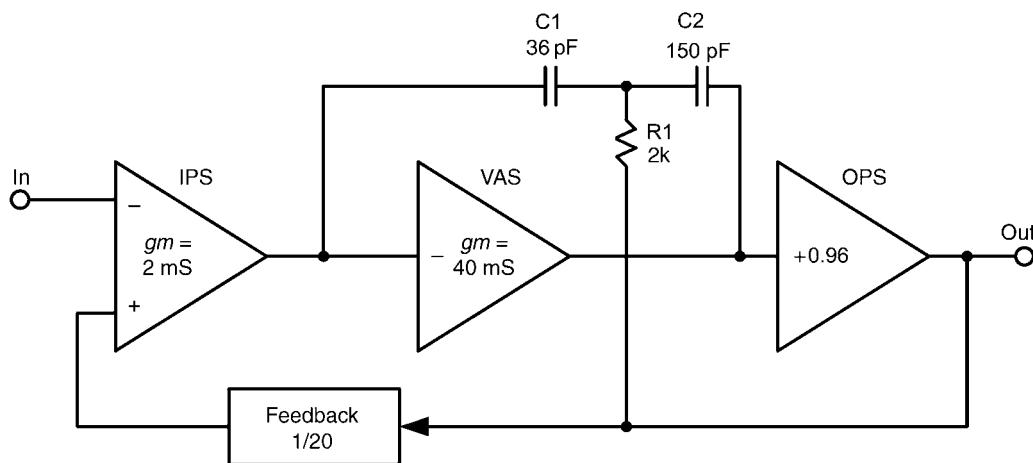
FIGURE 9.9   Amplifier with transitional Miller compensation.

very high frequencies, the two capacitors dominate the resistor and create an ordinary Miller compensation loop that has an effective C_M that is approximately the value of the two capacitors in series.

At low frequencies, the resistor is more conductive than C2, and the output stage is effectively enclosed within the local feedback compensation loop. TMC is well behaved and does not create the frequency response peaking and overshoot that necessarily accompanies TPC. Moreover, TMC reduces distortion by putting more local feedback around the output stage instead of by merely increasing global feedback in a certain frequency band. The global negative feedback rolls off at 6 dB per octave in the TMC scheme. This is the same as with conventional Miller compensation. TMC is very effective in reducing amplifier distortion because it introduces some local feedback around the output stage, where feedback is often needed most. Because the Miller compensation tap-off *transitions* from the output stage to the VAS at high frequencies, it does not suffer the instabilities introduced by IMC.

9.6 The Summing Node Pole

The resistance of the conventional feedback network in combination with the capacitance at the input of the LTP forms a pole that should not be neglected. If the resistance of the feedback network at the summing node is 1 kΩ and the capacitance seen looking into the LTP is 5 pF, a pole will be formed at about 32 MHz. This is not too bad, but the effective input capacitance of the LTP may be more than 5 pF in some cases. For example, if a JFET complementary differential pair input stage employs the 2SK389/2SK170 pair, each with typical gate-drain capacitance of 6 pF, the total capacitance seen will be 12 pF (even ignoring impedance effects of gate-source capacitance). This argues for the use of a low-impedance feedback network.

Another pole can sneak into the summing operation if the source impedance to the amplifier input side of the LTP is significant at high frequencies. For this reason it is usually a good idea to position the usual input LPF shunt capacitor electrically close to the input base of the LTP (I always separate it by at least 100 Ω for the sake of HF stability, however).

References

1. Cordell, R. R., "A MOSFET Power Amplifier with Error Correction," *Journal of the Audio Engineering Society,* vol. 32, January 1984; available at www.cordellaudio.com.
2. Stuart, E. Numerous Postings in DIYaudio Solid State Threads Concerning Negative Feedback; available at (www.diyaudio.com).

This page intentionally left blank

Output Stage Design and Crossover Distortion

The output stage is in many ways the most important part of a power amplifier. It is surely the most difficult section in which to reduce distortion when all reasonable measures have been taken to reduce distortion in the input and VAS stages. There is also a lot more money tied up in the output stage.

The output stage discussion was begun in Chapter 5. Concepts of crossover distortion were introduced and other classes and topologies were covered. Here we focus on the emitter follower (EF) output stage. The CFP output stage was discussed and was found to have some serious challenges and shortcomings, so it will not be discussed further. However, many concepts discussed here also apply to CFP output stages.

10.1   The Class AB Output Stage

The class AB output stage is the workhorse of most audio power amplifiers. This stage, shown in simple form in Figure 10.1, was examined in some detail in Chapters 3 and 5, where a simple power amplifier was evolved to a fairly high-performing design of conventional topology.

The output stage of Figure 10.1 is the classic Locanthi T circuit [1, 2], which will also be referred to here as a Triple EF or simply a Triple. This is my preferred BJT output stage, as it provides far higher performance than a simple Darlington output stage (a Double EF).

It will also be assumed throughout this chapter that the output stage is being driven in voltage mode. This loosely means that the output impedance of the VAS is much lower than the input impedance of the output stage. Bear in mind that the output impedance of the VAS is often fairly low, especially at high frequencies, due to the shunt feedback created by Miller compensation. Assuming predriver and driver transistor beta of 100 and output transistor beta of 50, the current gain of the Triple is 500,000, meaning that its input impedance is about 1 MΩ even when driving a 2-Ω load.

The voltage gain of the output stage is determined by the voltage divider formed by the output stage emitter follower output impedance and the loudspeaker load impedance. The output impedance of each half of the output stage is approximately the sum of the dynamic emitter resistance re' and the external emitter resistance R_E. The output impedance of the stage is thus approximately equal to R_E when $re' = R_E$.
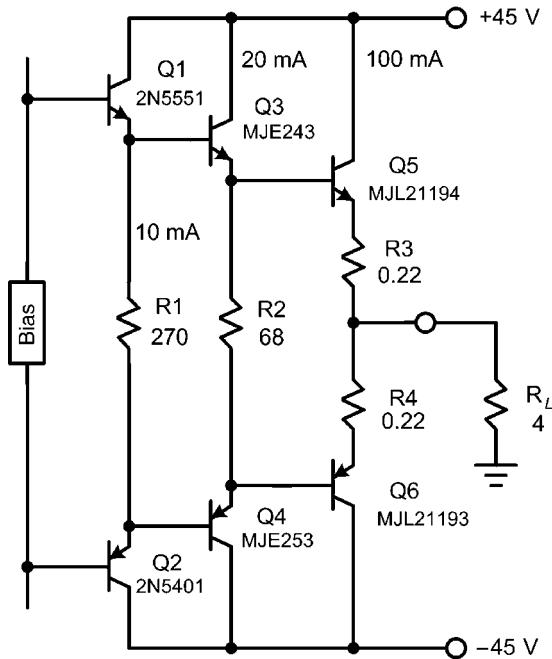
Figure 10.1 A simple class AB output stage using a Triple.

Class B or Class AB?

In a class B amplifier, the top and bottom halves each conduct for one-half cycle and the handoff from one side to the other is abrupt. In a class AB amplifier, the stage behaves largely like a class B amplifier, but some overlap of conduction is permitted, so that the transition of contribution to the output signal is a bit more smooth and broad. In the most widely used output stage, a small *optimum* bias is applied, called the *quiescent bias* I_q. In the region of $\pm 2I_q$ the stage is essentially in class A, with both transistors contributing transconductance. This chapter is focused exclusively on class AB output stages. Other authors have described this mode of operation as class B, and this is really just a matter of semantics [3].

10.2   Static Crossover Distortion

When the contribution to the output signal is transitioned from one half to the other half of the output stage, the effective output impedance of the output stage may change. This changes its gain into the load and causes static crossover distortion. This phenomenon was discussed at length in Chapter 5.

If the gain of the output stage is plotted as a function of the current being driven into the load, a so-called wingspread plot results [3]. Such a plot is shown in Figure 10.2 for the Triple output stage of Figure 10.1 biased at optimum quiescent current and at values of half and twice optimum current. This stage employs 0.22-Ω emitter resistors and its theoretical optimum bias is 118 mA, the ideal gain for the output stage is unity,
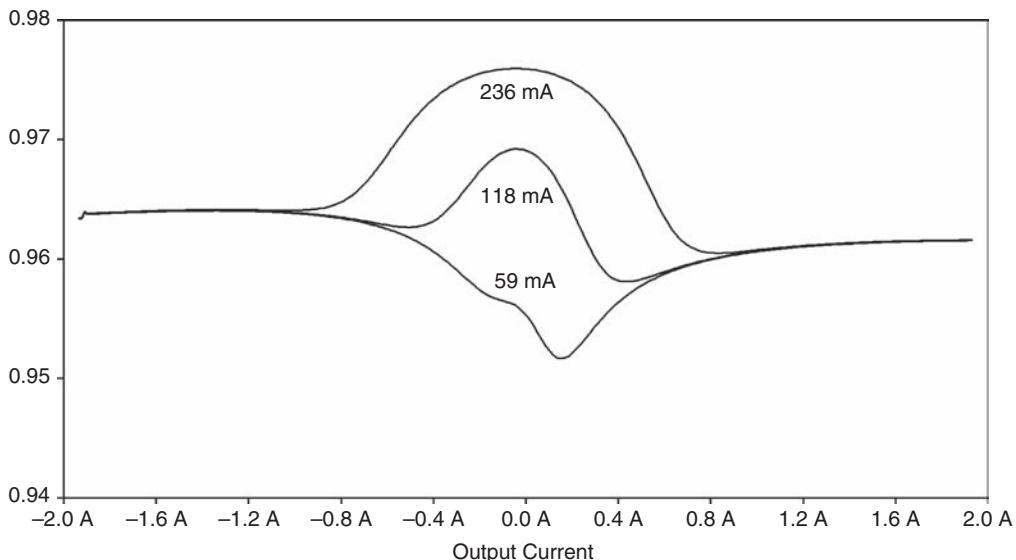
FIGURE 10.2   Wingspread plot illustrating the crossover distortion mechanism.

while a typical gain is on the order of 0.95 (95%) when driving a 4-Ω load. The peak-to-peak gain variation for the optimum bias case in Figure 10.2 is about 1.1%.

If a class AB output stage is overbiased, *gm* doubling can occur [3]. Suppose that the quiescent bias current of the output stage is sufficiently large that the intrinsic emitter resistance ($re' = 1/gm$) of the top and bottom transistors is much smaller than the resistance of the emitter resistors R_E. Under these conditions, the output impedance of the output stage will approach $R_E/2$. The effective transconductance of the output stage will be $2/R_E$. If the output voltage swings positive to produce a current into the load greater than twice its quiescent current, then only the top transistor will be conducting and the output stage impedance will be equal to R_E. Under these conditions the output stage transconductance is simply $1/R_E$. Thus we find that the effective transconductance of the output stage has nearly doubled in the *crossover* region where both top and bottom halves of the output stage conduct. The output stage transconductance has actually been cut in half outside the crossover region.

Evidence of *gm* doubling can be seen in Figure 10.2 for the overbiased case. If the nominal gain at high current was 0.94 and the gain rose to 0.97 in the crossover region (half the loss from unity), this would represent full *gm* doubling, which can only be approached in practice.

So-called *gm* doubling can happen when a conventional class AB design is unintentionally overbiased or it can happen in class AB designs that are deliberately overbiased to achieve a larger crossover region. We call these *class AAB* designs. The *gm*-doubling phenomenon also occurs in class A amplifiers when they are called on to deliver more than twice their quiescent current into the load. This will often happen in class A designs when they drive low-impedance loads to substantial power levels, where they effectively transition into class AB operation.
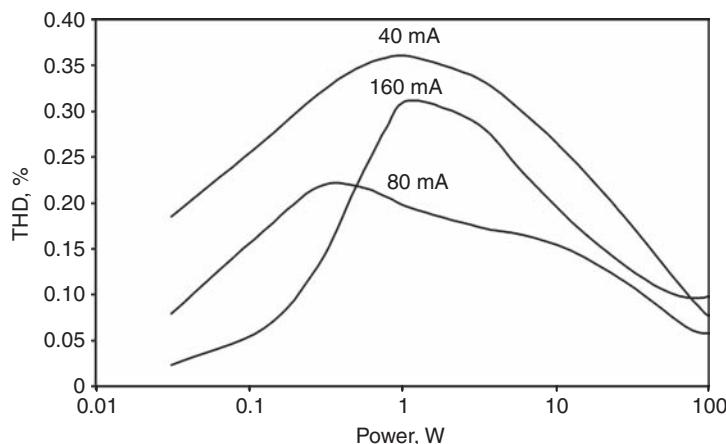
FIGURE 10.3   Crossover distortion versus power level.

Because crossover distortion is largely a function of output current, it will always be larger for loads that have lower impedance. Virtually no crossover distortion will be produced when an amplifier is under a no-load condition.

Crossover Distortion as a Function of Signal Level

Crossover distortion is small at very small signal levels where the class AB output stage is operating within its class A region, extending to peak output current equal to about twice I_q. Crossover distortion also tends to be low at high output levels where the crossover region of nonlinearity is only a small fraction of the signal swing. Crossover distortion is usually highest at low power levels. Figure 10.3 shows crossover distortion of the output stage of Figure 10.1 as a function of power level when driving 4 Ω. It can be seen to peak at about 0.5W. The other two curves show crossover distortion when I_q is one-half and twice the optimum value. It is notable here that the optimum bias is 80 mA, somewhat less than the theoretical value of 118 mA. This reflects some ohmic resistance contributions to effective R_E from the power transistors.

10.3   Optimum Bias and Bias Stability

Static crossover distortion is minimized when the variation in output impedance through the crossover region is minimized. This variation occurs as a result of the changes in transconductance with current of the upper and lower output transistors. The variation is thus a function of net output current, not net output voltage.

Assume ideal output transistors, each with an emitter resistor R_E. The emitter resistor serves to stabilize the bias current by providing a resistance across which a voltage drop will establish the bias current. However, it also plays a critical role in determining crossover distortion.

The bias spreader is usually implemented with a V_{be} multiplier. Part or all of the V_{be} multiplier circuit is usually mounted on the output transistor heat sink so that long-term output stage temperature can be tracked, providing a measure of temperature compensation. In Chapter 14 the use of more sophisticated output transistors that

include built-in temperature-sensing diodes will be discussed. These permit the design of bias spreaders that track internal output transistor temperature changes much more quickly and accurately.

Setting the Bias

The output stage bias is inevitably a function of heat sink temperature and junction temperature of the output transistors. It is also a function of the temperatures of the predriver and driver transistors. Under what conditions should the quiescent bias be set? Should it be set while the amplifier is at idle after it has stabilized? Should it be set by a distortion measurement? If so, at what power level into what load impedance? In what way is the degree of thermal compensation established in the amplifier design? This will affect the biasing process as well. These issues will be addressed in Chapter 14.

Bias Stability

Bias stability is important to class AB output stages because crossover distortion is sensitive to the quiescent bias current I_q. Figure 10.4 shows a plot of simulated crossover distortion as a function of quiescent bias current for the simple class AB output stage of Figure 10.1 driven from a voltage source. The stage is driving a 4-Ω load. Shown on the plot are THD-1 and the amplitudes of the individual odd harmonics up to the seventh harmonic. The even harmonics are of less interest. The power level is set to be 1 W. Notice that the different harmonics do not share the same minimum. These curves show that it is much safer to err on the high side when setting the bias current.

  Stability of the quiescent bias current can be a challenge because of the temperature variations in the output transistors and because it only takes a few millivolts to produce a 10% change in quiescent bias current.

Dynamic Bias Stability

Dynamic bias stability refers to the behavior of the output stage quiescent bias as a function of output transistor junction temperature changes caused by real program
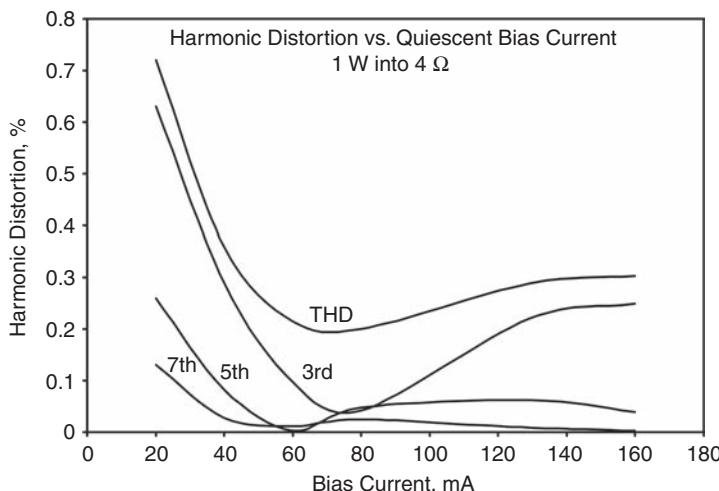
Figure 10.4 Crossover distortion versus quiescent bias current.

material. This does not show up under ordinary continuous sine wave testing on the bench. Dynamic bias tracking error can lead to conditions of overbias or underbias after the average power of the program material changes. This problem will be discussed in detail in Chapter 14.

The Bias Spreader

The V_{be} multiplier and minor variations on it are almost universally employed for the biasing of output stages. However, there are some challenges in designing it to provide good thermal bias stability and temperature tracking of the output transistors. Tracking is important because just 10 mV of error represents a large fraction of the ideal 26 mV which should appear across each emitter resistor. Tracking is made difficult because of the numerous time constants involved, particularly the very slow time constant of the heat sink on which the temperature sensing transistor or diode is usually mounted. The temperature of the power transistor junction can change much more quickly than that of the temperature-tracking device.

The ideal 52 mV that appears emitter to emitter at the output devices is the result of a subtraction of multiple junction drops from the bias spreader voltage. In the case of an output Triple, a spreader voltage on the order of nearly 4 V is required, from which 6 V_{be} will be subtracted to arrive at the 52-mV number. This process introduces increased sensitivity and opportunity for error. Often, several of those V_{be}s are associated with predriver and driver transistors not mounted on the heat sink, and are therefore not at the same temperature as the output transistors. This means that only a fraction of the bias spreader voltage should be temperature compensated by the heat sink temperature. The finite impedance of the bias spreader can also introduce changes in bias voltage if the VAS bias current is not well controlled. Bias spreader design will be covered in detail in Chapter 14.

10.4   Output Stage Driver Circuits

So far we have discussed output stages with simple or ideal drivers. In reality, the driver must be considered an integral part of the output stage. The two most common driver arrangements for emitter follower (common collector) output stages were discussed briefly in Chapters 3 and 5. These are the Darlington and the Triple, with one and two EF stages preceding the output transistors respectively.

Darlington Output Stage

The Darlington output stage consists of two emitter followers in tandem. It produces approximately unity gain and a current gain that is the product of the betas of the driver and output transistors. If the beta of the driver is 100 and that of the output transistor is 50, then the current gain is 5000. If the amplifier is driving a 4-Ω load, the VAS will see a net load of about 20 kΩ, significantly limiting its gain. If beta droop at high current causes driver and output transistor β to fall by a factor of 2, the VAS load could decrease to 5 kΩ. If the VAS produces a swing of 40 V peak for a 100-W/8-Ω amplifier, it will have to swing 8 mA peak.

Figure 10.5 shows a Darlington output stage with the bias spreader depicted as a box and with driver emitter resistors returned to the output node. The driver transistors in this common arrangement operate in class AB (they turn off shortly after the output transistor turns off).
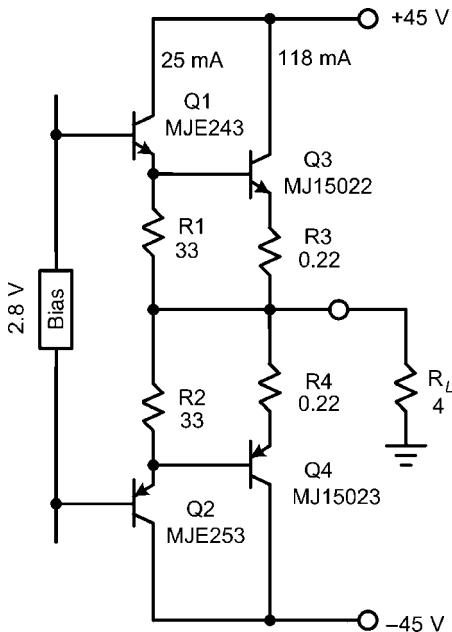
FIGURE 10.5 A simple Darlington output stage.

The Triple

An output stage Triple employs three transistors to achieve increased current gain. The most popular Triple is the common collector Triple. It simply adds an additional predriver emitter follower to the output stage, increasing total current gain by an additional factor of 100 if the β of the predriver is 100. With a total current gain of about 500,000 and a Z_{in} of about 2 MΩ with a 4-Ω load, it imposes a much lighter load on the VAS.

The most common Triple is the Locanthi T circuit, developed by Bart Locanthi in the late 1960s [1, 2]. This is the output stage shown in Figure 10.1. The predriver and driver emitter resistors are each returned to the emitter of the complementary device. This allows for improved turnoff of the subsequent device by reverse bias. It also increases the input impedance of the output stage because the emitter resistors have essentially no signal across them. The predriver and driver stages in this arrangement operate in class A. This stage requires a bias spread of about six V_{be} (about 4 V).

The Diamond Driver

The *diamond driver* [4, 5] is a four-transistor arrangement in which the first emitter followers are folded, or upside-down, as shown in Figure 10.6. It is a more complex circuit because it requires a pair of current sources to bias the folded emitter follower. An output stage driven by a diamond driver can be considered as another form of Triple, which we will call a *diamond buffer Triple* (DBT).

The collector voltages of the folded emitter followers move with the signal because they are bootstrapped by the signals at the emitters of the opposite driver transistors. This mitigates the nonlinear effects of their collector-base capacitances on the VAS output
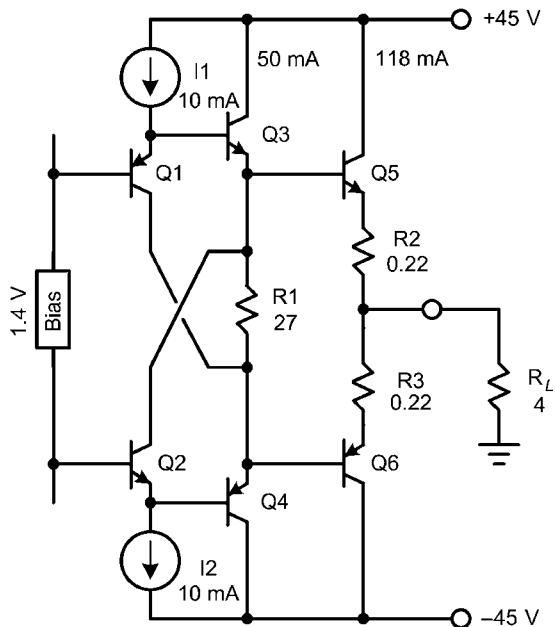
Figure 10.6   A diamond buffer driver in an output stage.

node. The Early effect in the predrivers is also greatly reduced. This arrangement permits the use of fast, low-voltage transistors for the predriver. Power dissipation in the predriver is also much smaller. Most of the dissipation that was once in the predriver is now in the current source, whose signal characteristics have little influence on the signal path.

The V_{be} drops of the predriver and driver cancel, leaving the bias spreader to provide only the spread required by the output transistors. If the predriver and driver transistors are bolted together, the temperature dependence of their V_{be} drops will largely cancel. A TO-126 predriver can be bolted to a TO-220 driver, separated by an insulator. The bias spreader then need only to correct the temperature dependence of the output transistor base-emitter junctions. Less opportunity for error is introduced into the driver chain than in the conventional triple EF arrangement. The drivers and predrivers all can be mounted together on an aluminum bar that spans across the amplifier PWB so they are all at the same temperature and there is some modest common heat sinking.

The current source feeding the folded EF predriver limits the amount of current that can be driven into the base of the driver transistor (unlike the situation with the conventional Triple). This can reduce the chances of catastrophic failure under some conditions like output short circuits.

If a diode is connected from the emitter of the folded EF to a fixed voltage, a Baker clamp is conveniently formed whose capacitance effects are buffered from the VAS by the predriver. Such a connection is shown in Figure 10.7. D1 and D2 are connected to positive and negative clipping voltages. Additional diodes (D3 and D4) are needed from base to emitter of the predriver to prevent excessive reverse biasing of
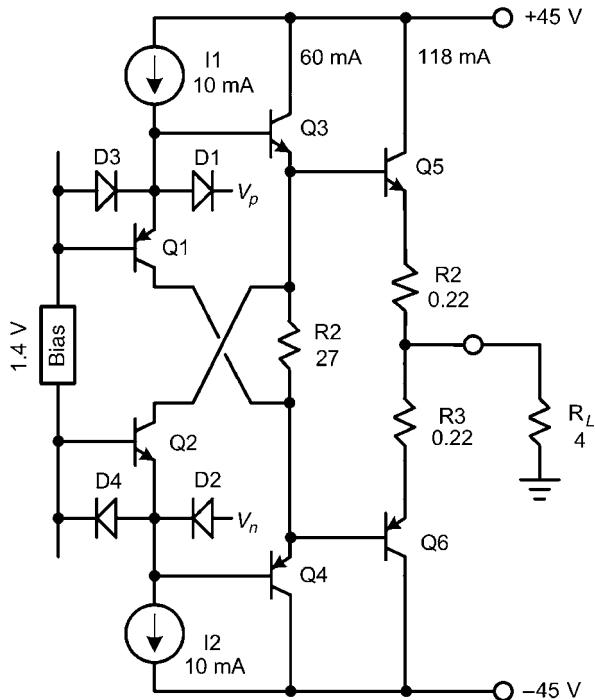
Figure 10.7   A diamond driver with a flying Baker clamp.

the base-emitter junction when the clamping action takes effect. These diodes also prevent the VAS transistors from saturating. D3 and D4 float with the signal, so their capacitance effects are essentially eliminated. This diode can be a small, fast diode. The arrangement is here referred to as a *flying Baker clamp*.

10.5   Output Transistor Matching Considerations

The audio signal passes through the top output transistors on the positive half-cycle and through the bottom transistors on the negative half-cycle. The signal takes two different paths through the output stage depending on the direction of net current flow to the load. If the behavior of the top and bottom halves is not the same, even-order distortion will result.

Beta Matching

If the current gain of the upper half of the output stage is different from that of the lower half, the load on the VAS will be different on the positive and negative half-cycles of signal current swing, creating second harmonic distortion. This effect is greatly reduced by the use of a Triple. In such a case, if the VAS output impedance is low at higher frequencies (where output stage distortion counts most), the output transistor will behave as if it is being driven by a voltage source and beta mismatch will matter much less.

Emitter and Base Resistance Matching

The voltage gain of the output stage when driving a loudspeaker load depends on the effective output resistance of the stage, which in turn is roughly the sum of the dynamic resistance of the output transistor (re') and the external emitter resistance R_E. The dynamic resistance of the output transistor is simply the inverse of its transconductance. When both output transistors are passing current in the crossover region, the net output resistance is that of the parallel combination of these resistances.

As illustrated in Figure 10.8, the dynamic resistance of the transistor as seen looking into the emitter is the sum of the intrinsic emitter resistance re' plus an ohmic component due to base and emitter resistances. The dynamic emitter resistance thus depends on the collector current of the device plus the effects of the transistor's base and emitter resistances.

It is not unusual for the ohmic base resistance RB of a power transistor to be a few ohms. If $RB = 3\ \Omega$ and $\beta = 50$, then the effective ohmic resistance seen at the emitter terminal due to RB is about 0.06 Ω. The ohmic base resistance of a power transistor often decreases at high collector current due to *emitter crowding* [6]. If these resistances (or βs) of the upper and lower output transistors are different, a different output transistor gm will result. This will lead to slightly different voltage gain for the upper and lower halves, which will lead to distortion.

Base Stopper Resistors

Sometimes series base resistors are added to promote better stability in the output stage. This is more often the case when several output transistors are connected in parallel. It reduces interactions among the paralleled output transistors that can lead to instability or oscillation.

The base stopper resistors *stop* the fall of impedance seen looking into the base of the output transistor as frequency increases. They place a minimum value on this impedance and prevent it from going negative under conditions of capacitive loading at the emitter. They *stop* oscillation. Small-signal simulations may not show the instability that is of concern because the ohmic base resistance of the transistor may not have
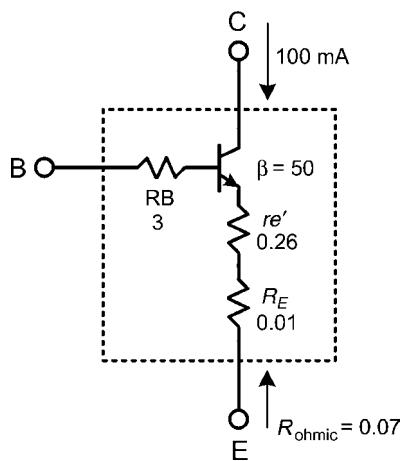
Figure 10.8 Dynamic emitter resistance components.

been reduced by emitter crowding under the quiescent conditions of the small-signal simulation. The base stopper resistors also tame parasitic oscillations by reducing the Q of resonant circuits involving the base terminal of the transistor and associated inductances and capacitances.

If base stopper resistors are employed, the voltage drop across them can be a significant function of base current, and this will lead to dependence of output stage gain (and bias) on the power transistor β and matching of β among the NPN and PNP output transistors with their individual base stopper resistors. Base stopper resistors should not be made larger than necessary. In many cases as little as $2\ \Omega$ is sufficient.

The base stopper resistor is just a further extension of RB. It will thus contribute to effective emitter resistance and rob transconductance in the same way as RB. By itself, a 5-Ω base stopper resistor with an output transistor whose $\beta = 50$, will add a full $0.1\ \Omega$ to the transistor's ohmic component of emitter resistance. This ohmic addition can influence the effective value of emitter resistance and alter the optimum quiescent bias current required for minimum crossover distortion. Conversely, if an output stage was designed for optimum bias with $R_E = 0.22\ \Omega$ for an ideal transistor, the actual value of R_E with the real transistor might have to be smaller. These effects can be seen in Figures 10.3 and 10.4 where the optimum bias current for the output stage is less than the theoretical optimum value.

10.6   Dynamic Crossover Distortion

Transistors do not turn off instantaneously. This is especially true of power transistors because they are slower than small-signal transistors. As the signal current goes through crossover in a class AB output stage at high frequencies, the rate of change of current can be substantial, and it can be difficult for the transistor turning off to do so fast enough.

The failure to turn off quickly and cleanly can result in a brief period when both transistors are conducting together (not just the quiescent bias current). This is variously referred to as *common mode conduction*, *totem pole conduction*, *conduction overlap*, *cross-conduction,* or *shoot-through current*. The resulting impairment to output stage behavior is called *dynamic crossover distortion*. Figure 10.9 shows the simulated collector current waveforms of the power transistors in a class AB output stage being driven hard at 20 kHz. Notice the separation of the two waveforms at the crossover point. It is well in excess of the quiescent bias current. This is evidence of cross-conduction. Notice also the sharper edge of the current waveform of the transistor turning off.

Cross-conduction results when the transistor turning on must conduct additional current to overcome that of the transistor that is turning off too slowly. Obviously, any hope of an optimal-biased class AB crossover transition goes out the window under these conditions. In many amplifiers the power supply current will rise at high frequencies when driving a load to high levels. This is a symptom of cross-conduction. In some cases cross-conduction can lead to destruction of the amplifier.

Transistor Turn-Off Current Requirements

Consider a 100-W/8-Ω amplifier delivering 200 W into a 4-Ω load at 20 kHz. Voltage slew rate will be 5 V/µs and the corresponding current slew rate will be 1.25 A/µs. If the f_T of the transistor is known and the rate at which it needs to turn off (in amperes per
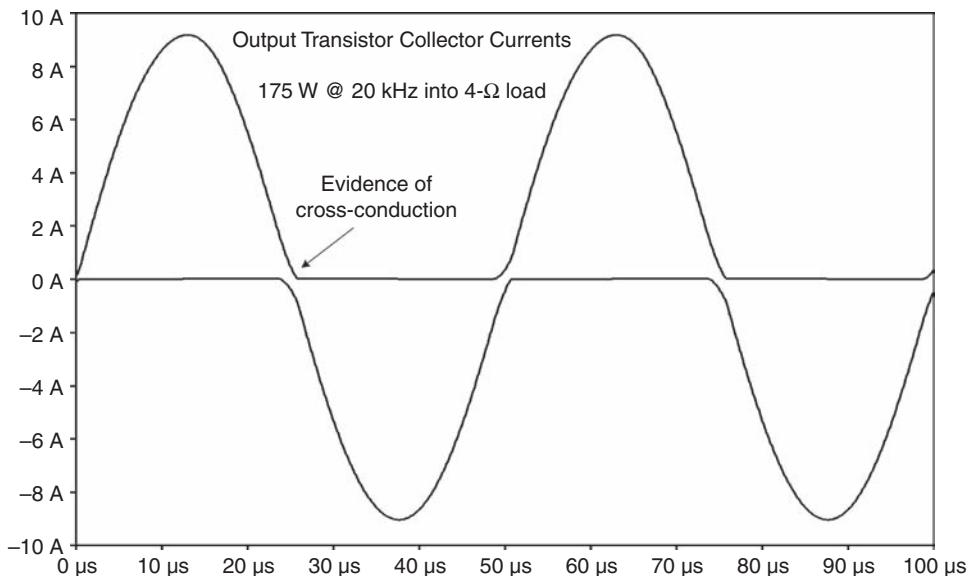
FIGURE 10.9 Output transistor current waveform.

microsecond) is known, then the base current required to be pulled out of the base can be calculated. For a BJT, the hybrid-pi input capacitance is approximately

$$C\pi = gm/(2\pi * f_T) \tag{10.1}$$

For a respectable 4-MHz power BJT (MJL21193/4) biased at 150 mA, $C\pi = 0.24$ μF. At higher collector current $C\pi$ will be much larger. At only 1 A, $C\pi$ will be a whopping 1.6 μF! The rate of voltage change at the base is

$$dV_{be}/dt = I_b/C\pi \tag{10.2}$$

where I_b is the base-discharge current. In a conventional output stage with an EF driver, that current can be no more than the driver bias current. Substituting for $C\pi$, we have

$$dV_{be}/dt = I_b * 2\pi * f_T/gm \tag{10.3}$$

The collector current slew rate dI_c/dt is merely $gm * dV_{be}/dt$, so we have, re-arranging,

$$dI_c/dt = 2\pi * f_T * I_b \tag{10.4}$$

Required base turn-off current is then

$$I_b = \mathrm{ISR}/(2\pi * f_T) \tag{10.5}$$

where ISR is the output current slew rate.

Notice that I_c and gm are not in this simple equation. Notice also that the number of paralleled output devices does not appear in this equation. If the number of devices are doubled, current per device gets halved and $C\pi$ per device gets halved, so total charge that must be removed from all of the bases for a given ISR remains the same. However,

effects of collector-base capacitance have been ignored in this simple estimate. Current flowing through the collector-base capacitance when the signal voltage is changing rapidly will subtract from the available base turn-off current.

An Example BJT Power Transistor

For a conventional power transistor with $f_T = 4$ MHz and a healthy $I_b = 50$ mA, the achievable current slew rate is only 1.2 A/µs. This is just equal to the current slew rate for the amplifier example above, where 200 W was being driven into a 4-Ω load at 20 kHz. To put this in perspective, bear in mind that the peak output voltage is 40 V and the peak output current is 10 A.

As a sanity check, consider the case where the transistor is turning off and its operating current is 1A. This will be at a point in the waveform where the current rate of change is near its maximum value of 1.2 A/µs. As mentioned above, $C\pi$ will be 1.6 µF at this point. The voltage rate of change across the base-emitter junction will be $I_b/C\pi = $ 0.031 V/µs. Intrinsic transconductance of the transistor will be about 40 S. The rate of change in the transistor collector current will be about 40 ∗ 0.031 V/µs = 1.24 A/µs.

Figure 10.10 shows the collector current of the driver transistor under these conditions with the exception that driver bias current has been reduced to 20 mA. When the collector current of the emitter follower driver transistor goes to zero, it has lost control of the output transistor and is unable to make it turn off faster.

Because a push-pull class AB output stage is assumed, the opposite power transistor may be turning on and contributing to the total demanded output current slew rate. It is therefore arguable that the transistor turning off only needs to be turning off at a rate of about 0.6 A/µs in order to achieve the total current rate of change of 1.2 A/µs demanded by 40 V peak at 20 kHz into a 4-Ω load. If the PNP power transistor must turn on in order to decrease the current being sourced into a resistive load while the output voltage is still positive, distortion will surely be created, however.
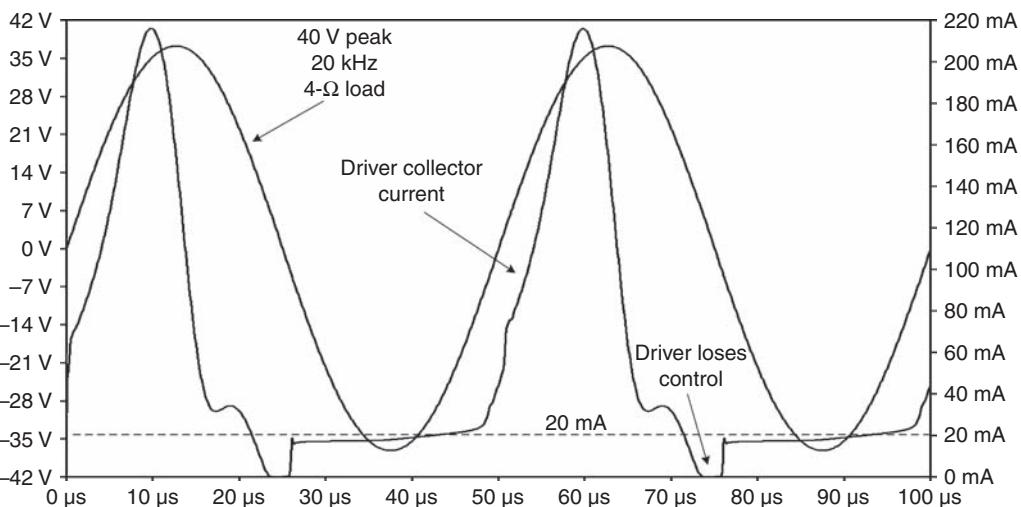
Figure 10.10   Driver collector current as it loses control of the output transistor.
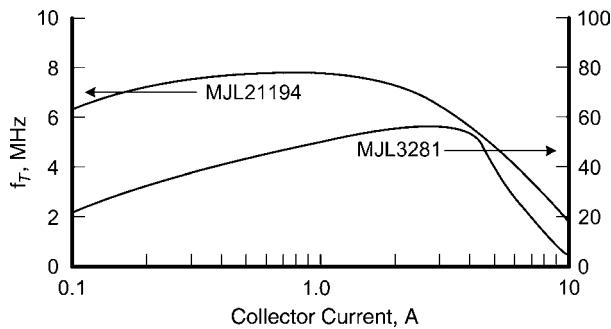
Figure 10.11   Power transistor f_T versus collector current.

The situation is better for BJT *ring emitter transistors* (RETs) or devices with similar advanced structures that provide higher f_T. The ON Semiconductor MJL3281 devices are a good example. Even at $I_q = 150$ mA, these devices still manage a respectable f_T on the order of 20 MHz. This means that with a base-discharge current of 50 mA, each device is capable of turning off at a rate of about 6 A/μs.

Figure 10.11 shows power transistor f_T as a function of collector current for a nominal 4-MHz transistor and a RET. Notice the decline of f_T for both devices at low and high collector current.

Turning Off the Transistor under Conditions of Beta Droop and f_T Droop

An additional concern is turning off the output power transistor in the vicinity of its maximum current at the peak of a sinusoid (when driving a resistive load). This is different than the other challenge of turning off the transistor during high *di/dt* in the crossover region.

Here the problem occurs when the transistor β and f_T become very low at high power under conditions of low V_{ce} and high I_c. A lot of current flows into the base as the peak amplitude of the signal is approached. This high base current is necessary to turn on the transistor to the high demanded current level in light of the decreased β at low V_{ce}.

Just after the peak, the rate of change of collector current becomes reversed, and turnoff of the transistor must begin. All of that charge in the base must be pulled back out of the base. This tends to be a bigger problem at high frequencies.

The Role of Collector-Base Capacitance

Consider once again a 100-W/8-Ω amplifier delivering full power of 200 W into a 4-Ω load at 20 kHz. Voltage slew rate (VSR) will be 5 V/μs and the corresponding current slew rate will be 1.25 A/μs. The voltage slew rate of 5 V/μs will cause a current to flow in the output transistor collector-base capacitance that will tend to oppose transistor turnoff.

For C_{cb} of 500 pF, this current will be VSR ∗ C_{cb} = 5 V/μs ∗ 500 pF = 2.5 mA. This is small compared to the amount of reverse base current needed for turn-off (here 50 mA for f_T = 4 MHz), but bear in mind that an output stage employing N paralleled output pairs will suffer a loss in turn-off current of N times 2.5 mA in this example. This current's proportion of the total required turn-off current will increase with the number of paralleled pairs because the total amount of minority carrier charge in the output transistor(s) will remain about the same as more devices are added.

Higher voltage slew rates delivered into lighter loads will increase the relative proportion of this component of turnoff current even further. Consider a 200-W/8-Ω amplifier with four output pairs delivering 20 V/μs to an 8-Ω load. I_{Ccb} will be 40 mA. Under these conditions ISR = 2.5 A/μs. If transistor f_T is 20 MHz, I_b required for sweep-out of stored charge carriers is only $I_b = $ ISR$/2\pi f_T = 20$ mA, which is less by a factor of 2 than the current through C_{cb}. Finally, it is important to bear in mind that C_{cb} becomes much larger at signal amplitudes near clipping, where V_{cb} is small.

The Speedup Capacitor

We have seen that the emitter follower driver is much more effective in turning on the output transistor than in turning it off quickly. Of course, the driver transistor on the opposite side would be in a good position to turn off the output transistor. Figure 10.12 shows an output Triple that employs a *speedup capacitor*. The capacitor works by resisting voltage change from base to base of the output transistors. This allows the complementary driver to contribute in pulling current out of the base of the transistor being turned off. Under AC conditions, it effectively provides push-pull drive for the bases of the output transistors.

Quite a number of amplifiers use the speedup capacitor and it does reduce crossconduction current and high-frequency distortion on sinusoidal tests. The amount of the capacitance must be considered. If it is to provide turnoff current to the base of one of the power transistors, it will accumulate an increased voltage and it will begin to allow a larger spread voltage between the bases of the output devices, corresponding to the increased common-mode current. If the speedup capacitor is small, it may be ineffective in drawing charge out of the base of the power transistor because it will charge up
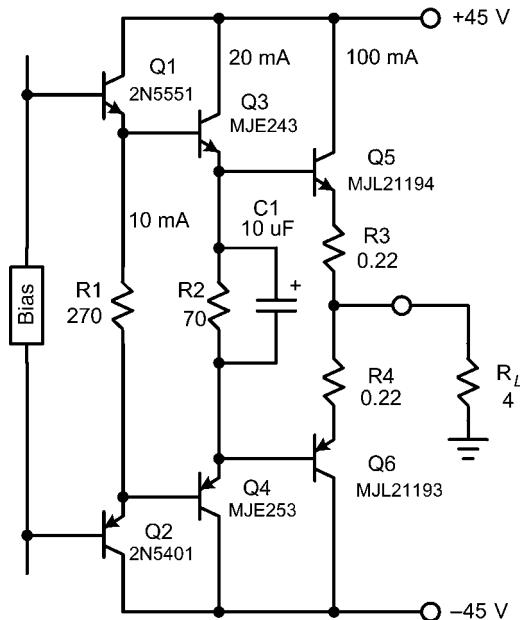
FIGURE 10.12   A Triple with a speedup capacitor.

quickly. If it is large, and does its job, it may leave the output stage in an overbiased state just after the cross-conduction event. This may not be a bad thing, given the alternative.

Suppose that a 10-μF speedup capacitor is asked to deliver 60 mA of turnoff current over an interval of 10 μs (corresponding to 1/5 cycle at 20 kHz). The capacitor will acquire a charge of 60 mV. If each R_E is 0.22 Ω, this added V_{spread} will correspond to increased bias current of 136 mA. Note that this is on the order of typical I_q.

Suppose a 10-μF speedup capacitor is being used with a driver biased at only 20 mA, as shown in Figure 10.12. The driver emitter resistor is 70 Ω. The time constant of 70 Ω and 10 μF is 700 μs. More importantly, the 20 mA of available driver discharge current will require 300 μs to discharge the speedup capacitor back to the nominal spread voltage, corresponding to 3 cycles at 10 kHz. During this time one or both driver transistors will be conducting less than its normal class A bias current. Because the speedup capacitor stores charge, it can have a lasting effect on the behavior of the output stage after the transistor base discharge event. The use of a larger speedup capacitor will do a better job of sweeping out stored minority carriers, but it will lengthen the hangover period. Pick your poison. The speedup capacitor may not be the panacea that some think it to be. Caution is always required when a capacitor is used in a nonlinear circuit.

Current Slew Rate Requirements

Consider a beefy 100-W/8-Ω amplifier driving a brief 20-kHz sinusoidal burst into a 2-Ω load, corresponding to 400 W. Voltage slew rate will be 5 V/μs and ISR will be 2.5 A/μs. If the amplifier uses 4-MHz power transistors, driver bias current will have to be 100 mA in order to handle this transient signal cleanly (assuming no speedup capacitor). These figures may seem extreme, but they are cause for pause.

10.7   The Output Emitter Resistors

The main purpose of the emitter resistors in a class AB output stage is to properly help set a stable quiescent bias current. In the case of paralleled output pairs, the emitter resistors also promote current sharing among the output transistors. However, the emitter resistance also plays an important role in controlling crossover distortion.

Power Dissipation

The emitter resistors in an output stage are called on to carry high currents, and so must be sized accordingly. This often means that the resistors must be physically large and well ventilated. The power dissipation can be estimated easily by recognizing that the emitter resistors together account for an amplifier output resistance that is in series with the load. Power dissipated in the emitter resistors is proportional to the net emitter resistance as compared to the load resistance.

Consider a 100-W/8-Ω amplifier delivering 200 W into a 4-Ω load. Assume that the amplifier employs two output pairs and that each transistor has an emitter resistor of 0.2 Ω. The output resistance to be used in the estimate is then the output resistance of the output stage, which is 0.1 Ω. If 200 W is being dissipated in a 4-Ω load, then 5 W will be dissipated in the emitter resistors. Because there are four of them, each one will be called on to dissipate 1.25 W. It is important to stress that this is average power dissipation over a cycle.

The peak current delivered to the load is 10 A. This means that each emitter resistor must be capable of handling peak current of 5 A. In some cases, this will govern the required size of the emitter resistors. The peak voltage drop across the emitter resistors will be 1 V, and the peak power dissipation for each resistor will be 5 W.

Inductance

It is usually recommended that the output stage emitter resistors be noninductive. However, there is little evidence that anyone has taken the trouble to measure the inductance of ordinary wire-wound emitter resistors and to quantify their effect. I am also unaware of any good technical analysis of emitter resistor inductance and its actual effect on output stage behavior. However, given the switching nature of a class AB output stage, one would instinctively assume that very low inductance in the emitter resistors is important.

The inductance of several typical inductive power resistors in the usual range of values used for emitter resistors was measured. The results indicate that conventional (inductive) wire-wound resistors in the 0.1- to 0.5-Ω range commonly used as emitter resistors in power output stages can be expected to have between 16 nH and 70 nH of parasitic inductance. Inductance appears to be smaller with smaller resistances, as expected. A safe worst-case estimate for typical modern output stages would be 120 nH for a 0.33-Ω wire-wound resistor. The axial and radial versions of the 0.33-Ω resistor had nearly identical values of inductance. At the other extreme, a pair of 0.68-Ω metal oxide 2-W resistors in parallel had a very low inductance of 25 nH. This is little more than that of a 1-inch trace.

One thing that must be considered in estimating the impact of small amounts of inductance in the emitter resistors is the expected current rate of change (ISR) in the resistor and the resulting inductive component of the voltage drop. The rate of change will be greatest near the crossover region, where the power transistor is in the process of turning on or turning off. Using ISR = 2.5 A/μs from the example above, each resistor will see 1.25 A/μs. If resistor inductance is 100 nH, we have an inductive voltage drop of 125 mV. This is not insignificant.

Paralleled Emitter Resistors

One approach to reducing inductance and increasing power dissipation without resort to large wire-wound resistors is to parallel several smaller power resistors to achieve the necessary resistance and power dissipation. Two 3-W metal oxide resistors can be connected in parallel to obtain a suitable noninductive emitter resistor. The penalty here is an increase in occupied board space unless the resistors are stacked.

10.8   Output Networks

Emitter followers are the basis of most output stages. They can be picky about their load when it comes to local high-frequency stability. Emitter followers can become unstable if they are lightly loaded at high frequencies or if they are called on to drive a capacitive load.

A capacitive load can also introduce another pole into the output stage frequency response, possibly destabilizing the global negative feedback loop. For these reasons, most amplifiers incorporate an output network that controls the impedance seen by the
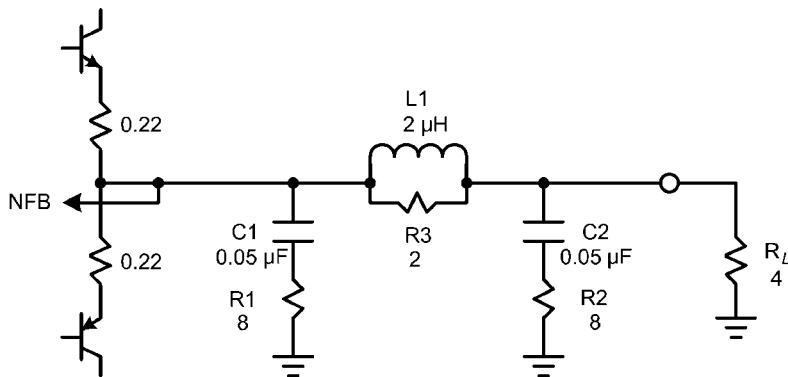
FIGURE 10.13   An output network arrangement.

output stage and isolates the load from the output stage at high frequencies. This helps to make the amplifier stable with the great variety of unknown loads it may be presented with by speaker cables and loudspeakers.

Figure 10.13 illustrates a simplified output stage with an output network and a load. The network includes a series R-C Zobel network to ground on the input side and a parallel R-L network in series with the signal path to the load. For generality, a second Zobel network is shown on the output side of the network for variants that will be discussed later.

The Zobel Network

The series combination of R1 and C1 shunting the output node is called a Zobel network. The purpose of the Zobel network is to ensure that the emitter follower output stage sees at least some resistive loading out to very high frequencies. This is important if the amplifier has no load or if the loudspeaker load becomes inductive at high frequencies.

Power dissipation in the Zobel network's resistor must be considered. At minimum, the resistor in the Zobel network should have a sufficient power dissipation rating to withstand continuous operation of the amplifier at full power at 20 kHz. Consider a 100-W/8-Ω amplifier with a typical Zobel network consisting of 0.05 μF and 8 Ω. This combination will be resistive at frequencies above about 400 kHz. The impedance of the capacitor will be about 159 Ω at 20 kHz. If the output voltage is 28 V RMS, the current in the network will be 176 mA. The power dissipation in the resistor will be 0.25 W. However, in the unfortunate event that the amplifier breaks into a high-power oscillation at ultrasonic frequencies, a small Zobel network resistor will likely get fried. For this reason, Zobel network resistors are often very oversized.

Because the function of the Zobel network is to maintain a resistive load, it is important that the resistor be noninductive. The load presented by the Zobel network should remain resistive up to at least the f_T of the power transistors. An 8-Ω wire-wound resistor with 500-nH inductance will become inductive at frequencies above 2.5 MHz. This argues against the use of wire-wound resistors in the Zobel network unless they are noninductive. Metal oxide resistors with adequate dissipation are a better choice.

Distributed Zobel Networks

The Zobel network is often built with fairly large components in order to dissipate the power that will be present under high-frequency conditions, especially sine wave testing. Such big components are not usually very good out to very high frequencies.

An attractive alternative is to use multiple smaller Zobel networks in parallel, where each Zobel network is placed very close to one output transistor pair. Smaller components can be used; they can be less inductive, and they can more effectively damp out high-frequency resonances. Such an approach provides a better high-frequency shunt path for output stages employing multiple output pairs in parallel. This can be more important when fast output transistors are being used. An output stage employing four pairs might include four Zobel networks, each consisting of a 33-Ω, 2-W metal oxide resistor and a 0.01-μF polypropylene film or COG ceramic capacitor.

The Series L-R Network

Most amplifiers include a small inductor in series with the output, usually with inductance between 0.5 μH and 5 μH. At high frequencies the impedance of the inductor increases and isolates the output stage and the global feedback takeoff point from capacitive loads. The inductor is shunted by a small resistor (1–10 Ω) that helps damp out resonances that the inductor might have in combination with load capacitance.

A combination of 1 μH and 2 Ω might be employed in a high-performance amplifier. At very high frequencies the output stage will never see load impedance less than 2 Ω, even if the output is shunted by a large capacitance with low ESR. The impedance of the 1-μH inductor is 2 Ω at about 3 MHz. At frequencies above 3 MHz the load seen by the output stage will be substantially resistive regardless of what kind of load is connected to the amplifier output. The coil will reduce the amplifier's damping factor at high frequencies. The impedance of a 1-μH inductor at 20 kHz is about 0.13 Ω, implying a damping factor of 62 at 20 kHz.

Details of the amplifier output stage and global feedback compensation will govern how small an inductance can be used without risk of instability when driving difficult high-frequency loads. Amplifiers with low open-loop output impedance at high frequencies will usually permit the use of a smaller inductor.

The Effect of the Coil on Sound Quality

Some high-end-amplifier designers claim that the presence of the output coil degrades the sound. It is hard to justify this solely on the basis of its impact on frequency and phase response when small inductances are used. A 1-μH output coil feeding a 4-Ω speaker load will cause a frequency response droop of less than 0.01 dB at 20 kHz. However, some amplifiers employ a 5-μH inductor in parallel with a 5-Ω resistor. Such a combination reduces the damping factor to only 13 at 20 kHz.

The coil must always be implemented as an air-core coil for best sound quality. Coils implemented with steel or ferrites will suffer nonlinearity, in some cases due to the approach of core saturation. Fortunately, air-core coils with values on the order of only 1 μH are quite small. The coil should be kept away from magnetic materials like steel for the same reason. The coil should also be kept away from devices or circuitry sensitive to radiation from it or from which it can pick up radiation, such as power wires carrying half-wave-rectified signal currents.

Variations on the Networks

In some cases the shunt Zobel network will be placed on the output (downstream) side of the output L-R network, as shown with R2 and C2 present in Figure 10.13 and with R1 and C1 absent. This will normally work adequately, since at high frequencies the resistor across the coil will act as part of the series resistance of the Zobel network, ensuring loading of the output stage that extends to high frequencies.

Sometimes, the series resistance of the Zobel network in this position (R2) will be eliminated, allowing the shunt resistor across the output coil to effectively take on this duty as well. Placing the Zobel network on the downstream side of the coil can help with physical design, getting it off of the amplifier printed wiring board and perhaps out at the speaker terminals. However, this can also compromise the integrity of the load it provides for the output stage at very high frequencies due to the increased wiring inductance in the path to the Zobel network.

There may also be concerns about where the Zobel is returned to ground (local to the output stage or local to the speaker return). One advantage of the downstream Zobel network is that it provides some degree of high-frequency termination directly at the speaker terminals, possibly reducing the opportunity of EMI ingress from the external world via the speaker cables.

The Pi Output Network

A further variation on output networks combines the advantages of the two approaches above. In this case a Zobel network is placed on both sides of the output coil as shown in Figure 10.13 when all of the components are present. The upstream Zobel network provides a low-inductance load for the output stage to very high frequencies and allows high-frequency currents to circulate local to the output stage. The downstream Zobel network provides a good resistive termination right at the speaker terminals at high frequencies, helping to reduce RFI ingress and damp resonances with, or reflections from, the speaker cables. Once again, in some cases the downstream Zobel is implemented without a series resistor, reducing it to merely a shunt capacitor.

Eliminating the Output Coil

Some designers do not employ an output coil in an attempt to eliminate its perceived influence on sound quality. This incurs some risk of instability when driving unusually capacitive loads with little effective series resistance.

In seeking to do without the output coil, three things must be considered.

- Local output stage stability
- Global negative feedback loop stability
- How bad a capacitive load one is willing to tolerate

The likelihood of trouble operating without an output coil can be reduced by employing a large number of output devices operating in parallel so as to greatly reduce effective output impedance. In some cases, the judicious use of base stopper resistors can also help. Finally, amplifiers that have a stiff, high-speed output stage and do not have a high gain crossover frequency for their negative feedback may better tolerate the absence of a coil. I believe that the risk of eliminating the output coil does not justify the perceived gain as long as the value of the output coil is not greater than 1 μH.

10.9   Output Stage Frequency Response and Stability

As mentioned in Chapter 4, the excess phase shift introduced into the negative feedback loop by poles in the output stage is one of the main limitations on how high a gain crossover frequency can be chosen. The frequency locations of the numerous poles in an output stage are governed by several factors, including f_T of the driver and output devices, base resistances, and collector-base capacitances. Device bond wire inductances and external stray inductances can also play a role in influencing the frequency and phase response of the output stage. Finally, the load as seen by the output stage through the output network can have a large influence.

Figure 10.14 illustrates the gain and phase of the Triple EF output stage when it is driving a 4-Ω load with 0.01 μF in parallel. The output stage employs a single output pair (MJL21193/4) with $R_E = 0.22$ Ω and includes the output network of Figure 10.13. Gain and phase are simulated at the feedback takeoff point upstream of the output network. The Triple is driven from a source impedance of 100 Ω. Excess phase at 2 MHz is 20 degrees. Notice that there is no amplitude loss at 2 MHz; response is actually up by 0.4 dB at this frequency. The addition of 2-Ω base stopper resistors eliminates the peak and increases phase lag to 26 degrees. The use of 5-Ω base stopper resistors increases phase lag to 35 degrees.

Variation with Operating Point

The f_T of output transistors varies with current. It gets smaller at low currents. This can happen at the quiescent bias current value. The f_T will often peak in the neighborhood of 1 to 3 A. At high currents the f_T also droops, as does β. This effect was evident in Figure 10.11, where the f_T of the MJL21194 was shown as a function of collector current for V_{ce} of 10 V.
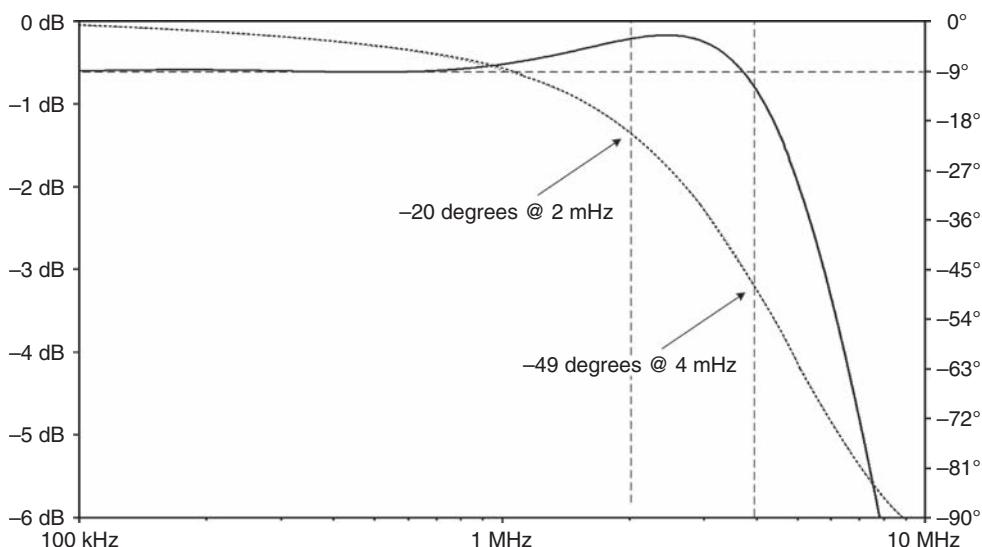
FIGURE 10.14   Gain and phase of the output Triple driving a 4-Ω load and 0.01 μF.

The f_T of output transistors also droops at lower collector-base voltages. This can be especially troublesome under conditions of output swings near clipping, where current is high and collector-base voltage is low, creating a double whammy working against f_T. The f_T of the MJL21194 drops by about 10% when V_{ce} falls from 10 to 5 V. Parasitic oscillations can result if too much excess phase shift results from the reduced f_T.

It is wise to simulate the amplifier with output transistors whose models are operating at the minimum expected f_T and maximum C_{cb}. This can be accomplished by doing an AC simulation with a large DC offset while driving a load resistance. This will simultaneously create conditions of high current and low V_{ce} in the output transistor, causing beta droop, f_T droop, and increased collector-base capacitance to come into play.

The collector-base capacitance of power transistors is not insignificant, often running into the hundreds of picofarads, depending on conditions. It also increases markedly at reduced V_{ce}. This means that things get worse for the frequency and phase response of the output stage under large-swing conditions that approach clipping. As an example, the On Semiconductor PNP MJL1302 has a C_{cb} equal to about 250 pF at 50 V. At 5 V it has climbed to 700 pF, and at 1 V it reaches 1200 pF. These numbers are of added concern when several output transistors are used in parallel.

When the output stage gets very close to clipping, the output transistors go into quasi-saturation, which in many respects is just a further exacerbation of the factors mentioned above. Unfortunately, some VAS circuits can drive the output stage in such a way that the slower output stage clips first. The global feedback loop then suffers from the potential instability created by quasi-saturation effects. This is a good argument for the use of Baker clamps in amplifiers where the VAS would otherwise cause the output stage to clip before the VAS. It is notable that output stages employing Triple emitter followers are less likely to clip before the VAS in many cases as a result of the larger number of V_{be} drops in the output stage. If the VAS can pull to within 1 V of the rail, then the output transistor emitter may reach within perhaps 3V of the rail. Even with $V_{ce} = 3$ V, some quasi-saturation effects are beginning to come into play.

Base Stopper Resistors

Base stopper resistors are sometimes added in series with the base of the output transistors to improve local output stage stability. This is more often seen in output stages where several devices are connected in parallel. Recognizing that an output stage emitter follower can have negative input impedance under some conditions (such as capacitive loading), the addition of a base series resistance can bring that negative impedance back to positive impedance. The base stopper resistor also maintains a lower limit on the total value of base resistance in light of reduced intrinsic base resistance of the output transistor under conditions of emitter crowding at high currents.

The use of base stopper resistors is not without a price. They add to the total base resistance of the output transistor and ultimately contribute to a reduction in the transconductance of the output transistor at high frequencies as the β_{AC} of the device decreases with increases in frequency. As explained earlier, the base stopper resistors can also influence the optimum class AB bias point by altering the ohmic resistance seen looking into the emitter of the output transistor.

Load Capacitance

Because the output stage has nonzero output impedance, placing any capacitive load on it will introduce a high-frequency pole and consequent frequency response roll-off

at high frequencies. It is important to recognize that the open-loop output impedance increases at high frequencies. The bottom line here is that feedback loop stability must be assessed with worst-case load impedances in place.

Excess Phase

The concept of *excess phase* recognizes that a circuit like an output stage may have many poles at higher frequencies, each adding some small amount of phase shift at frequencies in the range of the gain crossover frequency. These phase contributions add up, and sometimes are not accompanied by very much amplitude roll-off. For this reason, it is convenient to lump these parasitic high-frequency pole effects into what is called *excess phase*. A pole at 10 MHz will create a loss of only 0.04 dB at 1 MHz, but will introduce nearly 6 degrees of phase shift. Seven poles at 10 MHz will introduce almost 45 degrees of phase shift (the same as a single pole at the target frequency), but will introduce only 0.3 dB of loss, 1/10 that of a single pole at 1 MHz. In the vicinity of 1 MHz, the effect of these far-out poles is much like that of a constant time delay on the order of 125 ns.

Gain and Phase Margin

We have seen that the output stage plays a major role in establishing how high the gain crossover frequency can be made while retaining adequate loop stability. The gain and phase response of the output stage can vary considerably over different operating conditions. For this reason, it is important to design the power amplifier with adequately conservative feedback compensation so as to achieve generous gain and phase margins. It is crucial to avoid amplifier parasitic oscillations under all conditions of load and signal excursion, including clipping.

Stabilizing the Triple

The Triple has been strongly advocated throughout this book for BJT output stages. However, there is a dark side to the Triple. It tends to be more prone to local parasitic oscillations than the Darlington.

Emitter followers are prone to oscillate when they drive a capacitive load because their falling AC beta with frequency transforms the capacitive load impedance at the emitter into a negative resistance as seen at the base. Frequency-dependent negative resistance (FDNR) is always an invitation to oscillation. Bear in mind that the base-collector capacitance of a subsequent emitter follower can look like a capacitive load to an emitter follower. This is partly why the inclusion of a collector resistor or base resistor sometimes improves stability. The numerous terminal inductances and interelement capacitances like C_{bc} and C_{be} further contribute to instability by creating resonances and forming Colpitts and Hartley oscillator topologies. The Triple is more difficult to stabilize because it involves more EF stages that interact with each other.

Figure 10.15 shows an output Triple with the numerous parasitic inductances that may be found in transistors and their wiring. Bond wire inductance is usually on the order of 10–15 nH, while a 1-in. copper trace contributes about 20 nH. For purposes of simulation and illustration, every base terminal and every emitter terminal has a 35-nH inductor in series with it. Every collector terminal has 10 nH in series with it. Notice also the inclusion of some common rail inductance. This can allow the formation of a feedback path from the collector of the output transistor back to the driver or predriver. Assume that there is no such thing as a solid AC ground at high frequencies.
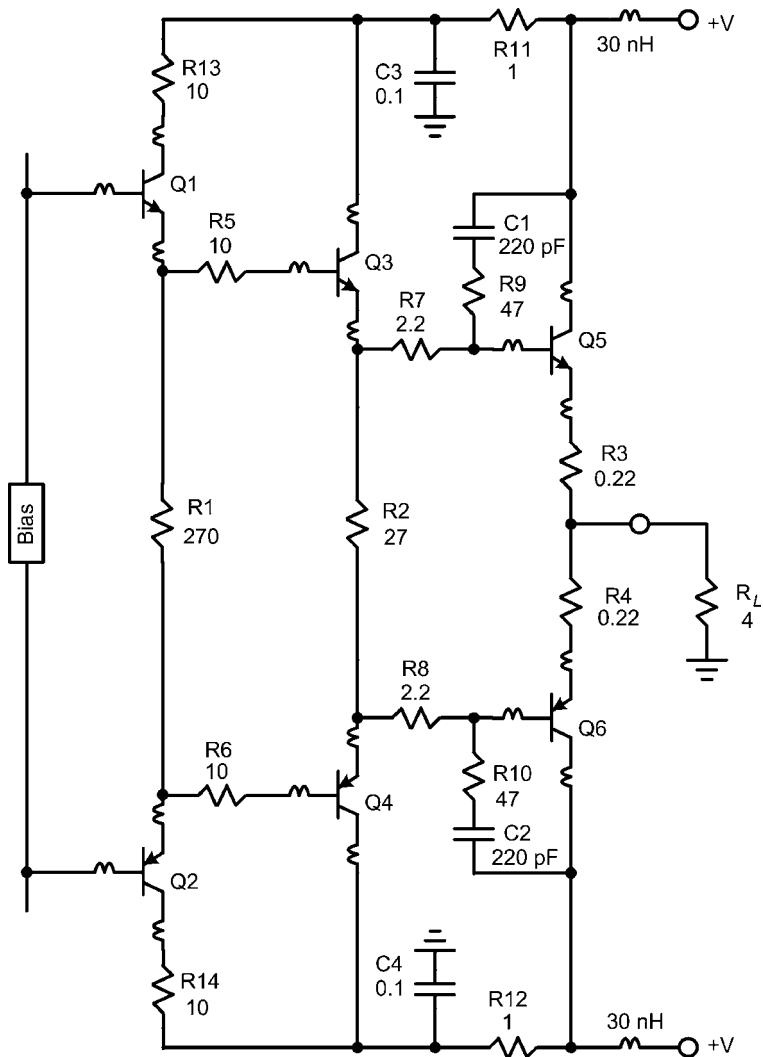
FIGURE 10.15   An output Triple with stray inductances shown.

Figure 10.15 also shows some circuit precautions that suppress instability. Both the output transistors and drivers incorporate base stopper resistors. Placing small base stopper resistors in the bases of the driver transistors in a Triple provides a stability advantage often overlooked by designers. Emitter followers that are isolated from each other by a resistance equal to at least $4/gm$ of the driving stage are much more stable (my rule of thumb). Small resistances in series with EF collectors can also help stability. This is shown for the predriver transistors.

Base stopper resistors prevent the formation of negative impedances and damp resonances. Other circuit approaches that damp resonances and kill oscillator Q are also helpful. Base-collector Zobel networks on the output transistors help damp resonances

formed by C_{bc} and terminal inductances. Shown also is a high-frequency R-C filter in the rail between the output transistors and the preceding driver stages. This acts in two ways. First, it breaks the feedback path via the common rail at high frequencies. Second, it acts as a Zobel network on the supply rail to dampen resonances there. This R-C filter is an opportunity for stabilization that many designers overlook.

The inclusion of ferrite beads in collector or base leads is a popular and effective practice for stabilizing circuits. Ferrite beads provide impedance that rises from zero at DC to some resistive value (often 10–100 Ω) at frequencies in the megahertz range. The resistive component of their impedance serves to damp resonances. However, their use is generally frowned on in audiophile circles because of their potential for introducing nonlinearity.

Good layout is important, but it alone is often not enough. Designers should strive for a layout-robust circuit design. Even the best, tightest layout cannot completely eliminate inductances and the formation of oscillator topologies. Many of the precautions shown in Figure 10.15 are very inexpensive to implement. However, it is also true that not all of them together are necessary in a given design.

10.10   Sizing the Output Stage

The output stage is where the money is in an amplifier (with the possible exception of the power supply). It includes expensive power transistors and expensive heat sinks.

Power Dissipation

Power amplifier output stages are not 100% efficient. This means that power is wasted in the form of heat. The power dissipation in an output stage is simply the power delivered to the output stage from the supply rails less the amount of power being delivered to the load. It was shown in Chapter 5 that the maximum power dissipation in an output stage does not occur when the amplifier is producing maximum output, but rather when it is producing a lesser amount, sometimes on the order of 1/3 rated power. Choosing the number of output pairs to provide adequate static power dissipation is only the first step, and is usually not sufficient to guarantee reliable operation. Sizing the output stage for power dissipation will be discussed in detail in Chapter 14.

Safe Operating Area

Power transistors cannot dissipate rated power under all conditions, even when that power is properly derated for worst-case temperature conditions. This reduced capability is usually evidenced at higher operating voltages and is attributed to an effect called *secondary breakdown*. One cause of secondary breakdown is thinning of the base at high voltage. At higher voltages the collector-base junction depletion region widens and causes the base region to become thinner. This can make the device more prone to uneven heat distribution across the die and lead to hot spots. Because the temperature coefficient of current as a function of voltage is positive for BJTs, the hot spots will conduct more current, making them still hotter and eventually leading to localized thermal runaway. Power transistors must always be operated within their safe operating area (SOA).

The key thing to bear in mind with SOA is that resistive loads do not tax the output stage nearly as much as reactive loads. Because load currents and output voltages are

out of phase with a reactive load, it is possible for one half of the output stage to be sourcing significant current to the load when it has a high voltage across it. Safe operating area is both an amplifier protection issue and an output stage sizing issue. SOA and protection circuits are discussed in detail in Chapter 15.

10.11   Delivering High Current

While the focus on amplifier clipping is most often on voltage clipping, it is equally important that amplifiers do not clip by failing to deliver the amount of output current demanded by the load. Such a failure can happen as a result of the output stage not having enough current gain (especially when beta droop occurs at high current) or it can happen as a result of protection circuits limiting the amount of output current to protect the output transistors from a safe area violation or a short circuit.

Driving Low-Impedance Loads

When you design an amplifier, you must choose the lowest load impedance into which the amplifier will be able to operate satisfactorily. This is the simplest aspect of determining how much output current must be delivered. Given a value of resistive load impedance and maximum output voltage swing, the peak output current can be calculated. We saw examples of such calculations in Chapter 1. A 100-W/8-Ω amplifier driving a 4-Ω resistive load to 40 V peak can be called on to deliver 10 A. Ignoring power supply sag, the amplifier could be confronted with the task of delivering 20 A into a 2-Ω resistive load. Things get worse, however.

Loudspeaker Peak Current Requirements

The model of a simple loudspeaker is largely that of a parallel resonance. The resonance is electromechanical. It is created by the compliance of the suspension and the mass of the cone. As such, this resonance stores energy, often in the form of cone velocity. The cone velocity creates counter emf; the loudspeaker acts like an electric generator. The counter emf usually opposes current flow in the voice coil. The impedance of the loudspeaker rises at the resonant frequency. This would cause most to think that the resonance effect would result in a lighter load on the amplifier and less peak load current. However, if the phase of the driving signal becomes opposite to that of the emf created by the velocity of the cone, much larger currents can result [7, 8]. Under some conditions the current required to drive a loudspeaker load can be twice that required to drive an equivalent resistive load. This phenomenon is discussed in detail in Chapter 18.

Beta Droop

The current gain of power transistors tends to fall off rapidly above a certain collector current. This is called *beta droop*. While a power transistor might have a beta of 80 at 1 A, the beta might fall to 20 or less at a collector current of 10 A. This makes it much harder for the amplifier to deliver high current to the load. This can also endanger the driver transistor because it will be asked to supply very high base current to the output transistor. Figure 10.16 illustrates the β versus I_c characteristic for the PNP MJL21193 power transistor at a collector-emitter voltage of 5 V. Beta drops to about 17 at 10 A.

Consider the 100-W/8-Ω amplifier above when it must deliver 20 A on rare transient occasions into a 2-Ω resistive load. A conservatively designed 100-W/8-Ω amplifier
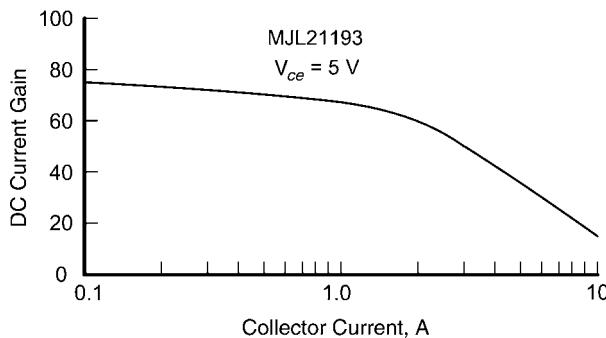
Figure 10.16   Beta versus I_c for the MJL21193.

would include two pairs of MJL21193/21194 output devices. Each pair would be called on to produce 10 A on a transient basis. Current gain for the PNP MJL21193 can be as low as 20 at 10 A. The driver transistor will thus be called on to deliver 1 A. Some driver transistors may already be experiencing some beta droop themselves at 1 A. The beta of the PNP MJE253 falls to about 35 at 1 A. In a simple Darlington output stage, the VAS would then be called on to deliver 29 mA, more than many VAS designs are able to produce (surely without distortion). This illustration underlines the importance of employing an output Triple if high current is to be delivered into difficult loads by the amplifier. It also argues for larger driver transistors like the MJE15032/33 pair.

Newer transistors often do not suffer as much beta droop at 10 A. The current gain of the NJL3281/1302 is 60 at 10 A and falls to about 35 at 15 A. Delivery of high current into difficult loads is one area in which vertical power MOSFET output stages excel, since they do not suffer from beta droop.

f_T Droop

The speed of a power transistor also degrades at high current. This is referred to as f_T droop. The MJE21193 has an f_T of about 7 MHz at a collector current of 1A, but this falls to less than 2 MHz at 10 A with V_{ce} less than 10 V. This means that the amplifier is operating with slower output transistors when it is delivering high current into the load. This can compromise feedback loop stability. It is another good reason to parallel output transistors.

Safe Operating Area of the Driver

The SOA of the driver transistor can also be taxed when the amplifier is called on to deliver high current, especially in light of the fact that the β of the power transistors falls at high currents. Under these conditions, the driver will still try to supply the increased base current required by the output transistor in order to drive the load. In some cases the failure of the output stage begins with the driver transistor entering second break-down. The shorted driver transistor may then take out the power transistor. It is not always possible to know which came first in such a failure situation when all you have left is a pile of melted silicon.

Bear in mind that the driver in a Locanthi Triple operates in class A, and conducts over the full cycle. This can tax SOA in an amplifier with a generous driver bias current of 50 mA and 70-V rails. The driver must be able to handle 50 mA at nearly 140 V. The MJE15032/33 drivers can handle about 150 mA at 140 V.

The message here is that the drivers should be generously sized and that output protection circuits should be designed with protection of the drivers in mind as well. If an amplifier is built with numerous output pairs to increase output SOA, the SOA of the drivers must also be increased. In some cases, a single driver transistor of the same type as the output transistor is a good choice. Indeed, the f_T of RET output transistors makes them plenty fast enough to serve as drivers in an output Triple arrangement. The caveat here is that the predriver bias current must be sufficient to drive the larger collector-base capacitance of the driver transistor.

10.12   Driving Paralleled Output Stages

Most power amplifiers rated at 100 W and above into 8 Ω employ paralleled output transistors to achieve adequate power dissipation, current handling, safe area, and current gain when driving heavy loads. This can introduce some technical challenges.

Output Transistor Current Sharing

A hotter transistor wants to conduct more current. This makes it still hotter, causing it to draw even more current. Even if this process does not lead to thermal runaway, it can easily cause very uneven sharing of load current among the multiple transistors in a paralleled output stage.

Beta droop may mitigate this to some extent, but this will apply less where the high transistor power dissipation is a result of high voltage rather than high current. For example, a power transistor conducting 3 A with 30 V across it will be dissipating 90 W, but it will be operating near its peak beta. Output transistors with matched betas will tend to share current more effectively. Increased emitter resistance will also help significantly.

Output Transistor Capacitances

Some larger amplifiers connect as many as four to ten pairs of output transistors in parallel. It is especially important to bear in mind that the collector-base capacitance of all of these transistors adds up and can become a significant sum. While C_{cb} under normal collector-base voltage conditions is often on the order of only 200 pF, this value can increase to nearly 1000 pF per device under large-swing conditions where the collector-base voltage becomes small. Such a large capacitive load can have small-signal and large-signal effects on the performance of the output stage. In a small-signal sense, the bandwidth of the output stage can decrease and global feedback stability may be reduced. Under large-signal high-frequency conditions, the driver may not be able to discharge this capacitance quickly enough.

The base-emitter capacitances of paralleled output devices will also add up, but the result of this is reduced by the bootstrapping effect of the output emitter followers. Output stages with more paralleled devices will often tend to have gain that is closer to unity, so the increased bootstrapping effect tends to offset the effect of the larger number of base-emitter junctions connected in parallel.

10.13   Advanced Output Transistors

The On Semiconductor ThermalTrak™ output transistors will be discussed at length in Chapter 14, but their electrical characteristics are worth mentioning here [9,10]. They are made with an advanced high-speed perforated emitter process that puts them in the

general class of ring emitter transistors (RETs). This means that they have high f_T and good safe operating area.

The On Semiconductor data sheet for the NJL3281/1302 complementary par of ThermalTrak™ transistors shows typical β to be quite flat at about 100 for most operating currents, falling to about 70 at 9 A [9]. Peak f_T is about 50 MHz at about 3 A, but is still about 20 MHz at 100 mA. At about 6 A, f_T has fallen to about 20 MHz. These transistors suffer much less beta droop and f_T droop than most other BJT power transistors. Collector-base capacitance is about 600 pF at V_{cb} = 10 V. Safe operating area for the device is almost 100 W at 100 V.

References

1. Locanthi, Bart N., "Operational Amplifier Circuit for Hi-Fi," *Electronics World*, pp. 39–41, January 1967.
2. Locanthi, Bart N, "An Ultra-low Distortion Direct-current Amplifier," *Journal of the Audio Engineering Society,* vol. 15, no. 3, pp. 290–294, July 1967.
3. Self, Douglas, *Audio Power Amplifier Design Handbook,* 5th ed., Focal Press, 2009.
4. Jung, Walt, "Op-Amp Audio–Realizing High Performance Buffers, Part 2," *Electronic Design*, October 1, 1998.
5. Williams, Jim, "High Speed Amplifier Techniques," *Linear Technology Corporation,* AN-47, August 1991.
6. Massobrio, Giuseppe, and Paolo, Antognetti, *Semiconductor Device Modeling with SPICE,* 2d ed., New York, McGraw-Hill, 1993.
7. Otala, M., and Lammasniemi, J., "Intermodulation Distortion in the Amplifier Loudspeaker Interface," 59th Convention of the Audio Engineering Society, preprint No. 1336, February 1978.
8. Cordell, R. R., "Open-loop Output Impedance and Interface Intermodulation Distortion in Audio Power Amplifiers," 64th Convention of the Audio Engineering Society, preprint no. 1537, 1982; available at www.cordellaudio.com.
9. ON Semiconductor datasheets for NJL3281D and NJL1302D, www.onsemi.com, June 2006.
10. *ThermalTrak^{TM} Audio Output Transistors*, Mark Busier, ON Semiconductor, AND8196/D, www.onsemi.com, February 2005.

This page intentionally left blank

MOSFET Power Amplifiers

While the majority of audio power amplifiers employ *bipolar junction transistors* (BJT) for their output stage, the power MOSFET presents an alternative with some significant advantages. These include high speed, freedom from secondary breakdown, and ease of driving them to very high currents.

Figure 11.1 shows a simple lateral MOSFET amplifier using the same kind of IPS-VAS that was discussed earlier in connection with BJT amplifiers. This design is much like that of Figure 3.8, the main difference being that Q10 and Q11 have been replaced by lateral power MOSFETs (2SK1056 and 2SJ160) [1]. The V_{be} multiplier is set to a slightly higher bias spreading voltage to accommodate the larger V_{gs} of the MOSFETs as compared to V_{be} of BJT output transistors. The MOSFETs are typically biased at a quiescent current of about 150 mA, where their V_{gs} is about 0.7 V. The V_{be} multiplier is usually not mounted on the heat sink with lateral MOSFET power amplifiers because the temperature coefficient of drain current for a given gate voltage for a lateral MOSFET at the typical bias current is nearly zero. At higher currents, the temperature coefficient becomes negative, promoting good temperature stability.

Notice also the absence of source resistors in this design. Many MOSFET power amplifiers do not employ source resistors because they are not very effective in promoting bias stability or current sharing among paralleled devices (unless they are of an unreasonably large value). Source resistors are also not required as part of the overall crossover distortion management scheme.

MOSFETs do not require DC current drive into the gate, so some designers do not employ drivers (here Q8 and Q9) and instead drive the MOSFETs directly from the high-impedance VAS output. This is not usually a good practice in my opinion because the MOSFETs do need drive current to charge and discharge their input capacitances at high frequencies.

The MOSFET power amplifier also employs gate stopper resistors (R17 and R18) in series with the MOSFET gates. These resistors are often required with power MOSFETs to prevent parasitic oscillations. Values between 100 Ω and 500 Ω are often used.

The design of Figure 11.1 would be changed very little if vertical power MOSFETs were employed instead of the lateral MOSFETs. Vertical MOSFETs typically require a higher V_{gs} turn-on voltage, so the bias spreading voltage will be larger. Some vertical MOSFETs, like the 2SJ201/2SK1530, have a V_{gs} of about 1.7 V at the typical quiescent bias current of 150 mA, whereas others, like the IRFP240/IRFP9240, have a V_{gs} on the order of 4 V at 150 mA [2, 3].

The V_{be} multiplier is still used as the bias spreader, but with vertical MOSFETs some or all of the V_{be} multiplier arrangement will be mounted on the heat sink for bias
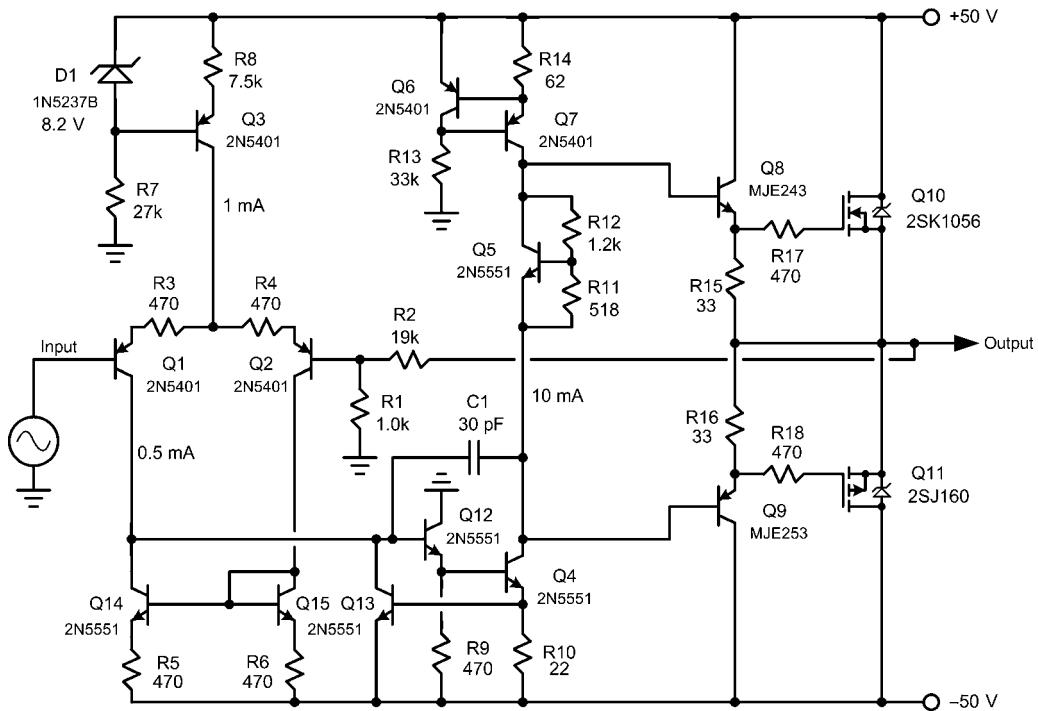
FIGURE 11.1   A simple lateral MOSFET power amplifier.

temperature compensation, as is done with BJT designs. This is so because vertical MOSFETs have a negative temperature coefficient of gate voltage at typical values of quiescent current (on the order of 150 mA).

11.1   MOSFET Types and Characteristics

Lateral MOSFETs were the first to be applied to power amplifiers in widespread production, perhaps the most well known being the Hafler MOSFET amplifiers [4], which employed Hitachi lateral MOSFETs like the Hitachi 2SJ56/2SK176. Other popular lateral MOSFETs included the Hitachi 2SJ49/2SK134 complementary pair [5]. Unfortunately, these devices are no longer available.

Vertical MOSFETs matured at a later point in time, their development spurred by their use in switching power supplies. They are characterized by higher transconductance and higher peak current capability.

Some have argued that vertical power MOSFETs were designed for switching applications and are not suitable for use in analog audio circuits. This is simply not true. What matters are the actual device characteristics, not the primary application for which the parts were made. It is true that the driving application often influences the optimization of certain characteristics over others, but the effect of this on other applications (good or bad) is usually just coincidental.

Lateral MOSFET Structure

The modern power MOSFET is made possible by many of the same advanced techniques that are employed in MOS large-scale integrated circuits, including fine-line photolithography, self-aligned polysilicon gates, and ion implantation. Two planar structures, one lateral MOSFET and one vertical DMOS, are currently the most suitable devices for audio applications. Both are available in complementary pairs, offer suitable current and voltage ratings, and are realized with a cellular structure that provides the equivalent of thousands of small-geometry MOSFETs connected in parallel.

The structure of the lateral power MOSFET is illustrated in Figure 11.2a. The N-channel device shown is similar to small-signal MOSFETs found in integrated circuits, except that a lightly doped n-type drift region is placed between the gate and the n+ drain contact to increase the drain-to-source breakdown voltage by decreasing the gradient of the electric field. Current flows laterally from drain to source when a positive bias on the silicon gate inverts the p-type body region to form a conducting n-type channel. Note that the arrows in Figure 11.2a illustrate the direction of carrier flow rather than conventional current flow. The device is fabricated by a self-aligned process where the source and drain diffusions are made using the previously formed gate as part of the mask. Alignment of the gate with the source and drain diffusions thus occurs naturally, and the channel length is equal to the gate length less the sum of the out-diffusion distances of the source and drain regions under the gate. Small gate structures are required to realize the short channels needed to achieve high transconductance and low on resistance.

While providing high breakdown voltage, the lightly doped drift region tends to increase on resistance. This partly explains why higher voltage power MOSFETs tend to have higher on resistance. A further disadvantage of this structure is that all of the source, gate, and drain interconnect lies on the surface, resulting in fairly large chip area for a given amount of active channel area, which in turn limits transconductance per unit area. Series gate resistance also tends to be fairly high (about 40 Ω) as a result, limiting maximum device speed. Lateral power MOSFETs have been widely used in audio amplifiers. Examples of this structure are the Hitachi 2SK-134 (N-channel) and 2SJ-49 (P-channel). Desirable features of these devices include a threshold voltage of only a
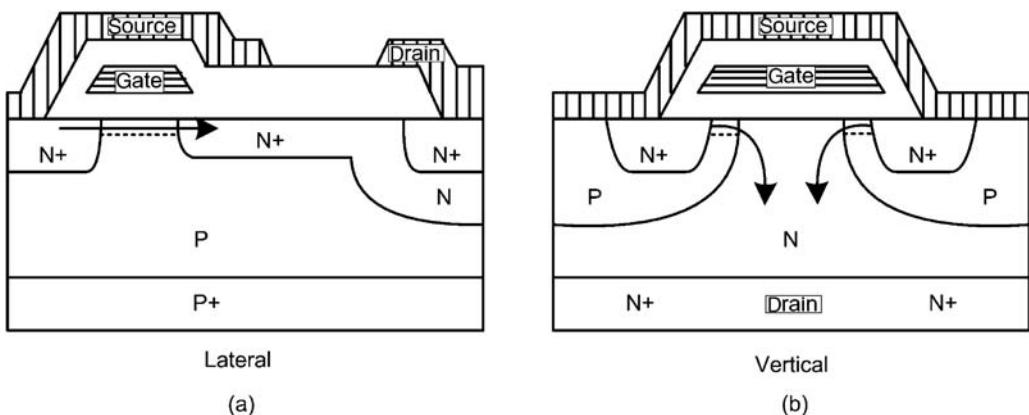
FIGURE 11.2 Structures of N-channel lateral and vertical power MOSFETs.

few tenths of a volt and a zero temperature coefficient of drain current versus gate voltage at a drain current of about 100 mA, providing good bias stability.

Vertical MOSFET Structure

A more advanced power MOSFET design is the vertical DMOS structure illustrated in Figure 11.2b. When a positive gate bias inverts the p-type body region into a conducting N-channel, current initially flows vertically from the drain contact on the back of the chip through the lightly doped n-type drift region to the channel, where it then flows laterally through the channel to the source contact. The double-diffused structure begins with an n-type wafer that includes a lightly doped epitaxial layer. The p-type body region and the n+ source contact are then diffused into the wafer in that order. Because both diffusions use the same mask edge on either side of the gate, channel length is the difference of the out-diffusion distances of the body and source regions. As a result, short channels are easily realized without heavy dependence on photolithographic resolution. Short channels permit high transconductance and low on resistance. The geometry and dimensions of the n-type drift region are such that its effective resistance can be much smaller than that of the drift region for the lateral devices. This also aids in achieving low on resistance while retaining high voltage capability.

The vertical DMOS structure is much more compact and area efficient than the lateral structure because the source metallization covers the entire surface; the polysilicon gate interconnect is buried under the source metallization. Also, each gate provides two channels, one on each side. The amount of active channel area for a given chip area is thus higher than for the lateral geometry. The fact that source metallization areas can occupy virtually an entire side of the chip leads to high current capability. Finally, the length of the gate can be greater in this structure because it does not directly control channel length. This feature, combined with the compact structure, results in lower series gate resistance (about 6 Ω) and higher speed. Because of its many advantages, the planar vertical DMOS structure is the main-line power MOSFET technology. Examples of this cellular structure are the International Rectifier IRFP240 (N-channel) and IRFP9240 (P-channel).

11.2   MOSFET Advantages and Disadvantages

Power MOSFETs enjoy several advantages over BJTs when used in power amplifier output stages. The most well known is the ease with which they can be driven. While BJTs require input current to drive the base, MOSFETs have an almost infinite input resistance at DC. They only require input current to charge and discharge their internal capacitances. In a sense, the DC current gain of a MOSFET is virtually infinite.

This also means that the MOSFET is free from the problem of beta droop at high current that BJT power transistors suffer. As seen in earlier chapters, the beta of a BJT can droop as low as 20 in some cases at currents approaching 10 A. This makes them much more difficult to drive at high current and creates distortion. The f_T of BJTs also droops at high current, whereas the equivalent f_T of power MOSFETs actually tends to increase at high current.

Freedom from Second Breakdown and Device Protection

MOSFETs are generally free from the second breakdown phenomenon that haunts BJT power transistors at high voltage. The safe operating area for a MOSFET is usually
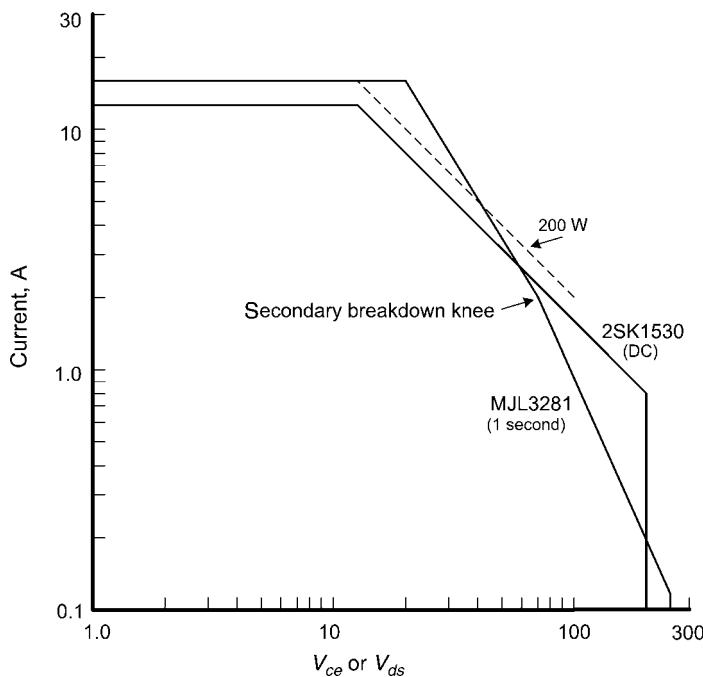
FIGURE 11.3   SOA comparison for BJT MJL3281 and MOSFET 2SK1530.

bounded by constant power dissipation. The point of device destruction is primarily a function of peak die temperature.

Figure 11.3 shows SOA plots for a MJL3281 BJT and a 2SK1530 vertical MOSFET. Notice the absence of the more steeply sloped line on the curve for the MOSFET. This is indicative of the absence of secondary breakdown in the MOSFET. The SOA curve for the 2SK1530 is for a DC condition, whereas that for the MJL3281 is for only 1 second. The 2SK1530 is rated at 150 W, whereas the MJL3281 is rated at 200 W. The dashed line on the plot represents constant dissipation of 200 W. The MJL3281 curve lies above the 200-W line at low voltages because the curve is restricted to 1 second. However, notice that it falls below the 200-W line above about 40 V.

Sustainable power dissipation for 100 ms at 100 V is a figure of merit that I like to use to compare devices for use in audio power amplifiers. The BJT MJL3281 can sustain 180 W, whereas the MOSFET 2SK1530 can sustain 290 W.

This does not mean that MOSFETs are indestructible, especially vertical MOSFETs. The inherent positive temperature coefficient of drain-source resistance over a wide range of current helps protect laterals and makes them quite resistant to burn out. The region of positive temperature coefficient of gate voltage and drain resistance for vertical MOSFETs begins at a much higher current level and does less to protect them from thermal runaway and localized hot spots on the die.

Because vertical power MOSFETs are inherently capable of very high current, they usually require protection from short circuits. The smaller maximum current capability of lateral MOSFETs, combined with their negative temperature coefficient of drain

current, means that lateral MOSFETs often do not require active short circuit protection and that they will survive a short circuit until a fuse has time to blow.

Fragile Gate Oxide

The thin gate oxide used to form the gate in MOSFETs often has a breakdown voltage of only about 20 V. Without protection, this is a serious source of vulnerability to destruction for MOSFETs. If this voltage is exceeded, a pinhole may develop in the gate oxide causing instant destruction of the device. Most lateral MOSFETs actually incorporate internal gate-source Zener protection diodes. Many vertical MOSFET power amplifier designs employ external Zener diodes to protect the gate from excessive voltages of either polarity. In other cases, it is possible to design driver circuits that are inherently unable to create excessive gate-source voltages.

In some amplifier designs, if the output is shorted or if the output stage is otherwise unable to supply the current demanded by the load, the driver circuitry will attempt to drive the output MOSFETs very hard, to excessive gate voltages, in an attempt to get the output stage to produce very high current. This is an example of where a MOSFET may be exposed to excessive gate-source voltage if it is unprotected. However, where gate protection Zener diodes are used, the driver may actually try to drive the load through the gate protection diodes, possibly leading to destruction of those diodes or the driver transistor.

The gate oxide can also be subjected to excessive voltages during high-frequency parasitic oscillations. The combination of circuit and bond wire inductances and the internal interelectrode capacitances of the MOSFET can create resonances where the internal gate voltage swing exceeds that of the external terminals of the device. External gate Zener diodes may not protect the gate oxide from excessive voltages under these conditions.

The Body Diode

Most power MOSFET transistors include a body diode that is fundamental to the semiconductor structure of the device. This diode will become forward biased if the source ever tries to swing beyond the rail to which the drain is connected. In switching applications, this diode is sometimes called a *freewheeling diode*. In audio amplifiers it performs the same function as the external rail catch diodes connected across BJT output transistors, protecting the output transistors from the inductive kick that can result from a loudspeaker when current flow is interrupted for some reason.

The body diode is usually quite fast, with a typical reverse recovery time on the order of 100 ns. The body diode has a reverse breakdown voltage that is the same as the rated drain-source voltage for the MOSFET. In reverse breakdown, the body diode can typically withstand the same or greater current than the maximum drain current rating of the MOSFET.

Supply of High Current

Lateral power MOSFETs are limited in their ability to deliver high current by their comparatively high drain-source resistance, and yet compete reasonably with BJTs overall. Vertical MOSFETs, on the other hand, are able to conduct very high current on a transient basis, largely because of their much lower $R_{ds(on)}$. A single vertical power MOSFET can conduct over 30 A on a transient basis and needs almost no drive current to do it. Figure 11.4 shows drain current as a function of gate voltage for typical lateral and vertical power MOSFETs.
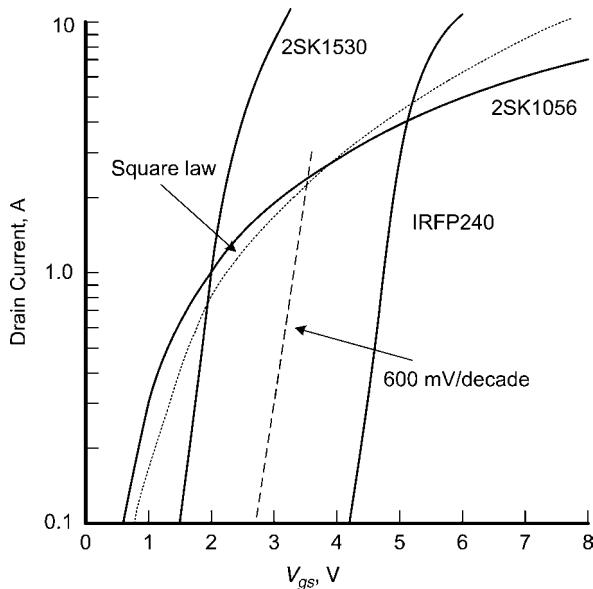
Figure 11.4 Typical drain current versus gate voltage for lateral and vertical power MOSFETs.

Notice that the forward bias required for 7 A is 8.3 V for the 2SK1056 lateral device whereas it is 2.8 V for the 2SK1530 vertical device and 5.6 V for the IRFP240. This is in spite of the fact that the vertical devices start out requiring a higher V_{gs} to turn on. The difference in V_{gs} from $I_d = 150$ mA to $I_d = 7$ A is 7.6 V for the lateral and about 1.2 V for the two vertical devices. The lateral device is incapable of delivering 10 A, whereas the 2SK1530 and IRFP240 vertical devices easily deliver 12 A and 50 A, respectively.

Table 11.1 shows the current that typically can be delivered from each device with strong forward gate drive and a V_{ds} of only 5 V. This is relevant because one may wish to evaluate maximum amplifier current delivery with a voltage drop from rail to output of no more than 5 V. If two output pairs are used to build a 100-W/8-Ω amplifier that is expected to be able to deliver 10 A into a 4-Ω load, the lateral devices are marginal by this criterion.

It is also notable in Figure 11.4 that the slope of I_d versus V_{gs} for the two vertical devices is very nearly 600 mV per decade over the range of interest from 300 mA to 3A. That is the slope of the dashed line drawn for reference between the curves of the two devices. Recall that the analogous slope for BJTs is 60 mV per decade. This implies that the *gm* of the vertical MOSFETs is about 1/10 of a BJT at a given current. It also suggests that their behavior in this region is more exponential than square law.

Device	Type	I_{max}, A
2SK1056	Lateral	6
2SK1530	Vertical	12
IRFP240	Vertical	35

Table 11.1 Maximum Drain Current at $V_{ds} = 5$ V

Device	Type	$R_{ds(on)}$, Ω
2SK1056	Lateral	0.55
2SK1530	Vertical	0.40
IRFP240	Vertical	0.18

TABLE 11.2 MOSFET on Resistance

In contrast, look at the I_d versus V_{gs} curve for the lateral 2SK1056. It is similar in shape to the square law curve plotted for reference with dotted lines. One is tempted to argue that the lateral device is more of a square law device in the region of interest than the vertical devices. Those who argue that the sound of lateral MOSFETs is superior to that of vertical MOSFETs might find comfort in this observation.
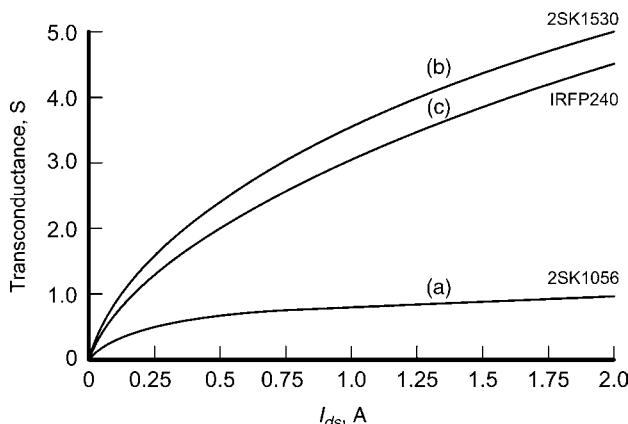
The Role of $R_{ds(on)}$

Power MOSFETs are often characterized by the parameter $R_{ds(on)}$. This is the effective value of resistance from drain to source when the MOSFET gate is strongly forward biased. It is essentially the slope of the I_d versus V_{ds} curve of the output characteristic curve in the linear region for high gate drive.

For an IRFP240, $R_{ds(on)}$ is specified as 0.18 Ω maximum with $V_{gs} = 10$ V and $I_d = 12$ A, implying that the drain-source voltage on the curves at this point is no more than 2.2 V. The $R_{ds(on)}$ specification is somewhat related to transconductance, but is of more use in switching applications than in linear applications. It is somewhat indicative of the maximum output that can be provided into a load under clipping conditions for a power amplifier. Table 11.2 shows typical values of $R_{ds(on)}$ for three MOSFETs.

Transconductance

One of the biggest differences between MOSFETs and BJTs is the transconductance. In very rough terms, MOSFETs have about 1/10 of the transconductance at a given current as BJTs. This factor typically ranges from 1/20 to 1/5. The ratio also depends on current because transconductance for a BJT is proportional to collector current while *gm* for a MOSFET is proportional to the square root of drain current. Figure 11.5 shows

FIGURE 11.5 Transconductance versus drain current for (a) 2SK1056, (b) 2SK1530, and (c) IRFP240.

transconductance as a function of current for a lateral MOSFET and two vertical MOSFETs. It is especially useful to compare the transconductance curves between the lateral and vertical MOSFETs.

Transconductance plays an important role in determining the amount of crossover distortion produced in push-pull class AB MOSFET output stages. In general, the smaller transconductance of MOSFETs places them at a disadvantage to BJTs in this regard due to what is called *transconductance droop* in the crossover region. This will be discussed in more detail in the section on crossover distortion below.

High Speed

The speed of a MOSFET can be characterized by equivalent f_T in the same way as a BJT. In the case of the MOSFET, the f_T is

$$f_T = gm/2\pi C_{in}$$

where C_{in} is the sum of the gate-source and gate-drain capacitances. The capacitance C_{in} does not generally increase significantly as current is increased (as is the case for the diffusion capacitance of a BJT). Therefore, the equivalent f_T of a MOSFET continues to rise with increased current as gm increases. As is often the case for BJTs, this estimate is made at 1 MHz (the estimate of f_T for a BJT is often taken as the value of AC beta at 1 MHz). The f_T is estimated at a current of 1 A for three MOSFETs in Table 11.3.

The transconductance of the IRFP240 is about 1 S at the typical class AB bias current of 150 mA. Its f_T under these conditions is about 120 MHz.

Transconductance Frequency Response

Transconductance can also be a function of frequency for MOSFETs as a result of gate resistance working against the gate-source capacitance. This is a special problem for lateral MOSFETs because they have higher gate resistances. Gate resistance for a lateral MOSFET is often on the order of 40 Ω, while for vertical MOSFETs it is on the order of 6 Ω or less. The transconductance for a typical lateral power MOSFET is down 3 dB at 2.5 MHz. This means that there will be excess phase created by this device that is not explained fully by its f_T.

The different device structure of the vertical MOSFETs results in much lower gate series resistance. For this reason the f_T estimates are more "real" for the vertical devices. The influence of gate series resistance on effective f_T of the MOSFET underlines the potential deleterious effect of large gate stopper resistors used with MOSFETs.

MOSFET Disadvantages and Caveats

MOSFETs have their disadvantages in comparison to BJTs as well. They are summarized here and will be discussed in later sections.

Device	Type	*gm*, S	C_{in}, pF	f_T, MHz
2SK1056	Lateral	1.0	620	250
2SK1530	Vertical	2.5	1100	360
IRFP240	Vertical	3.6	1300	440

TABLE 11.3 MOSFET f_T at a drain current of 1 A.

- Lower transconductance
- Higher required drive voltage
- Greater tendency to high-frequency oscillations
- Higher price in some cases, especially with laterals
- Fragile gate structure

MOSFETs versus Bipolar Transistors

BJTs have been the workhorse for audio power amplifiers since their inception as solid-state designs, and it will likely stay that way. BJTs have improved greatly over the years and are quite rugged and fast. MOSFETs didn't arrive until the late 1970s. At the time they were quite a bit more expensive than BJTs, but were arguably faster and more rugged.

MOSFET class AB biasing tends to be simpler and less critical, and the bias point is more stable with temperature. MOSFETs do not have an optimum class AB bias current. Instead, they operate better with greater bias as long as thermal objectives are met. For this reason, typical MOSFET power amplifiers operate at higher bias current per output pair and have a larger class A region of operation for small signals. However, their lower transconductance tends to result in higher measured values of static crossover distortion. Because of their high speed, MOSFET amplifiers are less prone to dynamic crossover distortion as a result of switch-off characteristics.

MOSFETs do not suffer from beta droop and f_T droop at high currents and are generally able to handle high peak currents better than BJTs. This is less so for lateral MOSFETs. The ease with which MOSFETs are driven also means that there is less stress on driver transistors when the amplifier is delivering high current to the load.

MOSFETs are a bit more prone to high-frequency parasitic oscillations as a result of their inherently higher speed. For this reason, circuit design and layout can require more care than for BJT designs.

11.3   Lateral versus Vertical Power MOSFETs

As a result of the structural differences, lateral devices have much higher $R_{ds(on)}$ than vertical devices and are not as adept at conducting high currents. Their gate structure also includes higher resistance, and this tends to limit their speed and performance at high frequencies. Although lateral MOSFETs are slower than vertical MOSFETs, they do tend to have reduced gate-source and gate-drain capacitances. Moreover, the gate-drain capacitance does not tend to rise substantially at low reverse gate-drain voltages, as it does in vertical devices.

The reduced turn-on voltage for lateral MOSFETs is initially appealing, but when you look at the forward bias required for high currents you quickly discover that any perceived advantage here disappears. This is a result of their smaller transconductance.

Whereas technically not as high performing as vertical MOSFETs, the sound of lateral MOSFETs is preferred by some as being more tubelike. Prices for vertical MOSFETs have fallen over the last 30 years, but the prices for lateral MOSFETs have risen and availability has decreased sharply.

11.4   Parasitic Oscillations

Vertical MOSFETs are about 10 times as fast as RET BJTs, with equivalent f_T in the range of over 100–500 MHz. Lateral MOSFETs are quite fast as well. For this reason, MOSFETs are more prone to parasitic oscillations due to stray inductances and capacitances in the surrounding circuitry. They are also sufficiently fast that their own internal bond wire inductance can come into play in parasitic oscillations.

Gate Stopper Resistors

The standard approach to controlling parasitic oscillations in MOSFETs is to employ gate stopper resistors in series with the gate of the device. These resistors are placed very close to the gate terminal of the MOSFET. The resistors tend to kill the speed of the MOSFETs and to damp out resonant circuits that may be formed by inductance operating in conjunction with gate capacitances.

Unfortunately, the practice of using gate stopper resistors discards one of the big advantages of the power MOSFETs, namely their speed. These resistors are often on the order of 100–500 Ω. It is easy to see that such a resistance up against a capacitance on the order of 1000 pF will result in a frequency roll-off in the vicinity of the low megahertz region. This will create excess phase in the output stage and limit the gain crossover frequency that can be employed for global negative feedback.

Parasitic oscillations become even more likely when power MOSFETs are connected in parallel, since more complex high-frequency interactions among the devices are then made possible [7]. Inevitably, individual gate stopper resistors, placed very close to the gate terminals, are necessary.

Origin of Parasitic Oscillations

A simplified analysis of the origin of such parasitic oscillations can provide insight into how to eliminate them with less brute force than simply the use of large-value gate stopper resistors. Some of the high-speed benefits of the MOSFETs can then be retained. The high-frequency parasitic oscillations are often caused by the inadvertent formation of oscillator topologies by the various inductances and capacitances present in the circuit. The Hartley and Colpitts oscillator topologies shown in Figure 11.6 are often the source for the parasitic oscillations [6].
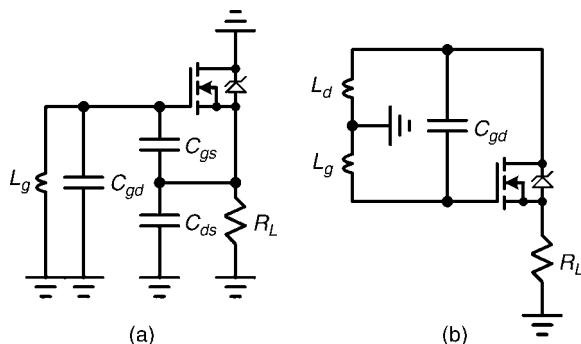
FIGURE 11.6   (a) Colpitts and (b) Hartley oscillator topologies.

The parasitic oscillations can often occur at quite high frequencies, from 25 MHz to 250 MHz. In some cases these oscillator topologies can be formed even in the absence of external inductances in the printed wiring board layout.

MOSFET Internal Inductances

The MOSFET internal bond wire and packaging inductances can play an important role in the formation of parasitic oscillators. The IRFP240 data sheet provides typical values of drain and gate inductances, as measured at the device leads 0.25 in. from the package [3]. The drain inductance is given as 5 nH, whereas the source inductance is given as 13 nH. The former is smaller because it does not involve a bond wire; the drain is in direct electrical contact with the package heat spreader. The gate inductance is not given, but it can be assumed to be approximately the same as the source inductance, since it includes a bond wire as well. For comparison, the inductance of a 1-in. trace on a printed wiring board is on the order of 20 nH.

It is instructive to calculate the resonant frequency of 13 nH with 1000 pF. It is 44 MHz. This frequency range is where such parasitic oscillations often occur. The reactance of each of these elements is 3.6 Ω at the resonant frequency of 44 MHz.

MOSFET Output Capacitance

The device structure of the vertical MOSFET creates a junction capacitance from drain to source called C_{ds}. This capacitance is a function of drain-source voltage. For an IRFP240, it is on the order of 1000 pF at 1 V, falling to 500 pF at 10 V, and falling still further to 200 pF at 50 V.

This capacitance represents a direct capacitive load on the source-follower output stage and can play a role in creating parasitic oscillations. This can be especially true when the output swings close to the rail, where C_{ds} becomes large. The total amount of this capacitance will also accumulate in designs where multiple output pairs are connected in parallel.

Fortunately, the amplifier's output Zobel network will place a fairly low resistance in parallel with this capacitance at high frequencies, helping to kill the Q of resonant circuits formed by this capacitance. This underlines the importance of having the drain power supply rail well bypassed locally to the circuit ground at high frequencies through very little stray inductance. It also suggests that the Zobel network should be located close to the output transistors. Alternatively, a high-frequency Zobel network with smaller resistance and capacitance values can be added close to the output transistors. Such a network might comprise a 1000 pF capacitor and a noninductive 1-Ω resistor.

Gate Zobel Networks

Rather than just killing the high-speed performance of the MOSFET, it is better to reduce the Q of the circuits involved in the oscillator topologies and damp out the oscillations. This can be done with series R-C Zobel networks like those used to shunt the output of power amplifiers [6]. These circuits look largely like open circuits at audio frequencies, but transition to a fairly low-value resistance at high frequencies. When placed in the gate circuit of a MOSFET, these networks provide a resistive shunt at the high frequencies where parasitic oscillators are likely to be formed.

These Zobel networks are usually best connected from gate to drain, rather than from gate to ground. This forms a damping loop with the drain that is more local at

high frequencies. Typical values for the components of a gate Zobel network are 47 Ω and 100 pF [6]. It is also important to minimize inductance in the gate line from the driver transistor. Recognize that only 100 nH of inductance has an impedance of 63 Ω at 100 MHz.

Ferrite Beads

Sometimes it is tempting for an amplifier designer to tame parasitic oscillations with strategically placed ferrite beads. These are often effective, but are frowned on in high-end audio circles as affecting the sound quality in a negative way.

Paralleled MOSFETs

Many power amplifiers of medium to high power require the use of multiple output pairs in parallel. The connection of MOSFETs in parallel increases the opportunity for parasitic oscillations, especially if the gates of the paralleled devices are not isolated at very high frequencies [7]. This means that individual gate stopper resistors are required for each device. It is also best that each gate have its own gate Zobel network if they are used.

Spotting Parasitic Oscillations

Finally, it is important to recognize that such parasitic oscillations may be difficult to spot with ordinary lab test equipment. It is desirable to have an oscilloscope with a bandwidth of at least 100 MHz in order to see some of these parasitic oscillations. Moreover, these oscillations will often show up only as brief bursts. This happens because the capacitances and transconductance of the MOSFET are a function of its operating point. It may be that the conditions for a parasitic oscillation are right only at certain places on a sine wave. Because gate-drain capacitance of MOSFETs increases dramatically under conditions of low V_{dg}, it is especially important to be watchful for parasitic oscillations at high output amplitudes at and near clipping.

The presence of parasitic oscillations will sometimes show up as increased harmonic distortion, but I have often seen this to be a subtle effect that can be dismissed as being merely the natural harmonic distortion created by the amplifier. Subtle increases in THD caused by parasitic oscillations are more likely to be noticed in an amplifier design that normally produces very low amounts of THD.

11.5   Biasing Power MOSFETs

Biasing power MOSFETs for class AB operation is different from that for BJTs in two ways. First, MOSFETs require greater forward bias at the gate than BJTs do at the base. Lateral MOSFETs typically require on the order of 0.7 V, but vertical MOSFETs can require up to 4 V. Some vertical MOSFETs like the 2SK1530 require only about 1.7 V, however. If MOSFETs requiring 4 V forward bias are combined with emitter follower drivers, the total bias spreading voltage will be on the order of 9.2 V. This compares to a typical bias spreading voltage of about 4.0 V for a BJT output Triple. This difference in required bias spreading voltage is not a problem for the traditional V_{be} multiplier or minor variants of it, but it does imply that the driver circuitry will require more voltage headroom in a MOSFET design. This is sometimes dealt with through the use of boosted power supplies for the circuits preceding the output stage.

TC_{Vgs} Crossover Current

The temperature coefficient of V_{gs} for MOSFETs is different from that for BJTs as well. Lateral power MOSFETs are characterized by a V_{gs} temperature coefficient that is nearly zero at typical quiescent bias currents on the order of 150 mA. This is illustrated in Figure 11.7a, where the I_d versus V_{gs} transfer characteristic for a 2SK1056 lateral MOSFET is illustrated for junction temperatures of 25°C and 75°C. It is easy to see that the temperature coefficient of V_{gs} (TC_{Vgs}) is zero at the point where the curves cross. At lower currents, the drain current is higher at high temperatures, indicating a negative TC of V_{gs}. At currents above the crossover point, drain current is smaller at high temperatures, indicating a positive TC of V_{gs}. Such a positive TC of V_{gs} makes for greater temperature stability, since higher junction temperature will result in smaller drain current and reduced power dissipation.

Because TC_{Vgs} for the lateral MOSFET is approximately zero at the quiescent bias level, the traditional V_{be} multiplier bias spreader need not be mounted on the heat sink. Notice also that the typical value of V_{gs} at the quiescent current for a lateral MOSFET is not very different than that for a BJT, so the V_{be} multiplier design will be very similar.

The situation is different for vertical MOSFETs. While the temperature coefficient of V_{be} for a BJT is about –2.2 mV/°C, the temperature coefficient for a 2SK1530 vertical power MOSFET is on the order of –4 mV/°C at a typical quiescent bias current of 150 mA. The TC_{Vgs} behavior of a 2SK1530 vertical MOSFET is illustrated in Figure 11.7b. Notice that there is still a current at which TC_{Vgs} is zero, but that it occurs at a very high current of about 8 A. The TC_{Vgs} crossover point for the IRFP240 (not shown) is at about 15 A and its TC_{Vgs} at 150 mA is about –6 mV/°C. This means that bias spreaders for vertical MOSFET output stages must incorporate some temperature compensation based on heat sink temperature.

Bias Spreaders for MOSFET Output Stages

Consider the IRFP240 vertical MOSFET. The –6 mV/°C TC_{Vgs} at the typical bias point of 150 mA may sound worse than for a BJT, but it is actually a much smaller percentage of the typical forward bias number (4 V for the vertical MOSFET compared
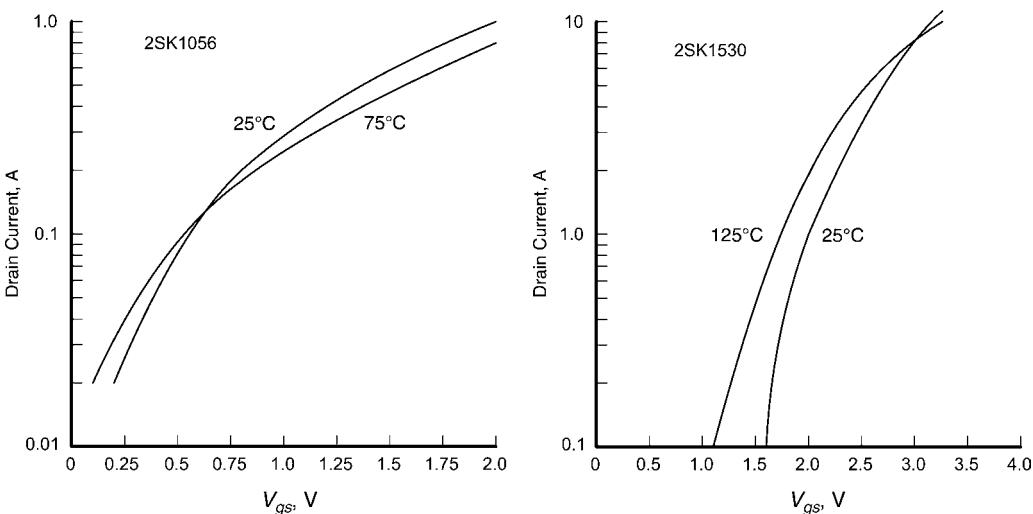
FIGURE 11.7 I_d versus V_{gs} at different temperatures for (a) lateral and (b) vertical MOSFETs.
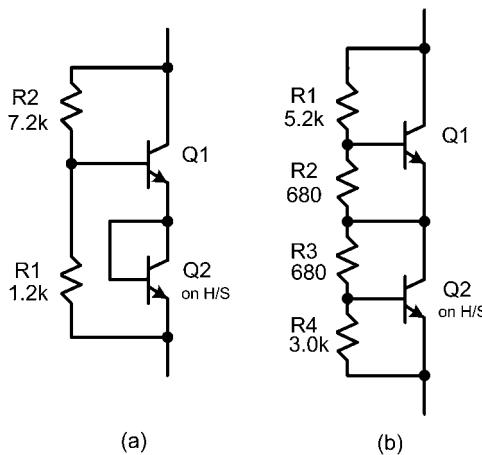
Figure 11.8 Bias spreader V_{be} multipliers for vertical MOSFET output stages.

to 0.7 V for the BJT). This means that a traditional one-transistor V_{be} multiplier with its transistor mounted on the heat sink will provide too much temperature compensation for a MOSFET design. In rough terms, it will provide –2.2 mV/°C multiplied by the ratio of V_{be} to V_{gs}, or about –14 mV/°C for the output device. This is about twice as much as needed. For this reason, a modified version of the V_{be} multiplier, with only a portion of its temperature sensing circuitry on the heat sink, is often used for vertical MOSFET output stages.

The V_{be} multipliers illustrated in Figure 11.8 can be used. The first bias spreader just adds a diode to the emitter circuit of the V_{be} multiplier. Only the diode is then mounted on the heat sink. The V_{be} multiplier is set to provide a spread of about 14 V_{be} (9.2 V), of which about half is compensated. The diode should be implemented as a diode-connected transistor. The second bias spreader consists of two V_{be} multipliers in series. The transistor for one of them is mounted on the heat sink. It also creates a spread of 14 V_{be}, of which 40% is compensated with the heat sink temperature. This permits significant freedom in picking the proportionality of the temperature compensation.

Dynamic Thermal Bias Stability

Mounting the V_{be} multiplier bias spreader (or a portion of it) on the heat sink provides for long-term bias stability against temperature variations by providing a form of biasing feedback. This feedback will be very slow-acting, since its action is governed by the long thermal time constant of the heat sink. This is true for both BJT and vertical MOSFET designs. As the temperature of the heat sink changes with program material over time, its temperature can lag what the temperature should really be for proper bias. As a result, bias may be too high or too low after the average power of the program material changes.

Imagine running the amplifier at 1/3 power for an extended period of time, with the average heat sink temperature reaching 60°C and the portion of the heat sink under the power transistor reaching 65°C (heat sinks are not isothermal). The transistor package may reach 75°C and the transistor junction may reach 90°C. If the temperature
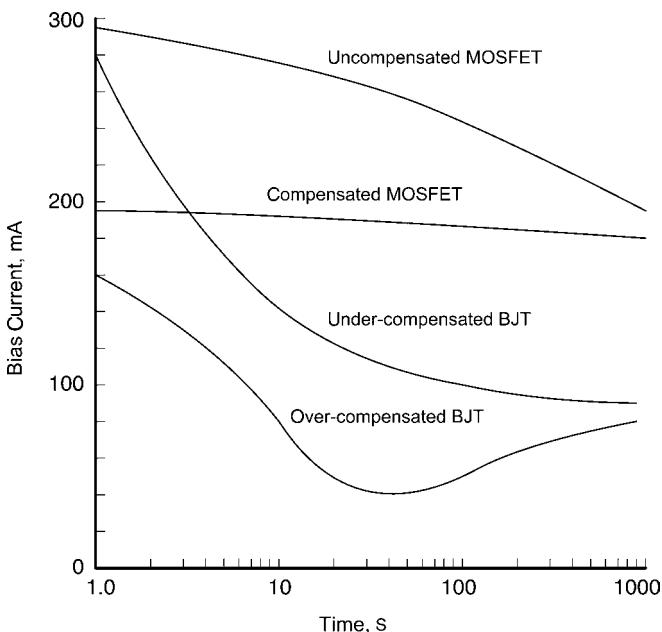
compensation was keeping the quiescent bias at its nominal value, it was compensating for quite a bit more than just the temperature rise of the heat sink. When the drive signal is removed, the junction, case, and local heat sink temperatures all move toward the average heat sink temperature with different time constants. This results in serious mistracking along the way.

Figure 11.9 shows the bias currents of a BJT and vertical MOSFET power amplifier as a function of time after a thermal step [6]. The BJT amplifier is configured to have the bias temperature compensation set to undercompensated and overcompensated. The MOSFET amplifier is set to have the bias uncompensated and properly compensated. When the temperature compensation is overcompensated, this means that a larger fraction of the bias spreader function is located on the heat sink. When the heat sink temperature rises, the bias voltage will be made to decrease a bit more than necessary. This fosters better overall bias stability.

Each amplifier was operated at 1/3 rated power into an 8-Ω load for 10 minutes. The signal was then removed and the bias current of the output stage was measured as a function of time. In an ideal amplifier, the bias current will not change with time. In an overcompensated amplifier, the bias can be expected to be too low immediately following removal of the signal and slowly rise to its nominal quiescent level. Immediately after the signal is removed, however, the output devices themselves are still quite hot, so the bias current actually takes a few seconds to fall to the underbias condition.

Figure 11.9 shows dramatically how much more thermally stable the MOSFET design is. The serious underbias that is evident in the BJT amplifier following removal of the signal can lead to crossover distortion that might not be revealed in static bench tests.

11.6   Crossover Distortion

Crossover distortion is one of the most insidious distortions in class AB power ampli-fiers. It occurs at fairly low signal levels and often contains a high-order distortion spec-trum that is more dissonant and difficult to remove with negative feedback. It is a result of the changing gain of the output stage as the signal current delivered to the load goes through zero (the crossover). We have seen how it originates in BJT output stages and the measures that must be taken to minimize it. MOSFET output stages are also subject to crossover distortion.

Static crossover distortion in BJT output stages is a result of the output impedance changing as the output current goes through zero. The output impedance forms a volt-age divider with the load impedance; as a result the gain of the output stage changes. The lower the value of the output impedance, the smaller the crossover distortion will be for a given percentage change in the output impedance.

The same is true for power MOSFET output stages, but the output impedance is generally quite a bit higher for a given amount of bias current. This is because the transconductance of a MOSFET is much smaller than that of a BJT. The transconduc-tance of a BJT at $I_c = 100$ mA is about 4 S. The transconductance of an IRFP240 biased at $I_d = 150$ mA is about 1 S. As a result, the sum of the transconductances of the upper and lower MOSFETs dips in the crossover region. This is referred to as *transconductance droop* [6].

Transconductance Droop

Typical transconductance characteristics as a function of drain current were shown in Figure 11.5. A class AB output stage comprises both an N-channel and a P-channel MOSFET. The transconductance of the source follower push-pull stage is thus the sum of the transconductances of the N- and P-channel devices. The output impedance of the push-pull output stage is simply the inverse of the sum of the transconductances.

The typical transconductance of different MOSFETs is shown in Table 11.4 for drain current values of 150 mA, 1 A, and 5 A.

Since both transistors are on at crossover, we should compare twice the *gm* of each transistor at the quiescent current with the *gm* of one transistor at 1 A. For the lateral device the transconductances are 0.8 S and 1.0 S, respectively, for a 20% transconduc-tance droop at crossover. This corresponds to the output impedance changing from 1.25 Ω to 1.0 Ω. With an 8-Ω load this corresponds to output stage gains of 0.86 and 0.89, respectively.

The vertical devices exhibit increased transconductance, but also a greater amount of increase in transconductance from quiescent current to 1 A. The comparison for the 2SK1530 is 1.4 S and 2.5 S, corresponding to output impedances of 0.7 Ω and 0.4 Ω,

Device	Type	I_d = 150 mA	I_d = 1 A	I_d = 5 A
2SK1056	Lateral	0.4 S	1.0 S	1.2 S
2SK1530	Vertical	0.7 S	2.5 S	4.5 S
IRFP240	Vertical	1.0 S	3.6 S	7.6 S

TABLE 11.4   Transconductances of Several MOSFETs
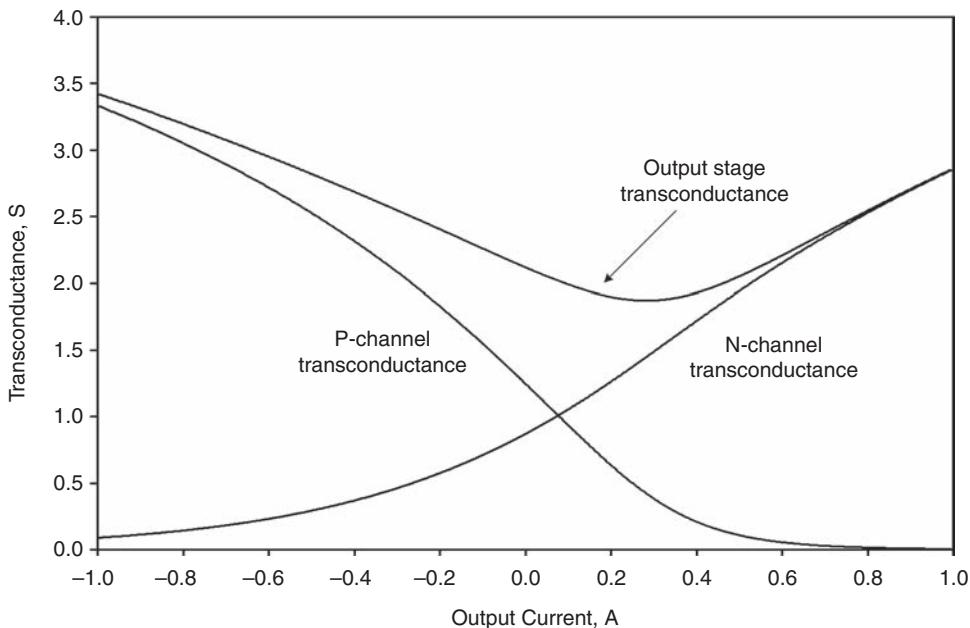
Figure 11.10   Illustration of transconductance droop for IRFP240/9240 output pair.

respectively. With an 8-Ω load this corresponds to output stage gains of 0.92 and 0.95, respectively.

The comparison for the IRFP9240 is 2.0 S and 3.6 S, corresponding to output impedances of 0.5 Ω and 0.28 Ω, respectively. With an 8-Ω load this corresponds to output stage gains of 0.94 and 0.97, respectively.

Figure 11.10 shows the transconductances of a complementary pair of vertical MOSFETs, the IRFP240 and the IRFP9240, as a function of output current from a class AB output stage. The curve in the center is the sum of the transconductances. It is easily seen that the total transconductance droops in the crossover region where the magnitude of the output current is small [6]. This corresponds to smaller gain in the output stage and thus static crossover distortion.

Absence of *gm* Doubling

When a BJT output stage is overbiased, its transconductance can be substantially larger in the crossover region than elsewhere because both transistors are on and contributing transconductance. The different transfer characteristics of MOSFETs, particularly vertical MOSFETs, make it almost impossible for *gm* doubling to occur. The MOSFETs would have to be operating at very high quiescent bias current for the *gm* at crossover to be substantially larger than that at output currents outside the crossover region. In general, more quiescent bias current is better for MOSFET output stages as long as no thermal problem results. If source resistors of significant value are used with MOSFET output stages, the possibility of *gm* doubling may arise, however. In some ways *gm* doubling is the opposite of transconductance droop.

Use of Source Resistors

Source resistors do not help very much with setting and equalizing bias current among paralleled MOSFETs, so they are often not used. However, sometimes they can be used to reduce crossover distortion in two ways. First, they can be used to reduce transconductance somewhat at high currents. This may reduce crossover distortion by reducing the relative amount of transconductance droop. Source resistors will have a larger effect on reducing transconductance at high current than at the low current in the crossover region. Figure 11.11 is similar to Figure 11.10, but includes source resistors to reduce transconductance variations.

Secondly, the use of different source resistances for the N- and P-channel MOSFETs may reduce crossover distortion slightly by improving the transconductance match of the devices. This has also been employed in the circuit used for Figure 11.11. The source resistor for the N-channel device is 0.15 Ω while the source resistor for the P-channel device is 0.22 Ω.

Wingspread Simulations

A *wingspread* simulation for a MOSFET output stage is shown below in Figure 11.12. It is a plot of output stage gain as a function of output current. It was carried out using EKV models created by the author for the IRFP240 and IRFP9240. These models are thought to be reasonable approximations to the behavior of the devices. The simulation is shown for three bias levels: 100 mA, 150 mA, and 250 mA. It is readily apparent that the higher bias yields reduced crossover distortion and that there is no evidence of *gm*
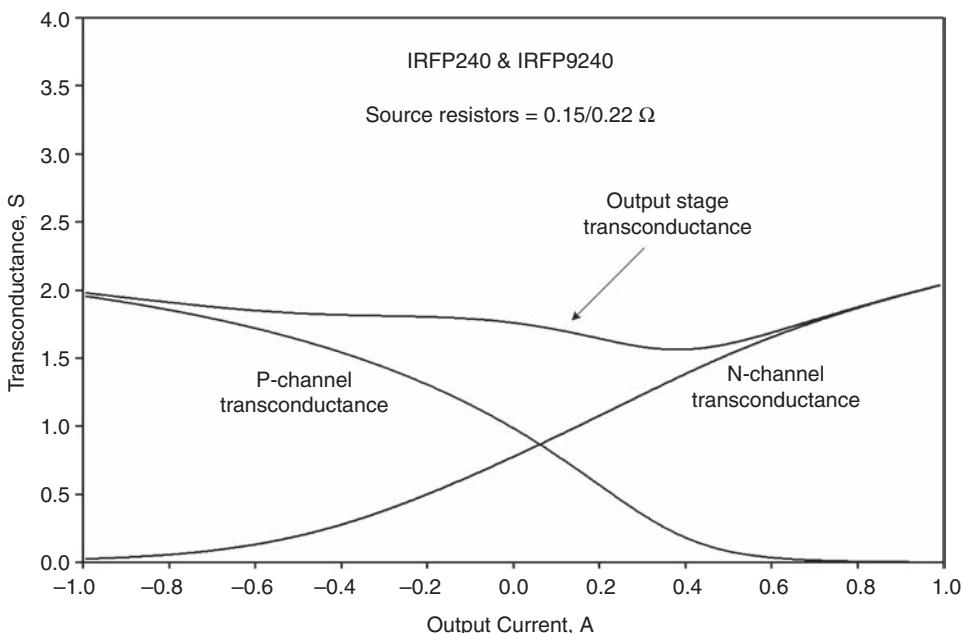
FIGURE 11.11 Transconductance versus output current when using source resistors for IRFP240/9240 output pair.
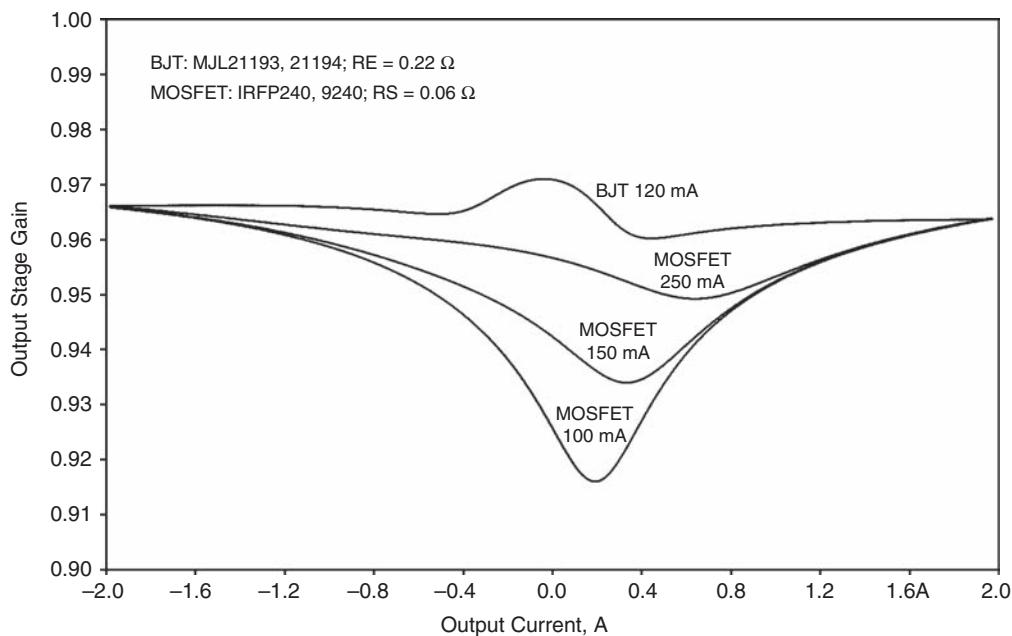
doubling. For comparison, the wingspread for a BJT output stage is also shown on the plot. The BJT output stage employs 0.22-Ω emitter resistors and is optimally biased at 120 mA. The MOSFET output stages include 0.06-Ω source resistors to make the BJT and MOSFET output stage gains equal at the output current extremes.

Memory Distortion

Memory distortion in output stages results when the history of output stage thermal variations with program material causes bias errors that can lead to increased crossover distortion [8]. This can be a significant concern with BJT output stages because of their sensitivity of bias point to temperature. As mentioned above, MOSFET output stages are inherently more temperature stable than BJT output stages, so they are less prone to memory distortion.

11.7   Driving Power MOSFETs

The high input impedance of power MOSFETs makes them much easier to drive than BJT output stages, but with a few caveats. In essence, they have almost infinite DC beta. This means that they are not plagued by beta droop when driving high currents.

The high DC input impedance of MOSFETs can make it tempting to drive them directly from the VAS, and indeed some amplifier designers do just that. This is generally not a good idea because the input capacitance of the power MOSFETs is not

insignificant, so the AC input impedance at higher frequencies definitely presents a loading effect on the VAS–and a nonlinear one at that.

Driving the Gate Capacitance

The gate capacitance of the MOSFET has two components: gate-source capacitance C_{gs} and gate-drain capacitance C_{gd}. As with BJTs in an emitter follower configuration, MOSFETs in a source follower configuration have their gate-source capacitance boot-strapped by the output signal. In contrast, the gate-drain capacitance is not boot-strapped. C_{gd} will sometimes dominate the effective input capacitance of the MOSFET output stage, especially when the output is near the rail and C_{gd} is large.

Gate-Source Capacitance

Since the gate-source voltage must change in order for the current of the MOSFET to change, the gate-source capacitance must be charged and discharged. C_{gs} is usually between 500 pF and 1500 pF and is relatively constant with changes in V_{gs} for vertical MOSFETs. While this capacitance can seem significant, its effective value is much smaller because it is bootstrapped by the output signal. The current through the capacitance is only in proportion to the signal voltage across C_{gs}. If the gain of the output stage when driving a load is 0.9 and C_{gs} is 1200 pF, the apparent load presented to the driver by the gate-source capacitance is only 120 pF.

Gate-Drain Capacitance

The drain voltage for a source follower output stage is at a fixed potential, while the gate voltage is changing at approximately the voltage rate of change of the amplifier output. The current required to charge and discharge the gate-drain capacitance C_{gd} is thus proportional to the rate of change of the output voltage.

The gate-drain capacitance for MOSFETs is usually small, but there is a major exception that is cause for concern. As shown by the plot of C_{gd} versus V_{dg} for the IRFP240 in Figure 11.13, the gate-drain capacitance becomes much larger for vertical MOSFETs
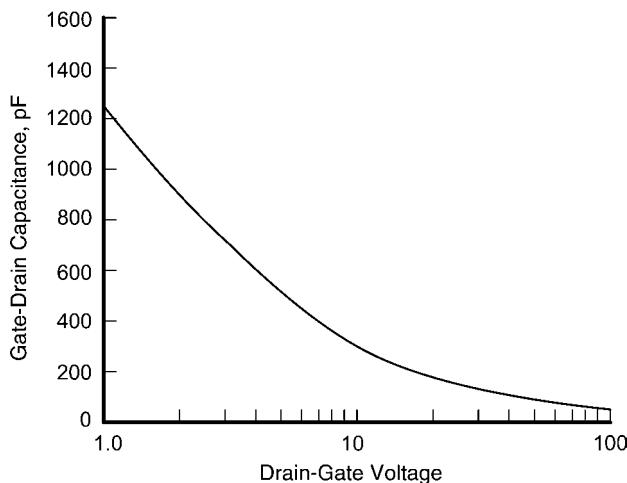
FIGURE 11.13 C_{gd} versus V_{ds} for IRFP240.

when the drain-to-gate voltage becomes small. At $V_{dg} = 50$ V, C_{gd} is only 50 pF. This climbs to 300 pF at 10 V and over 1200 pF at 1 V. C_{gd} can thus be quite large when the amplifier output is driven close to clipping. Fortunately, the voltage rate of change of program material is usually not at its maximum near clipping; it is more often greatest at smaller output voltage magnitudes. However, a square wave test signal will often exhibit its maximum rate of change just as its voltage begins to move away from the rail.

Required Drive Current versus Slew Rate

The drivers for a MOSFET output stage must be capable of providing adequate source and sink current to support the rated slew rate of the amplifier. The power MOSFET will often be driven with a BJT emitter follower. In such a case, the maximum available turnoff current is limited to the bias current of the driver stage. As with bipolar designs, if the turnoff drive current is not sufficient, there may be significant totem pole conduction through the output stage.

Consider an IRFP240/IRFP9240 output stage driving a 4-Ω load to 40 V peak with a slew rate of 100 V/μs. Output stage transconductance will be assumed to be at least 2 S and output stage gain will be at least 0.89. C_{gs} will be bootstrapped by a factor of about 10. If $C_{gs} = 1200$ pF, its apparent value will be about 120 pF. Even if C_{gd} is only 200 pF (the value at $V_{dg} = 20$ V), total capacitance that must be driven will be on the order of 320 pF. Required driver current will be 32 mA. Other demanding situations can be imagined where a high rate of change is required when the signal amplitude is near the rail, where C_{gd} is much higher. The message here is not to be complacent about required drive current for both turn-on and turn-off of MOSFETs under demanding dynamic signal conditions.

Excess Phase at Signal Peaks

The significant increase in C_{gd} when the signal is close to the rail can lead to degraded feedback loop stability in the vicinity of large signal peaks. The C_{gd} capacitance working against the source impedance feeding the MOSFET forms a pole whose frequency will decrease under these conditions. This is of special concern because C_{gd} will be usually working against a gate stopper resistance. Even if a relatively small gate stopper resistance of 47 Ω is used with an IRFP240 and C_{gd} increases to 1200 pF, that pole will be at about 3 MHz.

Driving Multiple Output Pairs

Many amplifiers employ multiple output pairs. This clearly can lead to increased capacitive loading on the driver. The paralleling action affects the C_{gs} and C_{gd} loading differently, however.

The apparent gate-source capacitance seen by the driver does not necessarily increase as expected. Recall that the gate-source capacitance is bootstrapped by the output signal. The closer the gain of the output stage is to unity, the more effective is the bootstrapping. If the added output pairs are each biased at the same quiescent current as the first, their presence will increase the total transconductance of the output stage and drive the output stage gain closer to unity, increasing the bootstrapping effect. In principle, the increased bootstrapping effect will offset the effect of the increase in total gate-source capacitance. Apparent input capacitance of the output stage due to C_{gs} will remain about the same.

The situation is not so rosy for C_{gd}. The gate-drain capacitance adds up with the introduction of multiple output pairs as expected. An amplifier with two output pairs will have twice as much C_{gd}. Under worst-case conditions with the output voltage near the rail, an amplifier with four pairs could present a 4800 pF load to the driver. This multiplication of C_{gd} is no different than that for C_{cb} in a BJT amplifier.

Maximum Drive Considerations

The fact that C_{gd} can climb to 1200 pF per output MOSFET when V_{dg} falls to 1 V is bad enough. However, C_{gd} continues to climb if the gate goes positive with respect to the drain voltage. In some amplifier designs that have boosted driver supplies this can happen. For this reason, I recommend that the amplifier not be able to drive the gate more positive than the rail.

Gate Protection

The thin gate oxide in MOSFETs often has a breakdown voltage of only about 20 V. Without protection, this is a serious source of vulnerability to destruction for MOSFETs. If this voltage is exceeded, the gate oxide may break down, causing instant destruction of the device. Many lateral MOSFETs actually incorporate internal gate Zener protection diodes, often with a breakdown of 15 V. Many vertical MOSFET power amplifier designs employ external Zener diodes to protect the gate from excessive voltages of either polarity. In other cases, it is possible to design driver circuits that inherently are unable to create excessive gate-source voltages. These will be discussed later in this chapter.

If the amplifier output is shorted or if the output stage is otherwise unable to supply the current demanded by the load, the driver may attempt to drive the MOSFETs to excessive gate voltages, in an attempt to get the output stage to produce very high current. This is an example of where a MOSFET may be exposed to excessive gate-source voltage if it is unprotected. However, even in the case where gate protection Zener diodes are used, the driver may actually try to drive the load through the protection diodes, possibly leading to destruction of those diodes or the driver transistor.

The gate oxide can also be subjected to excessive voltages during high-frequency parasitic oscillations. The combination of bond wire inductances and the internal capacitances of the MOSFET can create resonances by which the internal gate voltage swing exceeds that at the external terminals of the device. External gate Zener diodes may not protect the gate oxide from excessive voltages under these conditions.

Flying Catch Diodes

Figure 11.14 shows a driver circuit that incorporates so-called flying catch diodes. These diodes connect from each end of the bias spreader to the output node of the amplifier. They are normally reverse biased by the voltages at the ends of the bias spreader. These diodes will become forward biased when the gate drive voltage exceeds the magnitude of the bias spreader voltage. For example, if a vertical MOSFET is being used that requires $V_{gs} = 4$ V for a bias current of 150 mA, the maximum gate drive to that MOSFET will be limited to about 8 V by the catch diodes. This protects the gate from dangerous overdrive voltages without resort to gate Zener diodes. The diodes are referred to as flying catch diodes because both ends of the diode move with the signal.
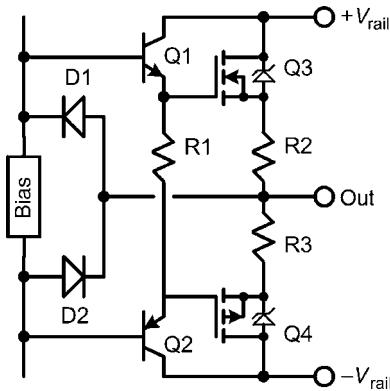
FIGURE 11.14   A MOSFET driver circuit employing flying catch diodes.

Natural Current Limiting

There is a second benefit from the use of the flying catch diodes. If the gate drive voltage is prevented from exceeding approximately twice the bias value, the maximum current that the MOSFET can deliver will be naturally limited. In the case of the IRFP240 the maximum current will be limited to approximately 30 A. The corresponding number for a 2SK1530 is about 12 A. We refer to this as *natural current limiting*.

If a smaller current limit is desired, a small source resistor can be added as shown in Figure 11.14. The voltage drop across the source resistor will subtract from the available gate drive, reducing the current limit. If a 0.1-Ω source resistor is used and 15 A flows, the available gate drive will be reduced by 1.5 V to 6.5 V. This is approximately the amount of gate drive required for the IRFP240 to conduct 15 A.

If for some unrelated reason a larger value of source resistor is used, the flying catch diodes can be connected to a voltage divider across the larger source resistor to retain the higher value of current limit. This is illustrated in Figure 11.15.

Short Circuit Protection

The flying catch diodes provide yet another opportunity in the form of short circuit protection. As mentioned above, the gate drive is limited to twice the bias spreading voltage. If the bias spreader is collapsed (shorted out), the output stage will be turned off and disabled because no gate drive will be available to either MOSFET. The VAS signal current will be dumped harmlessly into the output node. One approach to collapsing the bias spreader is to simply place a TRIAC across it that is triggered by an opto-coupler from circuitry that detects a short circuit condition. The amplifier then will be latched in a disabled state until power is cycled. Such behavior might not be desirable for a pro audio environment, but it is perfectly acceptable for home audio use.

Folded Drivers

Figure 11.16 illustrates an alternative way of driving a MOSFET output stage, referred to here as a *folded driver*. Because the MOSFETs require essentially no DC current to drive them, it is feasible to use an inverted driver EF that acts to turn-off the MOSFET rather than turn it on. Turn-on current is then provided by a current source. The current
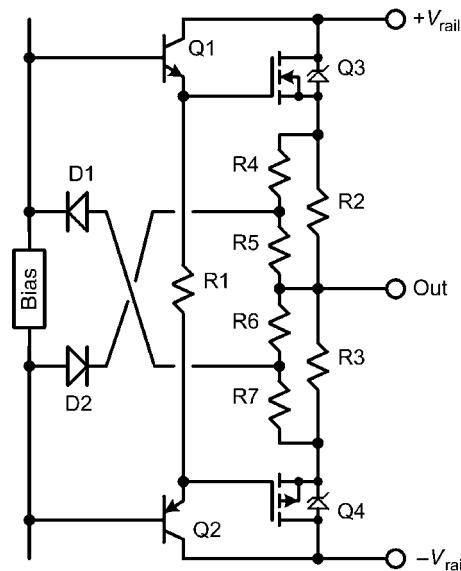
FIGURE 11.15   Adjustable natural current limiting with flying catch diodes.
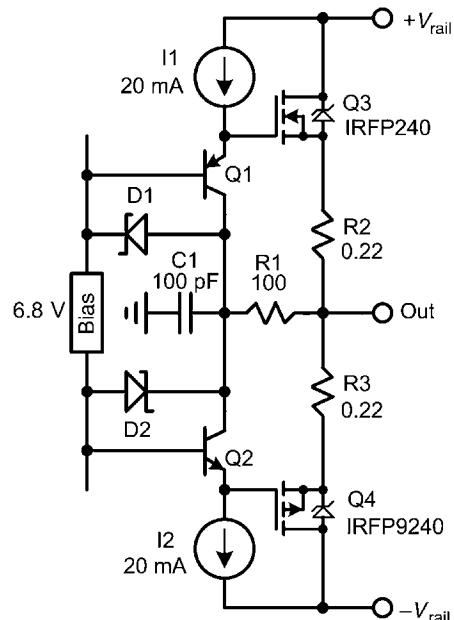
FIGURE 11.16   A MOSFET output stage with folded drivers.

must be able to provide adequate turn-on slew rate for the device (as opposed to adequate turn-off slew rate as in the conventional approach).

Notice that the collectors of the driver transistors are connected to the output node of the power amplifier. The unused drive current is thus dumped harmlessly into the output node. This means that there is low voltage across these transistors, allowing fast devices to be used. The signal from the output node is filtered somewhat at very high frequencies to avoid the possibility of feedback effects that might come into play at very high frequencies.

This approach has some advantages. First, the amount of gate drive is current limited. Secondly, the driver transistor can be a small, fast device if its collector is connected to the output node. The driver transistor controls the MOSFET by turning it off, shunting current from the current source to the output node. The driver transistor also draws charge out of the gate-source capacitance by shunting gate current right back to the source. Third, the current source, which bears virtually all of the driver power dissipation, need not have good signal-handling characteristics, since the signal does not pass through it. Fourth, the bootstrapping of the driver collectors greatly reduces the effects of their nonlinear collector-base capacitance and Early effect on loading of the VAS. The folded driver transistors also dissipate less power and experience less temperature rise. This helps overall output stage thermal bias stability.

The base-collector junction of the driver transistor also serves as the flying catch diode. In many cases the driver transistors can be allowed to saturate under natural current-limiting conditions without causing sticking. If the driver transistors must be kept out of saturation under these conditions, Shottky flying catch diodes can be incorporated as shown.

Boosted Driver Supplies

MOSFET output stages require more drive voltage than BJT output stages. Even lateral MOSFETs, with their relatively low gate threshold voltage, may require 8 V or more to drive them to high currents. This reduces VAS voltage headroom and results in a reduced power output capability for given rail voltages.

Better use is made of the available main power supply rail voltage if a boosted supply voltage is provided to the circuitry preceding the MOSFET output transistors [6]. The amount of current required from the boosted supply is small. However, the use of boosted supplies to allow drive of the gate above the rail supplying the drain of the output transistor may be unwise in light of the dramatically increased C_{gd} under such conditions.

11.8   Paralleling and Matching MOSFETs

Most power amplifiers require multiple output pairs, so issues in paralleling of MOSFETs must be considered. While bipolar transistors are regularly placed in parallel with small individual emitter ballast resistors, the paralleling issue is not as straightforward for power MOSFETs, at least in linear applications. It has been said that the negative temperature coefficients of transconductance and on resistance of MOSFETs act to suppress current hogging by one transistor, thus permitting easy paralleling of MOSFETs without ballast resistors. This appears to be true for hard-switching applications where the paralleled devices are all fully turned on together (i.e., channels fully

enhanced by forward gate voltage) so that current and dissipation imbalances are only a result of mismatch on resistance.

However, the issue is more complex for linear, and especially low-distortion, applications because the operating region of interest is not the fully turned-on region, but rather the linear region wherein drain current at a specified gate voltage is important. Specifically, recognizing that the gate threshold voltage specification for vertical power MOSFETs is 2–4 V for the IRFP240, for example, an examination of the gate transfer characteristics quickly shows that a very serious current imbalance can exist unless gate threshold voltages among paralleled devices are reasonably matched. It is also apparent that reasonable temperature differentials will not adequately reduce the imbalance. This is especially true if a common heat sink is employed. Because of the size of the worst-case threshold voltage differentials possible, the use of source ballast resistors is not a reasonable approach to achieving balance.

It thus appears that, for high-quality audio applications where paralleled devices are necessary, both threshold voltage and transconductance of paralleled devices should be matched. Matching that guarantees that all devices are carrying ±50% of their nominal current share in the quiescent bias state and ±25% of their share at high currents is probably adequate. For the IRFP240, V_{gs} matching of ±0.1 V at 150 mA and ± 0.25 V at 4 A will typically satisfy this matching criterion.

Fortunately, this is not as difficult as it sounds. With the manufacturing consistency in place for modern MOSFETs, most of the devices in a tube will be like peas in a pod. In many cases they will all have come from the same wafer. Moreover, if their threshold voltages are well matched, their transconductances will likely be well matched. For this reason, one can often get by with just matching V_{gs} at 150 mA.

11.9   Simulating MOSFET Power Amplifiers

Simulation of power amplifiers with SPICE can be very valuable, and this includes simulation of crossover distortion. However, extra caution is required in simulating MOSFET output stages, especially in regard to crossover distortion. The reason for this is that most SPICE models for power MOSFETs do not properly model the low-current region, sometimes called the weak inversion region. The MOSFET is generally thought of as a square law device.

$$I_d = K(V_{gs} - V_t)^2 \tag{11.1}$$

The simple square law equation for drain current goes to zero at the threshold voltage, causing a discontinuity in transconductance. This is simply not accurate for MOSFETs. In fact, at low currents, the MOSFET characteristic transitions to an exponential law that is much like that followed by BJTs, but with far different coefficients. Because the simulation of crossover distortion involves behavior of the devices at low currents (150 mA is considered to be in the transition region of the models), the normal SPICE models will give misleading results. There are better models for MOSFETs, one of which is called the EKV model [9]. However, EKV model parameters for power MOSFETs are extremely rare. The EKV model is discussed in depth in Chapter 20. With data sheet information and perhaps some low-current measurements, you can create an EKV model for a MOSFET and install it into LTspice.
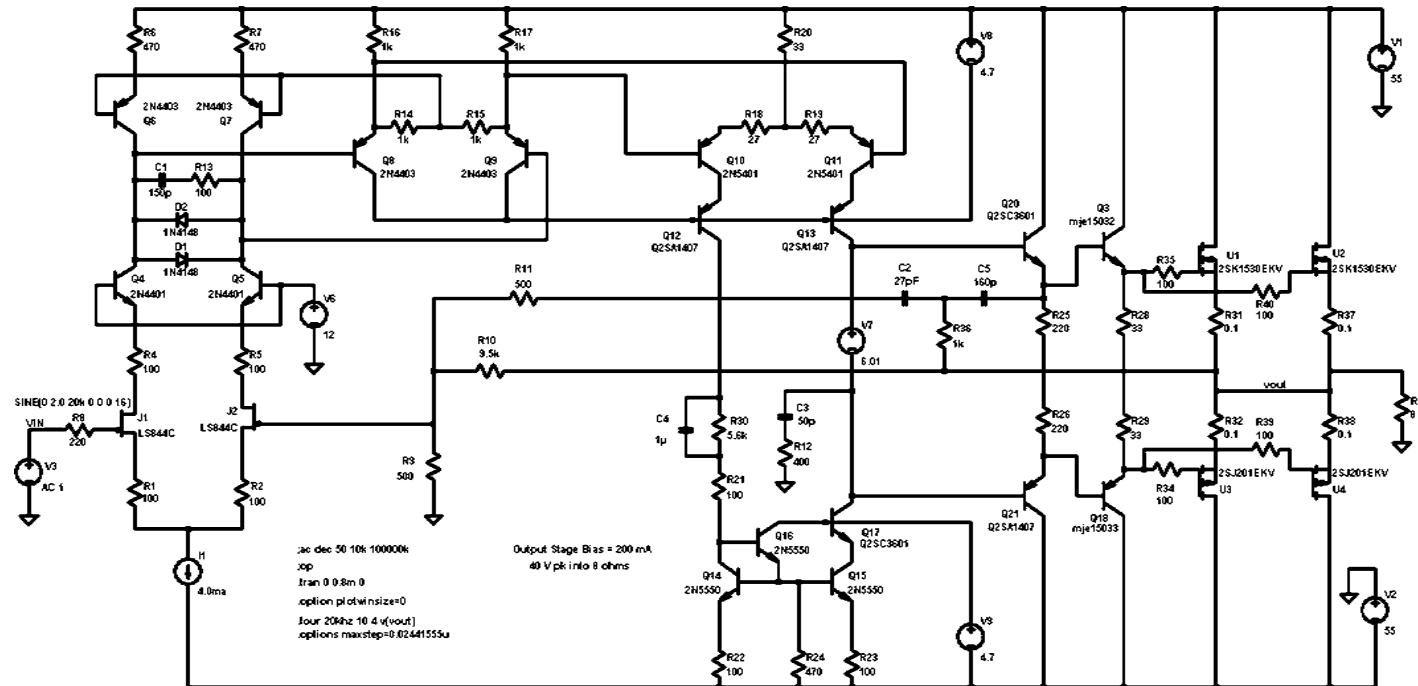
FIGURE 11.17 A high-performance MOSFET power amplifier.

High-Frequency Simulations

The gate-drain capacitance is highly nonlinear in MOSFETs and can become quite large when V_{dg} is small. This effect is not modeled well in most models available from manufacturers. In fact, many of their models are optimized for switching applications where different approaches to modeling C_{gs} may be satisfactory. Fortunately, the VDMOS model in LTspice does a good job of modeling C_{gd} that is equally well suited to linear applications. The VDMOS model should be used when the frequency response and gate drive current requirements of the MOSFET output stage matter the most. Unfortunately, the VDMOS model does not model subthreshold conduction, so the EKV model should be used for distortion simulations.

11.10 A MOSFET Power Amplifier Design

Figure 11.17 shows a MOSFET power amplifier based on the 2SK1530/2SJ201 vertical devices. The amplifier employs two output pairs and is suitable for 125 W/8 Ω. Each output pair is biased at 200 mA for low crossover distortion. The front end employs a cascoded LS844 JFET pair loaded with a differential current mirror and feeding a cascoded differential VAS [6]. The VAS includes a Darlington-cascode current mirror. Output offset is controlled by a DC servo (not shown). The amplifier uses transitional Miller compensation (TMC) as described in Chapter 9 [10]. In this amplifier the compensation encloses the input stage as in Miller input compensation [6]. The feedback compensation establishes a gain crossover frequency of 1 MHz. Simulations show that THD-20 at 125 W is less than 0.002% when driving an 8-Ω load. THD-20 does not increase at lower power levels, suggesting that crossover distortion is quite low. THD-20 is below 0.004% at 200 W driving a 4-Ω load. Slew rate is over 200 V/μs.

References

1. Renesas Data Sheet for 2SK1056/2SJ160.
2. Toshiba Data Sheet for 2SK1530/2SJ201.
3. Vishay Data Sheet for IRFP240/IRFP9240.
4. *Hitachi Power MOSFET Data Book HLN600,* Hitachi America, Ltd., 1983.
5. David Hafler Company, DH220 Power Amplifier.
6. Cordell, R. R., "A MOSFET Power Amplifier with Error Correction," *Journal of the Audio Engineering Society*, vol. 32, no. 1, pp. 2–17, January 1984; available at www.cordellaudio.com.
7. Oxner, E. S., "Analyzing and Controlling the Tendency for Oscillation of Parallel Power MOSFETs," *Proceedings Powercon*, vol. 10, 1983.
8. Sato, T., Higashiyama, K., and Jiko, H., "Amplifier Transient Crossover Distortion Resulting from Temperature Changes in the Output Power Transistors," presented at the 72d Convention of the Audio Engineering Society, *JAES* (Abstracts), vol. 30, pp. 949–950, December 1982, preprint 1896.
9. Enz, Christian C., and Vittoz, Eric A, *Charge-based MOS Transistor Modeling*, New York, Wiley, 2006.
10. Stuart, Edmond, Numerous Postings in DIYaudio Negative Feedback Thread.

This page intentionally left blank

Error Correction

Conventional negative feedback is not the only way to reduce distortion. Various error-correction techniques can be used in place of, or in connection with, negative feedback [1, 2, 3]. In this chapter we'll examine some of these techniques and study one of them in detail.

In virtually any well-designed power amplifier the output stage ultimately limits performance. It is here where both high voltages and large current swings are present, necessitating larger, more rugged devices that tend to be slower and less linear over their required operating range. The performance-limiting nature of the output stage is especially evident in class AB designs where the signals being handled by each half of the output stage have highly nonlinear half-wave-rectified waveforms and where crossover distortion is easily generated. In contrast, it is not difficult or prohibitively expensive to design front-end circuitry of exceptional linearity.

Overall negative feedback greatly improves amplifier performance, but it becomes progressively less effective as the frequency or speed of the errors being corrected increases. High-frequency crossover distortion is a good example. The philosophy here is based on the observation that only the output stage needs extra error correction and that such local error correction can be less complex and more effective.

While the power MOSFET has many advantages, it was pointed out in Chapter 11 that the lower transconductance of the MOSFET will result in moderate crossover distortion unless rather high bias currents are chosen. This effect was shown in Figure 11.10 where the individual and summed transconductances of both halves of a class AB MOSFET output stage were plotted as a function of net output current. The output stage transconductance is smaller in the crossover region, a phenomenon dubbed *transconductance droop* [2]. At a bias current of 150 mA and a load of 8 Ω, transconductance droop can result in open-loop output stage harmonic distortion on the order of 1% [2]. Mismatch in the transconductance characteristics of the top and bottom output devices also contributes to crossover distortion.

The primary focus of this chapter will be the application of error correction to MOSFET power amplifiers. However, output stage error correction can also be applied with advantage to BJT output stages, and that will be covered in this chapter as well.

12.1   Feed-Forward Error Correction

Figure 12.1 depicts a simple *feed-forward error correction* circuit. The idea is to calculate the error and then feed it forward and subtract it from the output. No loop is formed, so there are no stability concerns. The output stage is assumed to be a unity-gain stage with error injected. All forms of output stage error, including gain less than unity, are
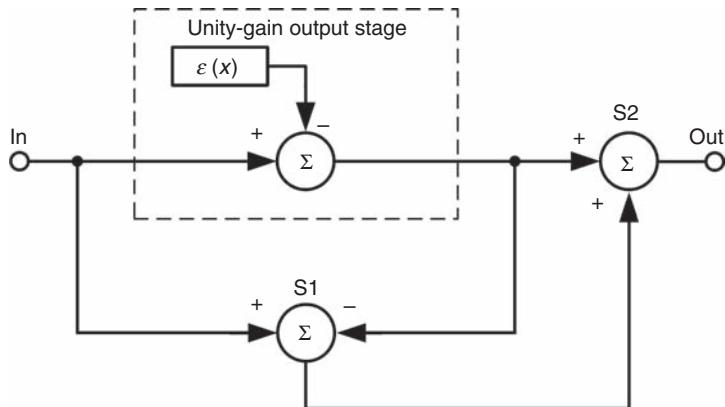
FIGURE 12.1 Feed-forward error correction.

represented by the source $\varepsilon(x)$. The error is subtracted from the unity-gain signal path to signify nominal gain less than unity. Summer S1 compares the input and output of the output stage and recovers $\varepsilon(x)$. Summer S2 adds $\varepsilon(x)$ back into the signal path to restore the signal to its original input value.

The problem with this kind of error correction is the difficulty with which an additional error signal can be passively added in a precise way to the output signal after the output stage. Making such a passive adding circuit at high power levels is difficult. It is even more difficult to do it in such a way as to not seriously compromise the output impedance. Any departures from the ideal signal will not be corrected after the summing network.

Reduced Effectiveness at High Frequencies

The cancellation of distortion with feed-forward requires that the error signal have just the right amplitude and phase. In principle, these can be adjusted with potentiometers, but this adds to cost and difficulty of setup. It is also generally the case that it becomes progressively more difficult to maintain the proper phase relationship as the frequency increases. Ultimately, this means that the amount of achievable distortion reduction through error correction decreases with increasing frequency, just as does the distortion reduction afforded by negative feedback.

12.2 Hawksford Error Correction

In 1980 Hawksford introduced a form of error correction that did not depend on a passive addition of the error signal to the output signal after the output stage [1]. Instead, as illustrated below, it fed back the error signal in a particular way. This will be referred to as *Hawksford error correction* (HEC). This technique is illustrated in Figure 12.2. As in Figure 12.1, the output stage is modeled as having exactly unity gain with an error voltage $\varepsilon(x)$ added. This error represents any departure from unity gain, whether it is a linear departure due to less than unity gain, a distortion due to transconductance non-linearity, or injected errors like power supply ripple. A differential amplifier, represented by summer S1, subtracts the output from the input of the power stage to arrive
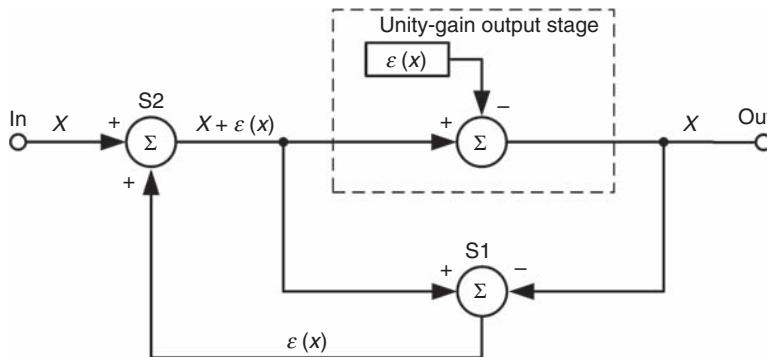
FIGURE 12.2 Hawksford error correction.

at $\varepsilon(x)$. This error signal is then added to the input of the power stage by summer S2 to provide that distorted input which is required for an undistorted output. Note that this is an error-cancellation technique like feed-forward as opposed to an error-reduction technique like negative feedback.

This technique is in a sense like the dual of feed-forward. It is less expensive because the point of summation is a low-power internal amplifier node. Like feed-forward, HEC tends to become less effective at very high frequencies because the required phase and amplitude matching for error cancellation becomes progressively more difficult to maintain. It can be shown that the required amplitude and phase matching are indeed identical to those for feed-forward. HEC also tends to become less effective at very high frequencies because, being a feedback loop (albeit not a traditional negative feedback loop), it requires some amount of frequency compensation for stability, which detracts from the phase and amplitude matching [2].

A Specialized Form of Negative Feedback

If the HEC circuit is redrawn as in Figure 12.3, it is apparent that there is a summer S5 with unity-gain positive feedback, around which there is a negative feedback loop (S4). In essence, the unity-gain positive feedback stage provides infinite forward gain and thus infinite negative feedback loop gain.
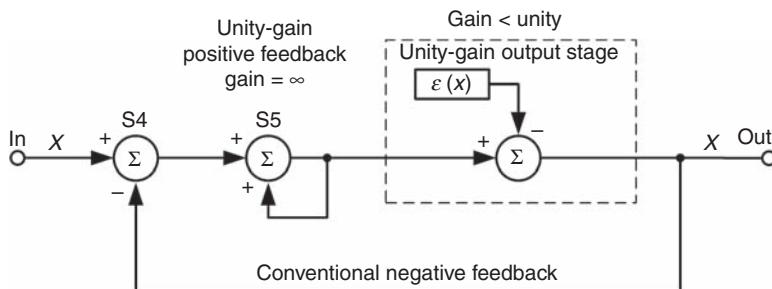
FIGURE 12.3 HEC viewed as negative feedback whose open-loop gain is enhanced by an embedded positive feedback loop.
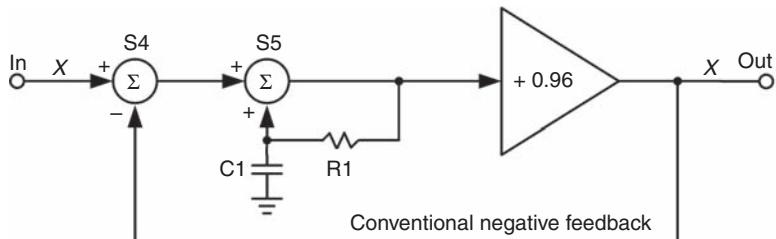
Figure 12.4   Compensating the error-correction loop.

If HEC is just another form of negative feedback, then what are its advantages? Those include simplicity of implementation and a tight local feedback loop. The negative feedback view of HEC also underlines the need for some form of frequency compensation of the loop. In the implementation to be discussed below, the forward path is compensated by feed-forward shunt capacitance that does not introduce a pole into the forward path of the output stage [2].

Frequency Compensation

Because HEC can be seen as a negative feedback loop with a high-gain stage formed by embedded positive feedback, it needs compensation just like any other negative feedback loop. A crude approach to compensating the *error correction* (EC) loop is illustrated in Figure 12.4, where the positive feedback view of the EC circuit is repeated, but with a compensating R-C circuit in the positive feedback path. It is easy to see that this network kills the loop gain of the EC circuit at high frequencies without placing a pole in the forward signal path. This helps avoid introducing additional phase lag into the global feedback loop of the main amplifier. This simplified example only reduces the EC loop gain to unity, so the practical implementation to be described is a bit different.

Effect on Output Impedance

The error-correction circuit seeks to force the gain of the output stage to unity under all conditions. Its output will then become load-independent. Increased loading will not cause the output to fall. This is equivalent to the output impedance being zero. As a result, the open-loop output impedance of an amplifier with EC is extremely low, even in the absence of global negative feedback. When global negative feedback is applied, the output impedance is driven even lower; this results in an extremely high damping factor out to quite high frequencies. The high-frequency damping factor for such an amplifier is largely dependent on the impedance of the output coil.

12.3   Error Correction for MOSFET Output Stages

The MOSFET output stage is an ideal candidate for the use of error correction. First, it profits greatly from error correction because the EC greatly mitigates transconductance droop. Secondly, the power MOSFET output stage is very fast and can provide the large bandwidth that allows HEC to work well.

Simplified Error-Correction Circuit

The simplified error-correction circuit of Figure 12.5 shows how an error amplifier can be interposed in the signal path of a vertical MOSFET output stage [2]. Emitter followers Q1 and Q2 isolate the high-impedance VAS output node from the output stage and provide a low-impedance signal for the error-correction summation process. They are fed from the VAS with voltages that are spread from nominal zero by ±11 V. This fixed voltage spread provided by Zener D1 powers the EC circuits and provides adequate headroom for the MOSFET bias voltages and V_{gs} signal swing. The signal path to the MOSFETs passes through EF predrivers Q5 and Q6 and drivers Q7 and Q8 to vertical MOSFET output transistors Q9 and Q10. The predrivers and drivers provide a high-current drive capability for the MOSFET gates and isolate the error-correction summing nodes from the MOSFET gate loads. Note that Q5 and Q6 can be fast, inexpensive small-signal transistors because their collectors are driven with the signals from Q1 and Q2.

Complementary transistors Q3 and Q4 make up the error amplifier, where the error-correction action takes place. The base and emitter circuits of Q3 and Q4 implement the function of summer S1 in Figure 12.2. The signal from the error amplifier is injected into the forward path by error current flowing through series resistors R1 and R2. The collector nodes of Q3 and Q4 play the role of summer S2 in Figure 12.2.
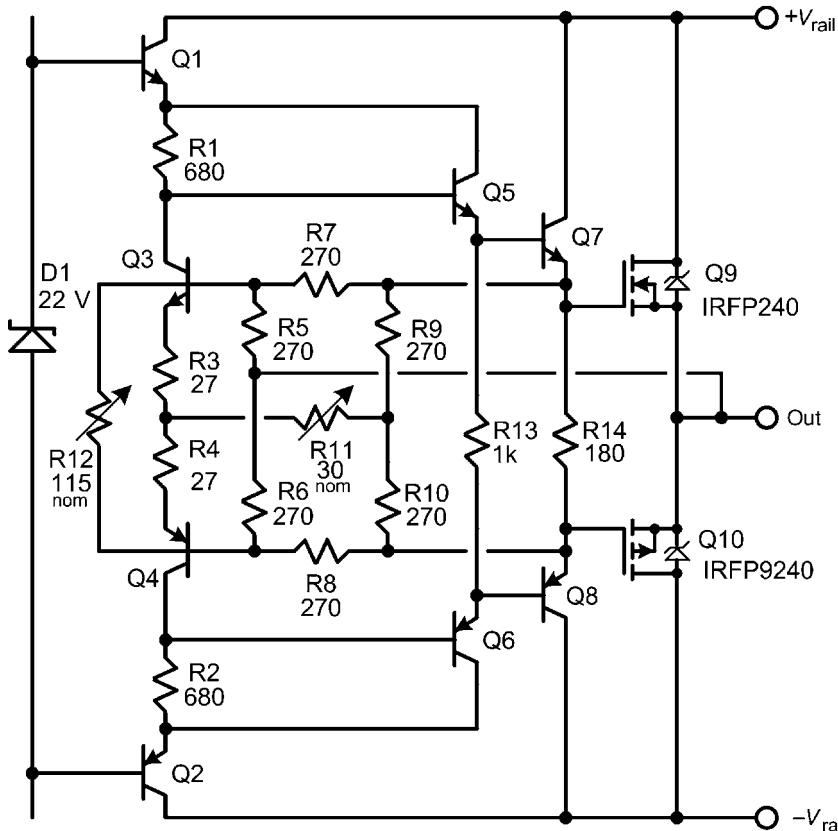
FIGURE 12.5 A simple error-correction circuit for a MOSFET output stage.

The error amplifier made up of Q3 and Q4 is a differential amplifier formed by complementary transistors. The inverting input is applied to the bases while the noninverting input is applied to the emitters. Emitter resistors R3 and R4 control the loop gain of the bias loops, provide emitter degeneration for the error amplifier, and improve stability.

In the context of Figure 12.2, MOSFETs Q9 and Q10 make up the output stage. The signal at their gates corresponds to the input signal supplied to the output stage by summer S2 in Figure 12.2. This signal makes its way back to the noninverting input of the error amplifier through R9, R10, and R11. A simple circuit analysis shows that the feedback loop formed from the emitters of Q7 and Q8 through the error amplifier and the summing node load resistors R1 and R2 has noninverting gain of unity. This corresponds to the behavior illustrated in Figures 12.2 and 12.3. The error correction condition is optimized when this gain is exactly unity, as optionally trimmed by R11. Adjustment of R11 nulls the distortion.

Transistors Q3 and Q4 also act as a V_{be} multiplier to implement the bias spreader for the MOSFET output stage. Q3 and Q4, in conjunction with bias adjust resistor R12, control the DC voltage drop across R1 and R2. They thus set the bias for the MOSFETs by means of a V_{be}-referenced feedback loop that also includes Q5, Q6, Q7, and Q8. The V_{be} drops of Q3 and Q4 together are multiplied by the combination of resistors R5–R8. Transistor Q3 is mounted on the heat sink to provide thermal feedback. Thus, about half of the total bias spread is compensated by the temperature of the heat sink. Q3 is preferably a fast TO-92 transistor embedded in a hole in the heat sink. The wiring to this transistor should be fairly short so as to avoid parasitic oscillations.

Error-Correction Circuit Operating Voltage

The error amplifier circuit floats with the signal and receives its operating voltage from the fixed bias spread provided to the EC circuit. The bias spread applied to the output transistors also plays a role in establishing the available operating voltage for the EC circuit. In the circuit of Figure 12.5, a fixed bias spreader provides the initial bias spread with which the error amplifier works. It is easy to see that the error-correction circuit requires additional headroom from the VAS. Because the error-correction circuit demands that the output stage have unity gain, it must provide all of the gate drive required by the MOSFETs to drive the load, even to very high currents.

Error-Correction Circuit Clipping

Under very high-current demands by the load, the error-correction circuit may not be able to provide all of the gate drive demanded by the output transistors. Under these conditions, one of the error amplifier transistors will go into cutoff. When this happens, any additional signal swing and gate drive must be provided by the VAS, meaning that the output stage gain for such large signal swings will fall somewhat below unity. Under these conditions, however, the MOSFETs are in a high-current state and their transconductance is quite high, so output stage gain will be fairly close to unity even without the action of the error-correction circuit. It is also possible that the error amplifier can clip by going into saturation. This should be avoided.

12.4   Stability and Compensation

Because error correction is a form of negative feedback, it must be stabilized in some way at high frequencies. As with conventional negative feedback, this is done by controlling the gain and phase in the local feedback loop so that stability is preserved.

Stability Considerations

It is important that the compensation of the local feedback loop formed by the error-correction scheme not interfere with the open-loop gain and phase of the amplifier. Otherwise, the gain crossover frequency of the global feedback loop will have to be reduced and the distortion reduction will be reduced. It is not desirable to achieve distortion reduction by error correction at the expense of distortion reduction by global negative feedback. The goal is to have an output stage with error correction that has little or no additional excess phase as compared to the same output stage without error correction.

The EC loop is active to fairly high frequencies, so its stability may be significantly affected by loading at the output of the amplifier. For this reason, it is important that the usual L-R network be placed in series with the amplifier output to isolate the output node from the load at high frequencies. It is also important to employ very good high-frequency layout and design techniques in the output stage when EC is being used.

Frequency Compensation Approach

Compensation of the error correction loop requires that the gain around that loop be reduced with frequency to achieve a gain crossover frequency, just as with an ordinary feedback loop. Because the EC loop is local, this gain crossover frequency can typically be at a higher frequency that used for the global feedback loop.

Figure 12.6 shows the addition of frequency compensation components to the basic EC circuit of Figure 12.5. The primary reduction of EC loop gain with frequency is
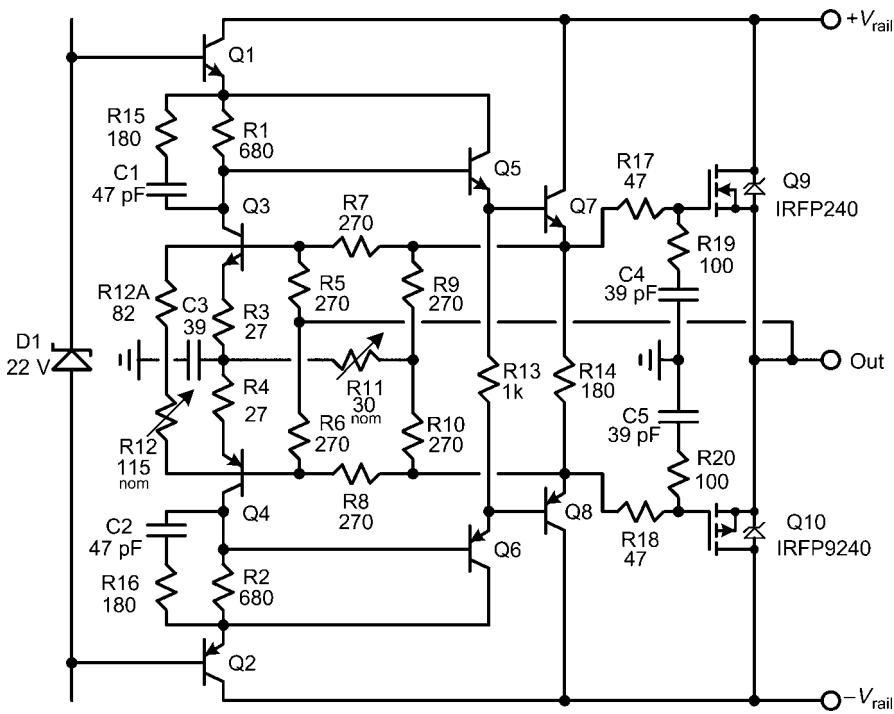
FIGURE 12.6 The error-correction circuit used in Ref. 2.

achieved with the series R-C networks that shunt the error amplifier collector load resistors R1 and R2. Clearly, if this impedance goes to zero, there will be no error-correction action and no error-correction loop gain. The important feature of this arrangement is that when it reduces gain of the EC loop, it does so by shunting the input signal around the error amplifier load resistor in a feed-forward fashion to the next emitter follower in the signal path. As such, this frequency compensation does not add phase lag to the overall open-loop amplifier.

C1 and C2 provide the primary means of frequency compensation by shunting R1 and R2. Resistors R15 and R16 in series with the compensation capacitors effectively place a zero in the loop of the EC circuit to improve phase margin. It is notable that at very high frequencies the collector-base capacitances of Q5 and Q6 create a further feed-forward bypass of the signal. As expected, the action of C1 and C2 at higher frequencies reduces the effectiveness of the error correction. However, in Ref. 2 the error correction still reduced THD by almost 30 dB even at 20 kHz.

The remaining element of the EC compensation scheme is the single capacitor C3 connected from the error amplifier emitter circuit to ground. This capacitor acts as a positive feedback loop spoiler. It upsets the balance of the EC circuit at high frequencies in such a way that the feedback loop gain of the inner positive feedback loop is decreased from unity, so that the forward gain contributed by the positive feedback loop falls with increasing frequency.

The gate stopper resistors (R17 and R18) and gate Zobel networks (R19, R20, C4, and C5) used in Ref. 2 for output stage stability are shown for completeness.

Simulation of Effective Gain Crossover Frequency

Estimating the effective gain crossover frequency of the error-correction circuit is not an easy matter. However, SPICE simulation can be used to evaluate it. SPICE simulation can also be used to evaluate the stability of the local error-correction feedback loop by viewing the frequency response and square-wave response of the error-corrected output stage by itself.

Figure 12.7 illustrates one way in which the EC loop can be broken in order to evaluate its loop gain. Recall that the EC circuit can be viewed as a negative feedback loop with an embedded high-gain stage formed by unity positive feedback as illustrated in Figure 12.2. The loop is broken in Figure 12.7 between the amplifier output (point *A*) and the input to the error amplifier (point *B*). The impedance at the output of the amplifier is much lower than the impedance at the input of the error amplifier. This means that the loop can be broken with little loss of accuracy by inserting an AC voltage source at the error amplifier side of the break and viewing the signal at the output of the amplifier. DC stability of the loop is not affected by breaking the loop in this way, so a large inductor is not needed to close this loop at DC. An AC test signal is merely injected into point *B* through a coupling capacitor.

Effect on the Global Feedback Loop

It is important that the error-correction circuit does not detract significantly from the phase margin and gain margin of the global negative feedback loop. Fortunately, when the EC loop gain diminishes and EC action is no longer in play, the output stage defaults to a conventional output stage. In principle, this output stage then exhibits no more excess phase than a conventional output stage of the same design.
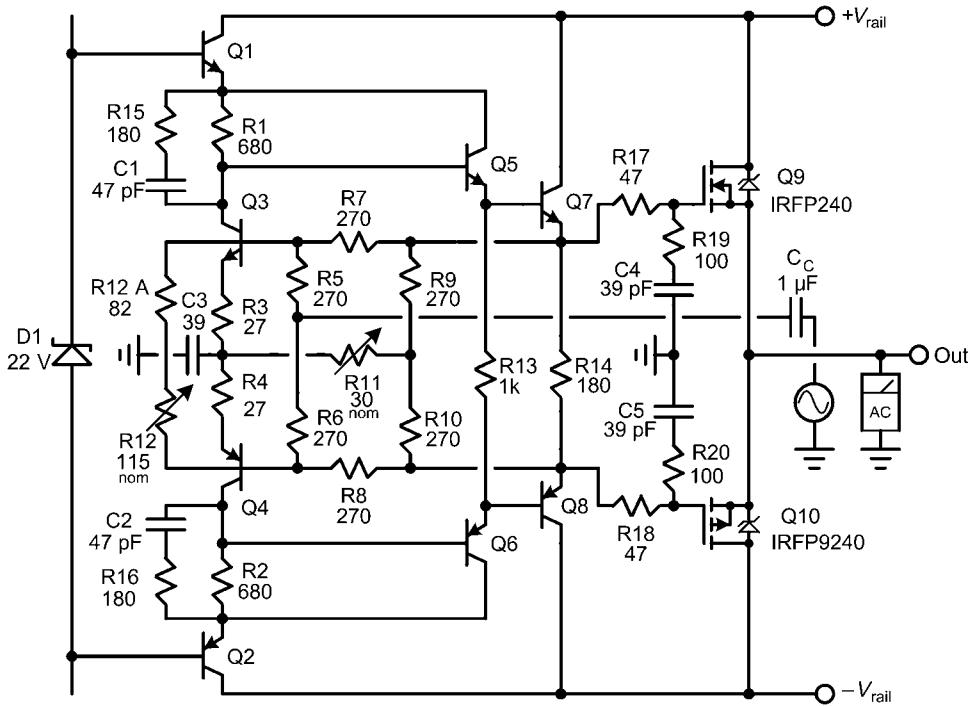
Figure 12.7 Breaking the loop for stability analysis.

To this end, the gain and phase of the EC output stage by itself should be evaluated by simulation with and without the error correction enabled. Error correction is easily disabled by removal of R11.

12.5 Performance and Design Issues

There are some performance-limiting issues and design nuances in the EC circuit shown in Figure 12.6 that will be discussed here. In some cases understanding these can point the way to improvements that can be made to the error-correction circuit.

Trimming

The amount of error correction is maximized by adjustment of the trim resistor R11 in Figure 12.6. Values too high or too low upset the balance of the circuit and result in less cancellation of distortion. The trim resistor can actually be adjusted for a null in the distortion. Interestingly, the polarity of the distortion residual actually changes as the trim resistor is changed from being too high to too low.

The presence of the trim resistor is seen by some as a disadvantage of error correction, suggesting that it forces a manufacturer to trim every amplifier manually while observing distortion on a distortion analyzer. This is not so. While it is true that such a procedure can be used to optimize the circuit, the amount to be gained must be put in perspective. It can be shown that a 1% error in the EC balance condition will still allow the error correction to reduce distortion by about 40 dB if that is the only impairment.

It is important to realize that the optimum value of trim resistor will be established by adjustment during the design process. The trim pot can subsequently be replaced with a fixed 1% resistor in production units. This procedure is known as *design centering*.

High-Frequency Limitations

It is well known that distortion at high frequencies in an amplifier is the most difficult distortion to reduce. This is certainly true for crossover distortion in the output stage. The necessary evil of high-frequency compensation for the EC loop upsets the EC balance condition at high frequencies. This results in a limitation on the amount of error correction that is available at high frequencies. This limitation cannot be overcome by any adjustment of the trim resistor, and usually dominates over trim resistor inaccuracies at high frequencies.

Given that high frequencies are where error correction is most needed, it is of relatively little value for the trim resistor to be substantially more optimal that achieves a similar degree of error correction at low frequencies. This is a further reason for arguing that a trim pot is superfluous for an EC circuit built with 1% resistors.

Nonlinearity in the Error Amplifier

The error-correction circuit sees any departure of the output stage from unity gain as an error, whether its origin is from a linear or nonlinear process. The EC will attempt to make the net gain of the output stage unity, regardless of load and (ideally) of frequency.

This means that all of the gate voltage increase required by the MOSFETs for production of signal current must be supplied by the EC circuit. Where high signal currents are involved, the difference in gate voltage drive from the quiescent state to the high-current state can be several volts. The production of a signal swing of several volts by an amplifier as simple as the error amplifier in Figure 12.6 can incur some distortion. The main cause of distortion is the dynamic emitter resistance of Q3 and Q4. The value of re' changes with error current and creates distortion.

Table 12.1 shows typical V_{gs} at 150 mA and 5 A for three different power MOSFETs. Also shown is the difference in V_{gs} for these two operating currents. This shows how much gate voltage swing is required when a single output pair is delivering 100 W into an 8-Ω load. Notice that the lateral MOSFET begins with a low value of V_{gs} but has a high value at 5 A due to its relatively low transconductance. This means that it must actually be driven harder than the vertical devices, and this suggests higher nonlinearity in the error amplifier.

Device	Type	$V_{gs,0.15 A}$	$V_{gs,5 A}$	ΔV_{gs}
IRFP240	Vertical	4.2	5.5	1.3
2SK1530	Vertical	1.6	2.8	1.2
2SK1056	Lateral	0.7	5.7	5.0

TABLE 12.1 V_{gs} for Three MOSFETs

Headroom and Clipping

The simple error amplifier will produce useful output only as long as the collector current of Q3 and Q4 is nonzero, so there must always be a sufficient voltage drop across the error amplifier load resistors R1 and R2. Increased gate drive for the output transistor is produced by reduction of the error amplifier transistor collector current. If the output MOSFET requires more gate drive than is available, that transistor will go into cutoff. Similarly, the error amplifier transistor on the opposite side should never saturate. This means that under maximum conditions of error correction, the emitter current of the error amplifier in the path of the output transistor that is off must not exceed the maximum collector current available through the load resistor. The available headroom is largely determined by the amount of fixed spreader voltage supplied by Q1 and Q2.

Boosted Rails

The added operating headroom required by the error-correction circuitry takes the form of increased fixed spreading voltage at the VAS. The fixed spreading voltage in the design of Ref. 2 was 22 V. This means that the available VAS voltage swing will be seriously limited if the VAS is powered from the same rail voltage as the output transistors. For this reason, it is advantageous to employ boosted supply rails for all circuits preceding the output transistors. This was also recommended in the previous chapter for conventional amplifiers employing MOSFETs because of their significant gate voltage drive requirements. It is doubly important here. It is still desirable to employ Baker clamps to limit VAS swing in light of the higher VAS supply voltage. Be mindful that with EC, the output stage has virtually unity gain.

Use with Low-V_{gs} MOSFETs

The EC circuit is partly powered from the bias spread provided to the output transistors. For output stages employing MOSFETs like the IRFP240/ IRFP 9240, this voltage spread is adequate because these devices have threshold voltages on the order of 4 V. This will not be the case for lateral MOSFETs with threshold voltages less than 1 V and may not be the case for other types of vertical MOSFETs with threshold voltages as low as 1.5 V (e.g., Toshiba 2SK1530/2SJ201). V_{gs} for the lateral 2SK1056 at a quiescent current of 100 mA can range from 0.2 V to 1.5 V. V_{gs} for a vertical 2SK1530 at 100 mA can range from 0.8 V to 2.8 V. The high percentage range of V_{gs} variation for such low-threshold devices can present other challenges for driver design, such as variation in the driver quiescent current when that current is set by a resistor connected between emitter follower driver transistors.

The EC circuit can be used with such low-threshold voltage MOSFETs, but some modification of the circuit is required to present the EC circuit with sufficient operating voltage. A simple approach is to introduce an additional voltage drop ahead of each of the output MOSFET gates. This might be as simple as introducing a diode or green LED in series with the emitters of the driver transistors, keeping the feedback to the EC error amplifier connected to the driver emitters while feeding the output transistors from the inner ends of the diodes or LEDs. However, if the drivers are biased at 50 mA, this will be too much current for ordinary LEDs.

An alternative approach is shown in Figure 12.8. Additional predriver transistors Q11 and Q12 are introduced into the signal path, and their outputs are used for the feedback
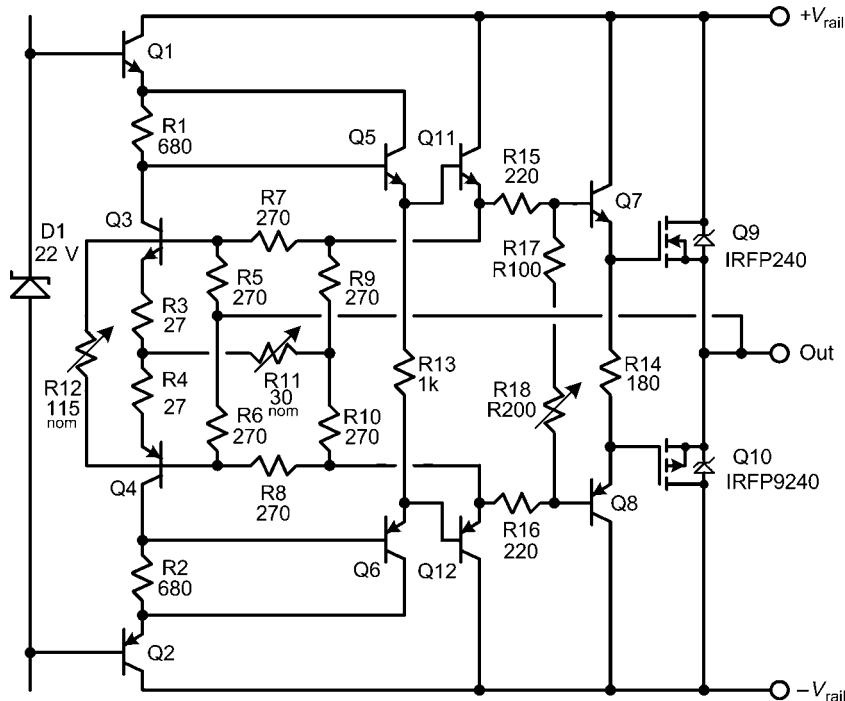
FIGURE 12.8   An EC circuit suitable for use with low-V_{gs} MOSFETs.

to the error amplifier. This introduces an additional V_{be} of drop in the path to the drivers. Further reduced voltage spread for the driver and output transistors is obtained from an attenuator formed by R15, R16, R17, and R18. Shunt resistor R18 can be trimmed in order to accommodate variation in the threshold voltages of the MOSFETs so that proper operating voltages for the EC circuit can be obtained. This approach also encloses the driver transistor in the error-correction loop, reducing distortion that it introduces. Notice, however, that the quiescent bias current of the driver transistors is still subject to considerable variation depending on the actual MOSFET output transistor threshold voltages. This is a potential issue for any amplifier that uses EFs to drive MOSFETs with a wide range of threshold voltages.

Error Correction for BJT Output Stages

Although Hawksford first described HEC in the context of BJT output stages, it has seen less application in BJT output stages. For one thing, the biasing arrangement is not necessarily advantageous. Secondly, BJT output stages do not need error correction as much, due to their higher transconductance. Finally, error correction does best when employed in connection with a very fast output stage, and even RET BJTs are not as fast as MOSFETs.

The circuit of Figure 12.8 can be used with BJT output transistors with little or no modification, where the situation and solution are really no different from those for lateral MOSFETs, whose threshold voltages are not too dissimilar to the V_{be} of a BJT.

Note, however, that the BJT output stage does not have such a wide range in turn-on voltages as the MOSFETs, so some of those problems of variability are much less. The turn-on voltage will always be nearly 0.6 V. For this reason, trimmer R22 can be eliminated.

One way in which EC can be used to advantage in a BJT design is to allow the BJT output stage to be somewhat overbiased. It will then incur some crossover distortion due to *gm* doubling. That distortion can be greatly reduced by error correction. The net advantage here is that the BJT amplifier can be overbiased and enjoy a larger class A operating region, while being more immune to the effects of dynamic bias errors caused by temperature swings with program material.

12.6   Circuit Refinements and Nuances

The simple error-correction circuit described thus far and used in Ref. 2 is very effective in reducing output stage distortion. The circuit adds only four transistors to what would otherwise be an output Triple (BJT or MOSFET). Given its simplicity, the circuit works amazingly well, in some cases providing 30 dB of distortion reduction at 20 kHz [2]. The MOSFET amplifier in Ref. 2 achieved THD below 0.001% at 20 kHz. However, these simple circuits have some limitations, and improvements can be made at little relative increase in parts cost.

Complementary Error Amplifier

Because the error amplifier consists of an NPN-PNP pair, it operates in a complementary fashion. When the signal current increases in one device, it decreases in the other device. This provides a desirable degree of second harmonic distortion reduction of the same type that accompanies the use of a conventional differential pair.

The assumption behind this distortion mitigation is that the output signals of the two error amplifier transistors both have the same effect on the amplifier output signal. Unfortunately, this is not always the case with the simple EC circuit described earlier. When one of the output transistors is in the off state during class AB operation, the output of one of the error amplifier transistors is largely ignored. This is because the drive signal paths for the N-channel and P-channel MOSFETs are independent.

Ideally, the signal voltages at the collectors of the two error amplifier transistors will be identical. For this reason, it is allowable to couple these two collectors together with a capacitor. When this is done, both collector currents will be forced to exert the same influence on the output signal, regardless of the on or off state of the associated output transistors. In effect, the signal contributions of the two transistors are merged immediately rather than at the output node of the amplifier. This simple arrangement is illustrated in Figure 12.9.where C6 provides an AC short circuit between the collectors of Q3 and Q4, forcing them to act as a differential pair even though they are of opposite polarity. C6 need not be large, since its most important contribution is at high frequencies where the need for error correction is greater. A value of 1 μF is adequate.

CFP Error Amplifier

The nonlinearity of the error amplifier is caused by signal-dependent changes of *re'*. If each transistor in the error amplifier is replaced with a *complementary feedback pair* (CFP), this effect will be greatly reduced. The CFP is implemented by the addition of Q11 and
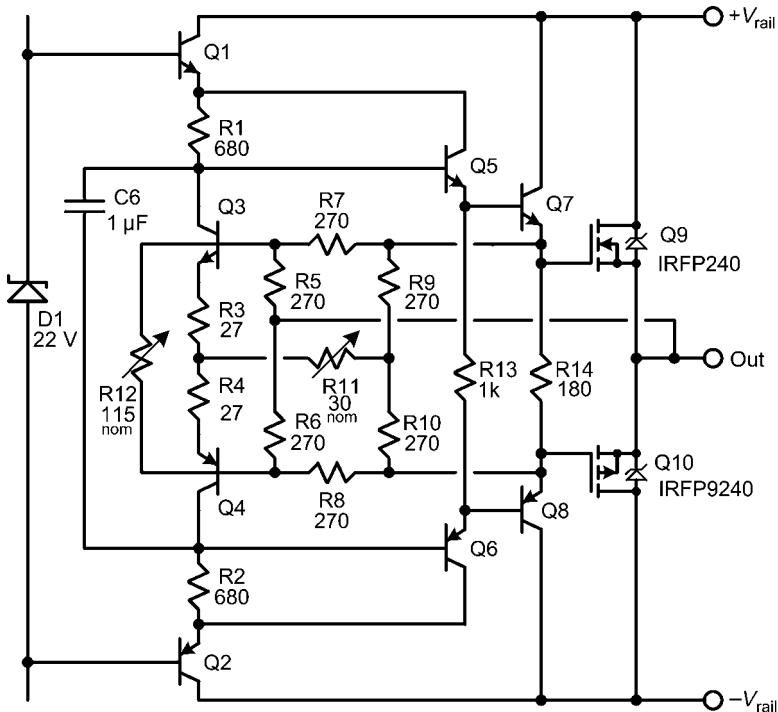
FIGURE 12.9   Capacitor C6 forces complementary behavior of the error amplifier.

Q12 to the error amplifier as shown in Figure 12.10. The bias current of the input transistor of the CFP can be set at about 1/10 of the CFP overall. The effective transconductance of the error amplifier transistors is greatly increased by the use of the CFP. This virtually eliminates the nonlinearity caused by re' variation.

A further advantage of the CFP error amplifier is that the effective beta of the CFP is much larger than that of a single transistor. This reduces the load placed on the resistive summing network and further improves linearity. A cost associated with the CFP is voltage headroom. The CFP will add at least $1V_{be}$ of required supply voltage to each driver rail.

Cascoded Drivers

All of the transistors in the error correction circuitry should be as fast as possible. This allows for a higher local loop gain crossover frequency and lighter EC compensation, which will lead to increased EC effectiveness at high frequencies.

The driver transistors (Q7, Q8) in the arrangements described so far must dissipate considerable power if their bias current is sufficient to quickly turn off the output MOSFETs. Bias current of 50 mA and quiescent V_{ce} of 60 V are not uncommon for these drivers. This corresponds to power dissipation of 3 W. Suitable driver transistors that can handle this dissipation will usually be slower than small-signal transistors.

The driver transistors can be cascoded as shown in Figure 12.10. Cascode transistors Q13 and Q14 are fed from input emitter followers Q1 and Q2. The bases of the cascodes and the collectors of the drivers thus move with the signal. Q13 and Q14 bear
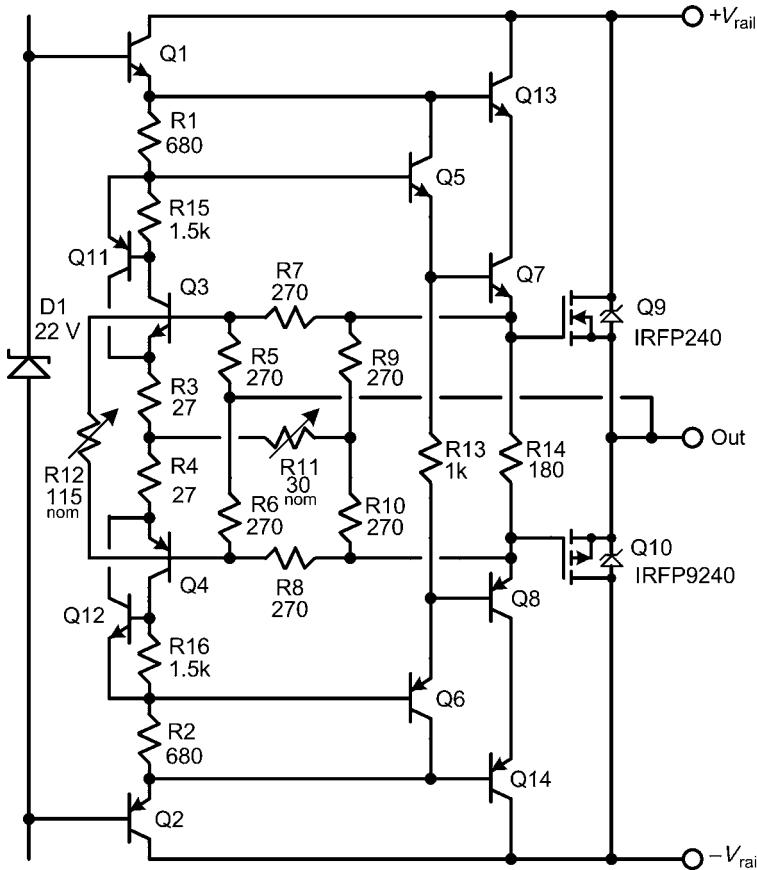
FIGURE 12.10 Use of a CFP-based error amplifier and cascoded drivers.

the greatest portion of the power dissipation. Since they are not really in the signal path, they can be slower devices without affecting EC circuit speed. The actual driver transistors then see a much smaller collector-emitter voltage (about 5.4 V) and dissipate much less power (about 270 mW). As a result, they can be fast, small-signal transistors. Driver transistors Q7 and Q8 in this configuration also operate at fairly low temperature. This improves bias temperature stability.

References

1. Hawksford, M. J., "Distortion Correction in Audio Power Amplifiers," presented at the 65th Convention of the Audio Engineering Society, *JAES* (Abstracts), vol. 28, pp. 364–366, May, 1980; preprint 1574.
2. Cordell, R. R., "A MOSFET Power Amplifier with Error Correction," *Journal of the Audio Engineering Society*, vol. 32, no. 1, pp. 2–19, January, 1984; available at www. cordellaudio.com.
3. Didden, J., "The paX Amplifier," *audioXpress*, pp. 6–15, August and pp. 10–15, September, 2009.

This page intentionally left blank

CHAPTER **13**

Other Sources of Distortion

The discussions on distortion have so far focused on well-understood distortions that are caused by nonlinearities largely in semiconductor devices. Examples are the nonlinear relationships of current to base or gate voltage, Early effect wherein transistor current gain is a function of collector voltage, or junction capacitance that is a function of reverse bias.

These kinds of nonlinearity produce many types of distortions. Harmonic and CCIF IM distortion are just different ways of measuring the symptoms of such nonlinearities. This is also the case with many other distortions, such as TIM [1]. Here we focus on other sources of distortion that must be considered as well. In many cases, these distortions result from the way in which the circuits are implemented, either as a result of other component imperfections or as layout-related matters.

In many cases, minimizing these distortions requires a great amount of attention to detail, such as layout, ground topology, and power supply bypassing. It is a shame that in some cases these sources of distortion can ruin an otherwise finely designed amplifier. Although some of these sources of distortion have been touched on in other chapters, they can often easily be overlooked. For that reason, each will be discussed here.

13.1 Distortion Mechanisms

Nonlinear distortion occurs as a result of a variety of sources, but these sources often share many of the same distortion-creating mechanisms. In the most general terms, distortion occurs when one or more parameters of an active or passive device change as a function of the signal. Examples include changing transistor current gain as a function of signal voltage and changing junction capacitance as a function of signal voltage. If a resistance changes as a result of signal-dependent temperature, this will also create nonlinear distortion.

Another trait of nonlinear distortion is that a small-signal characteristic of the amplifier changes as a function of signal excursion. The most common example is when the incremental gain of the amplifier changes over the signal swing. If the gain is higher on positive swings and lower on negative swings, this corresponds to second-order distortion. If the gain is smaller for large signal deviations from zero, this corresponds to third-order distortion. If instead the frequency response or phase response of the amplifier changes with signal, this is also a form of nonlinear distortion. Anything that changes as a function of signal is a likely source of distortion.

13.2   Early Effect Distortion

The current gain of a transistor is mildly dependent on the collector-base voltage. This is referred to as the Early effect. To the extent that the gain of an amplifier stage is dependent on the current gain of the transistor, the Early effect can cause distortion. The Early effect was discussed in Chapter 2. Early effect distortion is minimized by employing cascodes (which reduce signal-dependent collector-base voltage changes) or by designing stages whose gain is less dependent on transistor current gain. A common-emitter stage preceded by an emitter follower suffers less Early effect distortion because beta changes in the common emitter (CE) transistor have less influence.

13.3   Junction Capacitance Distortion

The capacitance of P-N junctions in transistors and diodes is a function of voltage. This means that the frequency response of a gain stage may change with signal voltage. This in turn means that the gain at high frequencies can be modulated. Whenever gain changes as a function of signal voltage, this is a nonlinearity that can cause distortion.

A good example of this distortion is the Miller effect in a gain stage. A larger value of collector-base capacitance will reduce high-frequency gain of the stage. In some amplifiers with simple Miller feedback compensation, the collector-base capacitance of the VAS transistor forms a part of the total compensation capacitance. The gain crossover frequency then becomes a function of signal, resulting in small in-band gain and phase changes that are signal-dependent [2]. Consider the collector-base capacitance of the 2N4401 NPN small-signal transistor. It is 9 pF at 0 V, 4.5 pF at 5 V, and 1.5 pF at 50 V.

It is also important to recognize that the gate of a JFET forms a reverse-biased P-N junction with the source-drain channel of the JFET. This junction will also be subject to modulation of its capacitance by the signal voltage.

MOSFET Gate Capacitance Nonlinearity

Just as with P-N junctions, the gate capacitance in a MOSFET can also change with voltage, so the same sort of nonlinearity and distortion can occur. Although the capacitor formed by a MOSFET gate has an insulator as its dielectric, there still exists a depletion region in the doped silicon underneath the gate. Increased amounts of reverse bias on the gate increase the width of this depletion region and effectively move the plate further away, decreasing capacitance.

The most serious example of this is the increased gate-drain capacitance C_{gd} of a vertical power MOSFET when the reverse bias of the gate with respect to the drain becomes small. Most of the time, the reverse bias from gate to drain is large. When the output signal is at zero and the gate is at a nominal forward bias voltage of a couple of volts, the reverse bias will be nearly equal to the rail voltage. When the audio signal swings to a large value (approaching clipping), the amount of this reverse bias will decrease to a low value, sometimes close to zero. When this happens, C_{gd} may increase very substantially. It can literally increase from 50 pF to over 500 pF as the drain-source voltage approaches zero.

13.4   Grounding Distortion

There exist very distorted half-wave-rectified signal currents in class AB output stages. Current flows from the positive rail on positive half-cycles and from the negative rail on negative half-cycles. Sometimes these nonlinear currents can make their way into the grounding circuit, causing nonlinear voltage drops across the finite resistance of ground traces.

A good example is the bypassing of the main rails of the output stage. Those bypass capacitors will be carrying substantial amounts of the nonlinear currents. The better those capacitors are, the greater percentage of that current they will carry. That current has to be returned to ground somewhere. If that current is dumped into a ground that signal circuits depend on, distortion will be coupled into the signal path. This is one reason why star grounds and other features of grounding architecture are so important. It is very important that bypass capacitors not form AC ground loops that can destroy the star grounding architecture at high frequencies. Always remember that signal currents (including nonlinear signal currents) will tend to take the path of least impedance. Sometimes the strategic placement of a small resistance will effectively break a ground loop and make a great improvement.

13.5   Power Rail Distortion

All of the stages in a power amplifier have some amount of *power supply rejection ratio* (PSRR). This describes the degree to which the stage can suppress the influence of noise and distortion on the power supply lines on the signal output of the stage. The power supply rail will often contain a mixture of rectifier ripple, noise, hum, and distortion components. This is especially true of the high-current main rails that supply the output stage. If any of this hash gets into a signal stage, it will make its way to the amplifier output. Nonlinear signals on power supply rails will thus result in amplifier distortion.

There are two basic ways to reduce distortion from the power rails. The first is to minimize the garbage appearing on the power rails. This can be done by employing generous R-C filtering in the power supply lines or by regulating the power supply lines. Sometimes a *soft* form of regulation is implemented with a pass transistor acting as an emitter follower for the power supply voltage. This will often take the form of a *capacitance multiplier*. Such an arrangement is shown in Figure 13.1. A nice feature of this
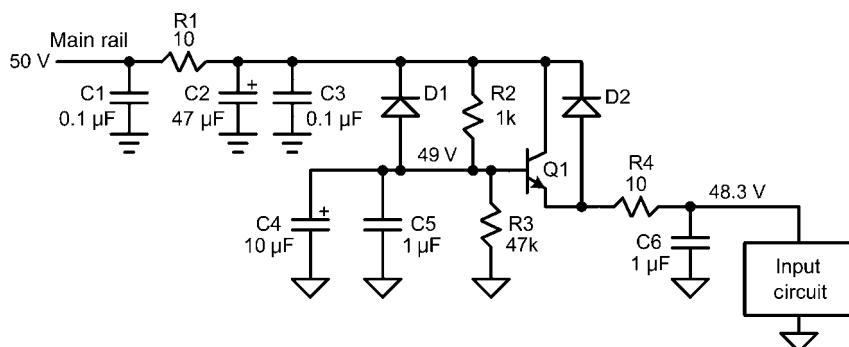
FIGURE 13.1   Filtering the power supply with a capacitance multiplier.

arrangement is that the filtering capacitor can have its ground referenced to the ground of the circuit that will be employing the resulting power rail.

The second approach is to design the individual amplifier stages to have higher PSRR out to higher frequencies. In many cases the PSRR of an amplifier stage will fall with increasing frequency. Differential circuits and cascode circuits often exhibit better power supply rejection up to higher frequencies.

Output Stage Power Supply Rejection

Although the output stage is usually just an emitter follower or source follower with some drivers in front of it, it is not immune to power supply garbage. This is largely because of the Early effect in the output transistors (or its analogous effect in MOSFETs). This is a weak effect in an emitter follower or source follower arrangement, but the amplitude of the garbage on the rails at this point is often quite large. This is of special concern when the output swings close to the rails. This effect is reduced in designs employing cascoded output stages. Splitting the power supply reservoir capacitors and separating them by as little as 0.1 Ω can make a big improvement here.

13.6   Input Common Mode Distortion

An often-neglected source of distortion results from the common mode signal swing on the input differential pair of a noninverting power amplifier. The common mode voltage is simply equal to the input signal swing, which may be on the order of a couple of volts.

The distortion can result from the collector-base voltages of the LTP changing with signal, causing beta to change via the Early effect. It can also result from changes in the collector-base junction capacitances as a result of their voltage dependence on V_{cb}. Nonlinear output impedance of the tail current source may also create common mode distortion. Techniques for minimizing input common mode distortion were discussed in Chapter 7.

An input stage that has better common mode rejection will tend to have smaller common mode distortion. Conversely, steps taken to reduce common mode distortion will often improve common mode rejection. Noise on power supply rails is often seen as common mode noise by the input stage. For this reason, input stages with good common mode rejection will tend to have better PSRR.

Testing for Common Mode Distortion

One way to test for the presence of common mode distortion is to drive the amplifier through a resistor connected to the inverting input, with no signal applied to the conventional noninverting input. This forces the amplifier to operate in the inverting mode, where there is no common mode signal swing on the input LTP. If distortion is significantly reduced under these conditions, it is likely that there is common mode distortion.

13.7   Resistor Distortion

Some resistors can change their value slightly as a function of the voltage across them or the current through them. These effects are quite small and very difficult to measure in most resistors of reasonable quality. In some cases carbon composition resistors will

show this effect. Sometimes the interface between the material of the resistor element and the resistor leads can develop some nonlinear voltage drop.

The feedback network resistors are especially important because they play a direct role in setting the gain of the amplifier. There is nearly a one-to-one dependence of gain-on resistor value; a 1% change in resistance will cause a 1% change in gain. The sensitivity of gain to change in the value of other resistors in the open-loop portions of the amplifier is usually much less (it is reduced by the feedback factor).

All resistors have a temperature coefficient of resistance. In many cases this might be on the order of 100 ppm/°C. Because the body of the resistor has a thermal time constant (its temperature will not change instantly), the effect of signal amplitude on resistance through heating will usually take place at low frequencies. This effect is particularly important in the feedback network resistors because the full signal swing of the amplifier output is across the network. This may cause significant short-term power dissipation and signal-dependent heating of the resistor. This effect is exacerbated when smaller values of feedback network resistance are used in pursuit of lower input stage noise [3].

Suppose a resistor's temperature swings by 10°C peak to peak. If the resistor has a TC of 100 ppm/°C, then the resistance will swing by 0.1% peak to peak, and distortion on the order of 0.05% may result. Suppose we have a feedback resistance of 4 kΩ and the amplifier output swings by 40 V peak. This will result in a peak current of 10 mA and peak power dissipation of 400 mW. Almost all of this power dissipation is in the series feedback resistor. It is easy to see how this could swing the temperature of the resistor by several degrees Centigrade at sufficiently low frequencies. A 6.81-kΩ 1/4-W metal film resistor subjected to 40 V DC dissipated 230 mW and its resistance changed by 0.06%.

Figure 13.2 shows the measured distortion of a 1/4-W metal film resistor as a function of frequency. The 1-kΩ resistor was subjected to an average power dissipation of
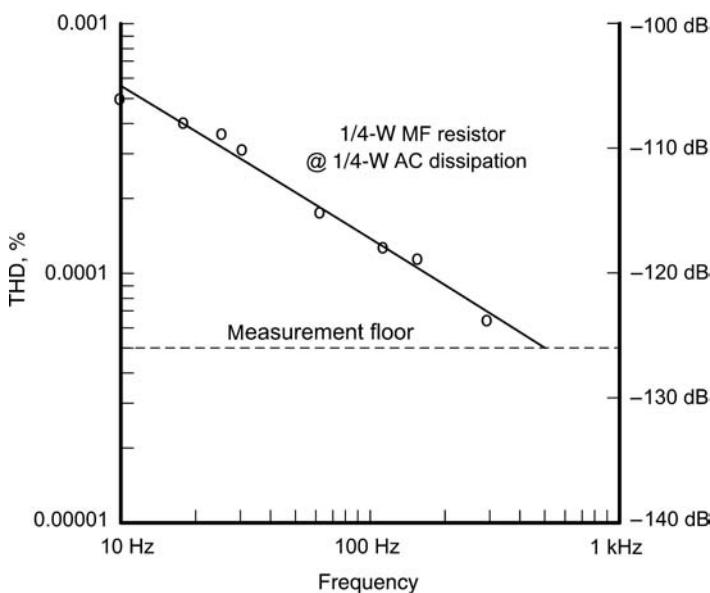
FIGURE 13.2 THD of 1/4-W resistor versus frequency at 1/4-W dissipation.

1/4 W. Distortion was measured by forming two 20-dB attenuators. One employed the resistor under test in the series arm and the other employed a 2-W version of the same resistor in its series arm. The difference of the outputs of the two attenuators was then amplified and analyzed. This technique virtually eliminates the influence of distortion from the driving amplifier and enhances the sensitivity of the spectrum analyzer used for measurement. Resistor distortion was primarily of third order and decreased with frequency, as expected.

The lesson here is to employ resistors of larger power dissipation in the feedback network, especially in the series feedback resistor. In some cases series-parallel combinations can be employed to achieve higher total power dissipation.

13.8   Capacitor Distortion

Some capacitors change their capacitance as a function of voltage. This is especially so for electrolytic capacitors and is also a problem with certain types of ceramic capacitors. Voltage-dependent capacitance variation will cause distortion at frequencies where the value of capacitance plays a role in setting the gain. For example, variation in the value of a coupling capacitor will change the 3-dB low-frequency cutoff frequency of the circuit, resulting in signal-dependent gain and phase at very low frequencies. Similarly, a small-value Miller compensation capacitor will alter the high-frequency response of an amplifier if its value changes with signal. The Miller compensation capacitor usually has the full signal swing across it.

Quality film capacitors have virtually no voltage dependence of capacitance. Ceramic capacitors with an NPO (COG) dielectric have very little voltage dependence, but ceramic capacitors with other dielectrics may have significant voltage dependence and should be avoided.

The biggest offender in most power amplifiers is the electrolytic capacitor commonly found in the shunt leg of the negative feedback network. Electrolytic capacitors have numerous forms of distortion. If electrolytic capacitors must be used in this location, large-value nonpolarized types should be employed. The use of a large value will reduce the amount of signal voltage that appears across the capacitor with program material, reducing somewhat the resulting distortion. These capacitors should be bypassed with a film capacitor of at least 1 μF. The low ESR of the film capacitor will effectively short out the electrolytic capacitor at high frequencies, limiting the damage done by the electrolytic to lower frequencies. Back-to-back diodes will often be placed in parallel across the electrolytic capacitor to protect it and the input stage from a large DC voltage if the amplifier output goes to the rail.

Figure 13.3a shows the THD of the voltage across a 100 μF, 16-V polarized electrolytic capacitor as a function of frequency. The capacitor is driven by a 5-kΩ resistor with a 20-V RMS input, corresponding to a 50-W amplifier with a low-value feedback resistor. Signal current in the capacitor is 4 mA RMS. THD reaches almost 0.01% at 20 Hz. Bear in mind that this is the distortion of the voltage across the capacitor; the resulting amplifier distortion will be smaller. The signal voltage across the capacitor at 20 Hz is about 300 mV. The frequency response of an amplifier built with this arrangement would be down by 3 dB at about 6 Hz.

Figure 13.3b shows the result when a 100-μF, 100-V audio-grade NP electrolytic capacitor is substituted. The capacitor is designed for use in loudspeaker crossovers and is not expensive. Its distortion is about 25 dB less than that of the low-voltage
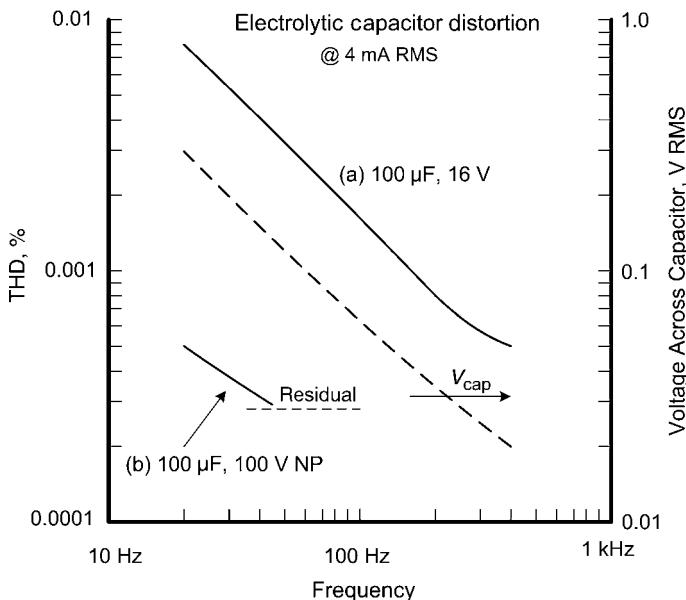
FIGURE 13.3 THD versus frequency for a 100-µF nonpolarized electrolytic capacitor.

polarized capacitor. If you must use an electrolytic capacitor in the feedback network, use an NP capacitor with a substantial voltage rating.

13.9 Inductor and Magnetic Distortions

The use of inductors is frowned upon in audio power amplifiers, so few, if any, are found in the signal path. The usual series output coil is a widespread exception. The absence of inductors does not mean that there are no nonlinear magnetic effects, so other magnetic effects will be examined here as well.

Magnetic Core Distortion

Magnetic materials have a magnetization curve that is nonlinear. The degree to which a magnetic material can be magnetized is ultimately limited. In an inductor or a transformer, this is referred to as *core saturation*. If the magnetization of the core approaches the saturation point, the inductance decreases. The simplest example of this is when an inductor is carrying DC current. As the current increases, the inductance will decrease. In general, the inductance of coils with ferrous cores is nonlinear.

A serious example of a nonlinearity that can be introduced into an amplifier is the use of an output coil with a ferrite core. This might be done to obtain adequate inductance with a smaller coil. The loudspeaker currents flowing in the output coil may cause saturation effects in the coil that will lead to increased distortion, especially at high frequencies. For this reason, output coils should always be constructed as air-core coils. This is not a serious problem because the value needed is usually 5 µH or less.

Distortion from Proximity to Ferrous Materials

A more subtle form of magnetic distortion can occur when the output coil is in close proximity to a magnetic material, such as a steel chassis. This can influence the inductance and can also introduce nonlinear losses into the inductor. For this reason output coils should be kept away from ferrous materials.

Ferrite Beads

The insertion of a ferrite bead in the base or collector of a transistor can often tame a parasitic oscillation. The ferrite bead acts somewhat like an inductor at middle frequencies and then experiences loss at high frequencies, ultimately behaving like a resistor. The loss introduced by the ferrite bead tends to damp resonant circuits and reduce the tendency to oscillate. The ferrite bead is a nonlinear passive device whose use in the signal path is frowned on. How much measurable distortion it introduces when used in a transistor base or in the collector of an emitter follower is debatable. The safest approach is to avoid the use of ferrite beads.

13.10   Magnetic Induction Distortion

There are very distorted signals running around in class AB amplifiers. The biggest source of these is the nonlinear half-wave-rectified current in the output stage. Current flows from the positive rail on positive half-cycles and from the negative rail on negative half-cycles. The magnetic fields created by these currents can induce nonlinear voltages in nearby signal lines, coupling distortion into the signal path [4].

Minimizing Magnetic Induction Distortion

The most important step in reducing magnetic induction distortion is to reduce the emission of nonlinear magnetic fields and then to keep as much distance from them to signal-carrying wires as possible. Twisting the positive and negative rail supply wires together can be quite helpful in reducing the emissions from these lines. This is effective because the sum of the currents (and thus the magnetic fields) of the positive and negative rail wires is a linear representation of the amplifier's output current signal. Bypassing the positive rail directly to the negative rail with low-ESR capacitors right at the output stage can improve matters by forcing fast-changing currents to circulate locally rather than through the wires back to the power supply.

The physical arrangement of the PNP and NPN output transistors on the heat sink can also have a significant effect on nonlinear magnetic fields emitted by output stage wiring. Interleaving the PNP and NPN power transistors on the heat sink is superior to grouping all of the PNP transistors on one end and all of the NPN transistors on the other end.

Arranging the emitting and pickup wires to be at right angles is also helpful. Reducing the susceptibility of signal lines to induction by magnetic fields can be accomplished by twisting the leads together with ground lines. The input and feedback signals are the most vulnerable to magnetic induction distortion.

13.11   Fuse, Relay, and Connector Distortion

Many amplifiers employ fuses or relays in the output signal path for protection or muting. These devices can cause distortion because of the high currents flowing through them.

Fuse Distortion

When high current passes through a fuse, it heats up the fuse element by causing a small voltage drop that leads to power dissipation and temperature rise. The fuse element must therefore be resistive for this process to take place. The fuse blows when the temperature rises to the melting point of the fuse element. The fuse element has a positive temperature coefficient of resistance, so the process is accelerated as more current flows through the fuse.

At low frequencies the audio signal can heat up and cool down the fuse element within a single cycle, causing the resistance of the fuse to vary as a function of the signal amplitude. This leads to distortion because the attenuation of the fuse resistance against the load impedance changes as a function of signal swing [5]. Fuses are often undersized with respect to the peak audio current they may be called on to pass, recognizing that a smaller fuse will provide relatively more protection and that with normal audio signals, such high currents are brief events much shorter than the time constant of the fuse element. The cold resistance of a 2-A 3AG fuse was measured to be 78 mΩ, while its resistance when passing 2-A DC was 113 mΩ. This represents a 45% increase in fuse resistance.

The distortion of a fuse can be measured by looking at the voltage across the fuse with a sinusoidal signal current passing through it. The fuse under test is put in the ground leg of an 8-Ω load resistor so that the signal voltage across the fuse can be easily analyzed. This technique largely takes the distortion of the driving source out of the picture. Figure 13.4a is a plot of fuse distortion versus frequency when a 2-A fast-blow 3AG fuse is passing a 2-A RMS sine wave signal. As expected, fuse distortion increases dramatically at low frequencies. Signal voltage across the fuse was 250 mV. Amplifier THD (due to the fuse) is calculated by normalizing the fuse distortion voltage to the amplifier output voltage. The resulting amplifier distortion is shown in Figure 13.4b. Amplifier distortion is lower than fuse distortion by a factor of 64 because of the small voltage across the fuse compared to the total signal voltage. At 20 Hz, amplifier distortion due to the fuse is calculated to be 0.0033%.

Relay Distortion

All contacts have some resistance. Sometimes that resistance can change as a function of the current flowing through them. This gives rise to distortion. When a relay is placed in series with an amplifier output line, the contact resistance will form a voltage divider with the load impedance, causing a tiny amount of attenuation. If the contact resistance varies with the signal, this attenuation will vary with the signal and distortion will result.

Not all relay contacts are alike, and some are much less prone to distortion than others. The tendency to distortion will depend on the contact metallurgy, the condition of the contacts, the contact area, and the contact pressure. High-current relays will often produce less distortion because the starting contact resistance is smaller and the current density in the contact is smaller. However, it is unwise to generalize that high-current relays (like automotive relays) will always yield lower distortion.

The distortion produced by a relay can be measured in the same way as that of a fuse. The output of a power amplifier is passed through an 8-Ω resistor that is connected to ground through the closed contacts of the relay under test. The voltage drop across the relay can be fed to a distortion analyzer or a spectrum analyzer. In some cases that voltage may have to be amplified before being applied to the input of the analyzer.
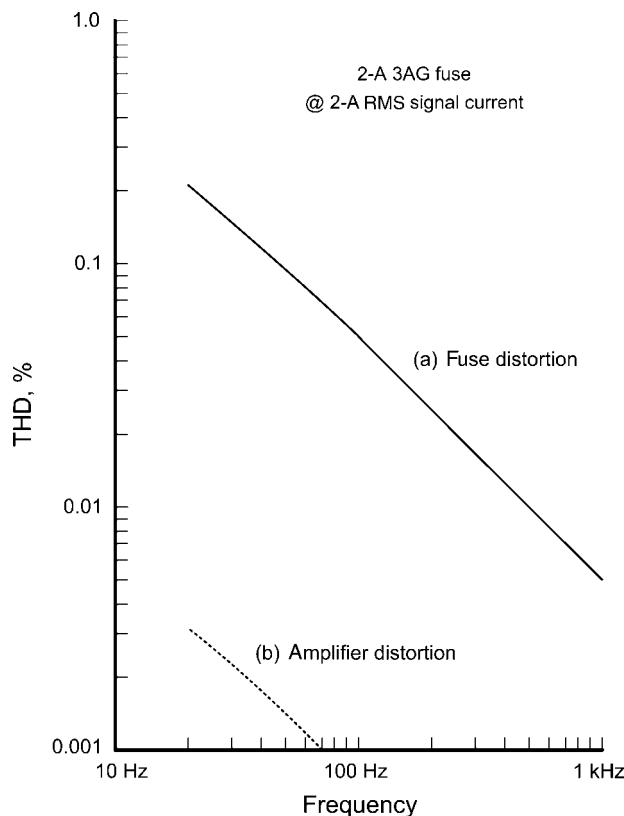
FIGURE 13.4   THD versus frequency for a 2-A fuse passing 2 A RMS.

The test setup is shown in Figure 13.5. A 16-V, 1-kHz test signal is applied to an 8-Ω resistor, producing a current of 2 A RMS. This corresponds to a power level of 32 W. The relay under test is placed in the ground leg of the resistor. A spectrum analyzer is connected across the closed relay contacts. With this setup, the analyzer's response at 1 kHz is reflective of the resistance of the relay contacts, while harmonics in the spectrum represent distortion. Six relays were tested. The good news is that one of the relays was
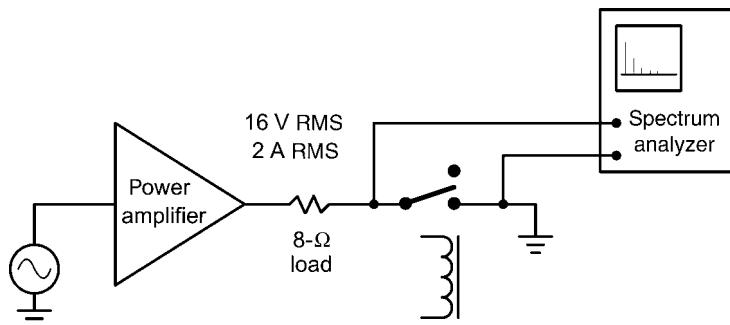
FIGURE 13.5   Test setup for measuring relay distortion.

exceptionally good; the bad news is that some were surprisingly bad. This means that relays for this kind of application need to be selected carefully.

The magnitude of the fundamental displayed on the spectrum analyzer was used to infer the contact resistance by dividing it by 2 A RMS. The in-service amplifier distortion attributable to the relay was calculated by normalizing the magnitude of each distortion component of the relay voltage to the 16-V amplifier output operating level. This test procedure does a good job of isolating relay distortion from amplifier distortion.

Relays 1, 3, and 5 were of medium performance, with resistance ranging from 25 mΩ down to 1.3 mΩ, and third order distortion on the analyzer ranging from –56 dB through –64 dB, corresponding to 0.001% (–100 dB) to 0.0004% (–108 dB) of added amplifier distortion. Third-order distortion predominated on most relays.

Relays 2 and 6 were notably bad, each with 25-mΩ contact resistance and third-order distortion as bad as –50 dB on the analyzer, corresponding to in-service third-order distortion of 0.002% (–94 dB). Relay 6 had a spectrum characterized by quite a bit of grunge above the analyzer noise floor.

Relay 4 was the clear winner. This was an 80-A automotive relay. It had a third-order distortion reading of –91 dB on the analyzer, corresponding to 0.00002% (–135 dB).

Although Relay 4 was the only "automotive" relay in the test, it would be wrong to conclude that an automotive relay will always be better than others for an audio application. It would also be premature to conclude that the higher current rating is responsible for the enhanced performance, on the basis of the variability among the other relays that were rated at 30 A.

There is no evidence that contact resistance is a good predictor of relay distortion performance. It is tempting to speculate that the contact surface chemistry plays a large role in the distortion performance; two different sets of contacts might exhibit the same resistance, but with different amounts of nonlinearity in that resistance.

Self has reported some frequency dependence of relay distortion, speculating that soft iron in the swinger may be responsible for increased distortion at high frequencies [6]. The plot in Figure 13.6 shows distortion of six relays as a function of frequency from 1 kHz to 16 kHz. This was a different group of relays than those mentioned above. The distortion was measured with the arrangement of Figure 13.5 with a 2-A signal flowing through the contacts.. The THD shown is that of the small fundamental signal that appears directly across the contacts. Contact resistance ranged from 1.3–11 mΩ, corresponding to signal levels of 2.6–22 mV.

These are believed to be representative relays, but it is not known what material is used in these relays. Three relays exhibit frequency dependence and three do not. The distortion of Relay D was below the residual for that relay, so it may exhibit some frequency dependence at very low distortion levels. With one exception, third-harmonic distortion dominated the measurements. Second-harmonic distortion dominated for Relay A. Distortion voltage across the contacts at 16 kHz for the three best relays was below 16 μV RMS, corresponding to 0.0001% distortion at the 16 V RMS operating level of the amplifier. Distortion does increase with frequency in some relays, but is not a problem if it remains very low at high frequencies.

The spread in net distortion among these relays was a remarkable 33 dB at 16 kHz, but the worst relays had distortion that was flat with frequency. Pick your speaker relays wisely.

Because distortion can be a function of the condition of the contacts, the performance of a new relay may not be representative of that relay after it is worn or abused. For
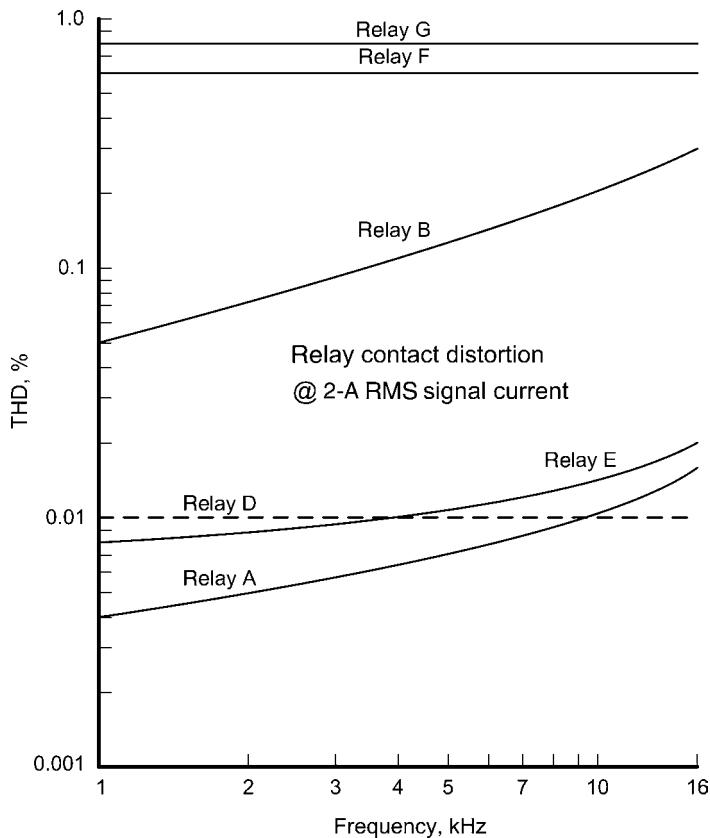
Figure 13.6   Relay contact distortion as a function of frequency for three relays. Distortion is measured across the contacts with 2-A RMS signal current flowing.

example, if the relay is frequently opened or closed when there is a large signal present, this can cause some pitting of the contacts that may lead to increased distortion.

Fuse or relay distortion can be reduced if the device is enclosed within the global negative feedback loop. Approaches to doing this are discussed in Chapter 15. The key consideration is what happens to the feedback loop when the device opens.

Connector Distortion
As with relays, any connector consists of a pair of metal-metal contacts. As such, the interface will exhibit contact resistance which may be nonlinear and which can be a source of distortion. This will be especially the case with loudspeaker connections (banana plugs in particular).

Distortion in banana plugs was measured using the same kind of testing that was applied to relay contacts. For this simple spot test, an ordinary banana plug and jack combination was compared with an expensive one. For the ordinary pair, the jack was gold plated in its interior, but the plug was merely nickel plated. In the more expensive pair, both were of very substantial construction and fully gold plated.

Interestingly, the banana plugs showed more second harmonic than third, and the ordinary plug combination was slightly better than the expensive one in this regard. Both plug combinations show a connector resistance of about 13 mΩ. All normalized distortion spectra were between –142 dB (0.000004%) and –135 dB (0.000016%). These are very encouraging numbers, but they are based on a very small sample. Both sets of connectors were brand new. I think it is very important that we err on the conservative side with any kind of connectors, especially the ones that may become loose with time.

13.12   Load-Induced Distortion

Don't overlook the possibility of distortion artifacts induced by the load resistor when testing an amplifier. Large wire-wound resistors can sometimes be quite nonlinear as a result of the way in which the resistive element is attached to the terminals. The nonlinear load of such a resistor can cause falsely high distortion readings for amplifiers with very low distortion levels.

It is also possible to be fooled by distortion in a simulated speaker load. If a passive speaker simulator network uses an inductor with a ferrous core, the distorted current that flows in the load can induce distortion in the amplifier, especially if the amplifier does not have a very low damping factor.

13.13   EMI-Induced Distortion

Amplifiers are subject to *radio frequency interference* (RFI), more commonly referred to as *electromagnetic interference* (EMI). Electric drills, light dimmers, radio stations, WIFI, and cell phones are common sources of EMI. Amplifiers are susceptible to EMI through three conductive ports: the input port, the output port, and the mains port. If EMI gets into an amplifier, it can show up as noise or buzzing which alone is objectionable. This is not distortion as such. It is additive noise. However, if the EMI disturbs amplifier stage operating points or intermodulates with the audio signal, then nonlinear distortion can result. Any EMI effect that is correlated with the audio signal will be perceived as nonlinear distortion. Distortion created by EMI is discussed in greater detail in Chapter 18.

13.14   Thermally Induced Distortion (Memory Distortion)

Whenever a temperature change can affect the gain or operating point of an amplifier, distortion may result when the program material contains low frequencies or when the short-term program power changes with time. This is sometimes called memory distortion.

This type of distortion was discussed in the cases of resistor and fuse distortion. If the gain of an amplifier stage changes with temperature, then it can also cause distortion at low frequencies or intermodulation with higher frequencies. Thermal distortion is often much lower at high frequencies because the thermal inertia of the affected elements prevents the temperature from changing too much with faster signal swings. However, it should be kept in mind that the local thermal time constant of a transistor junction can be on the order of milliseconds.

Memory distortion will not show up with conventional steady-state tests like THD-1 and THD-20. Memory distortions can sometimes be unmasked with an intermodulation distortion test where a large, very low frequency signal is added to a higher frequency

signal and the resulting amplitude modulation of the higher frequency is measured. This is how the SMPTE IM test works, where frequencies of 60 and 7000 Hz are mixed in a 4:1 ratio. For thermal distortion, better results will be obtained if the low frequency is 20 Hz. Thermal distortion may also show up as increased THD at low frequencies like 20 Hz. These symptoms can be confused with distortion from electrolytic capacitors in feedback networks, however.

A special form of thermal distortion occurs in the output stage of a class AB power amplifier [7]. Here the critical idle bias can be disturbed by junction temperature changes in the output transistors that are too fast to be tracked out by the bias temperature compensation. This will often result in idle bias errors that are dependent on the recent history of the signal. In some cases following a loud passage, the output stage may be temporarily underbiased after the program material returns to a low level; this will result in increased crossover distortion.

References

1. Cordell, R. R., "A Fully In-band Multitone Test for Transient Intermodulation Distortion," *Journal of the Audio Engineering Society*, vol. 29, no. 9, pp. 578–586, September 1981; available at www.cordellaudio.com.
2. Cordell, R. R., "Phase Intermodulation Distortion–Instrumentation and Measurements," *Journal of the Audio Engineering Society*, vol. 31, no. 3, pp. 114–124, March 1983; available at www.cordellaudio.com.
3. Cordell, R. R., "A MOSFET Power Amplifier with Error Correction," *Journal of the Audio Engineering Society*, vol. 32, no. 1/2, pp. 2–17, January 1984; available at www .cordellaudio.com.
4. Cherry, E. M., "A New Distortion Mechanism in Class B Amplifiers," *Journal of the Audio Engineering Society*, vol. 29, no. 5, pp. 327–328, May 1981.
5. Slone, G. R., *High-Power Audio Amplifier Construction Manual*, New York, McGraw-Hill, 1999.
6. Self, D., *Audio Power Amplifier Design Handbook*, 5th ed., Focal Press, 2009.
7. Sato, T., Higashiyama, K. and Jiko, H. "Amplifier Transient Crossover Distortion Resulting from Temperature Changes in the Output Power Transistors," presented at the 72d Convention of the Audio Engineering Society, *JAES* (Abstracts), vol. 30, pp. 949–950, December 1982, preprint 1896.

Real-World Design Considerations

P art 3 addresses those real-world design considerations that come into play when designing a high-performance amplifier that must operate in the real world. These include power supply design and grounding architectures, short circuit and safe area protection, and control of amplifier behavior when driving difficult loads. Thermal design and the oft-overlooked matter of thermal stability are given special attention. The use of advanced power transistors that include internal temperature monitoring means improved thermal stability is covered in depth.

The ways in which amplifiers misbehave often account for sonic differences. How amplifiers clip is an example. These issues are discussed in Chapter 17. The world is full of electromagnetic interference, and it is only getting worse. The challenges presented by EMI ingress and egress via the input, output, and mains ports of the amplifier is one of the topics covered thoroughly in Chapter 18.

This page intentionally left blank

Output Stage Thermal Design and Stability

Audio power amplifiers are not all that efficient, so they tend to produce a lot of heat. This has several implications. First, the amplifier must provide adequate means to get rid of the heat without excessive temperature buildup and consequent loss of reliability or risk of destruction. This requires heat sinks, which add to cost, physical size, and weight.

Another issue in thermal design is that of thermal stability. It can often be the case that when power transistors get hot, they tend to increase their current flow. This can lead to thermal runaway and destruction.

At higher temperatures the safe operating area of power transistors decreases. This means that protection circuitry must be more conservatively designed if the amplifier is to safely operate at higher temperatures. This in turn means that, for a given size or cost of output stage, the amplifier will be less able to supply high currents to difficult loads.

The effect of temperature variations on output stage bias levels is important to sound quality. The crossover distortion produced by a class AB output stage depends strongly on the output stage quiescent bias being at the right value. If poor temperature control and stability characterize the design, substantial increases in crossover distortion may occur either on a continuous or a transient basis. In some cases an amplifier that is run hot with high levels of program material will become underbiased after the high-amplitude program material is removed. This will leave the amplifier vulnerable to crossover distortion on subsequent low-level passages.

The thermal design of class AB output stages will be the primary focus of this chapter. Of course, many of the concepts presented here will be equally applicable to other types of output stages.

14.1   Power Dissipation versus Power and Load

Although it might seem intuitive that a power amplifier produces the most heat when it is putting out the most power, this is not generally so. The top curve in Figure 14.1 shows that the power dissipation (wasted heat) for an idealized 100-W class A amplifier actually decreases as the output power increases. This is so because the current drawn from the output stage power rails by a class A output stage is constant, regardless of output power. The idealized class A amplifier must

Power Dissipation vs. Power Output
Idealized amplifiers
Rail-to-rail swing
40-V supply rails

(a) Class A

(b) Class AB, 4 Ω
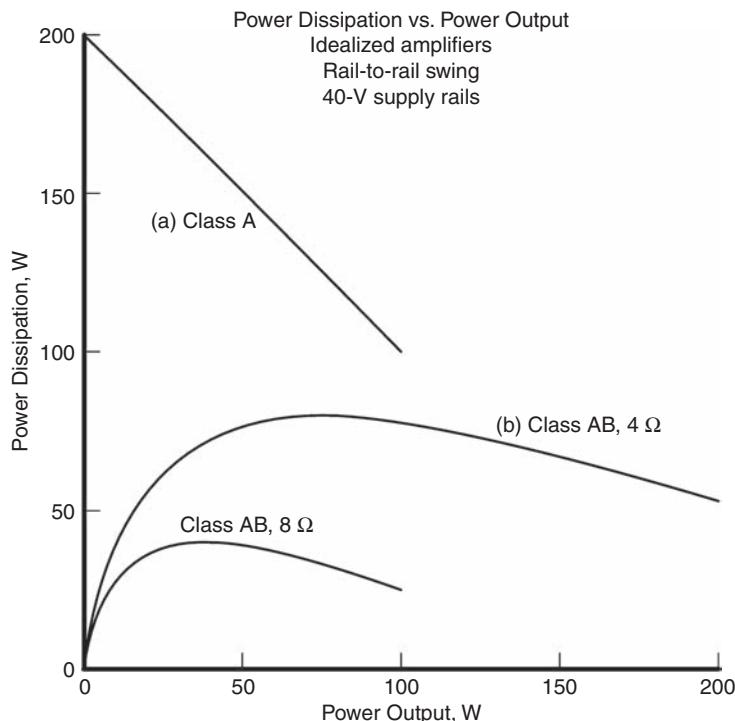
Class AB, 8 Ω

FIGURE 14.1   Power dissipation of a 100-W/8-Ω amplifier versus power output. (a) Class A. (b) Class AB. (c) Class AB driving 4-Ω load.

have ±40 V rails and an idle current of 2.5 A in order to remain in class A when driving an 8-Ω load to 100 W (40 V peak, 5 A peak). When the amplifier is at idle, all of this power is being dissipated as heat. When the amplifier is putting out its maximum power into the load, that maximum power is being dissipated in the load instead of in the amplifier. The laws of power conservation dictate that the amount of power being dissipated as heat in the amplifier will be less by the amount of output power. The important principle here is that power dissipation is simply average DC input power less the output power.

The more interesting curves in Figure 14.1 are the curves for an idealized 100-W/8-Ω class AB power amplifier delivering its power into 8-Ω and 4-Ω loads. Notice that the output stage power dissipation when driving an 8-Ω load is at its maximum value when the output power is at approximately 1/3 of its maximum value. The peak in power dissipation as a function of signal voltage occurs because power input to the amplifier increases linearly with signal voltage, whereas power being delivered by the amplifier increases as the square of the signal voltage. The peak in power dissipation explains why the FTC amplifier specification rule required that amplifiers be *preconditioned* at 1/3 of their rated power into an 8-Ω load for 1 hour [1]. This seems a fairly brutal test for an amplifier until one realizes that often the same amplifier will be called on to deliver nearly its same output voltage into a 4-Ω load.

14.2   Thermal Design Concepts and Thermal Models

Thermal analysis is key to thermal design. Fortunately, there are electrical analogs to thermal "circuits" that allow many electrical engineering concepts (particularly Ohm's law) to be applied to thermal analysis.

Figure 14.2 illustrates an electrical model for thermal analysis. It is a very simple model of a power transistor mounted on a heat sink. The model is an electrical analog for the thermal behavior of the system and can actually be simulated with SPICE. Resistors represent thermal resistance and current sources represent heat sources. A 1-Ω resistor corresponds to a thermal resistance θ of 1°C/W, while a 1-A current source corresponds to a power dissipation (or heat source) of 1 W. Node voltages correspond to temperatures in degrees Celsius relative to the ambient. Ground corresponds to the ambient temperature (usually 25°C). Capacitances are the analog of thermal mass. A 1-W heat source flowing into a 1-Farad thermal capacitance will raise the temperature 1°C in 1 second. One Farad of capacitance corresponds to 1 J/°C of thermal mass.

R1 in Figure 14.2 represents the thermal resistance from junction to case of the transistor, called θ_{jc}. Here it is 0.63°C/W, representing a typical 200-W power transistor in a TO-264 package and having a maximum junction operating temperature of 150°C. Shunt capacitor C1 represents the thermal mass of the die itself. The die has little physical size and mass, and its thermal mass is correspondingly very small. This means that the die temperature can change quickly, with a short-time constant. The value of C1 is 36,000 μF (36,000 μJ/°C). The thermal time constant τ_1 of R1 and C1 is about 23 ms. Voltage across R1 represents junction temperature rise above the case temperature. Voltage across C1 represents the junction temperature rise over ambient in degrees Celsius.

R2 models the thermal resistance of the insulator that separates the case of the transistor (usually the collector terminal) from the heat sink. This thermal resistance is designated θ_{cs}, meaning resistance from case to sink. This resistance depends heavily on the material and thickness of the insulator, and the area of contact. The most common material employed for insulators is mica. The value shown is 0.4°C/W, representative of an insulator for the larger TO-264 transistor package. The insulator's thermal resistance will be higher for the smaller TO-3P or TO-247 packages. The thermal mass of the transistor package is represented by C2, here 9 Farads (9 J/°C). The thermal time constant τ_2 of R2 and C2 is about 3.6 seconds. The voltage across C2 represents the case temperature rise over ambient in degrees Celsius.

The heat sink is modeled by R3 and C3, here 1.3°C/W and 960 F, respectively. The corresponding time constant τ_3 is about 1250 seconds (about 21 minutes). The voltage
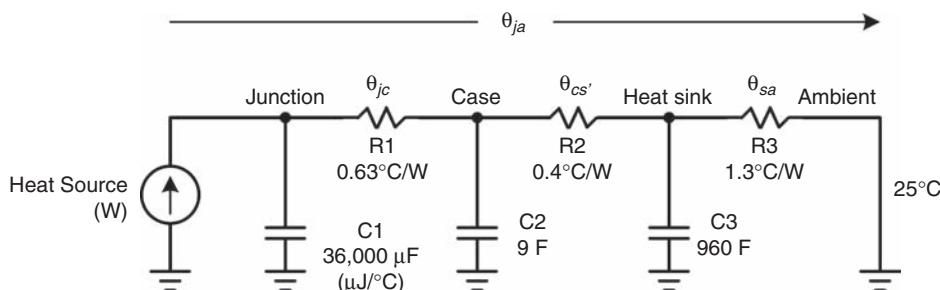
Figure 14.2   Thermal model for a power transistor mounted to a heat sink.

across C3 represents the heat sink temperature rise over ambient in degrees Celsius. Notice that each of the three thermal time constants is separated by more than an order of magnitude in time.

Temperature versus Log Time Plots

Temperature changes can take place over very short time intervals or very long time intervals. For this reason it is best to plot temperature changes as a function of log time. The slope of the resulting curve is in degrees Celsius per decade.

Figure 14.3 shows plots of junction, case, and heat sink temperature as a function of log time when a power dissipation of 40 W is applied to the model. The junction temperature curve shows three distinct regions with different slopes. These represent the three different time constants involved in determining the junction temperature.

Figure 14.4 shows plots of the same three temperatures following removal of the heat source. Notice that the junction temperature falls very quickly to the case temperature and then that falls fairly quickly to the heat sink temperature.

Thermal Attenuation

When the transistor is dissipating power it is easy to see that the series string of thermal resistances causes the junction temperature to be significantly higher than the heat sink temperature. There is so-called thermal attenuation from the junction to the heat sink. It means that during prolonged dissipation, the junction temperature remains significantly elevated over the heat sink temperature. In Figure 14.2, heat sink temperature rise over ambient will only be 56% of the junction temperature rise over ambient. This can be seen in Figure 14.4. However, when power dissipated by the transistor stops, the junction temperature falls to that of the heat sink within seconds. Heat sink temperature is not a
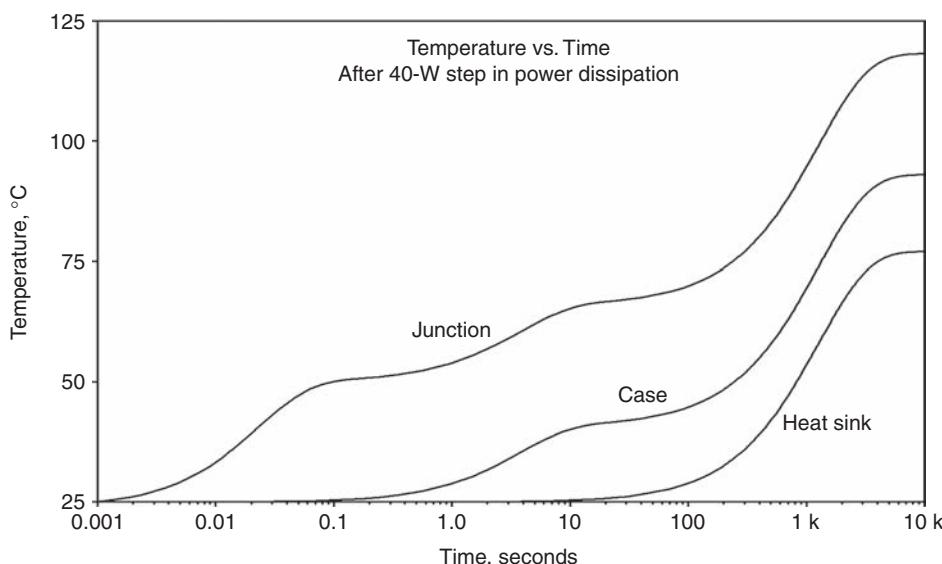
FIGURE 14.3   Junction, case, and heat sink temperature versus log time.
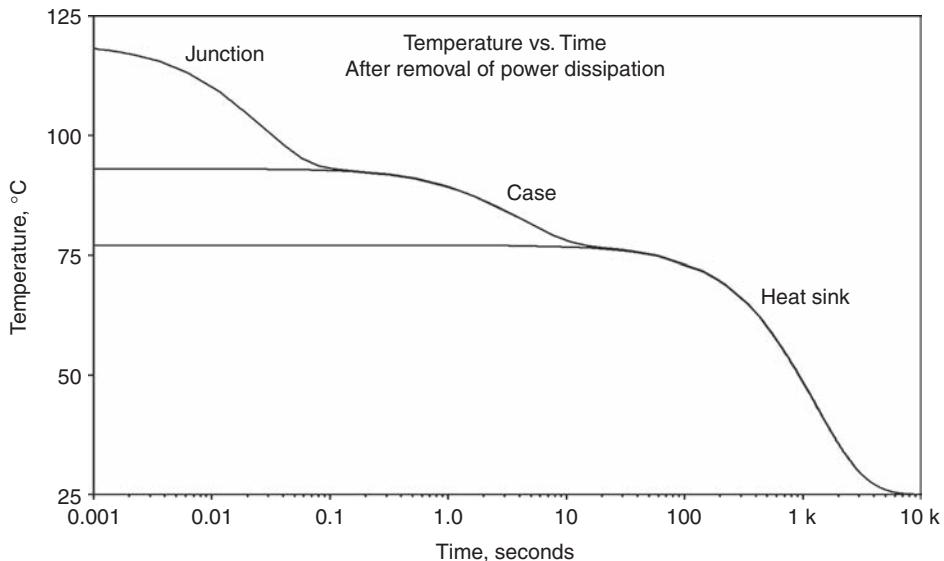
FIGURE 14.4 Junction, case, and heat sink temperature after removal of heat source.

good representation of junction temperature, even absent the time-dependent effects introduced by thermal mass and thermal time constants.

Lumped and Distributed Models

The models discussed above are highly simplified lumped models that do not accurately take into account the fact that heat travels as a diffusion process. For this reason, distributed models that include multiple R-C elements to model each part of the process are often used to obtain more accurate results.

Transient Thermal Impedance

Some power transistors are characterized by *transient thermal impedance* (TTI). This is often the case with MOSFETs, but is rarely the case with BJTs. The TTI curve is a valuable way of estimating the peak junction temperature when a power pulse is applied to the device. It recognizes the thermal mass of the parts of the transistor and the fact that heat diffuses through the device in a three-dimensional way. Because it takes distributed thermal mass into account, it is referred to as thermal impedance rather than a thermal resistance.

Figure 14.5 illustrates a TTI curve for an IRFP240 power MOSFET [2]. At long time intervals the value is simply the *DC* value of thermal resistance from junction to case. In this case that is 0.83°C/W. The maximum junction temperature for this 150-W device is 150°C. For shorter time intervals the effective impedance from junction to case (TTI) is smaller. This impedance can be used to infer the peak junction temperature reached at the end of a pulse of power of the given time duration. For example, at 10 ms, the TTI is 0.42°C/W, about half the DC value. If the case temperature is 70°C, a rise of 80°C is permitted at the junction with a 0.42°C/W rate for 10 ms. The allowable transient power
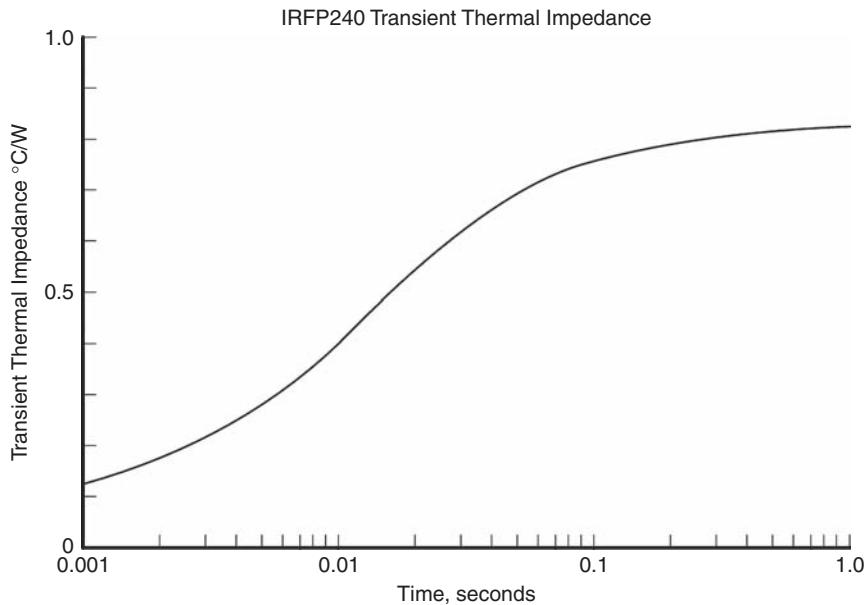
Figure 14.5   Transient thermal impedance curve for an IRFP240 power MOSFET.

dissipation under these conditions is then 80°C/0.42°C/W = 190 W. The real action in the TTI curve is around 10 ms, implying that the time constant is of this order of magnitude. The thermal time constant appears to actually be about 17 ms.

The published operating boundary criterion for this device is simple: Never let the peak junction temperature exceed 150°C. This is actually very conservative. The maximum junction temperature in plastic-packed devices is dictated by packaging reliability considerations. It is not the die-failure temperature.

Thermal Simulation

Having the electrical analog to the thermal circuit makes it possible to arrange for SPICE simulations to predict thermal behavior and gain insight. Using current sources as heat sources and the kinds of thermal models described above, simulations can be carried out where node voltages represent temperatures.

Simulations can also be created that combine the thermal and electrical aspects into a single "electrothermal" simulation. Such simulations can be used to evaluate thermal stability. Bear in mind that this kind of simulation does not necessarily use the temperature models in SPICE, but instead uses controlled voltage sources to alter effective transistor V_{be} drops as a function of the temperature (which is represented as a voltage elsewhere). For example, if the voltage of a node in a simulation signifies transistor junction temperature above the reference 25°C, a voltage source driven by a function of the voltage representing the transistor's junction temperature can be placed in series with the transistor's base. If the node voltage representing junction temperature is represented in volts per degree Celsius, then the scaling factor for the voltage source would be 0.0022, representing a 2.2 mV/°C temperature coefficient of V_{be}.
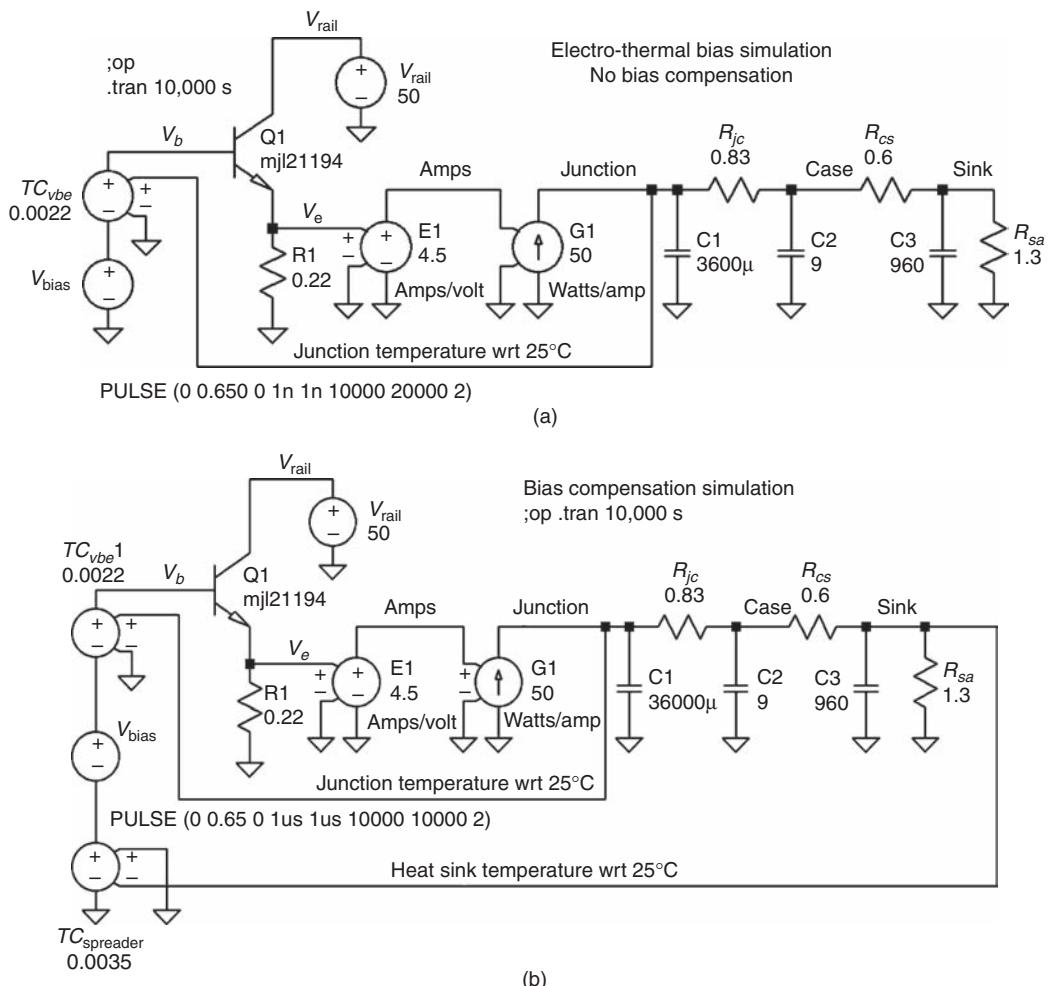
FIGURE 14.6 (a) Electrothermal simulation of a transistor mounted on a heat sink. (b) Transistor's bias is controlled by a V_{be} multiplier.

Figure 14.6a illustrates an example of an electrothermal simulation of a transistor mounted on a heat sink, where the base is driven with a constant voltage and the emitter is terminated with a 0.22-Ω resistor. Junction power dissipation is converted to current in this simple arrangement by scaling collector current, since collector voltage is almost constant. In a more accurate approach, dissipation is arrived at by multiplying collector voltage by collector current.

Electrothermal simulations in SPICE can be used to evaluate a complete bias loop, including the V_{be} multiplier and the output transistors. In this case, the controlled voltage source placed in series with the emitter of the V_{be} multiplier transistor would represent the temperature of the heat sink. In this way the dynamics of thermal lag in temperature compensation can be evaluated. Such a simulation approach is illustrated in Figure 14.6b.

Measuring Heat Sink Thermal Resistance

It is often desirable to measure the thermal characteristics of a heat sink in the lab. This may be because the information is not available on the data sheet or because the device is unusual or a custom component. A custom or surplus heat sink would be an example. Often, the chassis of an amplifier provides some of the heat sink capability and its contribution needs to be evaluated.

One of the most common approaches to measuring thermal resistance is to mount a metal-cased 50-W power resistor on the heat sink or other material in question and apply a known number of watts to the resistor. At the same time, an IC temperature sensor can be mounted to the heat sink to monitor the temperature rise. The thermal resistance is then easily calculated. By observing the rate of rise of temperature, the thermal mass can also be inferred. Alternatively, you can raise the heat sink to a known high temperature, remove the heat source, and record the time it takes for the temperature to fall to 63% of the difference between the ambient and the starting temperatures. This time value is then the time constant of the thermal capacitance and the known thermal resistance of the heat sink.

Figure 14.7 shows a simple schematic for using the three-terminal LM34 Fahrenheit temperature sensor. The output is a linear 10 mV/°F. The LM35 is a similar device that reads directly in degrees Celsius with a 10-mV/°C output. This handy device comes in a TO-92 package that can be placed in a 3/32-in. hole drilled in a heat sink and filled with some thermal grease. The LM35 is also available in a TO-220 package that can be mounted to the heat sink.

It is sometimes desirable to use a power transistor as a heat sensor in laboratory measurements. Here the V_{be} versus temperature characteristic of the transistor needs to be characterized at a known current flow when the transistor is diode connected. This can be accomplished by putting the transistor and an accurate thermometer in an oven. Take several data points, and allow a long time for the temperature to stabilize between data points. In some experiments, the transistor to be calibrated will be one that is used actively in an experiment, where a high current may be passed through it that will heat it up. That high current is then replaced with the calibration test current and the temperature is inferred from the V_{be}. Do not simply assume that the temperature coefficient
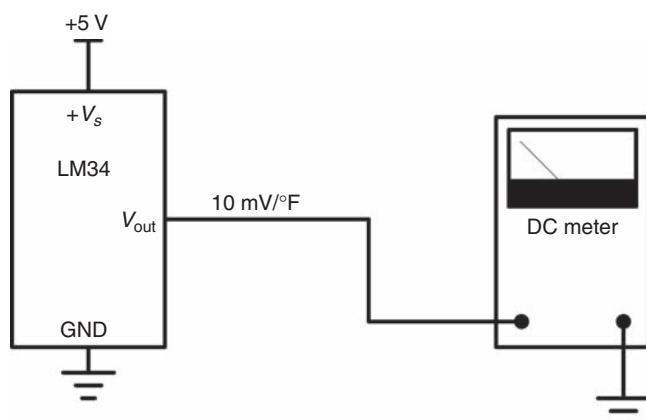
FIGURE 14.7   Using an LM34 to make temperature measurements.

of V_{be} (TC_{Vbe}) is –2.2 mV/°C. The actual value depends on many factors, including operating current, temperature, and the device's internal characteristics.

There is another approach to making temperature measurements with diodes or diode-connected transistors. Recall that the transconductance gm of a transistor is temperature dependent. It depends on the quantity $V_T = kT/q$, which is linearly dependent on absolute temperature T. Transconductance is simply I/V_T. Transconductance thus decreases linearly with increases in temperature. Conversely, the intrinsic emitter resistance re' of a transistor increases linearly with absolute temperature. That resistance is simply equal to kT/qI. A direct indication of absolute temperature can be obtained if a transistor is operated at a known DC bias current and its AC junction resistance is measured. If a transistor is biased at 100 μA, it's re' will be about 250 Ω. If an AC signal of 10 μA RMS is applied to its emitter, the resulting voltage will be about 2.5 mV. This will correspond to room temperature (about 290°C) and will linearly increase with temperature. In reality there is a transistor characteristic known as the ideality factor η. The value of η is approximately 1.015 for a 2N3904 transistor. This correction factor must be used to divide the equation to arrive at absolute temperature in degrees Kelvin. We then have

$$T = re'qI/k\eta \tag{15.1}$$

Another area sometimes in need of actual measurement is the effective resistance from case to heat sink for a power transistor, taking into account the insulator. In this case, the transistor can be mounted to a large heat sink using the insulator and thermal grease (if applicable). The transistor is then energized to heat up the arrangement with known power dissipation to a stable temperature. Temperature sensors mounted on the heat sink and on the case of the transistor can then be used to evaluate the temperature rise of the transistor case. Alternatively, the power transistor itself can be used as the case temperature sensor. The operating current is replaced with the transistor's temperature calibration test current and the case temperature is quickly inferred from V_{be}, before it has a chance to fall to the temperature of the heat sink.

A handheld infrared thermometer can also be a useful tool for thermal investigations. Most of them are equipped with laser targeting. Choose one with a good distance-to-spot ratio of at least 10:1. This means that a 1-in. area can be measured from a distance of 10 in. This is important when trying to measure the case temperature of a power transistor. Also be aware that the color of the surface can influence temperature readings made by the infrared technique.

14.3 Transistor Power Ratings

A power transistor is rated at 150 W if its junction temperature remains below its maximum value when dissipating 150 W and its case is held at 25°C. A transistor rated at 150 W with a typical maximum junction temperature of 150°C will be allowed to have its junction temperature rise by 125°C above the 25°C ambient when it is dissipating 150 W. Its thermal resistance θ_{jc} from junction to case must then be 125/150 = 0.83°C/W.

In most situations the transistor case must be electrically insulated from the heat sink with a mica insulator or an insulator made of some other material. This will add thermal resistance from case to heat sink (θ_{cs}) on the order of another 0.5°C/W. This will raise the total thermal resistance from junction to heat sink in the example to 1.33°C/W. If this transistor is to dissipate 50 W, then the heat sink temperature must be held to no more than 150 – 1.33 ∗ 50 = 83.5°C. In practice we almost never want the heat sink temperature

Package	Area, mm²	Pad θ_{cs}, °C/W	Kapton θ_{cs}, °C/W
TO-220	88	2.0	1.3
TO-247	183	0.96	0.64
TO-264	317	0.56	0.37

TABLE **14.1**   Thermal Resistance of Transistor Insulators

to exceed 70°C, so the maximum power this transistor can dissipate on average will be about $(150 – 70)/1.33 = 60$ W.

Transistor Insulators

The thermal resistance of an insulator depends on its thickness and its material. Just as with an electrical resistance, the thermal equivalent of ohms per square ($\Omega/\square$) is used to characterize insulators. In the case of insulators the term is degrees Celsius per Watt per square (°C/W/$\square$).

The net thermal resistance of the insulator for a transistor depends on the contact area of the metal portion of the package of the transistor. For a TO-247 package, this area is about 183 mm², while for a TO-264, it is about 317 mm². As an interesting reference point, the thermal resistance of a TO-247 case to a heat sink without an insulator is about 0.25°C/W when the interface is greased with thermal compound. Some numbers are shown in Table 14.1 for a typical *pad*-type insulating material. The last column in the table shows estimates for an insulator made from Kapton.

There are numerous different insulator materials. Some require thermal grease to fill in the microscopic valleys (irregularities) in the mating metal surfaces while others perform this function themselves. We will assume typical thermal insulator θ_{cs} for TO-247 and TO-264 packages as 0.8°C/W and 0.5°C/W, respectively.

14.4   Sizing the Heat Sink

One of the key design decisions is sizing the heat sink. More is better from a performance and robustness point of view, but more is not the optimum solution in terms of cost, size, and weight. Four key questions must be asked.

- What is the maximum power that will be dissipated?
- What is the maximum tolerable heat sink temperature?
- What is the maximum tolerable transistor junction temperature?
- What is the net thermal resistance from junction to the heat sink?

Depending on the numbers, the answers to either the second or third question will often dominate the decision about how big the heat sink must be. The thermal resistances from the junctions to the heat sink of all of the output transistors are effectively in parallel for purposes of calculating the net thermal resistance from the junctions to the heat sink.

Figure 14.2 illustrated the thermal resistance path from the transistor junction to the ambient. The first resistance encountered is from junction to case, designated θ_{jc}. The second is from the transistor case to the heat sink, θ_{cs}, which is dominated by the thermal

resistance of the insulator. The third resistance is θ_{sa}, representing the thermal resistance of the heat sink to ambient air. The total thermal resistance from junction to ambient is θ_{ja}. The junction temperature rise above ambient is $P_j * \theta_{ja}$. Junction temperature T_j will then be $T_j = T_a + P_j\theta_{ja}$.

Output Stage Power Dissipation

Consider a 150-W amplifier design with two pairs of MJL21193/4 output transistors. These transistors have θ_{jc} of 0.63°C/W and a 150°C maximum junction temperature. The devices are in the larger TO-264 package, which has more surface area than the standard TO-3P package. An insulator thermal resistance of 0.5°C/W will be assumed. The total thermal resistance to heat sink θ_{js} is then 1.1°C/W for each device.

Output voltage at 150 W into 8 Ω will be 49 V peak, with a peak current of 6.1 A. Average current per rail will be 1.9 A. Assume that 5-V headroom is needed from the rail to the peak output voltage, making the required rail voltage 54 V at full load. For simplicity, we will assume a stiff power supply and nominal mains voltage. Power input to the amplifier at rated power is the product of 1.9 A and the rail-to-rail voltage of 108 V, which is 205 W. With 150 W being dissipated in the load, 55 W will be dissipated in the output stage.

The worst-case power dissipation will occur at an output power level near 1/3 of rated power. Assume that the amplifier will support 1/3 of rated power to the point where the thermal circuit breaker opens at 70°C. At 50 W, output voltage will be 28 V peak and output current will be 3.5 A peak. Average power supply current will be 1.1 A per rail. Input power will be 119 W. With 50 W being dissipated in the load, 69 W will be dissipated in the output stage. This comes to 17 W for each of the four output transistors.

To keep things in perspective, bear in mind that if 0.22-Ω emitter resistors are used, optimal class AB bias current will total about 236 mA, resulting in quiescent power dissipation of about 25 W.

Required Heat Sink Thermal Resistance

If we assume a 25°C ambient, the heat sink will be allowed to rise by 45°C to its 70°C cutout value while dissipating 69 W. This requires a heat sink thermal resistance θ_{sa} of 0.65°C/W.

Power Dissipation into Reactive Loads

Power dissipation for a given load impedance may be greater if that impedance is reactive. This is because the power factor is nonideal for a reactive load; this means that the reactive portion of the load does not dissipate power. In the worst case of driving a purely reactive load, the load dissipates no power, but the power input to the output stage may be essentially the same. For example, the 150-W amplifier dissipates 69 W when driving an 8-Ω load at 1/3 power. However, when driving an 8-Ω purely reactive load, the power input is 205 W with no power being dissipated in the load, so the output stage dissipation is the full 205 W. This is far worse than the 1/3-power worst case for a resistive load. The example here is extreme and unlikely to ever occur in the real world.

Transistor Junction Temperature

The transistor junction temperature should now be checked. Each transistor is dissipating 17.3 W with a thermal resistance from junction to heat sink θ_{js} of 1.13°C/W.

This results in a junction rise of 20°C, for a junction temperature of 90°C when the heat sink is at 70°C. This leaves a comfortable margin of 60°C to the rated maximum junction temperature of 150°C. This allows for driving lower-impedance loads and for safe operating area allowance.

The junction temperature should also be checked when driving a 2-Ω load at 1/3 of the maximum (2-Ω) power. This check is done when the heat sink temperature is 70°C, the point at which the thermal breaker on the heat sink will open. This check is necessary because a reviewer may run the amplifier into a 2-Ω load until thermal shutdown occurs. It will be assumed that the power supply is very stiff and sags only 10% from its nominal 54-V value under the 1/3-power condition at 2 Ω. The rail is thus at about 49 V. It is further assumed that increased headroom of 7 V is required from the rail. Under these conditions, the full-power output is 42 V peak, corresponding to 2-Ω *rated* power of 441 W, one-third of which is 147 W. Power input will be 374 W and dissipation will be 227 W, or 57 W per transistor. With θ_{js} = 1.13°C/W, junction temperature rise will be 64°C, resulting in T_j = 134°C. This is a marginally safe junction temperature for this difficult testing condition.

The Thermal Breaker

A key element in protection of the amplifier is the thermal breaker. This sets an upper limit on operating heat sink temperature and actually makes maximum transistor junction temperature planning easier. A cutout temperature of 70°C is a good choice. The device can be as simple as a mechanical thermal switch mounted on the heat sink that interrupts the mains supply. An alternative solution is to employ an IC temperature sensor like the National LM34. This can be arranged with an accurate threshold circuit so that it can open a mains relay or disable the amplifier in some other way until power is cycled. A second threshold can be incorporated to activate a warning LED when the heat sink temperature reaches 60°C.

The Finger Test

As a convenient rule of thumb, you would generally like the heat sink temperature to be less than 60°C under strenuous operating conditions. It turns out that 60°C is approximately the highest temperature at which you can keep your finger on a surface for at least 30 seconds. For example, you might wish to design the amplifier so that you can run it at 1/3 power into an 8-Ω load for 1 hour and still be able to put your finger on the heat sink for 30 seconds. For such an amplifier, you might also set the thermal breaker to operate at 70°C. Any temperature over 70°C is considered a burn hazard. At 70°C you have time to remove your hand before a burn occurs.

The Heat Sink Is Not Isothermal

Aluminum has a very finite thermal resistance. This means that there will be thermal drops across the heat sink. In particular, the heat sink will be hotter in the vicinity of a power transistor. This can add to the effective thermal resistance of the heat sink as seen by the transistor, and so eat into thermal margins.

Sizing the Output Stage

Sizing the output stage is one of the most basic decisions in designing an amplifier if one is to achieve the desired performance and reliable operation. Much but not all of it

involves thermal considerations. There are several constraints that must be obeyed. Often, one constraint will dominate and set the size of the output stage. These constraints include

- Static power dissipation in the output stage
- Safe operating area
- Thermal bias stability
- Peak output current
- Beta droop (for BJTs)
- fT droop (for BJTs)

This topic was discussed in Chapter 10, and will be touched on here in respect to the thermal considerations.

Because things tend to scale, it is not unreasonable to make a recommendation of number of output pairs needed for a given power output rating into 8 Ω. The amplifier in the above example was reasonable, from a junction temperature point of view, at one output pair per 75 W of rated power into 8 Ω. That amplifier benefited from the use of large TO-264 200 W power transistors. On the other hand, it was deliberately designed to withstand the punishment of operating at 1/3 power into a 2-Ω load until the thermal breaker opened.

A simple rule of thumb is to take the rated power into 8 Ω, divide by 75, and round up to the next integer number of pairs. Recognize that this rule of thumb does not take SOA into account. That will be discussed in the next chapter. Depending on the type of protection employed, that consideration may trump worst-case average junction temperature considerations.

Table 14.2 provides a generalized rule of thumb for choosing the number of output pairs to use. This is based on a thermal breaker temperature of 70°C and rated power into a resistive 8-Ω load. It assumes that a maximum junction temperature of 150°C is reached by the time the thermal breaker opens, under conditions of driving 1/3 rated power (at 2 Ω) into a 2-Ω load. The table assumes that this output stage dissipation is $(227/150) * 75 \approx 114$ W for every 75 W of rated power into 8 Ω. The ratio $227/150$ comes from the exercise above where the maximum power dissipation of a 150-W/8-Ω amplifier driving 2 Ω at 1/3 the 2-Ω maximum power was 227 W. This is thus used as a scaling factor.

The numbers are based on the generic estimate listed in the table for net thermal resistance from junction to heat sink θ_{js}, including the insulator. The column labeled P_j is the estimated allowable power dissipation per transistor with the heat sink at 70°C. The number of output pairs is simply the power dissipation of 114 W divided by twice the available power dissipation for each output device. Figure 14.8 illustrates how the recommended number of output pairs climbs with increased power rating into 8 Ω.

Package	P_{diss}, W	θ_{js}, °C/W	P_j, W	Pairs/75 W
TO-247	150	1.6	50	1.14
TO-264	200	1.1	73	0.78

TABLE 14.2 Minimum Required Number of Output Pairs
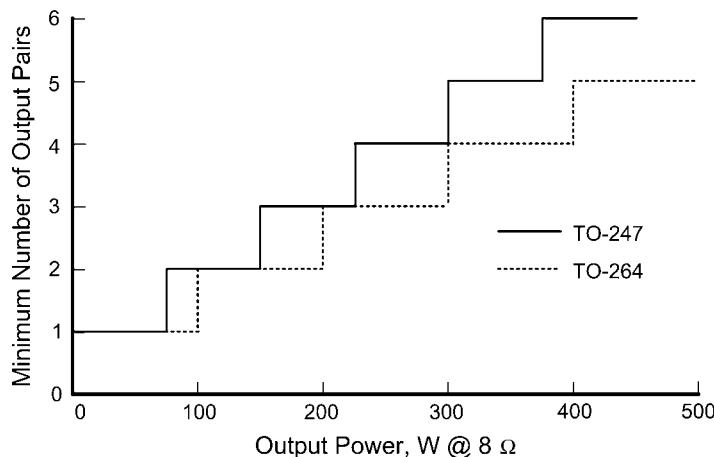
Figure 14.8 Recommended number of output transistors versus rated power into 8 Ω.

We can see that a 150-W amplifier just misses the criteria if it is implemented with two pair of TO-247 transistors (should have 2.3 pairs). We can also see that a 200-W amplifier just misses with two pairs of TO-264 devices (should have 2.1 pairs).

Modern output transistors are relatively inexpensive. For this reason, it is best to err on the side of conservatism when determining the number of output pairs to employ in an amplifier design. This approach also provides added SOA margin and may allow the use of less invasive protection circuits.

14.5 The Bias Spreader and Temperature Compensation

The quiescent bias current I_q in a class AB output stage plays an important role in controlling crossover distortion. This is especially true for BJT output stages where there exists an optimum value of bias. In theory, this optimum bias places 26 mV across each of the output transistor emitter resistors. The bias current requirements are less precise for MOSFET output stages, where more bias current is usually better. Proper bias in the case of MOSFETs is still important if for no other reason than avoidance of overheating. In this section the focus will be on BJT output stages because their bias-setting requirements are more critical, but most of the concepts apply equally to MOSFET output stages.

As explained in earlier chapters, BJTs have a positive temperature coefficient of current. If V_{be} is held constant and temperature increases, collector current increases. More often this is stated in terms of the V_{be} that corresponds to a given collector current as a function of temperature. This is referred to here as TC_{Vbe}. For most BJTs, it is about –2.2 mV/°C.

This means that as the transistor heats up, the bias spreader should provide it with a smaller V_{be} so as to maintain I_q at the desired fixed value. The most commonly used measure of the output transistor temperature is the heat sink temperature. Temperature compensation is usually accomplished by implementing the bias spreader with a V_{be} multiplier whose transistor is physically attached to the heat sink. As the temperature of the heat sink increases, the V_{be} multiplier voltage decreases, reducing the bias voltage applied to the output transistor in accordance with its reduced V_{be}.

The V_{be} Multiplier

Figure 14.9a shows the conventional V_{be} multiplier that has been described in numerous places in earlier chapters. Most of the VAS bias current I_{VAS} flows through Q1. Here I_{VAS} is assumed to be 10 mA. Resistors R1 and R2 form a voltage divider to feed the base of Q1. One V_{be} must appear across R1 for Q1 to be turned on. The remainder of the bias-spreading voltage will appear across R2. If R1 is 700 Ω and R2 is 2100 Ω, then the total bias spread will be $4V_{be}$ if base current in Q1 is negligible. The V_{be} multiplication factor is thus 4. About 1 mA will flow in the divider and about 9 mA will flow in Q1.

If Q1 has a β of 100, then its base current will be 90 µA and an additional 189 mV will be added to the drop across R2 and to the total bias-spreading voltage. Because β is temperature dependent, this constitutes a source of error in the V_{be} multiplier.

The usual bypass capacitor should be placed across the bias spreader to ensure stability and maintain low spreader impedance to high frequencies. Transistor Q1 will usually be mounted on the heat sink to temperature-compensate the junction drops of the output transistors. Sometimes Q1 will be implemented with a TO-126 device or something similar that is conveniently mounted to the heat sink. High-frequency stability precautions should be taken in light of the wiring inductance that may be encountered between the transistor on the heat sink and the remainder of the bias spreader on the circuit board. A 0.01-µF capacitor connected from collector to base of Q1 right at Q1 usually helps by converting Q1 into a diode-connected transistor at high frequencies.

Figure 14.9b shows a more practical version of the bias spreader where trimming resistor R1A has been added in series with R1 to provide for adjustment of the output stage quiescent bias I_q. If for some reason the trimming resistor fails to open, the bias spreader fails safely by defaulting to a multiplication value of unity.

V_{be} Multiplier Impedance

The intrinsic emitter resistance re' of Q1 will be about 2.9 Ω and the dynamic impedance of the bias spreader will be greater than this by the V_{be} multiplication factor of 4, or about 12 Ω. This means that if I_{VAS} increases by 1 mA (10%), the bias spread will increase by 12 mV. This is a significant fraction of the 52 mV that should appear across the output stage emitter resistors for optimum class AB bias.

This error can be reduced by a simple compensation scheme that is sometimes used. As shown in Figure 14.9c, a resistor is inserted in the collector circuit of the
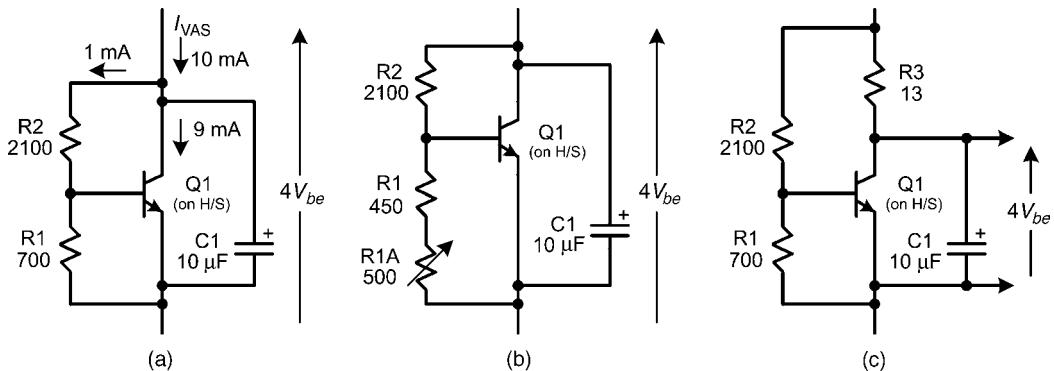
FIGURE 14.9   Conventional V_{be} multiplier bias spreader.

V_{be} multiplier. As I_{VAS} increases, total spreader voltage increases, but so does the drop across the collector resistor. The voltage drop across this resistor acts to reduce spreader voltage applied to the output stage. If the value of this resistor is the same as the DC impedance of the spreader, the effect will be nearly compensated. Because the impedance of the spreader is a function of bias current, this approach will be optimum at only one bias current level. Fortunately, the error curve is very broad and shallow.

Figure 14.10 shows a typical arrangement with the bias spreader of Figure 14.9 providing bias for an output stage Triple. Here the V_{be} multiplication factor is set to 6, with R2 increased to 3500 Ω. The spread is thus $6V_{be}$, with all V_{be} drops being controlled by the heat sink temperature if Q1 is mounted on the heat sink. This arrangement would work well in theory if the predriver and driver transistors were also mounted on the heat sink, placing them at the same temperature as the output transistors.

In some designs the driver transistors are mounted to the heat sink because they also dissipate moderate power, but the predrivers are often not mounted on the heat sink. In other designs neither the predrivers nor the drivers are mounted on the heat sink. Thus, not all of the $6V_{be}$ supplied by the bias spreader should be compensated by heat sink temperature. If all of them are compensated, then the output stage may be overcompensated, meaning that when the heat sink is hot, the bias-spreading voltage will be too small and I_q will be too low. Depending on the details of the output stage and the transistor mountings, some fraction of the six V_{be} supplied by the bias spreader should be compensated by heat sink temperature.
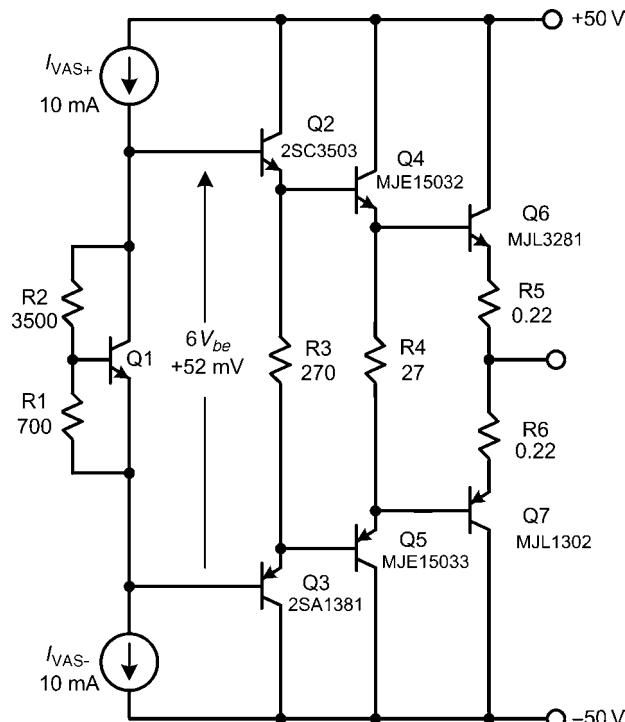
FIGURE 14.10 Conventional bias spreader driving a Triple output stage.

If the predrivers and drivers are not mounted on the heat sink, then in principle only two of the V_{be} of spread should be sensitive to heat sink temperature. In practice, this will often result in an undercompensated output stage because the actual junction temperature of the output transistor is higher than that of the heat sink, especially under conditions of significant power output. Recall that there is thermal attenuation between the junction and the heat sink. For this reason, somewhat more than the theoretical $2V_{be}$ of compensated bias spread is appropriate. When bias stability and thermal bias modulation are discussed below, it will be seen that the situation is somewhat more complex.

V_{be} Multiplier Variations

The need to obtain different amounts of compensated and uncompensated bias spreading leads to the use of V_{be} multipliers where part of the multiplier is mounted on the heat sink and part is mounted on the circuit board and exposed to the board ambient. We will refer to these as split bias spreaders. Figure 14.11a shows a simple variant where diode-connected transistor Q2 is inserted in series with the emitter of Q1. Transistor Q2 is mounted remotely on the heat sink while Q1 is mounted on the board. To achieve the same $6V_{be}$ drop, R1 is set to 1400 Ω and R2 is set to 2800 Ω. In this case half of the bias spread is compensated. This technically overcompensates the output stage, but that may be desirable in light of thermal attenuation from junction to heat sink. There will be situations where it is preferred to employ a real diode for temperature sensing instead of a diode-connected transistor, but the considerations are the same (see the discussion on ThermalTrak transistors™ in Section 14.8).

Figure 14.11b shows a different approach where Q2 is also configured as a V_{be} multiplier. This allows a completely flexible choice of the relative amount of compensation. The arrangement shown compensates four of the total spread of six V_{be}s.

Figure 14.11c is a complementary bias spreader employing an NPN and a PNP transistor with emitters connected. Here we assume that Q2 is mounted on the heat sink. This arrangement provides 50% compensation.

Figure 14.11d shows a bias spreader that employs a remote diode on the heat sink while also providing the flexibility of choosing the degree of compensation over a wide range. By means of diode-connected Q2, both R1 and R3 have $1V_{be}$ across them (for convenience we will often refer to the voltage drop of a forward-biased diode like D1 as $1V_{be}$). With the values shown, the degree of compensation is about 50%. If R3 is made
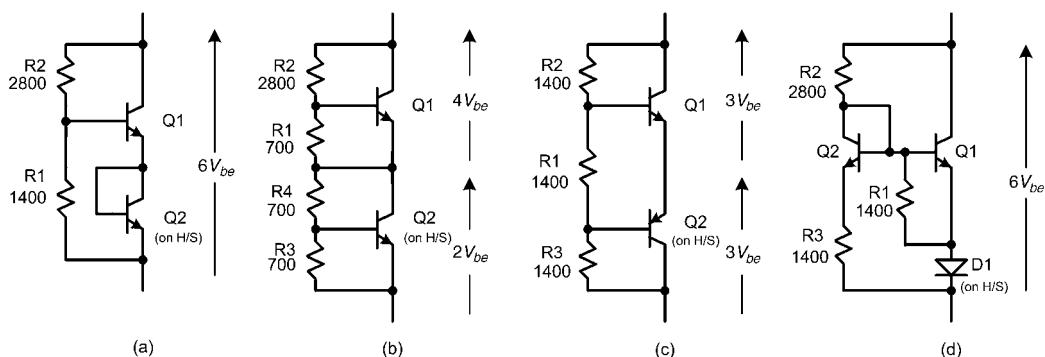
FIGURE 14.11   Four different split bias spreader arrangements.

much larger than R1, compensation will be quite small because most of the influence will come from the uncompensated V_{be} of Q1. If R1 is made much larger than R3, compensation will be quite high because most of the influence comes from the compensated diode drop of D1. Notice in this case the V_{be} of Q2 largely cancels the influence of Q1 in the current path through R3.

Darlington Bias Spreaders

There is sometimes concern about the error introduced by the base current in a conventional V_{be} multiplier. Figure 14.12a shows a bias spreader that employs a Darlington arrangement. Base current drawn from the divider formed by R1 and R2 is reduced by a factor of about 9 with the values shown. This arrangement multiplies two V_{be}s (those of Q1 and Q2) by a factor of 3 to arrive at the $6V_{be}$ spreading voltage. If Q1 is placed on the heat sink, compensation will be about 50%.

Figure 14.12b shows how the addition of R4 enables different contributions of compensated and uncompensated bias spreading by the two transistors. Reducing R4 and increasing R1 decreases the proportion of spread contributed by Q1. The fact that either Q1 or Q2 can be the transistor placed on the heat sink makes a wide range of compensation available.

Figure 14.12c illustrates a folded Darlington bias spreader. As shown, the V_{be} drops of Q1 and Q2 cancel out, leaving the full spreading influence to D1. This is useful when it is preferred to remote a diode to the heat sink instead of a transistor.

CFP Bias Spreaders

The single transistor in the conventional V_{be} multiplier can be replaced with a *complementary feedback pair* (CFP). The local feedback in the CFP greatly increases the stiffness of the bias spreader (lower impedance across its terminals) and greatly reduces the influence of transistor β on the action of the spreader.

Figure 14.13a illustrates a straightforward CFP bias spreader that produces a six-V_{be} spread. R1 and R2 perform the usual bias-setting function, with one V_{be} appearing across R1 and the remainder of the spread across R2. Q1 performs the primary function of the bias spreader, while R3 and Q2 complete the CFP. If the total spread is $6V_{be}$, $5V_{be}$
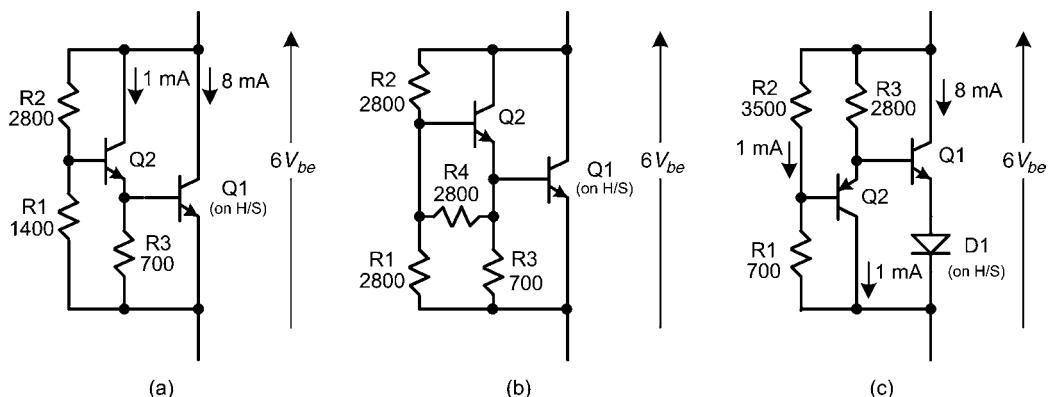
Figure 14.12   Darlington V_{be} multipliers.
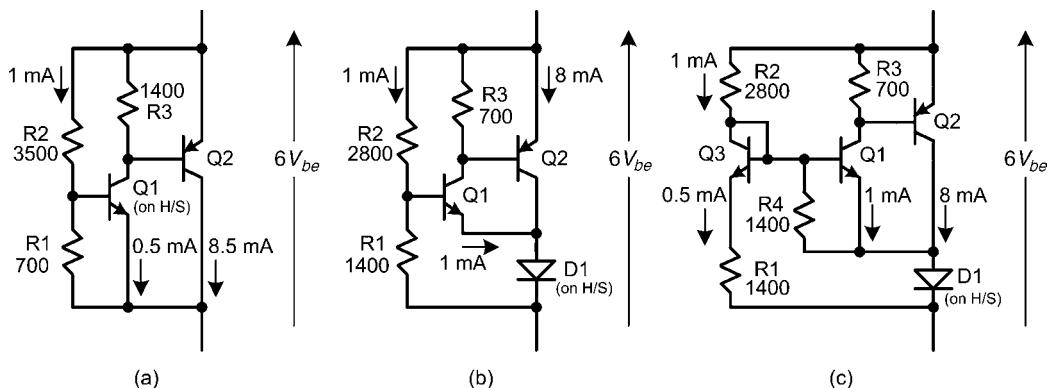
FIGURE 14.13   Three variations of the CFP bias spreader.

will appear across R2. Although the VAS bias current is 10 mA, only 0.5 mA is flowing through Q1. This means that the base current of Q1 is much smaller than in the one-transistor designs. Errors caused by β variations in Q1 will be much smaller.

Caution regarding high-frequency stability is always advised when using a CFP. In most cases the usual bypass capacitor across the spreader will be sufficient. A small resistor, here on the order of 50 Ω, can also be placed in series with the emitter of Q2 without seriously degrading performance. This reduces the loop gain of the CFP. Bias spreader impedance will be less than 2 Ω.

A remote temperature-sensing diode on the heat sink can be employed in the arrangement of Figure 14.13b. Here diode D1 is simply added in series with the emitter of the CFP. The voltage across R1 is now $2V_{be}$, only $1V_{be}$ of which is sensitive to the heat sink temperature. This bias spreader is 50% compensated. The remote diode should be bypassed at the spreader to avoid potential instability caused by wiring inductance to the diode.

If an intermediate value of temperature compensation is desired, the arrangement of Figure 14.13c is useful. Here a diode is placed in series with R1 to cancel the voltage drop effect of Q1 so that only one V_{be} (that of D1) appears across R1. The added diode is conveniently implemented as transistor Q3 that can be identical to Q1. R4 is added to make the current flow in R2 dependent on a portion of the uncompensated V_{be} of Q1. R1 and R4 each see one junction drop. If the nominal values of R1 and R4 are set to be equal, the degree of compensation will be 50%. This circuit is analogous to that of Figure 14.11d.

Location of the Sensing Junction

When the V_{be} multiplier or a portion of it is mounted on the heat sink it should be as close as possible to the heat source. Self has advocated mounting the sensing junction on the case of one of the power transistors so that it can react more quickly and with less thermal attenuation [3]. This is a useful approach, and a number of amplifier manufacturers have adopted it with various physical design approaches. Far superior results are obtained with the ThermalTrak™ line of output transistors by ON Semiconductor [4,5,6] to be discussed below in Section 14.8. These devices include a temperature-sensing diode inside the power transistor package right next to the transistor die.

Isothermal Bias Spreader and Driver Circuit

The Triple output stage generally provides superior performance in large part because of its much higher current gain and better isolation of the load from the VAS. However, it stacks up $6V_{be}$ of voltage drop that must be provided by the bias spreader. These six V_{be} all can come from different thermal environments and different conditions that affect the power dissipation and temperature of their corresponding transistors. As a result, thermal bias stability of the Triple can be more challenging than that of some other output stage designs. Here one approach to improving thermal stability of the Triple will be discussed.

Consider the case where the predrivers and drivers of a Triple output stage are mounted together on their own single heat sink on the circuit board. This heat sink could be as simple as an aluminum bar extending partly across the circuit board. It acts as a heat spreader. Assume also that Q1 of the V_{be} multiplier is mounted on this bar. These five transistors will then be essentially at the same temperature. The V_{be} of Q1 will track those of the predrivers and drivers very well. Now assume that the bias spreader incorporates a remote sensing diode mounted on the main heat sink, using one of the bias spreader circuits like those discussed above. The arrangement can now accurately take into account the two groups of V_{be} drops in the desired proportion. This approach can significantly improve the bias stability of the Triple.

Thermal Attenuation Revisited

Consider again the 150-W power amplifier with 54-V rails discussed above. It uses two output pairs wherein each transistor has thermal resistance from junction to heat sink of 1.1-°C/W (using the TO-264 package). The required heat sink was determined to have a thermal resistance to ambient of 0.65°C/W based on an allowed rise to 70°C when the output stage was dissipating 69 W (at 1/3 rated power into 8 Ω). This means that θ_{sa} for each output transistor is 2.6°C/W. The thermal attenuation from junction to heat sink is then 2.6/(2.6 + 1.1) = 0.7. This means that if the transistor junction temperature rises by a sustained 20°C, the heat sink will ultimately rise by 14°C.

Suppose the designer decides to be conservative and sets the bias compensation so that the bias is still correct when the amplifier is dissipating 35 W with a continuous sine wave. Under these conditions the heat sink will have risen by 23°C to 48°C (assuming a 25°C ambient). The junction temperature will have risen by 34°C to 58°C (remember, each of the four output transistors is dissipating only 8.75 W). The bias spreader will have to be designed to supply about 1.5 times the correction that would normally be created by the heat sink temperature rise. This is due to the thermal attenuation that is in effect when the transistor junction is dissipating continuous power. In rough terms, if the output stage needs two V_{be}s of temperature-compensated bias in theory, it will in practice really need three V_{be}s that are compensated. As a result of the 11°C difference in rise between the junction and the heat sink, the bias spreader will have backed off the bias voltage by about 2.2 mV/°C times 11°C or by 24 mV (as compared to the case where there was no thermal attenuation).

Now consider what happens when the signal is removed. Assuming that quiescent dissipation is small by comparison, the junction temperature "relaxes" back to the heat sink temperature with a time constant of less than 10 seconds. The heat sink temperature does not change significantly for quite some time. The bias spreader sees the same conditions and continues to supply a bias voltage that has been backed off by 24 mV to account for higher junction temperature rise than heat sink rise. However, there is no longer such an extra junction temperature rise. The output stage is now underbiased.

Setting the Bias and the Temperature Compensation

Under what conditions should you set the quiescent bias? In what way is the degree of thermal compensation established in the amplifier design? These are the questions to be addressed here. These two processes will be a bit interactive during the design process, but once the degree of thermal compensation is established and fixed by design, setting the bias will be fairly straightforward.

One procedure for designing the bias spreader for the proper amount of temperature compensation begins with a simple static bias adjustment. Assume for the moment that the bias spreader has been initially configured to provide a reasonable amount of temperature compensation. The bias is set to the low end of the range and the amplifier is turned on. While monitoring the emitter-to-emitter voltage, the bias is set for $2V_q = 52$ mV or whatever value has been determined to be optimal for the design. The amplifier is then allowed to reach thermal equilibrium over an extended period of time with no signal applied. The bias is retrimmed to the desired value during this time.

Bear in mind that if two output pairs with 0.22-Ω emitter resistors are used, optimal class AB bias current will total about 236 mA, resulting in quiescent power dissipation of about 25 W. This will raise the quiescent heat sink temperature by 16°C to 41°C if θ_{sa} of the heat sink is 0.65°C/W.

A reasonable objective for temperature compensation is to have the quiescent bias current be the same when the heat sink is hot as when it is only warm (some may choose a slightly different criteria). Assuming that the quiescent bias has been set as above, the amplifier is then driven at 1/3 power into a load for 15 minutes. This heats up the heat sink. The input signal is then removed, and the bias voltage is checked about 20 seconds later. If the bias voltage is too high, the amplifier is undercompensated. If it is too low, the amplifier is overcompensated. The bias spreader is altered and the process is repeated.

A dynamic approach to bias setting using a THD measurement can be optionally used after the adjustments and design revisions above have been carried out. The bias setting can be trimmed based on actual harmonic distortion measurements taken at the amplifier power level where crossover distortion is estimated to be greatest. The peak in crossover distortion will occur at different percentages of full power for different designs, but will often be in the range of 3% of full power. The dynamic adjustment procedure is best applied while measuring THD-20 into a 4-Ω load. The bias adjustment is done after the amplifier has reached thermal equilibrium driving the load at the selected power level. In this case, the heat sink will be warmer than in the static approach. Suppose that the power amplifier described earlier is operated at 5 W into a 4-Ω load. Under these conditions it will dissipate about 49 W. This is a surprisingly high amount considering that the amplifier is delivering only 5 W. The heat sink temperature will rise to 57°C if its θ_{sa} is 0.65°C/W. The difference in quiescent heat sink temperature and the temperature at 5 W into 4 Ω will be about 57°C – 41°C = 16°C (recall that idle dissipation is assumed to be about 25 W).

There are many compromises in setting the temperature compensation and choosing the conditions for setting the bias. It is easy to say *Just set $2V_q = 52$ mV*, but the imperfect thermal dynamics of the output stage make that easier said than done. There is no right answer. Bias will be wrong under some conditions. The approach described above is just one of many possible choices.

Biasing Lateral Power MOSFETs

The biasing requirements for class AB output stages based on lateral power MOSFETs are much like those for BJT output stages, but in many ways are much more forgiving.

MOSFET TC_{VGS} vs. Drain Current
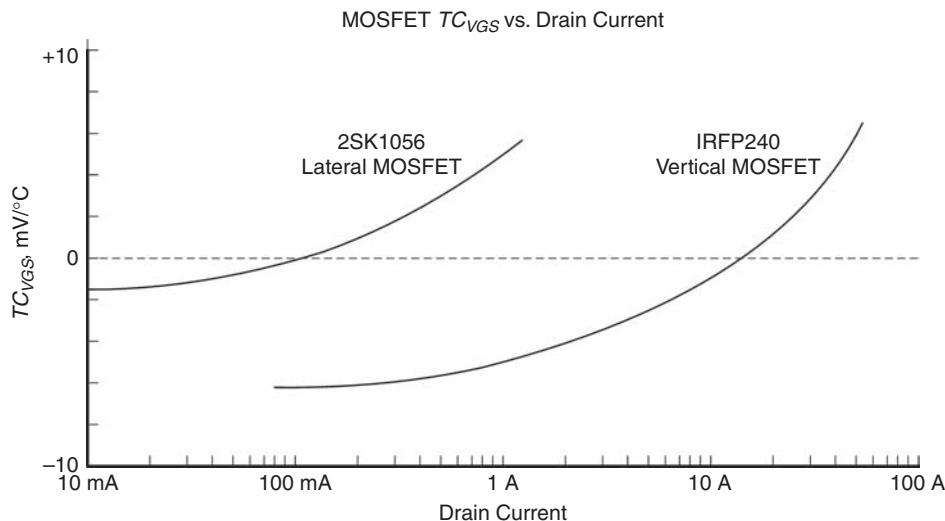
Figure 14.14   Temperature coefficient of V_{gs} versus drain current for typical lateral and vertical MOSFETs.

The temperature coefficient of BJT V_{be} (TC_{Vbe}) for constant collector current is about –2.2 mV/°C. This is what gives rise to the temperature instability and potential for thermal runaway in BJT output transistors. In contrast, TC_{Vgs} for lateral power MOSFETs is negative at drain currents below about 100 mA and transitions from a negative value to a positive value as drain current increases. Conveniently, TC_{Vgs} passes through zero at a drain current typically lying somewhere between 100 mA and 300 mA. This is close to the typical bias current value used for a MOSFET output stage, so the result is a rather stable bias current over temperature. For this reason an ordinary V_{be} multiplier is used for the bias spreader with the bias spreader transistor mounted on the board instead of the heat sink. Figure 14.14 compares TC_{Vgs} for lateral and vertical MOSFETs.

Biasing Vertical Power MOSFETs

The biasing requirements for vertical power MOSFETs lie between those of BJTs and those of lateral MOSFETs. The TC_{Vgs} of gate voltage for vertical MOSFETs starts out negative at low drain currents and transitions to a positive value as drain current increases, as shown in Figure 14.14. This behavior is similar to that for lateral devices, but the transition through zero TC_{Vgs} occurs at a much higher drain current, usually on the order of several amperes. This level of drain current is much higher than the typical 150-mA bias current. As a result, in the operating region for typical bias currents, TC_{Vgs} for vertical MOSFETs is negative (about –6 mV/°C).

Bias spreaders for vertical MOSFET output stages are much like those used for BJT output stages, with a portion of the spreading voltage compensated by heat sink temperature. The ratio of TC_{Vbe} to V_{be} is (–2.2 mV/°C)/0.7 V = 0.0031/°C, while the ratio of TC_{Vgs} to V_{gs} for an IRFP240 is about (–6 mV/°C)/4 V = 0.0015/°C. This means that the required percentage compensation for the base spreader will typically be smaller for vertical MOSFET output stages. Vertical power MOSFETs tend to have significantly greater thermal stability than BJTs, and the penalty for being overbiased is smaller.

14.6   Thermal Bias Stability

The biasing schemes described above actually constitute a thermal feedback system. As the transistor junction heats up, it heats up the heat sink, which in turn heats up the bias-spreader-sensing element. This then reduces the V_{be} applied to the power transistor, reducing its current. The reduced current then results in reduced power dissipation that then results in reduced temperature. Clearly a negative feedback loop has been formed. As with any negative feedback system, stability must be considered. As can be seen from a thermal circuit equivalent like that in Figure 14.2, there are several points of thermal inertia separated by thermal resistances. This is equivalent to electrical poles in the feedback loop. However, the thermal inertia of the heat sink forms a very dominant pole.

In contrast, a conventional bias temperature compensation scheme is not predominantly a negative feedback system when output stage power dissipation is dominated by program material rather than quiescent bias current. There the change in bias point that the bias spreader is trying to manage is not the dominant influence on the temperature. The dominant influence on the temperature is the program material and the power dissipation it creates. In this situation, the bias temperature compensation scheme is really more of a sluggish feed-forward scheme. The loop gain of the negative feedback aspect of its operation is quite small.

These aspects of bias stability involving the bias spreader will be referred to as *global bias stability*.

Local Bias Stability

Many power amplifiers incorporate multiple pairs of output transistors, and current sharing among those transistors is a concern. The dynamic behavior of this current sharing is referred to as *local bias stability*. Larger values of emitter resistor R_E promote better current sharing. However, it is often possible to achieve lower crossover distortion with smaller emitter resistors. There is thus a trade-off between bias stability and crossover distortion.

The use of small-value emitter resistors can lead to current hogging by one of the output transistors (I consider 0.15 Ω or less to be small). This is a local positive feedback phenomenon. A transistor that is conducting more current (for whatever reason) will run hotter. The negative TC_{Vbe} will then cause the transistor's current to increase. The increased bias current, in combination with the rail voltage across the transistor, will cause an increase in the transistor's power dissipation. That transistor will then get hotter still. The key observation here is that an increase in bias current causes a further increase in bias current. In some cases this may result in a thermal runaway cycle. This behavior can be more pronounced in amplifiers using more output pairs.

Local thermal stability can be estimated by some simple mathematical considerations. For local thermal stability, the heat sink is assumed not to change in temperature. No matter how big the heat sink is, local thermal stability can be a concern.

Figure 14.15 illustrates the local positive thermal feedback loop formed by these effects. The open-loop gain A is set to unity; in the absence of these effects the change at the output would simply be the same as the change at the input. In Figure 14.15 the input is the bias current setting $I_{q,\text{in}}$. The output is the bias current result $I_{q,\text{out}}$. The analysis could also be carried out with other variables, such as temperature or power dissipation, as the input and output. The gain G of the circuit is $\Delta I_{q,\text{out}}/\Delta I_{q,\text{in}}$. You can think of
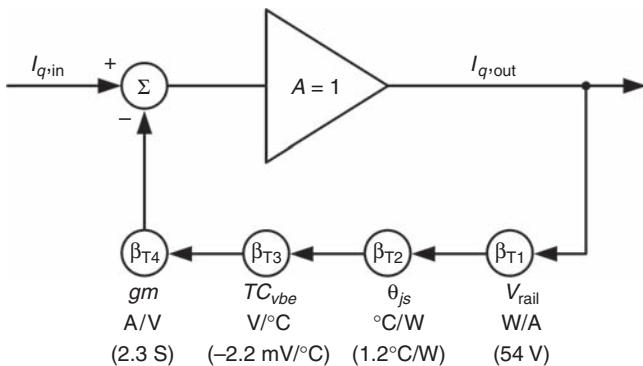
FIGURE 14.15   Local positive thermal feedback around the output transistor.

$\Delta I_{q,in}$ as a disturbance. Remember, this analysis is for one output transistor with the temperature of the heat sink constant in the time frame of the analysis. The time constants in this thermal feedback circuit are much faster than that of the heat sink.

The feedback path comprises four gain elements that together account for the thermal feedback factor β_T. The first element β_{T1} converts increased bias current to increased power dissipation. It is numerically equal to the rail voltage. The second element β_{T2} converts increased power dissipation to junction temperature rise. It corresponds to θ_{js}. The third element β_{T3} converts junction temperature rise to decreased V_{be}. It corresponds to TC_{Vbe} in millivolts per degree Celsius. The fourth element β_{T4} converts decreased V_{be} to increased bias current. It has units of amperes per volt and corresponds to transconductance gm. The feedback factor β_T is summarized by the equation below.

$$\beta_T = -TC_{Vbe} * gm * V_{rail} * \theta_{js} \tag{15.2}$$

In the equation above, β_T is considered to be a positive number for convenience. Assume that the negative sign is incorporated into the feedback summer. Remember that TC_{Vbe} is a negative number.

Consider a typical 150-W amplifier with 54-V rails and two pairs of TO-264 output transistors. Each transistor has $R_E = 0.22\ \Omega$ and is optimally biased at 118 mA, making its net transconductance, including R_E, equal to 2.3 S. Assume further that the thermal impedance from junction to heat sink for each transistor is $\theta_{js} = 1.1°C/W$.

$$\beta_T = 2.2\ mV/°C * 2.3\ S * 54\ V * 1.1°C/W = 0.30 \tag{15.3}$$

Recognizing that the unit of transconductance siemens has units of amperes per volt, we see that β_T is dimensionless, as expected.

Notice that the relevant thermal resistance is from junction to heat sink. In this analysis, it is assumed that the heat sink temperature remains constant over short periods of time and that there is no temperature-compensating effect occurring in the bias spreader. In the simple feedback system of Figure 14.15, closed-loop thermal gain is given by

$$G_T = A/(1 - A * \beta_T) \tag{15.4}$$

where A is the forward gain and β_T is the feedback factor. The product $A\beta_T$ is the loop gain. For negative feedback, $A\beta_T$ is negative, so the denominator grows with increased

amounts of negative feedback. When $A\beta$ is positive, we have positive feedback. In that case, $A\beta$ subtracts from the unity term and decreases the denominator with increased positive loop gain. This in turn increases G_T. When $A\beta$ goes to +1, the denominator goes to zero and G_T goes to infinity, and we have thermal runaway.

In the analysis here, open-loop gain A is set to unity, so the gain equation becomes

$$G_T = 1/(1 - \beta_T) \tag{15.5}$$

In the example above where $\beta_T = 0.30$, we have $G_T = 1.43$. This means that bias current changes (or temperature changes) will be multiplied by the factor 1.43 over what they would have been had there not been the local positive thermal feedback loop in play to enhance the thermal gain. When the value of β_T goes to unity, the denominator goes to zero and we have infinite gain and thermal runaway.

Now consider a 250-W power amplifier designed using 0.1-Ω emitter resistors and optimally biased in class AB at 260 mA per output pair for the theoretical 26 mV across each R_E. Ignoring the real-world effects of intrinsic base resistance and possible gate stopper resistance in calculating effective gm for each output transistor, we get $gm = 5$ S. Assume that the rail voltage is 70 V. Assume further that the output stage is built with 150 W TO-247 devices, with $\theta_{jc} = 0.83°C/W$ and 0.8°C/W insulator thermal resistance. Thermal resistance from junction to heat sink θ_{js} will thus be 1.6°C/W.

We have

$$\beta_T = 2.2 \text{ mV/°C} * 5 \text{ S} * 70 \text{ V} * 1.6°C/W = 1.23 \tag{15.6}$$

This amplifier is in deep trouble with respect to thermal bias stability, with a positive thermal feedback factor β_T greater than unity.

As a sanity check, we can "walk" around the loop starting with an assumed junction temperature increase of 10°C. This will cause a 22-mV decrease in V_{be}, which will in turn, through gm, cause a 110-mA increase in bias current. With a rail voltage of 70 V, power dissipation in the transistor will increase by 7.7 W. With junction to heat sink resistance of 1.6°C/W, this will result in a junction temperature rise of an additional 12.3°C. Because this is greater than the starting assumption of 10°C, there is greater than unity positive feedback and the transistor is off to the races.

This thermal stability analysis presents a strong case for employing more output devices in parallel with larger R_E. In the example above, if the number of output devices is doubled, each device can have $R_E = 0.22\ \Omega$ while keeping static crossover distortion about the same. This will reduce β_T by a factor of almost 2. Effective total θ_{js} will also be halved, further improving global bias stability. Additional advantages include increased SOA, reduced β droop, and reduced f_T droop. However, the driver circuits must be able to drive the increased collector base capacitance of the larger number of output transistors.

The evaluation of short-term local thermal stability by the calculation of β_T is of course a simplified approximation to the real word. There are other effects that are ignored, some of which are aggravating and some of which are mitigating. That gm increases with current is aggravating. That transistor current gain increases with temperature is aggravating. That base resistance decreases effective gm is mitigating.

The β_T analysis of thermal stability is very convenient and also applies to MOSFET output stages. Because the reaction time of the heat sink is so slow, local thermal runaway can happen in seconds.

Base Stopper Resistors and Thermal Bias Stability

Base stopper resistors are often placed in series with the bases of BJT output transistors to improve high-frequency stability. These resistors will create a DC voltage drop which is proportional to base current and which will factor into the bias current setting. This voltage drop will depend on transistor β and may be different among paralleled output transistors that are not matched for β. In some cases this can lead to current hogging. A transistor with higher β will conduct more current, get hotter, and have its β increase further. This effect will be more pronounced with output stages where very low-value emitter resistors are used.

Consider an output transistor with β = 40, bias current of 170 mA, and a 10-Ω base stopper resistor. Base current will be 4.3 mA and the DC drop across the base stopper resistor will be 43 mV. If another transistor in parallel with the first one has β = 60, the drop across its base stopper resistor will only be 28 mV. If the dynamic emitter resistance is 0.15 Ω and R_E = 0.15 Ω, then the difference of 15 mV will cause a difference in collector current of 50 mA. Beware of thermal instability that is exacerbated by the use of large base stopper resistors.

Measuring Thermal Bias Stability

Once an amplifier is built, it is desirable to evaluate its thermal bias stability. One certainly does not want it to show a tendency to destructive thermal runaway. However, even if that is not the case, one wants it to be thermally stable in regard to maintaining the optimum class AB bias current level under all static and dynamic temperature conditions.

Dynamic bias stability refers to the behavior of the output stage quiescent bias as a function of output transistor junction temperature changes caused by real program material. This does not show up under ordinary continuous sine wave testing on the bench. Dynamic bias mistracking can lead to conditions of overbias or underbias after the average power of the program material changes.

One way to evaluate dynamic bias stability is to place a meter across the emitter resistors of one of the output pairs, emitter to emitter. This is where one theoretically will see a 52-mV drop in an optimally biased class AB output stage ($2V_q$). In practice, this voltage will often be somewhat less than 52 mV.

Measure $2V_q$ when the amplifier has first been turned on. Measure it again after 1 hour (no signal). This will provide an indication of static bias temperature stability. Now run the amplifier at 1/3 rated power with an 8-Ω load until the heat sinks get too hot to touch (about 60°C). Ignore the bias voltage reading while the amplifier is providing a signal to the load. Remove the signal and record the bias voltage as a function of time. Variations in $2V_q$ are reflective of dynamic bias instability.

Bias Stability of MOSFETs versus BJTs

Figure 14.16 presents the results of such an exercise for four amplifier designs: an undercompensated bipolar, an overcompensated bipolar, an uncompensated MOSFET, and the slightly overcompensated MOSFET design in Ref. 7. All of the amplifiers had identical rail voltages, power ratings (50 W), and heat sinks.

The first 10 seconds illustrate the effect of the faster power transistor thermal time constant, while the remaining time illustrates the heat sink time constant. Notice that both bipolar cases are actually very overbiased during and immediately following the
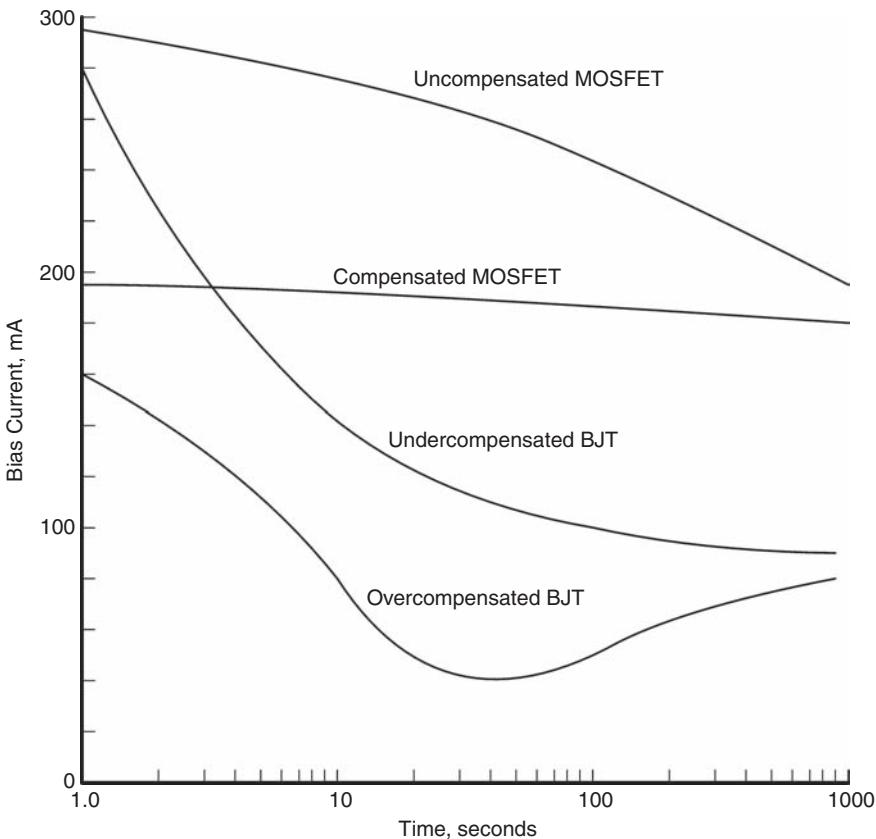
FIGURE 14.16   Bias current versus time for BJT and vertical MOSFET amplifiers.

high-dissipation "program" interval because the power transistor junctions run hotter than the heat sink due to thermal resistance from junction to heat sink. Overcompensation cannot reduce this effectively and will result in a seriously underbiased condition at other times. In comparison, the compensated MOSFET design has much greater short-term and long-term thermal bias stability. Even the uncompensated MOSFET design has better thermal performance than the bipolar designs; this suggests that smaller vertical MOSFET amplifiers (say, below 50 W) with good heat sinking can probably be made without thermal feedback.

14.7   Thermal Lag Distortion

Thermal lag distortion is probably the most insidious form of what some people call *memory distortion*. The pacing of the program material causes a modulation of the output stage power dissipation and temperature at subsonic to low audio frequencies, and this modulates the output stage bias. As we saw above, the output stage bias control in a BJT amplifier cannot keep up with the changing power dissipation in the output stage, often leaving the output stage underbiased after cessation of a high-power program material interval.

Thermal lag distortion is most directly caused by the phenomenon of thermal attenuation and is exacerbated by the long time constant of the heat sink when the bias spreader temperature-sensing element is mounted on the heat sink. The use of ThermalTrak™ BJT output devices with their internal temperature-sensing diode greatly reduces thermal lag distortion. These transistors will be discussed in the next section.

MOSFET power amplifiers are far less susceptible to thermal lag distortion for two reasons. First, they are far more temperature stable than BJT-based amplifiers. Second, with most MOSFET power amplifiers, more bias is better, as opposed to the optimum value that must be observed with BJT class AB output stages. Thus, the performance of a MOSFET output stage is less affected by the minor bias current variations that occur with program material.

14.8   ThermalTrak™ Power Transistors

Many problems with output stage bias stability have been mitigated by the introduction of the ThermalTrak™ line of output transistors by ON Semiconductor® [4, 5, 6]. These transistors incorporate an electrically isolated tracking diode inside the transistor in close thermal contact with the output transistor die. This enables the junction temperature of the tracking diode to much more closely track that of the power transistor than by common approaches using temperature compensation transistors mounted on the heat sink (or even on the exterior of the power transistor package). The NJL3281D (NPN) and NJL1302D (PNP) are good examples of these transistors [5]. These devices are rated at 15 A, 260 V, and 200 W. They have typical f_T of 30 MHz and also have very good Safe Operating Area (1.1 A at 100 V). The transistors come in a 5-pin TO-264 package.

In this section we'll show how one or more of the tracking diodes in the ThermalTrak™ output transistors of an output stage can be properly used in a V_{be}-multiplier-based bias spreader. It is notable that the use of ThermalTrak™ transistors can greatly reduce thermal lag distortion.

Construction and Physical Characteristics

The NJL3281D consists of a power transistor die and a MUR120 diode die mounted together on the copper header of a TO-264 package. The header is electrically connected to the collector of the transistor. The diode is mounted to the header but is electrically insulated from it. Figure 14.17 illustrates conceptually the construction of the ThermalTrak™ transistor and its pin-out. The physical arrangement allows the diode junction temperature to be virtually the same as the temperature of the copper header. This allows it to react much more quickly to transistor junction temperature changes than an external temperature-sensing diode. While the time constant of the heat sink is on the order of minutes, the thermal response time of the diode to changes in the header temperature is on the order of hundreds of milliseconds.

The actual junction of the power transistor is still thermally separated from the header by the junction-to-case thermal resistance of the transistor die, so there is still some thermal attenuation from the junction temperature to the temperature of the internal sensing diode. However, this thermal attenuation is much smaller than in any arrangement using an external temperature-sensing junction.
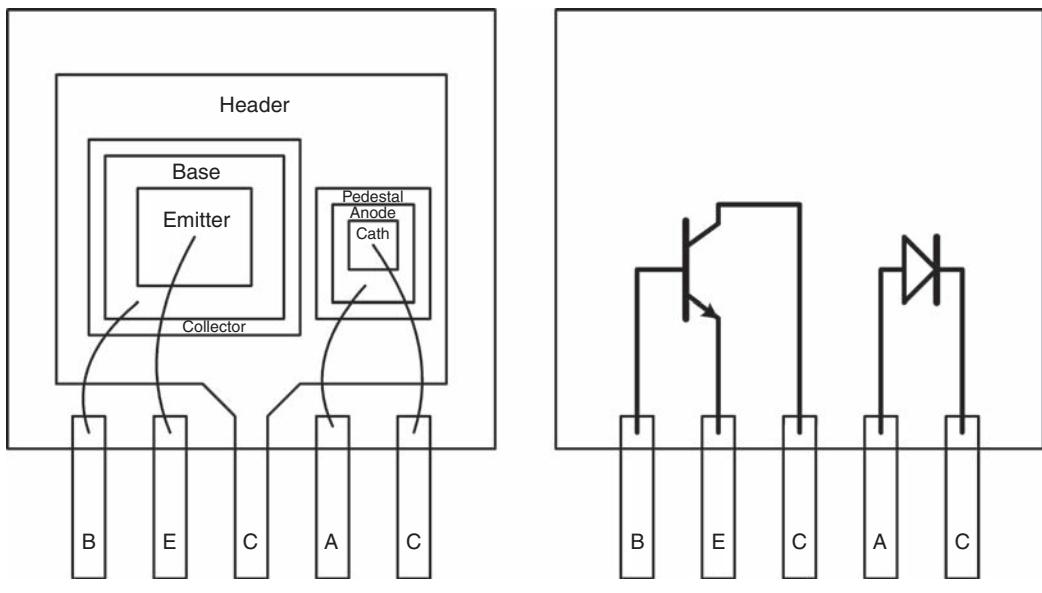
Figure 14.17   ThermalTrak™ output transistor illustration.

Bias Spreaders Employing ThermalTrak™ Transistors

Numerous bias spreader arrangements were discussed in Section 14.5 and many of them can be adapted for use with ThermalTrak™ transistors and their tracking diodes. The same principles apply, including those governing the choice of temperature compensation percentage. The bias spreaders employing remote sensing diodes, like those in Figures 14.11a and 14.11d, 14.12c, and 14.13b and 14.11c are particularly good candidates.

There is one important difference, however. It is important that at least one tracking diode from each of the NPN and PNP output transistors be included in the bias spreader. The reason for this is related to power transistor junction temperature changes at low frequencies. The reaction time of the tracking diodes is fairly fast, so it is desirable to take advantage of the complementary nature of the junction temperature changes of the NPN and PNP output transistors. For this reason the bias spreaders should be designed to employ two remote diodes.

The MUR120 is a 1-A SWITCHMODE™ power rectifier with a junction area that is large by comparison to those of the small-signal transistors usually employed in bias spreaders. Its forward junction drop is only about 600 mV at 25°C at a junction current of 10 mA, which is a typical VAS bias current. This compares to about 750 mV for a small-signal transistor like the 2N5550 operating at 10 mA. This will affect somewhat the distribution of junction drops being multiplied by the V_{be} multiplier. Finally, the slope of the temperature coefficient of junction voltage for the MUR120 (TC_{TTD}) at 10 mA is about –1.7 mV/°C, while TC_{Vbe} for the NJL3281 is about –2.1 mV/°C at its typical bias current of 118 mA ($R_E = 0.22\ \Omega$). This must also be taken into account in establishing the compensation percentage for the bias spreader.

Figure 14.18a shows a simple bias spreader employing a conventional V_{be} multiplier that includes two of the internal diodes from a ThermalTrak™ output transistor, TTD1 and TTD2. The tracking diodes are simply placed in series with a conventional V_{be}
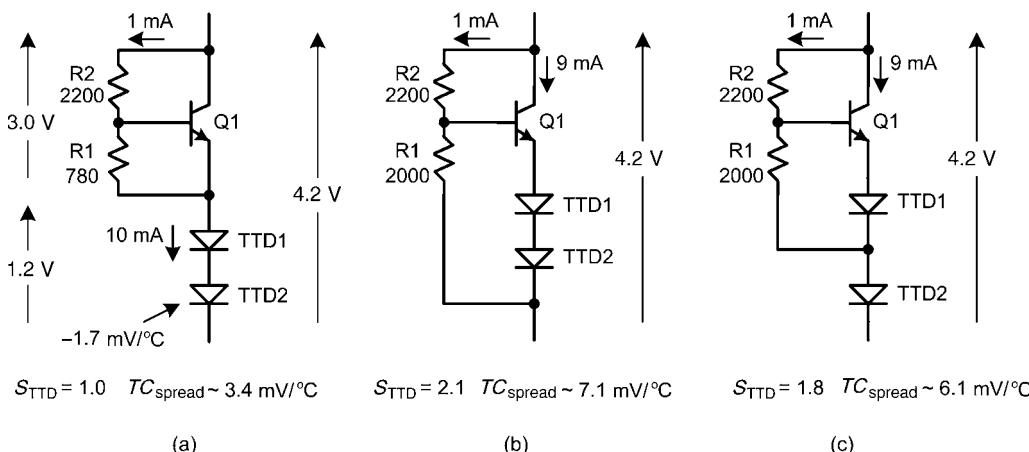
FIGURE 14.18 Three bias spreaders for ThermalTrak output transistors.

multiplier. Q1 is not mounted on the heat sink and has no role in temperature compensation of the output transistors. The bias spreader is designed for an output Triple and produces a nominal spread of about 4.2 V. The tracking diodes introduce the temperature effects of the output transistors, while the V_{be} multiplier transistor takes care of controlling that part of the bias spread necessary for the predriver and driver transistors. Sensitivity to the tracking diode TC (S_{TTD}) is unity. This bias spreader likely has too little compensation for the output transistors because TC_{TTD} is only about 80% of TC_{Vbe} for the output transistors. TC_{spread} for this bias spreader is only –3.4 mV/°C, while the output pair requires –4.2 mV/°C.

Figure 14.18b is a bias spreader that represents the opposite extreme. It encloses the two tracking diodes inside the V_{be} multiplier loop. As a result, TC_{TTD} is multiplied. The overall multiplier ratio in the spreader of Figure 14.18b is about 2.1; this is what is required to obtain the nominal spread of 4.2 V. As a result, TC_{spread} is about 7.1 mV/°C. S_{TTD} is about 2.1. This is more compensation than needed.

An intermediate solution is obviously needed. The spreader of Figure 14.18c is a tempting choice, but it still yields an estimated TC_{spread} of 6 mV/°C. The temperature coefficient is larger than one might expect because the multiplier ratio has increased, enhancing the influence of TTD1. A more significant concern is that the compensating influence of TTD1 and TTD2 is no longer equal; this degrades the balance brought by using one tracking diode from each of the top and bottom output transistors.

The bias spreader arrangement of Figure 14.19a is equally sensitive to TTD1 and TTD2 while providing a selectable value for TC_{spread}. R1 and R3 control the proportion of temperature coefficient introduced by the output transistor temperature. A larger ratio of R1/R3 provides increased S_{TTD}. With R1 = 1.3 kΩ and R3 = 5.0 kΩ, S_{TTD} is about 1.3, yielding TC_{spread} of about 4.4 mV/°C. This is just slightly more than the –4.2 mV/°C required for the output stage. However, slight overcompensation is often preferred.

Many other bias spreader arrangements can also be used with the ThermalTrak™ transistors. Figure 14.19b shows a Darlington bias spreader that yields a fixed TC_{spread} of about –5.3 mV/°C. It can be adjusted downward by adding a resistor (not shown)
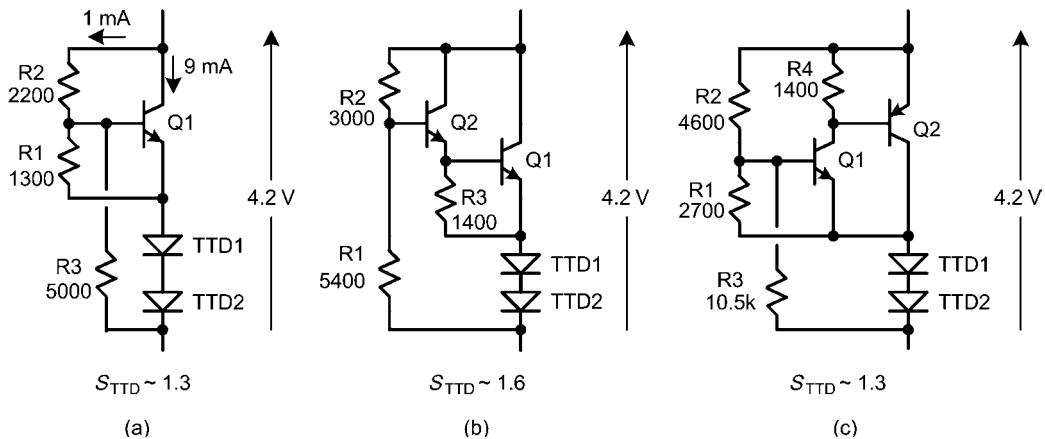
Figure 14.19   Bias spreaders with selectable temperature compensation.

between the base of Q2 and the anode of TTD1 in similar fashion to what was done in Figure 14.19a.

Figure 14.19c shows a CFP bias spreader that performs analogously to the spreader of Figure 4.19a. Spreader impedance is reduced, but not by as much as with a conventional CFP bias spreader as described in Section 14.5. This is because the tracking diodes must remain outside the CFP loop in order to have most of the 10-mA VAS bias current flowing through them. Spreader impedance is estimated to be about 7.3 Ω, less than half that of Figure 4.19a.

Tracking Diode Temperature Characteristics

Forward-biased silicon junctions do not always have a temperature coefficient of −2.2 mV/°C. This is just a convenient approximation. The actual number depends on several factors but in particular on the relative current density in the junction. The temperature coefficient is also a function of temperature.

Figure 14.20 shows the measured junction voltages for the ThermalTrak™ power transistor and tracking diode as a function of temperature. V_{be} is shown for 100 mA, while V_{TTD} is shown for 12.5 mA, 25 mA, and 50 mA. Notice that operating the tracking diode at 25 mA provides a voltage match to transistor V_{be} at 25 °C, but it has the wrong slope. Operating the diode at 12.5 mA, near the typical VAS bias current level, results in reduced V_{TTD} and about the same slope as at 25 mA. There is really no advantage to operating the diode at higher current as long as the slight difference in bias voltage can be made up.

Thermal Model

Figure 14.21 shows a thermal model for the ThermalTrak™ transistor with emphasis on the action of the tracking diode. This model was arrived at by measurement of a ThermalTrak™ transistor under several different conditions, combined with SPICE simulation of the model. The current represents the heat source in watts while the R-C ladder represents the path of heat flow from the source to the heat sink, with voltage representing temperature above ambient temperature in degrees Celsius. R1 represents θ_{jc}.
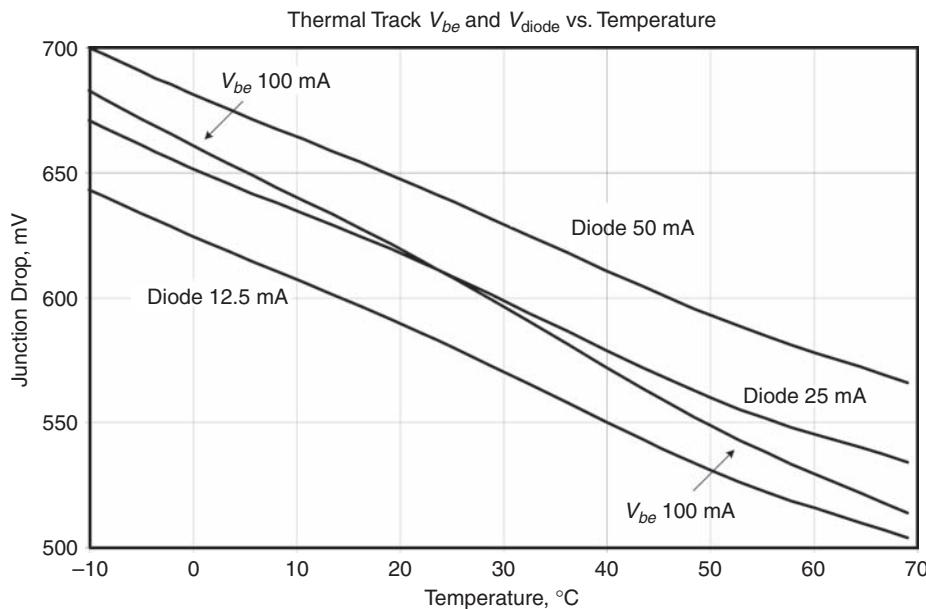
FIGURE 14.20 V_{be} and tracking diode drop versus temperature for different tracking diode current.
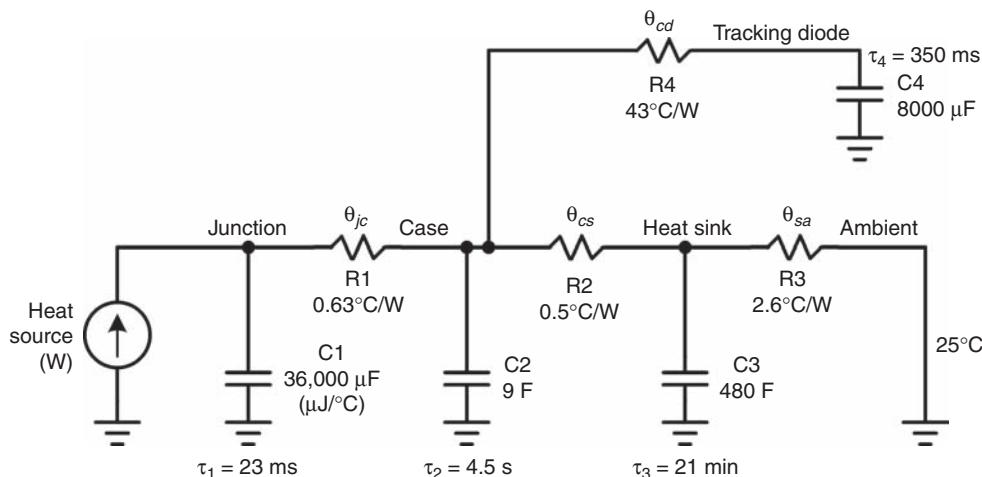
FIGURE 14.21   Tracking diode thermal model.

Here it is 0.63°C/W, representing the 200-W power transistor in a TO-264 package and having a maximum junction operating temperature of 150°C. Shunt capacitor C1 represents the thermal mass of the die itself. The capacitance of 36,000 μF has units of microjoules per degree Celsius. C2, at 9 F, represents the thermal mass of the copper header. R2 represents insulator thermal resistance $\theta_{cs} = 0.5$°C/W. R3 corresponds to this transistor's share of a heat sink with $\theta_{sa} = 0.65$°C/W. This transistor is assumed to be part of the 150-W amplifier described earlier in which there were two output pairs. Thus, θ_{sa} for

this model is 2.6°C/W. C3 = 480 F is this transistor's share of the heat sink thermal mass.

The tracking diode is affixed to the copper header with insulating epoxy that, combined with the smaller area of the tracking diode, results in thermal resistance $R4 = 43$°C/W from header to diode. At the same time, the thermal mass of the diode, represented by C4, is only 8000 μF.

Tracking Diode Response Time

The tracking diode in a ThermalTrak™ transistor is mounted on the same heat spreader (header) as the die of the power transistor, putting it in intimate thermal contact with the power transistor. There is still thermal attenuation and thermal delay in this arrangement, but it is far less than that encountered by conventional temperature compensation arrangements employing tracking diodes external to the power transistor. The thermal time constant of the tracking diode is $\tau_4 = 350$ ms. It is useful to note that the thermal time constant for the transistor with respect to the header is $\tau_1 = 23$ ms. Both of these time constants are fairly small compared to the time constant of the copper header with respect to the heat sink, $\tau_2 = 4.5$ seconds. The time constant for the heat sink is $\tau_3 = 1250$ seconds, or about 21 minutes.

Figure 14.22 illustrates measured diode thermal response time for four diodes used with the same ThermalTrak™ power transistor. The first diode is the internal ThermalTrak™ diode. The second one is affixed to the transistor package surface
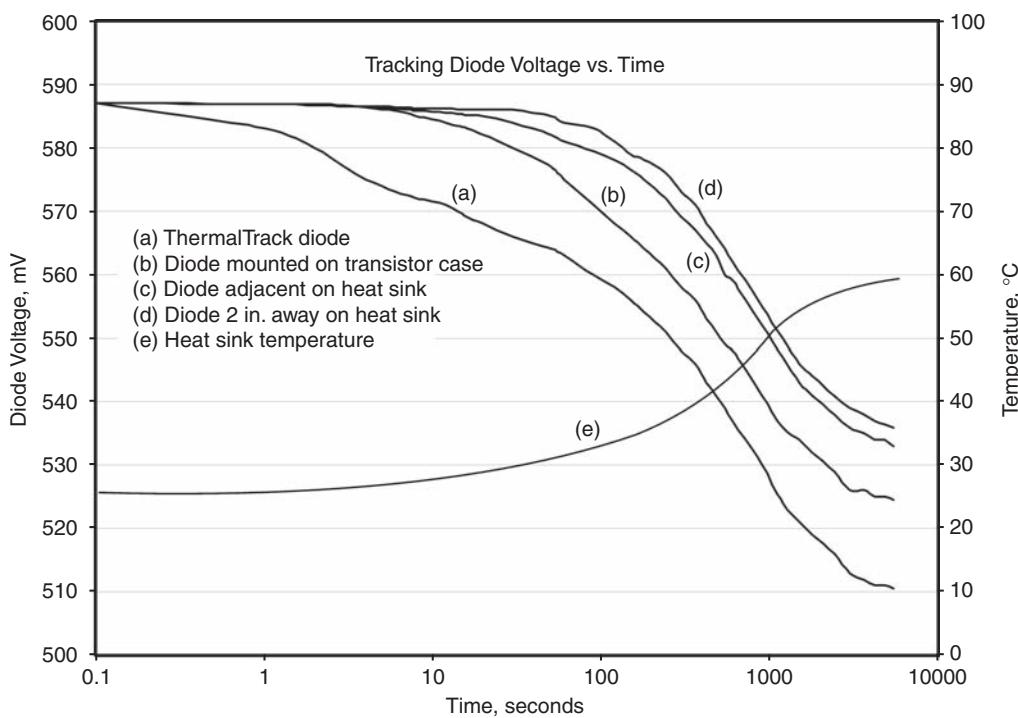
FIGURE 14.22 Measured diode thermal response time.

with thermal grease and some mechanical pressure. The third diode is mounted on the heat sink right at the power transistor, and the fourth diode is attached to the heat sink 2 in. away from the power transistor. All four diodes were run at 10 mA. The three external diodes were ThermalTrak™ diodes in other ThermalTrak™ transistors whose BJT devices were left unconnected. The power transistor was then operated at 25 W.

The plot in Figure 14.22 shows the junction voltage of each diode as a function of logarithmic time in seconds. The ThermalTrak™ sense diode reacted much more quickly than the external diodes. The ThermalTrak™ diode voltage dropped 5 mV in 1.5 seconds. The package-mounted diode took 27 seconds to drop by 5 mV. The diode mounted on the heat sink directly adjacent to the power transistor required 50 seconds to drop by 5 mV. The diode mounted 2 in. from the power transistor required 105 seconds to drop by 5 mV. The curve in Figure 14.22e shows the heat sink temperature as measured close to the power transistor.

Thermal Attenuation

Thermal attenuation can also be seen in Figure 14.22 by looking at the final value of junction drop for the four diodes. The actual junction of the ThermalTrak™ transistor is still thermally separated from the header by the junction-to-case thermal resistance of the device, so there is still some thermal attenuation from the junction to the internal sensing diode. However, this attenuation is much smaller than that for the external sensing diodes. Notice that beyond about 200 seconds all four diodes generally track the changes in heat sink temperature. The difference in the near-final values at 90 minutes illustrates the effect of thermal attenuation. Relative to the ThermalTrak™ diode, the external diodes exhibit thermal attenuation factors of 0.82, 0.71, and 0.67.

Compensation of Predriver and Driver

It is always important to bear in mind that not all V_{be} drops in an output stage are created equal. Those in the output transistors are subject to the greatest thermal variations, while those in the predriver and driver are subject to rather small temperature variations once they warm up and reach a stable temperature. This means that they should not be temperature-compensated in the same way as the output transistors, if at all. A significant choice to be made is how to provide heat sinking for the drivers, which will each dissipate 2.5 W to 4 W when biased at 50 mA. The drivers can be mounted on the main heat sink or they can include their own heat sink. The predrivers usually do not require heat sinks, although in some situations it may be advantageous to mount them on the main heat sink as well.

Any driver or predriver transistors that are mounted on the heat sink should be temperature-compensated by a V_{be} multiplier (or portion thereof) that is also mounted on the heat sink. In principle, if both drivers and pre-drivers are mounted on the heat sink, Q1 of the bias spreaders of Figures 14.18 and 14.19 should also be mounted on the heat sink. Alternatively, the five devices can be mounted on a separate isothermal bar on the circuit board that serves as a heat sink.

Bias as a Function of Time

The effectiveness of temperature compensation using the ThermalTrak™ transistors was evaluated by measuring V_q as a function of time after an amplifier using the devices

was allowed to cool down with no program material after having been run at high dissipation for 10 minutes.

The amplifier used for these tests employed an output Triple and two ThermalTrak™ output pairs with nominal 55-V power rails. The amplifier included two bias spreaders, one of which was selected for each test. The conventional design used a split bias spreader like that in Figure 14.11b, with one transistor mounted on the heat sink and the other transistor mounted on a common heat spreader bar on which the pre-drivers and drivers were also mounted. The ThermalTrak™ bias spreader was implemented with the circuit of Figure 14.19a, with R1 = 820, R2 = 1k, R3 = 1.2k, and R3A = 500. The single transistor in this bias spreader was mounted on the common heat spreader bar used for the pre-drivers and drivers.

Component values for proper bias compensation were determined by measuring V_q as the temperature of the heat sink was raised and lowered. Compensation was adjusted so that the same value of V_q was obtained when the heat sink temperature was 60 degrees Celsius as when it was at room temperature. An LM35 Celsius temperature monitor was mounted to the heat sink to measure heat sink temperature. The temperature of the heat sink was elevated by applying power to a pair of 50-W resistors mounted on the heat sink. A fan was used to cool down the heat sink in a timely fashion.

A dynamic bias stability test of the amplifier was then conducted. The output stage bias was adjusted to $V_q = 26$ mV in the quiescent state. The amplifier was then operated at 50 W (near 1/3 maximum power) for an extended period of time with the fan speed adjusted to obtain a final heat sink temperature of 60 degrees Celsius. The input signal was then removed and V_q was measured as a function of time. Figure 14.23 shows the
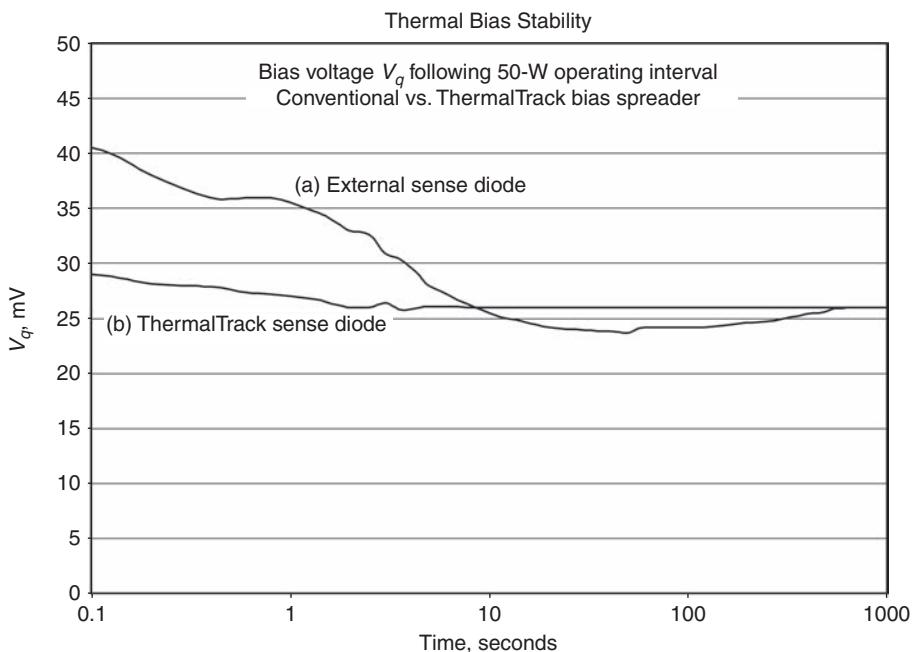
Figure 14.23   Bias (V_q) as a function of time after a thermal step.

results of this test for both the conventional and ThermalTrak™ bias spreaders. It is quite apparent that during high-dissipation signal intervals the amplifier is seriously over-biased, with V_q in excess of 41 mV. This is due to transistor junction and package heating that is not taken into account by the bias spreader transistor that is mounted on the heat sink. This behavior is evidenced by the fairly rapid decay of the over-bias condition after the signal is removed. However, notice that it has a fairly long tail, crossing through 26 mV at about 9 seconds and then exhibiting some undershoot.

In stark contrast, when using the ThermalTrak™ bias spreader, V_q rises to only about 29 mV during the program interval and settles to 26 mV in little more than 1 second. This is dramatic evidence of the improvement gained by use of the ThermalTrak™ transistors.

THD as a Function of Bias Setting

Crossover distortion of the output stage was then measured as a function of the initial setting of V_q, which was set when the amplifier was in thermal equilibrium and passing no signal. Crossover distortion of the output stage was measured by closing the global feedback loop from a center-tap on the driver bias resistor that is connected between the emitters of the driver transistors in the Locanthi T circuit. This technique exposes the open-loop distortion of the output stage. Static crossover distortion was measured at 1 kHz at an operating level of 4.5W while driving an 8-Ω load. As a sanity check, the distortion was measured under no-load conditions and was less than 0.001%. When the 8-Ω load was connected, the crossover distortion appeared as expected.

The output stage bias voltage V_q was adjusted to various values from 5 mV to 30 mV under stabilized quiescent conditions. The amplifier was then operated at 4.5 W and THD-1 was measured for each bias setting. The 4.5-W operating level is in an operating power range that is sensitive to crossover distortion. These measurements were conducted using both the conventional bias spreader and the one based on the Thermal-Trak™ transistors. The results when using the conventional bias spreader are shown in Figure 14.24a.

It is especially notable that the minimum amount of crossover distortion when using the conventional bias spreader occurred at a bias setting of V_q = 9 mV, when in theory the number should be 26 mV. This suggests that the junction and case of the power transistor heat up (even at only 4.5 W output) and effectively increase the bias current while the signal is present. This tends to agree with the observation above that amplifiers are actually operating at increased bias current under signal conditions. In this case, the distortion residual could actually be seen to decrease with time after the signal was applied.

Equally notable is the depth of the crossover distortion minimum and the fact that the distortion percentage changes over a range of 5:1 as the bias setting is changed from the optimum value to an over-bias value. Bear in mind that this is the open-loop distortion of the output stage.

The results for the same amplifier using a bias spreader based on the ThermalTrak™ technology are shown in Figure 14.24b. Here we see the same crossover distortion behavior, but the bias voltage V_q that yields the minimum value of crossover distortion is at a higher value of 14 mV. Changes in the level of the distortion residual with time after the signal was applied were still observable, but to a much lesser degree. This suggests that the temperature compensation that I used was good but not optimal.

The reduced value of V_q for minimum crossover distortion may be partly attributable to output transistor base resistance effects that cause the optimum bias to occur at
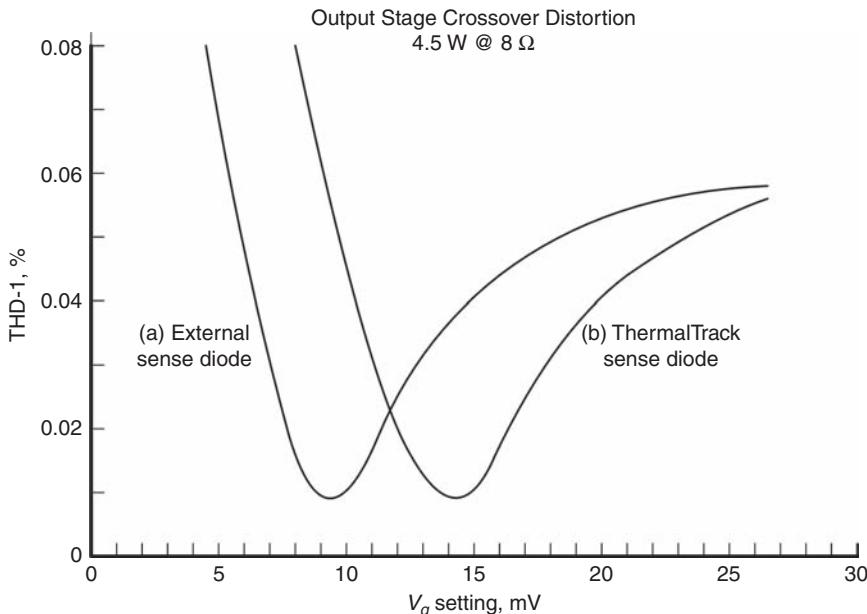
FIGURE 14.24 Output stage crossover distortion as a function of initial bias setting V_q.

a lower bias current than the expected 26 mV. This amplifier employed 2.2-Ω base stopper resistors which also contribute to this phenomenon.

ThermalTrak™ Transistors as Part of a Monitoring and Protection Scheme

If some of the ThermalTrak™ diodes are not used as part of the bias spreader, they can be used as output transistor temperature monitors. In this way, they can function as over-temperature devices that might be more accurate and responsive than thermal cut-outs mounted on the heat sink. There is, of course, a higher level of circuit complexity implied.

References

1. Federal Trade Commission (FTC), "Power Output Claims for Amplifiers Utilized in Home Entertainment Products," CFR 16, Part 432, 1974.
2. Vishay IRFP240 data sheet information on transient thermal impedance.
3. Self, D., *Audio Power Amplifier Design Handbook*, 5th ed., Focal Press, 2009.
4. U.S. Patent 7,279,983, "Output Amplifier Structure with Bias Compensation," October 9, 2007.
5. ON Semiconductor data sheets for NJL3281D/NJL1302D, June 2006.
6. Busier, M., *ThermalTrak™ Audio Output Transistors*, ON Semiconductor AND8196/D, February 2005, www.onsemi.com.
7. Cordell, R. R., "A MOSFET Power Amplifier with Error Correction," *Journal of the Audio Engineering Society*, vol. 32, no. 1, pp. 2–17, January 1984; available at www.cordellaudio.com.

This page intentionally left blank

Safe Area and Short Circuit Protection

A mplifier output stages are subject to abuse from the outside world that lies beyond the speaker connectors. An obvious source of abuse is a short circuit. A less obvious one is a loudspeaker load that creates dangerous combinations of voltage and current in the output stage.

Output transistors can be destroyed by overheating or by sudden high currents when more than a certain amount of voltage is across them. There are three things to be concerned about: (1) long-term power dissipation and average junction temperature, (2) transient power dissipation and peak junction temperature, and (3) secondary breakdown.

It is the job of an amplifier's protection circuits to prevent any kind of abuse from destroying the power transistors or any other part of the output stage, such as the driver transistors. Just as importantly, the protection circuit must prevent the expensive loud-speakers from being damaged by amplifier misbehavior. Often when an output stage fails, it will drive the output to a high DC voltage because the failure mechanism of output transistors usually results in a short circuit from collector to emitter.

This chapter provides an overview of protection issues, but not an in-depth treatment, especially with respect to protection circuit design details. Many other texts do a good job of treating protection circuits in greater depth [1, 2].

15.1 Power Transistor Safe Operating Area

The safe operating area for a power transistor is one of the most important specifications for protection circuit design and sizing of the output stage. Figure 15.1 shows a typical BJT power transistor safe operating area diagram. The device here is the Fairchild 2SC5200 (AKA FJL4315) [3]. This is a 15-A, 230-V, 150-W power transistor in a TO-264 plastic package. The rated maximum junction temperature for this transistor is 150°C. The horizontal voltage and vertical current axes of the SOA diagram are logarithmic, so a constant power boundary is a straight line. The DC SOA for the device is shown as the innermost boundary. Other boundaries are shown for 100-ms and 10-ms pulses.

The DC SOA line is the boundary of voltage and current conditions that the device can tolerate indefinitely. At low DC voltages the safe area is limited by the maximum rated current of 15 A. At V_{ce} above 10 V, the safe area is bounded with a sloped line that corresponds to 150-W power dissipation. If the case of the transistor is held at 25°C, this
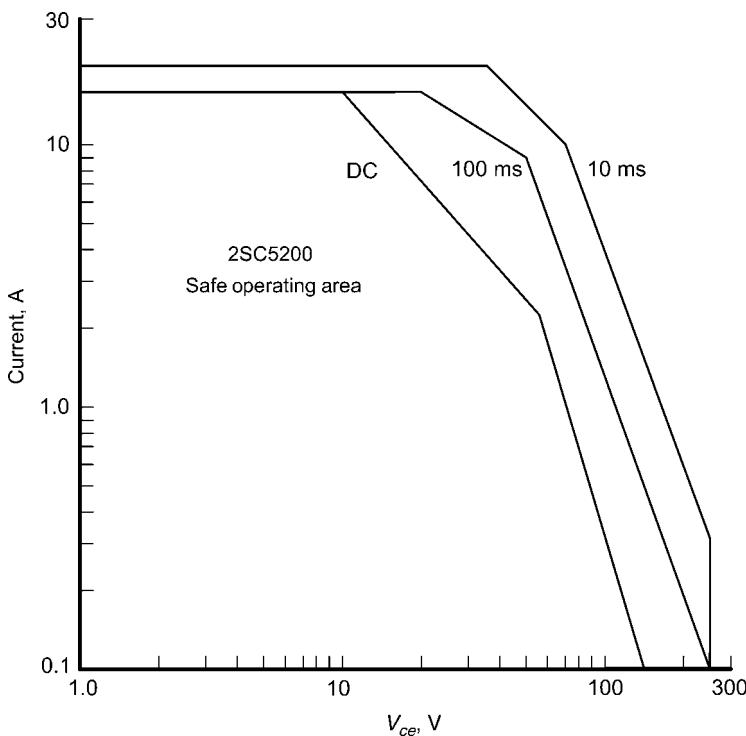
Figure 15.1   Safe operating area of the Fairchild 2SC5200.

line defines the voltage and current combinations that will keep the junction below its maximum rated temperature of 150°C. At 60 V there is a break in the slope of the line where allowed operating current begins to fall off more steeply. In this region the maximum power dissipation starts to become smaller with increases in voltage. This is where device capability is limited by secondary breakdown. Notice the rather low sustainable power dissipation of only 9 W ($I_c = 40$ mA) at the maximum voltage rating of the device. More importantly, the device can dissipate about 50 W at $V_{ce} = 100$ V.

The SOA boundary can also be plotted on linear coordinates, as shown in Figure 15.2. The linear presentation is more useful when plotting load lines to see if the SOA boundary is violated.

Yet another way to illustrate the SOA boundary is to plot allowable power dissipation as a function of V_{ce}. This will be shown in Figure 15.8. This illustrates the view of secondary breakdown corresponding to reduced power dissipation at high V_{ce}.

Secondary Breakdown Mechanism

The allowable power dissipation for a transistor decreases at higher V_{ce} because of hot spots that develop in the transistor structure. At high voltages the base thins because of the increased size of the base-collector depletion region. The thinner base has higher resistivity, allowing voltage drops across the base to influence the distribution of emitter current. This causes *emitter crowding,* in which most of the current conduction moves to the edges of the emitter, where there is less base voltage drop due to base resistivity.

Current hogging is the result, causing those areas to have higher local power dissipation. Transistors draw more current as they get hotter, so these hot spots dissipate still more power in what leads to a regenerative process that can progress very quickly and lead to destruction of the device.

Temperature Derating of SOA

The curves in Figure 15.1 define the SOA when the transistor case is held at 25°C. This is almost never the case, so these curves must be derated in consideration of the maximum anticipated operating case temperature. The derating of the constant-power portion if the SOA is straightforward. As explained in Chapter 14, a simple thermal analysis to keep the junction below its maximum rated temperature is all that is needed. Given the rated junction operating temperature of 150°C, the power dissipation is derated to about 64% (96 W) when the case is at 70°C. It is notable that the 150°C maximum junction temperature is due to a plastic packaging and reliability limitation. The MJ15024 in a metal TO-3 package, for example, sports a 200°C maximum operating junction temperature.

Derating of the second breakdown region is not as straightforward. Because the secondary breakdown failure mechanism is different from that for power dissipation, the way in which it is derated for higher case temperature is not the same. Fortunately, the appropriate derating is usually less severe. In some cases, it is derated as if the peak allowable junction temperature is much higher, like 250°C. This makes a big difference for plastic devices where the maximum specified junction temperature may only be 150°C. Using 250°C, if the case temperature rose to 70°C, then the second-breakdown derating factor would be $(250 - 70)/(250 - 25) = 80\%$ instead of $(150 - 70)/(150 - 25) = 64\%$.

Transient SOA

SOA curves like those in Figure 15.1 illustrate that the device can exhibit greater SOA for brief intervals. This conforms to the model of keeping peak junction temperature below a certain point, taking into account the thermal inertia of the device die. Sometimes this effect is described by what is called the *transient thermal impedance (TTI)* discussed in Chapter 14. For some transistors power dissipation is doubled for a 100-ms pulse and doubled again for a 10- ms pulse. This means that a 150 W device can withstand 600 W for 10 ms.

Similarly, allowed second-breakdown SOA may be greater by factors of 1.7 at 100 ms and 3–5 at 10 ms. At $V_{ce} = 100$ V, the Fairchild 2SC5200 can withstand 0.5 A at DC, 0.8 A for 100 ms, and 3 A for 10 ms [3].

The increased SOA capabilities for short pulses like 100 ms and 10 ms are important for audio amplifier applications because the instantaneous peak power caused by a 20-Hz sinusoid, for example, will last for much less than the 25-ms half-cycle time when one polarity of output transistor is conducting. This means that brief excursions outside the traditional DC SOA boundaries can be tolerated.

Long-Term Reliability and Destruct Point

DC SOA is about die temperature and long-term reliability, not the device destruct point. Ignoring secondary breakdown for the moment, the typical 150°C junction temperature limit for a plastic-packaged power device is set by long-term reliability criteria,

perhaps something like 1% failure in 10 years of continuous duty at the limit. Indeed, this is often a package consideration, not a device limit. Heat is the enemy of reliability. For this reason, it is clear that margin must exist between the rated junction temperature and the destruct junction temperature–quite a bit of it, in fact. Bear in mind that a linear voltage regulator could be operating continuously on any part of the SOA boundary with some amount of reliability for years (assuming that it is properly derated for temperature).

Managing Risk

The discussions above show that designing an output stage and protection to assure that the load conditions never cause the derated DC SOA boundary to be violated is quite conservative in respect to the possibility of device destruction. Nevertheless, it is better to be safe than sorry, so it is recommended to err on the safe side when designing the protection circuits. The price paid for this will be a slightly higher probability that protection will be triggered. For those designers who opt for little or no protection, the discussions above can help lend insight to the nature of the risk involved.

15.2   Output Stage Safe Operating Area

In this section we discuss how different loads may cause the operating conditions of the output transistors to approach or even violate the SOA boundaries. This sets the stage for proper sizing of the output stage and the design of appropriate protection circuits.

Resistive Loads

The most fundamental and optimistic calculation of required safe area is for a resistive load. A resistive load line is plotted as a straight line on linear V-I coordinates. A typical plot for a 4-Ω load plotted against the linear version of the SOA curve is shown in Figure 15.2. This represents an ideal 100-W/8-Ω amplifier with 40-V rails driving a 4-Ω load with a single 2SC5200 on the high side of the output stage. The dotted portion of the curve at higher V_{ce} is an extension of the constant-power curve. It helps to illustrate the allowable operating region lost due to secondary breakdown.

In a class AB output stage with a resistive load the transistor current is greatest at maximum signal swing where the output voltage approaches the power supply rail. This is where the voltage across the transistor is conveniently lowest. By the same token, when the output is at its zero voltage crossing and more negative, current through the upper transistor is very low or zero. This is why resistive loads are fairly benign in terms of stressing the SOA boundaries of the transistor.

The instantaneous output transistor power dissipation in an ideal amplifier when feeding a resistive load is at its maximum when driving the load to half the rail voltage. That maximum is one-half of the full average power capability into the load. A 100-W/8-Ω amplifier driving 40 V peak into a 4-Ω load (200 W full power) will dissipate a peak instantaneous power of 100 W when the load voltage is 20 V.

Reactive Loads

Loudspeakers present reactive loads, and these can be far more taxing of the SOA than resistive loads [4, 5]. Consider a pure 8-Ω capacitive load driven by a 40-V sinusoid, as shown in Figure 15.3. Such reactive load impedance is designated as j8 Ω. The current
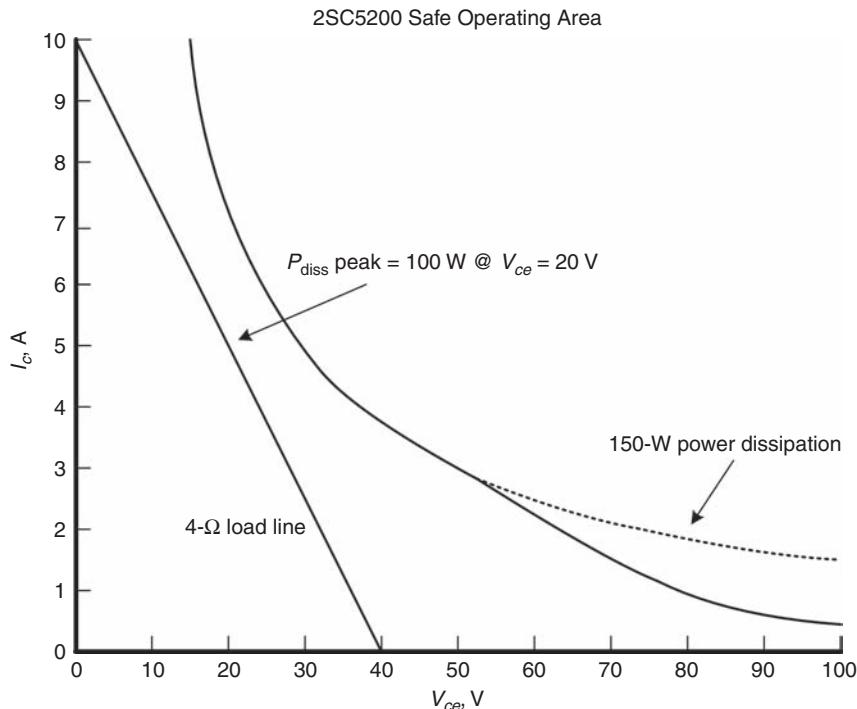
FIGURE 15.2   A 4-Ω load line plotted with a safe area curve on linear coordinates.

leads the voltage by 90°. The load line is a circle. In this case, the maximum load current occurs when the output voltage is zero and the output transistor has the full rail voltage across it. Instantaneous dissipation at this point is 200 W. This severely stresses the SOA boundary of the device. Notice that there is significant positive current flow even when the output is negative and the transistor has more than the rail voltage across it. The same holds true for a purely inductive load. The current lags the voltage by 90°, again forming a circular load line. A resistive 8-Ω load line has also been plotted as a straight line for reference.

Most real loudspeaker loads are not purely reactive, and virtually always have some effective resistance in series with the reactance. Often, this resistance will be the DC voice coil resistance of the woofer, referred to as R_e. This resistance is often on the order of 75% of the rated impedance of a loudspeaker (if it is rated honestly). In these cases an elliptical load line results. Such an elliptical load line with an impedance of 5.7 Ω plus j5.7 Ω is also shown in Figure 15.3. This load has a phase angle of 45° and a modulus of 8 Ω.

If only the positive-current portion of the load line is plotted as a function of $V_{ce} = V_{rail} - V_{out}$, the *V-I* combination can be plotted on linear coordinates along with the SOA curve, as shown in Figure 15.4. Here V_{rail} has been set to 45 V, corresponding to a 100-W/8-Ω amplifier. The 45° elliptical load line with $|Z| = 9$ Ω has been plotted with the SOA boundary of the 2SC5200. This reactive load line corresponds to a loudspeaker with $R_e = 6.4$ Ω. The resistive 8-Ω load line is also plotted for reference.
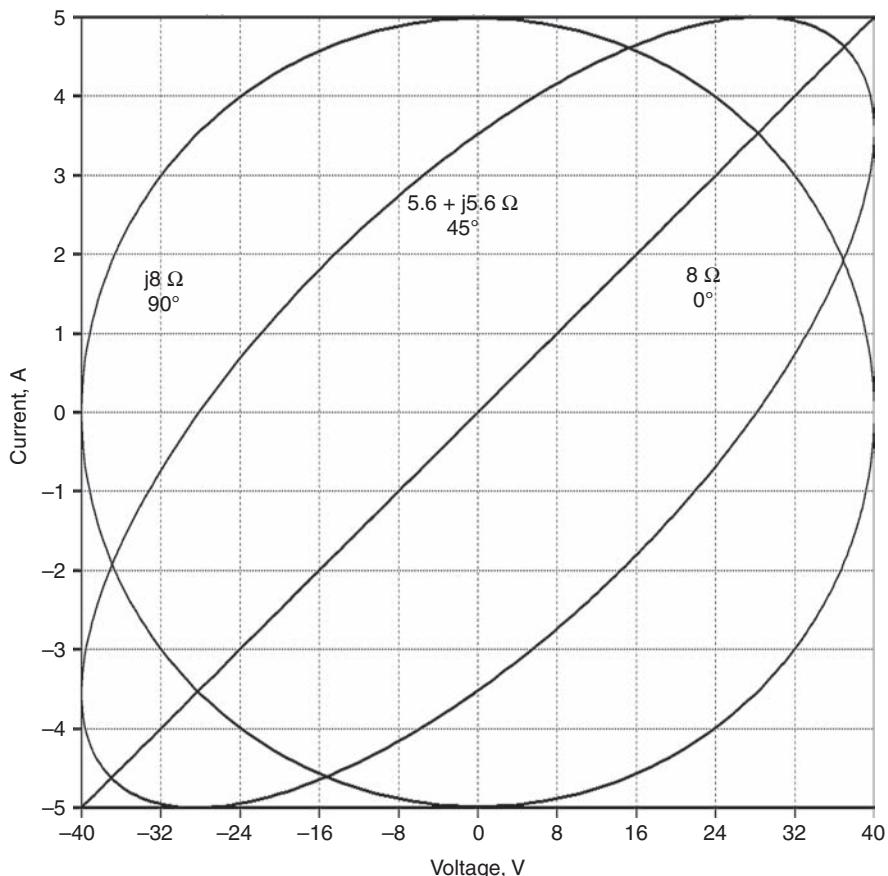
FIGURE 15.3   Circular load line of a purely reactive 8-Ω load and elliptical load line of a partially reactive 8-Ω load.

Impedance and Conductance as a Function of Phase Angle

Figure 15.5 shows a simple electrical model of a woofer in a closed box. A key observation is that there is a fixed value of resistance R_e in series with the reactive elements. This resistance represents the voice coil resistance. Even multiway loudspeaker systems with much more complex models usually have a minimum DC resistance effectively in series with the reactive elements. To first order, when the loudspeaker impedance is at its minimum, it is this resistance with a phase angle φ of 0° that is presented to the amplifier. A good example of this is a vented loudspeaker system, where the resistance drops no lower than R_e at the tuning frequency of the port. What this means is that when the impedance of the loudspeaker becomes reactive and has a nonzero phase angle, it becomes that way by the addition of reactive impedance, increasing the magnitude of the impedance of the load.
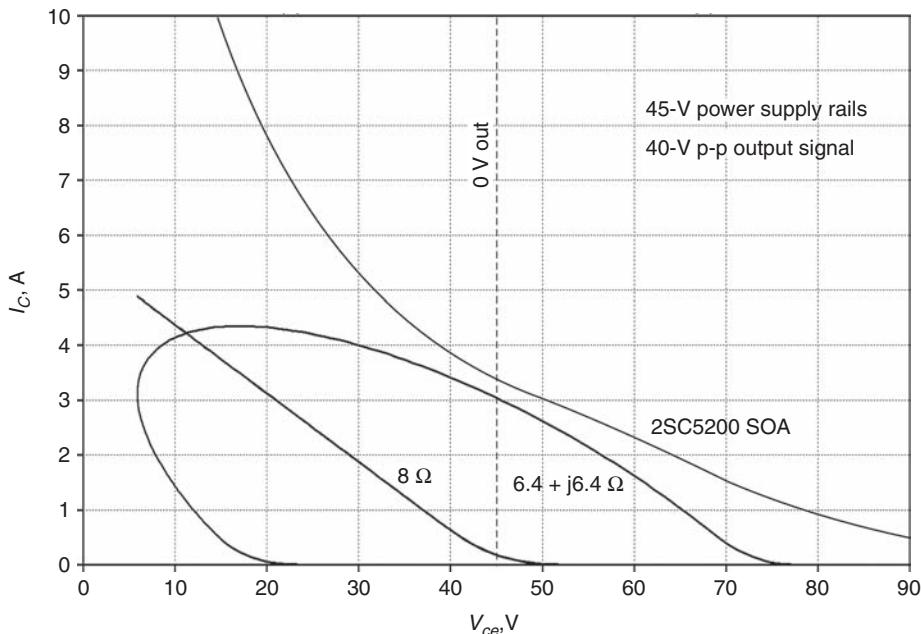
FIGURE 15.4 Positive-current portion of the reactive load line plotted against V_{ce}.
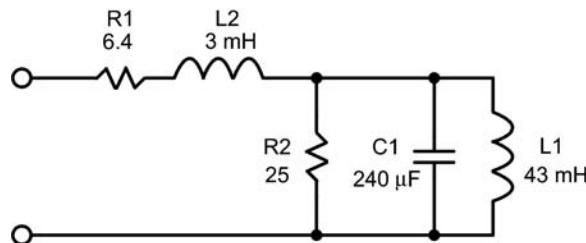
FIGURE 15.5 Electrical model of a woofer in a sealed enclosure.

The magnitude of the impedance is referred to as its modulus, designated by $|Z|$. Similarly its inverse, the magnitude of its admittance, is designated by $|Y|$. As the phase angle ϕ increases, $|Z|$ must necessarily increase and $|Y|$ must decrease [4]. This reality is easily apparent by looking at the impedance curve for a woofer. Such a curve is shown later in Figure 18.2. A woofer with $R_e = 6.4\ \Omega$ cannot have $|Z| = 6.4\ \Omega$ with a non-zero phase angle. As $|Z|$ increases from its minimum, $|\phi|$ increases toward 90°, but the current flow decreases, mitigating the effect of the nonzero $|\phi|$. An amplifier designed for a minimum load impedance of 4 Ω need not be designed to handle a load with a modulus of 4 Ω and a phase angle of 60°, for example.

As a simple example, consider a right triangle where the X axis is the real component of impedance and the Y axis is the imaginary component. The length of the hypotenuse
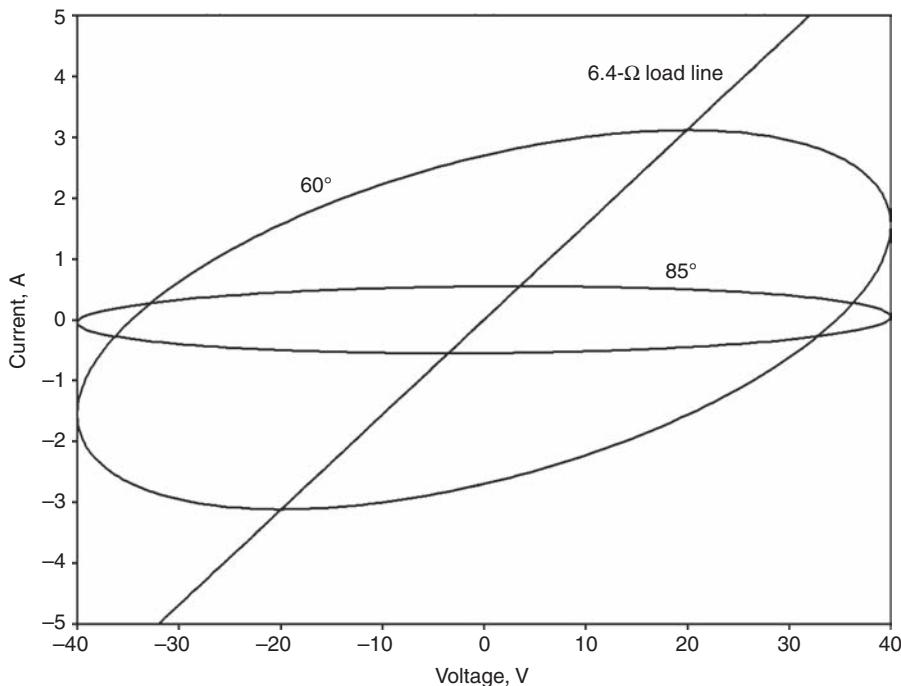
FIGURE 15.6 Load impedance curves for |ɸ| = 0°, 60°, and 85° when R_e is held constant at 6.4 Ω.

represents |Z|. If the real component is 1 Ω and the imaginary component is 2 Ω, |Z| = √5 = 2.2 Ω and |ɸ| = 60°. A 4-Ω loudspeaker with R_e = 3.2 Ω and a 60° angle will have |Z| = 7 Ω.

Figure 15.6 shows the impedance plot for |ɸ| = 0°, 60°, and 85°, when R_e is held constant at 6.4 Ω. This is analogous to Figure 15.3, but here R_e rather than |Z| has been held constant. Notice how the size of the curve becomes smaller and tilts away from the 45° resistive line as |ɸ| becomes larger.

Overlapped Elliptical Load Lines

An audio power amplifier must be able to safely drive many combinations of load impedance and phase angle. It turns out, however, that if a large number of elliptical load lines with different phase angles but the same minimum impedance R_e are overlapped, the maximum SOA boundary of the collection of load lines is a straight line with an equivalent resistive load line value of $2R_e$ [1], as shown in Figure 15.7. In contrast to the resistive load line, this virtual load line extends to $2V_{rail}$ (which is why its equivalent resistance is twice R_e). We can thus observe that the composite V-I locus for a reactive load with series resistance R_e is bounded by a resistive load line that extends from 0 V to twice the rail voltage and whose resistance is twice R_e. This is a valuable observation because it allows the evaluation of the general case without resort to every combination of reactive elements.
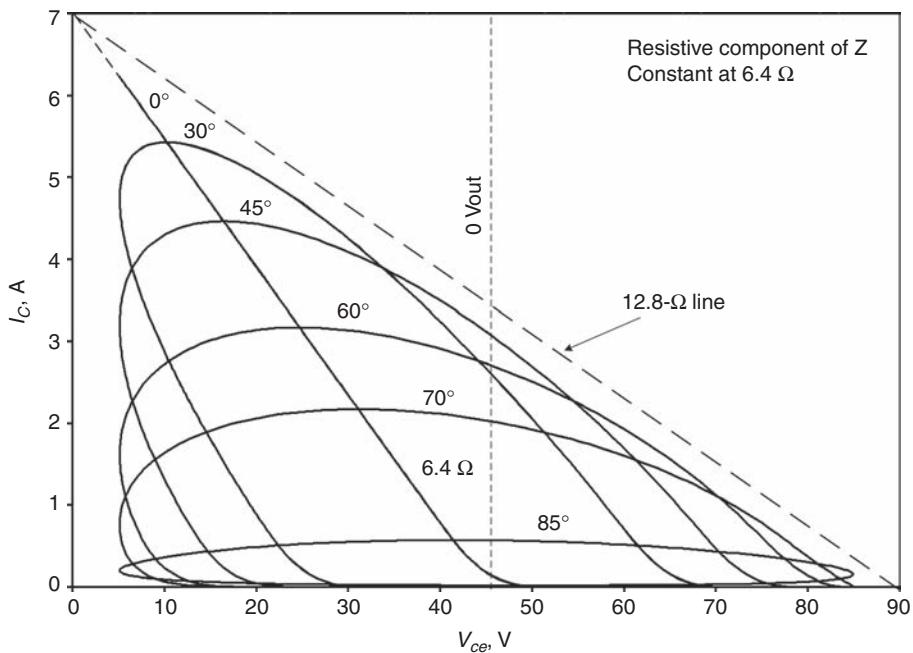
Figure 15.7 Overlapped elliptical load lines with ϕ = 0°, 30°, 45°, 60°, and 85° when R_e is always 6.4 Ω.

The above data can also be displayed on a power versus V_{ce} plot. Recall that the SOA for a transistor can be plotted this way. The constant-power portion of the SOA boundary will be a horizontal straight line. That line will then fall toward 0 for V_{ce} above the secondary breakdown knee voltage. If the transistor dissipation versus V_{ce} is plotted for the loads used in Figure 15.7, the diagram of Figure 15.8 results. For some, this presentation of the SOA boundary and transistor instantaneous dissipation may be easier to grasp. The allowable power dissipation is flat out to the SOA knee and then falls with increasing V_{ce}. Examination of the plot reveals that allowable power dissipation in the secondary breakdown region often falls off roughly as the square of V_{ce}. The Fairchild 2SC5200 can dissipate about 48 W at 100 V, but only 12 W at 200 V. The specified rate of falloff varies somewhat by manufacturer, but this behavior is not unusual.

15.3 Short Circuit Protection

Short circuits happen. Without some sort of protection, enormous output currents can flow into a short circuit. The low output impedance of the amplifier will cause large currents to flow even when there is no signal present, since the feedback will be removed by the short- and the open-loop gain of the amplifier will magnify even a small offset in the amplifier's forward path. If a short circuit occurs, each output transistor will have the full rail voltage across it, assuming that the output is at 0 V as a result of a short to
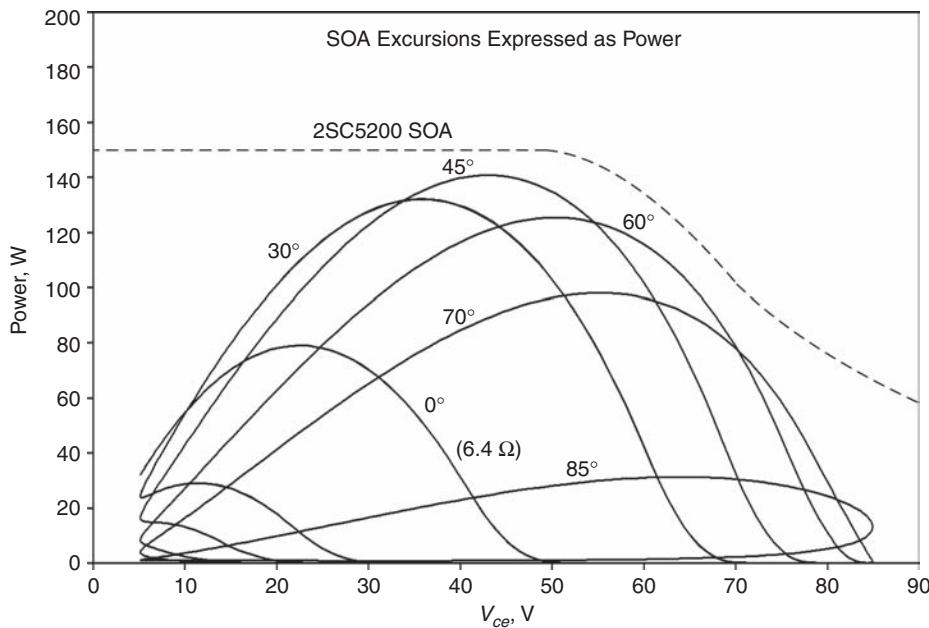
Figure 15.8 SOA and transistor stress plotted in terms of power.

ground. The simultaneous high current and high voltage will surely violate the SOA of the output transistors.

The driver transistors are in danger under these conditions as well. In attempting to supply very large currents into the short circuit, the output transistors will suffer serious beta droop, demanding more base current from the driver transistors. Indeed, the driver transistors may attempt to help drive the short circuit load through the base-emitter junction of the output transistor. The result will often be that the driver transistor's SOA will be violated as well. Indeed, sometimes the driver transistor is destroyed first.

Speaker Fuses

Speaker fuses are commonly used to provide some protection for both the loudspeaker and the output stage. Fuses do not act very fast, but in some cases a very robust output stage will be able to blow the fuse before it destroys itself. Fuses are designed to withstand their rated current indefinitely and to blow within a given amount of time for a given amount of overload. Figure 15.9 illustrates a typical fuse characteristic [6] for a conventional 2-A 3AG fuse. The fuse will survive 120 seconds at a current of 200% of rated value. Notice how great the overload must be for it to blow in just 10 ms (21 A).

As mentioned in Chapter 13, speaker fuses are a source of low-frequency distortion because their resistance is a function of current and time. The mechanism by which they blow depends fundamentally on resistance that increases when the element heats up due to current flow. Cold resistance for a 2-A fuse is about 70 mΩ. Sometimes speaker fuses are enclosed within the feedback loop to reduce distortion caused by them and to retain damping factor.
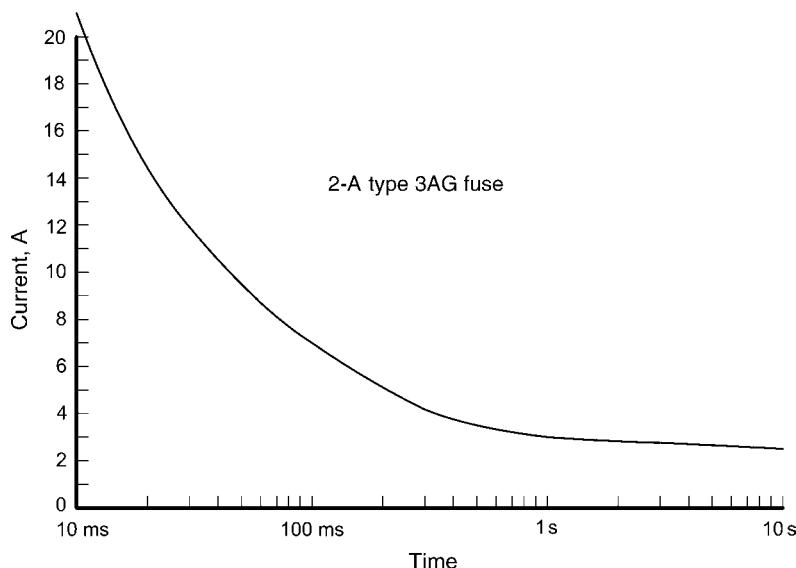
Figure 15.9 Typical fuse characteristic for a 2-A type 3AG fuse.

Rail Fuses

Fuses placed in the power supply rails to the output stage can also provide some protection against short circuits. Once again, they will provide protection only if they are faster in blowing than the output stage is in destroying itself. They have the advantage of not being in the signal path. If only one rail fuse blows there is the risk of the circuitry supplied by that polarity being reverse-biased and possibly suffering damage. For that reason, each rail should have a reverse protection diode to ground.

Current Limiting

A common approach to short circuit protection is current limiting of the output stage. If the peak current can be limited to a reasonable value, this may allow time for a fuse to blow or for a protection relay to be opened. A 100-W/8-Ω amplifier must be able to deliver 10 A peak into a 4-Ω load. On the other hand, 40-V rails across the output stage with 10 A in the event of a short circuit will create 400 W of power dissipation. This underlines the fact that simple current limiting by itself is not enough.

In some cases the action of current limiters can be delayed by the incorporation of an R-C time constant to prevent the activation of the circuit on very short high-current bursts, recognizing the ability of the power transistors to survive brief overloads. The selection of the amount of delay can be a delicate balancing act. The reaction time must be long enough to provide the output current needed by legitimate loads at high power levels at low frequencies. This should include continuous sine wave testing at 20 Hz into the lowest-rated load impedance.

A Simple Current Limiter

Active current limiting employs a transistor that turns on to rob base drive current from the output transistor when the output current exceeds the threshold. An example of this
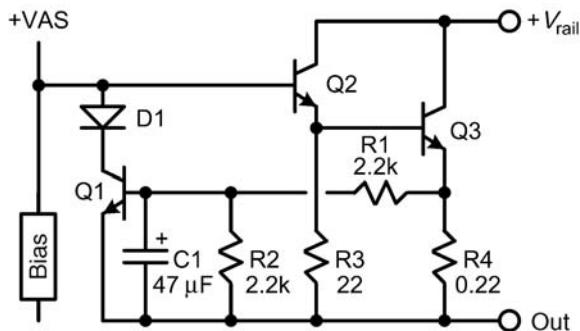
FIGURE 15.10   Simple current-limiting circuit.

is shown in Figure 15.10, where the top half of a Darlington output stage is shown with a current-limiting circuit set to a limit of about 5 A by the voltage divider formed by R1 and R2. If the voltage across the emitter resistor R_E exceeds 1.1 V, Q1 turns on and robs base drive from the output transistor by shunting the node from the VAS to the output node. This action turns the output stage into a current source, eliminating its damping influence on the loudspeaker and possibly allowing the energy stored in the loudspeaker to create a flyback pulse. This makes a terrible sound and can sometimes damage a tweeter.

The current-limiting circuit design presumes that the VAS is current limited in some way. D1 protects Q1 from negative voltages that can be present when the bottom half of the output stage is conducting. C1 slows the circuit down by introducing a 50-ms time constant to permit higher current for brief intervals. The current limit and time constant chosen here are just illustrative.

Current-limiting circuits like these must also be designed with recognition that when active, these circuits create a negative feedback loop whose stability must be considered. In practice, this will occur only during the beginning of the turn-on of the current limiter and the turn-off of the current limiter. The presence of C1 helps reduce the likelihood of oscillations.

Natural Current Limiting
Sometimes the driver circuit can be designed so that clamping diodes limit the amount of base or gate voltage drive to a specific amount. Doing so essentially limits the amount of voltage that can be dropped across the emitter resistor, and thus the maximum amount of current that can be sourced. The *flying catch* diodes discussed in Chapter 11 accomplish this. Such an arrangement is shown in Figure 15.11.

The Darlington output stage shown requires a bias spreading voltage of about 2.6 V, of which about 1.3 V is needed to turn on Q1 and Q3 when the top half of the output stage is conducting. Current-limiting action occurs when the bottom end of the bias spreader rises to one diode drop above the output node. This will happen when high current is passing through R_2. In the circuit shown, current limiting will begin when about 1.9 V appears across R_2. This corresponds to a current limit of about 8.5 A, which is rather high. This current limiter is difficult to delay, but is simple in its operation and does not involve feedback. It is suitable for fast, simple, high-limit short circuit protection.
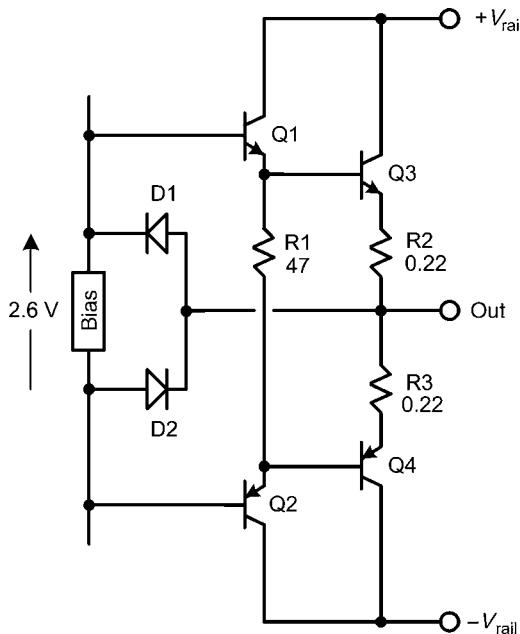
FIGURE 15.11 Natural current limiting with flying catch diodes.

Different driver and bias spreader arrangements can be made to yield higher or lower limiting thresholds. In some cases this circuit will have a very high current limit threshold and its main function will be to allow the use of the shutdown circuit below and to limit catastrophic damage to the output stage in certain failure modes.

Shutdown Circuits

Some short circuit protection circuits act by electronically shutting down the output stage when the output current exceeds a certain value. This value of current can be made to be a function of the output voltage, and the action of this circuit can be delayed by the use of an R-C time constant. Such a shutdown circuit is usually configured to latch and stay in the shutdown mode until the mains power is cycled. This protection behavior is usually undesirable in professional sound reinforcement applications, however.

Figure 15.12 shows such a circuit that operates in conjunction with the natural current-limiting circuit shown above. It operates by collapsing the bias spreader. When a short circuit is detected, a TRIAC is fired that shorts out the bias spreader. With flying catch diodes in place, this effectively shuts down the output stage. Current from the VAS will flow harmlessly into the load through D1 or D2. A simple circuit using an opto-coupler is shown for sensing high current and firing the TRIAC. If the voltage drop across either emitter resistor exceeds the forward voltage of the opto-coupler LED, the circuit will fire the TRIAC. VAS bias current will keep the TRIAC on until power is cycled. This circuit can be made very fast and is a good candidate for protecting MOSFET output stages.

Other similar approaches to electronic shutdown can be employed as well. For example, a transistor which can short out the bias spreader and which can be driven by an opto-coupler can be used in place of the TRIAC. Such a shunting transistor can also
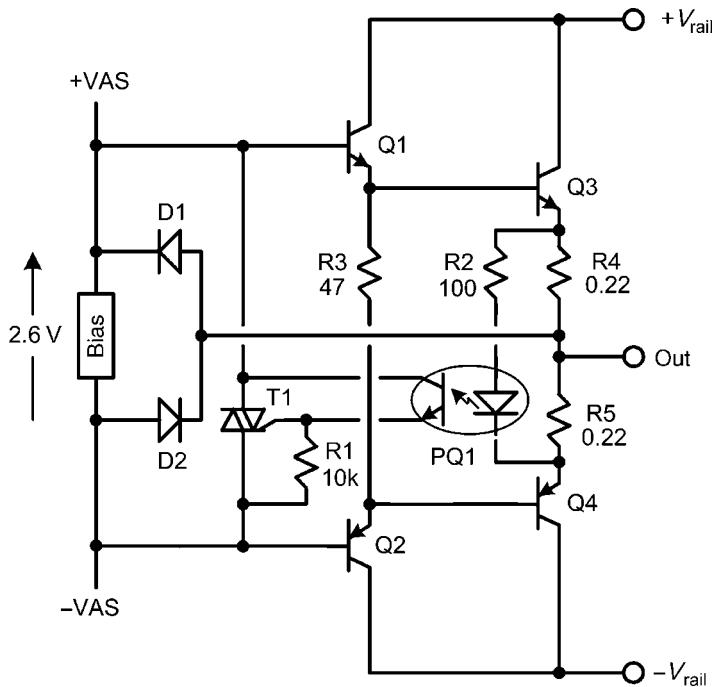
FIGURE **15.12** A TRIAC disables the output stage by collapsing the bias spreader.

be employed as part of a *retry* circuit to turn off the TRIAC after a delay period or when an output impedance sensor has indicated that the short has cleared. A simple relay can also be used to collapse the bias spreader.

Speaker Relays

A relay in series with the speaker line can be used to provide short circuit protection if it is driven by a circuit that senses an overcurrent condition. Relays are not always adequately fast, but they are often faster than fuses. Speaker relays are often incorporated into the overall protection scheme for other reasons as well, including protecting the loudspeaker from DC offset at the output of a failed amplifier and for power-on/power-off muting. These functions will be discussed in Section 15.8.

Load-Sensing Circuits

In more sophisticated amplifiers, circuitry is sometimes employed to electronically sense the condition of the load circuit for a short circuit during intervals when the speaker relay is open or when the output stage has been electronically shut down. Such circuitry can permit the protection circuits to reset once the short circuit in the load has been removed. The circuit can also be used to prevent the closing of the speaker relay at turn-on unless the load is deemed safe. Such circuits can be as simple as monitoring the DC output voltage across the load when a small direct current is passed through the load. Such a simple circuit obviously protects only against a DC short circuit or a load that has unreasonably low DC resistance (such as an excessive number of speakers connected in parallel).
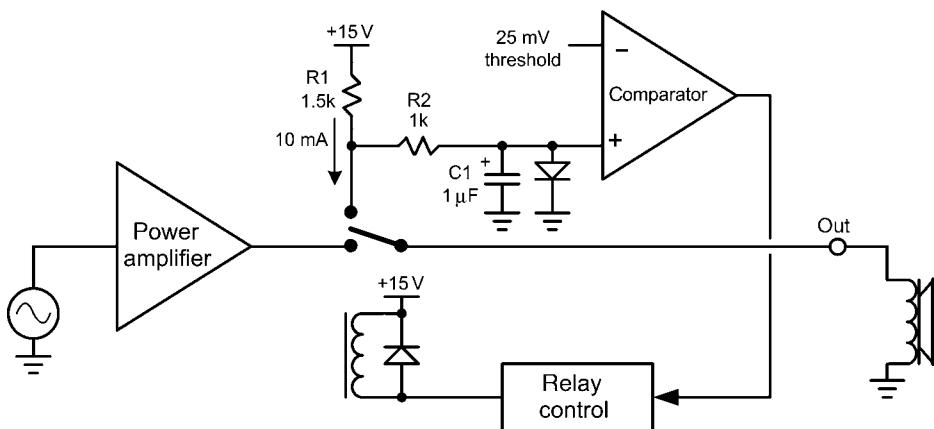
FIGURE 15.13   A simple load-sensing circuit.

Figure 15.13 shows a simple load-sensing circuit of this kind implemented in combination with a speaker relay. A current of 10 mA is applied by R1 to the loudspeaker through the normally closed contacts when the relay is open. The DC voltage will be 10 mV for every ohm of loudspeaker DC resistance (DCR). If the amplifier is designed to require no less than 2.5 Ω of DCR, the threshold for comparator U1 is set to 25 mV. The sensed voltage is filtered by R2 and C1 to reduce the effects of noise. D1 prevents the sense voltage from going above one junction drop when the relay is closed during normal amplifier operation. When the output of the comparator is positive it allows the relay control circuit to complete its speaker relay closure sequence. If the amplifier goes into a fault mode that causes K1 to be opened, the output of the load-sensing circuit can be used as one of a number of criteria to allow the amplifier to come back into operation and connect the loudspeaker.

15.4   Safe-Area-Limiting Circuits

Although short circuit protection is certainly a form of *safe area limiting,* this term is more often used to describe more sophisticated circuits that are intended to keep the output stage transistors within their safe operating area during signal excursions into reactive loads with dangerous load lines. These circuits are often called *V-I* limiters because they usually limit the current to an amount that is governed by the voltage across the transistor at any given moment. These circuits often incorporate some delay so that the larger transient safe area capability of the output transistors can be utilized.

The challenge for *V-I* limiters is to follow the curved SOA boundary of the transistors as accurately as possible. This maximizes the use of the available SOA and minimizes the unnecessary activation of these circuits. *V-I* limiters have gained a reputation as being sonically intrusive. When properly designed and not being called on to act, they should not degrade the sound. However, many years ago they were designed to protect relatively undersized output stages, making them much more intrusive. With more robust output transistors and larger output stages common today, *V-I* limiters can be designed with high triggering thresholds. Of course, the newer output stages are less likely to need *V-I* limiters at all.

Single-Slope *V-I* Limiters

The simplest form of *V-I* limiter merely makes the current limiting threshold of Figure 15.10 smaller when V_{ce} is larger. This means that the threshold is larger for larger output voltage. When the output signal is near the power rail, this is when the highest output current is likely to be needed, and this is also when the output transistor can handle the highest amount of current and still be within its SOA. This is good for resistive loads, but such a limiter will be more likely to act in the case of a reactive load, where high currents may flow at smaller output voltages. Modulating the current-limiting threshold by the output voltage creates a single slope of current limit as a function of output voltage. The steepness of this slope is easily adjusted.

Figure 15.14 shows a simple single-slope *V-I* limiter circuit. It is largely the same as the current limiter circuit in Figure 15.10, with the mere addition of two resistors R5 and R6. These resistors simply inject current into the protection transistor's base circuit that is proportional to V_{ce} of the power transistor. This makes the current-limiting transistor turn on at a lower output current when there is a larger voltage across the output transistor.

Figure 15.15 shows how the action of a single-slope *V-I* limiter maps onto the SOA boundary of a power transistor. It can be seen that its action is only a coarse approximation to the actual available SOA and that a lot of the available SOA of the transistor is wasted. This means that the amplifier will go into protection more often than it must.
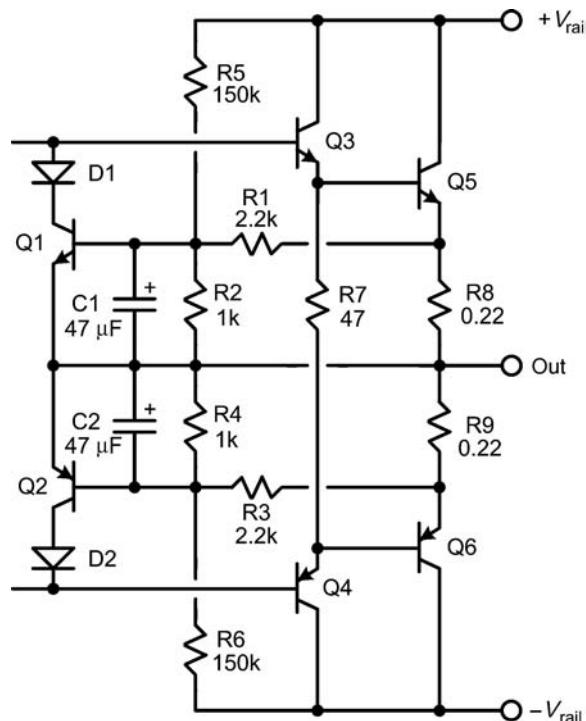
FIGURE 15.14 A single-slope *V-I* limiter.
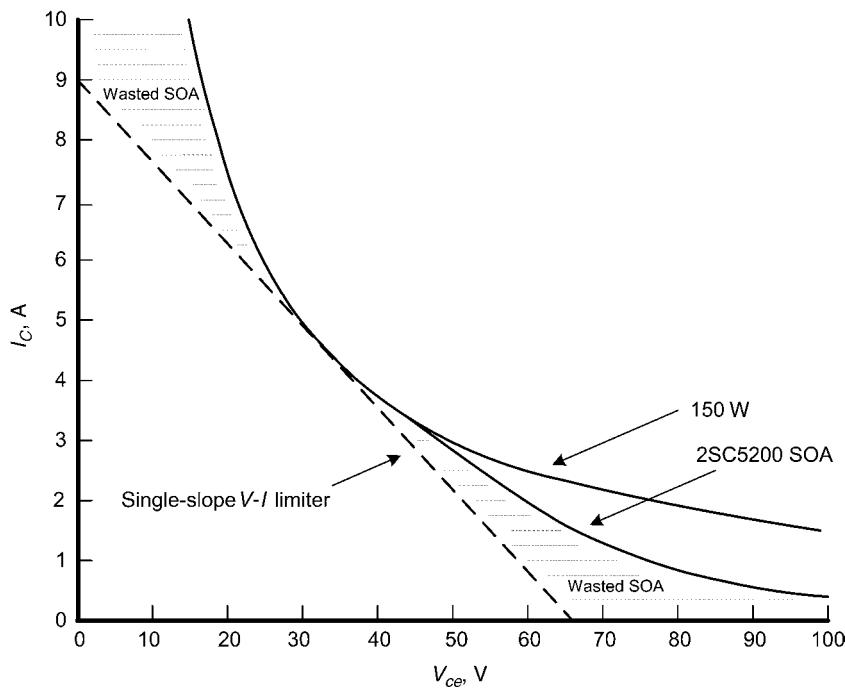
FIGURE 15.15 Single-slope *V-I* limiter action plotted with SOA curve.

Multi-Slope *V-I* Limiters

The *V-I*-limiting fit to the actual SOA boundary can be made more accurate if more than one slope is incorporated into the circuit. In practice, there is a law of diminishing returns as more slope segments are added. On the other hand, the resistors, diodes, and Zeners required to do so are quite inexpensive. The reactive load lines plotted against the SOA curve in Figure 15.8 provide guidance as to where more protection slopes can provide the most benefit. A number of other texts do a fine job of describing such *V-I* limiters in detail [1, 2].

Figure 15.16 illustrates a simple three-slope *V-I* limiter. Referring to the top half, R5 sets the nominal slope in the central region of operation, as in the single-slope design. For output signals larger than about 15 V, D3 turns on and R7 pulls current from the base node of Q1, increasing the current-limiting threshold. For output signals less than about –15 V, D4 turns on and R8 sources current to the base of Q1, reducing the current-limiting threshold. The breakpoint voltages shown in Figure 15.16 are conveniently derived from ±15 V supplies assumed to be available. If other breakpoint voltages are desired, they can be supplied by replacing R7 and R8 with resistive voltage dividers. Analogous circuitry is used on the bottom half of the output stage.

Drawbacks of *V-I* Limiters

V-I limiters would be fine if they never had to act. Unfortunately, when they do act, they create terrible sounds and can cause damage to tweeters. Depending on their sophistication and the nature of the loudspeaker load, they sometimes act unnecessarily.
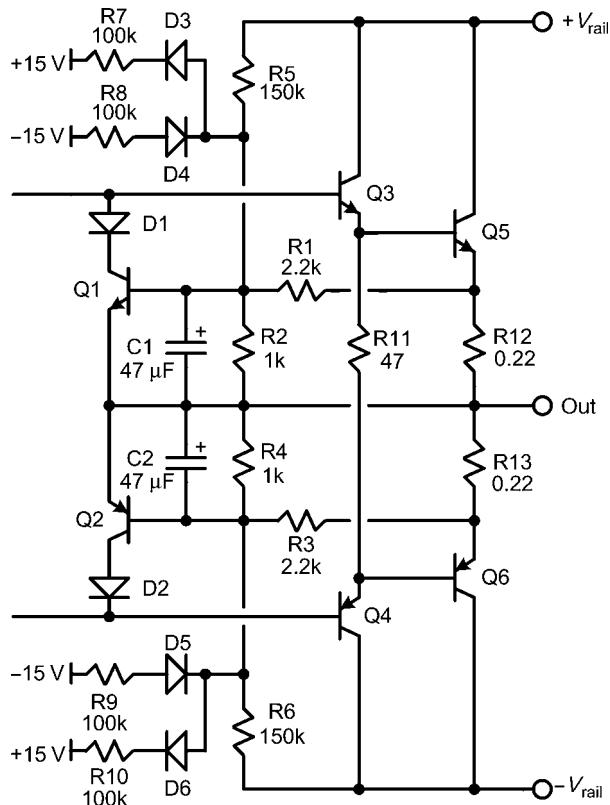
FIGURE 15.16   Three-slope *V-I* limiter.

If *V-I* limiters only acted to clip the signal amplitude, as with ordinary clipping of an amplifier, they would not be so bad. Unfortunately, in most cases the *V-I* limiter causes the output stage to change from a voltage source to a current source when the *V-I* limiter engages. When this happens, there is almost surely a lot of stored energy in the loudspeaker and crossover network. This stored energy wants to cause current to flow somewhere and be dissipated. With the output stage in a current source mode of operation, this may not be possible. As a result, a large inductive spike or kick may result, often transitioning the output voltage to that of the opposite rail (i.e., in a direction opposite to that in which the output stage was changing the signal).

This spike will be very audible, and its large amplitude may cause damage to the loudspeaker's tweeter. The action of a *V-I* limiter can turn an amplifier into a *tweeter eater*. The stored energy in the loudspeaker drivers and crossover will find its way to a place where it can be dissipated. The stored energy in the woofer and crossover coil(s) may be transferred to the tweeter.

It is also worth noting that a *V-I* limiter creates a negative resistance effect. This happens because the current limit is a function of the voltage across the output transistor. Once the output transistor reaches its current limit, the speaker current will cause the voltage across the transistor to increase, further reducing its current limit. This results in a fast regenerative turnoff of that transistor.

Flyback Protection Diodes

The inductive flyback caused by the action of a *V-I* limiter with an inductive load can produce large voltage spikes that may endanger the output transistors. If the spike causes the output node of the amplifier to go beyond the power supply rail, the power transistor will be subjected to reverse polarity and may be destroyed. For this reason, catch diodes are almost universally installed from the amplifier output node to each of the power rails to prevent the output node from going more than one diode drop outside the voltage defined by the rails. In some amplifiers that employ speaker relays, rail-clamping diodes are placed on the speaker side of the relay as well. If the relay opens when there is a large amount of stored energy in the loudspeaker, the clamping diodes will provide some protection for the relay contacts by limiting the flyback voltage to the rail voltage.

Avoiding the Use of *V-I* Limiters

The best *V-I* limiter is no *V-I* limiter. Avoiding the *V-I* limiter generally means building a more expensive output stage with greater total safe operating area. Over the years this has become more practical with the availability of power transistors boasting greater SOA and a reduced tendency to second breakdown. Such amplifiers still need short circuit protection. If these amplifiers are well designed and can survive a short circuit, they will often not need *V-I* limiters for purposes of adequate SOA when driving reactive loads. There will always be some risk, however. For example, if such an amplifier is called on to drive a highly reactive load with a very low effective series resistance of, say, 1 Ω, it might be in danger. A compromise condition is to design such an amplifier with a V-I limiter that is set for such high thresholds that it will only activate under conditions of extreme abuse. If executed well, such a V-I limiter will never activate in normal use and will be sonically transparent.

15.5   Testing Safe-Area-Limiting Circuits

Safe-area-limiting circuits can be tested by the use of large inductors and capacitors connected to the amplifier output to emulate a complex loudspeaker load, but this is not easy, especially in regard to obtaining an appropriate inductor that will not saturate under such conditions. Figure 15.5 showed a simplified electrical equivalent of an 8-Ω woofer in a closed box speaker system with a resonant frequency of 50 Hz. A 43-mH inductor and a 240-μF capacitor are required. Unlike the situation with a crossover inductor, some resistance in the inductor is not a problem and can be taken out of the 6.4-Ω series power resistor without serious damage to the behavior of the model. A motor starter capacitor can be used, as audio quality is not a big issue here. It is straightforward to extend this SOA load to emulate a two-way or three-way loudspeaker system.

Another possibility for SOA testing is to back-drive the amplifier under test from another larger, laboratory *load amplifier* through a load resistance. Such an arrangement is shown in Figure 15.17 [7]. If the amplifier under test is not fed with an input, its output will normally try to stay at zero, where the full rail voltage will be across each output transistor. This is often close to the most vulnerable situation encountered with realistic loads. The load amplifier can be driven with a sine wave at low frequencies that will exercise the output current at the fixed output voltage. One can then observe at what amplitude the amplifier under test goes into protection by seeing its output suddenly deviate from 0 V. Driving the load amplifier with a tone burst can further reveal the dynamics of the *V-I* limiter.
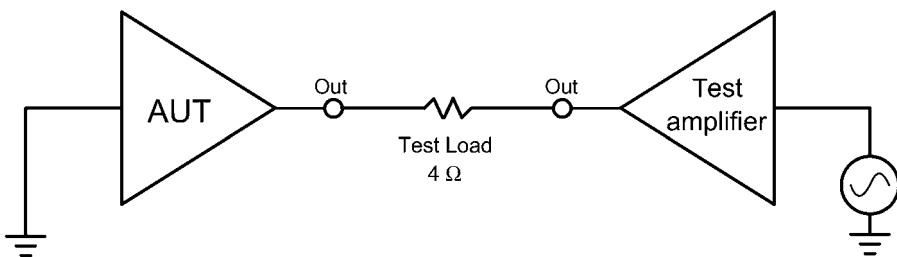
FIGURE 15.17   Back driving an amplifier to test SOA protection.

Another similar test can be carried out with two low-frequency sine waves at different frequencies. The second signal is applied to the input of the amplifier under test. As the sine wave signals beat against each other, virtually all combinations of voltage and current conditions for the amplifier will be exercised. The difference frequency of these two signals can be made large or small to exercise the SOA circuit's time constants in different ways.

Finally, the load amplifier can be configured with active filter circuitry to emulate a loudspeaker with chosen reactive load characteristics [7].

Simulation of Protection Circuits

SPICE simulation is directly applicable to the analysis of *V-I*-limiting circuits and can provide a great deal of insight. Simulation allows the examination of *V-I* limiter behavior with nearly arbitrarily complex loudspeaker loads that would be difficult to emulate with real passive components in the laboratory. It goes without saying that the use of real loudspeakers should be avoided when evaluating *V-I* limiter circuits at high power levels. The testing of amplifier protection circuits in the real world can be dangerous to the amplifier, so it is wise to carry out protection simulations before doing laboratory tests.

15.6   Protection Circuits for MOSFETs

The absence of secondary breakdown in MOSFETs means that most of the time they will not need *V-I* limiting for purposes of the usual safe area protection. This does not mean that they do not need protection. While lateral MOSFET amplifiers tend to be forgiving, vertical MOSFET amplifiers are not very forgiving of short circuits. This is because the vertical MOSFETs will gleefully try to put huge amounts of current into a short circuit load, unhindered by BJT realities like beta droop or lateral MOSFET realities like significant $R_{DS(on)}$ with a positive temperature coefficient. For this reason, fast-acting short circuit protection is desirable for vertical MOSFET power amplifiers. This was discussed in Chapter 11, Section 11.7. The fast electronic shutdown circuit for the output stage as described in Section 15.3 is especially useful here. If flying catch diodes are used as described previously, the shutdown circuit can be as simple as a small TRIAC or transistor that collapses the bias spreader, as was shown in Figure 16.12.

15.7   Protecting the Driver Transistors

If an output transistor is unable to drive the load (especially under short circuit conditions), the driver transistor may try to drive the load through the base-emitter junction of the BJT output transistor. This condition can also occur when the output is trying to

drive a very low-impedance load to high current where the output transistors are suffering from serious high-current beta droop. The smaller driver transistor may fail due to secondary breakdown. Safe operating area of the driver transistors must be considered. These concerns were discussed in Chapters 10 and 11. The protection of the output stage can be made more conservative to take into account the need to protect the driver transistors.

15.8   Loudspeaker Protection Circuits

It is very important to protect the loudspeaker from the results of an amplifier failure. Output transistors often fail shorted, meaning that the full power supply rail voltage may be applied to the output terminal of the amplifier. It is important that such a dangerous voltage be removed quickly, before it can do damage to the loudspeaker. Sometimes a speaker fuse or a rail fuse will blow quickly enough to protect the loudspeaker. In other cases a circuit that senses DC on the output of the amplifier will open a speaker relay, fire a crowbar TRIAC, or close a relay that shorts the amplifier output to ground. In the case of arrangements that deliberately short the output to ground under a fault condition, it is important that the amplifier can survive a short circuit by design.

Amplifiers that employ a DC servo naturally have a good monitoring point for excessive DC offset at the output of the amplifier. If the magnitude of the voltage at the output of the servo integrator is greater than some fraction of its range, the speaker relay is opened.

Speaker Fuses

Speaker fuses are inexpensive and not very interesting technically. They will usually protect a loudspeaker against a gross malady like an amplifier output stuck at the rail, but if the fuses are big enough to be reliable against demanding program material and low-impedance loads, they will be less protective of the loudspeaker. A 5-A standard-blow fuse in a 100-W/8-Ω amplifier stuck at its 50-V rail and delivering 7.8 A DC into an 8-Ω loudspeaker with 6.4-Ω DCR will survive for fully 5 seconds [6]. Do your expensive loudspeakers want that? Fuses also introduce thermal distortion and can suffer degradation of their contacts that will also lead to distortion.

The Speaker Relay and Its Control

The ubiquitous speaker relay is the most common first line of defense for loudspeakers. Key to its operation is its control circuit. Space does not permit a detailed discussion of such circuits, and there is good coverage elsewhere [1, 2]. Moreover, their design is usually straightforward given a good understanding of the functions that should be performed and the pitfalls to be avoided. A good speaker relay control circuit provides a comprehensive protection system and a well-behaved amplifier. Functions to be performed by the speaker relay system may include

- Protection against excessive DC at the speaker terminals
- Muting and thump elimination at turn-on and turn-off
- Power supply monitoring
- Speaker impedance monitoring
- Amplifier short circuit protection
- Retry after a delay following a fault

Protection of the loudspeaker from excessive DC at the output of the amplifier is important because most electronic protection circuits will not prevent application of the rail voltage to the loudspeaker if an output transistor fails shorted. The key issue in activating DC protection is the time constant. It should be long enough so that it does not trigger on legitimate high-amplitude low-frequency signals, including during amplifier testing down to at least 10 Hz.

Many amplifiers produce a thump when power is applied or removed. This is not necessarily a sign of bad amplifier design, but it is annoying and potentially damaging to loudspeakers. The speaker relay should be closed only after a delay following turn-on and should be opened immediately on turn-off before the rails collapse. The latter usually requires a power supply circuit that quickly detects loss of AC mains power. When turn-off is detected, it is also important to reset the turn-on delay timing circuit so that a full turn-on mute delay will occur if power is suddenly restored.

The DC power supplies should be monitored and verified to be within proper limits before the turn-on delay circuit is allowed to begin its sequence. It is especially important that turn-on not be allowed if one rail is down. Verification of the rail voltages should occur downstream from any rail fuses.

Simple circuits that test the speaker load resistance before the speaker relay is closed can be used to prevent the turn-on mute timer from proceeding. In some designs it is desirable for the relay control circuit to execute a retry following a fault. Such a retry may often incorporate a delay similar to that of the power-on mute delay.

Many of these functions can be conveniently implemented with an LM339 quad comparator. A small power MOSFET makes a good relay driver in such circuits. It requires virtually no gate drive current, its gate drive can be the full voltage of a +15 V supply, and a relay catch diode is not required to protect the transistor, as it is built into the MOSFET as the body diode. The body diode will permit a much higher relay coil flyback voltage than the usual silicon diode that is forward biased as soon as the coil voltage reverses. That slows down release of the relay. The higher reverse coil voltage allowed by the MOSFET allows faster release.

The TA7317 Loudspeaker Protection IC

No discussion of loudspeaker protection circuits would be complete without mention of the popular TA7317 integrated circuit expressly designed by Toshiba for the protection of loudspeakers [8]. This device is a 9-pin SIP for controlling a speaker relay. It performs the following functions:

- Over-current protection
- DC protection for the loudspeakers for two channels
- Delayed turn-on muting
- Fast turn-off muting
- Retry after about 3 seconds

Figure 15.18 shows a typical application circuit employing the TA7317. The IC is a convenient collection of transistors that provides the above functions. Most of its action is controlled by about 15 external passive components. The output at pin 6 controls the speaker relay with an open-collector Darlington driver. When the relay is energized, the loudspeaker is connected to the amplifier. Pin 6 can tolerate up to +60 V and can sink up
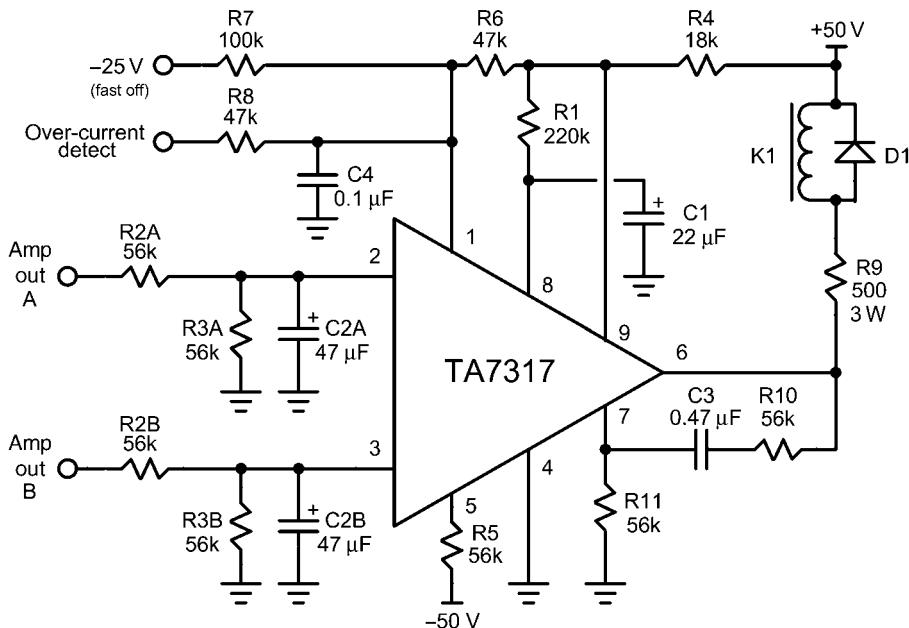
FIGURE 15.18 Typical protection circuit using the TA7317.

to 130 mA through the relay. Although the relay is powered here from a +50 V main rail, it can be powered from a low-voltage supply instead. The relay driver is controlled by a Schmitt trigger that provides hysteresis to prevent relay chatter.

Positive supply current is sourced to pin 9, where the voltage is shunt regulated internally to +3.1 V. R4 limits the current to the shunt regulator to about 2.5 mA. The supply current can be sourced from a lower-voltage supply like +15 V if desired. R5 provides 3 mA of negative bias current from a negative power supply.

The voltage applied to pin 8 controls muting. When power is applied, the voltage at pin 8 rises toward the 3.1-V supply at a rate controlled by R1 and C1. When the voltage on pin 8 reaches about +1.3 V, the speaker relay will be closed. If C1 = 22 μF and R1 is 100 kΩ, initial mute time is 2 seconds.

Pin 1 controls fast-off muting and over-current protection. It is connected to the base of an internal transistor whose emitter is connected to ground. When turned on, that transistor will discharge the pin 8 node and open the relay. If for any reason current is allowed to flow into pin 1, the relay will thus be opened. R6 sources a current of 50–170 μA to pin 1, depending on the voltage at pin 1. R7 sinks about 250 μA from pin 1, overcoming the current from R6. R7 is powered from a –25-V supply. This supply comprises a rectifier, small filter capacitor, and bleeder resistor (typically 1 μF and 15 kΩ). Its output will fall very quickly when power is removed. On shutoff, the current through R6 will drive pin 1 positive and quickly open the relay.

Over-current shutdown is controlled by current-limiting resistor R8, which sources current into the pin 1 node to open the relay. R8 is fed from an overcurrent detection circuit within the amplifier that supplies positive rail voltage when the current limit has been exceeded. When the over-current detect voltage goes to the positive rail, pin 1 goes

to $+1V_{be}$ and the relay is opened. A circuit similar to the opto-isolator circuit in Figure 15.12 can be used as the over-current sensor in the amplifier's output stage if it is connected to activate a PNP transistor whose emitter is connected to the positive rail.

Pins 2 and 3 are for DC detection for each of two channels. If the voltage at either pin goes high or low by $1V_{be}$, the relay will be opened. External components R2 and C2 filter the signal out and provide a delay for DC detection. R2 and R3 form an attenuator from the amplifier output signal to pin 2 (or 3). C2 must be large enough to prevent legitimate low-frequency signals from activating the protection circuit. If R2 = R3 = 56 kΩ and C2 = 47 μF, a DC level of 30 V will trigger shutdown in about 70 ms. A DC level of about 3 V will trigger the circuit in about 1 second.

R10, R11, and C13 act as a speedup circuit for opening of the relay by providing some initial positive feedback. When the relay is opened for any reason C1 of the turn-on mute circuit is discharged, forcing a new turn-on delay sequence. This means that the device will execute a retry after a few seconds. If the cause of the problem has been removed, normal operation will resume.

Protecting the Speaker Relay

When a speaker relay does its job by breaking the circuit to the loudspeaker, it may suffer damage from arcing. Pitted contacts may result. That will lead to increased relay distortion (see Section 11 of Chapter 13). Opening a circuit in the presence of significant DC current flow can be particularly harmful (this can happen when the amplifier output goes to the rail). Relays are not good at breaking DC at high currents due to continuous arcing. Indeed, relays are usually rated for less current and voltage when used in a DC circuit. For these reasons it is important to use speaker relays with adequate contact area and generous current ratings; too many amplifiers employ flimsy speaker relays.

Figure 15.19 shows some circuitry that can be used to reduce the likelihood of contact damage when relay K1 opens. Always remember that the output stage Zobel network (R1-C1) must be placed upstream from the relay, since amplifier stability must be preserved when the relay is open. A second Zobel network (R2-C2) on the downstream side of the output coil in a pi network arrangement can be placed after the relay. This will reduce slightly the open-circuit voltage rate of change when the relay opens. An R-C snubber (R3-C3) placed across the relay contacts can reduce the chance of arcing when the relay opens. The capacitor slows the rate of change of the voltage across the
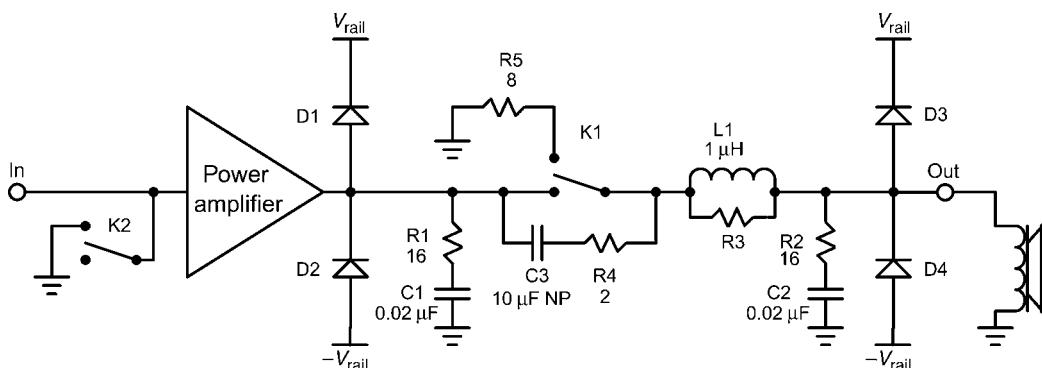
FIGURE 15.19   Some relay contact protection approaches.

contacts on opening while the series resistor prevents excessive current flow through the capacitor if a voltage difference exists when the contacts close. This network will cause some audio leakage during the muting time. Relay K2 can be used to kill the audio input to the amplifier during muting, preventing any significant voltage differential across the K1 contacts when they close. Resistor R5 provides a path for speaker current flow when K1 closes its NC contacts.

It is also important to limit the maximum voltage that can appear across the relay contacts as a result of flyback from an inductive speaker load. This is no different than the reason for the traditional rail catch diodes (D1-D2) that are placed from emitter to collector of BJT output transistors. A second set of such catch diodes (D3-D4) should be placed on the downstream side of the relay contacts.

Closing the Feedback Loop Around a Protection Device

Fuses and relays in the signal path can introduce distortion, so it is tempting to enclose them in the global negative feedback loop so that their distortion will be reduced by feedback. This is fine, but with one major caveat. When the protection device opens, the feedback loop will be opened and the amplifier will operate open loop, possibly resulting in damage and undesired effects. If the loop is closed around a relay and that relay is used for turn-on mute delay, nasty signals could be initially presented to the loudspeaker while the feedback loop stabilizes. This could be especially problematic if the DC output of the amplifier has drifted to a high offset value. For this reason it is wise to keep the feedback loop closed in some way when the protection device is open. Figure 15.20a shows one approach to enclosing a speaker relay or a fuse in the feedback loop.

R1 and R2 make up the usual feedback network, but R3 is also put in the path to the amplifier output terminal after speaker relay K1. R3, at 100 Ω, allows the injection of negative feedback by diodes D1 and D2 even when the output is a short circuit. In normal operation the signal present at the junction of R3 and R2 is slightly less than the full amplifier swing. R4 and R5 attenuate slightly the output of the amplifier before

(a)
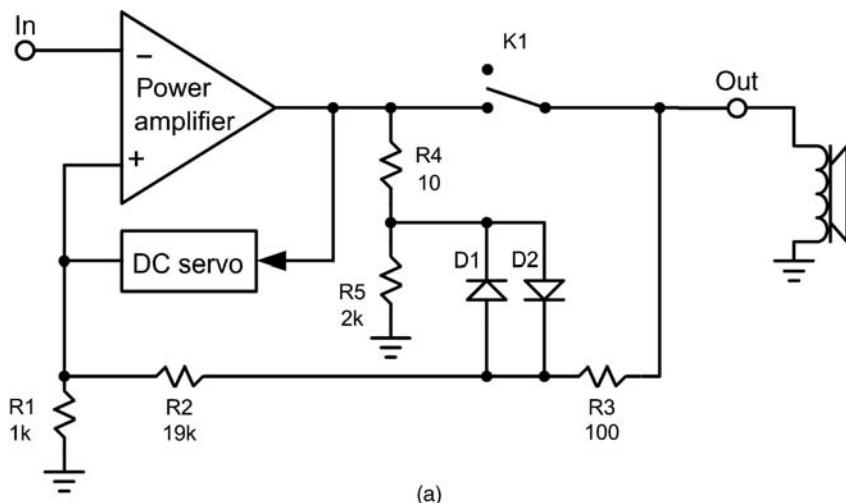
FIGURE 15.20   Enclosing the speaker relay in the global feedback loop.
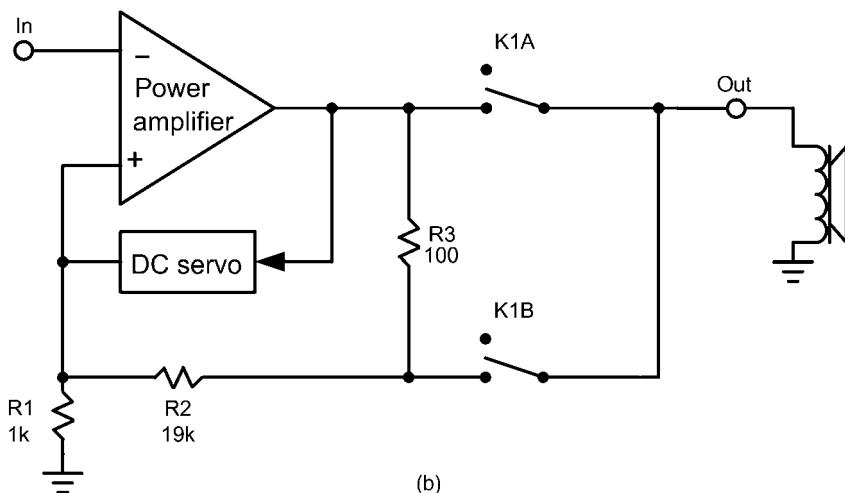
FIGURE 15.20   Enclosing the speaker relay in the global feedback loop. (*Continued*)

application to diodes D1 and D2 so that in normal operation there is no signal across the diodes to cause distortion.

A second approach that uses a second set of relay contacts is shown in Figure 15.20b. Resistor R3 provides negative feedback directly from the amplifier output node when the K1A speaker relay contacts are open. When the relay is closed, the K1B contacts short the feedback takeoff point to the downstream side of the K1A contacts, enclosing K1A in the feedback loop.

Notice that this amplifier uses a DC servo and that the servo takes its feedback directly from the amplifier output so that it can drive the DC output level to 0 even when K1 is open. There are many variations and improvements that can be made to this approach. Notice that in Figure 15.20a a small amount of signal and possible thump will be allowed to sneak through R3 to the loudspeaker during the muting periods. In such amplifier designs it is also wise to short out the input signal during the muting interval.

Crowbar Circuits

Crowbar circuits act by deliberately placing a dead short across the output of the amplifier to protect the loudspeaker. These circuits will usually be triggered by the presence of an excessive DC offset at the output of the amplifier. A TRIAC or relay is usually employed for this function. When crowbar protection is used, the amplifier should obviously be designed to withstand an output short circuit. Nevertheless, the priority for the crowbar circuit is to protect the loudspeaker.

Avoiding Speaker Relays

If electronic shutdown circuits and an output crowbar are used, the speaker relay can be avoided entirely. The muting function can also be handled by the electronic shutdown circuit if some aspects of its operation are designed to be non-latching.

Protection Processors

Together the control of amplifier and loudspeaker protection circuits can become complex. An attractive alternative is to use a small processor (like a PIC) to control these functions. In some cases, the processor I/O will be interfaced to portions of the amplifier through opto-couplers.

References

1. Duncan, Ben, *High Performance Audio Power Amplifiers*, Newnes, 1996.
2. Slone, G. Randy, *High-Power Audio Amplifier Construction Manual*, New York, McGraw-Hill, 1999.
3. Fairchild data sheet for 2SC5200/FJL4315.
4. Howard, Keith, "Heavy Load: How Loudspeakers Torture Amplifiers," *Stereophile,* July 2007.
5. Benjamin, E., "Audio Power Amplifiers for Loudspeaker Loads," *JAES,* vol. 42, no. 9, September 1994; available from www.aes.org.
6. Littelfuse data sheet for 2-Amp fuse (3AG).
7. Dymond, Harry C. P., and Phil Mellor, "An Active Load and Test Method for Evaluating the Efficiency of Audio Power Amplifiers," *J. Audio Eng. Soc.,* vol. 58, no. 5, pp. 394–408, May 2010.
8. TA7317 Audio Protection IC data sheet, Toshiba, 1989.

This page intentionally left blank

Power Supplies and Grounding

$\mathbf{P}$ ower supply design and grounding arrangements are too often the stepchild of the creative process when it comes to audio amplifier design. Poor power supply and grounding techniques can ruin an otherwise outstanding design by allowing grunge into the signal path in many different ways. Poor power supply regulation and inadequate power supply current capability can impair amplifier performance and limit the ability of amplifiers to drive difficult loads, especially at low frequencies.

16.1   The Design of the Power Supply

The power supply must convert the AC mains voltage into reliable and stable negative and positive DC rails. It must provide adequately small ripple and sufficient reserve current and regulation. Mains noise must not be communicated to the circuit side of the power supply.

Figure 16.1 shows a typical power supply for an audio power amplifier. In its simplest form it consists of a power transformer with a center-tapped secondary feeding a high-current bridge rectifier that produces positive and negative rails that are filtered by large reservoir capacitors. The design shown employs a 240 volt-ampere (VA) toroid with a pair of secondary windings each rated at 42 V RMS. The arrangement shown produces about 59 V DC on each rail with no load and about 52 V DC with a 2-A load on each rail.

Bleeder resistors are connected across the reservoir capacitors. This assures that the rail voltages fall to zero in a reasonable time after power is removed. So-called X capacitors are connected across the primary and the secondary windings to reduce noise. X capacitors used on the mains side must be of the type designed for continuous connection across the mains. They should be mounted on the mains side of the power switch close to the mains wiring entrance and should be shunted by a bleeder resistor to discharge any residual voltage that may be present after power is disconnected. IEC power inlet connectors with integral EMI filters usually include X capacitors.

Alternative Supply Arrangements

An alternative arrangement employs two secondary windings and two bridge rectifiers as shown in Figure 16.2. One possible advantage to this design is that it avoids the circulation of direct current through the transformer windings when the positive and negative rail load currents are different. The flow of direct current through transformer windings (primary or secondary) should be avoided, as it can degrade transformer
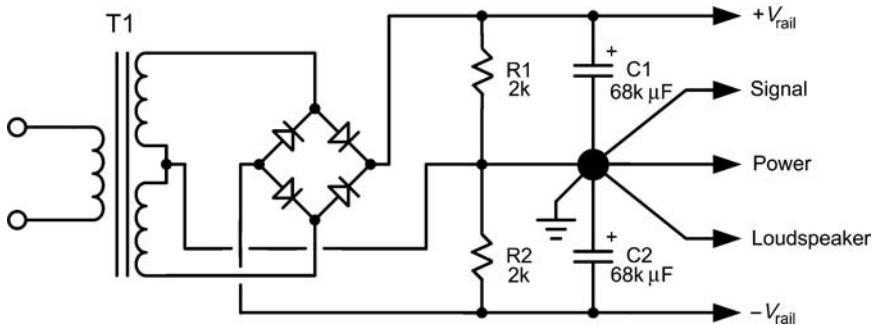
FIGURE 16.1   A typical amplifier power supply.
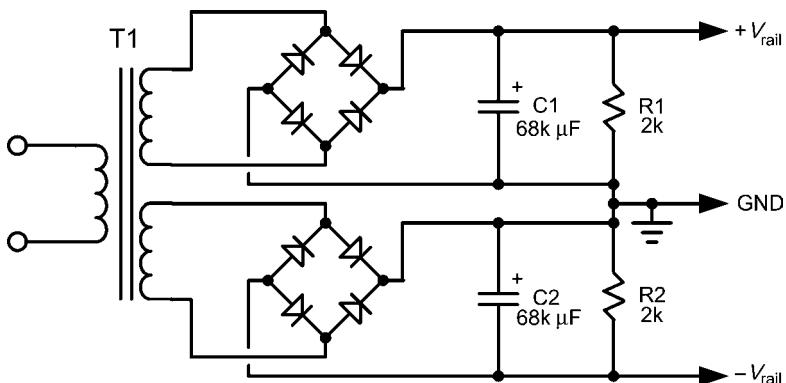
FIGURE 16.2   An alternative rectifier arrangement.

performance and sometimes create transformer buzzing. Toroid transformers are some-times more sensitive to this effect than transformers of conventional construction.

The rectifier current pulses for each half of the supply do not circulate through ground, but rather circulate locally. This may improve management of rectifier noise. Indeed, there is no direct connection of the secondary winding(s) to ground. This also means that the transformer is only connected to the amplifier during the brief rectifier conduction inter-vals. This may reduce the opportunity for mains EMI to enter the amplifier circuits. There does not appear to be universal agreement on the potential benefits of this connection.

This arrangement comes at a price. It suffers twice the voltage loss through the bridge rectifiers and costs more because of the doubling of the number of rectifiers. The added cost is not insignificant if expensive fast-recovery rectifiers are employed. On a fixed budget, I would opt for better rectifiers in the conventional arrangement.

Boosted Supply Rails

A number of amplifier designs employ boosted rails for the IPS and VAS circuits. The availability of slightly higher rail voltages for these circuits provides extra headroom to reduce distortion or allow the introduction of VAS cascodes without wasting output stage headroom on the main high-current rails. The boosted rails also make the intro-duction of Baker clamps more convenient. Boosted supplies will often add 5–10 V to the main rails. Although boosted supplies represent an increase in complexity of the power

supply, it is important to recognize that the current demands on them are very small compared to those on the main rails.

The most common way to realize boosted supplies is to add two low-current windings to the main windings of the power transformer, connected to the "ends" of the main winding of the transformer in Figure 16.1. The higher resulting AC voltages are then rectified with a single full-wave bridge equipped with its own small reservoir capacitors. In such an arrangement, when the output stage drags down the main rails, the boosted rails will not be dragged down with them because they have their own reservoir capacitors. Similarly, the boosted rails will tend to have smaller ripple voltages on them. There are many other ways to realize boosted supplies, including the use of a small dual-secondary auxiliary transformer if a main transformer with custom boost windings is not available.

Power Supply Stiffness and Regulation

The ideal power supply has infinite *stiffness,* meaning that its output voltage will not change as a result of differing output current demands. This is referred to as *load regulation.* An amplifier built with an extremely stiff power supply will come close to putting out twice as much power into a 4-Ω load as into an 8-Ω load, and in some cases four times as much power into a 2-Ω load (assuming no output stage limitation).

An important trade-off in stiffness of the power supply is the amplifier's *dynamic headroom,* which is the ratio of maximum short-term burst power to maximum continuous power. This reflects the fact that the amplifier can produce more power when the power supply is lightly loaded and can maintain high rail voltage for a brief period of time due to the charge stored in its reservoir capacitors. Eventually the rails will sag under the continuous power conditions and maximum output power will be smaller. A power supply with less stiffness will produce an amplifier with more dynamic headroom. Having significant dynamic headroom is good because it provides reserve power for signal peaks without costly increases in the power supply. However, sound quality may suffer because of the increased rail voltage fluctuations.

Figure 16.3 shows the output voltage of the power supply of Figure 16.1 as a function of load current drawn from each of the rails. This power supply employs a pair of
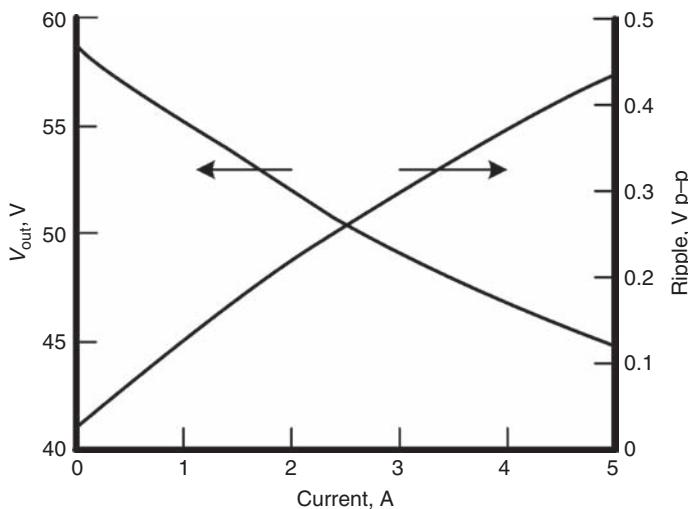
FIGURE 16.3   Output voltage as a function of load current; $R_{eff} = 2.6~\Omega$.

68,000 µF reservoir capacitors. The ripple voltage is shown as a function of load current on the right-hand scale.

Effective Power Supply Resistance

The curve shown in Figure 16.3 illustrates that it is not a bad approximation to assign an effective power supply resistance R_{eff} to each rail of the power supply for estimating power supply sag in typical power amplifiers. The effective resistance here is about 2.6 Ω for each rail at load currents greater than 1/10 of the full amount shown.

The transformer's primary and secondary winding resistances influence power supply regulation. The primary resistance for this 240 VA transformer is 1.7 Ω and the secondary resistance (end-to-end) is 1.1 Ω. The mains voltage for these tests was 119 V and the mains impedance was 0.3 Ω.

16.2   Sizing the Transformer

Picking the power transformer can be tricky because the VA and current ratings for power transformers are often given for AC loads, even though the relevant application here is for rectified DC loads. The same goes for load regulation. The VA rating is the product of the AC output voltage and the rated AC output current. The rated output current will typically be that current where the core temperature reaches 60°C and is often the point where the AC output voltage sags between 5% and 10% from the no-load value. The transformer of Figure 16.1 sags from 90 V RMS at no load to 84 V RMS at its rated load of 2.8 A AC, for a sag of 7%.

Many manufacturers rate their transformers in volt-amperes assuming a resistive AC load. This is far from reality for a DC power supply for an audio amplifier, with very high peak rectifier currents and small conduction angles. Figure 16.4 shows the rectifier current waveform when the power supply of Figure 16.1 is supplying 2 A to each rail. The scale is 2 A per division.
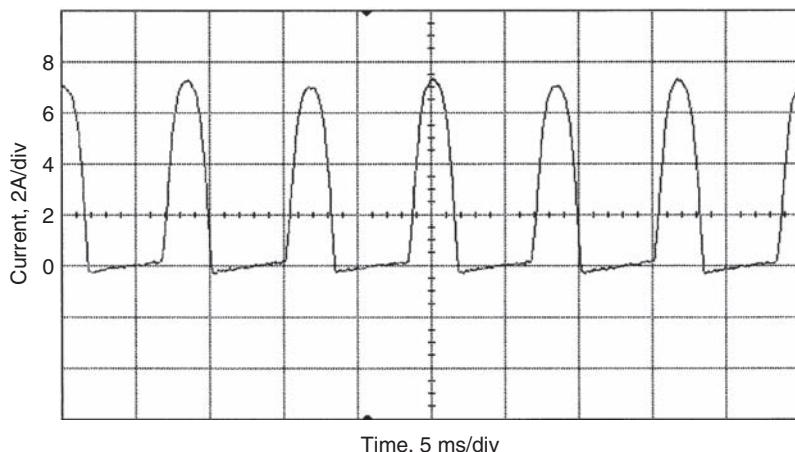
Figure 16.4   Rectifier current waveform when load current is 2 A.
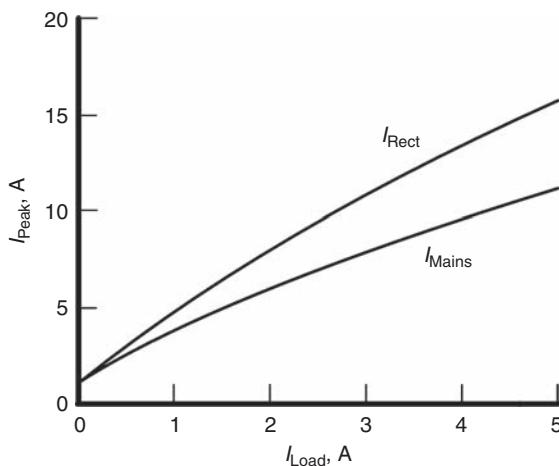
FIGURE 16.5   Peak rectifier current and mains current versus load current.

Figure 16.5 shows the peak rectifier current as a function of load current for the power supply. The peak rectifier current does not increase linearly with load current because the rectifier *conduction angle* increases with load current as well, increasing the area under the conduction pulse. The second curve shows the peak currents as seen at the mains side of the power transformer.

There is no right or wrong choice of transformer because different transformers will largely affect the stiffness of the power supply as described above. To first order, one chooses a hefty enough transformer to achieve the degree of stiffness (load regulation) that is desired. Bear in mind that a transformer may be rated for its maximum VA on the basis of core temperature for continuous duty at that load, but in the case of an audio power amplifier the average load is much smaller. For consumer audio, sag under peak load is more important than core temperature.

VA Rating Rules of Thumb

A good rule of thumb is to employ a transformer with a VA rating that is twice the maximum rated power to be delivered by the amplifier. The 240-VA transformer in the power supply of Figure 16.1 sags by 5 V on each rail when the amplifier output is increased from 5 W to 125 W with a load impedance of 8 Ω. The rail voltages sag an additional 4 V down to 48 V when the amplifier is delivering 200 W into a 4-Ω load.

VA versus Weight

The 240-VA toroidal transformer weighs 2.3 kg. This suggests that a reasonable approximation is 104 VA/kg. This is useful in estimating the VA of an unknown surplus power transformer. Other toroidal transformers appear to range between 100 and 140 VA/kg.

Toroid versus Conventional

Toroidal power transformers tend to be more efficient than transformers of conventional construction. They also better confine the noisy magnetic fields that result from large

rectifier spikes. There is little cost premium for toroidal transformers. Some claim that transformers with C-core or EI construction sound better, but this is unsubstantiated.

The advantages of toroidal transformers over conventional laminated transformers include [1]

- High efficiency
- Small size
- Low mechanical hum and buzz
- Low stray magnetic field
- Low no-load losses
- Light weight
- More available turns/layer
- Less copper length due to longer effective bobbin length
- Magnetic field running in grain-oriented direction of the steel

It is very important that the bolt through the center of the toroid not be allowed to create a shorted turn by having both ends of it conductively tied to the chassis. One end of the bolt should float. It is also undesirable to mount one toroid on top of the other.

Modifying Toroidal Transformers

Sometimes a different voltage or an additional winding is needed on the power transformer. A good example is a pair of extra windings to implement a boosted rail supply. Toroidal power transformers lend themselves ideally to this because of their open construction. Additional turns can easily be wound on the transformer by hand if the number of turns is not great. The first thing to do when contemplating such a modification is to measure the voltage per turn of the transformer. Wind 10 turns of wire on the toroid, measure the voltage on this added winding, and divide by 10.

The 240-VA transformer used in the power supply of Figure 16.1 has 0.36 V/T. Twenty turns will yield 7.2 V RMS, enough to provide a rail boost of about 9 V DC depending on the boost rectifier architecture. For this application the wire gauge of the added turns can be quite small. The number of volts per turn will vary somewhat by manufacturer and details of construction, but it appears to increase very roughly as the square root of the VA rating of the transformer.

16.3   Sizing the Rectifier

The rectifier in a conventional power supply is subjected to very high peak currents that have a fairly low conduction angle (duty cycle). These very high peak currents cause substantial voltage drops across the rectifier junctions, resulting in some reduction of the output voltage and in heating of the rectifier.

A common mistake is to undersize the rectifier by thinking in terms of the maximum delivered DC current. In such a case excessive rectifier forward voltage drops will occur and reliability of the rectifier will be degraded. Bridge rectifiers rated at 35–50 A are recommended for audio power amplifiers. The rectifier should be bolted to the chassis to keep it cool. The typical voltage drop for each diode in a 35 A full wave bridge is about 1.0–1.2 V at a peak current of 30 A.

16.4   Sizing the Reservoir Capacitors

The primary job of the reservoir capacitors is to maintain the output voltage during the time between charging pulses from the rectifier; this will reduce ripple. Calculating the ripple for a given load current and reservoir capacitor is fairly straightforward. The peak-to-peak 120-Hz ripple will be a sawtooth waveform at 120 Hz. The peak-to-peak ripple voltage can be approximated by recognizing that the voltage developed across a capacitor is $V = I * T/C$, where T will be 8.3 ms for a full-wave rectifier operating at 60 Hz. For the circuit of Figure 16.1 operating at a load of 2 A and with 68,000 µF reservoir capacitance (0.068 F), the ripple on each rail is estimated to be $2.0 * 8.3e - 3/6.8e - 2 = 0.24$ V.

The measured value for that circuit is 0.2 V p-p, as shown in Figure 16.6. The slope of the rising edge is indicative of peak rectifier current, while the slope of the falling edge is indicative of the load current. Bear in mind that capacitor tolerances are wide. The 68,000-µF capacitor used here actually measured about 80,000 µF.

While the reservoir capacitor is important for minimizing ripple, a large reservoir capacitor is also desirable for providing very high output current on a transient basis for brief bursts of program material.

Equivalent Series Resistance (ESR) and Inductance (ESL)

Figure 16.7a shows a simplified equivalent circuit for a high-quality 50,000-µF reservoir capacitor. It is important to recognize that the reservoir capacitors have some *equivalent series resistance (ESR)* and that the extremely high-peak currents of the rectifiers will create some voltage drop across the ESR independent of how large the capacitance is. This resistance varies considerably with the type and construction of the capacitor, but a value of 12 mΩ is not unusual. This means that a 7-A rectifier pulse may create a drop of 84 mV across the capacitor. Some evidence of this effect can be seen at the positive peaks of the ripple waveform in Figure 16.6.
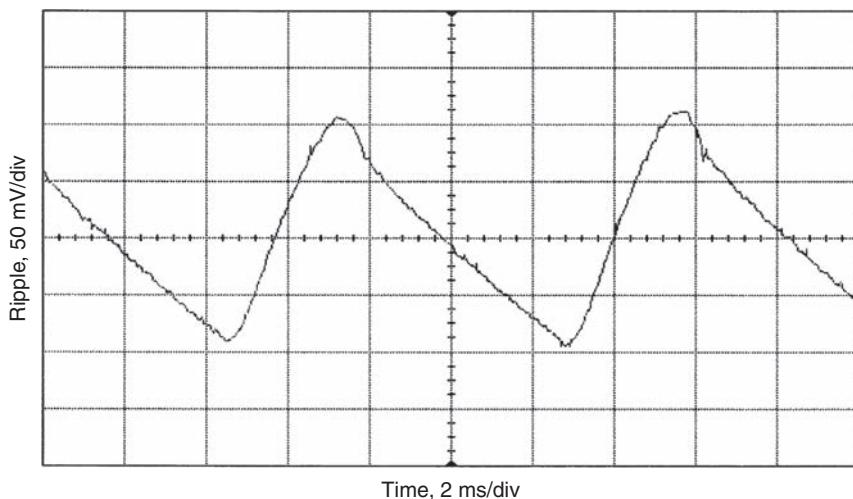
FIGURE 16.6   The ripple waveform for the circuit of Figure 16.1 with a 2-A load.
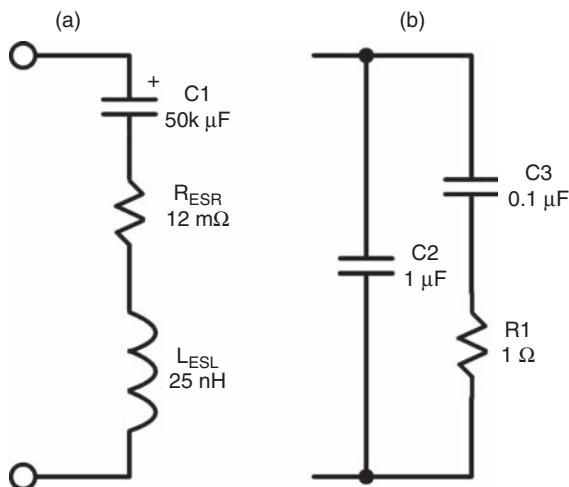
Figure 16.7 (a) Simplified equivalent circuit for a 50,000-μF reservoir capacitor. (b) A bypass/snubber arrangement.

Most capacitors also have a modest amount of *equivalent series inductance (ESL)*. This is often the result of the way they are constructed with windings. This means that at high frequencies the impedance of the capacitors actually starts to rise instead of continuing to decrease. The 25-nH value for the capacitor of Figure 16.7 is quite low.

Reservoir capacitors are sometimes also characterized by a resonant frequency, where their impedance dips almost to the value of the ESR when the capacitance and inductance series resonate. This is often in the range of tens to hundreds of kHz.

Bypasses and Snubbers for Reservoir Capacitors

Because large reservoir capacitors are far from perfect at high frequencies, performance can be improved by the addition of extra filtering components that have better high-frequency characteristics. One example is shown in Figure 16.7b. The most common approach is to bypass the reservoir capacitors with a quality film capacitor of 1 μF or more as done with C2 in the figure. This will generally assure that the combined impedance will continue to fall at high frequencies above the resonant frequency of the reservoir capacitor. Even with a bypass capacitor in place there often remains the possibility of impedance peaks due to wiring and component inductances that can form tank circuits at high frequencies. The addition of the 1-μF capacitor in Figure 16.7b actually created a resonance at about 1 MHz where the net impedance more than doubled to about 0.3 Ω.

For this reason a high-frequency *snubber* circuit can be added as well. The snubber in Figure 16.7b consists of R1 and C3. It is not unlike a Zobel network. At high frequencies it transitions to a damping circuit with a resistive behavior. Notice that 0.1 μF and 1 Ω are used here. The transition from capacitive to resistive for this network occurs at about 1.6 MHz. It is important that the capacitor has low ESR and ESL. This snubber will not do much for the 1-MHz resonance, but will help at higher frequencies. Finally, connection of a low-ESR/ESL 100-μF electrolytic capacitor across the reservoir capacitor can be very helpful. Its ESR can actually help damp resonances like the one at 1 MHz mentioned here.
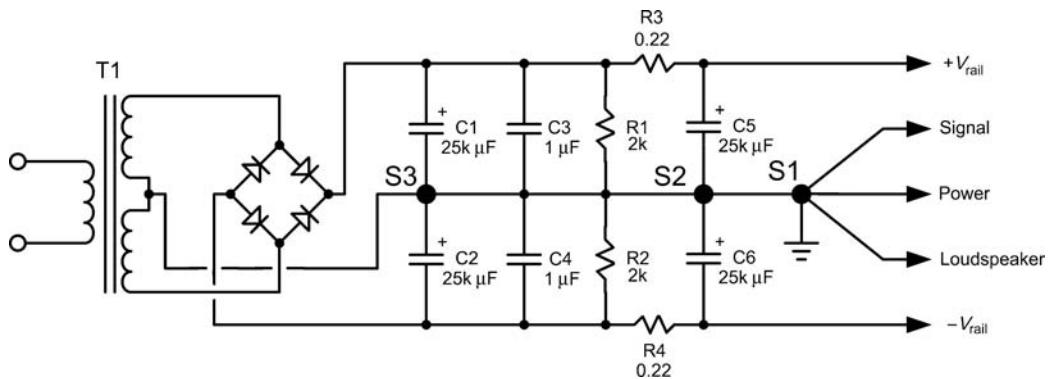
Figure 16.8 Split reservoir capacitor arrangement.

Split Reservoir Capacitors

Often two smaller reservoir capacitors will have an advantage over a single reservoir capacitor in terms of both ESR and ESL. If two reservoir capacitors are used, an additional advantage can be had by placing a small resistor in series in the rail line between them, as shown in Figure 16.8. A 0.22-Ω resistor is much smaller than the typical power supply effective resistance, and yet it can have a remarkable effect on reducing ripple and high-frequency noise content. Consider that the corner frequency of a 25,000-µF second reservoir capacitor against a 0.22-Ω resistor is only 30 Hz. This means that the 120-Hz ripple frequency will be attenuated by an additional 12 dB in this arrangement. This is a case where it is good if the resistor is an inductive wire-wound type; the added inductance can only help. The added 0.22 Ω of rail resistance is fairly small compared with the effective power supply rail resistance of 2.6 Ω, so that any added voltage loss is of little concern. Notice that the grounds for the two sets of capacitors should be physically separated in the grounding topology as shown in Figure 16.8. This will be discussed further in Section 16.9 on grounding.

16.5 Rectifier Speed

During the forward conduction pulse the peak current through the rectifier diode can be very high. As with any P-N junction, there exists a large stored charge in the form of minority carriers during this time. When the driving AC waveform decreases below the DC level stored in the reservoir capacitor on the other side of the diode, the diode must turn off, but it cannot do that instantaneously as a result of the stored charge. This charge must be sucked out of the diode by means of reverse current flow through the diode. The amount of time it takes to pull out this charge is a measure of the diode's speed and is referred to as its *reverse recovery time* (t_{rr}). The pulse of reverse current flow is especially undesirable because it can lead to RF emissions.

The power supply of Figure 16.1 uses an ordinary 35-A bridge rectifier. The reverse recovery current manifested itself as a 500 mA p-p negative current pulse lasting 30 µs when the rectifier in the power supply turned off. The pulse had very sharp edges with rise times on the order of 1 µs. The load current for this test was 2A. The reverse recovery pulse is not visible in Figure 16.4 due to the limited bandwidth of that measurement.

Soft Recovery and Fast Recovery

Diodes that are designed to have a fast recovery will create less noise because the amount of energy that must be sucked out of them during turn-off is smaller, leading to much shorter duration of the reverse current interval and consequent turn-off spikes. One type of fast recovery diode is the *Fast Recovery Epitaxial Diode (FRED)* [2]. While a conventional bridge rectifier may have a rated reverse recovery time of 350 ns, a FRED may have a t_{rr} of 35 ns. The trade-off is that FREDs cost more and sometimes have a larger forward voltage drop at a given forward peak current.

At the end of the reverse current interval, the diode finally turns off and its current returns to zero (where it should be in the off state). Once the excess carriers are swept out of the junction, some diodes will have their reverse current go to zero very quickly, almost snapping back. This high rate of change of reverse current can create more noise at high frequencies. Diodes that are designed to have a *soft recovery* have a more gradual return to zero of their reverse current. The smaller rate of change of falling reverse current causes less production of high-frequency noise. Some of the better fast recovery diodes are also characterized by soft recovery. The Vishay HEXFRED® devices are a good example [3].

Rectifier Noise and Snubbers

Rectifier noise due to turn-on and turn-off can be reduced by using snubber networks across each diode in a bridge, as shown in Figure 16.9. The resistors shown are often not used, but can be helpful in damping resonance effects. The snubber networks should be mounted right on the rectifier terminals. The use of damping resistors makes this more difficult, so there is a trade-off.

Measuring Rectifier Performance

Measuring the voltage across a rectifier diode with an oscilloscope under actual high-current DC load conditions can be very revealing. The two things of greatest interest are the peak forward drop across the diode and the turn-off characteristic of the diode.
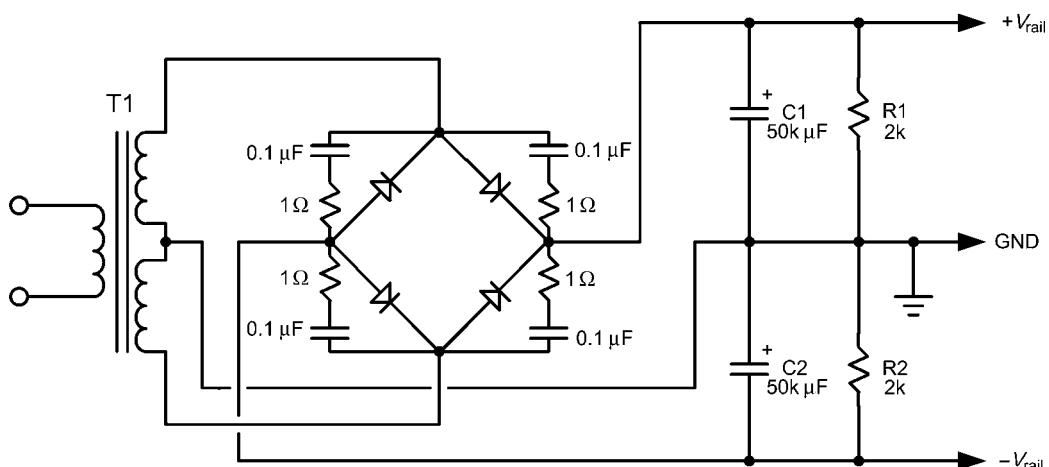
Figure 16.9 A bridge rectifier with snubber networks.
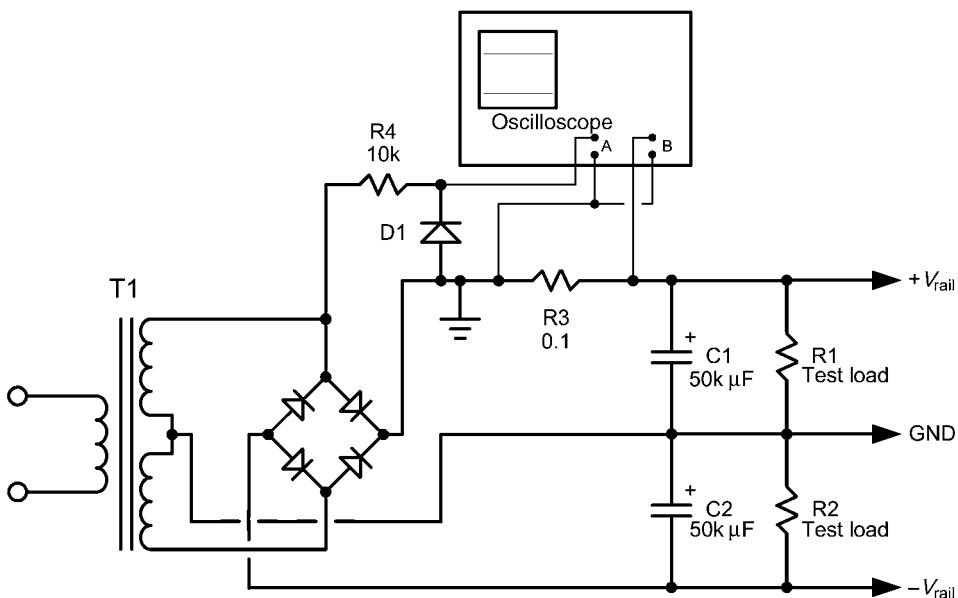
FIGURE 16.10   Measuring rectifier performance.

This measurement can be difficult to do in a conventional arrangement due to the common mode and reverse voltages present. However, by reconfiguring a bridge rectifier arrangement, one can do this. The key is to arrange the circuit so that one side of the diode, the cathode for example, is connected to ground. The remainder of the power supply is then allowed to float. Such an arrangement is shown in Figure 16.10.

The cathodes of the positive-output diodes of the bridge rectifier are connected to ground while the rest of the secondary DC rectifier circuit, reservoir capacitors, and dummy load resistors float. A 0.1-Ω resistor between the positive output of the bridge rectifier and the positive reservoir capacitor allows the measurement of rectifier current with an oscilloscope. If the scope probe is moved to one of the AC input sides of the bridge, the voltage drop across the bridge diode can be observed. However, the reverse voltage will be large, making it difficult to read the forward voltage. For this reason, a resistor-diode combination is employed to clamp the reverse voltage to one diode drop, allowing a more sensitive oscilloscope setting.

16.6   Regulation and Active Smoothing of the Supply

One might think that an ideal audio power amplifier would employ voltage-regulated power supplies. While this would often make a fine power amplifier, it would add greatly to the cost and power dissipation. An amplifier with regulated power supplies does not have any *dynamic headroom* because the power supply does not rise during low-power periods to be able to provide larger bursts of power on transients.

The job of a power supply regulated for constant output voltage is made even more difficult when you consider the mains voltage fluctuations. If you design the supply to deliver a fixed voltage under conditions of worst-case low mains voltage (without
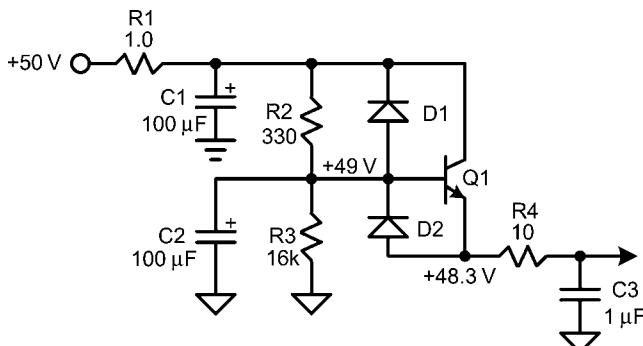
FIGURE 16.11 A capacitance multiplier filter.

falling out of regulation), then the voltage regulator (assuming it is a linear regulator) will be dissipating a large amount of heat as it throws away the extra rail voltage under conditions of worst-case high mains voltage.

Switching power supplies, on the other hand, usually produce a regulated output without the penalty of wasted power. These are discussed in Section 16.13.

Regulation of Input and VAS Power Supplies

It makes much more sense to regulate the power supplies feeding the input circuits and VAS because these circuits consume much less current. This is an alternative to the usual R-C filtering of the main supply that is used to power these circuits. Once again, regulation to a fixed voltage deprives the amplifier of operation at higher output power levels that are possible when the mains voltage is above the minimum value. For this reason, capacitance multiplier filters are often used for these circuits. Such a circuit is shown in Figure 16.11. The headroom loss can be designed to be less than 2 V if ripple on the main power supply is not excessive. A further advantage is that the filtered output of the capacitance multiplier can be referenced to the quiet ground without dumping a lot of ripple current into that ground.

Q1 is the pass transistor while R2 and R3 drop the input voltage by 1 V so that Q1 operates with 1-V collector to base. An additional 0.7 V is dropped through the base-emitter junction to arrive at the output voltage. R1 and C1 prefilter the input to the capacitance multiplier. C2 is the multiplier capacitor and it forms a pole at 5 Hz for filtering purposes. Diodes D1 and D2 protect Q1 from voltage reversals. Vertical power MOSFETs also make good pass transistors for capacitance multipliers if you are willing to tolerate a bit more voltage drop, which will be on the order of the threshold voltage or a bit more.

16.7   SPICE Simulation of Power Supplies

Simulating a power supply with SPICE is not always the first thing that comes to mind, but it can be valuable and provide a lot of insight. In particular, it can help in understanding peak rectifier currents, rectifier turn-off issues, the effect of snubbers, and the behavior of different kinds of reservoir capacitors and arrangements. The accuracy of the results can be greatly improved by having good models for the components used in

a power supply, but valuable insight can be gained even with very approximate models. For the more adventurous, some of the power supply components can be modeled by straightforward measurements. These include transformer winding resistances and inductances, rectifier V-I characteristics, and reservoir capacitor ESR and ESL. It is also wise to include estimates of parasitic wiring inductances in these simulations.

16.8   Soft-Start Circuits

All amplifiers are characterized by *inrush current* when they are turned on. At minimum, this burst of mains current is required to quickly charge up the reservoir capacitors. Some transformers, toroids in particular, also can draw an initial large magnetizing current depending on where in the AC cycle the power is applied. The inrush current for large amplifiers employing efficient toroid power transformers and large amounts of reservoir capacitance can be very high. Figure 16.12 shows the AC inrush current for the power supply of Figure 16.1. Peaks in excess of 40 A can be seen. In some extreme cases this could damage power switch contacts or even blow circuit breakers. In other cases the inrush current can degrade reservoir capacitors. Bear in mind that the power supply of Figure 16.1 is not for a big amplifier.

Passive Soft-Start Circuits

Passive soft-start circuits rely on a temperature-dependant resistance placed in series with the mains line. Such devices are called *power thermistors* or *negative temperature coefficient resistors (NTC)*. At room temperature these devices typically have a resistance on the order of 1 Ω to 5 Ω. This puts a limit on the inrush current. Under load, these devices heat up and their resistance falls, often to tenths of an ohm or less. These devices get hot, sometimes reaching temperatures of 180°C. The NTC device also takes time to cool
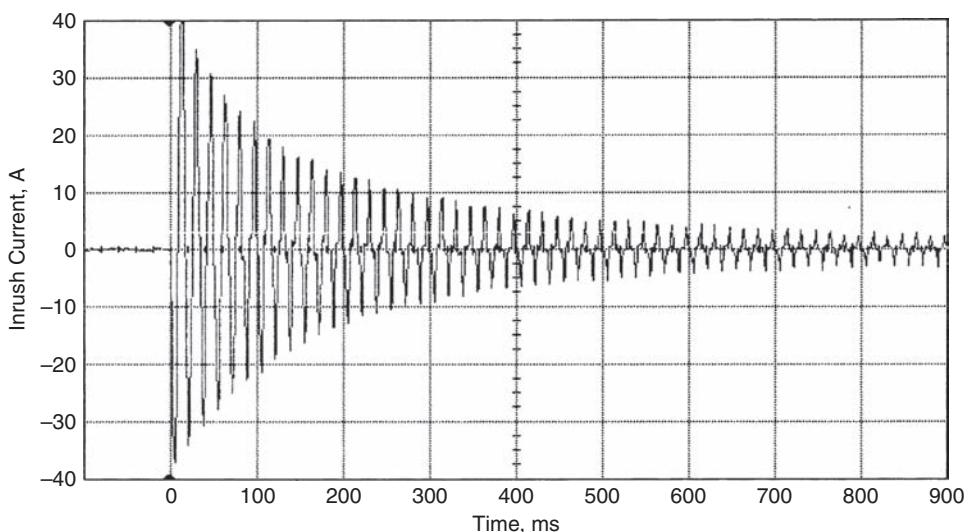
FIGURE 16.12   AC inrush current waveform for the power supply of Figure 16.1.

down and increase its resistance after power is shut off. This means that if power is restored quickly after turn-off, an unexpectedly high surge current may result.

The high peak currents encountered at the transformer primary under load due to rectifier spikes also raise concerns about the resistance introduced by a passive inrush controller. The size of these peaks is shown in Figure 16.5. When the supply is loaded with 2 A on each rail, these peaks are about 6 A. A passive inrush controller might be rated at 0.1 Ω under full load and 0.2 Ω under 50% load. These are RMS current values expressed as a percentage of the rated load current of the inrush controller.

When a power amplifier is operating at low sound levels most of the time, the resistance of the inrush controller may be quite a bit higher. This may deprive the amplifier of some headroom when a loud passage suddenly occurs. The popular CL30 inrush current limiter exhibits a resistance of 0.4 Ω in the power supply of Figure 16.1 when the power supply is delivering 1.5A. At a load of only 0.5 A, the resistance of the inrush limiter rises to 0.8 Ω. A resistance of 0.4 Ω may not seem like much in the AC line until one looks at the peak rectifier current pulses. This device drops the mains peaks by almost 3 V under these conditions.

Active Soft-Start Circuits

Active soft-start circuits usually employ a relay or TRIAC in series with the mains line and in parallel with a soft-start resistance. The controlled switch shorts out a conventional resistor or a passive soft-start device after a fixed period of time or after the power supply rail voltages have come up to a certain point. Such a circuit is illustrated in Figure 16.13. If a conventional resistance is used for the soft-start, safety measures must be implemented to ensure that the resistor does not overheat in the event that the control circuitry does not activate the shunting device within a few seconds. It is much preferred that an NTC device be used for this reason. The use of a shunting switch across an NTC device also allows it to cool down during normal amplifier operation, increasing its life, and avoiding the problem of large inrush currents if the power is restored shortly after shutoff.
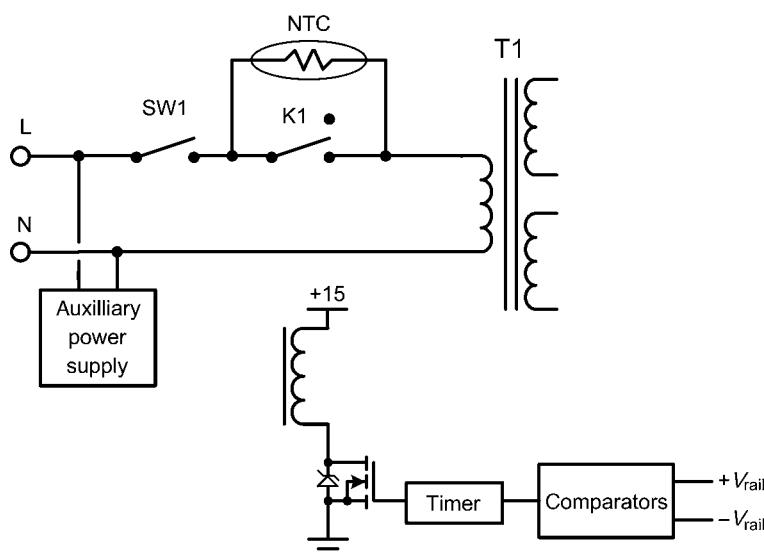
Figure 16.13   An active soft-start circuit.

The control circuitry activates a vertical MOSFET relay driver a short time after both rail voltages are detected to be above a chosen minimum value. The circuitry opens the relay immediately on detection of a power-off condition. The control circuitry can be powered by a small auxiliary supply that does not require inrush control or the control circuit can be designed in such a way that it becomes properly operational during the time when the reservoir capacitors are charging. Many variations of these circuits are possible. An always-on auxiliary supply powered from a class B transformer may be employed in any case for auto-on or remote control circuitry.

16.9   Grounding Architectures

Ground is the reference for all signals in an amplifier, but not all grounds are the same. Currents flowing through grounds create voltage drops, even across seemingly heavy grounds. All ground paths have resistance and inductance, no matter how small. Magnetic fields can also induce voltages across ground conductors. The most obvious symptom of poor or inadequate grounding is hum and noise. However, a much more insidious result of poor grounding is distortion. Any ground "noise" that is correlated to the program signal in any way is considered distortion.

Noisy and Quiet Grounds

In simple terms, there are two kinds of grounds—quiet signal grounds and noisy power grounds. All signal voltages that are single-ended should be referenced to quiet grounds. Quiet grounds are distinguished as grounds that have little or no current flowing through them.

When Ground Is Not Ground

Most ground points in an amplifier are interconnected with wires (never use the chassis). These wires have very finite impedance due to resistance and *self-inductance*. Heavy currents flowing through these wires will cause significant voltage drops. This is especially so for high frequencies or currents with sharp waveform edges (like rectifier spikes). Self-inductance of a 10-inch piece of 14-gauge wire is about 0.3 μH. Self inductance of a straight piece of wire is about 30 nH per inch, nearly independent of wire gauge. The impedance of 0.3 μH at 20 kHz is about 36 mΩ. The DCR of the 10-inch length of 14-gauge wire is about 2.5 mΩ. A loudspeaker return line carrying 5A RMS at 20 kHz through such a length of wire will cause a voltage drop of 180 mV.

Star Grounding

If all grounds are returned to a single point, then that point can be considered as the ground reference for the entire amplifier. This is the idea behind a *star ground* arrangement as illustrated in Figure 16.1. Here the two reservoir capacitors are connected by a short heavy bus bar or piece of heavy-gauge wire. The center of this heavy conductor is defined as the star, and all other ground connections are returned to this point, including the center tap of the power transformer. In the arrangement shown, separate ground lines are shown for the quiet ground, the power ground, and the loudspeaker return for each channel of a stereo amplifier.

If no current flows in a quiet ground connected to the center of the star, the potential on the quiet ground will remain unchanged; the same ground reference will exist at all

places in that node. This will be the *true* ground for the amplifier. The exception to this is if there is a voltage that is magnetically induced in the connection of the quiet ground to the star ground point. Heavy noise, ripple, and distorted audio currents can pass to the star ground without causing a disturbance to the quiet ground. Note that the "ground" potential at the far end of lines carrying such heavy currents will be moving with respect to the true ground reference at the star point.

There are some caveats, however. With heavy current flowing through it, the star ground node itself can develop some small voltage potentials among the several wires connected to it. In other words, it cannot really be a perfect equipotential point. Never use steel hardware to fasten together the elements of a star ground.

Star-on-Star Grounding

A star-on-star grounding architecture like that shown in Figure 16.8 is a better approach. All of the high-current rectifier spikes are resolved at the auxiliary star 3 ground (S3) independently of the main star ground. Split reservoir capacitor returns are merged at star 2. In addition to providing R-C filtering, resistors R3 and R4 prevent the formation of an AC ground loop among the reservoir capacitors. This arrangement keeps those dirty high currents away from the main star ground and keeps them from corrupting it.

An important concept is to have dirty currents circulate locally and be resolved before they are passed to a ground node involving other circuitry. If large electrolytic capacitors are used on the circuit board local to the output transistors, their grounds should be tied together before connection to another ground, such as the main star ground. This is because these capacitors are bypassing highly nonlinear class AB half-wave signal currents that should be resolved locally. The common ground of these capacitors can be thought of as another auxiliary star ground connected to the main star ground through a spoke.

The star-on-star approach is typical of the general approach to good grounding practice, namely, to follow the currents and beware of the voltage drops they can cause. More complex star-on-star grounding arrangements can be imagined when a thorough analysis of current flows is carried out. In many cases real amplifiers end up having some sort of a star-on-star grounding architecture without it having been intentionally designed that way.

Ground Corruption

One source of trouble that is often overlooked is the corruption of a quiet analog ground by currents injected into the ground by power supply bypass capacitors. This can happen when the main rail is routed to the input and VAS circuits through a small resistor or diode and then bypassed. Bypass capacitors can ruin an otherwise clean star grounding architecture by creating an AC ground loop and providing another path for alternating current flow.

Dual-Mono Designs

Even the best grounding architecture in a stereo amplifier cannot always prevent the formation of ground loops between the amplifier and the source (e.g., preamplifier). This can happen when the stereo pair of interconnects share the same ground at both ends of the interconnect cable. One way to avoid such ground loops is to completely isolate the power supplies of the two channels. The circuits of the two channels are then essentially floating with respect to each other. This is one advantage of dual-mono amplifier designs.

16.10   Radiated Magnetic Fields

The power transformer is usually the single biggest source of radiated magnetic fields. These fields can include both hum and rectifier spikes. However, any wiring that is carrying high currents can radiate a magnetic field that will induce voltages in nearby wiring. Toroidal power transformers can sometimes be rotated to minimize the impact of their radiated fields.

Antenna Loop Area

The best way to pick up an induced signal from a magnetic field is to build a loop with a fairly large area. Pickup from radiated magnetic fields is thus minimized by keeping the loop area small. This means that signal paths and their returns should be close to each other and not form a loop larger than absolutely necessary.

Circuit Path Crossing Angle

The possibility of magnetic coupling is maximized when wires pass parallel to each other. One wire carrying an aggressor current will create a magnetic field and induce a voltage into the victim wire. This transformer effect can be minimized if wires are crossed at a 90° angle.

16.11   Safety Circuits

Regardless of how good an amplifier sounds, safety must not be ignored. The two main aspects of safety are fire and the hazard of electrocution. The primary defense against fire is the line fuse or circuit breaker. A slow-blow characteristic is desirable, especially if an inrush limiting circuit is not used.

Safety Ground

Three-wire mains power cords include a safety ground as the third (green) wire. This wire runs right back to the house ground. This minimizes the danger if the neutral return path becomes open and is energized through the resistance of the load device (in this case the amplifier). The safety ground is connected to the chassis so that if there is a fault to the chassis it will be shunted by the safety ground. A typical fault that this guards against is a primary-secondary short in the power transformer.

Breaking Safety Ground Loops

Several pieces of interconnected equipment, each with a safety ground connected to its circuit ground, may form a ground loop. This is undesirable. One approach, similar to that used in Ref. 4 is illustrated in Figure 16.14. The safety ground is connected directly to the chassis ground. However, small-valued resistor R1 connects the safety ground to the circuit star ground. This is the only connection in normal operation, and the resistance breaks the ground loop. Back-to-back diodes D1 and D2 are connected in parallel with R1. In the event of a fault, the diodes conduct the fault current to the safety ground and prevent the circuit ground from ever deviating from the safety ground by more than one diode drop. In practice D1 and D2 are often replaced with a specially connected 35-A bridge rectifier wired in parallel with R1. The AC terminals are connected across R1 and the positive and negative "output" terminals of the bridge rectifier are
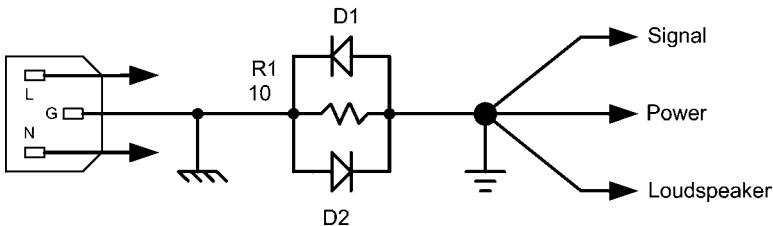
Figure 16.14 Breaking a safety ground loop.

shorted together. In this case the maximum allowed voltage drop between safety ground and circuit ground is about 1.4 V.

16.12 DC on the Mains

Although one would never think it to be there, DC voltages can exist on the mains power supply under some conditions. DC on the mains can cause the flow of direct current through the very low DC resistance of the primary of the power transformer, magnetizing the core. This can degrade transformer performance and sometimes cause audible buzzing. The cores of toroid transformers are more susceptible to the effects of DC on the mains. DC can be developed on the mains by the many loads shared among many utility customers. Some of those loads are highly nonlinear and may even employ half-wave rectification. Sometimes the presence of second harmonic distortion on the mains is accompanied with DC.

Some designers have taken measures to keep mains DC away from the transformer primary [4]. The obvious choice is to AC couple the mains through a large nonpolarized capacitor, but this is impractical and unreliable. Another approach is to place the AC terminals of a bridge rectifier in series with the mains circuit as shown in Figure 16.15.
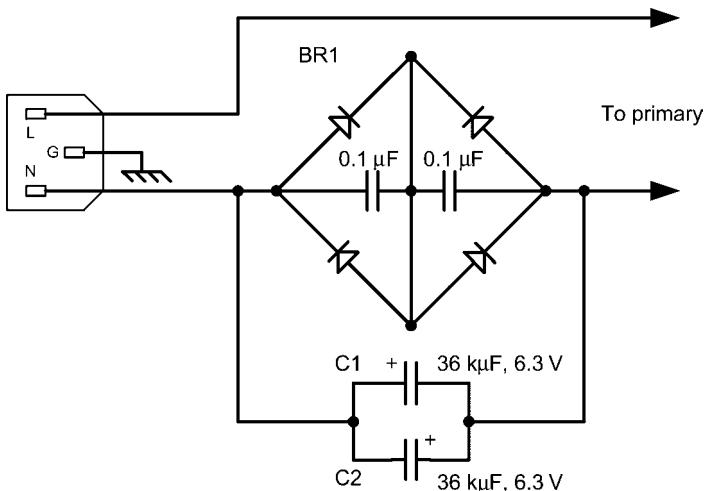
Figure 16.15 Keeping mains DC off the power transformer primary.

The positive and negative "outputs" of the bridge are then shorted together. This arrangement will create two junction drops before conduction can begin, so that any DC on the mains less than about 1.4 V will not be passed.

This approach can be combined with AC coupling by placing large electrolytic coupling capacitors C1 and C2 in parallel with the bridge. The capacitors can be rated at very low voltage and will always be protected by the bridge. The bridge rectifier diodes do not conduct under normal conditions so snubber capacitors are not necessary. C1 and C2 should have very low ESR and should be rated for high ripple current. This arrangement is not recommended for amplifiers that do not incorporate a soft-start circuit. This approach does not necessarily guard the transformer against the AC effects of second harmonics on the mains, however. DC mains blocking circuits are rarely seen on consumer power amplifiers.

16.13   Switching Power Supplies

Switching power supplies are beginning to make their way into more power amplifiers. They offer high efficiency while being compact and lightweight. Their use is becoming widespread in pro audio amplifiers and in home theater receivers where these qualities are especially important. They are also moving into some audiophile power amplifiers. Their advantages include regulated outputs at no penalty in power dissipation. Of course, this means that amplifiers using these supplies will often have little or no dynamic headroom.

Switching supplies typically operate by rectifying the mains voltage on the line side and storing the DC on a reservoir capacitor. This DC is then switched at a high frequency (several hundred kHz) to become AC to drive an isolating transformer. The secondary voltage is then rectified and stored on secondary reservoir capacitors. High-frequency transformers are smaller, lighter, and less expensive than transformers that operate at the mains frequency. The design of switching power supplies is highly specialized and will not be covered here. However, a glimpse of some of the technical issues can be gained from the material in Chapter 28 on class D amplifier design.

There are some caveats when switching supplies are used for audio power amplifiers. For one, they can be a prolific source of EMI. Secondly, because they operate and rectify at high frequencies, the traditional ripple problem is not as great. This can lead designers to employ smaller reservoir capacitors. This is not a good idea because it may deprive the amplifier of the large amount of energy storage necessary for reproduction of low-frequency transients.

There is also another phenomenon to watch out for. Switching power supplies are characterized by a constant power input for a given load current. If the mains voltage goes down, the current demanded from the mains will go up. Similarly, if the output voltage is constant and the load demands more current, the switcher will require more power from the mains and the front-end rectifier. If this causes the voltage at the input side to sag, still more current will be demanded by the switcher, since it is a constant-power device. The input will sag further and still more current will be demanded by the switcher. This is a potentially vicious circle.

This behavior is not unlike that of a negative resistance, and can lead to instability on the line side. Such a power amplifier at the end of a long run of 14-AWG house wiring will be more prone to such instability. This also argues for a large reservoir capacitor on the mains input rectifier to better handle amplifier transients. Amplifiers employing

switching power supplies may also be more vulnerable to trouble when driving a 2-Ω load; their current demands will be much higher and their power output capability will not fall gracefully from 4 times the 8-Ω power output value because the switching supply will try to remain perfectly stiff.

In principle some of the mains-side instability can be reduced. The negative impedance presented by the switching power supply can be reduced with the introduction of some dependence of the output voltage on the rectified mains voltage. This amounts to a deliberate, but controlled, degradation of the power supply regulation. If the rectified voltage on the mains side decreases, the voltage control circuit is directed to reduce the load-side output voltage by some chosen amount that is enough to keep the current demanded from the mains from increasing. This also allows the maximum output voltage of the amplifier to fall gracefully as the load becomes heavier. Without additional circuitry, this scheme will introduce some static dependency on the long-term mains voltage, which is undesirable.

References

1. Toroid Corporation of Maryland, Technical Bulletins.No. 1, 3, 4, www.toroid.com
2. IXYS VBE 26-12N07 data sheet for FRED 32A bridge rectifier.
3. Vishay data sheet for HFA25PB60 HEXFRED® Ultrafast Soft Recovery 25A diode.
4. Bryston 4B-SST amplifier.
5. National Semiconductor, AN-1849, "An Audio Amplifier Power Supply Design."

Clipping Control and Civilized Amplifier Behavior

The question is often asked why amplifiers with otherwise very good measured performance sound different. There are many possible reasons for this, but some of those reasons may lie in how the amplifier behaves under conditions for which it was not tested or optimized.

Overload conditions are a good example. Does the amplifier clip gracefully or does it create more than just a cleanly clipped waveform? Does the amplifier current limit prematurely under some conditions? Does the amplifier produce a burst of oscillation when it clips into certain kinds of loads?

17.1   The Incidence of Clipping

Amplifiers clip more frequently than some realize. This is especially the case on well-recorded music where the dynamic range has been well preserved. While low-power amplifiers are often thought to be more prone to clipping at realistic sound levels, even high-power amplifiers may clip when driving low-efficiency loudspeakers. Bear in mind that a loudspeaker with 84-dB sensitivity requires 10 times as much power as one with 94-dB sensitivity.

The dynamic range that must be reproduced is strongly influenced by the *crest factor* of the music being played. This is the ratio of the average power to the maximum power that occurs on peaks. Well-recorded music can have a crest factor exceeding 14 dB, while music from a typical FM station may have a crest factor of less than 3 dB. The latter is a result of processing that deliberately reduces dynamic range so that the station can sound louder while still remaining within its peak modulation limits. Music with a 14-dB crest factor will require 10 times the power of music with a 4-dB crest factor played at the same perceived sound level.

It is important to keep in mind that a 10-dB increase in sound level corresponds to a factor of 10 in power level. It is also important to recognize that the human perception of loudness corresponds more closely to the average power and that brief percussive transients are not bothersome. Consider program material with a 14-dB crest factor where loudspeakers with an efficiency of 83-dB SPL at 1 meter are being driven. Assume that realistic levels are being played such that the average SPL at 1 meter is 96 dB from each channel, on average (the level at the listening position will be considerably less). The average power must be +13 dB-W, or 20 W. The maximum power on the peaks will

be 14 dB higher, corresponding to a factor of 25. Thus the amplifier must be rated at no less than 500 W per channel if it is not to clip.

Clipping Experiments

Several experiments were carried out to evaluate clipping with real program material [1, 2]. The objective was to measure average power and peak power so as to be able to compare them and determine the crest factor of the program material. A special peak/average meter was designed and built for this purpose [3]. The average-responding side of the meter uses a true RMS IC with a moderately long time constant. Its output is calibrated in average power into an 8-Ω load. The peak-responding side of the meter employs a two-stage peak-hold detector that can resolve peaks as short as 10 μs with good accuracy. This circuit holds the highest peak for 3 seconds to allow time for the reading. This circuit is calibrated so that its peak voltage reading corresponds to equivalent average power into 8 Ω. If both meters are fed with a sine wave, their readings will be identical.

A percussive CD track was played through loudspeakers with a sensitivity of 84 dB. A 250-W amplifier was used. The music was played at a realistic but not overly loud level in a 400 square-foot hotel room. Average power hovered between 1 and 2 W. Power peaks exceeded 260 W, clipping the power amplifier.

17.2   Clipping and Sticking

Given the inevitability of clipping, it is important to consider the sonic behavior of the amplifier when it clips. Indeed, some believe that the more civilized way in which vacuum tube amplifiers clip is responsible for their perceived better sound (by some) in spite of their lower power.

The cleanest of solid-state power amplifiers will neatly clip the peaks off the signal. Many solid-state amplifiers will suffer what is called *sticking* or *overhang*. Such amplifiers go into clipping cleanly, but don't come out of clipping cleanly when the amplitude demanded by the program falls below the clipping point. Instead, such amplifiers *stick* to the higher clipped level for a brief instant and then fall more quickly down to the level required by the signal. Such a waveform is shown in Figure 17.1. Here we have also shown the waveform of the difference between the correct output and the actual output. Notice that the waveform includes spikes in the area where the sticking has occurred. These are noticeable and objectionable.

17.3   Negative Feedback and Clipping

Negative feedback can exacerbate undesirable clipping behavior. When clipping occurs, the error signal at the input of the amplifier becomes very large and may overload one or more stages of the amplifier. Those stages, having been overdriven, will take time to recover and get back to their proper signal voltages after the input is no longer being overdriven. The VAS is especially likely to become overloaded. Delays introduced by frequency compensation capacitors may lengthen the time required for recovery. It is especially important that output transistors not be allowed to saturate.

Negative feedback sharpens up the clipping edges. This happens largely because the gain from input to output at the onset of clipping attempts to go from the closed-loop
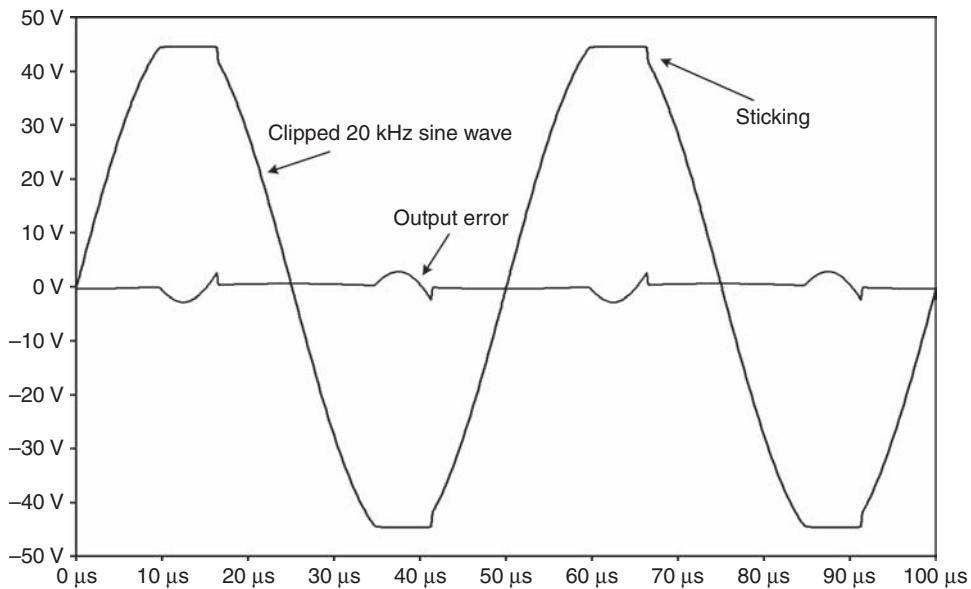
Figure 17.1   Output waveform of an amplifier that is clipping and sticking.

gain to the open-loop gain. This happens because there is no global negative feedback once the amplifier clips.

17.4   Baker Clamps

If an amplifier must clip it is important that it clips cleanly to achieve the highest sound quality. Ideally, power amplifiers should clip softly, but even when they clip hard, as most solid-state amplifiers do, it is important that there be no sticking or other failure to come out of the clipped state quickly.

It is also desirable that the amplifiers not lose their power supply rejection during clipping intervals, as that would allow ripple and grunge from the power supply to enter the signal path during the clipping interval. Amplifiers that clip to the main rail will essentially be applying the dirty main rail voltage directly to the loudspeaker under clipping conditions.

By proper design negative feedback amplifiers can be made to clip quite cleanly. In order to accomplish this it is very important that no transistors go into saturation. One approach to this is to employ so-called Baker clamps on the output of the VAS [4, 5]. These are diodes that will turn on and prevent the VAS output signal from swinging toward the rail beyond a certain point. This clamping action prevents the VAS transistor from saturating and also prevents the output transistors from saturating. In fact, it will be the turn-on of these diodes that actually causes the amplifier to clip before anything else in the amplifier's signal chain. These and other clamping circuits were discussed in Chapters 10 and 11.
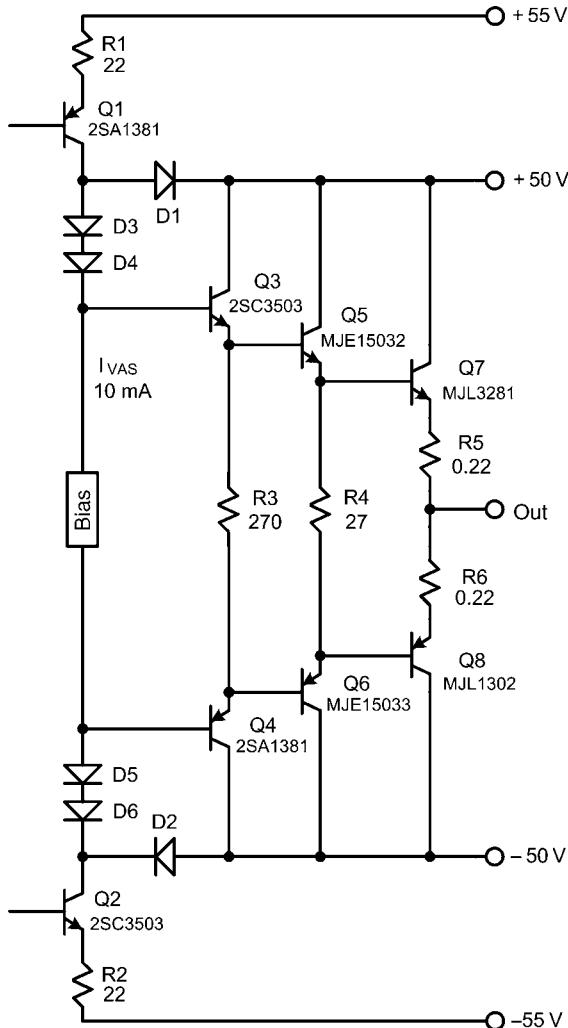
FIGURE 17.2 A simple power amplifier with a Baker clamp.

Figure 17.2 shows part of a simple power amplifier that incorporates a Baker clamp much like the one used in Ref. 4. VAS transistors Q1 and Q2 are powered from boosted supply rails operating several volts above the main rails. D1 and D2 are the Baker clamp diodes. They clamp the VAS output voltage to no more than one diode drop above the main rails. The Baker clamp in this amplifier thus clips at a voltage level that tracks the available power supply rail voltage. Diodes D3–D6 drop the VAS feed to the predrivers by two diode drops so that when clipping occurs Q3 and Q4 have one diode drop of V_{cb}. The Baker clamp thus keeps all of the output stage transistors out of saturation as well.

Flying Baker Clamps and Flying Catch Diodes

Other types of clamping arrangements were touched on previously in Chapters 10 and 11. Flying Baker clamps, discussed in Section 10.4, are arrangements in which both sides of the Baker clamp diode move with the signal until clipping occurs. This reduces nonlinear junction capacitance effects of the clamp diode and permits the use of a diode with a lower voltage rating. Flying catch diodes were discussed in Section 11.7 where catch diodes prevent the VAS node from going beyond a certain voltage from the output node when the output stage clips for any reason. If desired, fast Shottky diodes can be used in these arrangements.

Feedback Baker Clamps

Feedback Baker clamps keep the global feedback loop closed during clipping by diverting the clamping current back to the input of the amplifier, bypassing the output stage. As shown in Figure 17.3, the Baker clamp reference is provided from emitter followers Q9 and Q10 whose complementary collectors are joined. A signal is fed back from that junction to the input stage to complete the feedback connection around the amplifier
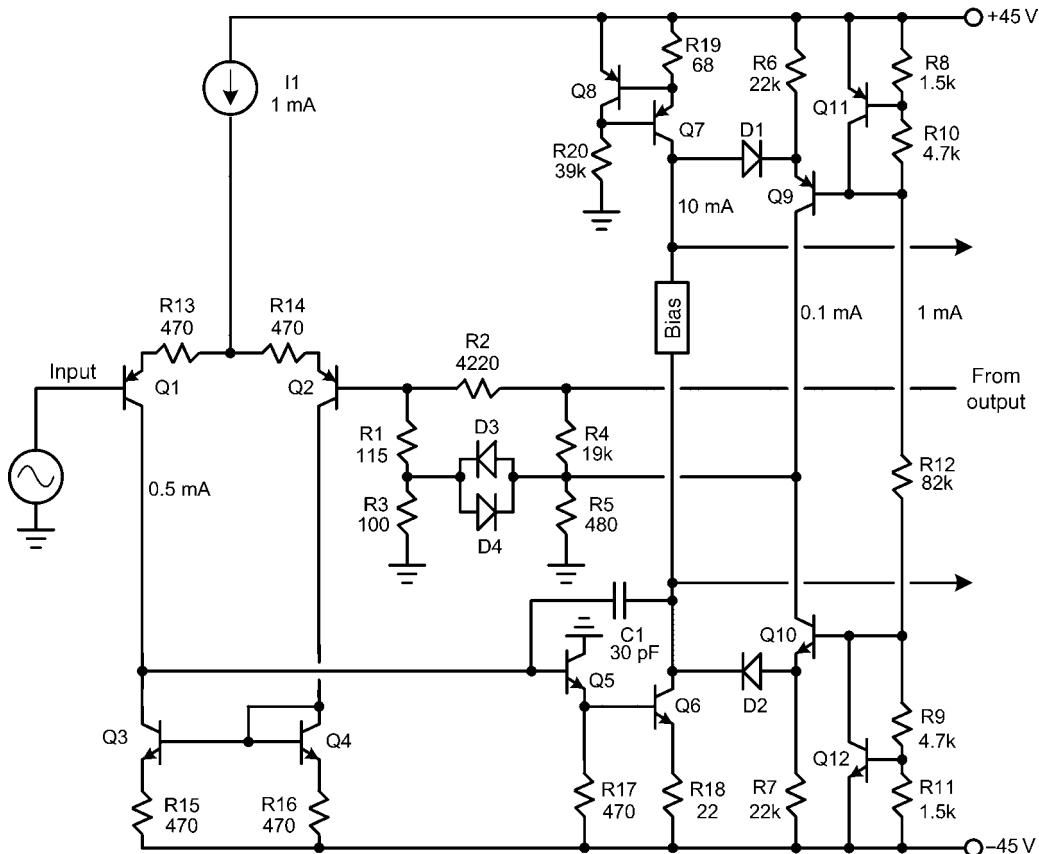
FIGURE 17.3   A power amplifier with a feedback Baker clamp.

when the Baker clamps are acting. This keeps the whole front end linear and prevents sticking. It is important that this bypass feedback loop be stable.

R1, R2, and R3 implement the normal global feedback network that is fed by the output stage, which is not shown. When Baker clamp diodes D1 or D2 conduct, their current is conducted by Q9 or Q10 to the junction of R4 and R5. These latter two resistors are fed by the amplifier output and create a voltage that is a replica of the voltage at the junction of R1 and R3. This arrangement keeps the signal voltage across isolating diodes D3 and D4 at zero during normal operation when the amplifier is not clipping. This eliminates the possibility of distortion currents being injected into the feedback node. When the amplifier clips, the diverted VAS current closes the feedback loop through D3 and D4. This allows the input stage to stay linear for input signals that far exceed the clipping point of the amplifier.

The use of the tapped shunt feedback resistor (R1, R3) illustrates the general case, but the clamp feedback can be connected directly to the feedback node if desired. The ratio of R1 and R3 allows some control of the behavior of the feedback Baker clamp under heavy-overload conditions. R4 and R5 must always be adjusted so that the normal signal voltage across D3 and D4 is zero for whatever ratio of R1 and R3 is chosen.

Q11 and Q12 are simply V_{be} multipliers that set how far from the rails the Baker clamp threshold is. As shown here, they produce a drop of $4V_{be}$ so that Q6 and Q7 will have one V_{be} of collector-base voltage when clipping occurs. This design is also compatible with amplifiers using boosted rails for the IPS-VAS.

Because the global feedback never disappears, the clipping afforded by the Baker clamp diodes here is a bit softer than without Baker clamp feedback.

17.5   Soft Clipping

The best amplifier is one that never clips. If clipping must occur, it is best accomplished with a passive circuit ahead of the amplifier input. Such a circuit can clip the signal quickly and cleanly, without creating sharp edges. Ordinary silicon diodes can fulfill this task. Of course, with soft clipping, there will be some gradual rise in THD prior to clipping. As a result, such amplifiers might not measure as well as amplifiers of the same rated power that are not preceded by a soft clip circuit.

The Klever Klipper

While diodes clipping to fixed thresholds can provide the desired soft-clipping behavior, they will not allow for the dynamic headroom normally available for brief signal bursts in normal amplifiers. Thus there is the need for dynamic clipping thresholds that track the available peak output of the amplifier in real time. Figure 17.4 shows what I call the Klever Klipper circuit [6].

Diodes D1 and D2 provide the soft-clip function in combination with R1. The soft-clip threshold voltages are created at op amps U1A and U1B. These voltages track the short-term average power supply rail voltage. Adaptive soft clipping occurs just shy of output amplifier hard clipping at any given power supply rail voltage condition. As a result, little or no dynamic headroom is sacrificed.

The Klever Klipper control circuit takes the negative rail supply voltage and scales it down to approximately 1/20 of its value, to roughly match the gain of the amplifier. This moving reference voltage is filtered by C1 and C2. The U1A buffer then adds one
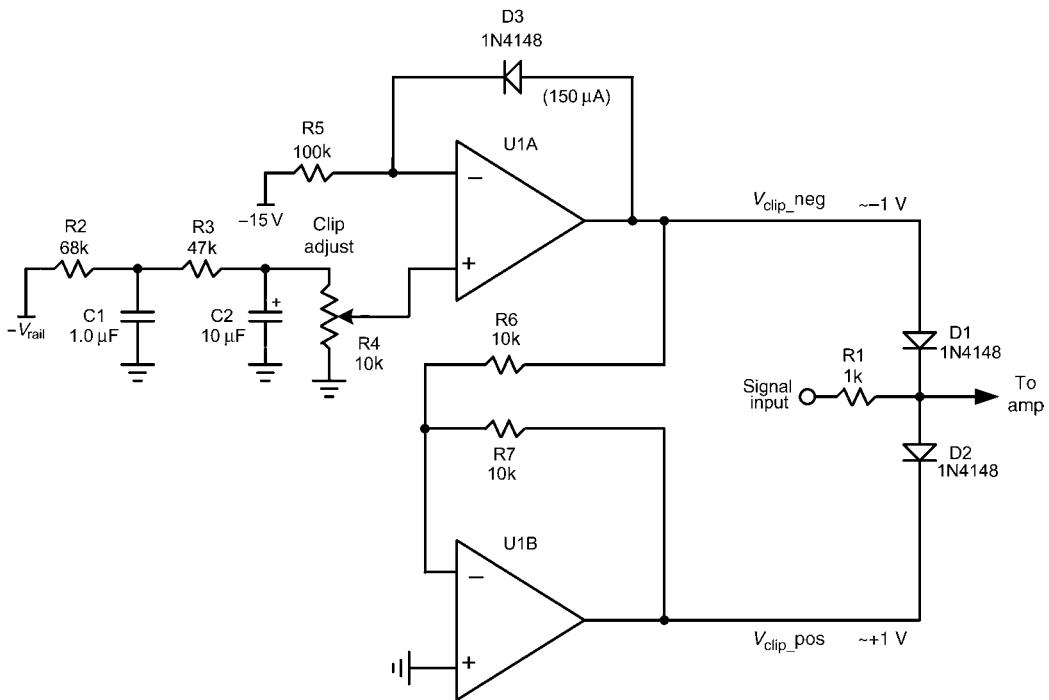
FIGURE 17.4 The Klever Klipper soft-clip circuit.

diode drop (D3) to this voltage to account for the approximate conducting diode drop of the soft-clip diodes when they begin to clip. The output of U1A is the negative clipping voltage that is applied to D1. U1B creates a positive version of this voltage for application to D2. This simple version of the circuit assumes that the positive and negative amplifier rails are of the same magnitude.

Clip adjustment potentiometer R4 is set with the amplifier operating at full power just at clipping into an 8-Ω load. Assuming that the pot starts at its maximum CW end, meaning least likelihood of causing soft clipping, the pot is then adjusted in a CCW direction until it just begins to soften the clipping to the point where it is controlling the clipping rather than clipping of the power amplifier itself. Figure 17.5 shows THD-1 as a function of power for a 50-W/8-Ω amplifier with and without the Klever Klipper engaged [6].

17.6 Current Limiting

Current limiting has been discussed previously in Chapter 15. It is mentioned here as a reminder that current clipping can happen just like voltage clipping. Once again, if it must happen, it should be done cleanly and with no signal artifacts other than the absence of the desired amount of signal swing. It is especially desirable that current limiting is not to be accompanied by flyback pulses. These can be caused by the stored energy in the inductive loudspeaker load. Such flyback pulses will be communicated
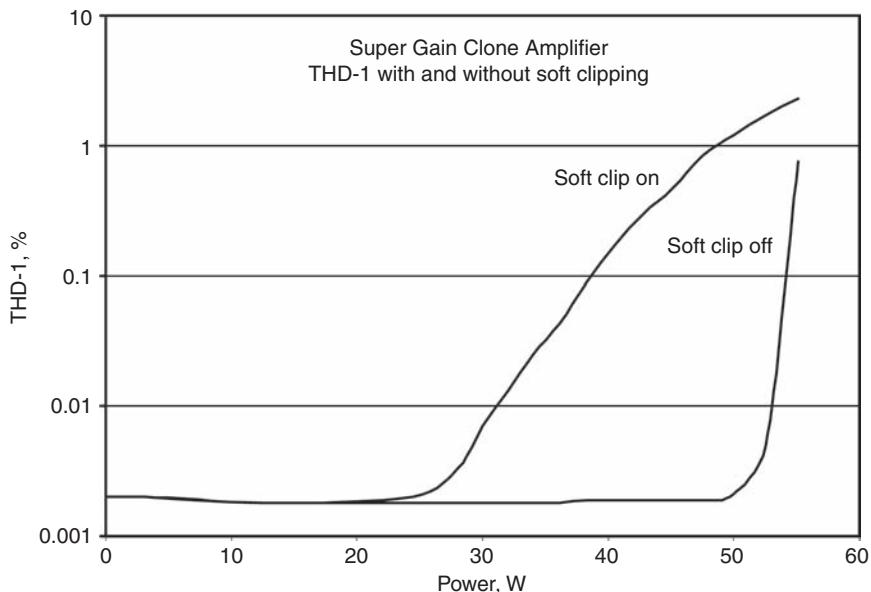
FIGURE 17.5   THD-1 versus power for an amplifier using the Klever Klipper.

directly to the tweeter through the crossover network. They will result in a very audible snapping sound and possible damage to the tweeter.

Active Current Limiting

Active current limiting is typically implemented with a feedback process (see Chapter 15, Section 3). It is the type of current limiting commonly found in V-I limiters. It tends to be quite abrupt and tends to cause the output of the amplifier to change from being a voltage source with low output impedance to a current source with high output impedance.

Natural Current Limiting

Natural current limiting results from the use of flying catch diodes as described in Section 3 of Chapter 15. This type of current limiting tends to be softer and tends to retain moderately low output impedance during current limiting.

17.7   Parasitic Oscillation Bursts

Another thing that can degrade the sound quality of an otherwise good-measuring amplifier is the occurrence of parasitic oscillation bursts. The operating points of many of the transistors in an amplifier signal path change quite a bit when there are large signal swings. Different operating points can cause altered transistor dynamic parameters like speed and capacitance. This can lead to a loss of feedback stability margin and possible parasitic oscillation bursts on signal peaks. This goes double when the amplifier clips.
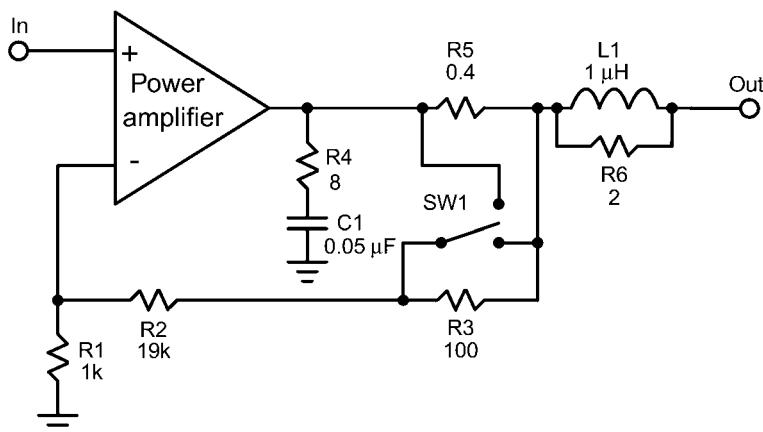
FIGURE 17.6   Selection of amplifier output impedance.

Amplifiers without negative feedback can also be prone to parasitic oscillations under certain signal swing and load conditions. These oscillations may be local in nature, such as in the case of an oscillating output emitter follower. Such parasitic oscillation bursts often may not show up on bench tests, especially when a resistive load is being used. A *parasitic oscillation sniffer* that can be used to detect bursts under a large variety of signal and load conditions is discussed in Chapter 23.

17.8   Optional Output Impedance

In some cases it is preferable to have controlled output impedance of a couple of tenths of an ohm. Some loudspeakers seem to sound better when fed with such a source. In some ways this is like the output impedance of a vacuum tube amplifier. This results in a low damping factor, often less than 20. A damping factor of 20 can be obtained by simply adding a 0.4-Ω noninductive power resistor in series with the output of the amplifier.

However, it is desirable to make the introduction of such a resistance into the output of the amplifier optional. This can be done with a relay across the added series resistor, but there is a more elegant way. The series resistor is placed between the output stage and the output coil. The negative feedback is then taken off either before or after the series resistor, as controlled by a small-signal relay. Figure 17.6 shows such an arrangement.

References

1. Rocky Mountain Audio Fest, Denver, CO, 2006.
2. Home Entertainment Show (HE2007), New York, 2007.
3. "A Peak/Average Power Level Meter," www.cordellaudio.com.
4. "The Apt1 Power Amplifier Owner's Manual," Apt Corporation, 1979.
5. Cordell, R. R., "A MOSFET Power Amplifier with Error Correction," *Journal of the Audio Engineering Society,* vol. 32, no. 1, pp. 2–17, January 1984; available at www .cordellaudio.com.
6. "The Super Gain Clone," www.cordellaudio.com.

This page intentionally left blank

Interfacing the Real World

More than any other component in the audio chain, the power amplifier must deal with the realities of the real world. This is particularly so because it drives the loudspeaker with high currents over typically unshielded cables and because the loudspeaker itself is an electromechanical device that makes for a highly complex load. Other realities include *electromagnetic interference* (EMI) ingress from the input and mains ports, rectifier noise, and other sources of trouble. Some aspects of the interface have already been covered in the earlier chapters on protection circuits and power supplies.

18.1   The Amplifier-Loudspeaker Interface

The fact that the power amplifier drives an electromechanical device distinguishes it from most of the other elements in the audio signal chain. The loudspeaker load has complex impedance and can store substantial amounts of energy. It can also require high currents to drive it.

The Loudspeaker Is Not a Resistive Load

The loudspeaker consists of multiple electromechanical drivers connected together by a passive LCR crossover network. Together, the elements of this arrangement form a complex nonlinear load for the amplifier. In some cases highly capacitive speaker cables add to the complexity. At radio frequencies there can be transmission line effects from the speaker cables as well. Figure 18.1 illustrates a simple equivalent electric circuit for a loudspeaker woofer in a sealed enclosure. Figure 18.2 shows the impedance curve for the driver of Figure 18.1.

Peak Output Current Requirements

The loudspeaker can store energy in many different ways, but the woofer velocity and displacement against the restoring force of the suspension are usually the two greatest ways in which energy is stored. Figure 18.3 shows the results of a SPICE simulation that reveals the high peak load currents that are possible under conditions where the loudspeaker is driven by a particular contrived waveform [1]. Other authors have also studied phenomena at the amplifier-loudspeaker interface [2, 3, 4].

The driving waveform in Figure 18.3 was deliberately chosen to maximize the expected peak load current. The signal swings between large positive and negative values, rather than simply starting from zero. The waveform begins at –28 V and remains there for 16 ms to allow load current to rise to at least 90% of its final value.

373
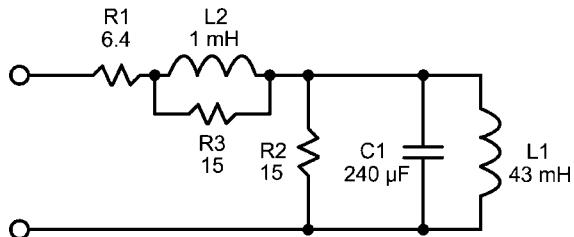
Figure 18.1   Electrical model of a loudspeaker woofer.
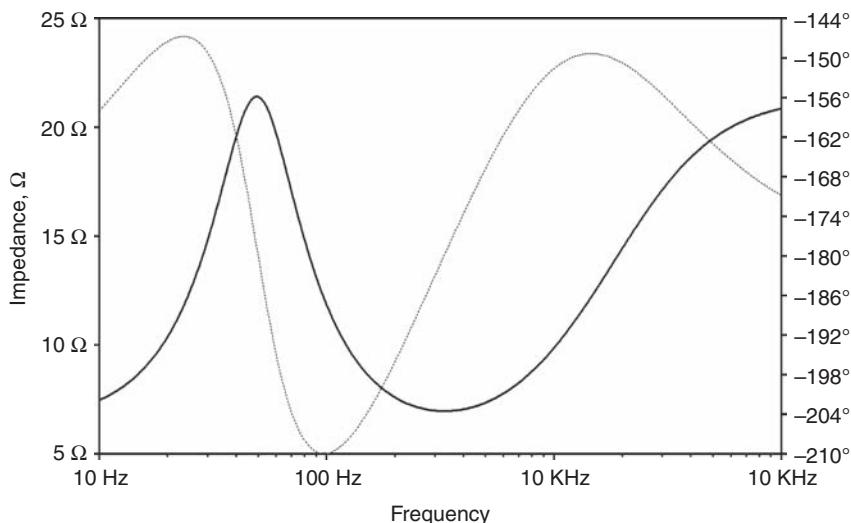
Figure 18.2   The impedance curve for the driver of Figure 18.1.
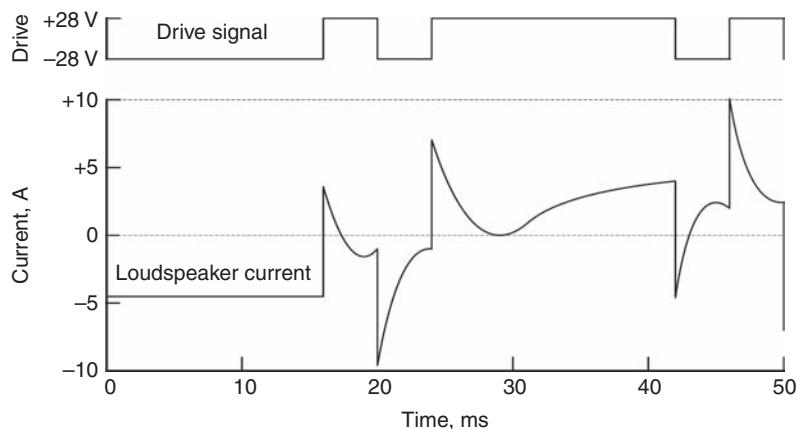
Figure 18.3   High peak load currents when the loudspeaker is driven with a contrived waveform.

The signal then goes to the positive extreme for 4 ms. At the end of this 4-ms interval the counter-emf of the loudspeaker is at its maximum (maximum cone velocity). The polarity is then reversed, going to the negative extreme. The counter-emf now opposes the new signal polarity and enhances the peak current flow. The very large negative current flow of nearly 10 A is the result. After 4 ms, the signal polarity goes back to the positive extreme and the sequence is repeated for the opposite polarity so that the average value of the signal is zero.

While an amplifier delivering this waveform to an 8-Ω resistive load would normally see a peak load current of about 3.5 A, we see from Figure 18.3 that the RLC load develops a peak load current of 10 A. While the probability and extent of this kind of occurrence in the real world with musical program material may be questioned, the exercise does provide some food for thought. The lesson to be learned here is to be prepared to handle larger currents than are encountered with a simple resistive load.

Transmission Line Effects of Speaker Cables

The loudspeaker cable is a transmission line that is usually misterminated. As such, it is subject to reflections, where energy is reflected back from one end to the other. Even if the speaker cable had a characteristic impedance of 8 Ω, it would probably be misterminated at the high frequencies where it matters most. In reality most loudspeaker cables have *characteristic impedance* Z_o between 50 Ω and 150 Ω. Transmission line effects are unlikely to matter much at frequencies in the audio band, but they can cause load impedance variations that can provoke amplifier instability at high frequencies.

Consider a speaker cable that is 10 feet long. The speed of light is on the order of 0.7 foot per nanosecond in cables with typical dielectrics. The propagation delay will be about 14 ns. The round-trip delay for a reflection will be about 28 ns. At a frequency whose period is 56 ns, this round-trip delay will represent 180°. This frequency is 18 MHz. An ideal transmission line with no far-end termination (at high frequencies) will exhibit very low impedance at this frequency. One with a shorted termination will exhibit very high impedance at this frequency. This frequency is well above the gain crossover frequency of virtually all audio power amplifiers, but it can be in the range where local output stage oscillations can be provoked in wideband output stages that are not isolated from the output by an L-R network. Amplifiers that misbehave under certain loading conditions will certainly sound different with different speaker cables.

Figure 18.4 shows the impedance versus frequency looking into the end of a 10-foot length of a very popular brand of speaker cable that employs a ZIP cord type of construction. The three plots are for the conditions where the far end is open, shorted, and terminated in the characteristic impedance of 120 Ω. The wild impedance gyrations in the open and shorted case may drive some amplifiers to instability. Bear in mind that the terminating impedance of a loudspeaker at frequencies above 1 MHz is anyone's guess. Figure 18.4c shows what a remarkable difference a proper termination makes even to frequencies approaching 100 MHz.

The data in Figure 18.4 suggests that a Zobel network located at the far end of the speaker cable is a good idea, even if it consists of little more than a 100-Ω resistor in series with a 0.01 μF capacitor. More complex networks that provide a controlled transition of the terminating impedance to 100 Ω as frequency increases can easily be imagined. Loudspeakers could also incorporate such a network internally.
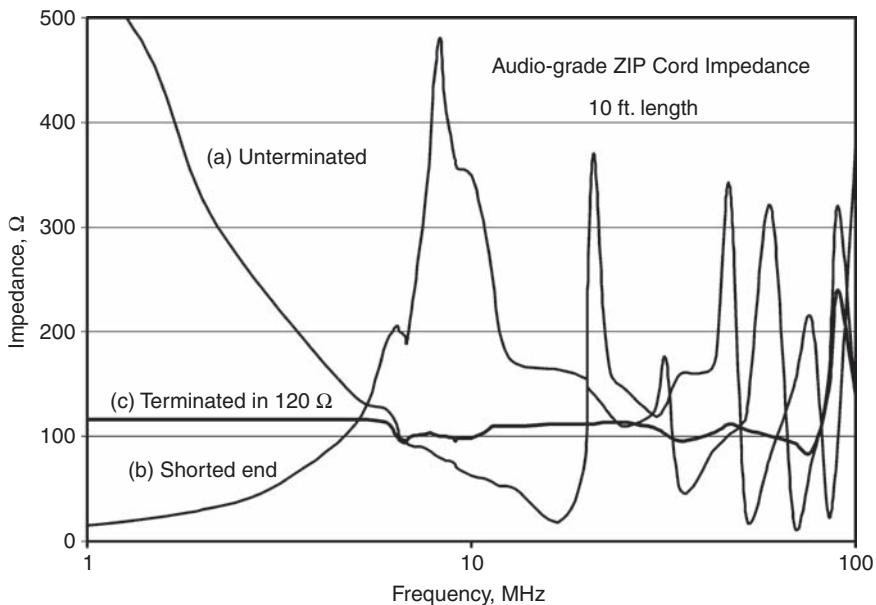
FIGURE 18.4 Impedance versus frequency looking into a 10-foot length of speaker cable. (a) Far end open. (b) Far end shorted. (c) Far end terminated.

18.2 EMI Ingress: Antennas Everywhere

Electromagnetic interference is all around us, across the complete frequency spectrum from the audio band up to several GHz and beyond. Operate a cell phone near your inexpensive powered computer loudspeakers, and you will likely hear the interference. Microwave ovens, light dimmers. and electric drills are other common sources of EMI.

These sources of interference can all create noise in the audio band, even though their frequencies are often way above the audio band. The noise, if present, is created by demodulation that creates audible artifacts. Noise is annoying, but is not the same as distortion. There are, however, mechanisms whereby the in-band noises created by EMI are correlated to the audio signal, and this then *is* distortion. Finally, one must ask the question: *If in the absence of the audio signal there is no audible noise from EMI, is it then safe to conclude that there must not be enough EMI to cause distortion of the audio signal?* It is tempting to say yes, but I am not so sure. The use of good RF design techniques is called for, even though these are audio amplifiers.

RFI and EMI

Radio Frequency Interference (RFI) and Electromagnetic Interference are treated as one and the same in this book. The term *EMI* is broader, so it will be used almost exclusively in these discussions.

EMI Ingress from the Amplifier Input

A monophonic amplifier driven by a well-designed shielded interconnect cable from the preamp should be subject to very little EMI from its input, assuming that the preamplifier

is not generating rogue high-frequency signals. However, such rogue high-frequency signals can sometimes originate with lower-quality SACD players. One SACD player tested produced a 100 mV RMS ultrasonic output at about 90 kHz. The power amplifier should be designed so that it can handle these rogue signals in stride without creating distortion. Heavy-handed attempts to filter them out in the power amplifier will likely cause phase and frequency response aberrations.

It is important to recognize that the interconnect cable is an unterminated transmission line. As such, it can exhibit unusual behavior at frequencies that are related to its quarter-wave frequency. As with the speaker cable, the quarter-wave frequency for a 10-foot length of interconnect cable will be about 18 MHz. A transmission line that is terminated in its characteristic impedance at only one end will usually be quite benign in terms of this kind of behavior. For this reason it is wise to terminate the interconnect cable at approximately its characteristic impedance Z_o at high frequencies with a Zobel network at the amplifier input. Most interconnect cables will have a characteristic impedance Z_o between 50 Ω and 100 Ω, so a 75-Ω termination at high frequencies is a good compromise. The network should begin to look resistive at least one octave below the quarter-wave frequency, here 18 MHz. A Zobel network consisting of a 75-Ω resistor and a 220-pF capacitor will satisfy this requirement.

It is best to place the Zobel network right at the input connector or at the input to the circuit board with the input connected to the circuit board via a short piece of coaxial cable. Figure 18.5 illustrates an amplifier input circuit that incorporates the Zobel network.

Many preamplifiers source-terminate the interconnect cable by their output impedance, even though this may not be a good approximation to the characteristic impedance of the interconnect cable. Good preamps with a low-impedance emitter follower or op amp output include at least 50 Ω of resistance in series with their output. Those that directly connect a low-impedance active circuit output to the interconnect cable seriously misterminate the line and risk oscillation. Most audio interconnect is similar to RG-58 or RG-59 coaxial cable, with Z_o of 50 Ω and 75 Ω, respectively. These cables have capacitances of 100 pF and 67 pF per meter, respectively. For those worried about the effect of a source terminating resistor on frequency response, bear in mind that the 3 dB-frequency of 600 Ω with 2 meters of RG-58 is about 1.3 MHz.
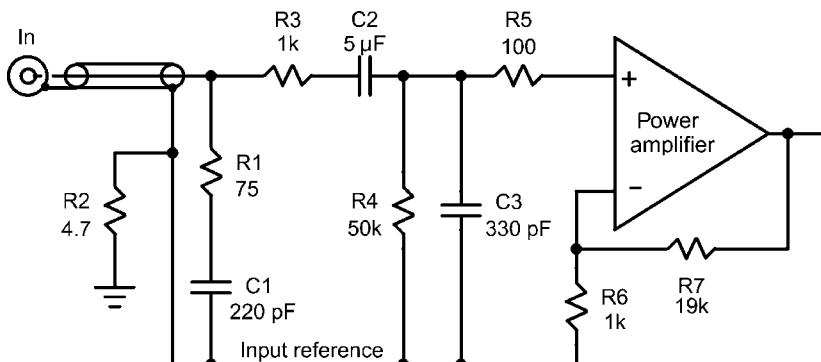
FIGURE 18.5 Amplifier input circuit with a Zobel network.

Implications for Input Stage Design

The need for immunity from EMI at the input means that the input stage must have good dynamic range and linearity up to high frequencies. This provides tolerance to EMI that makes its way to the input stage even after passing through whatever input low-pass filtering is in place. This also reduces the effects of any EMI that makes its way back to the input stage from the output of the amplifier (e.g., EMI picked up by the speaker cable antenna).

JFET input stages are especially good in this regard because the input of the stage does not include a forward-biased PN junction. Instead, the input sees a reverse-biased PN junction at the gate. The amount of voltage swing difference between the gate and source that would be required to cause rectification at the JFET input is typically greater than the threshold voltage of the device. The situation is different for a BJT input stage. The amount of voltage swing that is required between the base and emitter to disturb a conducting transistor is quite small; a differential as small as 60 mV will cause the transistor to conduct about 10 times less current, pushing it to near cutoff and essentially into rectification.

Things are not as bad for a BJT differential input stage if it is operated at a reasonable current and it incorporates significant emitter degeneration. In such a case, the potential at the emitter will largely follow the changes at the base caused by the EMI, and the PN base-emitter junction will not be pushed into rectification. At very high frequencies, however, the emitter may not do as well following the base. In this situation the stage will be more vulnerable to rectification from incident EMI. Large RF signal voltage acting on a nonlinear capacitance can also cause demodulation and other effects (this is related to the operating principle of *parametric amplifiers*).

EMI Ingress from the Loudspeaker Cable

The loudspeaker cable is a big antenna. As mentioned above, the propagation delay of a 10-foot length of speaker cable is about 14 ns. This corresponds to a quarter-wave line at 18 MHz. The speaker cable can act as a quarter-wave antenna at this frequency even though both conductors of the speaker cable may be intimately twisted together. Any inductance in the ground return of the speaker output of the amplifier will increase vulnerability to pickup of radio signals and other EMI at these high frequencies where the speaker cable is an effective antenna. The speaker return lead inside the amplifier may have self-inductance between its point of entry and the point where it reaches the star ground reference. Straight wire typically has self-inductance of about 30 nH per inch. A 6-inch ground return run will have 180 nH of inductance (there are many caveats here beyond the scope of this book). Its impedance at 100 MHz will be about 110 Ω. The impedance of this inductance may actually tune the antenna to some extent. In any case, RF that is developed across this length of wire may be able to cause some EMI vulnerability in the amplifier.

The loudspeaker hanging off the end of the speaker cable is also part of the antenna. The wiring inside the loudspeaker often forms a loop that can pick up EMI. The free-space capacitance of the loudspeaker hanging on the end of the speaker cable can also act to "tune" the antenna formed by the speaker cable. A large loudspeaker may have a free-space capacitance to ground on the order of 100 pF. If the common mode inductance of the speaker cable is 3 μH, this combination will have a resonance of about 9 MHz.

Implications for Output Network Design

It is important that EMI ingress from the output terminals not make its way into the amplifier in general and not make its way to the output stage in particular. The impedance at the output stage is nonlinear, especially in the crossover region. At the same time, the EMI signal will be impinging on PN junctions where rectification may be possible. The output network, consisting of a coil in parallel with a resistor and a Zobel network to ground on one or both sides of the coil, can be helpful in suppressing EMI ingress.

Implications for Feedback Network Design

Some amplifiers incorporate a phase lead capacitor across the feedback resistor. This often improves stability if it is not overdone (too large a capacitor). However, this capacitor provides a direct path for EMI from the speaker cable to enter the sensitive input stage. I prefer to achieve good feedback loop stability without resort to such a capacitor.

EMI Ingress from the Mains

Often the mains supply contains a lot of garbage, both in differential mode and common mode. Unfortunately, the mains safety ground also often contains garbage that can ultimately be conveyed to the power amplifier chassis ground. So-called X capacitors between the hot and neutral leads help to suppress differential-mode EMI, while capacitors from each of the hot and neutral leads to the safety ground help suppress common-mode EMI to some extent. EMI input filters integrated with the IEC power connector help.

Unfortunately, the power transformer does not always do a very good job of isolating EMI on the primary from the secondary. The capacitance from primary to secondary for one 500-VA toroidal power transformer measured over 1300 pF. Toroidal transformers usually have greater primary-secondary coupling capacitance than transformers of conventional construction. A 500-VA laminated E-I core transformer measured just under 600 pF.

EMI Distortion Mechanisms

EMI can cause audible noise to be generated even though the EMI itself may lie at very high frequencies. This happens as a result of nonlinear effects in the amplifier which either cause different elements of the EMI signal to intermodulate with each other or which cause rectification to occur so that AM detection of the EMI *carrier* occurs.

As long as the EMI causes only audible noise, this is not distortion per se. However, inevitably the voltage swing of the audio signal will affect in some way the behavior of the nonlinearity that brought the EMI down into the audio band. The EMI products are now correlated with the audio signal and bona fide distortion of the audio signal has occurred. Similarly, the presence of the EMI can affect the operating points of the circuitry within the amplifier, thereby causing distortion of the audio signal by impairing the operation of those circuits.

The big question is whether EMI can distort or otherwise impair the audio signal if the EMI is not audible by itself when there is no audio signal. In other words, if we can't hear noises produced by EMI, are we OK? Maybe not. For example, it could be the case that in the absence of an audio signal the amplifier has sufficient margins to handle the EMI without encountering enough nonlinearity to cause audible artifacts of the EMI to emerge. When the operating points are being moved around by an audio signal, those margins

may no longer be adequate and EMI may rear its ugly head only in the presence of the audio signal. One would hope, however, that such behavior would show up on a distortion test if the offending EMI is present when the distortion test is being carried out.

18.3   Input Filtering

The best defense against EMI at the input of the amplifier is input filtering that very substantially reduces the amplitude of any high frequency signal before it reaches the first active devices. Such filtering must be effective to very high frequencies in the GHz range; this is not always as easy as it seems. Filtering of the input signal in both the differential mode and the common mode (even for single-ended inputs) can be important. Placing some very high-frequency filtering immediately at the point where the signal is no longer in a coaxial environment is very helpful.

Achieving a Linear Phase Response

If multipole filtering is employed at the input of the amplifier, it is desirable that such filtering create a good approximation to a linear phase response to well beyond 20 kHz. This can be accomplished by placing multiple poles at successively higher frequencies. It then becomes possible to design the combined filter to have a better approximation to a flat time delay, where the phase lag introduced by the filter increases linearly with frequency. A simple rule of thumb is that each successive pole should be higher in frequency by one octave than the previous one in order to achieve a reasonable approximation to linear phase out to an octave beyond the highest pole frequency.

18.4   Input Ground Loops

Most stereo amplifiers are susceptible to input ground loops. This results from the two shielded interconnect cables carrying the left and right channels. In simple designs, the shields go to the same ground at both the source and amplifier ends. If the two interconnects do not follow exactly the same physical path, a loop will be formed and ground currents will flow in the loop. These ground currents, potentially representing hum and EMI, can induce garbage into the signal path.

Ground Break Resistor

The first order of business in dealing with the input ground loop problem is to minimize the circulating currents. This can be accomplished by putting resistance into the loop. The induced voltages are usually small, so even a few ohms will greatly reduce the amount of circulating ground current. This is commonly done in many power amplifiers by inserting a 4.7-Ω resistor between the input ground and the analog circuit ground. The negative feedback shunt resistor is returned to the input ground node. This is illustrated in Figure 18.5.

Balanced Inputs

Fully balanced amplifier inputs with true differential signals provide the best immunity to pickup of interference. Balanced inputs with high common mode rejection to high frequencies are most immune to EMI.

Interconnect Alternatives

Some single-ended interconnect arrangements employ a shielded twisted pair. In this case both the signal and the return for the signal (ground) are carried on a twisted pair so that the signal and return lines both experience exactly the same electromagnetic environment. The shield is connected to ground at only one end, usually the source end. This prevents the circulation of ground loop currents in the shield. While it does not prevent the circulation of ground loop currents in the ground return conductor, it reduces the effect by causing the same voltage to be induced into the signal conductor, forcing it into the common-mode signal domain.

18.5   Mains Filtering

Just about everything electric in your home (and your neighbor's home) is connected to the mains. As such, the mains network is a cesspool of EMI.

Line Filters

Prefabricated line filters are convenient and often quite effective. They are professionally designed and often well shielded. A more common and less-expensive approach is the line filter that is often built into an IEC receptacle. This has the advantage of being physically located right at the entrance of the power cord into the equipment, making it possible to stop the incoming EMI at the earliest point.

Ferrites and Inductors

The use of ferrites in audio amplifiers has gotten a bad reputation. These will often be in the form of ferrite beads and inductor cores. They can be in the signal path or in power supply circuits on either the mains side or the circuit side. Inductors in particular must be carefully placed because they can radiate electromagnetic fields. Toroidal inductors will be less prone to this, but are quite uncommon.

18.6   EMI Egress

A power amplifier can also create EMI that can disturb other components. The best example of this is rectifier EMI radiated through the mains power cable. It may appear as EMI that is conducted into other equipment via their power cords, or it may be electromagnetically coupled to signal interconnects that pass near the power amplifier's power cord. This kind of coupling must be avoided when carrying out sensitive distortion tests on power amplifiers. Rectifier noise was discussed at length in Chapter 16.

18.7   EMI Susceptibility Testing

As applied to audio amplifiers, EMI testing is an inexact science at best and completely absent at worst. Here we suggest a few procedures that can bring some experimentation and measurement into the picture.

Cell Phones and Electric Drills

Although they are certainly not calibrated instruments, cell phones, hair dryers, and electric drills operated in close proximity to a power amplifier can provide a helpful

qualitative indication of the amplifier's susceptibility to EMI. For these tests, the amplifier should be connected to a real source or an emulated source through interconnects of typical length. It should likewise be connected to a loudspeaker load or emulated loudspeaker load through speaker cable of typical length. The premise here is that susceptibility to such relatively high levels of local EMI will reveal itself as audible output from the amplifier or output that is measurable on an oscilloscope or spectrum analyzer.

EMI Generators

A slightly more scientific approach to EMI evaluation involves the use of toroidal inductors or power transformers through which an interconnect cable or speaker cable is passed. This causes the cable to become one-half turn of what amounts to a transformer. The transformer or inductor can then be excited by EMI using flyback techniques where a current is set up in the winding and then interrupted, resulting in a large flyback voltage. This can be done with a relay hooked up as a buzzer. One can also envision exciting the coil with a power MOSFET whose gate is turned on and off with some kind of generated signal, perhaps even a pseudo-random word generator.

References

1. Cordell, R. R., "Open-loop Output Impedance and Interface Intermodulation Distortion in Audio Power Amplifiers," 64th Convention of the AES, preprint 1537, 1982; available at www.cordellaudio.com.
2. Otala, M., and Lammasniemi, J., "Intermodulation Distortion in the Amplifier Loudspeaker Interface," 59th Convention of the Audio Engineering Society, preprint No. 1336, February 1978.
3. Cherry, E. M., and Cambrell, G. K., "Output Resistance and Intermodulation Distortion of Feedback Amplifiers," *J. Audio Eng. Soc.,* vol. 30, pp. 178–191, April 1982.
4. Otala, M., and Huttunen, O., "Peak Current Requirements of Commercial Loudspeaker Systems," *J. Audio Eng. Soc.*, vol. 35, no. 6, June 1987.

Simulation and Measurement

SPICE simulation can be extremely important to power amplifier design, and its use in this area is described in detail in Part 4. Even those designers with no SPICE experience will be able to employ this valuable tool. The excellent SPICE simulator LTspice, made available free of charge from Linear Technology Corporation, is the central focus. Accurate transistor models suitable for audio amplifier simulations can be difficult or impossible to obtain from manufacturers. This is especially so for BJT and MOSFET power output transistors. Chapter 20 is devoted to enabling you to create accurate models for transistors used in audio amplifier simulations, armed with only datasheet information and some simple measurements.

The many approaches to distortion measurement are also explained in Part 4. Much attention is paid to the techniques needed in order to achieve the high sensitivity required to measure the low-distortion designs discussed in the book. Less well-known distortion measurements, such as TIM, PIM, and IIM, are also covered here. In the quest for meaningful correspondence between listening and measurement results, other nontraditional amplifier tests are discussed as well.

This page intentionally left blank

SPICE Simulation

The SPICE circuit simulator has been around for over 30 years. Developed at U.C. Berkeley, the acronym stands for *Simulator with Integrated Circuit Emphasis* [1]. Because integrated circuits are almost impossible to breadboard and probe, there was a great need to simulate designs before committing to the expensive process of laying out and fabricating an integrated circuit. Although that was its original mission, it is equally useful for discrete circuits at the circuit board level.

This chapter is a brief audiocentric description of SPICE and its application to audio power amplifier design. It is definitely not a comprehensive treatment of SPICE, but it does provide quick access to most of the features and nuances needed for design of audio circuits. It is presented in a tutorial style. This chapter will not make a SPICE guru out of you, but it will arm you with most of the techniques that are valuable in the design and analysis of audio power amplifiers.

The use of SPICE simulation can save hours in reaching the point where you can build a working amplifier. Intuition is not always right when it comes to circuit design, and SPICE helps here.

19.1   LTspice

Although there are many SPICE packages available, one that stands out for audio amplifier design is LTspice from Linear Technology Corporation (LTC) [2,3]. The program is free, well supported, widely accepted, and easy to use. It is also one of the best-performing SPICE simulators. It is easily downloaded from the LTC site at www .linear.com.

All of the simulations done for this book were carried out with LTspice, and this discussion will focus on LTspice. Like most other software tools, LTspice has many options and capabilities (and a very large user manual). Here we will just scratch the surface to get you started in an efficient way. The 90-10 rule applies: 90% of what you need to do can be accomplished with 10% of the features. LTspice also comes with a good set of device libraries and a very helpful Educational directory where many example designs illustrate how LTspice is used.

Installation
Download the LTspice software from the LTC website at www.linear.com. After LTspice has been downloaded and installed, click on the icon that it places on the desktop. If you double click on the icon, the program will come up with a toolbar with most of the features grayed out.

The Toolbars

Familiarize yourself with the toolbar by placing the cursor under each icon and reading the name of the function that appears. Most of these functions are obvious. In most cases a click on the icon will activate the function. In some cases a window will appear and selections will be available. Details for these can be found in the LTspice manual or in Help. The functions listed below are used the most. The name of the item is followed by a description of the icon. A brief description of each function is also provided.

Save **(diskette)**

Saves the current schematic

Run **(runner)**

Runs the simulation

Cut **(scissors)**

Deletes elements from the schematic

Copy **(two pages)**

Copies windowed elements or groups of elements

Wire **(pencil and line)**

Places a wire

Ground **(ground symbol)**

Places a ground with its symbol

Label Net **(tag with A)**

Gives a node a name

Resistor, capacitor, inductor, diode

Places one of these frequently used components

Component **(AND gate)**

Places other components, like transistors, selected from a list

Move and Drag **(big hand, little hand)**

Windows an element and moves or drags it

Rotate and Mirror **(E with arrow)**

Rotates or mirrors an element when it is selected with *Move*

Text **(Aa)**

Adds text to the schematic

SPICE Directive **(.op)**

Defines aspects of the simulation to be run

Directory Organization

The LTspice material of greatest interest is located in two directories:

C:\Program Files\LTC\LTspiceIV\examples

C:\Program Files\LTC\LTspiceIV\lib

The …*examples* directory contains an *Educational* subdirectory where a great many example circuits are illustrated as simulations.

The …*lib* directory contains the models for the devices used in LTspice simulations. It contains three important sub-folders. The first is the …*cmp* folder where files for components are stored. This directory contains both passive and active components. An example file in this directory is the *standard.bjt* file. This single text file contains the SPICE models of all of the bipolar transistors supplied with LTspice and is the place where the user can append additional models. Adding models will be discussed later. If your copy of LTspice is in the *C:\\program files* directory, the full path for the *cmp* folder will be

C:\\program files\\LTC\\LTspiceIV\\lib\\cmp

The …*sub* folder contains subcircuits. These are circuits made up of components that can be used just like a component on a schematic. An op amp is a good example of a subcircuit. Every subcircuit requires a symbol. These are stored in the …*sym* folder. LTspice allows you to create your own components and subcircuits and store them in these folders. You can thus create your own libraries.

Control Panel

Go to the *Control Panel* by clicking on the hammer icon on the toolbar. There are many important controls here, most of which are best described in the LTspice documentation. A couple of controls will be explained as useful examples. Open the *Waveforms* tab, and notice that you can select thick lines for the plots and can change the color scheme for the plots. The color scheme for each of many traces can be selected. You can click on the background and set its color as well. In cases where a plot will be placed in a document, it may be desirable to put black traces on a white background. The color scheme selection also allows you to select the color scheme for the schematic and netlist presentations.

Under the *Operation* tab it is usually wise to select the option to automatically delete *raw files* to avoid saving unnecessarily large amounts of data. Under *Drafting Options* you may wish to have drawing grids visible and you may wish to draft with thick lines, especially if you will be placing the drawing in a document. You can also control the font.

Help

The Help files for LTspice are well organized and comprehensive. The examples shown in this chapter will quickly get you started, but many useful capabilities are not covered. Review the Help files to get a feeling for what is there and how it is organized.

The LTspice Users' Group

There is a very active, independent LTspice users' group on Yahoo. The users' group is at groups.yahoo.com/group/LTspice. Good discussions can be found there as well as many files for download and a good manual.

19.2   Schematic Capture

Schematic capture will be explained by actually creating a simple circuit comprising a differential pair amplifier stage. This demonstration circuit is shown below in Figure 19.1. The differential pair is operated with 1 mA in each transistor supplied by the 2-mA tail
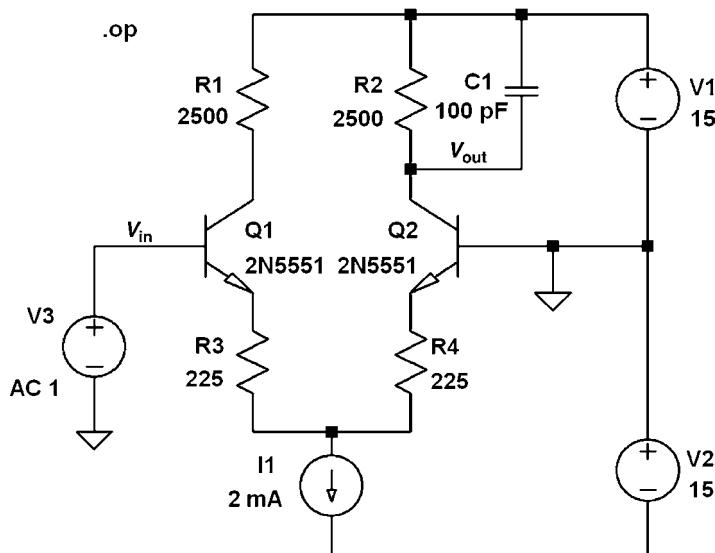
FIGURE **19.1** A simple circuit illustrating schematic capture.

current source I1. Emitter resistors R3 and R4 provide 10:1 emitter degeneration; that is, they reduce the gain by a factor of 10 compared to what it would be without degeneration. Collector load resistors R1 and R2 allow a nominal DC voltage drop of 2.5 V and provide for a differential gain of 10. The gain is 10 because each collector resistor is 10 times the value of the effective emitter resistance of its associated transistor. Single-ended gain to the output node V_{out} is 5, or about 14 dB. Capacitor C1 provides for some high-frequency roll-off by creating a pole at about 640 kHz.

Placing Components

Open LTspice and click on *File → New Schematic*. Place the resistors first. Click on the resistor toolbar button, bring the cursor to the location for the resistor, and click. R1 will be placed. Move the cursor to the position for R2 and click. R2 will be placed. Do the same for R3 and R4. Notice that the resistors are numbered in sequence as they are placed. Right-click to exit from the resistor placement mode. Right-click on R1, enter its value of 2500 in the dialog box that appears, and click *OK*. Enter the values for the other three resistors. Place capacitor C1 in the same fashion and enter its value as 100 p or 100 pF. Do not leave a space in this entry.

Place the voltage sources by clicking on the *Component* button on the toolbar. A list of available components will come up. Click on the component labeled *voltage*. The voltage source symbol will appear in a dialog box. Click *OK* and then place the voltage source by clicking on the location where it is to go. Click again on the locations for V2 and V3. Right-click to exit the voltage source entry mode. Right-click on V1 and enter its DC value of 15. Do the same for V2. Right-click on V3 and then click *advanced*. A dialog box will appear with many options describing the behavior of the voltage source. For now, simply enter *1* in the box for *AC Amplitude*. The button *(none)* under *Functions*

should be turned on. This prepares the voltage source to act as an AC voltage source for a small-signal AC simulation.

Click on the component button on the toolbar and select *current* from the list. Place the current source, and then right click on it to enter its value of 2 mA. Place the two ground symbols by clicking on the *Ground* button on the toolbar.

Picking and Placing Transistors

Place transistor Q1 by clicking on the *Component* button in the toolbar and selecting *npn* from the list that appears. Hit *OK* and place the transistor by clicking when it has been moved to the proper location. A second transistor will be attached to the cursor. Move the cursor up to the *Mirror* button on the toolbar and click it. This will flip the orientation of the transistor as needed for Q2. Now place the transistor. Right-click to exit transistor placement. Note that any component can be mirrored (*Ctrl* E) or rotated (*Ctrl* R) while it is attached to the cursor, including when using the *Move* command from the toolbar.

Right-click on Q1. A dialog box will appear, showing the type and some of the characteristics of Q1. At this point the information will be missing or generic. Click on *Pick New Transistor*. A list will appear showing all of the NPN transistors in the library. Select the 2N5551 and hit *OK*. Right-click on Q1 and notice now that the type and some of the characteristics are filled in. Define transistor Q2 in the same way.

Other Components and Subcircuit Libraries

When you clicked on the *Component* button in the toolbar, many different component selections appeared. Some of those were named in brackets. These are additional parts directories that can be accessed in the same way by double clicking on them. Take note especially of what lies in the *misc* directory.

Many of these components are constructed of so-called subcircuits, which are themselves circuits composed of numerous basic devices. A good example of a subcircuit is an operational amplifier. Subcircuits have symbols and can be placed on the schematic and used just like any other component.

Parameterized Elements

Sometimes it is desirable to parameterize the value of an element, like a resistor, rather than committing it to a fixed value. As we will see later, this can allow the value of the element to be stepped across a range of values, producing a simulation that has a family of curves. A component (like a resistor) is parameterized by placing a variable inside curly brackets where the component value would normally go. If the variable for a resistor is *Rseries,* the parameterization is completed by adding the SPICE directive

    .param Rseries=1k

where 1k is the nominal value of *Rseries*.

Completing the Schematic

Move the components into their desired position if necessary. Do this by clicking on the *Move* button on the toolbar and then windowing the component you wish to move. Move the component as desired and then left-click. Right-click to exit the *Move* mode. Note that you can move the component designation or the value in the same way. You can change the component designation by right clicking on the text of the designator.

Wire the circuit by clicking on the *Wire* button on the toolbar. Click on the beginning point of the wire and each place where it is to turn. Click on the final destination of the wire. Right-click to exit the wire mode. Do the same for all of the remaining wiring of the circuit. If any wire or component is put down that must be deleted, click on the *Cut* button on the toolbar, designated by a pair of scissors. Click on the element to be deleted, and it will be removed. Right-click to exit the *Cut* mode.

Add node names to selected nodes by clicking *Label Net* in the toolbar. A dialog box will appear. Enter the name for the node and click *OK*. A rectangle with a diamond at its bottom will be attached to the cursor. Place the diamond on the net in a convenient place and click. Right click to exit the *Label Net* mode. Label the base net of Q1 as V_{in} and the collector net of Q2 as V_{out}. Nodes with the same label will be connected for the simulation even if not connected by a wire in the schematic. This can sometimes reduce clutter on the schematic.

Add text to the schematic by clicking on the *Text* option in the toolbar. Type the desired text into the dialog box, hit *OK,* and place the text on the schematic. The schematic of the differential amplifier stage is now complete and should look like Figure 19.1.

Save the schematic to a directory of your choice. Call it *diffamp*. If you then look in that directory you will see a file named *diffamp.asc*. This is the schematic file.

The SPICE netlist can be obtained from the schematic by using the command *View → SPICE netlist*. Select all the text and copy it to the clipboard (*CtrlC*) to paste it into a different editor, like Notepad.

The schematic can be copied to an application like *Word* or *Paint* by typing *Ctrl-C* and putting it onto the clipboard. This is also true for plots. *Paint* can be used to convert the file to convenient formats like *TIF*, *GIF,* and *JPG*. The complete LTspice screen can be copied to the clipboard by clicking *Ctrl Print Screen*. This is useful for putting the material into a word document.

19.3   DC, AC, and Transient Simulation

The differential amplifier stage will be simulated in this section. The three most important and basic types of simulation are DC, AC, and transient. The DC simulation biases the circuit and shows all of the node voltages and operating points. The AC analysis shows small-signal frequency and phase response. The transient simulation shows the actual waveforms at different points in the circuit when the circuit is driven by an input signal. The result of a transient simulation is much like what one would see on an oscilloscope.

The DC Operating Point

Set up the DC simulation by clicking on *Simulate → Edit Simulation Cmd*. The simulation dialog box will appear with tabs for the following types of simulation:

- Transient
- AC Analysis
- DC sweep
- Noise
- DC Transfer
- DC operating point

Click on the tab for DC *operating point*. Note that *.op* will appear in the syntax box. This is the SPICE directive for a DC simulation. Hit *OK* and notice that a rectangle will be attached to the cursor. Place this rectangle on the schematic in a convenient place and click. The *.op* SPICE directive will now appear on the schematic.

The simulation is now ready to be run. Click on the *Run* button on the toolbar. The simulation will run quickly, and an information box will appear showing all of the node voltages in the circuit. Nodes you have named will appear with their names. Other nodes will be designated with sequential node numbers. Interpreting results is easier if you label all of the nets of interest. The box will also show the direct current flow in all of the transistors and passive elements. Note that the voltage at V_{out} is about 12.5 V, as expected, and that the collector current of each transistor is just shy of 1.0 mA.

Close the DC simulation information window and move the cursor over a component on the schematic. The lower left portion of the window will show the voltages, currents, and power dissipation for each component. Move the cursor over a wire. The information window will display its node name and voltage. This approach to viewing DC simulation results is usually much more convenient than viewing the results in the initial DC simulation results window.

The SPICE Error Log

There is more to the SPICE error log than one would think. It is not just telling you what is wrong. In the case of a DC operating point simulation, it reveals the operating point and small-signal model parameters for every transistor in the circuit.

Click on *View → Spice Error Log* and the information will appear. Information like DC and AC beta and f_T of the transistors at the actual operating point in the circuit can be very valuable. Virtually all of the important hybrid pi parameters are shown. This information provides good insight into how the model for the transistor is behaving. One can actually set up a circuit to bias the transistor at a chosen operating point and compare these numbers to the data sheet values for the transistor in order to see how well the model compares to the data sheet.

Convergence

LTspice is very good at converging to solutions, but there will be rare occurrences when the iteration limit is reached and the simulation fails. The message *Analysis Failed: Iteration limit reached* will be displayed.

This is often a result of the particular circuit topology being simulated and sometimes can be the result of a circuit design or schematic entry error. Apart from checking the circuit for errors, there are three things that can often solve the convergence problem. The first is to use the alternate solver available in LTspice. One can switch to the alternate solver by going to *Control Panel → SPICE* and selecting the alternate solver in the *Engine* area in the dialog box.

The second thing to try is more specific to power amplifiers and similar topologies. Connect a large-value resistor from the high-impedance VAS output node to ground. This resistor can often be as large as 1 MΩ or even 10 MΩ and still fix the convergence problem while causing minimal interference to normal circuit operation. Once convergence is achieved this way, the operating points of all of the transistors can be checked to see if something is wrong with the circuit itself. There is also the occasional case where the presence of a very large resistance to ground on the high-impedance node (e.g., 100 MΩ) can actually impede convergence.

I have also found that certain transistor models can be more prone to causing convergence problems. This possibility can be tested by temporarily changing one or more of the transistors to a different type. The VAS and predriver transistors connected to the high-impedance node are prime candidates in this case.

AC Analysis

Click on *Simulate → Edit Simulation Cmd* and then hit the *AC Analysis* tab in the dialog box to set up the AC simulation. Fill in the information requested. Select a decade sweep with 100 points per decade. Enter start and stop frequencies of 10k and 100Meg, respectively. The use of M for MHz will not work; *MEG* will work. Click *OK* and place the SPICE directive on the schematic in a convenient place by clicking there. Notice that the *.op* SPICE directive for the DC operating point will remain on the schematic but will change to *op*, signifying that it is not the simulation to be run this time.

Right-click on V3 and click on the *Advanced* box if necessary. Make sure that there is a *1* in the *AC Amplitude* box. The other boxes can remain blank. The circuit is now ready for AC analysis.

Click on *Run* in the toolbar. The AC analysis will be performed and a second window will come up with frequency labeled across the *X* axis. Place the cursor on the *Vout* net. The cursor will change to a red probe symbol. Click on the net. The frequency and phase response will appear in the plot window. Gain will be shown in dB on the left axis and phase will be shown in degrees on the right axis. Notice that the frequency response indicates approximately 14 dB of gain at low frequencies, as expected. Move the cursor over the frequency response curve at some low frequency and notice that the frequency, gain, and phase are shown numerically in the lower left corner of the main window. Move the cursor to the point on the curve where the gain is 11 dB, which is approximately 3 dB down. The frequency readout will indicate about 604 kHz, the 3-dB frequency of the circuit.

Move the mouse-probe to the collector net of Q1 and click. The frequency response at that point will also be shown. Notice that it exhibits very little reduction in gain even at 10 MHz. This is because there is no external capacitor connected to that node to create a significant HF roll-off.

Click in the area of the plot and then right-click. A list of options will appear. Select *Visible Traces*. A list of all possible traces to plot will appear. $V(V_{out})$ and $V(n001)$ will be highlighted because they have already been selected for plotting. Select an entry without deleting the others by control clicking on that entry. The status of an entry can be changed by control clicking on it as well. Do this for $I(C1)$ and hit *OK*. The plot of the current in C1 as a function of frequency will now appear.

Position the cursor over the V_{out} net. Push and hold down the left mouse button while the red probe is displayed. Hold down the button and move the probe cursor to the collector net of Q1. Notice that the probe color changes to black, signifying that it is now a negative probe. Release the left mouse button. A trace will appear showing the differential output voltage from the collector of Q1 to the collector of Q2. This curve will be up 6 dB compared to the single ended output curve, as expected.

Click in the area of the plot and see an entry in the toolbar called *Plot Options*. Select *Save Plot*. The same plot will automatically appear the next time the simulation is run.

Transient Simulation

Click on *Simulate → Edit Simulation Command* and then hit the *Transient* tab in the dialog box to set up the transient simulation. The transient simulation dialog box will appear. Enter 10 ms for *Stop Time*. All of the remaining boxes can be left blank. Hit *OK* and place the transient SPICE directive on the schematic.

Create the time-varying input for the transient simulation by right clicking on input voltage source V3. Because the *Advanced* dialog box was previously used to specify an AC source for AC simulation, that dialog box will again come up. In the function area, define the function by clicking the *Sine* button. Enter 0.1 in the amplitude box to generate a 0.1-V peak sine wave. Enter 1000 for the frequency and 10 for *Ncycles*.

Hit *Run*. The simulation will run and a waveform window will appear with time running from 0 to 10 ms along the *X* axis. Probe the V_{out} net, and the sine wave output of the amplifier stage will appear along with the voltage shown on the *Y* axis. Using the mouse, create a rectangle on the waveform window that extends left to right between a pair of cycle peaks and vertically from the bottom of the waveform to the top. Hold the mouse button. Notice the information box in the lower left corner of the screen. The period of the waveform is shown as *dx* equaling about 1000 μs and the peak-to-peak amplitude of the waveform indicated by *dy* as about 985 mV. Release the mouse button. This portion of the waveform will now appear zoomed in. Hit *Zoom Full Extents* in the toolbar to restore the waveform to its original presentation.

Probe the collector wire of Q1 and see the other output out of phase with V_{out}. Probe V_{in}, and see this smaller waveform presented swinging about zero volts and notice that the combined waveform presentation autoscaled by LTspice.

Move the cursor over C1 and see that the cursor changes to a representation of a clip-on ammeter. Click on C1 and see its current plotted in the plot window. Notice that it is 90° out of phase with respect to the voltage waveforms, as expected. The current in any of the wires in the circuit can be plotted by *Alt* left clicking on the wire.

Click on the display, then right-click on it and select *visible traces*. Clear all of the visible traces. Go back to the schematic window and probe from V_{out} to the collector of Q1. The differential output voltage will be displayed. Now click on V_{in} and see it displayed as well, with both traces scaled properly without the presence of a DC component on the output, making them easier to see and compare.

Right-click on V3 and set the function to a pulse. Enter $V_{initial}$ = –0.1, V_{on} = 0.1, *Tdelay* = 0, *Trise* = 10 ns, *Tfall* = 10 ns, *Ton* = 5 μs, *Tperiod* = 10 ns, and *Ncycles* = 10. This will create a 100-kHz square wave at V_{out} with 1 V p–p amplitude. Go into *Simulate > Edit Simulation Command* and enter a stop time of 100 μs in the transient dialog box. Hit *Run*, and then probe V_{out}. Ten cycles of the 100-kHz square wave will be shown. Notice the rounded leading edges due to the circuit bandwidth of less than 1 MHz.

Notice that in the *Transient* dialog box there was a place to enter *maximum timestep*. LTspice normally does a fairly good job of automatically adjusting the timestep in a transient simulation. The size of the timestep affects the accuracy of the simulation. In some critical simulations it is sometimes desirable to set a maximum timestep that LTspice is allowed to take. For the simulations done so far, it has been unnecessary to set a maximum timestep.

Transient simulations can create fairly large *.raw* files that will take up unnecessary space in the simulation directory. I recommend you have LTspice automatically delete

them after a run is closed. Go to the control panel by clicking on the hammer on the toolbar and select the *Operation* tab. Answer *Yes* to *Automatically delete .raw files*.

If you *Alt*-click a device in the schematic, a thermometer will appear and power dissipation of the device will be plotted. If you *Ctrl*-click the label of a waveform (at the top of the plot pane), a display box will appear that shows the RMS and average values of the waveform. If you do this for a power waveform of a device, the average power dissipation of the device will be displayed in the box. This is especially useful in looking at output stage transistors.

19.4   Distortion Analysis

The Fast Fourier Transform (FFT) capabilities built into LTspice make convenient and detailed distortion analysis possible. In this section distortion analysis will be illustrated by analyzing the distortion of the differential amplifier stage described above. Most conventional distortion analysis is carried out with a transient simulation employing a sinusoidal input. In preparation for the FFT analysis, attach the SPICE directive .option plotwinsize=0 to the schematic.

This turns off data compression that LTspice normally uses to save space. The accuracy and dynamic range of FFT analysis can be degraded when the data from a transient run are compressed. Data compression can also be disabled on the *Compression* tab of the control panel, but that setting will not be remembered the next time LTspice is invoked.

Run a transient simulation of the differential amplifier stage with a 1-kHz input with 0.1 V peak amplitude for 16 cycles. Note that when you click on the sine function, the new window that comes up will still have some of the boxes populated (left over from the square-wave run). Clear these boxes. Set the transient run duration for 16 ms and run the simulation. Click on V_{out} to obtain the output waveform. Its amplitude will be 1 V p–p.

FFT Spectral Plots

Click on the waveform window and then right-click on it. Select *View→FFT* at the bottom of the list of selections. In the *Time range to include* section, click the button *Specify a time range*. The *End Time* will already be listed as 16 ms or something very close to it. If it is not exactly 16 ms, enter 16 ms. Enter 8 ms in the *start time* box. This causes the FFT to be performed on the last eight cycles of the simulation, suppressing start-up artifacts. The default number of FFT points is 65,536, and this number is fine. Hit *OK*. A new window will appear with the FFT spectrum of the waveform shown in dBV as a function of frequency. Using the mouse, drag a window over the main area of interest in the spectral plot. This will provide a close-up view for measuring the harmonic amplitudes.

Place the cursor on the fundamental peak at 1 kHz and notice that the cursor value in the lower left corner of the window reads –9.5 dB. This is dB relative to 1 V RMS. Place the cursor on the second peak at 2 kHz, representing the second harmonic. It will read approximately –104 dB. The second harmonic is thus down about 94 dB, or at about 0.002%. Measure the third harmonic at 3 kHz in the same way. It will read about –79 dB, down about 69 dB from the fundamental, or at about 0.035%.

Notice that the fourth and fifth harmonics read –138 dB and –125 dB, respectively. The spectral noise floor, often called the *grass*, is at –142 dB. Notice also the large amount of spectra extending out to high frequencies. There are high-frequency artifacts at –81 dB, for example. This is evidence that the FFT has not been optimized.

Reading out the amplitudes of the spectral lines is made much easier by attaching a cursor to the spectral plot. Just left-click on the plot label and a crosshairs will appear. Right-click on the plot label, select one cursor, and hit *OK*. A readout box will appear showing the frequency and amplitude of the point on the plot where the cursor crosshairs are located. The crosshairs are dragged to the desired location by clicking on and holding at or near the crosshairs where the number 1 (designating cursor number 1) appears. You can also move the crosshairs left and right by convenient increments with the ← and → keys to zero in on a particular peak. These keys will usually land the crosshairs on a harmonic frequency of the fundamental. The step size of the cursor movement is the frequency increment corresponding to the period processed by the FFT. For example, if the number of cycles processed corresponds to the last 8 ms of the simulation, the step size will be 125 Hz.

Optimizing FFT Simulations

There are seven things that are important in optimizing the FFT:

1. Turn compression off
2. Simulate an adequate number of cycles
3. Simulate an integer number of cycles of the lowest frequency
4. Ignore an adequate number of cycles before beginning the FFT
5. Choose an appropriate number of FFT points
6. Choose a small enough and optimal maximum timestep
7. Beware of long time constants in the circuit

The first five items were satisfied above, but the timestep was left to SPICE to determine. Better results are achieved with the FFT when the maximum timestep size is limited to a small value that is related to the period of the sinusoid being simulated and to the length of time of the FFT analysis.

It has been recommended in the past that the maximum timestep be set to the FFT analysis time divided by 16,383 [4, 5]. This caused the timesteps of the transient simulation to coincide with the FFT sample points when the number of FFT points in the analysis time was 16,384. I have used this relationship over the years, even though the default number of FFT sample points in LTspice has increased in later releases, and it has always worked well for me. For an FFT analysis time of 8 ms, this corresponds to about 0.488 µs. Enter the SPICE directive .options maxstep=0.48831106u on the schematic.

Run the simulation again, noting that it will now take longer because of the smaller maximum timestep. Perform an FFT analysis on the result. Notice the significant reduction in spectra at higher frequencies. The high-frequency artifacts are at about –153 dB as compared with –81 dB in the previous simulation. Use the cursor to measure the fourth harmonic at 4 kHz. It will read about –153 dB, as compared with –138 dB above where maximum timestep control was not implemented. The grass is at about –162 dB as compared with the previous –142-dB number. These very substantial improvements in FFT resolution are due to the enforcement of the appropriate maximum timestep.

My experience has been that the above rule for maximum timestep may be conservative and that the precision of the chosen number is not sacred. A doubled maximum

timestep rounded up to 1 μs raised the high-frequency artifacts from –153 dB to –132 dB, but the other quoted numbers changed by an insignificant amount. My advice is to experiment with the maxstep number so that you get good results without resorting to an unnecessarily small number.

The FFT results can be degraded by the presence of circuitry with long settling times, such as AC-coupled inputs. Wherever possible, perform the FFT simulations on DC-coupled versions of the circuit. The number of cycles of the waveform that you employ for the FFT has a direct impact on the frequency resolution of the FFT. The width of the frequency bin for each spectral line will be $2/\text{FFT}_{time}$. A simulation with FFT processing of 8 ms of data will have spectral lines with a total width of 250 Hz.

The number of cycles that you simulate before starting the FFT analysis is a judgment call. The settling time is intended to ensure that all initial conditions and transients have had time to settle out so as not to affect the FFT results. For high-quality FFT results I recommend that you simulate 16 cycles and perform the FFT on the last eight cycles. Too small a settling time or too small an FFT time may result in artifacts and loss of FFT dynamic range. However, I have often obtained satisfactory results with as little as one cycle of simulation ignored before the FFT interval.

Total Harmonic Distortion

Total harmonic distortion (THD) for a sinusoidal transient simulation can be displayed in the SPICE error log by adding the *.four* SPICE directive to the schematic. Total harmonic distortion and the level of each harmonic will be listed up to the requested number of harmonics. Add the SPICE directive .four 1-kHz 10 8 V(V_{out}) to the differential pair schematic.

This directive specifies that the analysis will be done on a 1-kHz sine wave and that readout of the first 10 harmonics be provided. The number 8 indicates that the FFT is based on the last eight cycles of the waveform. Run the simulation, and then go to *View → SPICE Error Log*. THD will read about 0.035%. Second and third harmonic levels relative to the fundamental will read about 2*e*-5 and 3.5*e*-4, respectively.

19.5   Noise Analysis

Perform a noise analysis by going to *Simulate → Edit Simulation Command → Noise*. Fill in the dialog box with the output node to be measured, V(V_{out}), the input source (V3), the type of frequency plot (decade), number of points per decade (20), and start (1k) and stop (100k) frequency. Hit *OK* and place the resulting SPICE directive .noise V(Vout) V3 dec 20 1k 100k on the schematic.

Run the simulation. A plot window will appear, much like the one for AC analysis. Probe the V_{out} node and the plot of noise density versus frequency will be displayed. In this case it is fairly flat at about 16 nV/√Hz. The input-referred noise voltage is often of greater interest. It is just the output noise density divided by the gain of the circuit. With a single-ended gain of 5, the input-referred noise voltage for this differential stage is 3.2 nV/√Hz.

To put things in perspective, consider how much noise voltage is produced in a 20-kHz bandwidth. There are about 141 √Hz in a bandwidth of 20 kHz, so the total output noise in this bandwidth would be 2.3 μV. If the maximum useful output of the circuit were 5 V RMS, the SNR would be a factor of 2.17 million, corresponding to about 126 dB.
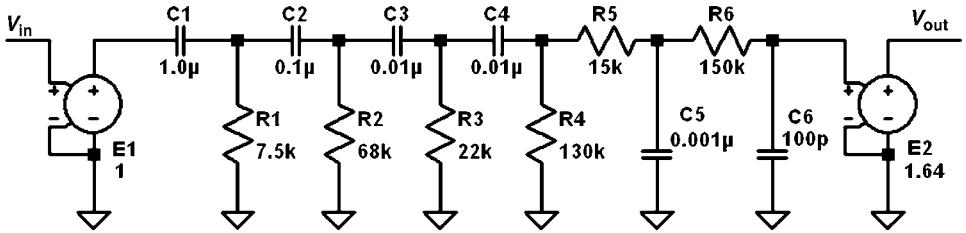
FIGURE 19.2 A-weighting noise filter.

Control-click on the trace label to see up a pop-up box that will display the total RMS noise on the plotted node over the plot frequency interval. This can be very helpful in deriving a signal-to-noise ratio.

Noise of Individual Contributors

The noise contribution of an individual component can be plotted by clicking on the component. The noise contribution for a transistor will include the effects from both its input voltage noise and input current noise.

Weighted Noise Simulations

As mentioned in Chapter 1, weighted noise measurements are often performed on amplifiers to better reflect those parts of the noise spectrum to which the ear is most sensitive. A good example of this is the A-weighting curve. This type of weighting can also be applied to simulations by following the circuit being simulated with a simulation circuit that implements the desired filter function. Figure 19.2 is a schematic of a filter that implements the A-weighting function. The voltage-controlled voltage source (VCVS) at the input buffers the signal. The VCVS at the output implements the necessary midband gain and buffers the output. This is a handy function to implement as a subcircuit.

19.6   Controlled Voltage and Current Sources

LTspice includes many types of voltage and current sources that can be controlled by voltages or currents. All of these sources can be assigned gain values. These provide a quick way of implementing certain functions within a simulation, such as buffering, chunks of gain, and so on.

The voltage-controlled voltage source (VCVS) can be used to implement voltage gain. It is designated by the letter *e* in the toolbar *Component* list. Setting its gain to unity implements an ideal buffer whose inputs and outputs are conveniently isolated. This allows one to pick off differential voltages, for example. Setting the gain to a very large number implements a near-ideal operational amplifier.

The voltage-dependent current source is designated by *g* (transconductance). LTspice also includes current-controlled voltage sources (*h*) and current-controlled current sources (*f*), but these are less frequently used. Their control current is the current flowing through a designated voltage source.

The circuit in Figure 19.3 subtracts an ideally amplified version of the input from the output to allow the viewing of the input-output error of the circuit. Go to the toolbar component selector and choose a VCVS by selecting the *e* listing. Place this on the
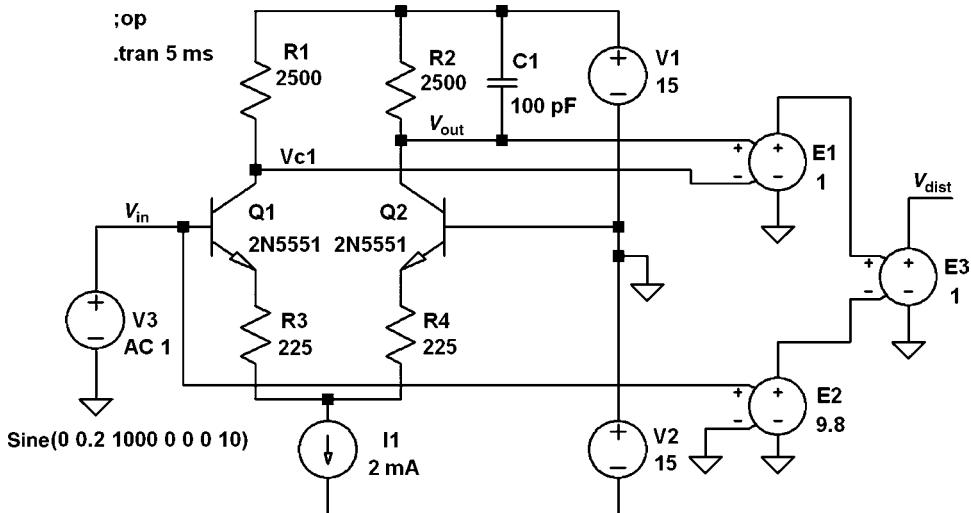
FIGURE 19.3   Simulation circuit for viewing input-output error.

schematic and connect it as shown. Right-click on the VCVS to set its gain. In the resulting dialog box highlight *Value* and type a gain of 1 in the box above. Place, connect, and set the gains of the other controlled sources *E2* and *E3*. *E1* merely derives the differential output voltage across the collectors of Q1 and Q2. *E2* multiplies the input signal by a value just slightly less than the differential gain of the stage. *E3* then takes the difference of the outputs of *E1* and *E2* and presents it as a distortion residual output.

Run the 1-kHz sinusoidal transient simulation for 5 ms with peak input amplitude of 0.1 V. Probe the V_{dist} node and see a small, slightly distorted replica of the sine wave. Rerun the simulation with a peak input voltage of 0.2 V and look at V_{dist}. Very visible distortion will now be evident as a result of the increased signal level.

19.7   Swept and Stepped Simulations

LTspice provides the capability to perform simulations where a source is swept or where a parameter or source is stepped for multiple simulations to produce useful plots.

DC Sweep

The *DC sweep* mode of simulation can be used to plot the input-output function of the differential stage of Figure 19.1. Go to *Simulate > Edit Simulation Cmd* and click on the *DC sweep* tab. A dialog box will come up. Select V3 as the source and pick a linear sweep. Enter start and stop voltage values of –1.0 and 1.0. Enter 0.01 for a sweep in increments of 10 mV. Hit *OK* and place the resulting SPICE directive on the schematic. Run the simulation and probe from the V_{out} net to the collector node of Q1. The transfer characteristic of the differential stage will be plotted. The DC sweep is also very useful in plotting transistor characteristics, such as I_c versus V_{be}.

DC Transfer

The DC Transfer mode of simulation provides a simple reading of the small-signal DC gain at a given operating point. Simply go to *Simulation → Edit Simulation Cmd → DC*

Transfer. Enter the output node V(V_{out}) and the name V3 of the source. Hit *Run* and a very simple result will be presented. The DC gain (transfer), the input impedance, and the output impedance will be shown. If this simulation is performed on a feedback amplifier, the low-frequency damping factor can be inferred from the output impedance. The DC gain of the amplifier is also conveniently shown.

Stepped Simulations

The *.step* command allows you to run multiple simulations with different parameter values and have the results plotted together as a family of curves. The stepped simulation can be illustrated by running the above DC sweep, but with the tail current source I1 stepped from 1 mA to 3 mA in increments of 0.5 mA. Add the *.step* SPICE directive shown below to the schematic.

.step I1 1mA 3mA 0.5mA

The syntax is simple. Listed in order are the source to be stepped, the starting value, the ending value, and the value of the increment.

Run the simulation and probe the differential output by dragging the mouse from the V_{out} net to the Q1 collector net. The resulting plot will show the differential transfer function for all six values of tail current. Notice that the output swing range before clipping occurs becomes smaller as tail current becomes smaller.

The stepped simulation is especially useful for plotting the output characteristic of a transistor, where V_{ce} is swept and base current is stepped. An AC analysis can also be stepped. Step the tail current in the AC analysis above from 0.1 mA to 2 mA in steps of 0.1 mA and see the effect on gain of the differential stage.

Example: A Wingspread Simulation

An important example of the use of stepped swept simulations is the so-called *wingspread* simulation of a class AB output stage [6]. This simulation shows the gain of the output stage as a function of output current for several different values of quiescent bias current I_q. This is valuable in evaluating crossover distortion.

The circuit of Figure 19.4 implements a wingspread simulation of a simple class AB output stage driving an 8-Ω load over a range of –10 V to +10 V. The two voltage sources $V_{spreadp}$ and $V_{spreadn}$ provide the bias spreading function and set the quiescent bias current. These voltage sources are parameterized by placing a variable inside curly brackets in place of the value of the voltage source. Here that variable is called V_{spread}. The parameterization is made complete by adding the SPICE directive.

.param Vspread=0.6

where 0.6 V is the nominal value of V_{spread}. The value of V_{spread} is then stepped for multiple simulations by adding the SPICE directive.

.step lin param Vspread 0.6 0.70 0.01

where the starting and ending points for V_{spread} are 0.6 V and 0.70 V, respectively. The stepping is done in increments of 10 mV. Each simulation is done in the *DC sweep* mode, where V_{in} is swept from –10 V to +10 V in increments of 0.1 V.

The gain of the output stage is plotted by adding a trace whose function is defined as $d[V(V_{out})]$. This is the derivative of V_{out} as a function of the input voltage. The resulting
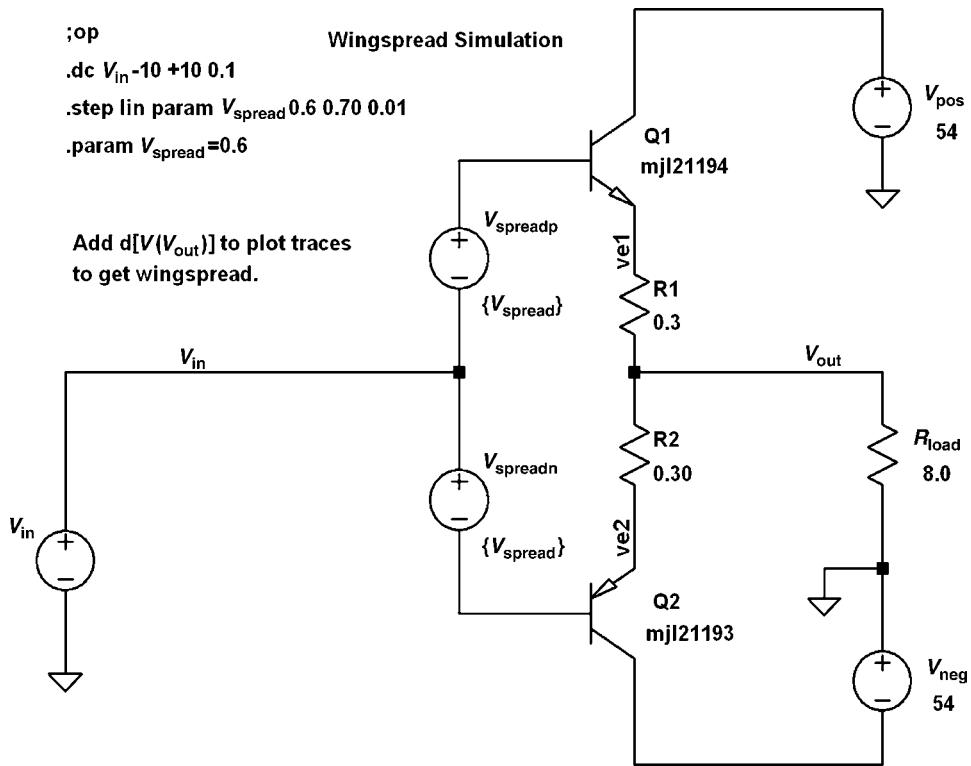
FIGURE 19.4   Wingspread simulation of a class AB output stage.

family of curves illustrates how crossover distortion is influenced by the quiescent bias of the output stage.

The nominal gain is about 0.95. With too little bias, the gain is seen to fall seriously at the crossover point to about 0.93. With the bias set too high, the gain is too high in the middle range of the crossover, at about 0.97, illustrating what is called *gm* doubling. Although an optimum compromise bias can be chosen, it is clear that there is no bias value that completely eliminates the crossover distortion.

19.8   Plotting Results

Many of the plotting capabilities of LTspice have been used and explained above. Some additional useful plotting functions are described here. At the top of the plot area (the plot plane) there is a label for each plot in the same color as the plotted trace. A convenient way to delete a trace is to click on the trace label with the scissors from the toolbar.

If you right-click on the trace label, a dialog box will be displayed. It allows you to change the color of the trace and to make the trace a function of the variable being plotted. For example, if the trace is V_{out}, you can make it become a trace of V_{out}^2. You can also define the trace as a function of V_{out} and other available variables. This is referred to as *waveform arithmetic*.

An especially useful capability for measuring points on the trace is to attach a cursor to it using the *Attach Cursor* box. This will display a set of crosshairs that always intersect on the trace and can be moved along the trace by the mouse (click on the crosshairs and drag the mouse). A display box will appear and show the horizontal and vertical values of the trace at the intersection. A second cursor can also be attached to the trace. In this case the display box will indicate the coordinates of the two cursors, their differences, and the slope between them. If two cursors are applied to the same edge of a square wave, the slope readout will correspond to the slew rate. If two cursors are placed on two successive positive edges of a waveform, the period will be read out as the corresponding frequency.

One can also add a trace to a plot. Click in the area of the plot and then right-click. A list of options will appear. Select *Add Trace*. A trace from the list of available traces can be added. Moreover, a function of one or more of the available traces can be typed into the function box. This capability will be described further below.

Right-click again in the plot window to get the options list. Click on *Grid*. This will toggle the display of grid lines on the plot. Plots can be copied to an application like *Word* or *Paint* by making the plot window active and hitting *Ctrl-C* to copy it to the clipboard.

In some cases there may be multiple traces on the plot plane that make viewing the results confusing. Traces in the plot plane can be displayed separately in an additional plot plane by right clicking in the original plot plane and then selecting *Add Plot Plane*. A blank plot plane will appear. Click on the waveform label of a trace and drag it to the new plot plane. One can add as many plot planes as desired and place the traces in any of them as desired by dragging them into the desired plot plane.

The default is to present plots with a black background. Sometimes this is undesirable, especially for printing. The background can be changed. Go to *Tools → Color Preferences*. Select *Background*, and then adjust the color sliders to obtain the desired color. Moving all three sliders to the right will provide a white background.

You can obtain the average and RMS values of a trace by control left clicking on the trace label.

Gummel Plot

The *Gummel plot* shows log of I_c and log of I_b versus V_{be} for a BJT. The Gummel plot illustrates the use of a logarithmic Y axis. The circuit of Figure 19.5 can be used to simulate
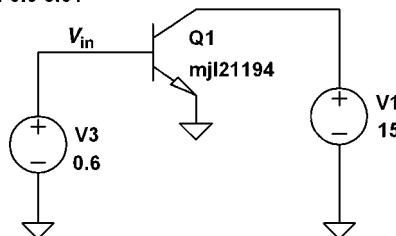
FIGURE 19.5 Generation of a Gummel plot for a transistor.

a transistor and obtain its Gummel plot. The MJL21194 NPN power transistor is used for illustration. This circuit merely applies a swept base-emitter voltage to the transistor under test. The base and collector currents are then probed to create the plot. Finally, the Y axis displaying current is given logarithmic coordinates by clicking the mouse just to the left of the Y axis. A dialog box will appear. Check the *logarithmic* box and enter the desired minimum value of current to display.

Beta versus I_c

Plotting the current gain of a transistor is a good way to illustrate the ability to plot functions of trace variables. The circuit of Figure 19.6 is used for this example. The emitter current of the power transistor is swept from 1 mA to 10 A with a decade sweep. Sweeping the emitter current introduces a small error due to the finite transistor beta. After the simulation is run, right-click on the plot plane and select *Add Trace*. In the dialog box enter the function $I_c(Q1)/I_b(Q1)$ and hit *OK*. Transistor beta will then be plotted. Notice how the current gain falls at both low and high current, illustrating so-called beta droop.

The small error created by sweeping emitter current instead of collector current can be corrected in the plot by changing the X-axis function that is plotted from the default swept value of emitter current to the value of the collector current. Simply left-click in the area below the X axis on the plot. A dialog box will appear. In the area labeled *quantity plotted* replace I1 with IC(Q1).

Transconductance versus I_c

This example illustrates the use of another function, the derivative function. Sweep the emitter current from 1 μA to 10 A. Add a trace with the function $1/[-d\{V(v_{e1})\}]$ to the simulation of Figure 19.6. This shows the inverse of the derivative of the emitter voltage with respect to emitter current, which is transconductance. Set the Y axis to be logarithmic from $1e$-5 to $1e$2. The log-log plot of transconductance versus transistor current will be a straight line over several decades, indicating that transconductance is proportional to operating current. However, the line begins to bend at currents above about 1 A, indicating the effect of ohmic transistor components on the transconductance at high current.

Beta vs. I_c Test Circuit

.dc dec I1 1 mA 10 10

Q1
mjl21194

V1
15

Add plot expression $I_c(Q1)/I_b(Q1)$
Y axis: log from 10 μA to 10 A

I1
100 mA

V2
15
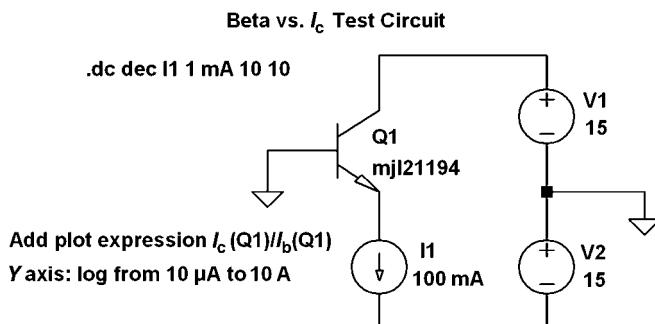
Figure 19.6   Sweeping the emitter current of a power transistor.

19.9   Subcircuits

Sometimes it is desired to employ the same circuit numerous times in a simulation. Subcircuits make it possible to name a circuit and store it in the simulation directory or in a library.

The *.subckt* SPICE directive allows you to name and define a subcircuit that can be put in a schematic multiple times merely by placing the corresponding instance repeatedly. One of the best examples of subcircuit use is an operational amplifier model that is composed of a collection of elements that may include transistors, resistors, and capacitors. Another example is a loudspeaker model that can be used to load an amplifier in a simulation. Even a simple low-pass filter can be realized as a subcircuit. When a subcircuit is specified, the circuit is expanded to a flat netlist before the simulation is run.

A circuit of your design can be defined as a subcircuit in the simulation directory or in the …*lib**sub* directory and can be used repeatedly in any circuit. If your copy of LTspice is located in the *C:**program files* directory, the full path for it will be

C:\program files\LTC\LTspiceIV\lib\sub

See the discussion below about creating a folder like …*lib**sub**mylib*.

Creating a Subcircuit

A subcircuit can be created by schematic capture. Go to *View → SPICE Netlist* with the schematic open. The netlist will appear in a box. Select all of the text and copy it using *Ctrl+C*. Then paste it into Notepad. Edit that netlist as necessary to make it into a subcircuit definition. This includes adding a first line that defines the circuit as a subcircuit. For a subcircuit named *LPF* it will look something like *.subckt LPF in out gnd*. A last line is added that looks something like *.ends LPF*. Delete extraneous lines like SPICE directives and voltage sources that were on the circuit schematic for purposes of simulation. The file is then named with a *.sub* file extension to become *LPF.sub*.

Shown below is how a simple first-order low-pass filter subcircuit is called in a *netlist*. Its instance is called U1 on the schematic. The instance name of the subcircuit is preceded by an *X* in the SPICE netlist.

XU1 Vin Vout 0 LPF1

The subcircuit that defines the 100-kHz LPF is shown below. Its filename should be *LPF1.sub*.

.subckt LPF1 in out gnd

R1 in out 10k

C1 out gnd 160pF

∗100-kHz first-order low-pass filter

.ends LPF1

It is helpful if the terminals in the *.subckt* line (here *in*, *out,* and *gnd*) are labeled in accordance with the pin names that will be put on the symbol. However, this is not entirely necessary, as the pin order in the symbol specification will correlate pin names between the symbol and the subcircuit definition.

The elements of the subcircuit can be parameterized and defined when the subcircuit is called in the SPICE netlist. The LPF below with parameterized *R* and *C* also includes a VCVS acting as a unity-gain output buffer. The intermediate node at the input to the VCVS was labeled N001 by LTspice.

.subckt LPF2 in out gnd

R1 in N001 {R}

C1 N001 gnd {C}

E1 out gnd N001 gnd 1

.ends LPF2

The parameterized subcircuit as it appears in the circuit netlist is

XU1 Vin Vout 0 LPF2 R=10k C=160pF

In the schematic of the circuit using the subcircuit, the *.param* directive is used for each of *R* and *C* in the usual way.

The Symbol Editor

Every model must have an associated symbol for entry onto the schematic. The symbols are defined in *.asy* files. LTspice has its own symbol editor for creating *.asy* symbol files. It can be used to create a symbol from scratch or to modify an existing symbol. The symbol editor can be accessed by going to *File → New Symbol*.

The usual drawing tools are available in the symbol editor. For example one can go to *Draw → (Line, Rectangle, Text)* to add those elements to the symbol. Scissors are available to delete elements.

After the symbol is drawn the connecting pins must be added. Go to *Edit → Add Pin/Port*. Fill in the *Label* with the pin name, hit the radio button for its desired location on the symbol perimeter, hit *OK*, and place the pin on the symbol.

The *Pin Table* contains the assigned (and visible) names of the pins and the order in which they appear on the SPICE line. Go to *View → Pin Table*. Double click on a pin in the left column to change its name. Double click on the numbers in the right column to rearrange their *Spice Order*. The order of the pins must correspond to the order of the pins listed in the .*sub* file.

The *Attribute Window* is used to select what attributes will be visibly attached to the symbol. These will often be the *InstName* and *Value*, where *Value* is the name of the part, i.e., *LPF1*. Go to *Edit → Attributes → Attribute Window*. Select a desired attribute to appear on the symbol and hit OK. The attribute will appear on the symbol attached to the cursor. Move the cursor to the desired location and click. Right click on it to enter the desired character string. Attributes can be removed with the scissors. Visible attributes can be changed by right clicking on them. This is not true for the instance name, which will be altered on the part when it is placed on the schematic.

The *Attribute Editor* allows you to set or modify both visible and hidden attributes of the symbol. Go to *Edit → Attributes → Attribute Editor*. Attributes that were added in the Attribute Window can be modified here as well. The hidden attributes (including those not selected to be visible in the Attribute Window) are also set here. These include *Prefix*, *SpiceModel*, and *ModelFile*. The prefix for a subcircuit should be *X*. Leave *Spice*

Model blank and enter the name of the *.sub* file for *ModelFile*. The *.asy* symbol file should be saved with the same name as the *.sub* file but with the *.asy* file extension.

Modifying an Existing Symbol

In many cases a suitable symbol for your subcircuit is already a standard one that is available in the simulator library. Sometimes, when a new device is created, one of the standard symbols must be modified. The symbol editor can be used to do this. Go into the …*lib**sym* directory and its subdirectories to find symbols that may work for your subcircuit. Then just choose one, copy it, and edit it to suit your needs. Rename it to the name of the device you are installing. Double-click on it and it will open in the symbol editor. Change its name and model attributes to reflect the name of the model file and what you want the symbol to say on its text on the schematic. The model name should be the same as the subcircuit name and subcircuit filename. Bear in mind that you can right-click on an existing symbol to see its visible attributes. You can *Ctrl* right-click on a symbol to access the attribute editor for it.

Summary for Creating the LPF1 Symbol

Here is a summary for creating the symbol for the subcircuit LPF1. Go into the *Symbol Editor* from the subcircuit schematic by hitting *File → New Symbol*. Go to *Draw → Rect* and draw a good-sized rectangle. It is helpful if the lines of the rectangle are on grid lines. Go to *Edit → Add Pin/Port*. Fill in the Label as *in*, select the *left* radio button to put it on the left edge, hit *OK* and place the pin on the left side of the rectangle. Place the *out* and *gnd* pins accordingly. Go to View → *Pin Table* and verify that the pin names are as desired and that the pin order corresponds to that in the *.subckt* definition. Notice that the pin order will be in the order that they were placed. Change the pin names or order if needed.

Go to *Edit → Attributes → Attribute Window*. Click on *inst name* and place it somewhere outside the rectangle. Go back into the Attribute Window and click on *Value* and place it somewhere inside the rectangle. Right-click on it and enter *LPF1* as the *string*. Go *into Edit → Attributes → Edit Attributes*. Select *Prefix* and enter *X*. Go back into Edit Attributes, select *ModelFile* and enter *LPF1.sub*. Save the file in the simulation directory as *LPF1.asy*. If desired, copy the symbol file to a library directory, such as …*lib**sym*\\ *mylib* (assuming that the *LPF1.sub* file was placed in …*lib**sub**mylib*).

Using the Subcircuit in a Schematic

With the subcircuit and corresponding symbol file in the simulation directory, the subcircuit can be used in the schematic just like a component. Click on the *Component* button. Scroll to the simulation directory and click on it. All of the subcircuits in the simulation directory will be listed. Click on the desired subcircuit, and its symbol will appear in the window. Hit *OK* and place it.

Installing Subcircuit Models in a Library

Subcircuit models can be accessed from a library that you can assemble. Create the folder …*lib**sub**mylib*. This is where the subcircuit file(s) will be stored. This folder will be available via the *Component* button. Place the *.sub* file in this folder. Similarly, create the folder …*lib**sym**mylib*. This is where the symbol file for the device should be stored.

To place the subcircuit on a schematic, click on the component button. Then double-click on *[mylib]* within the group of selections. A list will come up with all of the subcircuits that you have placed in *…\lib\sub\mylib*. Click on the one you want. Its symbol will appear in a window. Hit *OK* to place it on the schematic in the usual way. If you wish to go up one level back to the full component selection, double-click on *[..]*.

19.10   SPICE Models

Good models are at the heart of SPICE simulations. Most manufacturers provide models for their transistors and integrated circuits, and there are a great number of models available for other components, like transformers and loudspeakers. A tremendous amount of model information is available on the Web, both from manufacturer's sites and private sites.

Go to the Internet and search device manufacturers' websites. You can create your own model by modifying an existing one and renaming it. Software for creating models is also available at www.intusoft.com/spicemod.htm. Chapter 20 will cover device models and the creation or tweaking of them in much more detail. Here we will focus on using the models in the LTspice library and adding acquired models.

Bipolar Junction Transistors

BJTs are supported with the symbol names NPN and PNP. BJT models are located in the *standard.bjt* file in the *…\lib\cmp folder*. Many models are included in this one file. LTspice comes with this file populated with a large number of models, but you can add more models simply by pasting the transistor model file into the *standard.bjt* file. Those models will then be available via the component button just like any other BJT models. A simple SPICE model for a BJT is

.model 2N3904 NPN (IS=1E-14 VAF=100

+ Bf=300 IKF=0.4 XTB=1.5 BR=4

+ CJC=4E-12 CJE=8E-12 RB=20 RC=0.1 RE=0.1

+ TR=300E-9 TF=400E-12 ITF=1 VTF=2 XTF=3 Vceo=40)

This is the kind of model that can be pasted into the *standard.bjt* file. The meaning of each of the parameters in this file and how to tweak or derive them will be discussed in the next chapter.

To install a BJT model, start with the *.model* file in Windows Notepad. Set the file type to *All Files*. Append the file to *…\lib\cmp\standard.bjt* with a paste. It will then show up in the list of available transistors when using *pick new transistor*.

Junction Field Effect Transistors

The JFET transistor is chosen with a symbol name of NJF or PJF from the library. These correspond to N-channel and P-channel devices, respectively. A simple N-channel JFET model looks like

.model J310 NJF (BETA=0.004 VTO=-4 LAMBDA=0.06

+ CGS=16E-12 CGD=12E-12 PB=0.5 M=0.5 FC=0.5 N=1

+ RD=5 RS=30 IS=4E-14 KF=6E-18 AF=0.6)

JFET models can be added to the *standard.jft* file in the …*lib**cmp* folder with a simple paste operation.

Power MOSFETs

LTspice supports two different kinds of models for power MOSFETs. The first is the proprietary LTspice VDMOS model for vertical double-diffused power MOSFETs. It is supported in the library in much the same way as a BJT, with a *standard.mos* file in the …*lib**cmp* folder. It is placed using the component button by selecting *nmos* or *pmos*, placing the transistor, then right clicking on it to select the particular transistor. A simple VDMOS model looks like

> .model IRFP240 VDMOS (nchan Vto=4 Kp=0.1 Lambda=0.003
>
> + Rs=0.02 Rd=0.1 Cgdmax=30p Cgdmin=6p a=0.4
>
> + Cgs=40p Cjo=7p m=0.7 VJ=2.5 IS=4E-06 N=2.5)

Additional VDMOS models can be installed by pasting them into the *standard.mos* file. Such VDMOS files are not generally available from other than Linear Technology, but the next chapter shows how they can be created.

The second kind of power MOSFET model supported is based on a subcircuit that includes at its core a SPICE Level 1 MOSFET model like that used in an integrated circuit. The remainder of the subcircuit adds some of the peculiarities of power MOSFETs, such as the body diode and nonlinear gate-drain capacitance. This is the way much of the industry models power MOSFETs. Models in this form are widely available from vendors. A very simplified version of such a model (where gate-drain capacitance is constant) is shown below. Many vendor models have elaborate circuits within the subcircuit to attempt to model the nonlinear gate-drain capacitance, but many are not very accurate, especially for linear applications.

> .subckt IRFP240 1 2 3
>
> ∗pins: Drain Gate Source
>
> M1 9 7 8 8 MM
>
> D1 3 1 MD
>
> RS 8 3 0.05
>
> RD 9 1 0.1
>
> RG 2 7 5
>
> CGS 2 3 1e-9
>
> CGD 1 2 0.5e-9
>
> .MODEL MM NMOS LEVEL=1 IS=1e-32
>
> + VTO=4 LAMBDA=0.002 KP=3
>
> .MODEL MD D IS=1e-12 N=1
>
> + CJO=1e-09 VJ=4 M=1 FC=0.5
>
> .ENDS

The power MOSFET subcircuit is treated largely the same as any other subcircuit. However, its *.subckt* file should be saved with a *.mod* file extension instead of a *.sub* file

extension. Similarly, its *ModelFile* definition in the symbol attributes should have a *.mod* file extension instead of a *.sub* file extension.

Include Statements

The *.include* spice directive causes a file to be included in the simulation file as if it was written there. The *.include* directive can be used to put models or libraries of models or subcircuits in the simulation.

.include 2N3904.mod

The above directive will include the model of the 2N2904 BJT for use by the simulation. LTspice will first look for the file in the …*lib**sub directory*. If it is not found there, LTspice will look in the directory where the simulation is being run. Alternatively, a complete path name can be specified for the file. This could be a directory in your top-level simulation folder where you place your own models.

The *.include* directive applies to a single file, but that file can contain many models, just like the LTspice *standard.bjt* library file contains many BJT models. Your file of BJT models might be called *mybjt.bjt*.

You can place your own library of BJT models in the …*lib**sub* directory by placing the file *mybjt.bjt* there. The directive *.include mybjt.bjt* should then be placed on the schematic. Notice that the full pathname does not need to be included when this approach is used. The transistors in *mybjt.bjt* will not show up in "pick new transistor" if you right-click on a transistor, so you must edit the name of the transistor to be that of the one in *mybjt.bjt* that you want. You can also place the BJT library file in …*lib**sub*\ *mylib*. In that case the directive *.include mylib\mybjt.bjt* would be used.

Libraries

The *.lib* directive is similar to the *.include* directive. It includes the model and subcircuit definitions of the specified file in the simulation file. LTspice looks first in the …*lib*\ *cmp* directory when the *.lib* directive is used. It will then search the …*lib**sub* directory and finally the simulation directory. A complete path name can also be specified. In contrast, LTspice does not look for the file in the …*lib**cmp* directory when the *.include* directive is employed.

As an example, you can place your own library of BJT models in the …*lib**cmp* directory by placing the file *mybjt.bjt* in the …*lib**cmp* directory. The directive *.lib mybjt.bjt* should then be placed on the schematic. Notice that the full pathname does not need to be included when this approach is used. The transistors in *mybjt.bjt* will not show up in "pick new transistor" if you right-click on a transistor, so you must edit the name of a transistor on the schematic to be that of the one in *mybjt.bjt* that you want.

Indeed, the directive *.lib …\lib\cmp\standard.bjt* is automatically included by LTspice in the netlist whenever a BJT is used from the library in the usual way.

19.11   Simulating a Power Amplifier

Here I'll describe the simulation of the simple power amplifier first introduced in Chapter 1. This will provide a good start so that a *put it all together* understanding can be achieved. This template simulation can be modified extensively for use with virtually any amplifier design. Indeed, I usually begin with a previous amplifier schematic
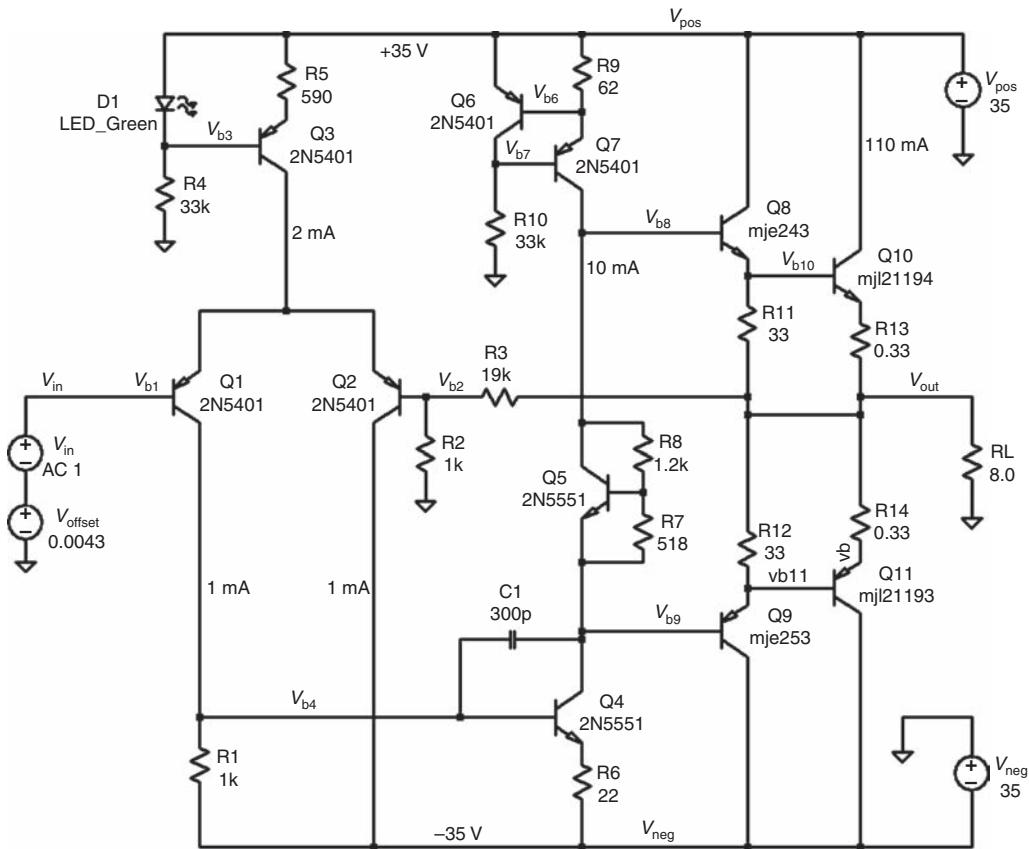
Figure 19.7 Power amplifier to be simulated.

and copy it to a new name and just modify it to the new design, reusing many of the components and SPICE directives. The simulation circuit is shown in Figure 19.7. Notice that it is in DC-coupled form to optimize FFT analysis.

DC Analysis

Select *Simulate → Edit Simulation Command → DC operating point*. Hit *OK*, and then hit *Run*. Check V_{out} in the pop-up simulation results window for acceptably low output offset. If necessary, adjust V_{offset} to obtain offset voltage of less than 1 mV at the output. Check the operating currents of the transistors. Click out of the simulation results box and go to *View → SPICE error log*. Look at the operating points and model parameters of the transistors in the circuit. Are they all operating at expected current levels? Are any transistors in saturation?

Close the SPICE error log and mouse over various circuit nodes to see their voltage levels in the lower left display window. The node number will also conveniently be displayed. Mouse over the *vt* and *vb* nodes in the output stage to infer the output stage operating bias. Under optimum conditions, these nodes would be at or a bit less than ±26 mV. However, this amplifier has been slightly overbiased. Mouse-over the resistors

to see their operating currents and power dissipations in the same display. Mouse-over the transistors to see their power dissipations.

Frequency Response

Select *Simulate → Edit Simulation Cmd → AC Analysis*. Select a decade sweep with 10 points per decade, a start frequency of 100, and a stop frequency of 1000k or 1Meg (note that M by itself is interpreted as *milli*).

Hit *OK* and hit *Run*. Probe V_{out} with the mouse. The frequency and phase response will appear in the plot window. Left-click on the trace label. A crosshairs cursor will appear. Mouse-over it and the number 1 will appear, designating cursor number 1. This crosshairs cursor will be attached to the gain trace. Move it to a low frequency and note that the gain is indicated as 26 dB in the pop-up display box. Move the cursor up in frequency until the gain is down by 3 dB. Note that the frequency is indicated as 539 kHz.

Click on *vb8*, the VAS output node. An additional trace showing frequency response to this new point will be added to the plot window. Drag the mouse in the plot window to zoom in on the pair of traces at 1 kHz. Notice from the spacing of the traces that the output stage has a small-signal gain loss of 0.35 dB.

1-kHz Transient Analysis

In this section a 1-kHz sine wave will be simulated by a transient analysis that will show voltages and currents in the circuit as a function of time. Select *Simulate→ Edit Simulation Command → Transient.* Set a stop time of 4 ms to simulate four cycles of the waveform.

Specify the signal source V_{in} to be a 1-kHz sine wave with amplitude of 1 V peak and comprising four cycles. This will produce an output of 20 V peak, corresponding to 25 W into the 8-Ω load. Run the simulation and click on the V_{out} node to see the expected output waveform. *Alt*-click on Q10's collector wire and see the class AB half-wave rectified current waveform for Q10.

Increase the input signal amplitude to 1.6 V peak, rerun the simulation, and probe V_{out}. Notice that there is no obvious clipping. *Alt*-click on Q1's collector wire to show the waveform for Q1's collector current. Notice the onset of clipping as revealed by the sharp peaks in the collector current of Q1. The amplifier just clips at 64 W.

Increase the input signal to 2 V peak to see the amplifier operating in fairly strong clipping. Here the amplifier is attempting to produce an output of 100 W. Probe V_{out} and see the obviously clipped output waveform. *Alt*-click on Q1's collector wire to show Q1's collector current waveform. Probe from the base of Q1 to the base of Q2 to see the negative feedback error signal. Notice how the error signal suddenly pops up to a large value on the peaks where clipping is occurring. Probe various nodes to see voltages and currents. Look especially for signs of transistor saturation and unusually large currents and evidence of sticking.

20-kHz Transient Analysis

In this section a 20-kHz sine wave will be simulated. Select *Simulate → Edit Simulation Command → Transient.* Set a stop time of 400 μs to capture eight cycles of the waveform.

Specify the signal source V_{in} to be a 20-kHz sine wave with amplitude of 1V peak and comprising 16 cycles (even though only eight cycles will be simulated at this time). This will produce an output of 20 V peak, corresponding to 25 W into the 8-Ω load. Run the simulation and click on the V_{out} node to see the expected output waveform.

Alt-click on Q1's collector wire to show Q1's collector current. Notice that it falls dangerously close to zero, indicating that the amplifier's input differential pair is operating at close to its maximum capability. This means that the amplifier is close to its slew rate limiting point. Mouse-over Miller compensation capacitor C1 and click on it to see its current. *Alt*-click on Q4's base wire to plot Q4's base current. Notice that most of the signal current supplied by the LTP is flowing into the compensation capacitor.

Increase the input signal amplitude to 1.3 V peak and run the simulation. Again plot the current in Q1's collector wire, seeing that it is clipped; this indicates that slew rate limiting is occurring. Plot the input differential error signal by dragging the mouse probe from the base of Q1 to the base of Q2, noting the large error voltage present when slew rate limiting is occurring.

Square-Wave Response

The 50-kHz square-wave response will now be simulated. Select *Simulate → Edit Simulation Command → Transient*. Choose a stop time of 80 μs to cover four cycles. Set the input source to provide a 50-kHz square wave with amplitude of 0.1 V peak. Set the initial voltage to –0.1 V and the pulse voltage to 0.1 V. Set 10 ns rise and fall times. Set a pulse time of 10 μs and a period of 20 μs.

Run the simulation and probe V_{out}, noting the rounded leading edges that result from the finite bandwidth of the amplifier. Probe the collector current in Q1's collector wire. The current waveform exhibits large pulses at the times of the square-wave edges. These current pulses are charging and discharging the compensation capacitor in order to produce the required output.

Increase the input amplitude to 0.2 V peak, rerun the simulation, and probe V_{out}. The amplifier is now exhibiting slew rate limiting. Window-in on the straight-sloped portion of a waveform edge. Right-click on the V_{out} label and select two cursors in the pop-up window. Manipulate the cursors to be 1 μs apart on the straight slope. Read the indicated slew rate in the bottom right portion of the information box. The slew rate is approximately 3 V/μs.

Close the information box and unzoom the plot. Probe the current in the collector wire of Q1. Notice the clipped spikes, indicative of slew rate limiting.

1-kHz Total Harmonic Distortion

Change the input voltage source to be a 1-kHz sine wave with amplitude of 1 V peak. This corresponds to 25 W into the 8-Ω load. Select *Simulate → Edit Simulation Command → Transient.* Set a stop time of 8 ms to simulate eight cycles of the waveform. Place the following three SPICE directives on the schematic:

    .option plotwinsize=0

    .maxstep=0.48831106u

    .four 1kHz 10 4 v(vout)

As described earlier, the first directive turns off compression for greater transient analysis accuracy. The second sets an optimum timestep for Fourier spectral analysis of the 1-kHz sine wave. The third causes a THD summary of the Fourier analysis to be printed in the SPICE error log result. The amplitudes of the first 10 harmonics,

normalized to that of the fundamental, will be printed. The Fourier analysis will be carried out during the last 4 periods of the 1-kHz sine wave.

Run the simulation and look at the information window at the bottom of the screen to view simulation progress. When the simulation is completed, click on *Vout* to plot its trace. Left-click and right-click in the plot window; then select *View→ FFT* from the pop-up window. The trace selection $V(V_{out})$ will already be highlighted in the list of available traces. Select *Specify a time range*. The *End Time* should already be shown as 8 ms. If it is not exact, enter 8 ms. Enter a *Start Time* of 4 ms. The first 4 ms allow the simulation to stabilize and the last 4 ms are analyzed by the FFT.

Hit *OK* and a new window will appear with the FFT results. Window-in on the range of interest, extending from about 1 kHz to about 20 kHz, and extending down to –140 dB. Mouse-over the peaks of the spectra and observe the corresponding amplitude in the bottom display window. The amplitudes are reported in dB with respect to 1 V (dBV). The fundamental at 1 kHz lies at about +23 dB, corresponding to 14.14 V RMS.

The second and third harmonics are at –55 dB and –59 dB, respectively. They are 78 dB and 82 dB below the fundamental, suggesting THD on the order of 0.013%, not including all of the higher harmonics. The fairly rich spectrum of higher harmonics suggests the presence of output stage crossover distortion.

Close the FFT window and click on the schematic window. Then hit *View → SPICE error log*. A list of the amplitudes of the first 10 harmonics, relative to the fundamental, will be shown. At the bottom of this list the THD will be shown as 0.016%. This display is often more convenient than looking at the raw spectral trace.

20-kHz THD

Total harmonic distortion at 20 kHz is one of the more difficult and stressful tests for an amplifier. Set the input source to a 20-kHz sine wave with amplitude of 1 V peak. This will produce 25 W into the 8-Ω load. Set a transient simulation stop time of 400 μs to simulate 8 cycles of the waveform. Alter the SPICE directives on the schematic as follows:

.maxstep=0.02441555u

.four 20kHz 10 4 v(vout)

Here four cycles, or 200 μs, will be processed by the FFT.

Run the transient simulation until it is completed. Click on V_{out} to display the output waveform. Left-click and right-click in the plot window and select *View→FFT* from the pop-up box. The end time should be listed as 400 μs. Enter 200 μs for the start time. Hit *OK,* and the FFT spectrum will come up in a new window. Note the substantially increased levels of distortion as compared to the 1-kHz simulation. With the fundamental at +23 dBv and the third harmonic at –23 dBV, the worst harmonic is only 46 dB down, suggesting THD of at least 0.5%. Notice that significant spectral lines are present out to fairly high frequencies. Bear in mind that the power level here is only half the rated 50 W.

Window-in on the plot region extending from about 20 kHz to about 500 kHz, and from +30 dBV down to –100 dBV. Sometimes this will require more than one windowing operation to obtain the properly zoomed area. This is the region of greatest interest, as harmonics more than 120 dB below the fundamental are of relatively little significance and may even be simulation artifacts.

A big advantage of 20-kHz THD simulations is the ability to view the higher harmonics. A major limitation of THD-20 lab measurements is that the THD analyzer sometimes limits the bandwidth of the residual to 80 kHz. This barely allows room for the second through fourth harmonics.

Close the FFT window and click on the schematic window. Go to *View → SPICE error log* and review the THD data. Note that these data are available even if the plot of output voltage and its FFT are not made. The total harmonic distortion reads 0.52%, with significant harmonic content out to the tenth harmonic.

This is surely not a good amplifier design and is one that would do poorly on the DIM-30 test for *Transient Intermodulation distortion* (*TIM*). This illustrates that such an amplifier will do poorly on a THD-20 test as well, especially when a spectral analysis of the harmonics out to at least 200 kHz is performed.

CCIF Intermodulation Distortion

The 19+20-kHz CCIF intermodulation test is implemented by feeding the amplifier a mixed combination of 19 kHz and 20 kHz sinusoids in equal proportions. The test is best conducted at or near a voltage swing corresponding to peak voltage at full power. For this amplifier the test will be conducted at a smaller total peak input level of 1 V, the same peak level that was used for the 20-kHz THD test. This corresponds to 25 W into 8 Ω.

The CCIF IM test produces intermodulation products at integer sum and difference combinations of the two test frequencies. These IM products are best viewed on a spectrum analyzer or with an FFT plot as will be done here. The order of the products is equal to the number of instances of the two test tone frequencies in the sum and difference equation that creates a given IM frequency product. Suppose frequency A is 20 kHz and frequency B is 19 kHz. The second-order product will be produced at A-B = 1 kHz. The fourth-order product will be produced at 2A-2B = 2 kHz.

The third-order product will be produced at 2B-A = 18 kHz. The fifth-order product will be produced at 3B-2A = 17 kHz. The seventh-order product will be produced at 4B-3A = 16 kHz. And so on. Notice that all of these components are in-band. Of course, there are many other components created with other sum/difference combinations of the test frequencies, many lying out of band. Of particular interest is the fact that the odd-order distortion products lie at intervals 1 kHz apart going down from 18 kHz and jumping two orders at every 1-kHz grid point. This produces a picket-fence appearance in the spectrum. The CCIF IM test is thus very capable of displaying high-order nonlinearities without resort to testing frequencies beyond the audio band.

Simulate the CCIF IM test by adding a second sinusoidal voltage source set for 19 kHz and a peak level of 0.5 V. This source can be simply placed in series with the existing 20-kHz source. Set the level of the 20-kHz source for 0.5 V peak.

The lowest frequency of interest in the simulation and FFT analysis is 1 kHz. Moreover, all of the IM products of interest are on a 1-kHz grid. For this reason, the FFT time should be an integer multiple of the 1-kHz period. Here the FFT will be performed on four cycles of the 1-kHz beat frequency.

Alter the SPICE directives on the schematic as follows:

.maxstep=0.12207776u

remove the .four 20kHz 10 4 v(vout) directive.

Here four cycles of the 1-kHz difference signal, or 4 ms, will be processed by the FFT. The *max step* is set to 0.5 times 4 ms/16,383. The FFT will be run with 65,536 points. The above selection of maximum timestep will provide an FFT analysis with grass that is below –120 dBv. Some experimentation with the FFT interval and the maximum timestep is often needed in simulations involving multiple tones in order to obtain a result with adequately low spurious grass.

Set the transient simulation for a stop time of 5.5 ms. The first 1.5 ms of the simulation is to be ignored by the FFT. The use of 1.5 ms causes the beginning and end of the FFT analysis to occur at a point where the 1-kHz beat signal goes approximately through zero. This helps slightly to reduce FFT windowing artifacts.

Run the transient simulation and click on V_{out}. Notice the beat-frequency action between the 19-kHz and 20-kHz sinusoids as they produce a signal envelope that goes from essentially zero amplitude to the full amplitude of 20 V peak.

Select the FFT. The stop time should be listed as 5.5 ms. Enter a start time of 1.5 ms and hit *OK*. The FFT will appear in a new window. Select the region of interest by windowing the plot from 1 kHz to about 50 kHz and from 30 dBv down to –160 dBv. Notice the picket fence of odd-order distortion spectra extending both above and below the pair of input sinusoids at 19 kHz and 20 kHz. There is also a prominent picket fence of intermodulation products centered at 39 kHz. The even-order products can be seen beginning at 1 kHz.

In a very good amplifier, all of the CCIF IM products will be 100 dB or more below the level of the two test tones. In the simulation of this amplifier, the test tones are at +17 dBv, while the third-order product at 18 kHz is at –34 dBV, down only 51 dB. The second-order product at 1 kHz is at –41 dBV, down by only 58 dB from the test tones. These are not very good results and are consistent with the poor high-frequency distortion results obtained from the THD-20 simulations.

Signal-to-Noise Ratio

LTspice can be used to perform a simulation that will predict the *signal-to-noise ratio* (SNR) of an amplifier in a number of different ways. One caveat is that environmental sources of noise, like power supply ripple and EMI, will not be taken into account. For this reason, noise predictions based on simulation may be a bit optimistic.

The bandwidth over which the noise is being characterized is of paramount importance. In the specification of power amplifiers there are usually three ways to characterize noise. The first is an unweighted wideband measurement where the bandwidth is substantially greater than the audio band, usually limited by the closed-loop bandwidth of the amplifier under test or by a filter in the test equipment. This yields the poorest signal-to-noise ratio, and often the actual measurement bandwidth is not specified. The second is the noise in a 20-kHz bandwidth. The effective noise bandwidth can be set at 20 kHz by using a first-order low-pass filter at 12.7 kHz (the noise bandwidth of a 20-kHz first-order filter is 31.4 kHz because it does not have a brick-wall characteristic). In general, the ENBW of a first-order filter is 1.57 times its 3-dB bandwidth.

The last is the A-weighted noise measurement (whose effective noise bandwidth is approximately 13.5 kHz. All of these were described briefly in Chapter 1. Simulation of A-weighted SNR can be conveniently carried out using the A-weighting filter subcircuit described earlier in Figure 19.2.

In a well-designed amplifier with very little hum, the SNR will be governed mainly by the high-frequency measurement bandwidth, since thermal noise is proportional to the square root of bandwidth.

Select *Simulate → Edit Simulation Command → Noise*. Set the output to $V(V_{out})$ and set the input to V_{in}. Select a decade sweep from 20 Hz to 20 kHz with 20 points per decade. Run the simulation and click on *Vout*. A plot of voltage noise will appear. The noise density will be flat at 86 nV/√Hz. Because the amplifier gain is 20, this corresponds to an input-referred noise of 4.3 nV/√Hz. *Ctrl*-click on the plot label. The RMS noise within the 20-kHz bandwidth is 12.2 μV RMS. This is 124 dB below the maximum 20 V RMS output of the amplifier at 50 W. The unweighted SNR with respect to 1 W is about 107 dB.

Click on R2, the feedback network shunt resistor. It contributes about 77 nV/√Hz to the total output noise of 86 nV/√Hz. Click on Q1. It contributes about 12 nV/√Hz. Click on Q2. It contributes about 30 nV/√Hz. Why the difference? Q2 contributes more noise because of its input current noise. The input current noise of Q1 is not a contributor because the impedance at its base is zero in this simulation.

Damping Factor and Output Impedance

The damping factor of a power amplifier is the factor by which the output impedance is smaller than 8 Ω. An amplifier with an output impedance of 0.08 Ω will have a damping factor of 100. The output impedance of an amplifier is usually a function of frequency.

The best way to measure the output impedance is to apply a known alternating current to the output of the amplifier and measure the resulting voltage at the output node. This is done while the input to the amplifier is connected to ground. This can best be accomplished by connecting a voltage source to the output through a resistor whose value is high compared with the expected output impedance of the amplifier. The voltage gain from this voltage source to the output node is then indicative of the output impedance. If 10 V is applied through an 800-Ω series resistor and 1 mV is measured at the amplifier output terminals, the DF is 100.

The way in which the output impedance changes with frequency can also be an indicator of stability. If the impedance rises sharply in a particular high-frequency region, this may indicate instability. If this frequency region is near the expected global feedback gain crossover frequency, then stability of the overall negative feedback loop may be inadequate. If instead the output impedance peak occurs at a much higher frequency, the possibility of a local instability, such as in the output stage, is suggested.

Stability

Select the *AC Analysis* tab in the simulation options and select a frequency range by decade from 10 kHz to 10 MHz. Probe the base node of Q2. This node should normally act like a unity-gain voltage follower to the input signal. You should see unity gain at this point with little or no gain peak. If this is done with a parameterized Miller compensation capacitor that is stepped in value, a family of stability curves will be produced.

Inferring Loop Gain

The open-loop gain (OLG) characteristic can be inferred by setting the closed-loop gain (CLG) very high. This *exposes* the open-loop gain. This will be reasonably accurate for OLG readings that are less than the high CLG for which the amplifier is configured. Change R3 in the simulated amplifier to 1 MΩ and carefully adjust input offset for small output offset, recognizing that the CLG has been set to about 1000. Run the AC simulation and see the open-loop gain. Above 10 kHz the gain drops below 60 dB. Above this

frequency the plot is a reasonable depiction of OLG. The gain crossover is at 400 kHz, where the OLG equals 26 dB, the normal CLG for the amplifier. Phase at this frequency is lagging by 101°, suggesting a phase margin of 79°.

Measuring Loop Gain

The negative feedback loop gain can be measured directly by breaking the loop. Replace R3 with a 1000-GH inductor. This will keep the feedback path closed at DC. Connect the base of Q1 to ground. Connect the AC source to the base of Q2 through the 19-kΩ resistor that was R3. Loop gain will be plotted directly. The plot now will go to 0 dB at 400 kHz.

Output Stage Power Dissipation

The instantaneous power dissipation of any component can be plotted. Move the cursor to that component and press the *Alt* key. A thermometer will appear on the cursor. Left-click and the power waveform will be displayed. If you do this for a transistor, its instantaneous power dissipation will be revealed. You can also do this for a voltage source.

The average of the waveform (here the average power dissipation) can be displayed in an information box. Simply *Control*-left-click on the label of the instantaneous power dissipation waveform. If you do this for the amplifier load resistor and subtract the result from the sum of the dissipations for the rail voltage sources, the power dissipation of the amplifier will be revealed. These procedures also prove very convenient for determining the power dissipation of output stage emitter resistors and Zobel networks.

Output Current Limiting

The maximum available output current of the power amplifier can be checked by back-driving current into the output of the amplifier from a voltage source connected to the output through a low-value resistance, typically 8 Ω or less. This is not unlike the technique for measuring output impedance, but is carried out in a large-signal sense. The input of the amplifier is grounded and the voltage at the output node of the amplifier is viewed in a transient simulation or a DC sweep. The point at which the voltage at the output of the amplifier suddenly becomes large is the point at which current limiting is occurring.

Notice that this technique measures output current limiting when the output voltage is near zero. Alternatively, one can measure output current limiting by driving large signals through the amplifier into progressively smaller output load resistances.

You can also adopt this technique to measure output current limiting at voltages other than zero by applying a DC offset to the amplifier, assuming the amplifier is DC coupled. This can be useful in evaluating the behavior of V-I limiting circuits used for safe area protection, as the current limit for these circuits is often made a function of the output voltage.

Safe Operating Area

Plot the voltage across the power transistor against its current, using the *XY* plot capability. Load the amplifier with a series *R-C* combination of 8 Ω and 30 μF. Run a transient simulation with a 1.4-V peak sinusoidal input at 1 kHz. Run the simulation with a start

time of 1.5 ms and a stop time of 4 ms. Plot I_c(Q10). You will see the expected half-wave current plot as a function of time.

With the plot plane active, move the cursor just below the *X* axis of the plot plane. A ruler will appear. Click on it. A dialog box will appear for the *X* axis. Normally it will show time as what is being plotted (*Quantity Plotted*) in a transient simulation, but you can type in an expression to plot in the window. Type the expression for the voltage across the output power transistor, $V(V_{pos}) - V(V_{out})$, into the *Quantity Plotted* box. You will now see a plot of collector current as a function of V_{ce} for the transistor. If you wish, you can make both axes logarithmic to portray the usual safe area plot. You can also do this for a loudspeaker load, plotting current as a function of voltage and getting an ellipse.

References

1. L.W. Nagel and D.O. Pederson, "Simulation Program with Integrated Circuit Emphasis," Proc. Sixteenth Midwest Symposium on Circuit Theory, Waterloo, Canada, April 12, 1973; available as Memorandum No. ERL-M382, Electronics Research Laboratory, University of California, Berkeley.
2. LTspice User's Manual; available at www.linear.com.
3. LTspice Users' Group, www.groups.yahoo.com/group/LTspice.
4. DIYaudio Forum, www.diyaudio.com.
5. Connors, Andy, private communication.
6. Self, D., *Audio Power Amplifier Design Handbook*, 5th ed., Focal Press, 2009.

This page intentionally left blank

SPICE Models and Libraries

This chapter covers the adjustment and creation of SPICE models for BJT, JFET, and power MOSFET devices.

SPICE is only as good as the models used with it. In some cases, manufacturer-supplied models are quite inaccurate. One would think that those models would almost perfectly fit the data supplied in the transistor specification sheet. However, in many cases they don't even get the basics accurate, like V_{be} versus I_c.

Often, manufacturers subcontract the generation of SPICE models, especially for older devices where SPICE models were not developed for the part when the part was new. Often, they will just give a paper specification sheet to the subcontractor and have him or her glean data from the sheet. That data will then be entered into an automated curve-fitting software tool that quickly spits out a model. This is why we often see SPICE parameters with a ridiculous number of decimal places when they are in reality not even within 10% of where they should be.

You can do a much better job creating a SPICE model armed only with the same datasheet information. SPICE models can also be created or improved with relatively simple laboratory measurements that you can make using standard test equipment.

We all know that many transistor parameters vary quite a bit. Transistor β, for example, may easily vary by a factor of 2 from part to part. Base-emitter voltage can also vary, especially from one manufacturer to another. We therefore know instinctively that high precision in SPICE parameters is not important. Yet, the *behavior* of the transistor that they model is important.

SPICE is extremely valuable even with the use of inaccurate off-the-shelf models. It provides insight and exposes design behavior. However, poor models may give misleading results, especially under certain conditions. Poor models will often lead to inaccurate results in distortion simulations. This can be especially important in BJT output stages where beta droop and f_T droop at high current cause distortion. If these effects are not modeled reasonably well, distortion results will be significantly in error under high-swing conditions.

This chapter addresses the quality and accuracy of manufacturers' SPICE models with a strong emphasis on those for power BJTs. The chapter also provides understanding of what each SPICE parameter means. It also illustrates possibilities for simplifying the models by showing which parameters are more important. We also show how to create or fine-tune a model from information on a data sheet. SPICE models can be extracted from laboratory measurements; you don't have to have expensive measuring equipment for this.

The emphasis is on BJT power transistors, but the techniques and procedures are applicable to small-signal and driver transistors as well. JFET and power MOSFET models are also covered. A substantial amount of material on device behavior, device operating equations, and SPICE parameter meanings is provided in this chapter that has been gleaned from many sources [1–4].

20.1   Verifying SPICE Models

Manufacturer-supplied SPICE models are helpful and convenient. Some manufacturers do a good job on their SPICE models, but others do not. For this reason, it is wise for the serious designer to verify manufacturers' SPICE models against the supplied data sheets for the transistor. Surprisingly, sometimes there will be significant errors, even in simple things.

SPICE models can be checked by simulating the transistor at a specified operating point. After running a DC operating point simulation in LTspice, you can go to View -> SPICE error log. There you will see the transistor parameters in effect at the chosen operating point. These include V_{be}, AC and DC beta, f_T, and many others.

For example, you might check the parameters of a power transistor at $V_{ce} = 20$ V and at collector currents of 0.1, 1.0, and 10 A. This will give a quick indication of how close the SPICE parameters are.

Figure 20.1 shows a simple simulation circuit for verifying the operating parameters of an NPN transistor, in this case the MJL21194 power transistor. The circuit does little more than cause the transistor to operate at a particular collector current with a specified V_{ce}. The simulation includes the option of sweeping the emitter current so that plots can be viewed.

The Hybrid Pi Model

The hybrid pi model was introduced in Chapter 2. It models the small-signal behavior of a transistor. A very simplified version of the model is shown below in Figure 20.2. The fundamental active element of the transistor is a voltage-controlled current source; namely a transconductance gm. The remainder of the model comprises passive parasitic components. AC current gain is taken into account by the base-emitter resistance r_π. Early effect is taken into account by r_o. Collector-base capacitance is shown as C_{cb}. Current gain roll-off with frequency (f_T) is modeled by C_π. Because this is a small-signal
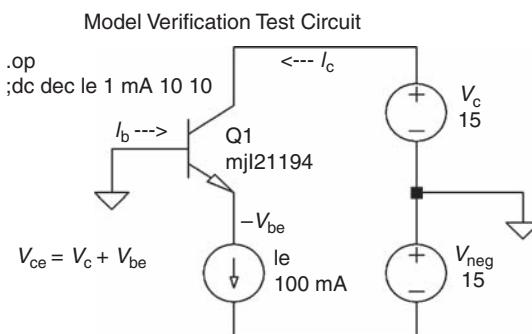
Figure 20.1   A simple SPICE simulation circuit for model verification.
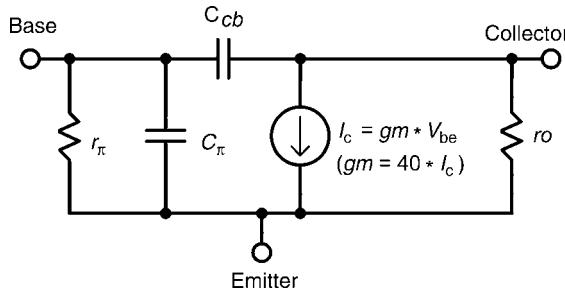
FIGURE 20.2 Hybrid pi model of a BJT.

model, element values will change with the operating point of the transistor. This behavior is what makes SPICE modeling more complex.

20.2 Tweaking SPICE Models

In some cases it may only be necessary to tweak a couple of key SPICE parameters in the model. In this section, we cover the most basic of tweaks, such as those for V_{be} and beta as a function of I_c. This will set the stage for what follows later where a complete SPICE model is actually created.

Perhaps the best example is that of getting V_{be} right at a low operating current. This is done by adjustment of the parameter IS (saturation current). The transistor is simulated at a chosen V_{ce} and I_c. V_{be} is then checked and compared to the datasheet value for the same operating point, and the error in millivolts is noted. A factor of 2 increase in the parameter IS will decrease V_{be} by 18 mV; a factor of 10 increase in IS will decrease V_{be} by 60 mV. This information guides the adjustment of IS to eliminate the V_{be} error.

A Typical SPICE Model File

A typical BJT model file is shown below. Throughout this chapter SPICE parameters like TF will be shown in capital letters, while a corresponding transistor parameter, typically at a given operating point, will be shown with a different designation, like τ_f. Similarly, the value of C_{jc} (C_{cb}) for a transistor will be governed largely by the SPICE parameter CJC.

.MODEL mjl21194 npn

+	IS=4e-12	BF=65	VAF=500	
+	IKF=14	ISE=1.2e-9	NE=2.0	NF=1.01
+	RB=3.4	RBM=0.1	IRB=1.0	RC=0.06
+	CJE=8e-9	MJE=0.35	VJE=0.5	RE=0.01
+	CJC=1e-9	MJC=0.5	VJC=0.6	FC=0.5
+	TF=21e-9	XTF=90	VTF=10	ITF=100
+	TR=100e-9	BR=5	VAR=100	NR=1.1
+	EG=1.1	XCJC=0.96	XTB=0.1	XTI=1.0
+	NC=4	ISC=0.3e-12	mfg=OnSemi060708	

The model may appear complex, but it is important to understand that it consists of primary and secondary parameters. The primary parameters include IS (V_{be}), BF (current gain), TF (f_T), CJE (base-emitter capacitance), and CJC (base-collector capacitance).

Many of the secondary parameters govern the detailed way in which the primary parameter elements are modulated by the transistor operating point. These secondary parameters are often less important and often can be left at their default values or their values as listed in the manufacturer's SPICE model. For example, MJC and VJC govern the way in which the parameter CJC acts when the voltage across the base collector junction changes. Similarly, IKF, NE, and ISE control beta droop at high and low collector current.

Base-Emitter Voltage

Adjustment of V_{be} is very straightforward. We just tweak IS to get V_{be} right at a single operating point. Figure 20.3 shows a plot of V_{be} versus log I_c. We note the approximate relationship

$$I_c = IS(e^{V_{be}/V_t} - 1) \qquad (20.1)$$

As mentioned above, V_{be} changes by 60 mV per decade of change in collector current. This also means that V_{be} changes by 18 mV for a doubling of collector current. If simulated V_{be} is high by 60 + 18 = 78 mV, IS should be increased by a factor of 20. If V_{be} is low by 60 – 18 mV, IS should be decreased by a factor of 5.

Notice, however, that V_{be} does not follow the logarithmic relationship dictated by (20.1) at high collector currents in Figure 20.3. This is largely due to the presence of base resistance.
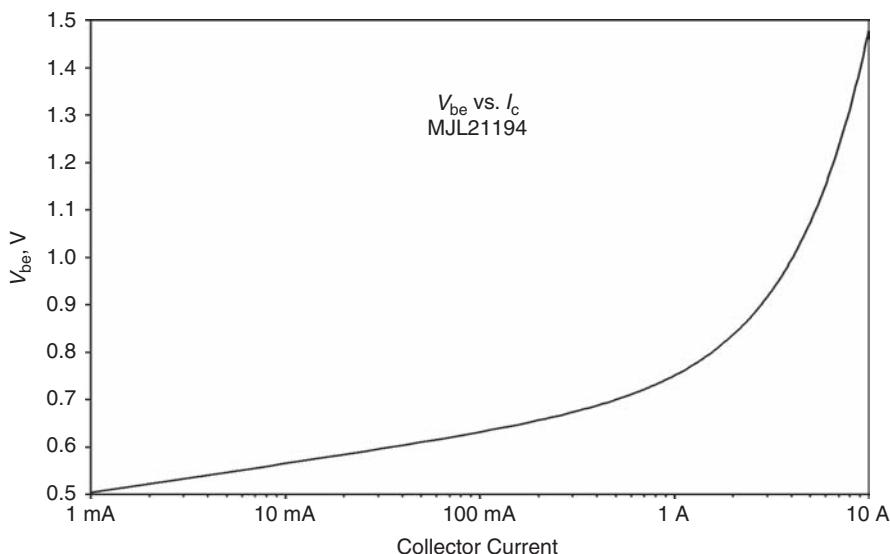
FIGURE 20.3 V_{be} versus log I_c for a typical power transistor.
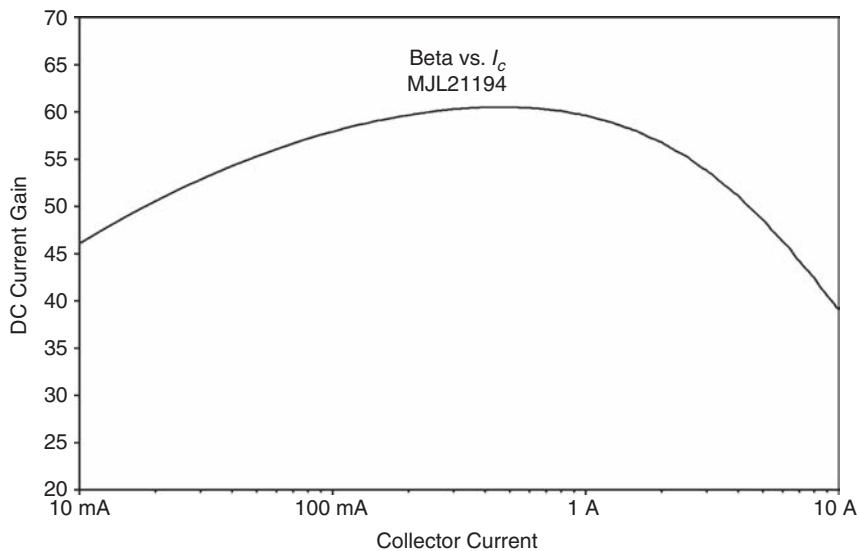
FIGURE 20.4   Current gain beta versus collector current.

Current Gain

A plot of beta versus log I_c is shown in Figure 20.4. The parameter BF does not always represent peak beta, but it controls it. BF can be tweaked to get beta correct at a single operating point. The current gain of a transistor can vary over a large range from one device to another, so getting beta exact is a foolish pursuit. We will, however, see later that properly modeling the behavior of beta as a function of collector current and voltage is important for power transistors.

Speed

The variation of f_T with collector current for a typical power transistor is illustrated in Figure 20.5. The SPICE parameter TF (transit time, τ_f) should be tweaked to get the transistor f_T correct at the collector current for which f_T is maximum. We note the idealized relationship

$$f_T = 1/(2\pi * \tau_f) \tag{20.2}$$
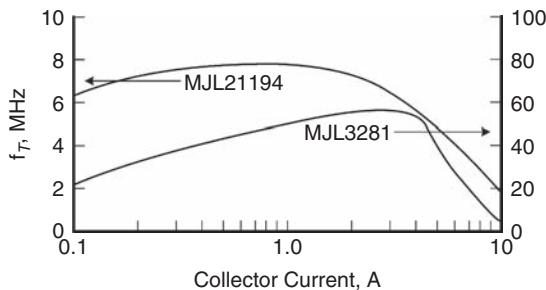
FIGURE 20.5   Transistor f_T as a function of collector current.

As will be discussed later, there are other factors that cause f_T at a given operating point to be smaller than the value given in (20.2). A simple simulation like that in Figure 20.1 can be run at any given DC operating point, and then the SPICE error log can be checked for the value of f_T at that operating point. If maximum f_T is too low, TF should be decreased.

Base-Emitter Capacitance

The base-emitter capacitance is tweaked by adjusting CJE. The value of the parameter CJE is defined at zero reverse junction voltage, so it is usually a bit more than (~ 2×) the base-emitter capacitance at $V_{be} = -2$ V. As before, simulate the transistor at a chosen operating point and check the value of C_{je} (also called C_{be} or C_{ib}) in the SPICE error log and adjust CJE accordingly.

Base-Collector Capacitance

The base-collector capacitance is tweaked by adjusting CJC. The value of the parameter CJC is defined at zero reverse junction voltage, so it is usually a bit more than (~ 1.3×) the base-collector capacitance at $V_{cb} = -2$ V. As before, simulate the transistor at a chosen operating point and check the value of C_{jc} (also called C_{cb} or C_{ob}) in the SPICE error log and adjust CJC accordingly.

20.3 Creating a SPICE Model

Many of the SPICE parameters interact, so the order in which they are established (and then iterated) can make a big difference in how quickly the process converges. In general, it is often best to start with a reasonable model, tweak certain values, and simulate to see how close the result is to the value under consideration. Then iterate.

It is important to bear in mind that almost none of these numbers is sacred and that some combinations may be heuristic and non-unique. The DC parameters should be optimized first. These include things like V_{be}, beta, and Early voltage.

The key to the approach is to realize that when LTspice is used to do a DC run on a simple one-transistor circuit, the operating parameters of the transistor are listed in the resulting SPICE error log. Thus, changes can be made to the model and then quickly evaluated by doing a DC simulation and checking the SPICE error log. Parameterized DC sweeps in the simple transistor simulation with plots can also be very helpful in evaluating and fine-tuning SPICE parameters to obtain accurate transistor behavior.

The manufacturer-supplied SPICE model for the transistor can be used as a starting point, but many of the parameters interact to a degree that may make this less valuable. In many cases, some of the parameters may be useful as a start, such as the capacitances.

In the example procedures described below, the focus is on establishing the SPICE model for a power transistor. This is because the errors in manufacturer SPICE models for power transistors are often more serious. Moreover, errors in power transistor models often have a greater influence on SPICE distortion simulations of power amplifiers. This is because the output transistors in a power amplifier typically operate over much larger extremes of voltage and current, experiencing larger degrees of beta droop, for example.

Gathering Datasheet Information

The first step in creating or revising a SPICE model is to carefully review the datasheet curves for the device and list some key characteristic values as a function of operating point. This data can be taken right off the graphs that are supplied with the data sheet. You can also use the program *Engauge Digitizer* (available at www.digitizer.sourceforge .net) to capture data from a .PNG or .JPG file of the data sheet. The data needed is described below.

Record V_{be} versus I_c from minimum to a reasonable maximum value of I_c. For a power transistor, this should typically include a minimum of four points at 100 mA, 1 A, 5 A, and 10 A.

Record beta versus I_c from a minimum to a maximum value of I_c, like those mentioned above. Record these data at both the higher and lower values of V_{ce} for which data are usually supplied (typically 5 V and 10 V).

Record f_T versus I_c. Do this for a minimum to a maximum value of I_c. Record these data at both the higher and lower values of V_{ce}.

Record C_{be} and C_{bc} versus reverse V_{be} and reverse V_{bc} at a low reverse voltage and a medium reverse voltage. For a power transistor this should typically include reverse junction voltages of 2 V and 10 V. In some cases the medium reverse voltage for the base emitter may be less than 10 V because for some transistors the reverse base-emitter breakdown is less than 10 V.

Measuring Device Data

In some cases, the best models will only result if some lab measurements are done on actual sample devices. This is because the range of current over which the data is shown in data sheets is sometimes not great enough or the precision of the information is not sufficient. This may especially be true for V_{be}-versus-I_c and beta-versus-I_c measurements in the range of I_c from 1 mA to 1 A. These measurements can be done without special-ized pulsed measurements in many cases, but should be done quickly so that junction temperature does not rise excessively and shift the parameters.

It is especially important to get low-current V_{be} versus I_c data in order to determine the parameter NF. The value of NF will usually be near unity. If supporting data cannot be gathered, NF should be set to unity. Defaulting NF to unity may just make it a bit more difficult to get good model matches.

Figure 20.6 illustrates a Gummel plot for a transistor. It is simply a plot of base cur-rent and collector current as a function of V_{be}. The base and collector currents are plotted on a log scale. The distance from the base current to the collector current is the current gain of the transistor at that point.

Figure 20.7 shows a measurement setup that can be used to gather data for the Gummel plot. The transistor is connected with a grounded emitter and a high resis-tance supplying current to the base. The collector current is measured by measuring the voltage drop across a small collector resistor. The base current is calculated from the applied base-voltage-source-voltage less the measured V_{be}, divided by the base resis-tance. The measured data can be entered into a spreadsheet.

Saturation Current and Nominal V_{be}

The V_{be} of a transistor is determined by the saturation current I_s. The saturation current parameter *IS* should be determined first, as it controls V_{be} at lower values of I_c. V_{be} at
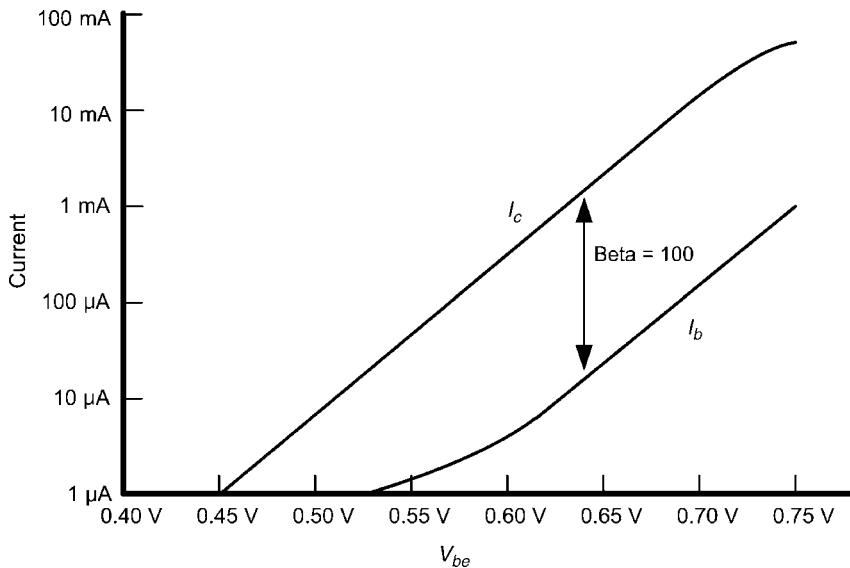
FIGURE 20.6 Transistor Gummel plot.
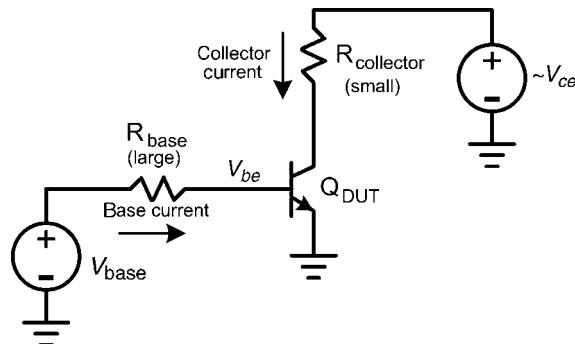
FIGURE 20.7 A measurement setup for gathering Gummel plot data.

higher current is influenced by *RB* and base current, and thus by beta. For this reason, estimation of RB will be done after BF is determined.

Beta is also influenced by V_{ce} via the Early effect. So before we adjust the BF parameter for β, we should make an estimate of the Early effect parameter VAF.

A good starting point for IS can be had by realizing that a value of IS = 200*e*-12 will result in a V_{be} of about 600 mV at a collector current of 100 mA. Keep in mind that a factor of 10 increase in *IS* will result in V_{be} being reduced by about 60 mV, while a factor of 2 change in IS will change V_{be} by about 18 mV. If, for example, V_{be} is 540 mV at 200 mA, then one might want to try increasing IS by a factor of 10 to account for the 60 mV shortfall from 600 mV, and another factor of 2 to account for the bias point being at 200 mA instead of 100 mA. This would result in an IS = 4000*e*-12 = 4*e*-9. The equation below governs I_c.

$$I_c = \text{IS}(e^{V_{be}/(\text{NF} * V_t)} - 1) \tag{20.3}$$

NF is the forward-mode ideality factor and is usually set equal to or near unity. While NF is usually defaulted to unity, it should be noted that NF affects the logarithmic slope of I_c as a function of V_{be}. For example, in the absence of base resistance, V_{be} will increase by approximately 60 mV for each decade increase in I_c. However, this is based on V_t being 26 mV and NF being unity. The effective value of V_t in the above equation is actually multiplied by NF.

If the effective value of V_t were 30 mV (corresponding to NF = 1.15), then the amount by which V_{be} increased with a decade increase in I_c would be approximately 69 mV (simply 1.15 ∗ 60 mV). If NF is greater than unity, not taking this into account can lead to some error in estimating RB from V_{be}-versus-I_c data. It will also cause an error in V_{be} versus I_c at low currents.

If we have V_{be}-versus-I_c data at four points each a decade apart, at 10 mA, 100 mA, 1 A, and 10 A, we can use the difference in V_{be} over the first decade to infer NF and IS (note that these interact). Then we can use the difference over the second decade, from 100 mA to 1 A, to infer RB. Finally, we can use the difference over the third decade, from 1 A to 10 A, to evaluate the reduction in effective base resistance at high base current that results from emitter crowding. The modeling of this is controlled by RBM and IKR.

The parameter NF should be established early in the modeling process. If NF is subsequently changed, then IS will also have to be changed. If IS has to be changed substantially, the value of ISE, which determines low-current beta droop, will have to be changed.

In the procedure below the values of IS and NF are determined. If the proper value of NF is not known, it should be set to unity. NF usually falls between 0.9 and 1.1. Setting BF to the transistor's peak beta value and RB to 5 Ω provides a better starting approximation in this procedure.

PROCEDURE 1 (determine IS and NF)

- Measure V_{be} versus I_c at collector currents from 1 mA to 100 mA.
- Record the ratio of observed decade changes in V_{be} to 60 mV.
- Record octave changes in V_{be} compared to 18 mV.
- Set NF as the average ratio to the ideal values of 60 mV and 18 mV.
- Typical NF will be between 0.9 and 1.1.
- Set initial BF = peak beta datasheet value.
- Set RB=5, RBM=0.1, IRB=10.
- Set IS so that simulated V_{be} is correct at I_c = 1 mA.
- Typical IS might be 1e-12 to 1000e-12.

Early Voltage

The Early voltage *VA* determines the output resistance of the transistor. In other words, if the base current is held constant and the collector-emitter voltage is increased, by how much will the collector current increase? The collector current will increase because the current gain of the transistor increases slightly as collector-base voltage is increased. The current gain, in turn, increases because the increased collector voltage causes the depletion region of the collector-base junction to enlarge, thinning the base.
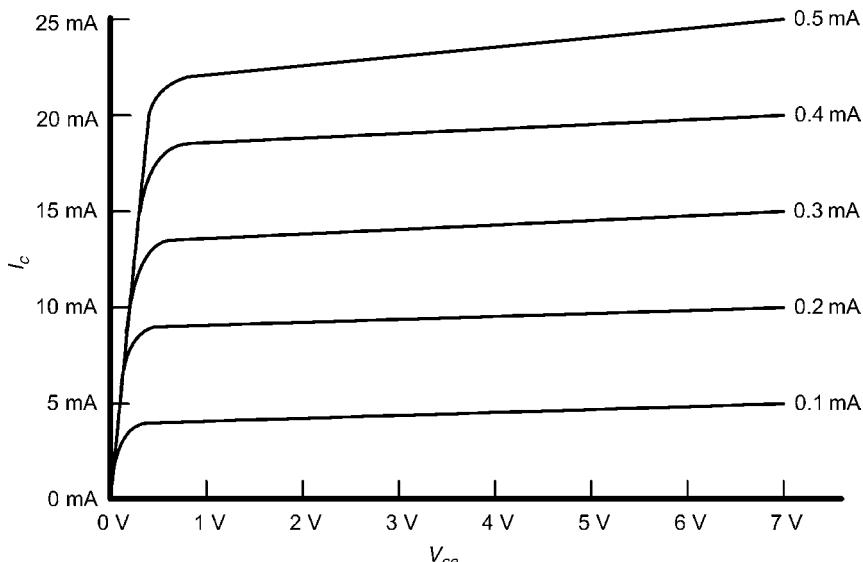
FIGURE 20.8 Transistor collector current characteristic.

Figure 20.8 illustrates a typical transistor output characteristic that would be provided on a data sheet.

Estimating *VA* can be done from the transistor's output curves. It is essentially governed by the way in which beta changes with V_{ce}. One way to find *VA* is to determine the slope of the I_c-versus-V_{ce} curve on the output characteristic at a medium value of I_c. This is output resistance r_o. We then know that $r_o = VA/I_c$, so

$$VA = r_o * I_c \qquad (20.4)$$

Of course, the value of I_c that is used for this calculation matters, but it does not change a lot over the range of V_{ce} that is being used because a reasonable Early voltage results in a relatively shallow slope. Once again, it is important to estimate *VA* first, because the presence of finite *VA* means that actual operating beta will be higher at the usual 20-V operating point for determining beta than at low voltages. The presence of *VA* can sometimes result in a beta that is higher than BF for this reason.

The value of *VA* for a high-voltage power transistor will usually be greater than its V_{ceo} voltage rating. Bear in mind that when V_{ce} is equal to *VA*, the beta has doubled with respect to its very low-V_{ce} value.

In the procedure below, the Early voltage parameter VAF will be estimated from the slope of the curves in the transistor output characteristic.

PROCEDURE 2 (determine VAF)

- Measure the I_c versus V_{ce} slope at a nominal collector current.
- This slope is r_o in ohms.
- Set $VAF = r_o * I_c$.
- Typical VAF might be twice rated maximum collector voltage.

Note that *VA* can be inferred from $\Delta\beta$ over a range ΔV_{ce} as

$$\text{VAF} = \Delta V_{ce} * \beta/\Delta\beta$$

Nominal Beta

The current gain beta of a transistor is readily found on the data sheet. Beta will often be given for different combinations of collector current and collector-emitter voltage. It is important to keep in mind that the Early effect has some effect on current gain.

Figure 20.4 above showed a typical beta-versus-I_c curve that might be found on a data sheet. It can be seen that there is reduced beta (beta droop) at low current and at high current. It can also be seen that beta is reduced at low V_{ce} when I_c is high.

Once VAF is set, we wish to establish a value of BF that results in the proper operating beta at a desirable operating current. This current should be chosen to lie at a sweet spot in the middle of the transistor's operating range. For a power transistor, this will often be around 1 A. For this purpose, we wish to have little or none of the low-current and high-current beta droop effects in play.

In the procedure below, nominal current gain will be set by the parameter BF. This will be approximately the peak beta of the transistor in many cases. The SPICE parameters ISE and NE affect low-current beta droop and will be set to eliminate that effect in this procedure. Similarly, IKF affects high-current beta droop and will be set to eliminate that effect in this procedure. Find beta from the specification sheet at $I_c = 1$ A and $V_{ce} = 20$ V.

PROCEDURE 3 (determine BF)

- Set NE=2.0 and ISE=1*e*-16 in the model.
- Set IKF=100.
- Set BF to the value of beta at I_c=1A and V_{ce}=20V.
- Typical BF might be 50-200.
- Verify beta with a DC simulation at this operating point.
- Adjust BF to obtain correct beta.

Beta Droop at High and Low Current

The current gain of a transistor is often fairly constant over a middle range of collector current. However, beta falls off at very low current and fairly high current. This is often referred to as beta droop. High-current beta droop is especially important in power transistors for amplifier output stages because of the high current they may be called on to handle. The procedure below will facilitate determination of the SPICE parameters that control the modeling of beta droop at low and high currents.

Beta droop at high current is first approximated by finding a value for the parameter IKF. Set IKF to a large value like 100. Check beta at 1 A and at 10 A; these two values should be about the same. Now introduce a lower value of IKF of about 10 A and observe how it has affected beta at 10 A and 1 A. Iterate until a reasonable fit is obtained. Some adjustment of BF may be necessary as well.

Now try to establish beta droop at low currents. Low-current beta droop is controlled by ISE and NE. The parameter NE is the base-emitter leakage emission coefficient.

It controls the slope of the I_b line on the Gummel plot in the low-current beta droop region. Keep NE at 2.0 and increase ISE until beta at 100 mA begins to fall toward the data-sheet value of beta at 100 mA. The SPICE default value of NE is 1.5, but a larger value often results in a better model in power transistors.

Figure 20.9 shows a Gummel plot that has been modified to show the effects that contribute to low-current beta droop. The key thing to recognize is that there are two contributors to base current that result in finite transistor current gain. The first component of base current is determined by BF. It creates a base current that is numerically equal to I_c/BF. If this were the only contributor, beta would equal BF and there would be no beta droop at low currents. The second component is created by the combination of ISE and NE. These create a current that is of the same exponential form as a base or collector current, but with a different slope that is controlled by NE. This latter component of base current tends to dominate at lower collector currents, causing transistor beta to be reduced.

$$I_b = I_c/\text{BF} + \text{ISE}(e^{V_{be}/(\text{NE} * V_t)} - 1) \tag{20.5}$$

while

$$I_c = \text{IS}(e^{V_{be}/(\text{NF} * V_t)} - 1) \tag{20.3}$$
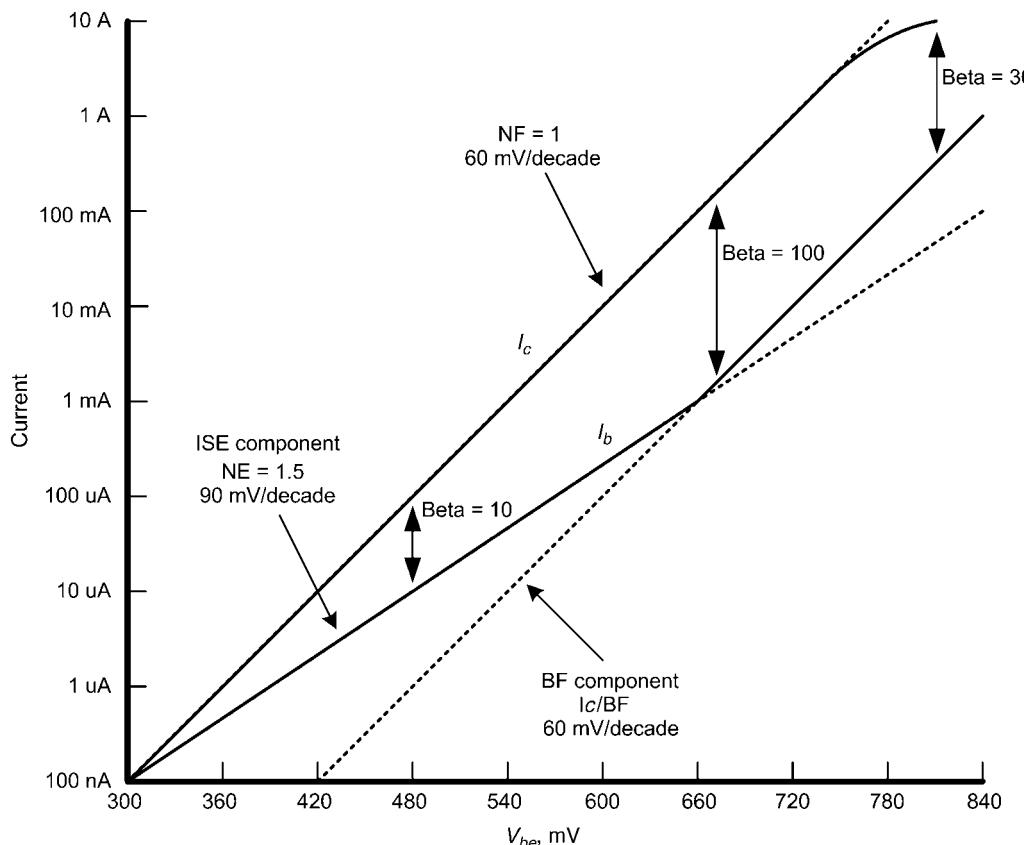
Figure 20.9 Transistor Gummel plot showing beta droop.

The parameter NE will virtually always be greater than NF. While NF is often close to unity, NE is often 1.5–2.0. This difference is what creates the difference in slope of the two contributors to base current on the Gummel plot. If NE = 1.5, for example, the slope of the ISE contributor will be 90 mV/decade. Because the difference in slope created by NF and NE is what determines low-current beta droop, it will often be the case that a transistor with a larger value of NF will need a correspondingly larger value of NE for a given degree of low-current beta droop behavior.

There is significant interaction between the IKF control of beta droop at high current and the ISE control of beta droop at low currents. While IKF attacks beta at 10 A, it also has a depressing effect on peak beta at 1 A. Similarly, while ISE attacks beta at 0.1 A, it also substantially reduces beta at 1 A. In other words, both IKF and ISE reduce beta at the nominal point of 1 A.

Indeed, because IKF reduces beta with increasing current even beginning at 1 A, it will have the effect of making beta at 0.1 A larger (in a relative sense) than that at 1 A before the introduction of ISE. This happens because IKF depresses beta more at 1 A than at 0.1 A. This interaction makes the needed effect of ISE to be even more aggressive in attempting to make beta lower at 0.1 A than at 1 A if low-current beta droop is being experienced at 0.1 A.

Similarly, the effect of ISE lingers so as to tend to reduce the high-current beta droop. As a result, when both IKF and ISE are introduced, BF will have to be increased to move beta back toward peak beta. If IKF is set first and beta from 1 A to 10 A looks good, and then ISE is adjusted to bring beta at 0.1 A down to below that at 1 A, then it will be found that not only does BF need to be increased, but IKF may need to be made more aggressive (a smaller value). As mentioned below, if BF becomes more than about twice the value of peak beta, the model may be questionable.

A significant part of the problem is that the influence of ISE is often not very strong as a function of I_c. Thus, achieving a significant effect at 0.1 A results in an undesired amount of effect at 1 A. Also, the effect at even 0.01 A is surprisingly less than one would expect. The Gummel slope NE affects this. A larger value tends to sharpen the effect of ISE as a function of I_c.

With many power transistors, beta droop at 0.1 A compared to 1 A is relatively insignificant, often being only 10%. Indeed, in some cases beta may be the same or greater at 0.1 A. For this reason, it may be unwise to try too hard to increase ISE aggressively to obtain the desired beta droop at 0.1 A. Such action may jeopardize the high-current beta droop match, which is much more important. A compromise is to introduce just enough ISE to bring beta at 0.1 A down to the value of beta at 1.0 A. A transistor with significant high-current and low-current beta droop will be more difficult to fit.

Figure 20.10 illustrates the effect of different values of NE on low-current beta droop by showing a Gummel plot with a family of curves having three different values of NE. As seen in the figure, changing ISE moves the more steeply sloped curve up and down, while changing NE adjusts its slope; together, they establish the point of intersection where low-current beta droop begins.

With some model parameter combinations, beta at nominal operating current can become hypersensitive to NE. This sensitivity occurs when the value of NE is chosen to be inadequately larger than NF, while seeking some moderate low-current beta droop. This results in the effects of the ISE contribution to base current still being large (and maybe dominant) even at the peak beta point. This can result in a very large value of BF being required to achieve correct peak beta. If BF is greater than twice the value of peak beta, this may be an indication of an unhealthy model.
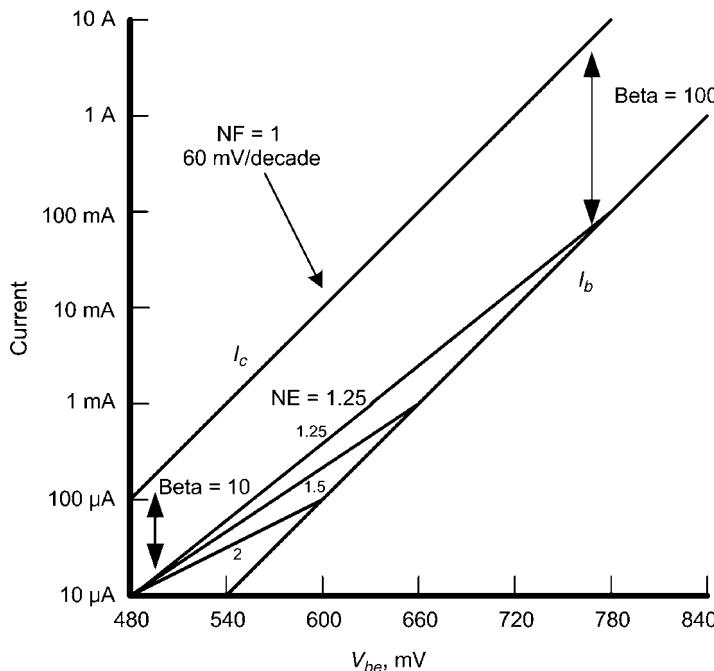
FIGURE 20.10   Effect of *NE* on beta versus I_c.

In the procedure below, the high-current and low-current beta droop parameters will be set. Be aware that this procedure can decrease simulated peak beta somewhat, so that some revision of BF may be needed.

PROCEDURE 4 (determine *IKF*, *NE*, and *ISE*)

- Set NE=2.0 and ISE=1e-16 in the model.
- Evaluate beta at 10A.
- Reduce IKF from 100 until beta at 10A is a good fit.
- Typical IKF might be 15–20.
- Re-check beta at 1A and adjust BF if necessary.
- Evaluate beta at 100 mA.
- Leave NE at the value of 2.0.
- Increase ISE until beta at 100 mA falls appropriately.
- Re-check beta at 1A.
- Increase BF as necessary, and re-check beta at 1A and at 10A
- Typical ISE might be 300∗IS.
- If beta at 1 mA is too low, choose a smaller value of NE and start over.

This procedure may require considerable iteration between the adjustment of low-current beta droop and high-current beta droop, all the while readjusting BF to

maintain proper peak beta. In some cases, adjusting for low-current beta droop before high-current beta droop may make the process converge more quickly.

In general, if the slope of low-current beta droop as a function of I_c is too shallow, use a larger value of NE, but recognize that this will necessitate the use of a larger value of ISE to obtain a given amount of low-current droop. If the slope is too steep, use a lower value of NE, closer to 1.5, recognizing that this will require a smaller value of ISE to obtain a given amount of low-current beta droop.

Establish RB

V_{be} at low current (e.g., 0.1 A) has already been established by the choice of IS. The value of RB has little effect on V_{be} at low current because base current is small and therefore the drop across RB is small.

Base resistance has an influence on V_{be} at higher collector currents. With reasonable values of beta as a function of I_c, we can now establish base resistance RB. The parameter RB corresponds to the value of base resistance r_{bb} at low and moderate currents. Actual base resistance effectively decreases at high current due to emitter crowding. Another term is introduced to allow for modulation of r_{bb} at high-base current. This term is RBM, the minimum value of resistance to which base resistance falls at high-base current.

It is important to realize that the excess V_{be} caused by voltage drop across r_{bb} is due to base current and thus is a function of beta. That is why it was important to establish beta prior to establishing RB. Moreover, beta droops at high currents, further increasing excess V_{be}, so it was important to establish high-current beta droop prior to this exercise as well.

RB can be established by choosing a value of RB that makes V_{be} correct at a medium current like 1 A. The influence of base resistance on V_{be} at a collector current of 1 A can be easily illustrated. Assume beta = 50. Base current I_b will then be 20 mA. If RB= 5, then an extra 100 mV will be added to V_{be} by RB.

Bear in mind the relation

$$I_c = IS(e^{V_{be}/(NF*V_t)} - 1) \tag{20.3}$$

See the comments above about the influence of nonunity values of forward ideality factor NF on the determination of RB. If NF is wrong, it will cause the change in V_{be} from 0.1 A to 1.0 A to be wrong. This "error" in V_{be} could then be wrongly attributed to RB.

In the procedure below, RB is determined by adjusting it to achieve the correct V_{be} at a medium value of collector current. Setting RBM = 0.1 and IRB = 10 in the model prevents modulation of RB by collector current.

PROCEDURE 5 (determine RB)

- Set IRB in the model to 10.
- Set RBM in the model to 0.1.
- Measure the value of V_{be} at $I_c = 1$ A.
- Adjust RB so that simulated V_{be} is correct at 1A.
- Check simulated V_{be} at 5 A; increase RB if necessary.
- Check simulated V_{be} at 10 A; it should be too high.
- If not, increase RB to make it so.
- Typical RB might be 3–5 Ω.

If IS and NF have been chosen correctly, the nonzero value of RB should cause an increase in V_{be} at high current above that which would be expected from the basic equation for V_{be} as a function of I_c. We refer to this ohmic drop across r_{bb} as excess V_{be}.

We should point out that the Gummel plot in Figure 20.6 is an idealized one that assumes no base resistance. With base resistance included, the I_b-versus-V_{be} line would tend to bend down at high currents along with the I_c-versus-V_{be} line.

Establish RB at High-Base Current

As mentioned above, the effective value of base resistance decreases at high collector current. The parameter IRB is the base current (not collector current) at which r_{bb} has fallen half way from RB to RBM. The parameters RBM and IRB may be omitted in simpler models, but may result in excessive V_{be} at high I_c (e.g., 10 A) where a reasonable value of RB has been chosen to properly reflect increased V_{be} at moderate current (e.g., 1 A).

Suppose beta has dropped to 33 at 10 A. Base current will now be 300 mA. If r_{bb}=5, then the excess V_{be} voltage drop across r_{bb} will be 1500 mV. If V_{be} was 700 mV at 1 A, then V_{be} will now be 2.2 V. This is way too high. A more typical value would be about 1.6 V. This is why RBM and IRB are needed to model the effective decrease in base resistance at high collector current.

To get the maximum slope of effective base resistance as a function of collector current (it will often be needed), set RBM to a very small value, on the order of 0.1 Ω or less. At the RBM point, excess V_{be} will then be 30 mV if base current at that point is 300 mA. The value of IRB can then be chosen to get V_{be} down to about what it should be at 10 A.

This adjustment of IRB will have some effect on the value of V_{be} at 1A (V_{be} will have been reduced a bit). Some iteration is then necessary. Often, V_{be} at middle currents like 1A will be a bit less than the datasheet value due to the limited slope of base resistance afforded by the model. This is a better compromise than allowing V_{be} to become unrealistically high at high currents.

In the procedure below, the model parameters RBM and IRB are determined. We will usually set the minimum base resistance RBM, to a very small value to achieve the highest slope of change in r_{bb} at high currents. We will then set the center of the transition point from RB to RBM. This is controlled by the parameter IRB, which is the base current (not collector current) at which r_{bb} has fallen half way from RB to RBM. IRB will be set to yield the best fit for V_{be} at high collector current.

PROCEDURE 6 (determine RBM and IRB)

- Set RBM = 0.1 Ω.
- Set IRB to a high value like 10 A.
- Simulate V_{be} at I_c = 10 A. V_{be} will be too high.
- Reduce IRB until V_{be} at I_c = 10 A falls to the correct value.
- Simulate V_{be} at I_c = 1 A, 2 A, 5 A.
- Iterate RB and IRB if necessary for a reasonable compromise fit.
- A typical value of IRB might be 1 (1 A base current)

This procedure is carried out with a DC sweep simulation of V_{be} versus log I_c from 100 mA to 10 A.

In evaluating the effect of excess V_{be} resulting from r_{bb}, it is helpful to bear in mind the following. If you know V_{be} at 100 mA, then ideally with no r_{bb} V_{be} at 1 A will be larger

by NF times 60 mV. Similarly, ideal V_{be} at 10 A will be greater than that at 1 A by NF times 60 mV. Were it not for decreasing r_{bb} at high collector currents, excess V_{be} would be far too much at very high currents.

Bear in mind that excess V_{be} at high currents and the choice of IRB depends on the amount of high-current beta droop and the choice of RBM. If the downward slope of change of r_{bb} is too high (as indicated by excess V_{be} not sufficient at high current), increase the value of RBM. Too high a slope in r_{bb} will result in inadequate excess V_{be} at high current.

Establish Nominal Transit Time and f_T

The speed of a transistor is mainly characterized by its f_T, the frequency at which its current gain has fallen to unity. The value of f_T, in turn, is primarily determined by the so-called transit time τ_f of the transistor. In this section the nominal peak f_T of the transistor will be established by setting the transit time τ_f. We start using the approximation that

$$f_T \approx 1/(2\pi * \tau_f) \tag{20.2}$$

at its highest point (if we are lucky). It is useful to note that $\tau_f = 10$ ns $=> f_T = 16$ MHz.

In the procedure below, the model parameter TF is set by finding the peak f_T of the transistor and setting TF so that the simulation yields this f_T at the operating point where f_T is at its peak. The parameter XTF controls f_T droop at high current. It is set to zero for this exercise so that there is no effect from high-current f_T droop. The SPICE parameter CJE will be set to a relatively small value so that low-current f_T droop effects largely disappear at the nominal peak f_T operating conditions.

PROCEDURE 7 (determine T_f)

- Find the peak f_T from the data sheet.
- Set XTF = 0 in the model.
- Set CJE to 1/10 of the value given in the model.
- Set TF = $1/(2\pi * f_T)$.
- Simulate f_T at the peak f_T operating point.
- Tweak TF if necessary.
- A typical value of TF would be 20e-9, corresponding to 8 MHz.

Establish f_T Droop at High Current

The f_T of a transistor declines at high operating current as a result of the Kirk effect [5]. It further declines at high operating current when V_{ce} is low. The f_T droop at high current (and low voltage) is established by

		Default
XTF	Coefficient for bias dependence of τ_f	0
VTF	Voltage for V_{bc} dependence of τ_f	∞
ITF	High-current dependence of τ_f	0

The f_T droop behavior at high current is modeled in SPICE by modulating the transition time by the variable *ATF* as

$$\tau_f = \text{ATF} * \text{TF} \tag{20.7}$$

The variable ATF is defined as

$$\text{ATF} = 1 + \text{XTF} * e^{(V_{bc}/(1.44*\text{VTF}))} * [I_c/(I_c + \text{ITF})]^2 \tag{20.8}$$

It is important to recognize that the value of V_{bc} in the above equation is negative, reflecting the reverse-biased condition of the base-collector junction. This means that the exponent is negative. The value of τ_f is multiplied by the factor ATF, where ATF = 1 + XTF at very high current while V_{bc} is still reasonably high (e.g., 10–20 V).

ITF controls the introduction of the factor XTF as I_c increases relative to ITF. The variable VTF will be discussed later in connection with f_T droop at low collector voltages.

The slope of the transition from nominal f_T to drooped f_T is controlled by the relationship of ITF to the current level at the high-current data point. If there is substantial f_T droop at 10 A and ITF is set to 10 A, then a medium slope of the droop transition results. This all assumes that the value of XTF has been set to achieve the proper level of f_T reduction at the high-current data point.

If instead ITF is made about 10 times the value of the current at the high-current data point, then nearly the maximum achievable slope between the medium-current region and the high-current region will be obtained. This assumes that a different value of XTF has been chosen to once again achieve the proper level of f_T reduction at the high-current data point.

Adequacy of the slope can be checked with an evaluation of f_T at 1 A and 10 A. Starting with ITF = 10 A is not unreasonable, but may often result in too shallow a slope in the transition region. A larger value of ITF may be necessary. Bear in mind that the choice of ITF directly affects the value of XTF required to achieve the desired amount of high-current f_T droop.

The f_T droop at high current for power BJTs often has a fairly steep slope. For this reason, it may often be that as much slope as possible is desired. This would lead to choosing a large value of ITF, like 100. In this case, the factor $I_c/(I_c + \text{ITF})$ will be 10/110 = 0.091 at I_c = 10 A, and the squared value will be 0.008, leading to an effective needed multiplier on XTF of 1/0.008 = 125. Of course, if one chooses ITF = 9 times the high-current data point, then the factor becomes 0.1 and the squared value becomes simply 0.01.

In the procedure below, the values of ITF and XTF in the model are determined so that f_T will fall at high collector currents in accordance with the datasheet information. The value of ITF is set to a large value of 100 so as to maximize the slope of beta droop in the high-current region, as this is usually necessary to obtain the best fit to the data. VTF here is set to a nominal value that will usually give a reasonable degree of beta droop at low collector voltages in the high-current operating region.

PROCEDURE 8 (determine XTF and ITF)

- Set ITF = 100.
- Set VTF = 10.
- Set XTF = 0.

- Simulate f_T at 10 A.
- Increase XTF to the point where f_T at 10 A falls to the desired value.
- Re-check f_T at 1 A; iterate TF and XTF as necessary.
- Also check f_T match at 3 A.
- Typical XTF may be 10–100.

Establish f_T Droop at Low Voltage and High Current

The droop of f_T at high current tends to become more pronounced at low collector-emitter voltages. This behavior is controlled by the parameter *VTF*. Once the f_T droop is established at V_{ce} = 10 V, one can then set the further amount of f_T droop experienced when V_{ce} is small, for example, 5 V. In actuality, it is more proper to refer to base-collector voltage V_{bc} as the controlling variable. Differences between V_{bc} and V_{be} on the specification sheet in the way that f_T droop is displayed should be noted.

In the procedure below, the VTF parameter will be set so that f_T at 10 A and 5 V is appropriately less than f_T at 10 V and 10 A. A smaller value of VTF causes greater f_T droop at low voltages. A value of VTF = 10 will often give satisfactory results. It is important to note that a different value of VTF will usually require a change in XTF in order to reestablish the proper amount of f_T droop at high current and nominal V_{ce}.

PROCEDURE 9 (determine VTF)

- Set VTF = 10, as used in establishing f_T droop at higher voltages.
- Simulate f_T at V_{ce} = 5 V and I_c = 10 A.
- See if adequate f_T reduction due to the lower voltage has occurred.
- If not, choose a smaller value of VTF.
- Adjust XTF for correct f_T droop at 10 V.
- Simulate f_T at 5 V and 10 A.
- A typical value of VTF is 10.

Establish f_T Droop at Low Current

The f_T of a transistor droops at low collector current because the base-emitter junction capacitance remains relatively fixed while both diffusion capacitance and transconductance decrease. This decreases f_T. Thus, low-current f_T droop is set by CJE.

Recall from the hybrid pi model that

$$f_T = gm/(2\pi * C_\pi)$$

or that

$$C_\pi = gm/(2\pi * f_T)$$

However, in reality,

$$C_\pi = C_{je} + gm * \tau_f$$

At high current, C_π is dominated by the product $gm * \tau_f$; this is the diffusion capacitance component of C_π. In the limit, $f_T \sim 1/(2\pi * \tau_f)$. However, at low current the somewhat

fixed value of junction capacitance C_{je} comes into play and decreases f_T by limiting how small C_π can go. At very low current, f_T devolves to $f_T = gm/(2\pi * C_{je})$. Because gm is proportional to collector current, one can see that under these conditions, f_T decreases directly as collector current decreases.

Consider a transistor operating at 100 mA with f_T of 8 MHz. Its gm will be 4S. If diffusion capacitance alone is considered, its C_π will be

$$C_\pi = 4/(6.28 * 7e6) = 80{,}000 \text{ pF}$$

If, instead, its f_T has actually sagged to 6.5 MHz due to the additional presence of the junction capacitance, then $C_\pi = 98{,}462$ pF, an increase of 18,462 pF. This increased amount of capacitance relates approximately to the junction capacitance C_{je}.

The junction capacitance at work here is a bit larger than CJE due to the forward bias of the base-emitter junction. Bear in mind that CJE is the capacitance of the base-emitter junction at zero bias.

The junction capacitance C_{je} is governed by the SPICE parameter CJE. We set CJE in the SPICE model by increasing it from a low value until the f_T at a low current (e.g., 100 mA) has drooped by the appropriate amount.

There is a compromise here. The resulting CJE may conflict with the datasheet value of C_{je} at low reverse base-emitter voltages like –2 V. This is because C_{je} is a function of reverse junction voltage. Adjusting the MJE and VJE may help this situation.

In the procedure below, the model parameters CJE, MJE, and VJE will be established to obtain the datasheet amount of f_T droop at low collector current. The most important parameter is CJE, while MJE and VJE can usually be set to typical values or those provided in the manufacturer's SPICE model, if available.

PROCEDURE 10 (determine CJE, MJE, and VJE)

- Note datasheet C_{je} at $V_{be} = -2$V and $V_{be} = -10$V.
- Set CJE $= 2 * C_{je}$ at –2V.
- Set MJE $= 0.5$.
- Set VJE $= 0.5$.
- Simulate f_T at 1 A and at 100 mA.
- See if low-current f_T droop is appropriate.
- If f_T droop is too great, decrease CJE.
- Tweak TF if peak f_T has fallen too much due to CJE.
- Simulate C_{je} at 0 V, 2 V, and 10 V, check match.

The parameter CJE will often be about double the value of C_{je} at 2-V reverse bias. Moreover, MJE = 0.5 and VJE = 0.5 are reasonable for the base-emitter junction. If the manufacturer's SPICE model is available, use their values for MJE and CJE. Otherwise, use 0.5 for both parameters. The error will not be serious.

For those interested, SPICE computes C_{je} as

$$C_{je} = \text{CJE} \left[1 - (V_{be}/\text{VJE}) \right]^{-\text{MJE}}$$

where *VJE* is the built-in potential and MJE is the capacitance exponent. Junction capacitances are usually of this form.

Determine Base-Collector Capacitance

In the procedure below, the base-collector capacitance C_{jc} (also called C_{bc} or C_{ob}) is established by setting CJC, MJC, and VJC. The parameters MJC and VJC are less important and will usually be set to typical values or those values found in the manufacturer's SPICE model, if available.

PROCEDURE 11 (determine CJC, MJC, and VJC)

- Set VJC = 0.6.
- Set MJC = 0.5.
- Read datasheet value of C_{jc} at –2V.
- Set CJC = 1.3 times C_{jc} at –2V.
- Check behavior of C_{jc} against data sheet.
- Adjust CJC as needed.

Check the Model

In the procedure below, the SPICE model that has been created is spot-checked for accuracy. This helps assure that no serious problems have crept into the model as it was being created, either by error or by unanticipated interactions.

PROCEDURE 12

- Check V_{be} at low, medium and high current.
- Check beta at low, medium, and high current.
- Check beta at low and high voltages.
- Check f_T at low, medium, and high current at medium V_{ce}.
- Check f_T at low, medium, and high current at low V_{ce}.
- Check C_{je} at low and medium reverse bias.
- Check C_{jc} at low and medium reverse bias.

All of these items can be checked by viewing the SPICE error log after performing a simple simulation that biases the transistor at the operating point of interest.

BJT Model Example

Below is a typical BJT power transistor model that was created using these procedures. The model is of the MJL21194 NPN transistor that has been used in several of the power amplifier examples in other chapters.

```
.MODEL mjl21194 npn
+   IS=4e-12     BF=65        VAF=500
+   IKF=14       ISE=1.2e-9   NE=2.0       NF=1.01
+   RB=3.4       RBM=0.1      IRB=1.0      RC=0.06
+   CJE=8e-9     MJE=0.35     VJE=0.5      RE=0.01
```

+	CJC=1e-9	MJC=0.5	VJC=0.6	FC=0.5
+	TF=21e-9	XTF=90	VTF=10	ITF=100
+	TR=100e-9	BR=5	VAR=100	NR=1.1
+	EG=1.1	XCJC=0.96	XTB=0.1	XTI=1.0
+	NC=4	ISC=0.3e-12	mfg=OnSemi060708	

20.4   JFET Models

JFETs operate on a different principle than BJTs. Think of a bar of N-type doped silicon connected from source to drain. This bar will have a resistance and act like a resistor. Now form a PN junction somewhere along the length of this bar by adding a region with P-type doping. As the P-type gate is reverse biased, a larger depletion region will be formed and this will begin to pinch off the region of conductivity in the N-type bar. This reduces current flow. This is called a *depletion device*. It is normally on (at zero gate-source voltage) and is turned off by controlling the amount of depletion by applying a negative voltage to its gate (for N-channel devices). The JFET will be nominally on and its degree of conductance will decrease as reverse bias on its gate is increased until the channel is completely pinched off.

The amount of reverse gate-source voltage that causes complete pinch-off of the channel is called the pinch-off voltage V_p or more commonly the threshold voltage V_T. Put differently, V_T is the gate-source voltage at which current flow begins as reverse bias is decreased from the threshold voltage value. The threshold voltage is often on the order of 0.5 V to 4 V for most small-signal JFETs.

For small values of V_{ds}, the JFET acts as a resistance whose value is controlled by the degree of channel pinch-off caused by the reverse bias of the gate junction. This is called the *linear* or *triode region*. JFETs are often used as voltage-controlled resistors in this region. As V_{ds} increases, it also tends to pinch off the channel by creating a reverse bias with the gate junction. This opposes increased I_d caused by V_{ds} and causes the JFET to enter into what is called the saturation region, where I_d is largely independent of V_{ds}. The demarcation between the linear region of operation and the saturation region occurs at the point where $V_{ds} = V_T$ if $V_{gs} = 0$. The discussion here will focus on JFET behavior in the saturation region.

DC Behavior of JFETs

The JFET *I-V* characteristic (I_d vs. V_{gs}) obeys a square law, rather than the exponential law applicable to BJTs. The simple model below is valid for $V_{ds} > V_T$ and does not take into account the influence of V_{ds} that is responsible for output resistance of the device.

$$I_d = \beta(V_{gs} - V_T)^2 \tag{20.9}$$

The equation is valid only for positive values of $(V_{gs} - V_T)$. The factor beta (not to be confused with BJT current gain) governs the transconductance of the device. The variable name K is sometimes used instead of beta. When $V_{gs} = V_T$, the $V_{gs} - V_T$ term is zero and no current flows. When $V_{gs} = 0$ V, the term is equal to V_T^2 and maximum current flows.

The maximum current that flows when $V_{gs} = 0$ V and $V_{ds} > V_T$ is referred to as I_{DSS}, a key JFET parameter usually specified on data sheets. Under these conditions the channel is at the edge of pinch-off and the current is largely self-limiting. The parameter beta

is the transconductance coefficient and is defined in terms of I_{DSS} and V_T. It has units of amperes per volt squared.

$$\beta = I_{DSS}/V_T^2 \qquad (20.10)$$

In real devices the drain-source voltage also has some influence on the drain current, even in the saturation region. This is not unlike the Early effect in BJT devices. The influence of V_{ds} on I_d is a result of what is called *channel length modulation,* described by the SPICE parameter LAMBDA (λ). The relationship below includes the effect of λ.

$$I_d = \beta(V_{gs} - V_T)^2 * (1 + \lambda V_{ds}) \qquad (20.11)$$

LAMBDA controls the output resistance of the JFET. Smaller values of λ correspond to higher output resistance r_0. LAMBDA is referred to as the *channel-length modulation parameter* and has the units of inverse volts (1/V).

Transconductance for a JFET at a given operating current is smaller than that of a BJT by a factor of about 10 in many cases. Its turn-on characteristic (once the threshold voltage has been overcome) is much less abrupt that that of a BJT.

The JFET SPICE Model

A typical model for a JFET is shown below. As with BJTs, there are primary and secondary model parameters, where the former are fairly fundamental and the latter are less important in many applications. The first line includes the primary parameters that govern DC behavior. BETA governs the transconductance above threshold, VTO is the threshold voltage, and LAMBDA controls the output resistance of the device.

.MODEL J310 NJF

+ BETA = 0.004 VTO = -3.75 LAMBDA = 58E-3

+ CGS=16E-12 CGD=12E-12

+ PB=0.52 M=0.54 FC=0.5 RD = 5 RS= 33 N=1

+ IS=41E-15 KF =5.6E-18 AF = 0.56

The second line includes the primary AC parameters, which are merely gate-source and gate-drain capacitance. The third line includes secondary parameters influencing the capacitance behavior and the drain and source parasitic resistances. The last line includes IS, which characterizes the saturation current of the gate junction, and parameters that govern the flicker noise of the device.

Creating and Tweaking the JFET Model

JFET behavior is mainly modeled by the three parameters BETA, VTO, and LAMBDA, and these are the only ones that will be discussed here. Numbers from manufacturers' models, if available, should generally suffice for the others. Manufacturers' JFET SPICE models are usually decent, but the large range of threshold voltage and I_{DSS} sometimes make creation of a model from measurements of real devices quite useful.

Measure I_{DSS} as the current that flows with $V_{gs} = 0$ V and $V_{ds} = 10$ V. Measure V_T as the reverse bias needed to reduce drain current to 1% of I_{DSS}. This is not necessarily the same as what the manufacturer specifies as V_{gs_off}, which may be specified at extremely low current values. Calculate BETA as $\beta = I_{DSS}/V_T^2$. Set VTO as the measured threshold

voltage (VTO is always a negative value, regardless of device polarity). Set LAMBDA = 0.002 as a starting value.

Simulate the family of *I-V* characteristics for the device and iterate the three parameters to obtain a good match. If the slope of the I_d-versus-V_{ds} curve at $V_{gs} = 0$ V is too shallow, increase LAMBDA. If the spacing of the curves as a function of V_{gs} is too small, increase BETA.

20.5 Vertical Power MOSFET Models

Unlike the JFET, the MOSFET power transistor is an enhancement-mode device; this means it is normally off at $V_{gs} = 0$ and must be turned on by increasing V_{gs} to a voltage greater than the threshold voltage. The MOSFET gate is insulated from the underlying source-drain structure by a thin oxide, forming capacitances to the source and drain nodes.

The DC characteristics of power MOSFETs are usually modeled in essentially the same way as those for small-signal MOSFETs like those used in integrated circuits. An example of the basic DC SPICE Level 1 model for a power MOSFET is shown below.

.MODEL IRFP244 NMOS LEVEL=1

+KP=2.9 VTO=4.2 LAMBDA=0.003

+CGSO=0 CGDO=0 IS=1e-32

The threshold voltage VTO is positive for enhancement mode N-channel devices and negative for P-channel enhancement devices. The parameter KP governs device transconductance. The drain current obeys a square-law relationship.

$$I_d = \tfrac{1}{2}\text{KP}(V_{gs} - V_T)^2 \qquad (20.12)$$

Notice the similarity to the JFET model. The threshold voltage V_T (VTO) is a positive number, reflecting the enhancement nature of the device. In comparison to the JFET model, the parameter KP serves the same transconductance function as beta.

The influence of V_{ds} on I_d is modeled in the MOSFET by the parameter LAMBDA as shown below. LAMBDA controls the output resistance of the MOSFET. The effect controlled by LAMBDA is not unlike the Early effect in BJT devices. Smaller values of λ correspond to higher output resistance r_0.

$$I_d = \tfrac{1}{2}\text{KP}(V_{gs} - V_T)^2 * (1 + \lambda V_{ds}) \qquad (20.13)$$

Establishing the DC Parameters

It is important to recognize that the threshold voltage cannot be accurately estimated just by looking at the datasheet plot of I_d versus V_{gs} where I_d appears to go to zero. This is because of subthreshold conduction that will be discussed later. It causes I_d to be larger than predicted by the square law at V_{gs} near threshold.

The parameters VTO and KP can easily be estimated by checking V_{gs} at two values of drain current that differ by a factor of 4. Recall the square-law relationship.

$$I_d = \tfrac{1}{2}\text{KP}(V_{gs} - V_T)^2$$

Consider the datasheet values of V_{gs} at 1 A and 4 A (V_{gs1} and V_{gs2}, respectively). We know that $(V_{gs} - V_T)^2$ at 4 A will be 4 times that at 1 A. Similarly, we know that $(V_{gs} - V_T)$

will be twice that at 4 A as at 1 A. We can use these relationships to yield estimates for VTO and KP.

$$\text{VTO} = 2V_{gs1} - V_{gs2}$$

$$\text{KP} = 2I_{d1}/(V_{gs1} - \text{VTO})^2$$

These may be useful starting values, but simulation of I_d versus V_{gs} and iteration to refine the fit will be necessary. As long as iteration is necessary, a useful alternative is to estimate VTO as the voltage where I_d for a power MOSFET is down to about 50 mA, then adjust KP as necessary to achieve the right V_{gs} at some medium current like 4 A. VTO and KP will have to be juggled to optimize the fit of I_d versus V_{gs}. The I_d-versus-V_{gs} curve may bow above or below the target curve at values of I_d that are smaller than the I_d value chosen for the initial setting of KP. If V_{gs} for $I_d = 2$ A is low, increase VTO and revise KP to obtain correct V_{gs} at 4 A.

The drain current of a MOSFET is a mild function of V_{ds}, resulting in output conductance. This is not unlike the Early effect in a BJT. This behavior is modeled by LAMBDA in the MOSFET model. Simulate I_d versus V_{ds} at a gate voltage that produces a medium value of drain current, like 3 A. Adjust LAMBDA so that the difference in I_d from $V_{ds} = 10$ V to $V_{ds} = 50$ V matches that on the device data sheet. In other words, adjust the shallow upward slope of the curve to be correct. LAMBDA will often be in the range of 0.001 to 0.1. Because LAMBDA works by influencing the effective value of KP, the value of KP used in the model may have to be trimmed a bit after LAMBDA is set. If the approximate value of LAMBDA is known beforehand, it should be put in the model before VTO and KP are adjusted.

The recommended procedure for creating a typical Level 1 power MOSFET model is

- Review the I_d versus V_{gs} datasheet curve.
- Estimate VTO as V_{gs} at I_d of about 50 mA.
- Set KP to a reasonable starting value, like 3.0.
- Set LAMBDA to a reasonable starting value, like 0.003.
- Simulate I_d versus V_{gs} of the model at the same V_{ds} as used for the datasheet curves.
- Adjust KP to get desired V_{gs} at 4 A.
- Juggle VTO and KP to get desired curve shape.
- If V_{gs} for $I_d = 2$ A is low, increase VTO and revise KP to obtain correct V_{gs} at 4 A.
- Simulate I_d versus V_{ds} at 2 A.
- Adjust LAMBDA to obtain the same slope as found on the device output curves.
- Iterate.

Gate-Source Capacitance

The gate-source capacitance C_{gs} for a vertical power MOSFET is fairly constant with changes in V_{gs}. Some engineers have been fooled into thinking that this capacitance increases dramatically by looking at the steep incline that begins at turn-on in the usual

gate charge plot provided in power MOSFET data sheets. In reality, this steep incline is caused by the transistor turning on and allowing the Miller effect on the gate-drain capacitance to take effect.

The input capacitance of a power MOSFET is referred to as C_{iss}, and this is usually what is plotted in data sheets. It is the sum of C_{gs} and C_{gd}. The rise in C_{gd} is what is responsible for the rise in C_{iss} at low V_{ds}. C_{gs} is about 1200 pF for an IRFP240. This is a fairly large capacitance, but it is bootstrapped to a much smaller effective value in a source follower output stage.

Gate-Drain Capacitance

The gate-drain capacitance C_{gd} becomes very large at low values of V_{ds}, as measured when $V_{gs} = 0$ V. The nonlinear nature and large maximum values of C_{gd} are a concern for audio amplifier design at high frequencies and high levels. If high slew rate is to be supported at output voltages near the rails, the driver must be able to source and sink the current required to charge and discharge this increased gate-drain capacitance.

The value of gate-drain capacitance for an IRFP240 MOSFET is plotted below in Figure 20.11 as a function of V_{ds} when $V_{gs} = 0$ V. At high V_{ds}, C_{gd} is a modest 50 pF. However, C_{gd} grows rapidly at reduced V_{ds}. At $V_{ds} = 10$ V it has already climbed to about 700 pF. At $V_{ds} = 1$ V, it is a very large 1250 pF. Note that C_{gd} is also referred to as C_{rss}.

C_{gd} Test Circuit

The individual interelectrode capacitances in a MOSFET can be difficult to isolate; when two terminals are shorted for a capacitance measurement, two of the three capacitances are being measured in parallel. It is possible to measure C_{gd} by driving an AC signal into the drain and then measuring the signal voltage that appears from gate to source while a shunting resistance is tied from gate to source. This resistor should have a resistance that is at least 10 times smaller than the reactance of the estimated C_{gs} capacitance at the test frequency. The attenuation of the applied AC signal from drain to gate can then be used to infer C_{gd}.
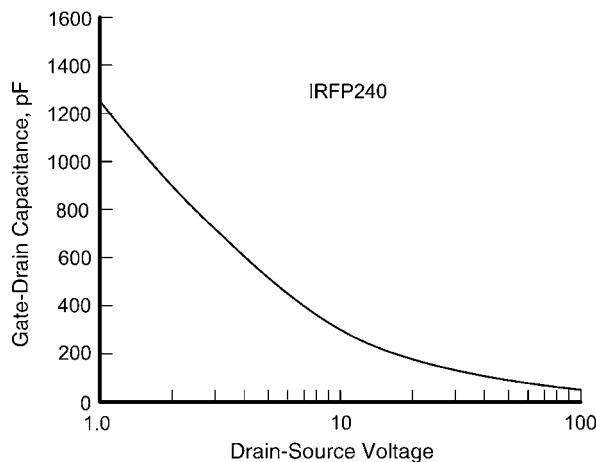
FIGURE 20.11   Power MOSFET C_{gd} versus V_{ds} for IRFP240.

The Subcircuit Model

The common SPICE model used for power MOSFETs comprises a basic core SPICE MOSFET model that is encapsulated in a subcircuit that includes additional components to model the drain-source body diode and the capacitance effects.

The power MOSFET C_{gd} nonlinearity is difficult to model. Some manufacturers have rather elaborate subcircuit models with numerous diodes and passive elements to model the capacitances. In those cases, it may be best to use the manufacturer's model and just tweak the DC core part of the model to obtain desired DC behavior. However, bear in mind that manufacturer's MOSFET SPICE models are created primarily for correct behavior in switching applications, not linear applications. Some of the subcircuits used to model the gate-drain capacitance can introduce nonlinearities that do not exist in the real device.

Figure 20.12 shows a schematic of a simple subcircuit model for a power MOSFET. This model employs only a diode for simulation of the nonlinear gate-drain capacitance. This is a very oversimplified approach for purposes of illustration only. Clearly, this model does not behave properly if the gate becomes forward-biased relative to the drain. Such a condition can occur in amplifiers that employ boosted supplies for the driver circuitry. MOSFET amplifier designs should avoid this condition because of the very high C_{gd} that results and the consequences for output stage bandwidth shrinkage and increased dynamic driver current requirements.

Shown below is a corresponding subcircuit model for the IRFP244.

```
*Drain Gate Source
.SUBCKT IRFP244 1 2 3
M1 10 20 30 MOSFET L=100u W=100u
RD 1 10 0.05
RG 2 20 3
RS 3 30 0.005
CGS 20 30 1000p
DGD 2 1 GDDIODE
DDS 3 1 DSDIODE
*
```
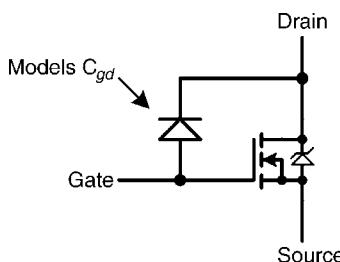

FIGURE 20.12 Subcircuit model schematic.

```
.MODEL MOSFET NMOS LEVEL=1
+KP=2.9 VTO=4.2 LAMBDA=0.003
+CGSO=10p CGDO=10p IS=1e-32
*
.MODEL DGDIODE D
+IS=1E-32 N=100 RS=10
+CJO=1200p M=0.5 VJ=0.5
*
.MODEL DSDIODE D
+IS=4E-6 N=1.0 RS=0.02
+CJO=1400p M=0.7 VJ=2.5
*
.ENDS
```

The parameters $L = 100\mu$ and $W = 100\mu$ are sometimes seen in the first line of the call to the MOSFET model. These parameters define what is called the *W/L ratio*. The appropriate *W/L* ratio when using the Level 1 SPICE model for power MOSFETs is usually unity. These parameters can be left off, as the default is unity. However, these parameters should be explicitly specified when using the EKV model to be discussed later.

Capacitor CGS models the relatively constant gate-source capacitance of the vertical MOSFET. For this reason, CGSO is set to a fairly small value in the core MOSFET model. Diode DGDIODE models the nonlinear gate-drain capacitance, so CGDO is set to a small value in the core MOSFET model. Diode DSDIODE models the body diode.

Although not shown, bond wire and package inductances can be incorporated into the model for improved modeling of behavior that might influence parasitic oscillations in a real circuit. The inductances for the bond wires can be increased somewhat to account for local board-level trace inductances as well. Typical values for bond wire inductances are 10 nH for gate and source and 5 nH for the drain.

Subthreshold Conduction

The DC behavior of the basic SPICE model is inaccurate at low current for V_{gs} in the vicinity of the threshold voltage and below. This is because weak inversion is not modeled in the Level 1 model. The power MOSFET does not behave as a square-law device in this region of operation. This is a problem for simulation of MOSFET amplifier biasing and crossover distortion.

The simple square-law equation for drain current goes to zero at the threshold voltage; this causes a discontinuity in transconductance. This is simply not accurate for MOSFETs. In fact, at low current, the MOSFET characteristic transitions to an exponential law that is much like that followed by BJTs, but with far different coefficients. Because the simulation of crossover distortion involves behavior of the devices at low current (150 mA is considered to be in the transition region of the model), the normal SPICE models will give misleading results. For example, at the threshold voltage, where the simple model would have $I_d = 0$, I_d for an IRFP240 is between 50 and 100 mA. There are better models for MOSFETs, one of which is called the EKV model. However, EKV model parameters for power MOSFETs are quite rare.

Applicability

The conventional subcircuit power MOSFET model is adequate for many power amplifier simulations with the major exception of crossover distortion. The subthreshold region is encountered as the signal passes through the crossover region in a class AB amplifier. The typical bias point of 150 mA often lies in the transition region between the subthreshold and square-law parts of the model, so that the actual bias voltage required to obtain the desired bias current may be off a bit.

Power Amplifier Design Concerns

Datasheet information on MOSFET C_{gd} is incomplete for the operating region relevant to audio. The data sheet usually plots C_{gd} for $V_{gs} = 0$ V. This is a condition that never occurs in audio amplifiers at low values of V_{ds} where C_{gd} becomes large. V_{ds} is small when the output is near the rails and the amplifier is sourcing considerable current, requiring V_{gs} to be quite positive, that is, nowhere near 0 V. The region of greatest concern relevant to audio is near clipping, where V_{ds} is 5 V or less and V_{gs} is >5 V, *and* where the source is largely still following the signal. This may have important implications for the behavior of C_{gs} and C_{ds} and how they influence effective C_{gd}.

The effect of the increased C_{gd} in source follower amplifier output stages largely manifests itself as a substantially increased need for dynamic gate drive current at output amplitudes near clipping. Output stage bandwidth also decreases as C_{gd} increases, especially if gate stopper resistors are employed. Consider the case where C_{gd} has risen to 1000 pF and a 50-Ω gate stopper resistor is in place. This combination will introduce a pole at 3.2 MHz. Increased C_{gd} is likely much more serious in MOSFET CFP output stages because of the increased influence of Miller effect in that arrangement.

20.6   LTspice™ VDMOS Models

The LTspice VDMOS model was created specifically for vertical double-diffused power MOSFETs. It eliminates the need for the subcircuit approach and incorporates modeling of the source-drain body diode and the nonlinear capacitances right into the model itself. As a result, the model runs faster and more accurately models the nonlinear capacitances. The VDMOS model uses the basic Level 1 SPICE core model for DC behavior of the power MOSFET, so subthreshold behavior is not modeled. A typical VDMOS model is shown below.

```
.MODEL IRFP244 VDMOS NCHAN
+KP=2.9 VTO=4.2 LAMBDA=0.003
+CGDMAX=2.3e-9 CGDMIN=6.3e-12 a=0.34
+CGS=1340p CJO=1300p M=0.68 VJ=2.5
+RS=0.05 RD=0.1 RDS=1e7 IS=4.0e-6 N=2.4
```

The second line defines the DC behavior in the same way as the conventional Level 1 SPICE model. The third line defines the behavior of the nonlinear gate-drain capacitance in a way unique to the VDMOS model. The fourth line defines the gate-source capacitance C_{gs} and the body diode capacitance C_{jo} (a junction capacitance).
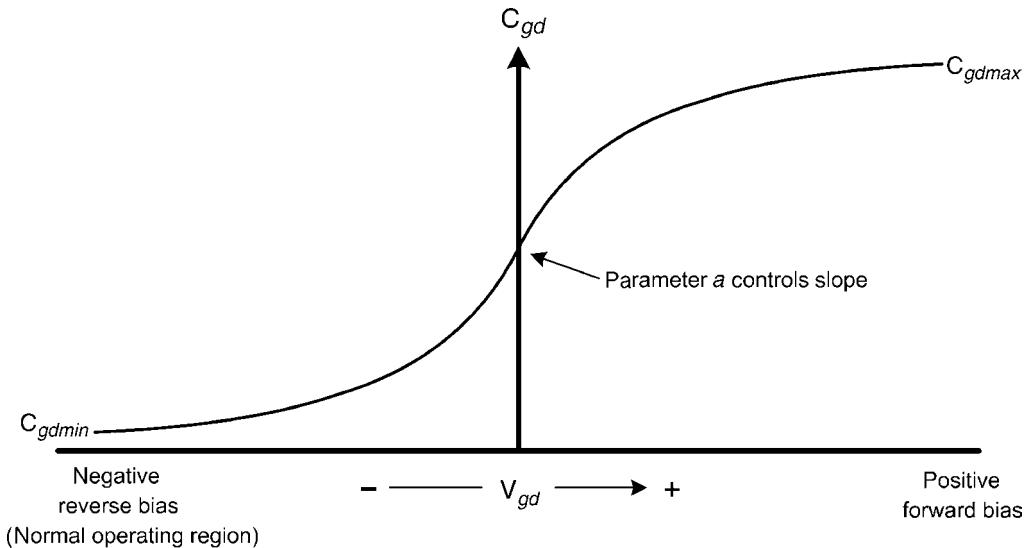
Figure 20.13 C_{gd} as a function of V_{gd} in the VDMOS model, for V_{gd} large negative to large positive.

The gate-drain capacitance is modeled as a nonlinear function of V_{gd} as illustrated in Figure 20.13 for an N-channel device. For negative values of V_{gd} (e.g., high drain-source voltage), C_{gd} becomes smaller, approaching C_{gdmin} at large values of reverse bias. For positive V_{gd}, C_{gd} increases to C_{gdmax}. The C_{gd} behavior is modeled by the parameters CGDMIN, CGDMAX, and a. The parameter a controls how abrupt the change of C_{gd} is as a function of V_{gd}. The default value of a is 1.0 and typical values lie between 0.3 and 1.0. The computation of C_{gd} by CGDMAX, CGDMIN, and a is described in the LTspice User Manual [6].

Establishing the Model Parameters

The behavior of C_{gd} is usually described on a data sheet with a plot of C_{gd} (C_{rss}) as a function of V_{ds}, with $V_{gs} = 0$. This means that V_{ds} is the same as the reverse-bias amount of V_{gd}. The plot often extends from $V_{ds} = 1$ V to $V_{ds} = V_{dsmax}$, where V_{dsmax} may be 50 V or more. C_{gd} is at its minimum value at V_{dsmax}. This can be seen in Figure 20.11. The VDMOS parameters are chosen to fit this curve.

The parameter C_{gdmin} can be chosen to equal the minimum value of C_{gd} on the plot, at V_{dsmax}, although often it will be chosen to be smaller. The parameter C_{gdmax} is not the same as the maximum value of C_{gd} on the plot at V_{ds} of 1 V or less. It can be seen from Figure 20.11 that C_{gdmax} is a larger value than this. Bear in mind that the parameter a controls the sharpness of the transition from C_{gdmin} to C_{gdmax} as V_{gd} changes from negative values to positive values.

To help establish the VDMOS parameters we define two factors that will be a function of the parameter a. The factor $F1 = C_{gd(1)}/C_{gd(10)}$, where $C_{gd(1)}$ and $C_{gd(10)}$ are the values of C_{gd} at V_{ds} equal to 1 V and 10 V. This factor captures the slope of the transition from the datasheet plot. Similarly, the factor $F2 = C_{gdmax}/C_{gd(1)}$ helps establish the parameter C_{gdmax} from the value of C_{gd} at $V_{ds} = 1$ V.

Figure 20.14 is a plot showing typical values of $F1$ and $F2$ as a function of the parameter a. In this plot the values of C_{gdmin} and C_{gdmax} were held constant. The plot provides
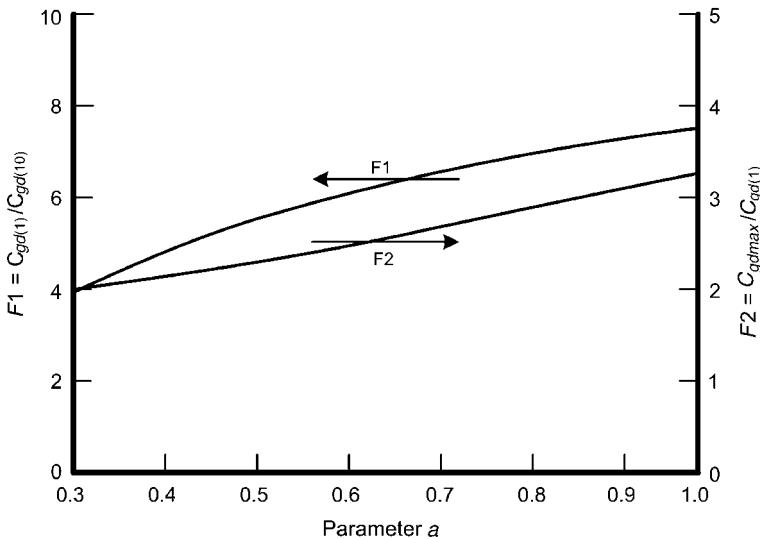
FIGURE 20.14 $F1 = C_{gd(1)}/C_{gd(10)}$ and $F2 = C_{gdmax}/C_{gd(1)}$ as a function of a.

insight into the influence of a. It also provides a means of estimating starting values of the parameters when fitting the data sheet plot. Increasing a increases the slope of the transition of C_{gd}, as can be seen by how it affects $F1$. Increasing a while C_{gdmax} is held constant decreases the value of $C_{gd(1)}$. The procedure below should be iterated as needed. The value of C_{gd} for the device model is found from simulation with $V_{gs} = 0$ and various values of V_{ds}. The simulated value of C_{gd} can be found by looking in the SPICE error log.

Below is a procedure for establishing C_{gdmin}, C_{gdmax}, and a.

- Find $F1 = C_{gd(1)}/C_{gd(10)}$ from the data sheet.
- Set a based on $F1$ and Figure 20.14.
- Find $F2 = C_{gdmax}/C_{gd(1)}$ from the data sheet.
- Set C_{gdmax} based on $F2$ and Figure 20.14.
- Set C_{gdmin} to 1/10 of the value of C_{gd} at V_{dsmax}.
- Simulate and adjust C_{gdmax} for correct $C_{gd(1)}$.
- Simulate and check $C_{gd(10)}$.
- If $C_{gd(10)}$ is high, increase transition slope by increasing a.
- If a was increased, increase C_{gdmax} to reestablish correct $C_{gd(1)}$.
- Adjust C_{gdmin} for correct C_{gd} at V_{dsmax}.
- Iterate as needed.

Applicability

The VDMOS model is suitable for most amplifier simulations, but it has the same limitations as the Level 1 MOSFET model insofar as its failure to model subthreshold behavior. For this reason crossover distortion simulations may be inaccurate. The VDMOS

model is much more convenient to use because it does not require a subcircuit and tends to model the nonlinear capacitances more accurately.

20.7   The EKV Model

The power MOSFET is not purely a square law device governed by the usual equation where I_d goes to zero at $V_{gs} = V_T$. The MOSFET has substantial subthreshold conduction in the so-called weak inversion region. Indeed, at very low current, the behavior of the device transitions from a square-law characteristic to an exponential characteristic that is much like that of the BJT. The basic SPICE model does not handle this behavior. It has I_d go to zero at the threshold voltage. The EKV model [7] is a more sophisticated model that accurately accounts for subthreshold behavior in power MOSFETs. The EKV model can be used to replace the DC core model in a subcircuit-based power MOSFET model. It does not contain the built-in body diode and the nonlinear gate-drain capacitance modeling. The EKV model is assigned as SPICE Level 12 in LTspice. A simple version of an EKV core model for the IRFP240 is shown below.

.MODEL MOSFET nmos level=12

+VTO=4.1 PHI=0.7 GAMMA=5.0

+KP=6.0 LAMBDA=100

The parameters in the second line establish the behavior in the weak inversion region where drain current is small. These parameters should be adjusted first. The parameters VTO, GAMMA, and PHI are adjusted to optimize the fit of I_d versus V_{gs} at low current. VTO is the threshold voltage parameter. Transconductance in the subthreshold region is controlled by drain current via an exponential that is dependent on GAMMA and PHI. I have found that GAMMA can be set to 5.0 for power MOSFETs without compromising the achievable fit to device data. Throughout the remainder of this section GAMMA is assumed to be 5.0.

The parameters KP and LAMBDA in the third line are associated with the DC characteristics in the strong-inversion region. In combination with VTO, they are analogous to the parameters in the conventional Level 1 square-law model. However, it is important to recognize that the value of KP may be quite different in the EKV model compared to its value in the Level 1 model for the same transistor. These parameters should be adjusted next. KP is adjusted to fit the I_d-versus-V_{gs} curve at moderate current well above the threshold voltage but at current levels that are not significantly limited by device resistances (primarily source resistance). KP is the transconductance parameter and has units of A/V^2.

Shown below is a corresponding subcircuit model for the IRFP240.

∗Drain Gate Source

.SUBCKT IRFP240 1 2 3

M1 10 20 30 MOSFET L=100u W=500u

RD 1 10 0.05

RG 2 20 3

RS 3 30 0.005

```
CGS 20 30 1000p

DGD 2 1 GDDIODE

DDS 3 1 DSDIODE

*

.MODEL MOSFET nmos level=12

+VTO=4.1 PHI=0.7  GAMMA=5.0

+KP=6.0 LAMBDA=100

+CGSO=10p CGDO=10p IS=1e-32

*

.MODEL DGDIODE D

+IS=1E-32 N=100 RS=10

+CJO=1200p M=0.5 VJ=0.5

*

.MODEL DSDIODE D

+IS=4E-12 N=1.0 RS=0.02

+CJO=1400p M=0.9 VJ=4.4

*

.ENDS
```

It is very important to recognize that KP in the EKV model can be numerically quite different from KP in the SPICE Level 1 model for the same transistor. KP in the EKV model will generally need to be larger to obtain the same I_d for a transistor with the same W/L ratio. KP in the EKV model will often be about 3–5 times larger than KP in the SPICE Level 1 model for the same transistor. The required value of KP in the EKV model is strongly influenced by PHI.

I have chosen to use the W/L ratio to bring KP in the EKV model into line with KP in the Level 1 model. The values $L = 100\mu$ and $W = 500\mu$ in the first line above create a W/L ratio of 5. This ratio is by default unity in the Level 1 model and was not shown earlier. Specific values for L and W should always be used in the EKV model for power MOSFETs, with L in the range of 100μ being a good number. Undesired behavior not relevant to power MOSFETs will occur, for example, if instead $L = 1\mu$ and $W = 5\mu$ are used. The value of W/L required to bring KP into conformance with the Level 1 value of KP is largely dependent on the choice of PHI and the resulting subthreshold slope created. I have found empirically that the desired value of W/L will be very roughly inversely proportional to 40 mS/mA divided by subthreshold slope in mS/mA.

Figure 20.15 shows how the choice of PHI affects subthreshold slope and required W/L ratio to achieve the same I_d in the EKV model as in the Level 1 model with the same value of KP. If subthreshold slope is known, required PHI can be found from the left-hand Y axis. Once PHI is determined, the recommended starting value of W/L can be found from the right-hand Y axis. We note that a subthreshold slope of 10 mS/mA corresponds to V_{ds} changing with I_d at a rate of 240 mV/decade. This is analogous to the familiar rule for BJTs where V_{be} changes by 60 mV/decade of increase in I_c. The relationships illustrated in Figure 20.14 are approximate, and are valid only for GAMMA = 5.0.
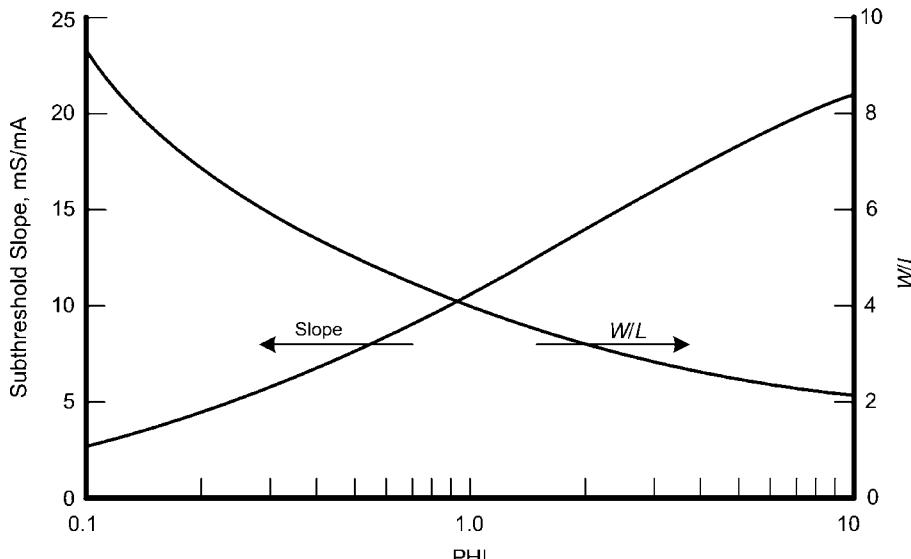
FIGURE 20.15   Subthreshold slope and desired value of *W/L* as a function of PHI.

The parameter LAMBDA is responsible for controlling I_d behavior as a function of V_{ds}. Adjust LAMBDA for the best fit to the I_d-versus-V_{ds} data (slope) at medium current like 2 A. As an example, the change in I_d from $V_{ds} = 10$ V to $V_{ds} = 50$ V at a nominal drain current of 2 A is about 100 mA for an IRFP240. This is the change that should be matched by adjusting LAMBDA when the model is simulated. While LAMBDA in the EKV model acts in the same way as LAMBDA in the Level 1 model, the numerical value of LAMBDA required for the same transistor behavior is quite different in the EKV model. While a value of LAMBDA of 0.003 is about right for the IRFP240 in the Level 1 model, the required value of LAMBDA is about 100 for the same device in the EKV model.

Those familiar with the EKV model know that there are many more parameters that have not been mentioned here. I have found that these can be left out of the model and remain at their default values while still allowing a very good model fit for power MOSFETs. In particular, THETA and *UCRIT* are left at their defaults in the model creation procedures here.

Figure 20.16 shows plots of log I_d versus V_{gs} for the conventional SPICE model and the EKV model. Notice the transition region around 100 mA where the EKV model correctly shows much more drain current than the standard SPICE model. The incorrect behavior of the simple square-law model will cause a large discontinuity in *gm* in the region of low current where V_{gs} will be close to V_T.

Subthreshold MOSFET Measurements

Few MOSFET data sheets show subthreshold I_d-versus-V_{gs} data, so the proper creation of an EKV model should include measurements of the subthreshold behavior. There are two pieces of data that are important. The first is the subthreshold slope in mS/mV. Alternatively this can be measured in millivolts per decade and converted to mS/mV by dividing 2400 by the former number. A relationship of 240 mV/decade thus corresponds
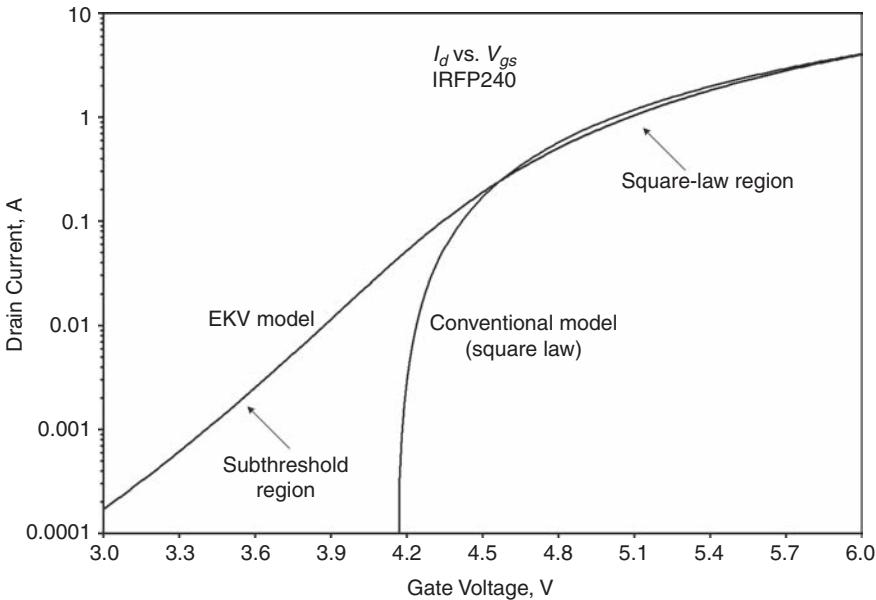
FIGURE 20.16   MOSFET I_d versus V_{gs} for conventional and EKV SPICE models.

to 10 mS/mA. The second piece of data is the amplitude of I_{ds} at a value of V_{gs} that is well into the subthreshold region. Put simply, slope and amplitude describe the subthreshold region. The necessary data can be obtained for a typical power MOSFET by measuring V_{gs} for values of I_d from 10 μA to 1 mA, that is, over two decades of I_d in the subthreshold region.

Model Creation Procedure

The procedure below summarizes the approach that can be taken to arrive at the parameters for the DC EKV power MOSFET model.

- Review the I_d versus V_{gs} datasheet curve.
- Estimate VTO as V_{gs} at I_d of about 50 mA.
- Set KP to a reasonable starting value, like 3.0.
- Set LAMBDA to a reasonable starting value, like 100.
- Measure subthreshold slope (typically 5–20 mS/mA).
- Set PHI based on Figure 20.15 (typically 0.5–3.0).
- Set W/L from Figure 20.15 by setting L=100μ and W as needed.
- W will typically be 200μ to 600μ.
- Set KP to Level 1 SPICE model value if available.
- Simulate I_d versus V_{gs} of the model at the same V_{ds} as used for the datasheet curves.
- Adjust KP to get desired V_{gs} at 4 A.

- Juggle VTO and KP to get desired curve shape.
- If V_{gs} for $I_d = 2$ A is low, increase VTO and revise KP to obtain correct V_{gs} at 4 A.
- Simulate I_d versus V_{ds} at 2 A.
- Adjust LAMBDA to obtain the same slope as found on the device output curves.
- Iterate.

I have found that the required value of LAMBDA in the EKV model (as created here) is much larger for a given target I_d-versus-V_{ds} slope (output conductance) than the corresponding value of LAMBDA for the Level 1 model.

Applicability

The EKV model is needed for reasonably accurate simulation of crossover distortion effects because it properly handles the subthreshold and transition region where crossover distortion issues are most prominent. The accuracy of the model in the subthreshold region is not critical; what is most important is that the subthreshold conduction is there, so that there is no discontinuity in *gm*.

20.8   Hybrid VDMOS-EKV Model

An alternative subcircuit power MOSFET model can be envisioned that combines the strong points of both the VDMOS and EKV models. In essence, the DC behavior is modeled with a SPICE EKV model while the body diode and nonlinear capacitances are modeled with a VDMOS model. Two MOSFETs, one modeled with the EKV model and another modeled with the VDMOS model, are connected in parallel in a subcircuit. The capacitances in the EKV model are set to zero, while the transconductance in the VDMOS model is set to zero. The hybrid model is more complex and takes longer to run, but this is not a problem for amplifier circuits because so few of the devices are used. Shown below is a subcircuit for a hybrid VDMOS-EKV model.

```
∗Drain Gate Source
∗
.SUBCKT IRFP244 1 2 3
M1 10 20 30 MOSFET1
M2 10 20 30 MOSFET2 L=100u W=500u
RD 1 10 0.05
RG 2 20 3
RS 3 30 0.005
∗
.MODEL MOSFET1 VDMOS NCHAN
+KP=0.0 VTO=4.2 LAMBDA=0.0
+CGDMAX=2.3e-9 CGDMIN=6.3e-12 a=0.34
+CGS=1340p CJO=1300p M=0.68 VJ=2.5
```

+RS=0 RD=0 RDS=1e7 IS=4.0e-6 N=2.4

*

.MODEL MOSFET2 NMOS LEVEL=12

+VTO=4.4 GAMMA=5.0 PHI=0.7

+KP=0.11 LAMBDA=100

*

.ENDS

Notice that the drain, gate, and source resistors are handled externally to the paralleled MOSFET models. This is not a perfect solution, but it is more important that these resistances be used to get the DC behavior correct, so they must be in the path of the EKV part of the model. Alternatively, these resistances could be included inside the EKV model.

20.9   Lateral Power MOSFETs

The discussion on power MOSFET modeling thus far has focused on vertical double-diffused power MOSFETs. The lateral power MOSFET has many of the same electrical characteristics and is modeled in the same way, but there are some distinctions worth noting. The lateral power MOSFET acts somewhat more like a conventional small-signal MOSFET that would be found in an IC.

Most importantly, C_{gd} for lateral MOSFETs is much smaller and exhibits relatively little nonlinearity. The 2SK1058/2SJ162 complementary pair of lateral MOSFETs typically have C_{gd} on the order of 50 pF or less [8]. Gate-source capacitance is generally between 500 pF and 1000 pF. The lateral MOSFET includes a body diode and its capacitance is typically on the order of 400 pF.

The lateral MOSFET can be modeled with the subcircuit model described in Section 20.5 with a simple fixed capacitor for C_{gd} as shown below.

*Drain Gate Source

.SUBCKT 2SK1058 1 2 3

M1 10 20 30 MOSFET

RD 1 10 0.5

RG 2 20 75

RS 3 30 0.5

CGS 20 30 400p

DDS 3 1 DSDIODE

*

.MODEL MOSFET NMOS LEVEL=1

+KP=1.5 VTO=0.5 LAMBDA=0.1

+CGSO=0 CGDO=50E-12 IS=1e-32

*

```
    .MODEL DSDIODE D
    +IS=2E-12 N=50 RS=0.05
    +CJO=1000E-12 M=0.9 VJ=0.3
    *
    .ENDS
```

The lateral power MOSFET devices have internal back-to-back Zener diodes from gate to source to limit V_{gs} to safe values. These diodes are not modeled above and usually need not be modeled for amplifier simulations where very large gate-source voltages are not applied. Typical breakdown voltage for these diodes is 15 V.

Like any MOSFET, the lateral MOSFET exhibits subthreshold conduction. However, weak inversion appears to play a smaller role in the normal region of operation of lateral MOSFETs in power amplifiers, so there appears to be less need to resort to something like the EKV model.

Lateral MOSFETs suffer from a fairly large value of internal gate resistance, on the order of 75 Ω as shown in the example model above. This creates a pole in the AC transconductance of the device. For $C_{gs} = 400$ pF, this pole is at 5.3 MHz. Unfortunately, it is customary to employ gate stopper resistors of 200–500 Ω with lateral MOSFETs for HF stability. This will bring the *gm* pole down to 1.4 MHz or below.

20.10   Installing Models

Place the subcircuit model file in the simulation directory and give it a *.mod* file extension. Take a symbol for the transistor and edit its attributes to include the name of the model file.

- Open the symbol.
- Go to Edit>Attributes>Edit Attributes.
- Enter the transistor name for *Value.*
- Enter the name of the model file on the *ModelFile* line.

To place a transistor modeled with a subcircuit on the schematic, click on the *Component* tab on the toolbar. A directory path to the library will appear in the top window. Click the down arrow to select another option. Select the simulation directory path. A list of available models in the local simulation directory will appear. Click on the desired device name. The symbol will come up in the large window. Hit *OK* and place the device.

References

1. Sedra, Adele, and Smith, Kenneth, *Microelectronic Circuits,* 6th ed. New York, Oxford University Press, 2010.
2. Roberts, G. W., and Sedra, A. S., *SPICE,* 2d ed., New York, Oxford University Press, 1997.
3. Frederiksen, T. M., *Intuitive IC Electronics: A Sophisticated Primer for Engineers and Technicians,* New York, McGraw-Hill, 1982.

4. Gray, P. R. and Meyer, R.G., *Analysis and Design of Analog Integrated Circuits,* 2d ed., New York, Wiley, 1984.
5. Kirk, C. T., "A Theory of Transistor Cut-off Frequency, f_T, Falloff at High Current Density," *IEEE Transactions on Electron Devices,* ED-9, March 1964.
6. LTspice User's Manual; available at www.linear.com.
7. Enz, C. C., and Vittoz, E. A, *Charge-based MOS Transistor Modeling,* New York, Wiley, 2006.
8. Renesas Tehnology 2SK1058 and 2SJ162 datasheets, www.renesas.com.

This page intentionally left blank

Audio Instrumentation

Designing and building an audio amplifier without test instrumentation is like flying blind.

For the better part of my many years in audio, test equipment was a limiting factor. It was expensive. I had access to great test equipment by Tektronix and HP at work, but not at home. Often I relied on kits from Heathkit and EICO, among others. Forget about a decent THD analyzer, much less a spectrum analyzer! As a result, I resorted to designing and building my own test equipment. That was a very satisfying endeavor, and even today in some situations it is really the way to go, especially if you need a custom or specialized function.

Fortunately, much has changed with the introduction of the modern PC. Although there is a lot of test equipment that is PC-based that uses a proprietary card that goes into a PC slot, there is more software-based electronic test equipment that is based on the ubiquitous sound card. Measurement capabilities are limited only by the performance of the sound card. That, coupled with the availability of very high-performance sound cards with sample rates as high as 192 kHz and word sizes as large as 24 bits, and you have the makings for a very valuable test bench at reasonable cost. Much of the software is available as shareware or freeware.

The industry evolution from analog test equipment to digital test equipment has put a lot of very good analog test equipment on the surplus block, including HP and Tektronix equipment that was once far out of the reach of the individual designer. Some of the traditional hardware-based instrumentation can be obtained at affordable prices from surplus outlets and on Ebay. In some cases the equipment may need repair, but in many cases the service manuals are available from various sources.

In this chapter we will describe audio testing instruments and methodology, both traditional and PC-based.

21.1   Basic Audio Test Instruments

The audio oscillator, the AC voltmeter and the oscilloscope are the most fundamental building blocks for testing and measuring power amplifiers.

Audio Oscillator

Choose an audio oscillator that will go as low as 10 Hz and as high as 1 MHz or more. It should have a constant output with frequency and preferably a decade attenuator to provide output levels over a wide range. The oscillator will be used for stability testing as well as frequency response measurements, thus the need for the high-frequency

capability. It should also have a square-wave output unless you also have a function generator. While it is nice to have a low-distortion oscillator, in most cases the low-distortion signal source will come from the THD analyzer if one is available. Good choices include the HP 651, 652, and 654 test oscillators. HP 200 series oscillators are also very good, but do not include decade attenuators. The Tektronix SG502 and SG505 are also excellent choices. Function generators are readily available, and you can get by with one as the sine-wave and square-wave test source if resources are very limited.

AC Voltmeter

A good AC voltmeter is a must. It should be very flat over the audio band and should go down to 1 mV full scale. For amplifier bandwidth and stability testing, it should have a bandwidth extending to at least 1 MHz. It need not be *true RMS* responding, but that feature helps provide more accuracy in noise and distortion measurements. The meters in the HP400 series are widely available on the surplus market and are an excellent choice. One of my favorites is the HP 400EL. It is flat to 10 MHz and has a scale that is linear in dB. The Tektronix DM502 is also a good candidate. The HP3400A is a very good *true RMS* meter.

Oscilloscope

Used analog oscilloscopes are widely available at low cost. The unit should have a bandwidth of at least 100 MHz to allow the viewing of parasitic oscillations. Tektronix portable oscilloscopes are probably the best choice and most widely available.

21.2   Dummy Loads

It is very important that amplifiers be properly loaded when they are tested. In fact, many vacuum tube amplifiers can be damaged if they are operated without a load. The load can be as simple as an 8-Ω power resistor for low-power investigations. Metal-cased 50-W power resistors mounted on heat sinks can support high-power measurements. In some cases a fan-cooled heat sink may be necessary.

Choose Load Resistors Wisely

Some wire-wound power resistors are poor performers and will induce distortion into the measurement. Applying a nonlinear load to an amplifier with finite output impedance will cause distortion. This kind of load resistor distortion may be caused by the way in which the wire-wound resistive element is affixed to the solder terminals. This behavior can be evaluated by placing a known-good small resistor in the return leg of the resistor under test. The distortion across the small resistor is then measured. The distortion measured in this way should be no larger than the distortion measured at the output of the amplifier under the same conditions.

Inductive versus Noninductive

It is usually recommended that dummy load resistors be noninductive. However, this is not absolutely necessary in most cases. The inductance of even fairly large wire-wound power resistors is typically less than 10 μH. For such an 8-Ω load resistor, the inductive reactance reaches 8 Ω at about 100 kHz. Non-inductive load resistors should be used for high-frequency stability testing.

A really high-quality noninductive load resistor can be made from a large array of series-parallel connected 3-W metal film resistors. An array of sixty-four 512-Ω resistors can be configured to provide a 192-W load. A second array can be connected in parallel to provide a 4-Ω load that can dissipate 384 W.

Power Dissipation and Cooling

The most straightforward approach to a high-power dummy load is to use several 50-W chassis-mountable 8-Ω power resistors and mount them on a large heat sink. One can also fan-cool the heat sink for the higher-power measurements if it is not sufficiently large. Fan cooling also works well if the dummy load is to be mounted in a ventilated box. A more sophisticated approach would be to monitor the temperature of the heat sink and energize the fan when the temperature exceeds 50 °C.

Connecting to the Dummy Load

Where high currents and low impedances are involved, it is wise to make Kelvin-like connections to the load. This can be done right at the output of the amplifier. This reduces the chance of high current flowing through load connectors introducing distortion. It can also be beneficial to pick off the amplifier output signal differentially to avoid forming ground loops. This makes the cable to the distortion analyzer less vulnerable to pickup of noise and rectifier spikes that may be in the amplifier power cord. Is it wise to place a 50-Ω resistor in series with the hot amplifier output terminal to avoid damage to the amplifier in the event of an accidental short circuit in the connection with the test equipment.

21.3   Simulated Loudspeaker Loads

More sophisticated amplifier testing can be carried out with simulated loudspeaker loads. This is done in some amplifier reviews to show the influence of load impedance on amplifier frequency response. This reveals behavior due to amplifier output impedance and damping factor. The results can be a real eye-opener and can sometimes explain differences heard among amplifiers that otherwise test the same. The frequency-dependent impedance of a loudspeaker load can also influence amplifier distortion. For small-signal frequency response tests, actual loudspeakers can be used as the load. The disadvantage here is that it is not a standardized load.

Figure 21.1 is a schematic for a simulated loudspeaker load. Even though it is not a real loudspeaker, power levels must be kept to reasonable levels unless the load is constructed from high-power components. The 6.4-Ω resistor represents the DC voice coil
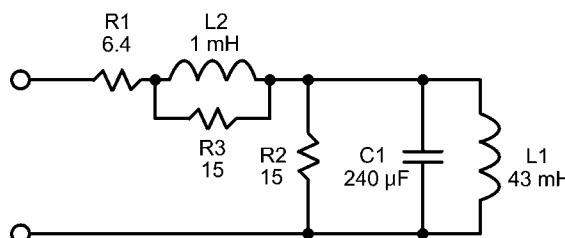
FIGURE 21.1   A passive simulated loudspeaker load.

resistance while the 280-µF capacitance and 43-mH inductance model the mechanical resonance. The 15-Ω resistors model the losses in the speaker and largely define the maximum impedance at resonance. The 1-mH inductor corresponds to the voice coil inductance. This model represents a single driver in a closed box with a resonance at 50 Hz. More complex models can easily be constructed to represent multiway loudspeaker systems with crossovers.

If the model of Figure 21.1 is implemented, it is important that the capacitor not be implemented as an electrolytic, but rather as a large Mylar or polypropylene metal film capacitor. The inductor must be rated for high current so that its core does not saturate under the testing power levels. One or more inductors used for high-power woofer crossovers are usually suitable. The inductor used in the load circuit here need not have very low resistance, as some resistance in L1 can be absorbed as a reduction in the value of R1.

For the more adventurous an active loudspeaker load can be built using a second power amplifier to back-drive the amplifier under test (AUT) through a load resistance equal to the DC voice coil resistance of the load to be simulated [1]. A second signal from the signal source is sent to the back-drive amplifier through an appropriate active filter to create at its output a signal representing the back-emf of the simulated loud-speaker. An alternative arrangement is to directly synthesize the desired impedance characteristic with the back-drive amplifier using appropriate feedback around it. The back-drive amplifier must have adequate power handling and SOA capability for this approach to be safe and reliable.

Protection Circuit Testing

Protection circuits like *V-I* limiters are more likely to act in the presence of a reactive load. For this reason, a simulated loudspeaker load can be used to test them. The use of such loads can get the bench testing a step closer to the real world where some amplifier anomalies may show up.

21.4   THD Analyzer

The most common distortion measurement is of total harmonic distortion. In this test a low-distortion sine wave is applied to the amplifier and the output is fed through a deep notch filter that eliminates the fundamental signal. Everything that remains is considered distortion. What remains will also include amplifier noise, so the test is actually referred to as *THD+N*. For detailed information on how THD analyzers work, see Ref. 2.

Figure 21.2 shows a block diagram of a THD analyzer. The output signal from the power amplifier is scaled down by an input attenuator and sent through a voltage-controlled notch filter. This filter removes the fundamental without adding significant attenuation at any of the harmonic frequencies. The residual contains the distortion and noise from the amplifier. It also contains a very small amount of the fundamental that has not been removed if the notch is not perfectly tuned for frequency and depth. This signal is compared to the input signal to create DC control signals that tune the notch filter for best rejection. This is referred to as the *autonull function.*

The input signal is also sent to an AGC circuit that includes a *voltage-controlled amplifier* (VCA). The AGC circuit adjusts the control voltage of the VCA to make the output signal amplitude equal to a reference level. A second identical VCA is put in the
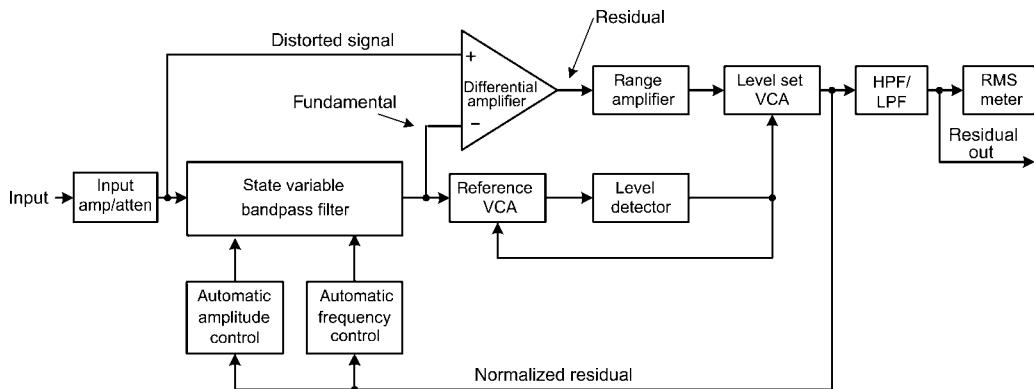
FIGURE 21.2   Block diagram of a typical THD analyzer.

path of the residual output from the notch filter. The second VCA is controlled by the same voltage as that for the first VCA. As a result, the amplitude of the residual is automatically scaled so that the output is representative of a percentage of the fundamental. The residual output is then low-pass filtered to establish the measurement bandwidth and limit noise. The measurement bandwidth is usually between 80 kHz and 200 kHz. Most THD analyzers include the low-distortion oscillator. Its frequency setting is synchronized with that of the analyzer notch filter for convenience.

Interpreting Results

The THD analyzer produces a single-number reading that is useful but certainly not complete in characterizing the distortion from the test. Virtually all THD analyzers provide the residual as a signal output. It is very common to view the residual in the time domain on an oscilloscope. This is useful for viewing crossover distortion. Sometimes the amplitude and wave shape can be seen to change with time as the output transistor temperature changes. Mains frequency-related distortion and noise are viewed by synchronizing the scope to the line frequency. The ability to view the distortion residual in the time domain usually can't be implemented by PC-based solutions.

Spectral Analysis

Much more frequency-domain information can be gathered by viewing the distortion residual on a *spectrum analyzer*. Although one could simply use a spectrum analyzer to directly view the amplifier output, using the THD analyzer to first notch out the fundamental greatly improves the useable dynamic range of the spectrum analyzer. The dynamic range of a good analog spectrum analyzer like the HP 3580A is only about 85 dB.

The spectrum analyzer not only allows one to view the individual harmonics in the spectrum, but also largely eliminates the noise. This is especially valuable when looking for crossover distortion at low power levels where the distortion may be buried in the noise. The typical rising curve of THD+N at low power levels can be due to either noise or crossover distortion.

Obtaining a THD Analyzer

THD analyzers are indispensable, yet expensive. The analyzers listed below can sometimes be obtained at reasonable prices. A very good THD analyzer has a THD+N *measurement floor* of less than 0.001% at 20 kHz with a 200-kHz measurement bandwidth. Some of these analyzers fall a bit short of that performance, but are nevertheless very valuable for amplifier evaluation.

- Audio Precision AP1
- Tek AA501/SG505
- HP 334A, 339A
- Amber 5500, 3501
- Sound Technology 1700, 1710

21.5   PC-Based Instruments

Good audio test equipment used to be expensive and often out of the reach of the average enthusiast. The PC has largely changed that, with the combination of high-performance sound cards and appropriate software. While PC-based instrumentation is not a complete substitute for traditional laboratory test equipment, it can provide many very important functions with surprisingly good performance and sophisticated functionality.

PC-based solutions include digital storage oscilloscopes (DSOs), signal generators, AC voltmeters, and spectrum analyzers. Some include THD analyzer functions. Much of the software is freeware or shareware. The level of performance that can be obtained depends mainly on the performance of the sound card. Useful functionality can even be had from the computer's standard onboard sound card.

Sound Card Software

Given a good sound card to get the input and output signals from the analog domain to the digital domain, the computing power of the PC can be used to carry out sophisticated analysis. The PC also provides a very user-friendly virtual front panel.

Most of the available software packages support the basic capabilities needed, but ease of use and quality of documentation vary widely. Many packages support sound card sampling rates up to 192 kHz and data widths of 24 bits (192/24), but some do not. Compatibility with the many different sound cards available also varies. Listed below is a sample of the numerous test/measurement software packages available.

- ARTA—www.fesb.hr/~mateljan/arta
- Audio Tester—www.audiotester.de
- Visual Analyzer—www.sillanumsoft.org
- RMAA—RightMark Audio Analyzer—http://audio.rightmark.org
- SpectraPlus—www.spectraplus.com
- Virtins Multi-Instrument 3.1—www.virtins.com

Sound Cards

Sound cards of very high quality can be had for less than $200. I recommend choosing one with 192/24 ADC to maximize useable frequency range and dynamic range. Excellent sound cards are available in both internal and external USB-based formats. Below is a brief list of some suitable sound cards.

- ESI Juli@—www.esi-audio.com
- Sound Blaster X-Fi—www.creative.com
- EMU 1212, 0202, 0404—www.emu.com
- Lynx L2, L22—www.lynxstudio.com
- Asus Xonar Essence—www.asus.com
- M-Audio Audiophile 192—www.m-audio.com

PC-Based Oscilloscopes

Although several of the soundcard-based PC instruments above support an oscillo-scope function, the bandwidth is strictly limited to the audio band (or just slightly beyond). There are PC-based Digital Storage Oscilloscopes (DSOs) designed as instruments employing special-purpose hardware that supports sample rates at 10 MHz to beyond 100 MHz. These solutions provide the higher bandwidth necessary for general-purpose oscilloscope use. They are also much more flexible in regard to input signal levels they can handle and often include probes.

The wideband DSOs depend on a special card that plugs into a slot in the computer or is attached via USB. Many of these instruments have data paths that are only 8 bits wide, but that is entirely satisfactory for the oscilloscope function. The software that comes with these devices is often capable of many other functions, such as FFT spectrum analysis. Three examples of these devices are listed below.

- ScopeCard—www.alazartech.com
- PicoScope—www.picotech.com
- Virtins (USB)—www.virtins.com

21.6   Purpose-Built Test Gear

Off-the-shelf test equipment often does not exist for the specialized needs of audio measurements. To fill this gap, many purpose-built *gadgets* can be very helpful. Many can be constructed with little difficulty. The dummy loads described above fall into this category, but many other functions are important. A very good example is an interface box for the sound card in a PC-based test setup.

Sound Card Interface Boxes

Sound cards are not designed for use as test instruments. They are designed for line-level sound processing. As such, it is important for both the safety and utility of the card to have an interface device between it and the equipment to be measured. Figure 21.3 is a block diagram of such an interface box.
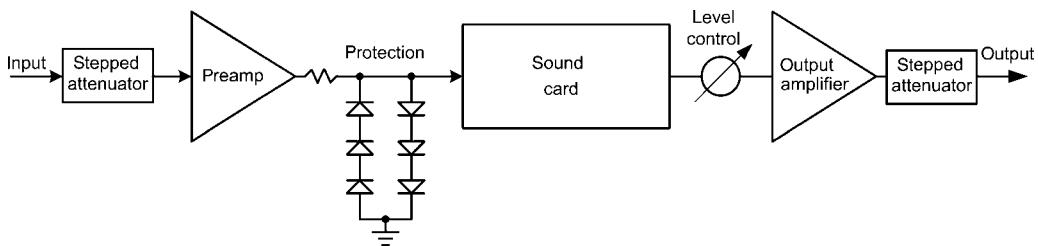
FIGURE 21.3   A sound card interface box.

The most important function is input attenuation and protection. The output level of power amplifiers can be well above the maximum input that can be handled by the sound card and can easily damage the device. For this reason a stepped attenuator followed by protection diodes should be implemented in the input interface. It is also desirable to implement a preamplifier in this part of the interface, so that very small signals can be analyzed without sacrificing available dynamic range of the sound card. The combination of attenuation and preamplification can enable the use of the sound card near its "sweet spot" input level. Differential inputs are another example of desirable functionality on this side of the interface. The 1200 series of balanced input line receivers made by THAT Corporation are a convenient high-performance solution [3]. The box might also incorporate A-weighting input filters to support SNR measurements if that function is not available in the software.

The output of the sound card should be buffered and amplified or attenuated. The buffering and amplification protects the sound card outputs and makes available signal levels up to 10V RMS. The attenuator allows signals in the millivolt range to be produced without sacrificing sound card dynamic range. A solid-state floating differential output stage would be convenient for driving differential amplifier inputs and for breaking ground loops. The model 1646 balanced driver IC made by THAT Corporation is a convenient high-performance solution [4].

The interface box might also take advantage of the two-channel capability of stereo soundcards, so that two-tone test signals can be generated, such as 19+20 kHz CCIF and 60+7000 Hz SMPTE IM. For this application, the box should include a very high-quality output summing operational amplifier. In such an arrangement the IM distortion of the composite test signal will not be dependent on the sound card electronics.

All of these functions can be easily implemented at low cost with high-quality operational amplifiers. The National LM4562 dual operational amplifier is an excellent choice [5].

The Distortion Magnifier

The *Distortion Magnifier* (DM) [6] increases the sensitivity of a THD analyzer or spectrum analyzer by subtracting most of the original test signal from the output of the *amplifier under test* (AUT) before it is applied to the input of the analyzer. If 90% of the test signal is subtracted, the distortion percentage in the resulting signal will be magnified by a factor of 10.

A block diagram of the DM is shown in Figure 21.4. The DM subtracts a version of the input signal from a scaled version of the signal from the AUT to form a deep (>60 dB) null at the fundamental. A controlled amount of the source signal is then added back to
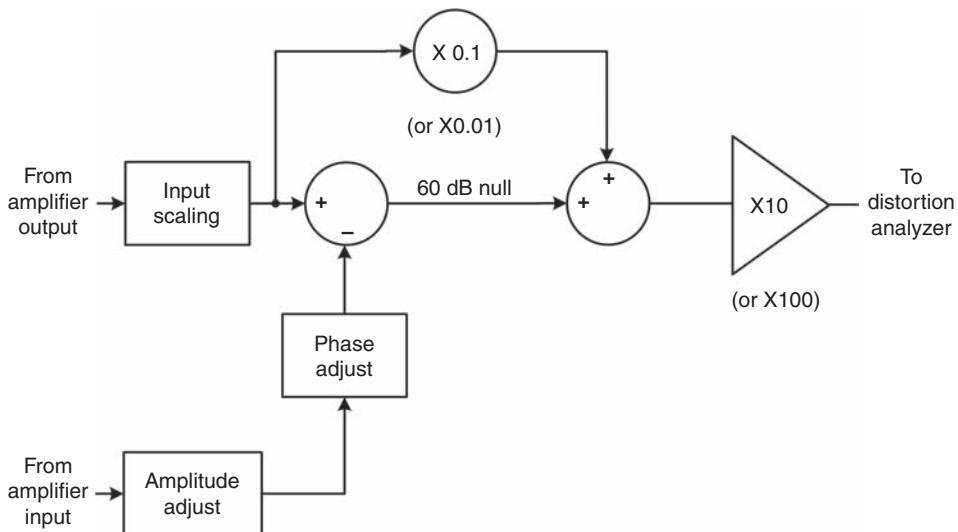
Figure 21.4   The Distortion Magnifier.

achieve a known amount of distortion magnification, either 20 dB or 40 dB. This also provides fundamental energy needed by the distortion analyzer to lock onto.

The DM magnifies the distortion of the AUT without magnifying the distortion (and noise) of the oscillator. Consider a THD analyzer whose lowest range is 0.003% FS. If the DM is placed in front of it with 40-dB magnification, that becomes 0.00003% FS. Of course, this result is generally noise-limited (often by the noise of the AUT). The distortion floor is also limited by the distortion of the op amps used to implement the DM. The noise limitation can be largely eliminated if the residual output of the THD analyzer is fed into a spectrum analyzer.

The DM includes coarse and fine amplitude and phase adjustments to optimize the null. The phase adjustment is simply a first-order LPF that constitutes a very simplified model of the AUT. Amplitude and phase must be tweaked a bit if the fundamental frequency is changed. Because of the simple model, there will be some amplitude and phase error at the higher harmonic frequencies that will detract a bit from the cancellation process, allowing a bit of oscillator noise and distortion to come through. A more complex model of the DUT high-frequency response can be used, but I have not found that necessary for my use. Similarly, the DM can incorporate low-frequency phase matching for low-frequency THD measurements on AC-coupled power amplifiers, but that has not been implemented. More detail on the Distortion Magnifier can be found in Ref. 6.

The DM is also useful in extending the dynamic range of analog spectrum analyzers and PC instruments using sound cards. With the DM set to 40 dB of magnification, the HP3580A, with its 85-dB dynamic range, can "see" down to about –125 dB.

Balanced Interfaces

Balanced input and output interfaces make low-noise, low-distortion measurements easier and help break ground loops among instrumentation and devices under test. Even if the target signals are single-ended, as often is the case with power amplifiers,

the use of balanced interfaces can help with sensitive measurements. Test signals from the AUT are fed to a differential amplifier [3]. Similarly, balanced versions of the test signals can be delivered to the AUT by implementing differential output buffers. The simplest balanced output buffer merely provides two polarities of the test signal, each referenced to ground. This does not help break ground loops. A more sophisticated arrangement implements an active floating differential output buffer—the electronic equivalent of an output transformer (mentioned above in connection with the sound card interface box) [4].

IM Test Signal Combiner

This device is simply a very low-distortion mixer with two inputs. It is used to generate the test signals for the SMPTE IM (60 + 7000 Hz, 4:1) CCIF IM (19 + 20 kHz, 1:1) and DIM (3.18 kHz square wave & 15 kHz, 4:1) distortion tests. The outputs of two oscillators are combined in the mixer by a very low-distortion op amp, so that IM products in the resulting test signal depend only on the low-distortion performance of the mixer and not the individual generators. If the combiner is to be used for DIM tests, it should include selectable first-order 30-kHz and 100-kHz low-pass filters in the output path.

Synchronous Tone-Burst Generator

Tone-burst testing can be valuable for power amplifiers when performance at very high power levels for brief intervals is needed. This obviates concerns about power dissipation and overheating. Such a test is used to measure short-term peak power output before the power rails have time to sag. This is the dynamic headroom test. Tone-burst testing can also be used to check peak current output available into extremely low load impedances. By controlling the number of cycles in the tone burst, the reaction time of protection circuits can also be evaluated.

Figure 21.5 shows a block diagram of a synchronous tone-burst generator. The generator enables and disables an externally supplied tone at zero crossings of the tone. The tone can be switched with a CMOS transmission gate that is buffered on both sides. The output circuit can optionally include an amplitude control and switched attenuator.
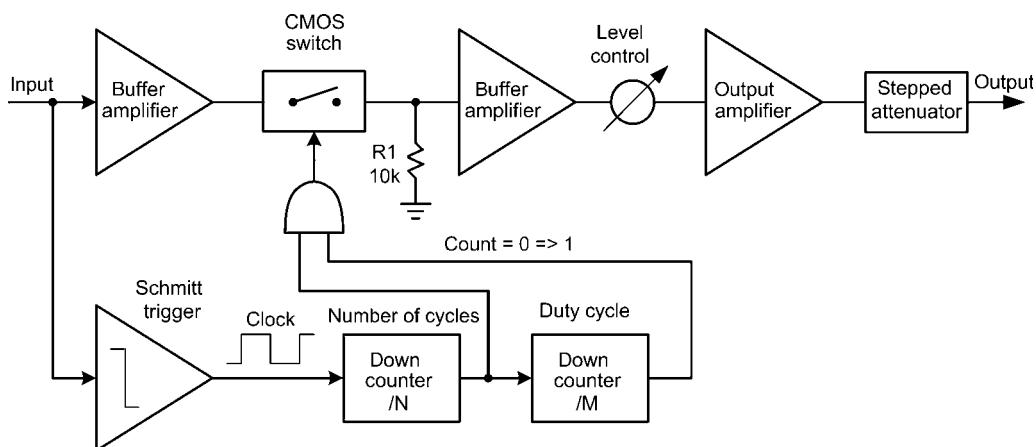
FIGURE 21.5   A synchronous tone-burst generator.

The control path begins with a squaring circuit that converts the incoming tone to a square wave that is suitable for clocking CMOS logic. Switching of the transmission gate is controlled by CMOS logic circuits. These operate synchronously with the clock. Counters are used to form the enable signal for the CMOS switch. The number of cycles N in the burst is controlled with one counter and the repetition rate M of the burst is controlled with a second counter. For example, if $N = 2$ and $M = 5$, a two-cycle burst will be generated once every ten cycles of the incoming tone. This corresponds to a 20% duty cycle ($1/M$). A sync signal is provided at the output of the tone-burst generator. This is just a replica of the digital switching signal used to control the CMOS switch.

Signal-to-Noise Measurement Preamp with A Weighting

This device enables accurate SNR measurements to be made if another piece of test equipment with this capability is not available. It is a high-gain preamp with controlled bandwidth and optional A-weighted frequency shaping. The unit should have a gain of 100 or 1000 in order to provide a sensitivity of 10 µV full scale when used with an external AC voltmeter (preferably true RMS, like the HP 3400A). The preamp should incorporate input protection. A power amplifier with a very good input-referred noise level of 5 nV/√Hz and a voltage gain of 20 will produce about 14 µV RMS at its output when the measurement bandwidth is limited to 20 kHz. A first-order LPF at 12.7 kHz has a noise bandwidth of 20 kHz. The amplifier will produce a smaller noise reading if the measurement is A-weighted. The equivalent noise bandwidth of the A-weighting function is 13.5 kHz.

Figure 21.6 is a schematic of an A-weighting filter that can be used for SNR measurements. The filter is an entirely passive R-C design that just needs to be buffered at its input and output and which needs a gain of 1.64 in one of the buffers to make up for loss and provide the +1.2 dB of gain at the 2.5-kHz pass-band peak.

Powering Purpose-Built Test Equipment

Most purpose-built audio test equipment requires very little power at typically ±15 V. Power can be supplied from a wall transformer with an AC output (14–20 V, at least 10 VA). Note that the lightly loaded output of a class B wall transformer is usually quite a bit more than the transformer's rated voltage. The power supply is illustrated in Figure 21.7. It can be housed in a separate project box containing the
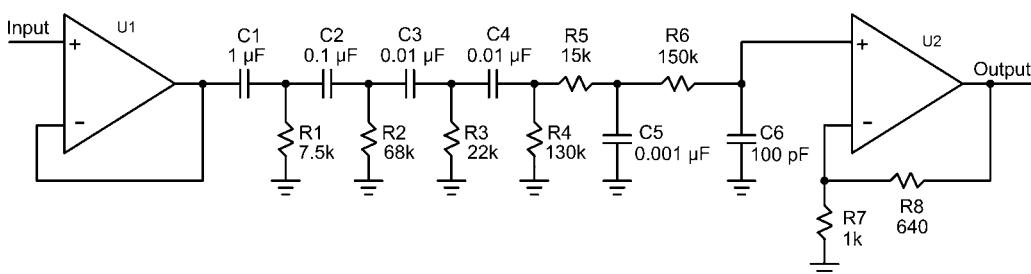
FIGURE 21.6 A-weighting filter.
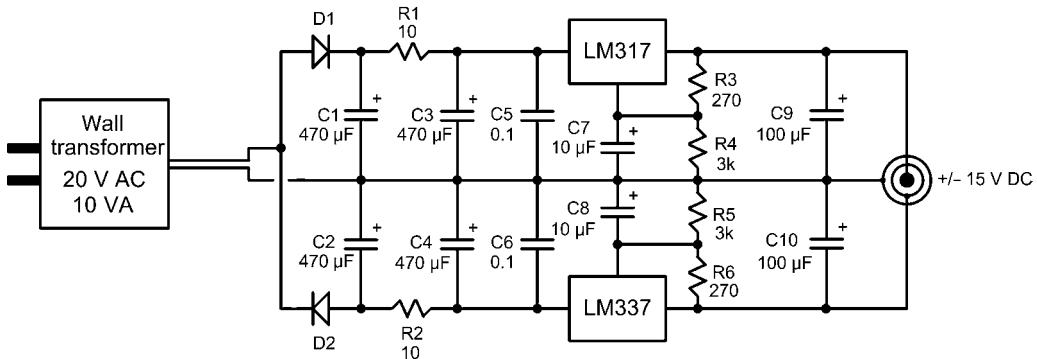
FIGURE 21.7   Wall transformer power supply for test gear.

half-wave rectifiers, filters, and regulators. The ±15 V is then supplied to the purpose-built test instruments with a three-wire interface. This keeps hum and noise out of the instrument. I use a single box to supply power to numerous purpose-built instruments at the same time.

References

1. Dymond, Harry C. P., and Mellor, Phil, "An Active Load and Test Method for Evaluating the Efficiency of Audio Power Amplifiers," *J. Audio Eng. Soc.,* vol. 58, no. 5, pp. 394–408, May 2010.
2. Cordell, R. R., "Build a High Performance THD Analyzer," *Audio,* vol. 65, July, August, September 1981; available at www.cordellaudio.com.
3. THAT Corporation 1200-series Ingenious differential line receiver data sheet; www.thatcorp.com.
4. THAT Corporation 1646-series Outsmarts balanced output driver data sheet; www.thatcorp.com.
5. National Semiconductor LM4562 dual operational amplifier data sheet; www.national.com.
6. Cordell, Bob, "The Distortion Magnifier," *Linear Audio,* vol. 0, September 2010; available from www.linearaudio.net.

Distortion and
Its Measurement

In this chapter we'll look at some distortion theory and some approaches to measuring distortion. Throughout the discussion it is important to distinguish between distortion mechanisms and distortion measurement techniques. Many of the mechanisms were discussed in Chapter 13.

22.1 Nonlinearity and Its Consequences

Nonlinearity is the underlying mechanism of distortion. When a circuit parameter changes as a function of signal, nonlinearity exists. Stimulation of the nonlinearity is also necessary for creation of distortion from that nonlinearity. Signal voltage or current is usually the stimulus at the location of the nonlinearity. The resulting distortion will usually be in proportion to the amplitude of the stimulus (or to a power of it). When the value of a capacitance changes as a function of signal voltage, that is a distortion mechanism that is stimulated by voltage. The consequences of that capacitance change are what a distortion test measures. If the capacitor is across a very low-impedance source, its signal-dependent capacitance change may not make much difference in the signal and measured distortion will be low.

More often, the capacitance will be associated with a resistance, causing a pole in the circuit to move up and down in frequency. One distortion test may measure the time-varying frequency response that results, while another test might measure the time-varying signal phase that results. Yet another test might measure the harmonic frequencies that are created. The same underlying nonlinearity will cause distortion to be seen by many different types of measurement. This is a very important point and is sometimes misunderstood.

This is why it is virtually impossible to have one type of measured distortion without having another type of measured distortion. Having said that, it is important to realize that different distortion measurements can have vastly different sensitivities to the same nonlinearity, depending on how effective they are in stimulating (exercising) that nonlinearity and how sensitive they are in measuring the resulting distortion products. This is why there are numerous different types of distortion tests. A given nonlinearity creates THD, TIM, and CCIF IM; these are just different ways of stimulating the nonlinearity and measuring its consequences.

High-frequency distortion is a very good example. It is largely a function of the rate of change of the stimulus that is exercising the amplifier. THD-20 and TIM are measuring the same nonlinearity by stimulating the amplifier with a high rate of change.

Indeed, a given type of distortion measurement is really the observation of the symptoms of the nonlinearity. An analogy here would be that in medicine the presence of many diseases is inferred from symptoms or from the presence of antibodies, not necessarily the disease itself.

The Order of a Nonlinearity

As signal level is increased, the increase in distortion percentage is a function of the order of the distortion being considered. For example, with second-order distortion, a 1-dB increase in signal level will cause the magnitude of the second-order distortion product to go up by 2 dB. This means that the distortion expressed as a percentage will go up by 1 dB. For example, if second harmonic distortion is 1% at a fundamental level of 1V RMS, then the second harmonic will rise to 2% at a fundamental level of 2V RMS.

For third-order distortion, a 1-dB increase in fundamental level will result in a 3-dB increase in the product magnitude and a 2-dB increase in the distortion percentage. If the third-order distortion is –80 dB relative to the fundamental at a fundamental level of 0 dBV, it will rise to –78 dB relative to the fundamental at a fundamental level of +1 dBV. Distortion of order n will go up by $(n – 1)$ dB relative to the fundamental when the signal level is increased by 1 dB.

This known behavior can be helpful in inferring whether the distortion component being observed (as on a spectrum analyzer) is from the source or the *amplifier under test* (*AUT*). Increase the level to the AUT by 1 dB. The magnitude of the third harmonic (for example) should go up by 3 dB. If it goes up by only 1 dB, it has probably originated in the source.

22.2   Total Harmonic Distortion

Total Harmonic Distortion (THD) is one of the most common measures of distortion. It is based on the fact that when a sine wave encounters a nonlinearity, harmonics will be created at integer multiples of the fundamental frequency of the sinusoid.

As explained in Chapter 21, the amplifier under test is fed a low-distortion sine wave. The fundamental frequency of the sine wave is removed with a very narrow and deep notch filter. What remains after the notch filter is the residual, consisting of noise and harmonics [1]. This is why the measurement is usually referred to as *THD+N*. The residual is passed through a low-pass filter that limits the measurement bandwidth to typically 80 kHz or 200 kHz. This improves the SNR of the measurement. The amplitude of the residual is displayed on the instrument meter as a distortion percentage and the residual signal is made available at an output jack for viewing with an oscilloscope or a spectrum analyzer [1].

Interpretation of THD

Single-number THD specifications are of limited use in characterizing the sound quality of an amplifier because they do not convey the nature of the distortion. For example, they do not distinguish between low-order and high-order distortions. Worse, single-number THD will often be quoted at 1 kHz, where it is easy to achieve very small

numbers. This is a big part of the reason why it is common in many circles to dismiss THD as having little or no relationship to perceived sound quality. Such a view paints THD with too broad a brush. THD is a much better indicator of amplifier performance when it is measured at high frequencies (THD-20) and a full spectral analysis is presented of the amplitudes of the individual harmonics.

Advantages of THD

While not an airtight guarantee of good sound, a very low THD number for an amplifier leaves little room for most other distortions to be present. By very low THD we mean THD well under 0.01% under all conditions with thorough testing and observation of the amplitudes of the harmonics. This is not the only path to good sound, however. Benign distortions that elevate THD readings may not audibly degrade sound quality. Second harmonic distortion would be an example.

Very low THD assures exceptional overall circuit linearity under static conditions. Low THD at all frequencies means that most other distortions will be very small as well. These include CCIF IM, SMPTE IM, TIM, and PIM. It is very difficult for these other measured distortions to exist without their also being at least small amounts of THD. This is especially so if the THD residual has been evaluated on a spectrum analyzer and if the THD has been measured in a bandwidth that is at least 10 times that of the fundamental.

Very low THD virtually guarantees the absence of audible crossover distortion. This is especially so if THD without noise is shown to be very small at lower power levels by the use of spectral analysis of the residual. There is also a stronger assurance if the measurements include loading with 2 Ω.

Very low THD-20 indicates that magnetic coupling distortions from power supply rails are absent. Magnetic coupling of the highly nonlinear half-wave-rectified signal currents in class AB output stages readily shows up as high-frequency THD. Very low THD also assures that power supply coupling distortions due to limited PSRR are very small. Low THD also indicates that ground-induced distortions due to imperfect grounding are very small.

Very low THD-20 suggests that parasitic oscillations are absent when driving the load used in the test setup. In thorough testing, these THD tests should be done with capacitive loads and simulated speaker loads. The presence of parasitic oscillations usually causes subtle increases in THD. These subtle increases will go unnoticed in amplifiers with higher THD.

Very low 20-Hz THD strongly suggests that many low-frequency thermal distortions are absent. These include fuse distortion, feedback resistor thermal distortion, and transistor junction thermal distortion. It also suggests that some measurable capacitor distortions, such as from electrolytic capacitors at low frequencies, are absent.

Very low THD at 20 Hz or 50 Hz virtually guarantees that power supply ripple and its harmonics are not entering the signal path. These will show up in the distortion residual even though they are not harmonics of the fundamental signal stimulating the amplifier.

Finally, low THD when driving a 2-Ω load assures that the amplifier has very good high-current capabilities. Effects of beta droop in the output stage will often be unmasked in this THD test.

In general, the attention to design detail and implementation necessary to achieve very low THD will tend to result in a better amplifier (as long as something stupid is not done to achieve low THD at the expense of something else).

Limitations of THD

THD-20 is one of the tougher and more revealing distortion measurements that can be done on an amplifier. However, the higher harmonics lie well above the audio band and many audio spectrum analyzers cannot display spectra above 50–100 kHz. If the THD analyzer has an 80-kHz filter engaged to improve its sensitivity, these harmonics will be attenuated. Single-number THD measurements do not tell the whole story because they do not distinguish between the low-order nonlinearities and the more troublesome high-order nonlinearities.

Single-number THD+N measurements are of limited value at low power levels because there is no way of knowing whether the reported THD+N level is primarily noise or crossover distortion.

Low THD does not assure the absence of many sonic shortcomings. For example, it does not reveal distortion resulting from thermal bias instability, as when an output stage becomes temporarily underbiased following a high-power interval. It also does not assure that there is no flabby low-end performance due to a sloppy power supply. Nor does it assure the absence of sonic degradation due to poor transient performance and ringing.

Low THD does not guarantee civilized amplifier behavior under clipping conditions or when protection circuits are activated. It does not indicate the absence of frequency response coloration due to the effects of frequency-dependent variations in load impedance (damping factor). It also does not assure the absence of poor sound quality resulting from unforeseen interactions with the loudspeaker load under dynamic conditions. Nor does it prove the absence of instability under all possible cable and loudspeaker loads.

Good THD readings do not assure that the amplifier is reproducing music faithfully in the presence of EMI ingress. It does not address some linear and nonlinear distortions that are less well understood, such as the influence on sound quality of passive component quality. In fairness to THD, many other distortion tests also do not reveal these sonic shortcomings.

Single-number midband THD, like THD-1 can give a misleading impression of good amplifier performance. This may be the single biggest reason why some eschew THD measurements, claiming that it has little correlation with sound quality. The fact that some amplifiers with relatively high THD sound very good further contributes to this impression.

22.3   SMPTE IM

SMPTE intermodulation distortion (*SMPTE IM*) is another distortion measure that has long been in use. It is based on the observation that nonlinearity can be represented as a change in the incremental gain of a circuit as a function of instantaneous signal amplitude. This measurement is also referred to as *amplitude intermodulation distortion* (*AIM*). The dynamic changes in incremental gain are observed by creating a test signal with a small-amplitude high-frequency *carrier* on top of a large-amplitude lower-frequency signal.

After the test signal passes through the amplifier under test, the low-frequency signal is filtered out and the carrier signal is AM-detected. The SMPTE IM test employs test signals at 60 and 7000 Hz mixed in a 4:1 ratio. A typical SMPTE IM measuring
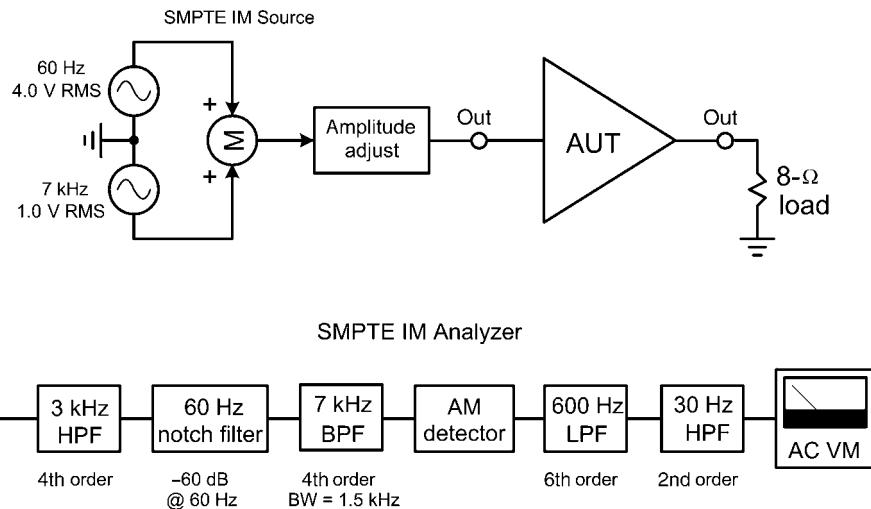
FIGURE 22.1 Measuring SMPTE intermodulation distortion.

arrangement is shown in Figure 22.1. The sensitivity of the analyzer is largely determined by the rejection characteristics of the various filters. Most SMPTE IM analyzers use a conventional rectifying AM demodulator, but better ones employ *synchronous detection* where phase-locked loops are required to recover the 7-kHz carrier. Synchronous detection does a far better job of keeping AUT noise out of the measurement.

22.4 CCIF IM

The CCIF IM distortion test takes advantage of the fact that if two tones are passed through a nonlinearity, spectral components will be created at frequencies of $mf_1 \pm nf_2$, where f_1 and f_2 are the frequencies of the two tones. This test, often referred to as the twin-tone test, is usually conducted with equal-level sine waves at 19 kHz (f_1) and 20 kHz (f_2). A second-order nonlinearity will produce a distortion component at 1 kHz, the difference of the two frequencies. Notice here that two frequencies are involved in the calculation of the distortion product frequency and that $m + n = 2$. This characterizes the nonlinearity as second-order. The sum of f_1 and f_2 always designates the order of the nonlinearity that the spectral component represents. The second-order nonlinearity will also produce a spectral *line* at 39 kHz, representing the $m + n$ component.

A third-order nonlinearity will produce components at $2f_1 - f_2 = 18$ kHz and $2f_2 - f_1 = 21$ kHz. A fifth-order nonlinearity will produce components at $3f_1 - 2f_2 = 17$ kHz and $3f_1 - 2f_2 = 22$ kHz. It is easy to see the progression as the order of the nonlinearity increases. Figure 22.2 shows a typical CCIF IM plot that illustrates the result when nonlinearities at second through seventh order are present.

Notice that the fourth-order nonlinearity shows up at $2f_2 - 2f_1 = 2$ kHz and that the sixth-order nonlinearity shows up at $3f_2 - 3f_1 = 3$ kHz. The CCIF IM test reflects even-order nonlinearities down to low frequencies. Early uses of the test simply employed a low-pass filter to attenuate the higher test frequencies so that the lower products could be measured with an AC voltmeter, with particular emphasis on the second-order
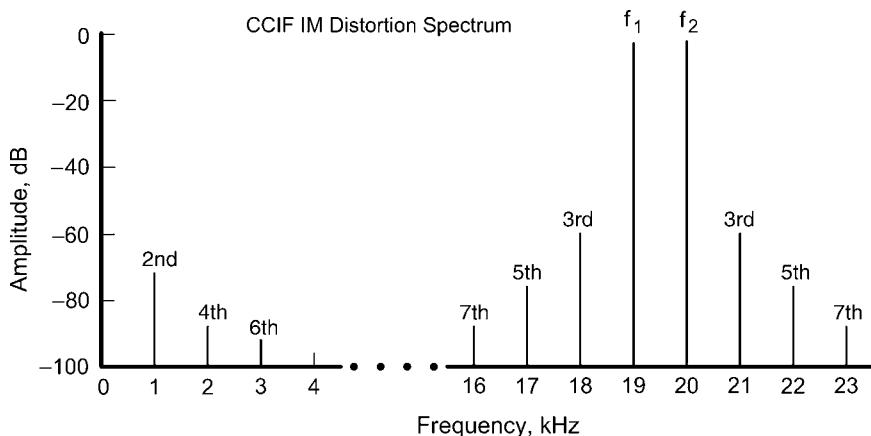
FIGURE 22.2   A CCIF IM plot.

product at 1 kHz. Unfortunately this was a very incomplete test. Proper use of the CCIF IM test requires the use of a spectrum analyzer. This enables the odd-order distortion products to be viewed.

The great advantage of the CCIF IM test is that representatives of all of the distortion orders are present in-band, allowing the use of spectrum analyzers of modestly high-frequency capability. The individual oscillators do not have to have very low distortion, and this is a major advantage of this test. However, the summing circuit where their outputs are combined must have very low distortion.

22.5   TIM and SID

Transient intermodulation distortion (TIM) received a great deal of attention in the 1970s and early 1980s [2–10]. It is a distortion mechanism that is often described in time-domain terms. It has wrongly been blamed on the use of large amounts of negative feedback and small open-loop bandwidth. If an input signal to a feedback amplifier changes very quickly–too fast for the output of the "slow" amplifier to respond–the input stage may be overloaded and clip. The stage will be overloaded by the large error signal that arises before the feedback from the output catches up to the input. The overload occurs because the input stage of a feedback amplifier is not usually designed to be able to handle the full amplitude of the input signal, since under normal conditions it needs to handle a much smaller error signal.

Slew Rate Limiting and Input Stage Stress

The *slew rate limiting* distortion mechanism was known many years before the term *TIM* was coined. TIM has in fact been described as *slewing-induced distortion* (*SID*) [7, 8]. *Hard TIM* occurs when the input stage clips and the amplifier is in slew rate limiting. *Soft TIM* occurs when the stress on the input stage increases as the slew rate limit is approached, resulting in input stage nonlinearity. It is important to recognize that TIM results from signal stress on the input stage.

Amplifiers with large amounts of negative feedback and small open-loop bandwidth can achieve very high slew rates. This is why large amounts of negative feedback
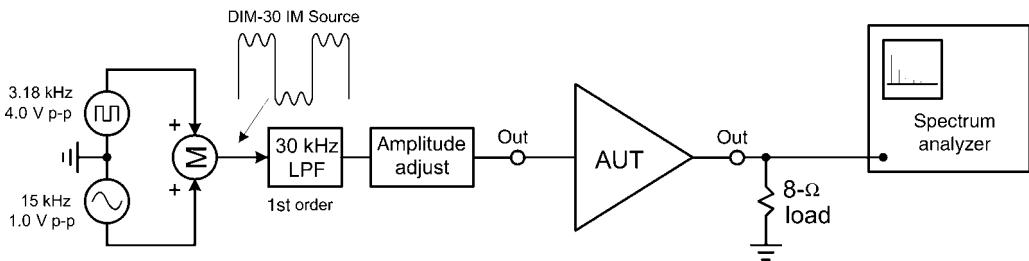
FIGURE 22.3 The DIM test for transient intermodulation distortion (TIM).

and small open-loop bandwidth are not a root cause of TIM. Poor amplifier design without adequate slew rate and input stage dynamic range is what is responsible for TIM [10].

The DIM Test

TIM is a dynamic distortion that results from fast changes in the signal. For this reason it is also a distortion that is more prominent at high frequencies. The original test developed for this distortion is referred to as *dynamic intermodulation distortion* (*DIM*) [11–13].

As shown in Figure 22.3, the DIM test signal consists of a 3.18-kHz square wave and a 15-kHz sine wave mixed in a 4:1 ratio. The combined signal is then low-pass filtered with a first-order network at 30 kHz (DIM-30) or 100 kHz (DIM-100). The fast edges of the square wave stress the amplifier at high frequencies with high-voltage rates of change while the 15-kHz carrier signal is modulated as a result. The result of the test must be viewed on a spectrum analyzer, and the amplitudes of all of the relevant spectral lines must be added on an RMS basis and then referred to the amplitude of the 15-kHz carrier. Notice that the square-wave portion of the input signal contains components at the fundamental and its odd harmonics. Each of those harmonics can interact with the 15-kHz fundamental on an $m \pm n$ basis. This means that nonlinearities of low order will still produce a very rich spectrum.

The dynamic range of the spectrum analyzer limits the measurement floor for the DIM-30 test. The popular HP 3580A audio spectrum analyzer has a dynamic range of 85 dB on a good day. The 15-kHz component of the DIM-30 test signal is down 14 dB from the full p–p amplitude of the composite DIM-30 test signal. This means that the measurement floor is at about –71 dB, or about 0.03%. Some newer spectrum analyzers based on high-performance sound cards should do much better.

THD-20 Will Always Accompany TIM

With some caveats, I have never seen an amplifier that had measurable TIM that did not also have measurable THD-20. The essential difference between these tests is that TIM exercises the amplifier with a high peak rate of change that has a small duty cycle, while THD-20 exercises the amplifier with a smaller rate of change but with a much larger duty cycle. The peak slew rate for a 20-kHz sine wave is 0.125 V/µs per volt of peak signal amplitude ($V/µs/V_{pk}$). The peak slew rate for the DIM-30 test signal is 0.319 $V/µs/V_{pk}$. A 20-kHz sine wave at 100 W into 8 Ω has a slew rate of 5 V/µs.

THD-20 will tend to track DIM fairly well as long as the amplifier is not pushed into slew rate limiting (hard TIM) by the higher peak slew rate of the DIM test signal.

THD-20 will often be about 4–7 dB below the DIM-30 number [14]. However, the measurement floor with a good THD analyzer (about 0.001% or –100 dB) lies well below that of the DIM-30 test. Because of the large rate of change applied to the amplifier in order to stimulate the high-frequency nonlinearity, it is possible for a DIM test to cause an amplifier to go into slew rate limiting when a THD-20 test would not. In this case it is possible to have large amounts of DIM with fairly small amounts of THD-20.

More often, low THD-20 virtually guarantees the absence of TIM, especially if the amplifier is known to have a healthy slew rate of 50 V/μs or more depending on power rating.

Recommended Amplifier Slew Rate

The maximum slew rate from a CD source is limited by the very steep anti-alias filtering required by the *Red Book* standard for audio CDs. A square wave recorded on a CD will have a slew rate of about twice that of a 20-kHz sine wave of the same peak amplitude, or about 0.25 V/μs/V_{pk}. Newer recoding standards, like SACD and high-rate PCM, increase this maximum, at least in principle. Many amplifier input stages begin to exhibit nonlinearity well before slew rate limiting occurs. For these reasons, it is wise to have an amplifier slew rate that is about 10 times that of a full-amplitude 20-kHz sine wave. For a 100-W amplifier this corresponds to 50 V/μs. The minimum recommended slew rate for a 400-W amplifier is 100 V/μs. These numbers are not difficult to achieve in practice, given a sufficiently fast output stage.

22.6   PIM

Nonlinearity can sometimes cause a change in the phase shift of a circuit as a function of instantaneous signal amplitude. This distortion mechanism is called *phase intermodulation distortion* (*PIM*) [15–18]. Some have also called it *FM distortion* (phase modulation is simply the integral of frequency modulation).

The PIM measurement is analogous to SMPTE IM (AIM), but involves phase modulation instead of amplitude modulation. 60-Hz and 7-kHz test signals are mixed in a 4:1 ratio and applied to the AUT. A simple example of a circuit that creates PIM is a nonlinear capacitance in an R-C low-pass filter arrangement. If the capacitance changes as a function of signal amplitude, the corner frequency of the low-pass filter will change and, correspondingly, the phase shift of the filter will change.

PIM is also created by AIM in a feedback amplifier. If the signal amplitude modulates the gain of the input stage, the changing open-loop gain of the amplifier will result in a changing closed-loop bandwidth, as illustrated in Figure 22.4. Just as in the passive case above without feedback, the movement of the closed-loop 3-dB frequency will cause a change in phase shift, which corresponds to PIM. This is an example of amplitude-to-phase conversion caused in this case by the action of the negative feedback loop. Only a portion of the AIM is converted to PIM, leaving AIM as well as PIM. For this reason, an amplifier of conventional design cannot exhibit PIM without also exhibiting AIM.

Differential Gain and Phase

The measurement of AIM and PIM is not new to the analog video world. There it is referred to as *differential gain and phase,* referring simply to gain and phase shift that are a function of signal.
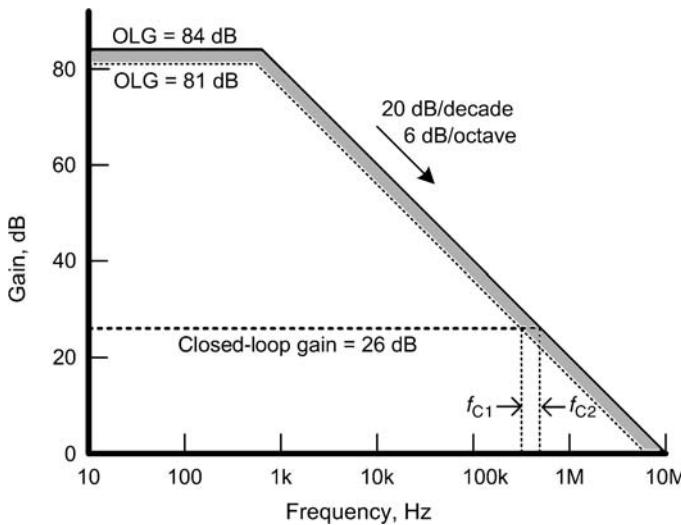
FIGURE 22.4 Creation of PIM by modulation of the open-loop gain.

Measuring PIM

PIM is measured in much the same way as AIM, but with a phase detector substituted for the AM detector. The test signal for PIM and AIM is the same [15–17]. A large low-frequency signal, typically 60 Hz, is used to cause the operating points in the amplifier to traverse a large-signal range. A smaller signal, typically 4 times smaller and at a high frequency like 7 kHz, then has its amplitude and phase modulations measured. Modulation on the small signal at 60 Hz or its harmonics is either AIM or PIM depending on whether amplitude or phase detection is used.

This is a more challenging measurement that usually requires a phase-locked-loop and synchronous detection, as described in Ref. 18. The arrangement is referred to as a coherent IM analyzer. The instrument uses in-phase and quadrature coherent detection to extract both conventional SMPTE IM (AIM) and PIM, respectively.

The 19+20-kHz CCIF test is also sensitive to PIM. Phase and amplitude distortions both create spectral lines at frequencies that have an $mf_1 \pm nf_2$ relationship. For this reason, an amplifier with PIM will exhibit spectral lines using the 19+20-kHz CCIF test. However, one will not be able to distinguish PIM from AIM with this test.

Negative Feedback and PIM

If the open-loop gain of a feedback amplifier is a function of signal swing (this is AIM), the gain crossover frequency of the global negative feedback around the amplifier will change. If the open-loop gain decreases, the gain crossover frequency and the closed-loop bandwidth of the amplifier will become smaller. When this happens, the amplifier will exhibit slightly higher in-band phase lag. This is PIM. The negative feedback has effectively caused some of the AIM to be converted to PIM. Put simply, movement of the closed-loop pole of a feedback amplifier is the source of feedback-generated PIM. Even though the closed-loop pole is well above the audio band (typically above 50 kHz), it causes a small amount of phase lag in-band, whose change creates PIM. For this reason, PIM has been blamed on negative feedback.

Moreover, PIM has wrongly been blamed on low open-loop bandwidth [15]. It seems intuitive that if movement of the closed-loop pole causes PIM, then the lower the frequency of the open-loop pole, the worse the PIM. This is not true. Consider a conventional Miller-compensated amplifier. Input stage *gm* and the size of the Miller capacitor set the gain crossover frequency for a given closed-loop gain. If you simply look at the calculation for gain crossover frequency as a function of input stage *gm* and Miller capacitor, you see that the open-loop bandwidth is not in the picture. Open-loop bandwidth does not play a role in determining the gain crossover frequency for a given nominal gain crossover frequency. For this reason, low open-loop bandwidth does not contribute to PIM.

PIM can be expressed in RMS degrees or in RMS nanoseconds. The amount of PIM generated by a given amount of input stage nonlinearity is mathematically derived in Ref. 18**.**

Input Stage Stress

Like TIM, PIM results from input stage stress that causes changes in the incremental gain of the input stage. In fact, for a given amount of negative feedback at 20 kHz, high feedback and correspondingly low open-loop bandwidth actually reduce input stage stress and therefore AIM and PIM. Bear in mind that the error signal at the input stage of a feedback amplifier is smaller if the open-loop gain is larger.

PIM in Amplifiers Without Negative Feedback

Amplifiers without negative feedback also have PIM. One common source of PIM in an amplifier without negative feedback is nonlinear junction capacitance that changes the bandwidth, and thus the phase shift, of the amplifier as a function of signal swing. Miller effect in the VAS from collector-base junction capacitance is an example. Another source can be the changing f_T of the output transistors affecting the bandwidth as their f_T droops at signal extremes.

Feedback amplifiers thus have PIM in the open loop even before negative feedback is applied. Interestingly, the application of negative feedback reduces this component of PIM in the same way that it reduces distortion from any other open-loop nonlinearity.

The results in Ref. 18 show that PIM is not a problem in contemporary amplifiers and that negative feedback reduces total PIM in most cases. The instrument built in Ref. 18 has a PIM measurement floor of 1 ns. An amplifier of ordinary design tested in Ref. 18 had PIM of less than 3 ns. The amplifier of Ref. 19 was also measured for PIM. It has very high negative feedback and very low open-loop bandwidth and measures less than 0.001% THD-20. It had measured PIM of only 0.04 ns (40 ps). That measurement required the use of a spectrum analyzer connected to the residual output of the coherent IM analyzer.

22.7   IIM

Interface intermodulation distortion (IIM) is caused by interaction of the load with the nonlinearity of the output impedance of a power amplifier [20, 21]. The nonlinearity can be stimulated by *back-emf* that originates in the loudspeaker. One example of this mechanism is the change in open-loop output impedance of the output stage as the output current goes through a zero crossing.

The output impedance of a feedback amplifier is approximately equal to its open-loop output impedance divided by the feedback factor. If the open-loop output impedance is large, the low closed-loop output impedance of the amplifier will depend on negative feedback for its reduction. IIM can thus be influenced by negative feedback. If the input stage experiences greater stress when the amplifier must deliver high currents, its incremental gain may decrease. This will decrease the amount of open-loop gain and reduce the amount of negative feedback. The change in feedback factor as a function of output current thus causes a change in closed-loop output impedance, and thus IIM.

Loudspeaker emf and Peak Current Requirements

The typical loudspeaker is anything but a benign resistive load. It is a reactive load that comprises mechanical elements that can store energy. This is especially the case with woofers, where significant electromotive force can be generated by cone motion. This can cause large excursions in output current that can stimulate the production of IIM.

The loudspeaker presents a fairly complex load to the amplifier, often with several significant resonances. The impedance can sometimes rise to over 10 times its rated value and fall to much less than 80% of its rated value (sometimes to less than half). The electromechanical system of the speaker (particularly the woofer) also represents an energy source and generation capability. Any movement of the cone will cause an emf to be generated by the voice coil or magnet system. This movement is often due to cone momentum developed by earlier excitation. The capability thus exists for the speaker to inject a signal back into the output of the amplifier. This can cause unexpectedly large currents to flow. These currents, in turn, can excite nonlinearity of the open-loop output impedance.

Figure 22.5 shows a simple RLC electrical model of a loudspeaker woofer in a closed box. The loudspeaker resonance is at 50 Hz. In this model, R represents the DC voice coil resistance, C accounts for the mass of the cone, and L accounts for the suspension compliance. The model ignores the effects of crossovers, other drivers, and so on. In all cases we make the conventional assumption that the minimum speaker impedance at low frequencies is equal to 80% of rated impedance.

Figure 22.6 shows the speaker current as a function of time when driven by the 28-V peak waveform shown. The driving waveform was deliberately chosen to maximize the expected peak load current [21]. The signal swings between large negative and positive values, rather than simply starting from zero. It stays at one extreme for 16 ms to allow load current to rise to at least 90% of its final value. A 4-ms pulse then follows, with the trailing edge of this pulse reversing the applied polarity just when the counter
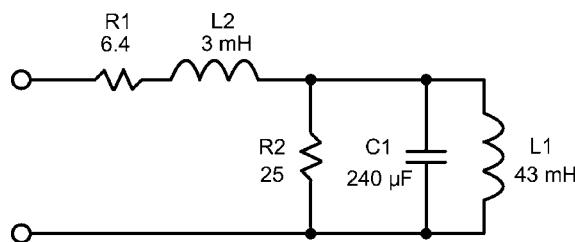
FIGURE 22.5 Loudspeaker model for simulation of peak current flow.
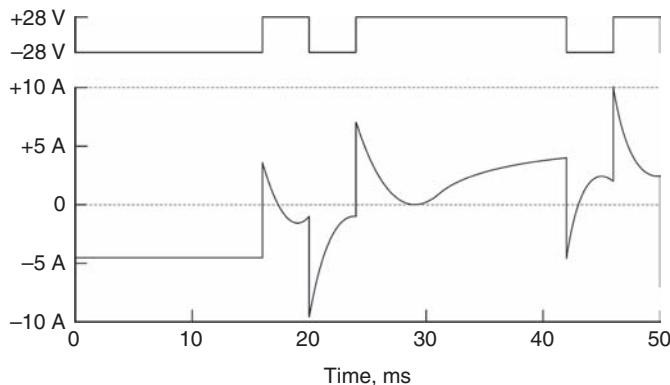
FIGURE 22.6 Peak loudspeaker currents with a special test signal.

emf of the speaker is at its maximum. This causes a large current to flow because the counter emf is now enhancing current flow rather than opposing it. The situation is then repeated for the opposite polarity sequence so that the average value of the signal is zero.

While an amplifier delivering this waveform to an 8-Ω resistive load would normally see a peak load current of about 3.5 A, we see here that the *RLC* load develops a peak load current of 10 A. While the probability and extent of this kind of occurrence in the real world with musical program material may be questioned, the exercise does provide some food for thought. The lesson to be learned here is to be prepared to handle larger currents than are encountered with a simple resistive load.

High-Current Amplifier Design

The message here is that the power amplifier should be designed for high-current output capability. Use an output stage with lots of current gain, employ a good number of output pairs, avoid current limiting and current limiters to the extent possible, and run the VAS at a healthy bias current (at least 10 mA). Note that a good number of MOSFET output pairs will provide very low open-loop output impedance because of their nearly infinite current gain at audio frequencies.

Measuring IIM

IIM is measured with a very interesting variation of the SMPTE IM arrangement. The IIM test is illustrated in Figure 22.7 [20]. Tones at 60 Hz and 1000 Hz are used in a 1:1 amplitude ratio. The 1-kHz carrier signal is fed forward through the amplifier. The amplifier is connected to an 8-Ω load resistor, the other end of which is tied to another amplifier instead of to ground. The second amplifier is fed the 60-Hz component of the IM test. The amplitude of the 60-Hz signal at its output is the same as the 1-kHz carrier signal at the output of the amplifier under test (AUT).

This is a back-feeding distortion test, where current is forced to flow in the output stage of the AUT. The current created by the 60-Hz back-feed signal will cause modulation of the 1-kHz carrier via the IIM distortion mechanism. The 60-Hz modulation present on the 1-kHz carrier at the output of the AUT is then measured and referenced to the 1-kHz signal level to arrive at a distortion number.
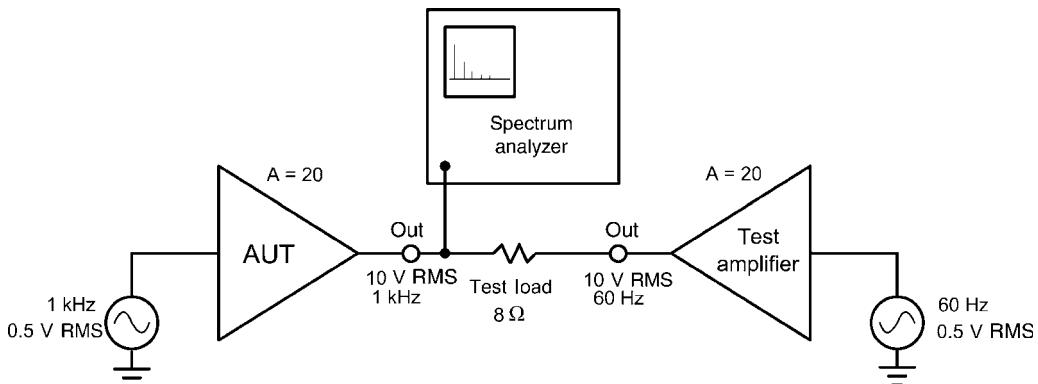
FIGURE 22.7   Measurement setup for interface intermodulation distortion.

Open-Loop Output Impedance

Open-loop output impedance plays a role in the creation of IIM. If it is nonlinear, it will contribute significantly to the IIM nonlinearity. Unfortunately, open-loop output impedance is sometimes misunderstood.

The high impedance of the VAS output node, combined with finite output stage current gain, makes it intuitive that open-loop output impedance should be high. This is only partially true. The shunt feedback on the VAS output node created by the Miller compensation capacitor greatly reduces the impedance at that node, especially at high frequencies. For this reason the open-loop output impedance of the amplifier is a function of frequency. It is naturally lower at high frequencies. This tends to compensate for the fact that there is less feedback at high frequencies to reduce output impedance when the loop is closed. Indeed, over a good part of the upper frequency range, the practice (intuitive to some) of adding VAS load resistors to reduce open-loop output impedance is both ineffective and harmful. It is ineffective because at upper frequencies the Miller shunt feedback has already reduced the impedance at that node much lower than the value of any reasonable VAS shunt resistors. It is harmful because the shunt resistors make the VAS work harder and create more distortion.

The amount by which Miller compensation reduces VAS output impedance is a strong function of the circuit design details. High impedance at the input node of the VAS tends to elevate the amount of shunt feedback provided by the compensation capacitor. The amplifier of Figure 3.10 can serve as an example to put the matter in perspective. The VAS output impedance at 1 kHz for that design is less than 5 kΩ. When that impedance is divided by the current gain of the Triple output stage (over 100,000), the VAS output impedance contribution to open-loop output impedance becomes a mere 50 mΩ. The VAS output impedance contribution will be much lower than this at higher frequencies.

The argument in Ref. 20 asserts that when open-loop output impedance is higher, negative feedback must play a greater role in keeping the output voltage from changing in the presence of counter emf from the loudspeaker. A larger error must circulate through the amplifier, as it were. In reality, the error signal amplitude is largely independent of the open-loop output impedance [21].

22.8 Multitone Intermodulation Distortion

The *multitone intermodulation (MIM)* distortion test employs three tones instead of the two tones used in the CCIF test [14]. This allows odd-order distortion products to be reflected to a low frequency in the audio band so that they can be measured without the need for a spectrum analyzer. This is also referred to as a *triple-beat* test because three tones create beat frequencies among them when they interact with nonlinearities. Three equal-level tones at 20.00 kHz, 10.05 kHz, and 9.00 kHz are fed to the AUT. If these three frequencies are designated as f_a, f_b and f_c, then an even-order nonlineairity will produce a beat frequency distortion product at $f_b - f_c = 1050$ Hz and an odd-order nonlinearity will produce a distortion product at $f_a - f_b - f_c = 950$ Hz.

The MIM distortion products can be measured with simple equipment. The output of the AUT is passed through a sixth-order 2-kHz LPF to discard the three high-frequency test tones. The signal is then passed through a fourth-order 1-kHz bandpass filter with a bandwidth of 150 Hz, which is wide enough to pass the distortion product frequencies at 950 Hz and 1050 Hz. This arrangement provides very good sensitivity because the noise bandwidth of the analyzer is quite small. Details of the test setup and how well it compares to THD-20 and DIM-30 tests can be found in Ref. 14. MIM produces smaller distortion percentage numbers, but it has a correspondingly lower measurement floor. MIM is largely sensitive to distortion products of only second and third order.

22.9 Highly Sensitive Distortion Measurement

Highly sensitive distortion measurements can be made using several pieces of test equipment together. The simplest example is the analysis of the residual output of a THD analyzer with a spectrum analyzer. Figure 22.8 illustrates how a combination of
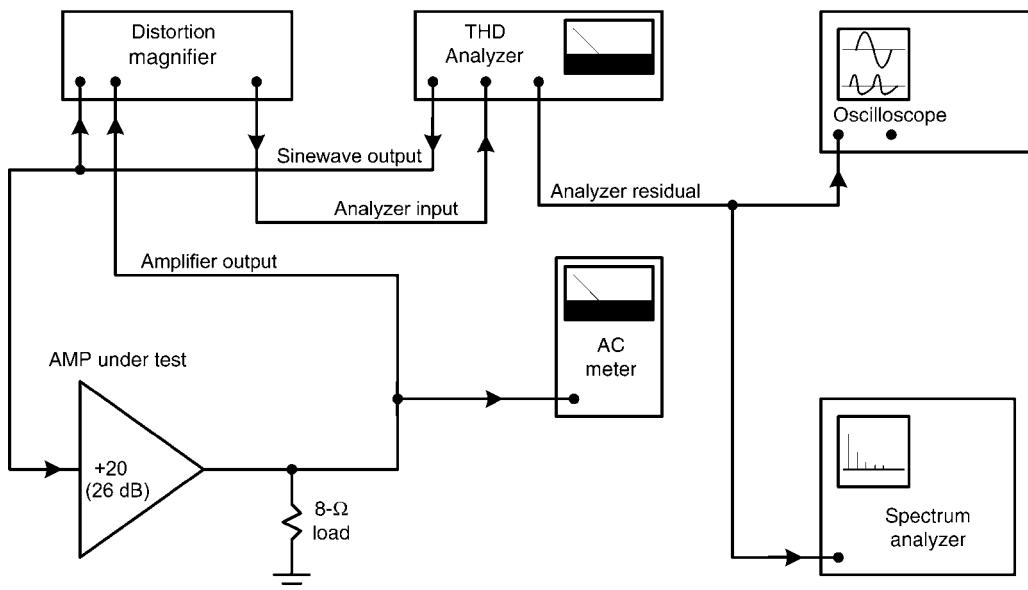
FIGURE 22.8 Highly sensitive distortion measurement.

instruments can be used to obtain very good measurements. The Distortion Magnifier described in Chapter 21 is placed in front of the THD analyzer to increase its dynamic range and measurement floor by 20 dB or 40 dB. This does not improve the noise floor as established by noise in the AUT, however. The spectrum analyzer is connected to the residual output of the THD analyzer. The small noise bandwidth afforded with spectrum analysis eliminates most of the AUT and THD analyzer noise from the measurement. The complete setup can provide a measurement floor well below –120 dB. The spectrum analyzer can be one based on a PC and soundcard.

22.10   Input-Referred Distortion Analysis

The effect of negative feedback on distortion is most easily understood by working backward from the output. We assume a perfect output and evaluate the input-referred distortion required to generate that perfect output, just as we do in calculating input-referred noise. Because the feedback signal under these conditions is perfect, the level of the input-referred distortion is the same for either open-loop or closed-loop conditions. Distortion percentage is reduced by feedback simply as a result of the larger pure component of the input signal required under closed-loop conditions. This technique is quite accurate when the referred distortion products are small compared to the total closed-loop input, that is, when closed-loop distortion is small. It is important to remember that the gain involved in referring a distortion product back to the input may be a strong function of frequency.

Consider one of the major contributors to IM distortion: output stage beta variations with current. The output stage requires a nonlinear driver current from the VAS to produce a perfect output. This results in an input-referred distortion voltage when the transconductance of the IPS-VAS is considered. Notice that the value of VAS load resistors (if present) will have virtually no effect on the level of this particular product because they have little effect on the transconductance.

Input Referral Breaks the Feedback Loop

While distortion analysis of the open-loop forward path of an amplifier can be difficult enough, a good understanding of distortion behavior can be even more difficult under closed-loop negative feedback conditions. For this reason, sometimes the technique of examining input-referred distortion can be helpful. This is not unlike input-referred noise techniques. By referring these phenomena back to the input, the feedback loop is effectively broken. When used in looking at distortion phenomena, it is essentially the process of answering the question, What distortion at the input would be required to produce a distortionless output?

Input Referral Demonstrates Why High Forward-Path Gain Reduces Distortion

This kind of analysis shows why a high gain in the forward path is more desirable—because it then takes less nonlinearity at the input to produce the perfect output. Of course in reality the output signal is not perfect, but it is close enough (by the action of the feedback) to make the approximation of the analysis valid. This approach may not preserve the harmonic content of the distortion representation, since there is a division involved. The approach is very useful for providing insight on effects of NFB on distortion. It also highlights the role of input stage stress in creating distortion.

References

1. Cordell, R. R., "Build a High Performance THD Analyzer," *Audio,* vol. 65, July–September 1981; available at www.cordellaudio.com.
2. Otala, M., *"Transient Distortion in Transistorized Audio Power Amplifiers," IEEE Transactions on Audio and Electro-acoustics,* vol. AU-18, pp. 234–239, September 1970.
3. Otala, M., and Leinonen, E., "The Theory of Transient Intermodulation Distortion," *IEEE Transactions on Acoustics, Speech and Signal Processing,* vol. ASSP-25, no. 1, pp. 2–8, February 1977.
4. Leach, W. M., "Transient IM Distortion in Power Amplifiers," *Audio,* pp. 34–41, February 1975.
5. Leach, W. M., "Suppression of Slew-rate and Transient Intermodulation Distortions in Audio Power Amplifiers," *J. Audio Eng. Soc.,* vol. 25, no. 7–8, pp. 466–473, July–August 1977.
6. Greiner, R. A., "Amp Design and Overload," *Audio,* pp. 50–62, November 1977.
7. Jung, W.G., Stephens, M. L., and Todd, C. C., "Slewing Induced Distortion and Its Effect on Audio Amplifier Performance – With Correlated Measurement Listening Results," AES preprint No. 1252 presented at the 57th AES Convention, Los Angeles, May 1977.
8. Jung, W. G., Stephens, M. L., Todd, C. C., "An Overview of SID and TIM," *Audio,* vol. 63, no. 6–8, June–August 1979.
9. Garde, P., "Transient Distortion in Feedback Amplifiers," *J. Audio Eng. Soc.,* vol. 26, no. 5, pp. 314–321, May 1978.
10. Cordell, R. R., "Another View of TIM," *Audio,* February, March 1980; available at www.cordellaudio.com.
11. Leinonen, E., Otala, M., and Curl, J., "A Method for Measuring Transient Intermodulation Distortion (TIM)," *J. Audio Eng. Soc.,* vol. 25, no. 4, pp. 170–177, April 1977.
12. Takahashi, S., and Tanaka, S., "A Method of Measuring Transient Intermodulation Distortion," 63rd Convention of the Audio Eng. Soc., preprint No, 1478, May 1979.
13. Leinon, E., and Otala, M., "Correlation Audio Distortion Measurements," *J. Audio Eng. Soc.,* vol. 26, no, 1–2, pp. 12–19, January–February 1978.
14. Cordell, R. R., "A Fully In-band Multitone Test for Transient Intermodulation Distortion," *Journal of the Audio Engineering Society,* vol. 29, September 1981; available at www.cordellaudio.com.
15. Otala, M., "Feedback-generated Phase Modulation in Audio Amplifiers," 65th Convention of the Audio Engineering Society, London, 1980; preprint No. 1576.
16. Otala, M., "Conversion of Amplitude Nonlinearities to Phase Nonlinearities in Feedback Audio Amplifiers," pp. 498–499, *Proc. of IEEE International Conference on Acoustics, Speech and Signal Processing,* Denver, CO, 1980.
17. Otala, M., "Phase Modulation and Intermodulation in Feedback Audio Amplifiers," 69th Convention of the Audio Engineering Society, Hamburg, 1981, preprint No. 1751.
18. Cordell, R. R., "Phase Intermodulation Distortion–Instrumentation and Measurements," *Journal of the Audio Engineering Society,* vol. 31, March 1983; available at www.cordellaudio.com.
19. Cordell, R. R., "A MOSFET Power Amplifier with Error Correction," *Journal of the Audio Engineering Society,* vol. 32, January 1984; available at www.cordellaudio.com.

20. Otala, M., and Lammasniemi, J., "Intermodulation Distortion in the Amplifier Loudspeaker Interface," 59th Convention of the Audio Engineering Society, preprint No. 1336, February 1978.

21. Cordell, R. R., "Open-loop Output Impedance and Interface Intermodulation Distortion in Audio Power Amplifiers," preprint No. 1537, 64th Convention of the AES, 1982; available at www.cordellaudio.com.

This page intentionally left blank

CHAPTER **23**

Other Amplifier Tests

E ven with the best conventional testing of amplifiers there remains a good deal of discrepancy between measurement results and perceived quality of sound. Some of this can be attributed to the many poorly controlled variables in subjective listening tests, but it is also likely that the relevant differences are measurable but they are not being measured. For example, the often relatively static conditions of conventional tests may not stimulate that which is responsible for two amplifiers having a different sound.

In this chapter some other tests not mentioned elsewhere in the book will be discussed. Most of these tests fall into the unconventional category. Amplifiers often sound different because they misbehave differently. One of the objectives of some of these tests is to get the amplifiers to misbehave.

23.1 Measuring Damping Factor

The importance of damping factor is sometimes underestimated, particularly in regard to its frequency dependence and its effect on frequency response. Every amplifier review should start with a frequency response measurement as seen at the terminals of the speaker system being used for the listening test. This would be very revealing in many cases. The effect of frequency response differences on perceived sound quality differences must never be underestimated.

Damping factor is defined as the ratio of 8 Ω to the output impedance of the amplifier. An amplifier whose output impedance is 0.16 Ω will have a damping factor of 50. The output impedance of the amplifier forms a voltage divider with the speaker load impedance, creating attenuation between the idealized output and the actual output. The damping factor can be inferred by measuring the amplifier frequency response under no-load and with a known-load. This is a fairly crude approach.

A better approach is to inject a signal current into the output of the amplifier and measure the resulting voltage. Such an arrangement is shown in Figure 23.1. This can be done by *back-feeding* from another amplifier through a 100-Ω 2-W resistor. The back-feeding amplifier is set for an output level of 10V RMS. This will create a "probe" signal current of approximately 100 mA RMS. The voltage across the output terminals of the amplifier under test (AUT) is then measured with an AC voltmeter. A 10-mV reading will correspond to an output impedance of 100 mΩ, which in turn corresponds to a DF of 80. The test frequency should be swept across the audio band to obtain a plot of output impedance versus frequency.

It is wise and instructive to view the signal at the output terminals on an oscilloscope as well. First, make sure that wideband noise from the amplifier is not dominating
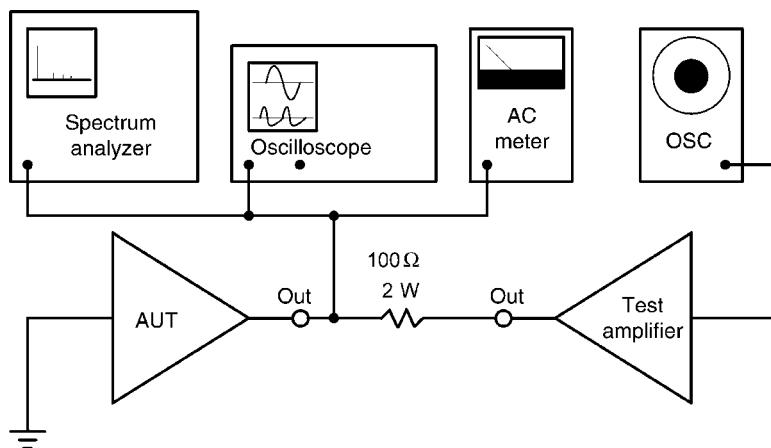
Figure 23.1 Measurement of damping factor.

the reading. If it is, insert a 100-kHz low-pass filter ahead of the AC voltmeter. Secondly, make sure that hum from the AUT is not dominating the reading. If it is, insert a high-pass filter ahead of the AC voltmeter and measure DF only above 1 kHz.

Finally, the oscilloscope waveform may unmask some crossover distortion whose percentage has been magnified by the DF. The signal at the output terminals of the AUT can also be viewed with a spectrum analyzer. This is especially useful when the damping factor is very high and the fundamental of the probing signal is very small.

Do not underestimate the influence of damping factor across the full audio frequency band. Some claim to be able to hear a 0.1-dB (1%) frequency response deviation. Some loudspeakers dip below 2 Ω somewhere in the frequency band. An output impedance of about 0.02 Ω is required to meet this combination of requirements, corresponding to a DF of about 400. This DF is virtually unattainable at frequencies above about 5 kHz. Expecting a DF of 400 out to high frequencies is unrealistic, but this exercise puts the importance of DF into perspective. A DF of 40 could lead to a 1-dB frequency response deviation when a speaker's impedance dips to 2 Ω. Loudspeaker impedances go through major changes in the vicinity of woofer resonances, but they often also go through significant gyrations in the vicinity of crossover frequencies, which can lead to coloration.

23.2 Sniffing Parasitic Oscillations

Some amplifiers are designed with inadequate stability margins and may break into bursts of parasitic oscillations under some signal and loading conditions. This can lead to audible differences that may not show up in conventional bench testing. Sometimes these oscillations will be visible as small bursts on a sine wave as viewed on a wideband oscilloscope. A purpose-built test instrument can be made to sniff such oscillations, even in the presence of music played through a loudspeaker and speaker cables. Such a device is shown in block diagram form in Figure 23.2.

The instrument comprises a sharp high-pass filter with a high-order cutoff at about 600 kHz. The filter can be implemented with a passive first-order HPF at the input followed by a pair of second-order active emitter follower filters. Rejection at 20 kHz is in
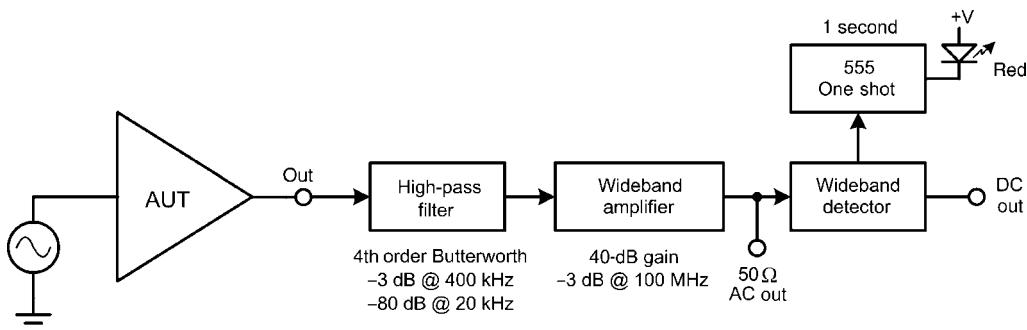
FIGURE 23.2 Block diagram of a parasitic oscillation sniffer.

excess of 80 dB. Total gain should be 100 with bandwidth out to beyond 100 MHz. The AC signal is available as a 50-Ω output that can be viewed on a wideband oscilloscope. The signal is also fed to a wideband peak detector for display of detected parasitic oscillation activity as a DC signal. If the signal strength is above a certain threshold, it will also trigger a 555 timer that will illuminate an LED for 1 second.

23.3   EMI Ingress Susceptibility

EMI ingress was discussed in Chapter 18. Here we discuss a possible method to test for EMI ingress susceptibility that is more objective than operating a cell phone or hair dryer near the amplifier under test. The idea is to generate an RF signal that can be applied to any of the three conductive EMI ingress ports of an amplifier (input, output, and mains). The test uses an RF multitone signal in the low MHz range with three tones whose intermodulation products lie in the audio band. These three tones are located at 990 kHz, 1001 kHz, and 2000 kHz. The intermodulation products of interest lie at 11 kHz (1001 – 990) and 9 kHz (2000 – 1001 – 990).

These signals can be generated by three audio generators and combined passively for injection into the amplifier port. An optional passive high-pass filter can be placed in the injection path if there is any concern about IM distortion created by interaction among the three oscillators (such interaction should be very small due to the isolating effect of the attenuation inherent in the summing process). The distortion products at 9 kHz and 11 kHz can be viewed at the output of the amplifier with a spectrum analyzer. They can also be viewed using a 10-kHz band-pass filter and an oscilloscope. Each frequency should be accurate within 0.1% to land the IM products to within 1 kHz of the target frequency. A frequency counter is a must in setting up the frequencies. Figure 23.3 illustrates how the EMI test signals might be injected into the three ports of the amplifier.

The test signal will be especially effective when injected at the input port because of the high impedance there and the ease of passive combining of the three tones. Caution must be used in selecting the input signal amplitude because some power amplifiers may still have significant gain at 1 MHz. Each tone should be applied with amplitude of 10 mV RMS. Three 1-V RMS tones can be fed to the amplifier input through 10-kΩ resistors. The input is shunted with a 100-Ω resistor to complete the input attenuator/combiner.
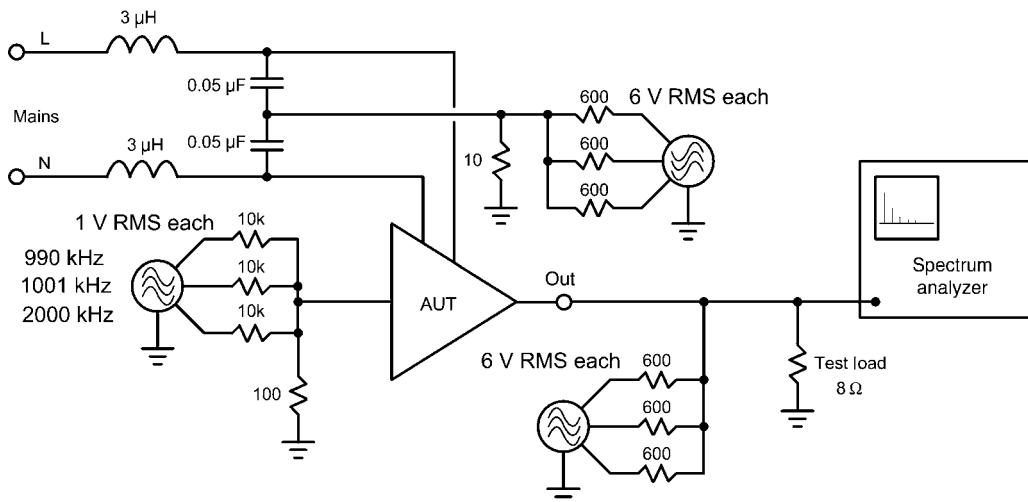
FIGURE 23.3 Injection of the RF multitone EMI test signals into the three ports of the amplifier.

The combining at the output port can take place directly at the output node of the amplifier with 10 mA RMS injected by each of the oscillators. This is simply accomplished by routing each signal through a 600-Ω resistor with the oscillator set to generate 6 V RMS into a 600-Ω load. This test should be done with a standard 8-Ω load connected across the output terminals. Notice that this test produces peak currents of 42 mA into the output port with a peak current rate of change of 56 mA/μs.

Signal combining and injection at the mains port requires a bit more thought. Caution must be observed in light of the high mains voltages involved. The test signal is most easily applied in the common mode to the mains input. A 3-μH air-core inductor can be connected in series with each of the hot and neutral lines (the impedance of each inductor equals about 19 Ω at 1 MHz). Each of those lines is connected to a summing point through a 0.05-μF, 600-V capacitor. Notice that this summing junction will have half the mains voltage on it in the absence of any loading at the summing point. The impedance of each 0.05-μF capacitor at 60 Hz is about 60 kΩ (it is about 3 Ω at 1 MHz). The summing node is connected to ground through a 10-Ω resistor and each of the tones is connected to the summing node through a 600-Ω resistor. With each tone set to 6 V RMS, 10 mA RMS is injected into the summing node by each tone. This will result in about 70 mV RMS for each tone in the common mode on the mains lines when the impedance of the series inductors is considered. Other arrangements are also possible. For example, a small air-core transformer can be used to inject the signal to one side or the other of the mains, or to both sides if the transformer has three windings.

23.4 Burst Power and Peak Current

Conventional tests do not adequately probe an amplifier's ability to deliver large bursts of power or output current on a momentary basis. The closest that they have come was the old dynamic headroom test. Tone-burst testing of amplifiers can help evaluate these short-term performance capabilities without damaging the amplifier. A 2-cycle tone

burst at 50 Hz with load resistances of 8 Ω, 4 Ω, 2 Ω, and 1 Ω can probe both an amplifier's short-term power capability (dynamic headroom) and its maximum current output capability. The duty cycle of the tone burst should be 10% or less. The tone-burst generator was discussed in Section 21.6.

23.5   PSRR Tests

The degree and quality of power supply rejection (PSRR) in a power amplifier can have an important influence on its sound quality. The rail voltages in a power amplifier move around a lot and are typically full of garbage. Every stage in the amplifier can be influenced by this noise, including the output stage. Input and VAS stages are influenced in accordance with the amount of power supply filtering in their supply lines and by the inherent ability of their circuits to reject the influence of power supply variation and noise.

PSRR tests are difficult and are almost never done except in the amplifier development stage. They are very invasive because they generally require that a disturbing signal be superimposed on a supply rail inside the amplifier.

PSRR at mains frequencies can be inferred. The amplifier is operated at full power at 1 kHz. A spectrum analyzer is then used to look for mains-frequency components at the output. If necessary, the useable dynamic range of the spectrum analyzer can be enhanced by using a filter to notch out the 1-kHz test signal at the output of the amplifier. If a THD analyzer is available, it can perform this function and its residual can be viewed on the spectrum analyzer. If the THD analyzer has a high-pass filter, it should be disabled for this test.

23.6   Low-Frequency Tests

It is often mistakenly thought that achieving low THD at low frequencies in a solid-state power amplifier is easy, especially when large amounts of negative feedback are available at low frequencies. This is not always so. This can lead to low-frequency performance being taken for granted and low frequency tests being overlooked. THD at 50 Hz (or lower) should be measured, and the residual subjected to spectral analysis. Some surprises are often in store. Such tests stress power supply rail rigidity and invite intermodulation with the 120-Hz ripple present on the power supply rails.

Beat Frequency Tests

Tests with a very low frequency component of output power variation can also stress an amplifier. Consider what may be called the low-frequency CCIF test. In this test sinusoidal signals of equal amplitude at 19 Hz and 20 Hz are applied to the amplifier. The output power of the amplifier then rises and falls in accordance with the 1-Hz beat frequency of the applied low-frequency tones.

This test can be particularly brutal and revealing, as the output stage is called on to change from no power output to full power output at a 1-Hz rate as the 19-Hz and 20-Hz signals beat against each other. This could reveal some thermal distortion mechanisms. No energy should be present in the output at 1 Hz, 2 Hz, 17 Hz, 18 Hz, or 39 Hz. If an analog spectrum analyzer is used for this test, the sweep can take quite some time because the analysis bandwidth must be set small.

23.7   Back-Feeding Tests

The IIM test proposed by Otala [1, 2] was an early example of employing a back-feed test to an amplifier. That test was similar to the SMPTE IM test, but using 60-Hz and 1000-Hz signals in a 1:1 ratio. However, the high-frequency signal was fed forward through the amplifier under test while the low-frequency signal was fed backward through a dummy load resistor from a laboratory amplifier. This test exercised the output current range of the output stage while evaluating any resultant modulation of the forward-propagated high-frequency signal. The back-feed testing concept can be generalized to many other useful testing procedures.

Back-Fed Beat Frequency Test

A variant of the low-frequency 19+20-Hz beat frequency test is to apply one of the tones in the forward direction and the other one via back feeding. Such a test exercises a large portion of the SOA of the output stage without resort to use of a reactive load. This test will really exercise the protection circuits. Such a test arrangement is shown in Figure 23.4.

Both amplifiers will be subjected to various combinations of high-voltage swing and high-current swing while the phase relationship between voltage and current will change, in some ways emulating what may be seen when driving a reactive load. This test is not for the faint of heart. The reference amplifier providing the back-feed signal should be a large hefty one with substantial SOA. The output of the AUT should be observed on an oscilloscope.

THD-20 in the Presence of Low-Frequency Back-Feed

This test feeds a 20-kHz test signal through the amplifier at the power level where crossover distortion is highest and THD-20 is measured. A 20-Hz back-drive signal is applied through an 8-Ω load resistor to produce a substantial back-feed current. THD-20 is measured and the residual is then viewed at the output of the THD analyzer. The change in the residual as a function of the low-frequency back-drive signal is noted. This allows you to see the effect of the larger output stage current swings on the THD distortion products. The effect of crossover distortion on the THD-20 will vary as the 20-kHz signal
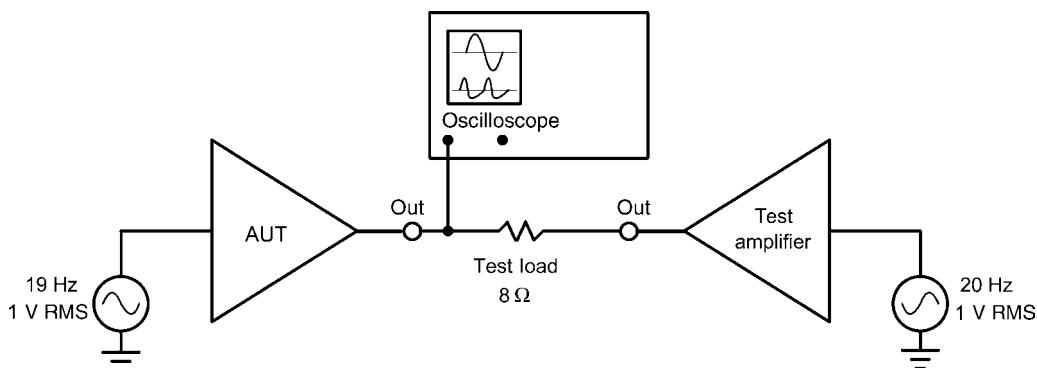
FIGURE 23.4   Two-tone back-feeding test using 19-Hz and 20-Hz test signals.

moves in and out of the crossover region. To perform this test you need a THD analyzer setup that has good rejection of the 20-Hz back-drive signal.

Current-Induced Distortion Tests

Two of the more villainous distortions in power amplifiers are output stage crossover distortion and pickup from class-AB half-wave-rectified signal currents. Both of these distortions are caused by signal current rather than signal voltage. These are *current-induced distortions* (CID). Both of these distortions have potentially broadband distortion spectra that are not at all benign.

To isolate the current-induced distortions the amplifier is forced to produce a significant output signal current without making it produce any significant voltage output. This can be done by back feeding current into the output of the amplifier through a load resistor from another amplifier. The amplitude of the distortion spectra present at the output of the amplifier under test is then observed with a spectrum analyzer.

One version of this test is implemented by feeding a 20-kHz sine wave at full power from one channel of a stereo amplifier through an 8-Ω load resistor into the output of the channel of the amplifier under test, whose input is grounded. The signal at the output terminals of the channel under test is then fed to a THD analyzer or an oscilloscope. Caution is advised with a test like this because it exercises a significant portion of the safe area of the output stage. With the output held essentially at ground, the peak current corresponding to the power output of the driving amplifier is drawn from the output stage while the full rail voltage of the amplifier under test is impressed across its output stage. In addition to unmasking crossover distortion, this test can also reveal distortion from poor PSRR, and distortion from nonlinear ground currents.

References

1. Otala, M., and Lammasniemi, J., "Intermodulation Distortion in the Amplifier Loudspeaker Interface," 59th Convention of the Audio Engineering Society, preprint No. 1336, February 1978.
2. Cordell, R. R., "Open-loop Output Impedance and Interface Intermodulation Distortion in Audio Power Amplifiers," preprint No. 1537, 64th Convention of the AES, 1982; available at www.cordellaudio.com.

This page intentionally left blank

Topics in Amplifier Design

Part 5 covers many of those other important topics that do not fit neatly into the other parts. Advanced designers as well as audiophiles will find many interesting discussions in this part. Some of the controversies in audio, such as the use of negative feedback, are addressed here. Chapter 25 discusses the challenges faced in the design of amplifiers that do not use negative feedback or which maintain wide open-loop bandwidth for those who believe these features to be important. Part 5 also covers other amplifier designs, such as fully balanced designs and power amplifiers that can be implemented all or in part with integrated circuits.

This page intentionally left blank

The Negative Feedback Controversy

The use of negative feedback has been controversial for many years in the hi-end audio community. Some argue that none should be used, while others argue that only small amounts should be used. Some argue that wide open-loop bandwidth is required to achieve the best sound quality. Some argue that global negative feedback is bad but that local negative feedback in IPS and VAS stages is OK.

24.1   How Negative Feedback Got Its Bad Rap

Negative feedback has gotten a mostly undeserved bad rap. Much of this is because poorly designed solid-state amplifiers of the 1970s happened to use large amounts of negative feedback. These were poor-performing designs in the first place, but negative feedback got the blame. Some designers carelessly believed that negative feedback could be used to linearize a design that was inherently not very linear to begin with.

Amplifier Limitations of the 1970s

Audio power amplifiers of the 1970s, being part of the early era of solid-state power amplifier technology, suffered many problems. These are some of the problems that contributed to poor sound quality.

- Slow power transistors with inadequate SOA
- Frequent use of quasi-complementary output stages
- Aggressive protection circuits that misbehaved
- Excessive crossover distortion
- Input stages with little dynamic range, leading to inadequate slew rate
- Poor stability margins and occasional parasitic oscillations
- Output coils wrapped around aluminum electrolytic power supply capacitors
- Poor capacitor choices

Guilt by Association

Most of these early designs achieved decent distortion measurements by using negative feedback, but nevertheless did not sound good. In a sense, the negative feedback allowed designers to make bad choices or cut corners. A very good example of such

499

poor choices was the use of undegenerated differential input stages in the misguided belief that the resulting higher gain would provide more negative feedback and lower distortion, at least in the midband. Those designers did not realize that they were crippling the amplifier's ability to deliver high slew rate. All of this was compounded by the fact that many designers were struggling to harness the new solid-state technology. Power transistors were slow and had poor SOA, and so required intrusive protection circuits.

It was not feedback itself that was responsible for the poor sound, but its inability to perform miracles on fundamentally poor circuit designs; that was the problem. Nevertheless, feedback got the blame for the poor sound. In a sense, a form of architectural profiling emerged, in which some treated any amplifier using negative feedback with suspicion.

TIM, PIM, and IIM

During the 1970s and early 1980s several researchers sought to identify logical and measurable phenomena that were correlated with poor sound [1–9]. This effort was noble, but often the wrong conclusions were drawn. In many cases a distortion mechanism would be identified and negative feedback would be given the blame. A measurement technique for the identified distortion would then be defined [8–11]. Those very measurements ultimately disproved the assertion that negative feedback was the villain [12–14].

The distortions that were identified do indeed exist and can be measured. That is not the controversy. The point is that negative feedback itself, when properly applied, does not exacerbate these distortions. All of these distortions are in fact quite measurable in amplifiers that do not even have any global negative feedback.

24.2   Negative Feedback and Open-Loop Bandwidth

It may seem intuitive to many that the open-loop bandwidth of a feedback amplifier should extend to the highest audio frequencies. This allows NFB to act equally on all frequencies. It was also demonstrated by Otala that error overshoot would occur in the input stage of a feedback amplifier when the open-loop bandwidth was substantially less than the low-pass filtered bandwidth of a square wave.

The amount of NFB applied at the highest audio frequencies (e.g., 20 kHz) is necessarily limited by feedback stability considerations. The open-loop gain must usually fall at 6 dB per octave so that the NFB loop gain reaches 0 dB at a sufficiently low unity-gain frequency, often on the order of 1 MHz or less. In such a case the NFB at 20 kHz will be about 34 dB. If the open-loop bandwidth is 20 kHz, the amount of NFB at low frequencies will also be about 34 dB. If the unity-gain frequency is kept the same and the open-loop bandwidth is allowed to decrease, the amount of negative feedback at lower frequencies will increase. For example, if the open-loop bandwidth is 1 kHz, the NFB at 1 kHz and below will be about 60 dB. This gives rise to the association of high feedback with bad sound, since high feedback occurs coincidentally with low open-loop bandwidth when the unity-gain frequency is held constant.

The Input Stage Error Signal

Figure 24.1 shows the input stage error signal for two amplifiers when driven with a 5-kHz square wave that is rolled off with a first-order filter at 30 kHz (as in the
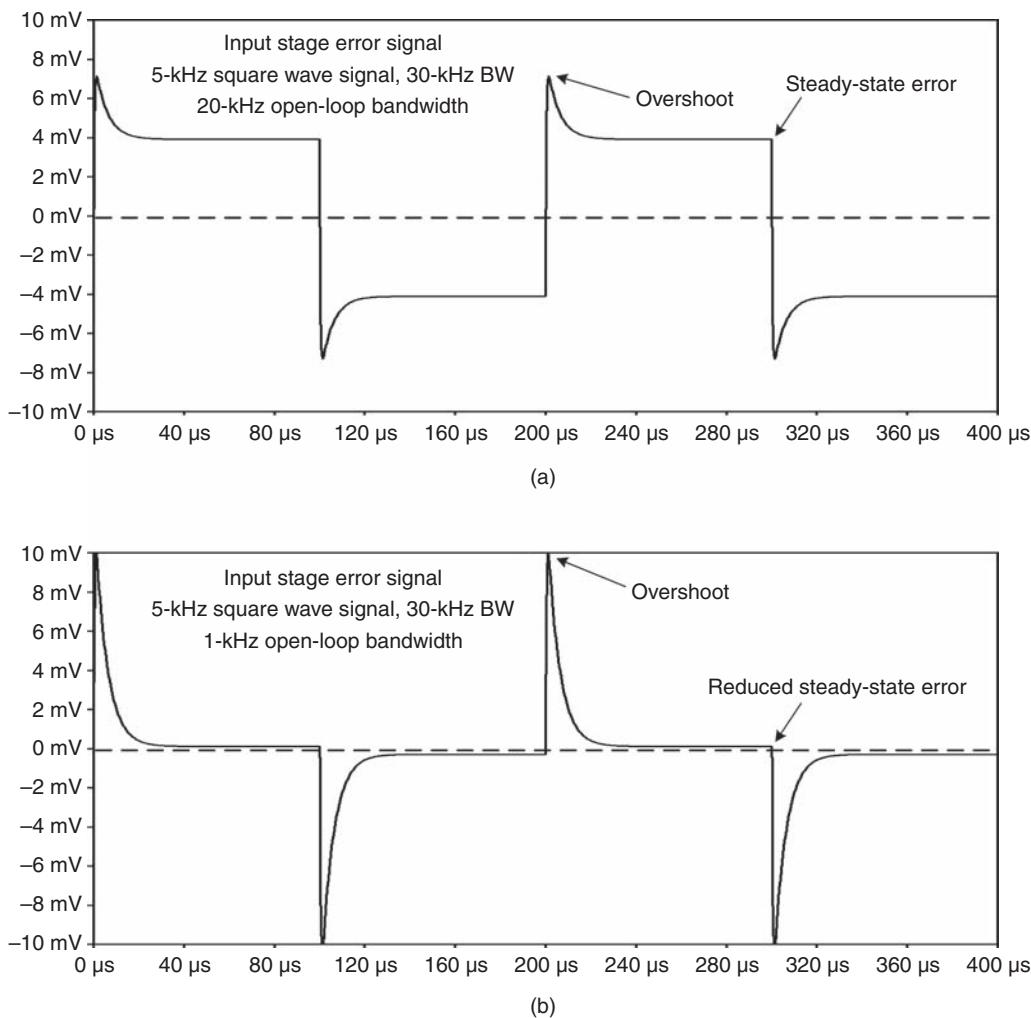
Figure 24.1 Input stage error signal. (a) With wide open-loop bandwidth, (b) With low open-loop bandwidth.

DIM-30 test). Both amplifiers have the same 500-kHz unity-gain frequency and the same amount of negative feedback at 20 kHz. The amplifier in Figure 24.1a has a 20-kHz open-loop bandwidth and open-loop gain of about 54 dB. The amplifier in Figure 24.1b has a 1-kHz open-loop bandwidth and open-loop gain of about 80 dB. Both amplifiers are driven to a peak output voltage of 2 V.

The early papers on TIM made much of the concern about the overshoot in amplifiers with low open-loop bandwidth. However, it is clear that when an apples-apples comparison is done, the "overshoot" is really created by a major *reduction* in error as time progresses. The peak stress on the input stage is similar in both cases (7 mV and 10 mV, respectively), but the average stress is much larger in the case where open-loop bandwidth has been made large.

24.3   Spectral Growth Distortion

If distortion products are created in the forward path of an amplifier, negative feedback will feed these new frequencies back to the input stage, where they will have another opportunity to mix with the input signal where the nonlinearities in the forward path are encountered. This *reentrant* distortion mechanism was described by Baxandall [15]. The process creates new spectral lines at frequencies where none may have existed in the open-loop amplifier. For this reason it is convenient to refer to this mechanism as *spectral growth distortion (SGD)*.

Baxandall's Findings

If a forward gain path with only second-order distortion is enclosed by negative feedback and fed a 1-kHz signal, the output will "initially" include a 2-kHz component. When this component is fed back to the input, it will mix with the input signal at the second-order nonlinearity to create a 3-kHz signal as a result of the sum and difference process that characterizes a second-order nonlinearity. On the next go-round, a 4-kHz component will be created. Baxandall showed this phenomenon by analyzing a single-stage JFET amplifier with negative feedback around it. The JFET was chosen because it creates mostly second harmonic distortion. The open-loop second harmonic distortion in his experiment was quite high, on the order of 10%. A similar circuit for illustrating SGD is shown in Figure 24.2.

It is important to note that the concept of negative feedback going around and around the loop as illustrated above is a simplistic abstraction. If that abstraction is taken too literally, it can lead to erroneous conclusions. In practice, the negative feedback traverses the loop in nanoseconds, an amount of time that is insignificant compared to the period of any frequencies in the audio band. Figure 24.3 is a plot showing the amplitudes of the different harmonic distortion components as a function of amount of NFB. This data comes from SPICE simulations of the simple JFET circuit of Figure 24.2.

As the value of negative feedback is increased, the percentage of second harmonic goes down, as expected. However, the higher-order harmonics, which start out very low, grow with increasing amounts of negative feedback as expected by the heuristic remixing argument presented above. Interestingly, after the amount of NFB exceeds about 15 dB, all harmonics decrease with increasing amounts of NFB. So, over a range of conditions, the application of negative feedback did indeed create or increase higher-order distortion products. Baxandall's work raised legitimate concerns about the
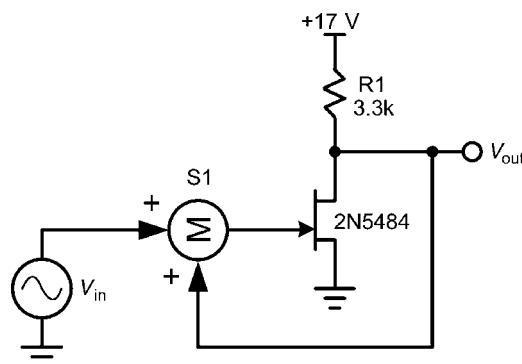
Figure 24.2   One-stage circuit for evaluating spectral growth distortion.
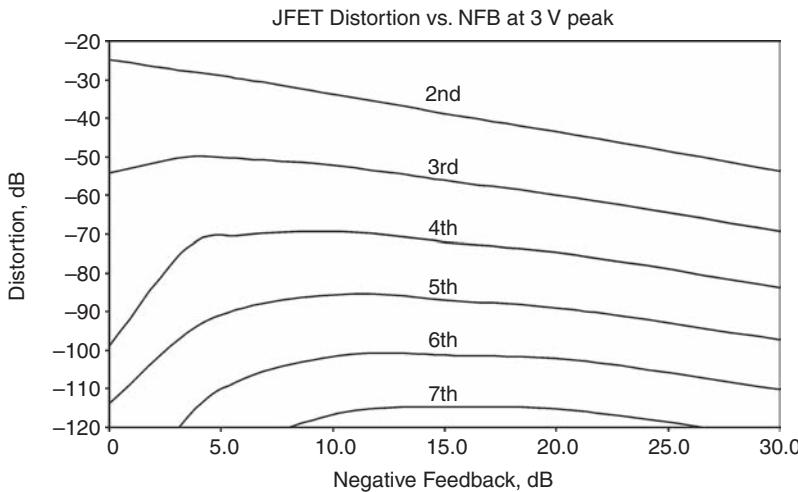
FIGURE 24.3 Harmonic distortion components versus amount of negative feedback.

distortion-reducing ability of negative feedback, and whether some benign distortion was being exchanged for less benign distortion.

Real-World Amplifiers

Baxandall's work was incomplete in that it only dealt with a single amplifier stage. Multistage amplifiers have a higher-order distortion characteristic due to the multiplication of individual characteristics that occur as the stages are cascaded.

Moreover, real circuits are not pure second order, but more often exponential. The BJT has an exponential characteristic that is naturally rich in high-order distortion components. Even real circuits implemented with square-law devices do not have a square-law characteristic. A JFET differential pair does not have a square-law characteristic. A class AB output stage certainly does not have a square-law characteristic. The bottom line is that real amplifiers have complex nonlinearities in their open loop to begin with. In many cases, any spectral growth that occurs may be smaller than these initial high-order products.

Baxandall was operating the JFET amplifier stage at a very high distortion level in order to demonstrate the point. Open-loop distortion was on the order of 10% in the single common-source stage he demonstrated. The effects described become much smaller at more reasonable operating levels, especially when one recognizes that the higher-order distortion products increase much faster with increases in signal level than the low-order products (e.g., fifth-order distortion products go up 5 dB for every dB increase in operating level.

Degeneration and SGD

SGD is not limited to global negative feedback. Indeed, Baxandall's experiment involved rather local feedback. It turns out that even emitter degeneration can be shown to exhibit the SGD Baxandall effect. A single-ended BJT amplifier stage exhibits spectral growth if its gain is reduced by applying NFB in the form of source degeneration, as shown in Figure 24.4.

Once the amount of total negative feedback exceeds about 20 dB the spectral growth stops and all orders of distortion decrease as feedback is increased. It is tempting
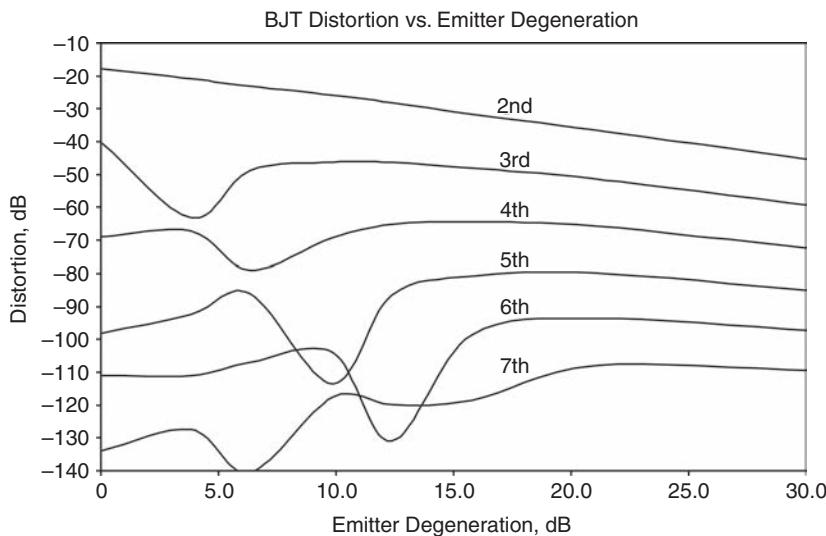
Figure 24.4   Harmonic distortion components versus amount of emitter degeneration NFB.

to generalize that this 20 dB number includes emitter degeneration or other local feedback. The existence of the SGD effect seems to make a good case for designing the amplifier for good open-loop linearity. The first 20 dB of feedback can be applied locally, typically as emitter degeneration, to get beyond the starting region of the SGD effect. The application of global negative feedback will then not be expected to cause any SGD.

SGD and Crossover Distortion

Crossover distortion is usually the biggest and most audible distortion in a properly designed amplifier. It starts out being rich in high-order products. Figure 24.5 shows
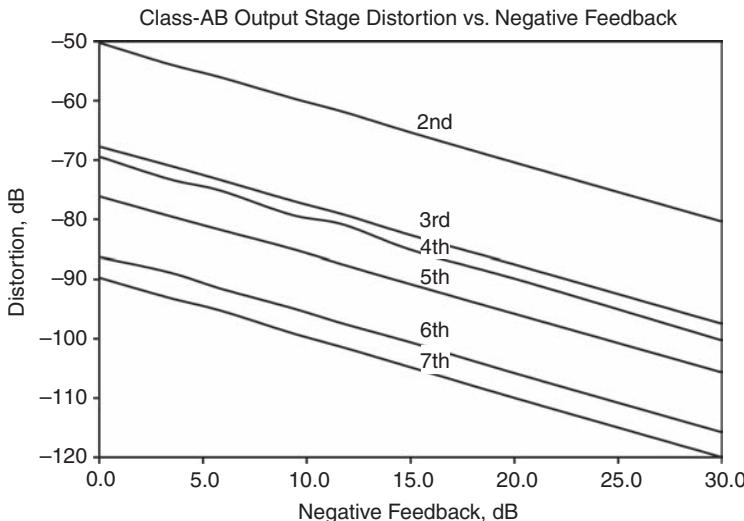
Figure 24.5   Harmonic distortion versus feedback for a class AB output stage.

that the application of NFB to an amplifier reduces all orders of crossover distortion, right from the beginning.

Although the Baxandall effect was an intriguing eye-opener, the audio community read too much into it, wrongly generalizing the results and asserting that feedback did not really reduce the net imperfection of the signal.

24.4   Global versus Local Feedback

Issues of open-loop bandwidth and frequency compensation largely pertain to global feedback loops that usually enclose virtually all of the amplifier stages. In contrast, local negative feedback rarely needs compensation and typically has very wide bandwidth. Emitter degeneration is a form of local negative feedback. Shunt feedback around a single stage is also local negative feedback.

Some who are opposed to the use of negative feedback are also opposed to the use of local feedback, but do not consider emitter degeneration to carry with it the supposed ills of negative feedback. Analysis shows that even emitter degeneration causes spectral growth distortion just like any other form of negative feedback.

24.5   Timeliness of Correction

Some critics of negative feedback argue that NFB represents an electronic attempt to correct an error after it has happened and that the finite time delay and sequence of events make the correction faulty. The electronic time-of-flight delay and phase delay due to feedback compensation do indeed exist, but these delays must be small in order for the circuit to be stable. In an amplifier with a 1-MHz unity-gain frequency the delay must certainly be less than 0.5 μs. This is 100 times smaller than the period of a 20-kHz sinusoid. This delay is merely a different way of recognizing that the distortion-reducing properties of negative feedback are less effective at very high frequencies. It does not suggest that negative feedback is failing to correct an error at 20 kHz.

24.6   EMI from the Speaker Cable

The speaker cable is a big antenna. The concern about negative feedback here is that EMI from the loudspeaker cable will get back to the input via the feedback path [16]. This concern is not completely unfounded. In fact, the use of a phase lead capacitor across the feedback resistor can make the input stage unnecessarily vulnerable to EMI that makes its way into the amplifier via the speaker cable. Such EMI will be attenuated by the shunting impedance of the output stage and by the feedback network before it arrives at the input stage. Nevertheless, this is a good reason to employ an input stage that has good signal-handling capability to high frequencies, such as a JFET stage or a well-degenerated BJT stage operated at a healthy bias current. Such an input stage is more resistant to EMI effects from the input port as well.

24.7   Stability and Burst Oscillations

An amplifier that does not employ global negative feedback does not need to be properly compensated (it does not need to be compensated at all) for global loop stability. Such amplifiers will tend to be less prone to burst oscillations due to global feedback loop instability. It is true that there are more possibilities to make a bad design with

negative feedback. Negative feedback is a powerful tool that can be abused. However, abandoning NFB does not ensure that a power amplifier will be free from burst oscillations. This is especially true of oscillations that can originate locally in the output stage.

24.8   Clipping Behavior

The use of global negative feedback does tend to alter the clipping behavior of an amplifier. It sharpens up clipping edges and makes the onset of clipping more abrupt. The use of Baker clamps in the amplifier design will make the abrupt clipping cleaner, but will usually not soften it. If you are going to clip your amplifier often, you may not want to use negative feedback. Guitar amplifier designers learned this many years ago. Soft clipping circuits can eliminate this problem by gradually clipping the input to the amplifier before the amplifier itself clips. Unfortunately, soft clip circuits are rare because they increase circuit complexity and they increase measured amplifier distortion at levels below clipping. It is notable that some amplifiers that do not employ negative feedback clip rather sharply as well.

References

1. Otala, M, "Transient Distortion in Transistorized Audio Power Amplifiers," *IEEE Transactions on Audio and Electro-acoustics*, vol. AU-18, pp. 234–239, September 1970.
2. M. Otala, and Leinonen, L., "The Theory of Transient Intermodulation Distortion," *IEEE Transactions on Acoustics, Speech and Signal Processing*, vol. ASSP-25, no. 1, pp. 2–8, February 1977.
3. Leach, W. M., "Transient IM Distortion in Power Amplifiers," *Audio*, pp. 34–41, February 1975.
4. Leach, W. M., "Suppression of Slew-rate and Transient Intermodulation Distortions in Audio Power Amplifiers," *J. Audio Eng. Soc.*, vol. 25, no. 7–8, pp. 466–473, July–August 1977.
5. Greiner, R. A., "Amp Design and Overload," *Audio*, pp. 50–62, November 1977.
6. Otala, M., "Feedback-generated Phase Modulation in Audio Amplifiers," 65th Convention of the Audio Engineering Society, preprint No. 1576, London, 1980.
7. Otala, M., "Conversion of Amplitude Nonlinearities to Phase Nonlinearities in Feedback Audio Amplifiers," *Proc. Of IEEE International Conference on Acoustics, Speek and Signal Processing*, pp. 498–499. Denver, CO, 1980.
8. Otala, M., "Phase Modulation and Intermodulation in Feedback Audio Amplifiers," 69th Convention of the Audio Engineering Society, preprint No. 1751, Hamburg, 1981.
9. Otala, M., and Lammasniemi, J., "Intermodulation Distortion in the Amplifier Loudspeaker Interface," 59th Convention of the Audio Engineering Society, preprint No. 1336, February 1978.
10. Leinonen, E., Otala, M., and Curl, J., "A Method for Measuring Transient Intermodulation Distortion (TIM)," *J. Audio Eng. Soc.*, vol. 25, no. 4, pp. 170–177, April 1977.
11. Leinon, E., and Otala, M., "Correlation Audio Distortion Measurements," *J. Audio Eng. Soc.*, vol. 26, no. 1–2, pp. 12–19, January–February 1978.

12. Cordell, R. R., "Another View of TIM," *Audio,* February–March, 1980; available at www.cordellaudio.com.
13. Cordell, R. R., "Phase Intermodulation Distortion–Instrumentation and Measurements," *Journal of the Audio Engineering Society,* vol. 31, March 1983; available at www.cordellaudio.com.
14. Cordell, R. R., "Open-loop Output Impedance and Interface Intermodulation Distortion in Audio Power Amplifiers," preprint No. 1537, 64th Convention of the AES, 1982; available at www.cordellaudio.com.
15. Baxandall, P. J., "Audio Power Amplifier Design–5," *Wireless World,* December 1978.
16. Thiele, A. N., "Load Stabilizing Networks for Audio Amplifiers," *J. Audio Eng. Soc.*, vol. 24, no. 1, pp. 20–23, January–February 1976.

This page intentionally left blank

Amplifiers Without Negative Feedback

Some designers eschew the use of negative feedback, while many others embrace it. There are two sides to this controversy, and both deserve exploration. In this chapter we'll look at the design trade-offs in amplifiers that use little or no negative feedback and discuss some approaches to high-quality implementations of these amplifiers.

The greatest focus here will be on amplifiers with no negative feedback of any kind, since this is the most difficult challenge. Amplifiers with no global negative feedback but with liberal use of local negative feedback (not enclosing the output stage) will also be discussed. Finally, although a bit off-topic, amplifiers with wide open-loop bandwidth will be discussed.

25.1 Design Trade-Offs and Challenges

The basic assumption here is that no-feedback amplifiers do not employ global negative feedback from the output of the amplifier. They may employ local negative feedback within the IPS, VAS, and driver circuits. However, some designers prefer a more strict definition of no-feedback and philosophically limit themselves to emitter degeneration. The challenges described here assume the more strict view of having no negative feedback.

The challenges in a *no-negative-feedback* (NNFB) amplifier design begin with the input stage. It must handle the full line-level signal swing with very low distortion. It will typically require a large amount of emitter degeneration to do this and noise will be increased as a result.

The VAS must be able to produce the full output swing of the amplifier with equally low distortion and with gain that is well defined by a load resistance. The substantial current swing required to drive the load resistance will create distortion. The large voltage swing at the output of the VAS may allow the Early effect to cause distortion as well.

The gain of most audio power amplifiers lies in the range of 20–30. The VAS gain must therefore be held at about 10–30 to allow at least unity gain for the input stage. This means that the VAS must be heavily degenerated; this may also increase VAS noise. Because the input stage gain will be typically small, much of the VAS noise will be referred back to the input, further compromising amplifier noise performance. Power supply noise making its way into the input stage and VAS will not be mitigated by

negative feedback, so inherent PSRR of these circuits must be high and the power rails must be very quiet.

The output stage is one of the most significant contributors to distortion in an amplifier, so any amplifier that does not include global negative feedback faces a big challenge here. Without feedback, it is especially important to minimize crossover distortion. The most straightforward way to do this is to use more pairs of output transistors optimally biased with fairly small emitter resistors. The amplifier will run hotter, but it will benefit from a larger class A region without *gm* doubling.

Beta droop in the output stage will cause signal-dependent loading on the VAS. This will cause distortion at the moderately high impedance output node of the VAS. For this reason, the current gain of the output stage must be made very high. An output Triple will provide adequate current gain, but four levels of output emitter followers (an output Quad) may be better able to minimize this distortion. The Early effect in the output transistors can also contribute distortion.

The damping factor in some NNFB amplifiers can be poor because there is no NFB to reduce output impedance. Fortunately, if more output pairs are used in combination with an output Quad, the damping factor will be good.

DC offset can be a problem for NNFB amplifiers because the amplifier gain will usually be maintained at its full value down to DC. In the absence of NFB, there is no feedback network shunt capacitor (often an electrolytic) to reduce gain down to unity at DC. Input stage DC offset is thus multiplied by the full gain of the NNFB amplifier. Moreover, because the input stage gain may be as low as unity in some designs, DC offsets in the VAS will add to offset problems. Strict adherence to the no-feedback philosophy rules out the use of a DC servo.

Input Stage Dynamic Range and Distortion

The input stage must handle the full input signal swing with generous margin so as not to distort. Large amounts of emitter degeneration are required and input noise characteristics may be compromised. It is very important to use balanced differential architectures to maintain good PSRR.

BJTs will usually perform better in this situation, but their input bias current and input noise current can exacerbate the DC offset problem and compromise SNR in some arrangements. Many prefer the sound of JFET inputs. In some cases JFET inputs are more resistant to EMI effects. However, the linearity of a JFET input stage is a bigger challenge. In some cases it is better to employ the JFETs as source follower buffers ahead of a BJT LTP.

Figure 25.1 shows a BJT and a JFET input pair. Each BJT emitter has a 650-Ω degeneration resistor to set the gain. This corresponds to a generous degeneration factor of 52:1. The degeneration resistors for the JFET pair are smaller, at 275 Ω because of the lower JFET transconductance.

Both stages have small-signal gain of 1.5 (to each side of the differential output) and tail current of 4 mA. Each stage has 2-kΩ load resistors to permit a theoretical maximum output of 8 V p–p on each side of the output. The nominal voltage drop across the collector resistors is 4 V. This eats into power supply headroom, and boosted supplies for the IPS and VAS are desirable in amplifiers like this. Figure 25.2 shows THD as a function of input level for each pair. Notice the substantially larger THD from the JFET pair. The JFET has smaller transconductance than the BJT for a given operating current, and
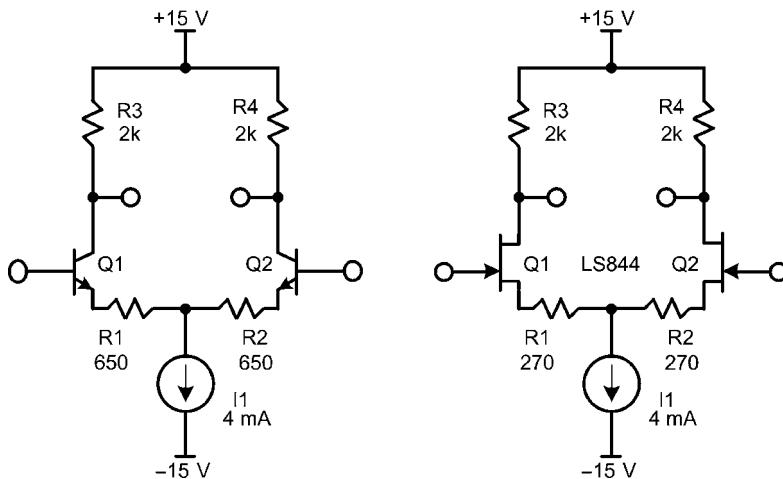
FIGURE 25.1   BJT and JFET input pairs each with a gain of 1.5 to one output.
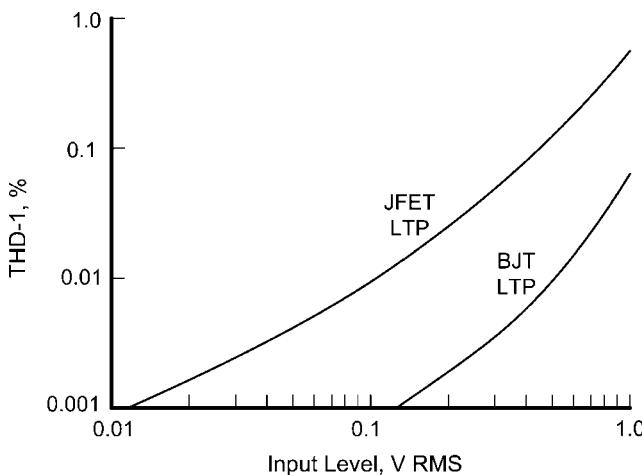
FIGURE 25.2   THD versus RMS input level for BJT and JFET input pairs.

so signal-dependent changes in transconductance of the JFET have a greater influence on incremental voltage gain of the stage. This results in higher distortion.

Whenever a large amount of emitter degeneration is used in an input stage, resistor noise is a concern. From Chapter 7 we know that resistor noise is:

$$E_n = 4.1 \text{ nV}/\sqrt{\text{Hz}}/\sqrt{\text{k}\Omega}$$

The total emitter-to-emitter resistance of the BJT pair is 1300 Ω, so the resistor noise contribution is 4.7 nV/$\sqrt{\text{Hz}}$. Simulation shows total input-referred noise of 5.8 nV/$\sqrt{\text{Hz}}$, reflecting additional smaller contributions from the transistors and load resistors. This is very good for a power amplifier, but input-referred VAS noise has not yet been considered.

For comparison, the simulated input noise of the JFET pair, using LS844 devices, is 5 nV/√Hz. Interestingly, the amount of resistance needed to degenerate the BJT LTP to the same transconductance as the JFET LTP makes the BJT circuit slightly noisier. Bear in mind that these simulations were done with zero-impedance input sources. Finite input source impedance will allow additional noise to be generated in the BJT case because of BJT input noise current.

JFET Input Buffers

The BJT IPS can be used while retaining its distortion advantage and eliminating its input current disadvantage by preceding both inputs with matched JFET source followers. The JFETs will add little noise in comparison to the noise of the degenerated BJT LTP and will eliminate DC input bias current and input current noise. This can actually mitigate DC off-set issues. Total input noise of this arrangement, shown in Figure 25.3, is 7.0 nV/√Hz.

Cascoding the Input Stage

It is especially desirable to employ a cascoded input stage to achieve better PSRR. Moreover, further reduction in common-mode input stage distortion can be had if the cascode bases are driven with a replica of the input common-mode signal so as to minimize the effects of common-mode nonlinearities.

Gain Allocation

Another issue that makes for difficulty in designing NNFB amplifiers is what to do with all the VAS gain. It is actually difficult to get that gain down. Shunting resistive loads are often used on the VAS output node to control the gain. This makes the VAS work harder and increases distortion. Large amounts of emitter degeneration are also often used in the VAS to control gain and reduce distortion. If local negative feedback is permitted, it can be used quite effectively to rid the VAS of much excess gain without compromising its distortion characteristics.

The forward gain in an amplifier without global negative feedback must be carefully controlled and allocated. Overall, best performance is achieved if the gain of the amplifier is made to be on the high side. A gain of about 30 is a good number. A simple
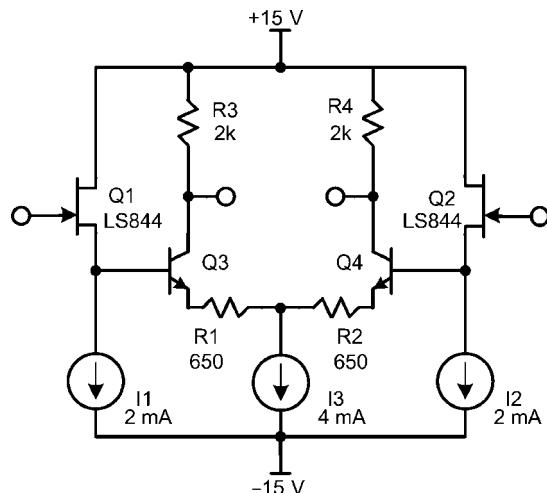
FIGURE 25.3   A BJT input stage preceded by JFET source followers.

allocation sets a differential gain of three in the input stage (1.5 to each output side) and a gain of 10 in the VAS.

Controlling VAS Gain

Achieving a gain of only 3 in the input stage is not difficult, but achieving a gain of only 10 in the VAS requires large emitter degeneration resistors if the VAS collector load resistor is to be of a reasonable value. The key challenge with the VAS is to achieve the large voltage swings with controlled gain and low distortion. Resistively loading the VAS output node to ground is necessary in designs that use no negative feedback of any kind. The changes in transistor current needed to create the large signal across the VAS load resistor tend to increase VAS distortion.

Consider the simple VAS of Figure 25.4a. It consists of a differential pair loaded by a current mirror. The differential-to-single-ended gain of the VAS is set to 10. The net load resistance on the single-ended output of the VAS is 10 kΩ. The quiescent bias of the top and bottom VAS transistors is 10 mA. This means that 20 mA can be driven into the 10-kΩ load resistance, producing a theoretical output voltage of 400 V p–p were it not for rail voltage limiting. A 100-W amplifier requires 80 V p–p. This means that the swing margin is 5:1. Only 1/5 of the theoretical swing is actually used; this means that the
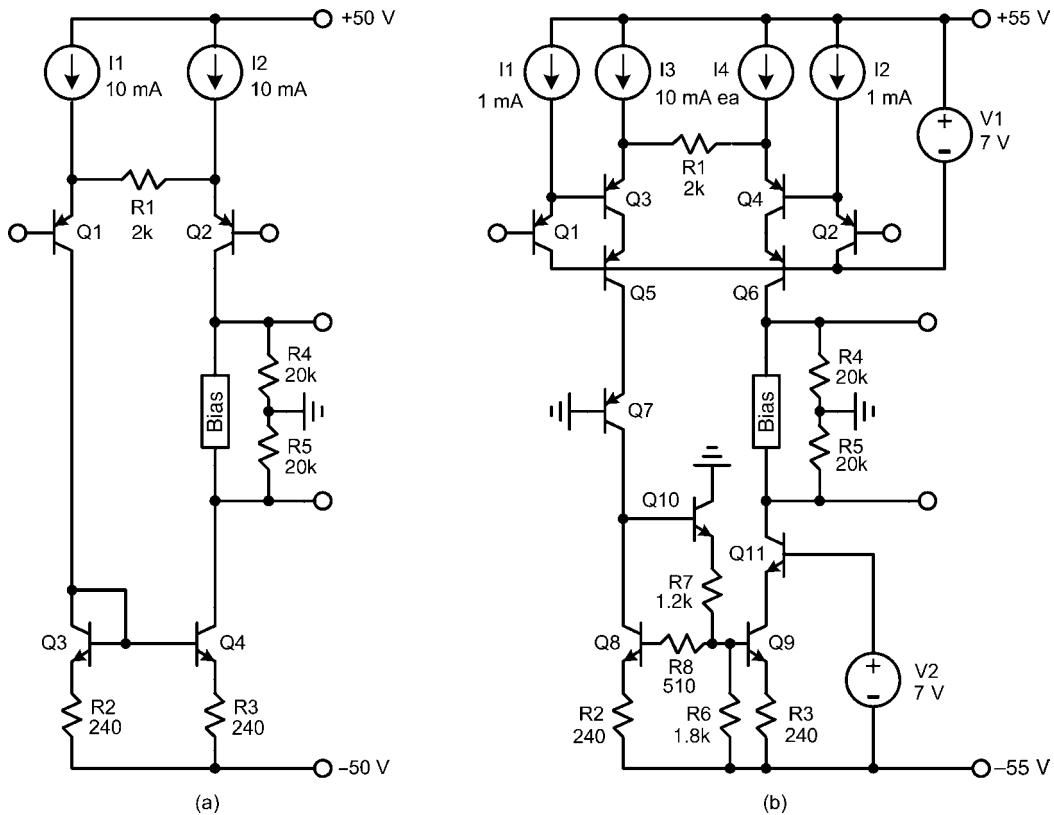
FIGURE 25.4 (a) A suitable VAS with a gain of 10. (b) An improved version.
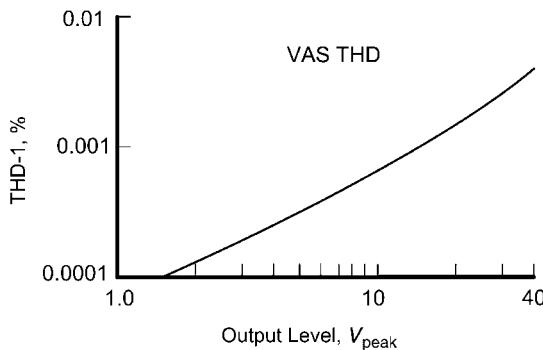
FIGURE 25.5   THD of the VAS of Figure 25.4b.

operating currents change by only 20% to generate the actual needed output swing. This reduces distortion due to current variations in the transistors.

To achieve a gain of only 10 to the single-ended output, a differential emitter degeneration resistance of 2 kΩ is required. The use of the twin emitter current source arrangement makes this possible without incurring very large DC drops across the emitter degeneration resistors that would be employed in a conventional circuit.

An improved practical version of the VAS is shown in Figure 25.4b. Input emitter followers have been added to isolate the VAS from the input stage and make loading on the input stage very light. The differential pair and the current mirror have been cascoded to reduce Early effect distortion. A second cascode has been added on the side driving the current mirror to equalize nominal quiescent collector voltages and power dissipations of the upper stage. Distortion of this VAS as a function of peak output signal level is shown in Figure 25.5. Simulated THD-1 at a peak output of 40 V is less than 0.004%.

VAS distortion can be strongly influenced by the types of transistors used. KSA 1381 devices were used for Q5, Q6, and Q7. KSC3503 devices were used for Q8, Q9, and Q11. These transistors have a very high Early effect figure of merit.

DC offset in the VAS can also be problematic for amplifiers that do not employ negative feedback or DC servos. This is partly a result of the high product of quiescent current and load resistance combined with relatively low VAS voltage gain. Even when precision resistors are used, current lost due to finite beta in Q7 and Q11 can result in DC offset. This effect is mitigated by base resistor R8. It introduces a beta-dependent voltage drop that creates a compensating offset current. The compensation is a crude approximation, but it is helpful. Resistor R7 causes the base-collector voltage of Q8 to be closer to that of Q9.

VAS Noise

With input stage differential gain of only 3.0, VAS noise must be considered. There are numerous contributors to VAS noise in the design of Figure 25.4b. Input-referred noise of the VAS is about 26 nV/√Hz, contributing about 8.8 nV/√Hz to amplifier input noise. This actually exceeds the noise contribution of the input stage. Unfortunately, DC compensation resistor R8 and transistor Q8 (as a result of R8) are the largest contributors here. Their contributions can be reduced if R8 is bypassed with a 10-μF capacitor. This will reduce total VAS noise by about 3 dB. The bypass capacitor also causes a slight

reduction in VAS distortion. Bear in mind that when I3 and I4 are replaced with real current sources, additional noise will be introduced.

To put this in perspective, I consider any amplifier with input noise less than 10 nV/√Hz to be very good.

Amplifiers with Local Negative Feedback

If local negative feedback is permitted, one can control the VAS gain with feedback and many of the design challenges are mitigated. The local feedback also makes the VAS stage more linear and reduces its output impedance. Local shunt feedback in the VAS would be an example of this. If local feedback is also extended to the input stage, dynamic range problems there will also be reduced, although then opportunities for balanced inputs may be diminished. Such *local* feedback encompassing more than one stage may have to incorporate frequency compensation. Such frequency compensation can be much lighter, however, since a higher closed-loop bandwidth is allowable when the slower output stage is not enclosed.

Output Stage Distortion

The class AB output stage is often the single largest source of distortion in any amplifier, whether global negative feedback is used or not. In amplifiers with no negative feedback, it is desirable to use an output stage with a large number of output pairs. This will provide a fairly large class A region and will reduce crossover distortion by reducing the nonlinear output impedance of the stage. Good thermal stability can be achieved by employing ThermalTrak™ output transistors. This may permit the use of smaller emitter resistors and correspondingly higher quiescent current, further reducing crossover distortion.

Four output pairs employing 0.15-Ω emitter resistors will have a total quiescent bias current on the order of 650 mA when optimally biased. The amplifier will be able to supply 1.3 A peak before exiting the class A region, corresponding to almost 7 W into 8 Ω. A 200-W version of such an amplifier with 65 V rails will dissipate about 85 W at idle. Figure 25.6 shows simulated THD-20 for the BJT output stage described here when driving 8-Ω and 4-Ω loads. 2.2-Ω base stopper resistors were used. Open-loop output stage distortion at 20 kHz is less than 0.1% when operating at 400 W into a 4-Ω load.
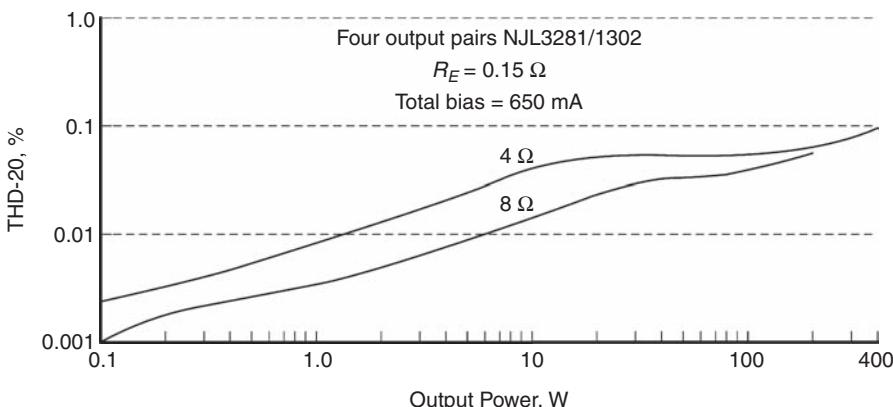
Figure 25.6   THD-20 versus level for a 200-W BJT output stage. (a) Driving 8 Ω. (b) Driving 4 Ω.
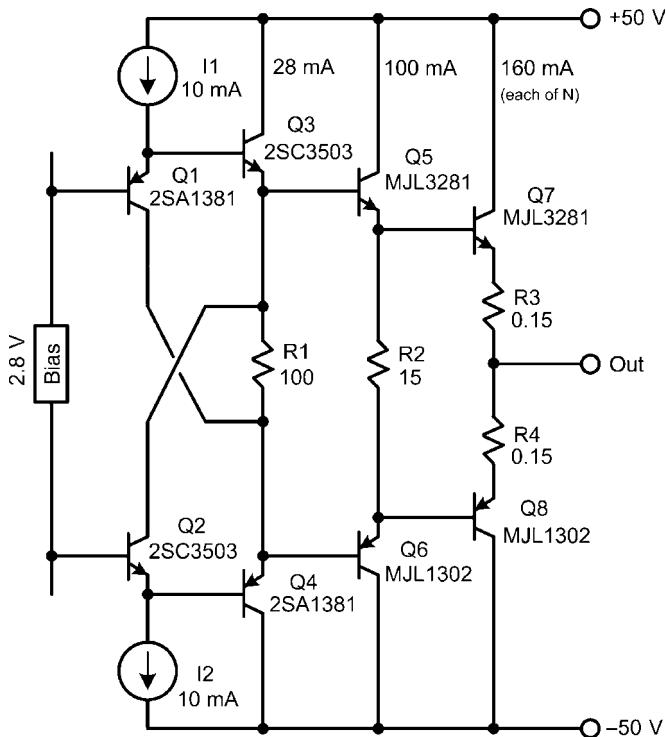
FIGURE 25.7   A BJT output Quad including a diamond buffer.

The output stage should be at minimum a Triple so as to present an extremely light load to the VAS. A Quadruple including a diamond driver may be helpful here. High current gain in the output drivers is also important in minimizing the output impedance of the amplifier. In essence, we want the output impedance to be entirely governed by the output transistor circuit, as if it were being driven by a voltage source instead of a VAS. This also means that the use of large base stopper resistors on the output and driver transistor bases should be avoided to the extent possible.

An output stage Quad using a diamond buffer to drive four output pairs is illustrated in Figure 25.7. Only one output pair is shown for clarity. Q1 and Q3 should be TO-126 devices bolted together to improve bias stability in the cancellation of their V_{be} drops. The driver transistors Q5 and Q6 are also ThermalTrak™ power devices.

Early effect in the emitter follower output stage should be minimized to reduce non-linearity and provide good rejection from the main power supply rails. For this reason, it is advantageous to cascode the output stage. This will cost headroom. It is also desirable to maintain a decent value of V_{ce} for the output transistors. This translates to a further price paid in amplifier power dissipation and need for higher power supply voltages.

MOSFET Output Stages

The use of MOSFET output transistors will result in somewhat more distortion in the NNFB amplifier because it is difficult to achieve adequate linearity in view of the transconductance droop problem. Nevertheless, four vertical MOSFET pairs with each pair biased
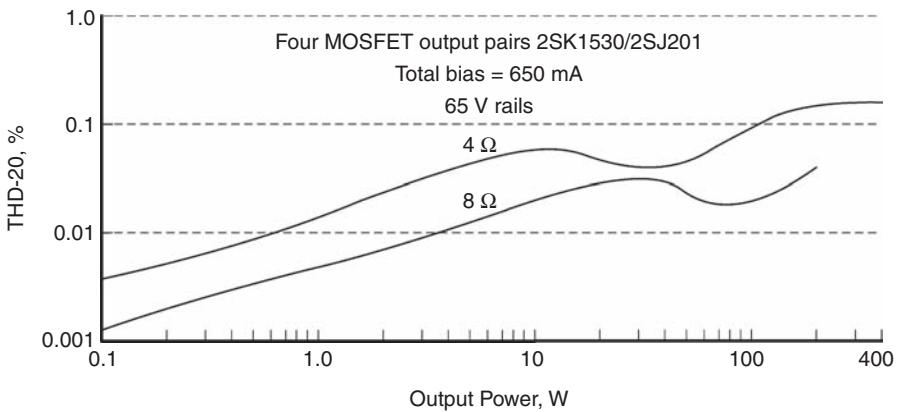
FIGURE 25.8 THD-20 versus level for a 200-W MOSFET output stage. (a) Driving 8 Ω. (b) Driving 4 Ω.

at 165 mA will be able to remain in the class A region up to a peak output current of 1.3 A, corresponding to about 7 W into 8 Ω. The transconductance of each MOSFET will average about 0.7 S at 165 mA, so the eight devices will provide total *gm* of about 5.6 S at the crossover point, corresponding to an output impedance of about 0.18 Ω.

Figure 25.8 shows simulated THD-20 for the MOSFET output stage described here when driving 8-Ω and 4-Ω loads. EKV models were used for the 2SJ201 and 2SK1530 power MOSFETs. Rail voltages of ±64 V are assumed. The MOSFET output stage is driven by a diamond buffer and includes asymmetrical source resistors for distortion reduction. The source resistors for the N-channel devices were 0.33 Ω, while those for the P-channel devices were 0.15Ω . Open-loop output stage distortion at 20 kHz is about 0.16% when operating at 400 W into a 4-Ω load. This is only 1.6 times that of the BJT stage described earlier, with both designs operating at the same bias current.

If bias current is increased to 250 mA per MOSFET and source resistances are reduced to 0.22 Ω and 0.1 Ω, THD-20 falls below 0.09%. The output stage will then dissipate 130 W under idle conditions.

Damping Factor

An amplifier without global negative feedback will tend to have higher output impedance because there is no impedance-reducing feedback involved. Achieving low output impedance first requires that there be large enough output stage current gain to make sure that VAS output impedance is completely inconsequential in determining output impedance. Consider a VAS with 10-kΩ output impedance paired with a total output stage current gain of 125,000 (a Triple with current gain of 50 in all transistors). The output impedance resulting from the VAS contribution will be 10 kΩ/125,000 = 0.08 Ω, corresponding to DF = 100. This is just on the border of acceptability, especially recognizing the likelihood of beta droop effects that will introduce nonlinearity into this impedance. A Quad, with four levels of emitter followers, can be used to provide enough additional current gain to take VAS output impedance completely out of the picture. The first two stages of the Quad can be realized with a diamond buffer as shown in Figure 25.7.

Once VAS output impedance effects are dealt with, the remainder is largely the output impedance from the output emitter resistors and output transistor intrinsic output impedance. The best approach here is to use a large number of output pairs in parallel, each with a fairly low-value emitter resistor of 0.15 Ω. Four output pairs, each

with R_E = 0.15 Ω and biased at 165 mA, will yield an output impedance contribution of about 0.038 Ω, corresponding to a healthy damping factor of 210.

The effect of intrinsic base resistance in the output transistors should not be neglected. A 4-Ω base resistance combined with a beta of 50 will result in 0.08 Ω of additional emitter resistance. An additional 4 Ω of base resistance in the form of a base stopper resistor will double this contribution. At high output current, where re' can be neglected, the actual output impedance could approach 0.3 Ω per pair when the 0.15-Ω emitter resistance is added to the effective emitter resistance. This underscores the need for output transistors with high current gain and minimal beta droop. Notice that the use of a larger number of pairs to reduce output impedance has the secondary effect of reducing beta droop effects. If the NPN and PNP output transistors have different amounts of intrinsic base resistance, it may be helpful to compensate for this by using slightly different values of base stopper resistance for the NPN and PNP output transistors.

Power Supply Rejection and Power Supply Design

Without negative feedback the amplifier is more vulnerable to power supply ripple and noise. For this reason, the circuits must be designed to have inherently high PSRR. This can be achieved by the use of a fully balanced design and liberal use of cascode stages. It is also important to have a very quiet power supply. The input and VAS stages should be fed with supply rails that have been filtered by capacitance multipliers. The extra headroom needed by these circuits dictates that boosted rails should be used to supply the IPS-VAS for best performance.

Output stage PSRR is often ignored in designs that use negative feedback. It cannot be ignored when global negative feedback is absent. Although it is intuitive that a simple emitter-follower stage would have good PSRR, the Early effect can degrade it. Fluctuations on the rail will modulate transistor beta and V_{be}, causing noise ingress. The consequences of the Early effect can be reduced (but not eliminated) by feeding the output transistors from a very low-impedance driver.

Beware that the Early effect will act on all three transistor stages in a Triple, causing a β^3 effect. At minimum, the collector rails of the predriver and driver transistors should receive extra R-C filtering.

A very high quality no-feedback amplifier should incorporate a capacitance multiplier filter into the main rails for the output stage if a cascoded stage is not used. This involves a cost in power supply headroom and amplifier power dissipation. It is also important to minimize the amount of magnetic induction noise and nonlinearity from the output stage half-wave rectified currents. Having a large class A region helps to reduce the production of such noise at small signal levels where it will not be masked by program material.

DC Offset

Without negative feedback there will be little correction for DC offset. It will be amplified by the full amount of the amplifier gain. We assume here that the use of a DC servo violates the mandate of no negative feedback. A fundamentally DC-stable design must be used, and some amount of offset trimming may be required. Although JFETs have a higher DC voltage offset than BJTs, they are likely to be better in regard to DC offset overall because they do not require input bias current. It is also possible to choose well-matched JFET input pairs. As mentioned earlier, DC offset and DC offset drift contributed by the VAS can also be problematic.

Balanced Inputs

Balanced inputs are naturally available by the balanced input of the degenerated LTP because it has no negative feedback connection to the opposite side. When balanced inputs are used, there is no common-mode signal at the input LTP.

25.2   Additional Design Techniques

Here we discuss some additional circuit techniques that can further improve the performance or versatility of an NNFB amplifier.

A Complementary IPS-VAS

The complementary IPS with unipolar JFETs described in Figure 7.13 can form the basis of a fully complementary IPS-VAS for an NNFB amplifier. As shown in Figure 25.9, the IPS employs BJT input transistors instead of JFETs. This keeps the distortion low. JFET source followers at the inputs provide very high-input impedance and freedom from input-bias current. The differential input stage operates at an equivalent tail current of 4 mA. The IPS can include a DC offset trim in the base circuit of the downward-firing PNP cascodes. The top and bottom differential outputs are resistively loaded and applied to LTP VAS stages through emitter follower buffers. The differential VAS stages employ twin 20-mA current sources with generous degeneration as described earlier. Output cascodes provide freedom from Early effect distortion.
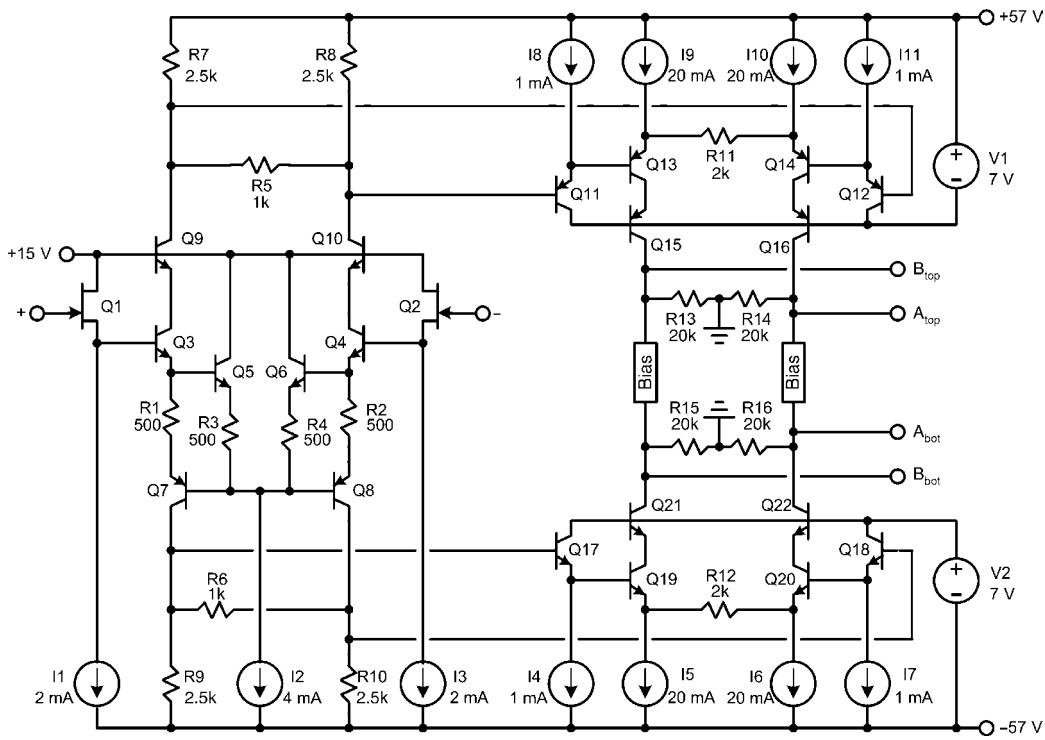
FIGURE 25.9   A complementary IPS-VAS for a balanced NNFB amplifier.

This VAS provides full-swing outputs of opposite polarity for free. These can be used to drive a pair of output stages to provide a balanced output. This configuration can have advantages in the way power supply current is used. It also provides four times the output power for given power supply rail voltages. Balanced output arrangements like this are especially easy to implement in no-feedback amplifiers.

The Cascomp Input Stage

The cascomp stage shown in Figure 25.10 is a low-distortion configuration often used with bipolar transistors. The circuit was designed for use in oscilloscopes where wide bandwidth and high linearity is required [1]. The cascomp linearizes the LTP by taking account of the nonlinear difference signals across the LTP emitters and injecting a compensating signal to cancel those differences. A cascode stage placed above the LTP creates a replica of these nonlinear differences. Across its emitters appear the same base-emitter signals, with their nonlinearities, as appear across the LTP emitters.

A second differential pair amplifies the difference of these nonlinear emitter signals and injects a correction signal at the collectors of the replica cascode in the opposite phase, using crossed collector connections. A second cascode stage above the replica cascode can optionally be incorporated to achieve high-voltage tolerance and improved power supply rejection. The cascomp architecture described here is a form of error feed-forward. A replica of the error is measured and then fed forward and added to the output to cancel the original error. Figure 25.11 compares THD versus output level for a conventional differential pair
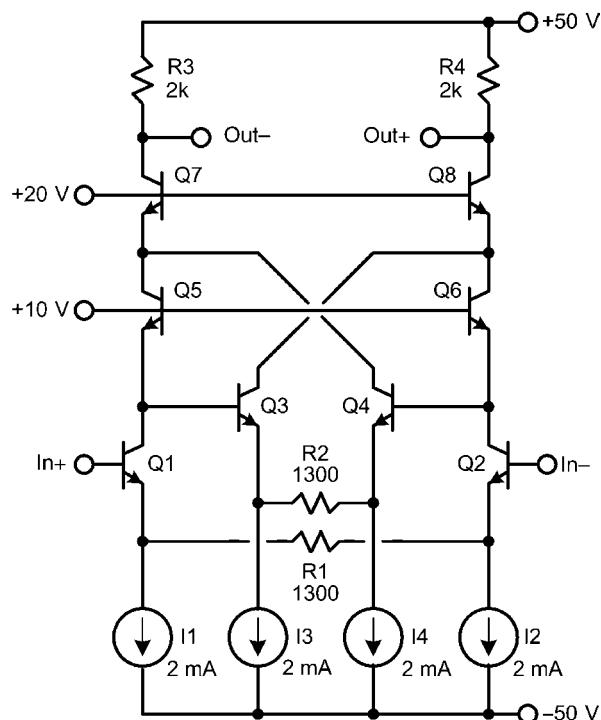
FIGURE 25.10 The Cascomp differential input stage.
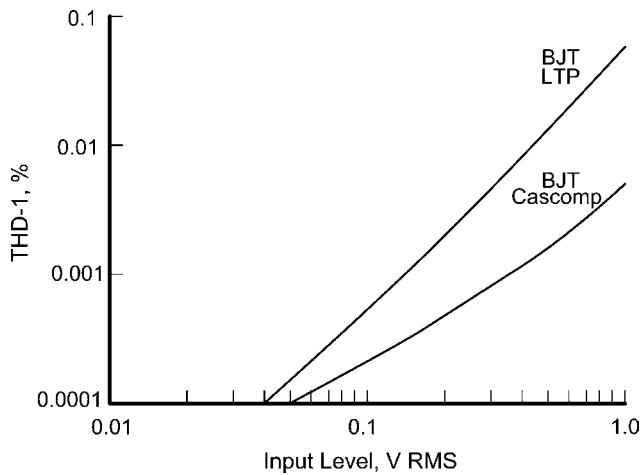
FIGURE 25.11 Cascomp THD versus differential pair THD.
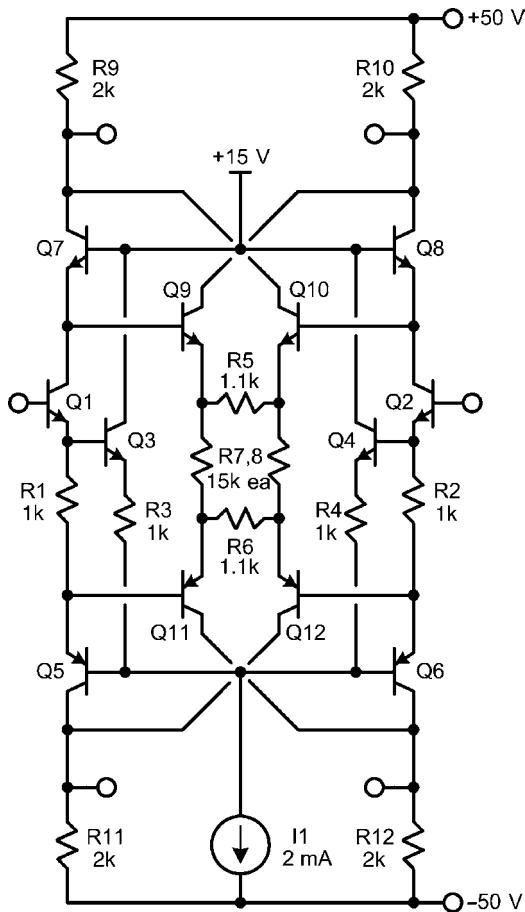
FIGURE 25.12 Complementary Cascomp input stage.
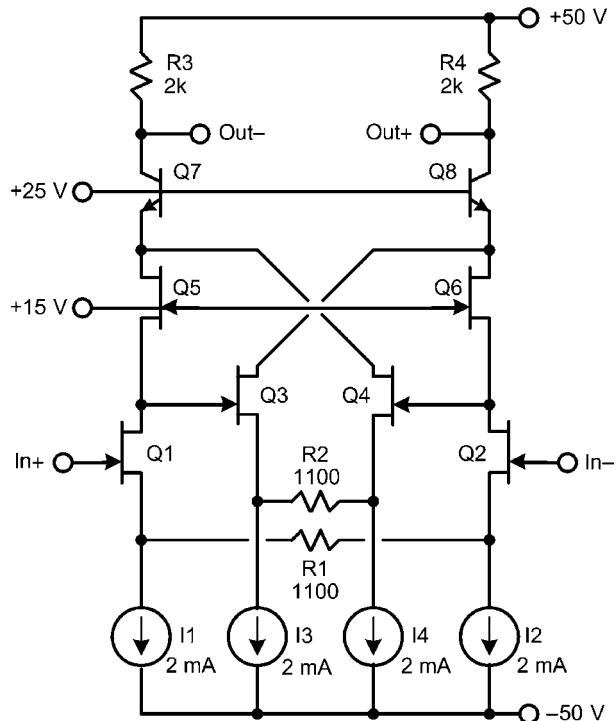
Figure 25.13   A JFET Cascomp.

and a cascomp, each with the same amount of emitter degeneration. The cascomp reduces distortion by a remarkable factor of 10 at high signal levels.

The cascomp technique can also be applied to complementary input stages, including the floating complementary IPS of Figure 25.9. This is illustrated in Figure 25.12. Q9 and Q10 perform the normal cascomp function while Q11 and Q12 harvest the correction current and add it to the bottom complementary circuitry.

The cascomp cell can also be used with the differential VAS stages illustrated in Figure 25.4. This can mitigate the VAS nonlinearities caused by the current swings necessary to drive the VAS load resistors.

Figure 25.13 illustrates a JFET cascomp input stage. I have not seen this used before. Although the gate-source voltage nonlinearities are different than base-emitter nonlinearities, the same error correction concept can be applied. All three JFET pairs should be matched to each other for best distortion cancellation. The JFET cascomp reduces distortion by a factor of over 6:1 at high signal levels. It may provide sufficient linearity to allow the use of JFETs instead of BJTs in input differential pairs where distortion must be kept very low.

25.3   An Example Design with No Feedback

Figure 25.14 shows a fully balanced 200-W amplifier that uses no negative feedback. This design is based on the principles discussed above. It employs the complementary IPS-VAS arrangement of Figure 25.9. The gain of the amplifier is 30. The IPS-VAS front
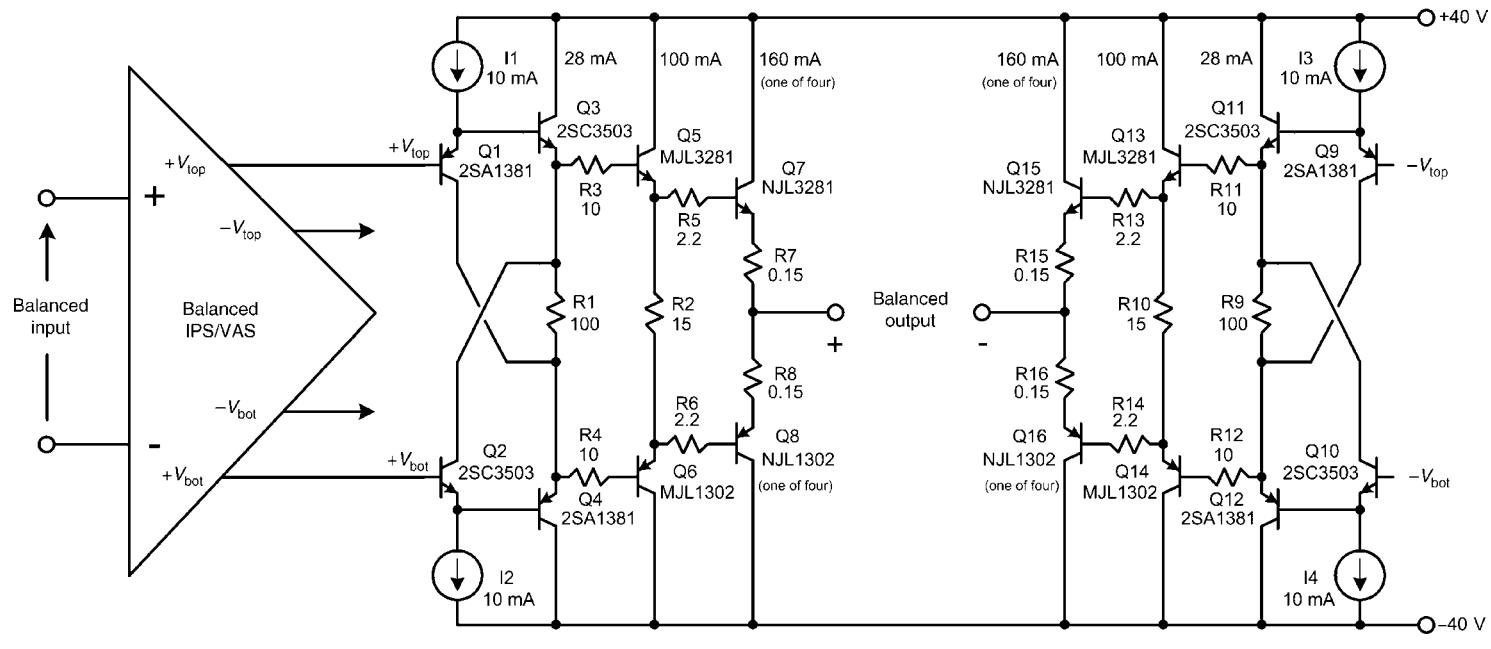
FIGURE 25.14 A 200-W balanced amplifier without negative feedback.

end is shown as a block in Figure 25.14, as it is the same as that illustrated in Figure 25.9. The bias spreaders are omitted for simplicity, but their design follows the approach described in Chapter 14 for use with ThermalTrak™ transistors.

Each of the two output stages uses four pair of ThermalTrak™ output transistors, each pair employing 0.15-Ω emitter resistors and biased at 163 mA for a total of 650 mA. With 40-V power rails, total idle dissipation is 104 W. The driver for each output stage is a Quad that includes a diamond driver as illustrated in Figure 25.7.

25.4   A Feedback Amplifier with Wide Open-Loop Bandwidth

It is often said in the low-feedback camp that amplifier open-loop bandwidth should be greater than 20 kHz. It has been shown that doing so does not reduce TIM or other distortions as long as closed-loop bandwidth and slew rate are held the same [2]. Nevertheless, some say that wide open-loop bandwidth sounds better, so we will discuss ways to achieve it.

Notice that this is not the same as designing an amplifier that makes minimal or no use of negative feedback. High amounts of negative feedback at 20 kHz and wide open-loop bandwidth are not mutually exclusive. In some of the approaches here we will make liberal use of local feedback and will also use as much global negative feedback as allowed by the chosen closed-loop bandwidth and stability criteria.

Achieving Wide Open-Loop Bandwidth

Wide open-loop bandwidth is often achieved by shunting the output of the VAS with resistances to ground. This makes the VAS work harder and increases distortion.

A much better way to limit the VAS bandwidth is to control it in a way that is analogous to the operation of the compensation capacitor. This means that it is controlled with negative feedback. In the IPS-VAS arrangement used in Ref. 3 and shown in Figure 7.16, this means tapping off a midpoint voltage across the bias spreader (or after the predriver emitter followers) and feeding back the signal with a resistor to the inverting input of the IPS, in parallel with the compensating capacitor. This is somewhat like using global negative feedback that does not enclose the output stage. Note also that we can vary the DC voltage at the tap-off point with a pot as a trimming adjustment of DC offset in the event that we choose not to use a DC servo.

With wide open-loop bandwidth at every point in the circuit, voltages and currents remain in phase at all points in the circuit. The error signal is also largely in phase with the input signal. In the IPS-VAS arrangement of Ref. 3, this can be accomplished by including a light shunt resistance across the collectors of the IPS cascodes. In addition, the load presented to the VAS by the resistive bandwidth-controlling feedback path is made low enough to keep the inherent stand-alone bandwidth of the VAS larger than 20 kHz.

A 200-W MOSFET Design

The design is shown in Figure 25.15. The open-loop bandwidth is set to 40 kHz, and the gain crossover frequency is set to 2 MHz. This would normally mean 34 dB of NFB up to 40 kHz. However, some mild increase in the slope of the open-loop frequency roll-off is used to make the open-loop response a closer approximation to linear phase in the upper part of the audio band. This slightly steeper roll-off provides a bit more feedback at
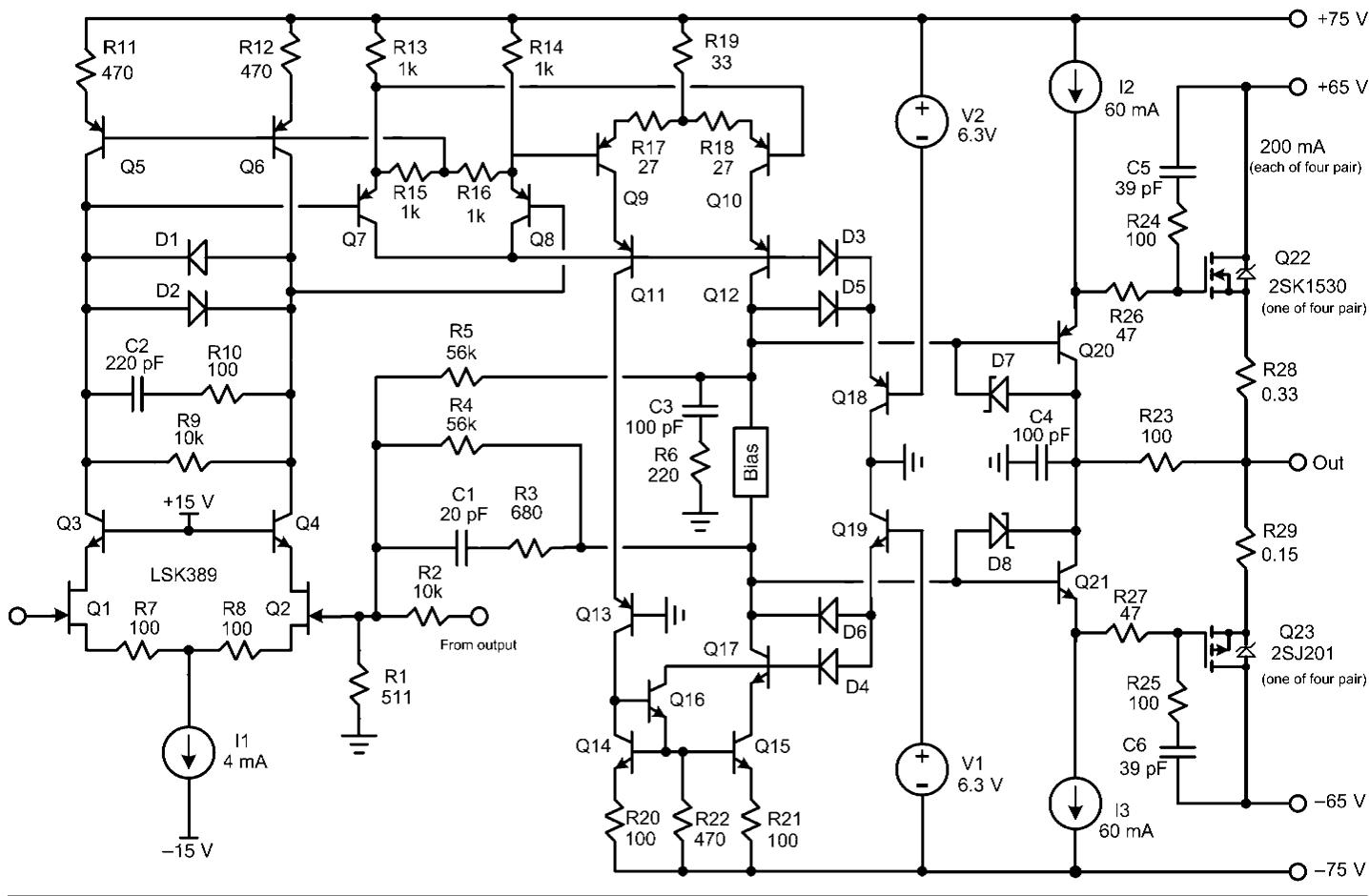
FIGURE 25.15 A MOSFET feedback amplifier with 40-kHz open-loop bandwidth.

40 kHz without introducing the overshoot that is usually associated with two-pole compensation. The output stage employs four pairs of vertical MOSFETs (2SJ201/2SK1530). Each pair is biased at 200 mA and optimized asymmetric source resistors are employed.

References

1. Quinn, P.A., "Feed-Forward Amplifier," U.S. Patent 4,146,844, March 27, 1979.
2. Cordell, R. R., "Another View of TIM," *Audio,* February–March, 1980; available at www.cordellaudio.com.
3. Cordell, R. R., "A MOSFET Power Amplifier with Error Correction," *Journal of the Audio Engineering Society,* vol. 32, January 1984; available at www.cordellaudio.com.

Balanced and Bridged Amplifiers

Balanced is beautiful–that's what a mentor of mine told me many years ago. In this chapter three aspects of differential operation of power amplifiers will be discussed. Single-ended power amplifiers that have balanced inputs will first be considered. These are the most common variant of differential operation in consumer audio. Most of these can also accommodate a single-ended input as well.

Bridged amplifiers will next be discussed. These amplifiers are actually best referred to as bridge-connected amplifiers, as they are usually composed of a stereo pair of amplifiers that are fed the same signal but fed in opposite phase. Twice the voltage is available across their output terminals, so in this configuration they can supply four times the power into a given load impedance. Some of these amplifiers can be configured to accept balanced inputs as well.

Balanced amplifiers will finally be discussed. These are much like bridged amplifiers, and differences will be highlighted. In some cases, amplifiers that are called balanced amplifiers are merely what used to be called bridged amplifiers. The term balanced is much more appealing than the term bridged.

26.1 Balanced Input Amplifiers

Most professional, and a number of hi-end audio power amplifiers incorporate balanced inputs using XLR connectors with pin 2 hot. This provides for improved rejection of external common mode noise.

Achieving balanced inputs for a single-ended (SE) power amplifier is not always straightforward, especially if the highest sound quality is to be maintained and if the amplifier must allow the user to operate the amplifier with either XLR balanced inputs or RCA single-ended inputs (with or without the need for a mode switch).

Gain and Input Impedance Considerations

Other important considerations include the gain of the amplifier in the two modes and the input impedance of the amplifier in the two modes. In particular, in the balanced input mode it is especially desirable that both the positive and negative inputs of the amplifier have the same input impedance so as to maintain the best possible common-mode rejection in the presence of finite driving impedances from the source.

Often, the incorporation of a balanced input capability will involve the introduction of additional circuitry and possible compromise of the signal-to-noise ratio of the
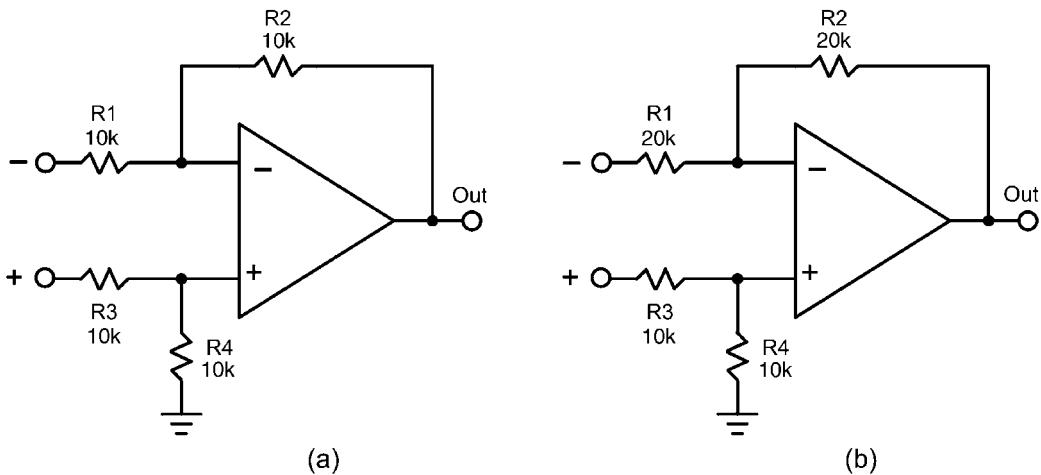
FIGURE **26.1**   Single op-amp differential-to-single-ended input circuits.

amplifier. In high-end applications, it is sometimes frowned on to use an op-amp, which is the obvious and easy choice in implementing a balanced input capability.

Single and Triple Op-Amp Solutions

An op-amp can be used to implement a differential-to-single-ended converter, as shown in Figure 26.1a. Notice that this circuit presents different load impedance to single-ended sources on the positive and negative inputs. A single-ended source on the positive input sees an input impedance of 20 kΩ. A single-ended source on the negative input sees an input impedance of 10 kΩ. A common-mode source sees 20 kΩ on each side for a net of 10 kΩ. If the source impedance on both sides of the source is the same, common-mode rejection will be acceptable if resistor tolerances are tight.

In Figure 26.1b the resistor values are chosen so that the positive and negative inputs exhibit the same input impedance to a single-ended source (the resistors on the inverting side have been doubled to 20 kΩ). However, when a balanced signal is applied (with each of its signals referenced to ground at the source), the signal current flowing in the plus and minus inputs is not the same. Similarly, if a common-mode signal is applied to both inputs, the current flowing into the positive input is larger than the current flowing into the negative input. This happens because the virtual short at the op-amp inputs forces 1/2 of the voltage at the positive input to appear at the negative terminal of the op-amp. Because most balanced sources are symmetrically referenced to ground, this imbalance can cause undesired effects. If the positive and negative source impedances are not identical, common-mode rejection (CMRR) will suffer.

The single op-amp solution also forces a compromise between input impedance and noise. The circuit as shown has single-ended input impedances of only 20 kΩ and yet puts 20-kΩ resistors in the signal path, generating noise. The 20-kΩ input impedance also forces the use of large-value input-blocking capacitors if they are to be used.

The three op-amp instrumentation amplifier shown in Figure 26.2 does not have these limitations. It can be used to achieve high common-mode rejection and symmetrical input impedances under all drive conditions. It also provides high input impedance while allowing the use of relatively low-value resistors in its implementation. However,
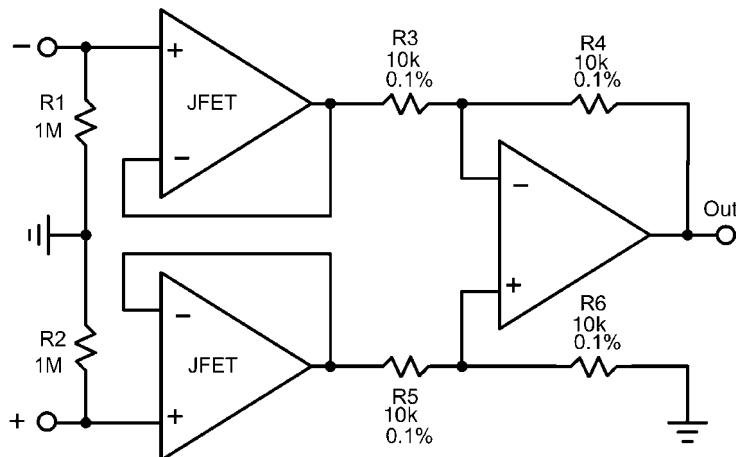
FIGURE 26.2   Triple op-amp instrumentation amplifier.

the circuit is more complex, and concerns about passing the signal through multiple op-amps are magnified.

The circuit is composed of unity-gain input buffers followed by a differential-SE converter with a gain of 1. Very high input impedances can be obtained by using low-noise JFET op-amps for the input buffers. The resistors surrounding the third op-amp should have 0.1% tolerance in order to maintain high CMRR.

Configuring the Power Amplifier as a Differential Amplifier

Another approach is to configure the main amplifier itself as a differential input ampli-fier in a way analogous to that of Figure 26.1a. This is illustrated in Figure 26.3a. Unfor-tunately, this results in relatively low input impedance on the inverting side because the
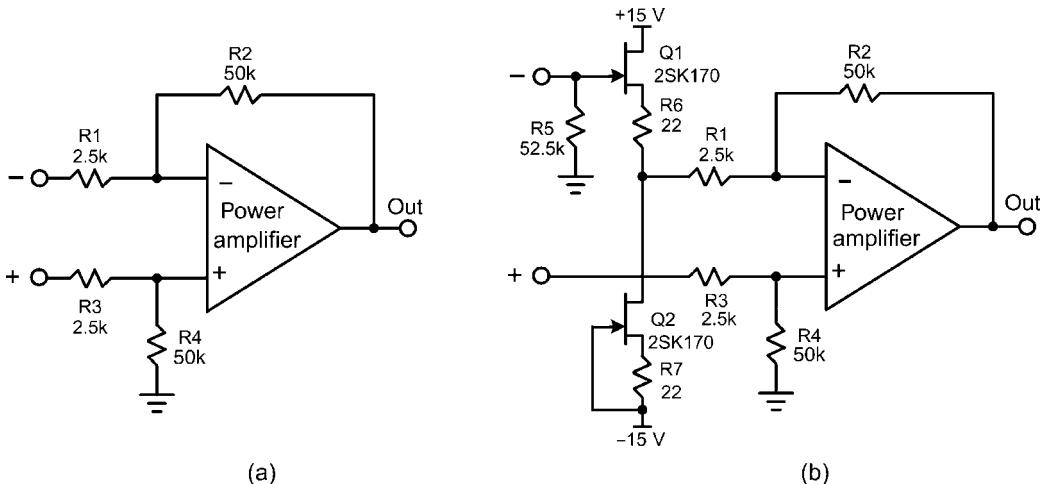
FIGURE 26.3   (a) Power amplifier configured as a differential amplifier. (b) With JFET input buffer on the inverting side.

power amplifier has gain on the order of 26 dB. It also forces up the choice in value of the amplifier's feedback resistor. For example, if one wants a single-ended-to-single-ended gain of 20, then the negative input resistor might be 2.5 kΩ and the feedback resistor might be 50 kΩ. This compromises amplifier input-referred noise and leaves the amplifier with low input impedance on the inverting input side. This arrangement will likely be unstable with an open input, as the amplifier is probably not unity-gain stable.

One solution to this is to buffer the inverting input side. This can be done with a discrete JFET source follower, but that will introduce some distortion into the inverting input signal path. Such an arrangement is shown in Figure 26.3b. This approach provides the same input impedances to both sides of the input when driven both in common mode and in single-ended mode. A single-ended/balanced mode switch can be used to short the inverting input of the arrangement to ground when SE inputs are used, providing a slightly improved SNR. The discrete JFET buffer can be made to have approximately no DC input-output offset if the two JFETs are matched.

A better solution is to use identical JFET input buffers on both the inverting and non-inverting input sides. The circuit can then be arranged so that the signal currents flowing in both buffers are made the same by equalizing the loading of the buffers. This will cause the buffers to act in a balanced, differential fashion, canceling out second harmonic distortion. Both of the differential inputs can have identical, high values of input impedance and both positive and negative signals encounter the same signal path for symmetry.

The discrete JFET input buffers must be run at fairly high currents to keep the distortion low, given the subsequent low impedances (on the order of 2.5k) that they must drive in the power amplifier's differential-to-single-ended conversion input stage. This arrangement is illustrated in Figure 26.4. R7 makes the load seen by the positive-side buffer nominally the same as that seen by the negative-side buffer. This makes the power amplifier part of an instrumentation amplifier arrangement. The finite output impedance of the discrete JFET buffers can detract from common-mode rejection, however.

The Differential Complementary Feedback Quad (DCFQ)

The differential buffer shown in Figure 26.5 is referred to here as a *differential complementary feedback Quad (DCFQ)*. It employs two JFETs and two BJTs in a differential
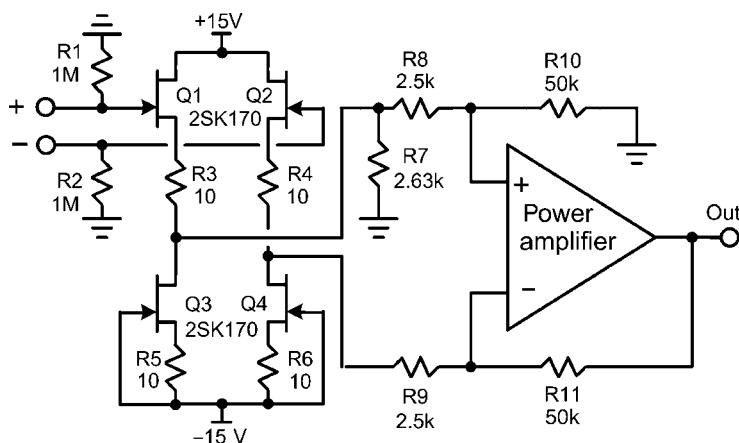
FIGURE 26.4   Configuring the power amplifier as a differential amplifier with dual input buffers.
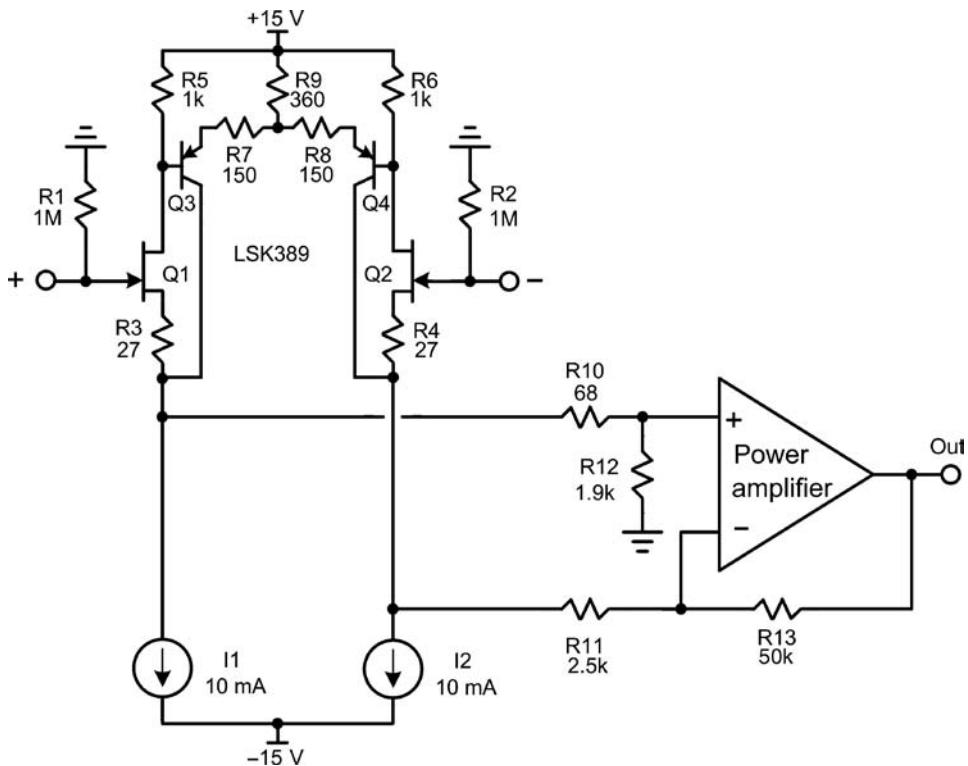
FIGURE 26.5 The differential complementary feedback Quad (DCFQ) buffer.

arrangement analogous to a pair of JFET-bipolar CFPs. This circuit provides a low-distortion, low-impedance drive to the subsequent differential amplifier arrangement of the power amplifier.

JFETs Q1 and Q2 form a pair of source-followers that are *helped* by their respective complements Q3 and Q4. The BJTs are arranged as a differential pair, resulting in much-improved bias stability as compared to using two individual JFET-bipolar CFPs. R3 and R4 drop the source voltages down to 0 V to form the output signals.

THD of the DCFQ stage is less than 0.002% under all conditions of positive, negative, and differential drive. This arrangement takes advantage of the good offset matching of the dual JFET, with pair-to-pair variations in V_{gs} resulting in only a common-mode offset that is ignored by the subsequent differential amplifier of the power amplifier. If desired, the common-mode level presented to the subsequent differential amplifier can be trimmed to zero with adjustment of R9. In principle, one could serve the currents in I1 and I2 to make the common-mode output DC level equal to zero.

26.2 Bridged Amplifiers

Bridged amplifiers are used widely where high power is required. This is especially so in the pro-sound arena. A simple bridged amplifier arrangement is illustrated in Figure 26.6. Two channels of a stereo amplifier are driven out of phase and the loudspeaker is connected across the hot outputs of the two amplifiers. A bridged power
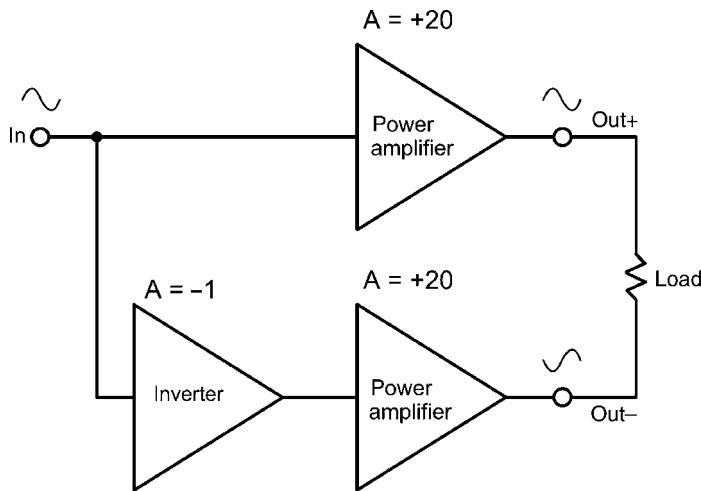
Figure 26.6 A bridged power amplifier.

amplifier can theoretically produce 4 times the power into a given load compared to its nonbridged counterpart (one channel of the stereo amplifier) using the same rail voltages. This is because the voltage across the loudspeaker is doubled and power goes as the square of voltage. Under these conditions, each of the two amplifiers "sees" an effective load resistance equal to half that of the loudspeaker impedance. For this reason, the bridged amplifier may produce somewhat less than 4 times the power.

Sound Quality

Bridged amplifiers have not always enjoyed a reputation for the highest-quality sound. This is partly because they are seeing half the impedance of the loudspeaker and the distortion of power amplifiers is virtually always higher when driving lower impedance loads. Moreover, the peak output current requirements are doubled, and some amplifiers may not be up to the task. Indeed, their protection circuits may be activating. Finally, bridged amplifiers are often abused. Each channel may not be rated to drive a 2-Ω load, but the amplifier may often be asked to drive a 4-Ω load in bridged mode.

Bridged amplifiers provide only half the damping factor into a given load because there are essentially two amplifier output impedances in series with the load. This can also detract from sound quality.

Power Supply Advantages

Amplifiers operating in bridged mode often enjoy some advantage in regard to the power supply. Single-ended amplifiers draw power from either the positive rail or the negative rail on each half-cycle of the signal. This current flows through ground. The duty cycle of current flow from each rail is only 50%. In bridged-mode current is being drawn from both rails simultaneously and little or none of the output current flows through ground. Each rail is being used 100% of the time. The waveform of the current being sourced by each rail is full wave rather than half wave.

26.3   Balanced Amplifiers

Any amplifier that can accept balanced inputs and produce balanced outputs can be called a *balanced amplifier*. However, there are degrees of balance. A bridged amplifier with a balanced input can be called a balanced amplifier, and many so-called balanced amplifiers are made that way. For the audiophile, balanced is beautiful and bridged is brawn. That is why the term *balanced* is preferred when what would otherwise be a bridged amplifier is marketed to the audiophile community.

True Balanced Amplifiers

True balanced amplifiers comprise a single amplifier whose circuitry is balanced from input to output, not two separate amplifiers wired together in bridged mode. One version of an amplifier without negative feedback described in Chapter 25 was a truly balanced design. Indeed, in some ways it is easier to design a true balanced amplifier in the absence of negative feedback.

Building the differential open-loop amplifier is not difficult. It is fairly straightforward to adopt a differential VAS arrangement and drive two copies of the output stage. Applying the negative feedback is where the added challenge lies.

Differential-Mode Feedback

The output of a balanced amplifier is a differential (balanced) signal. The information applied to the loudspeaker is in the differential mode. That means the negative feedback must be taken as the difference of the voltages existing across the two *hot* output terminals. The negative feedback must therefore be in the differential mode and be applied to the input circuits in the differential mode. One such arrangement is illustrated in Figure 26.7. The amplifier is operated in the inverting shunt feedback configuration insofar as the feedback is concerned. The differential feedback creates a virtual short across the differential input terminals of the open-loop amplifier. Differential input signal current is applied to these input nodes through input resistors R1 and R2. The positive and negative halves of the balanced input signal are buffered so that the amplifier can present high impedance to the source. This differential buffering function can be implemented with the DCFQ differential buffer shown in Figure 26.5.
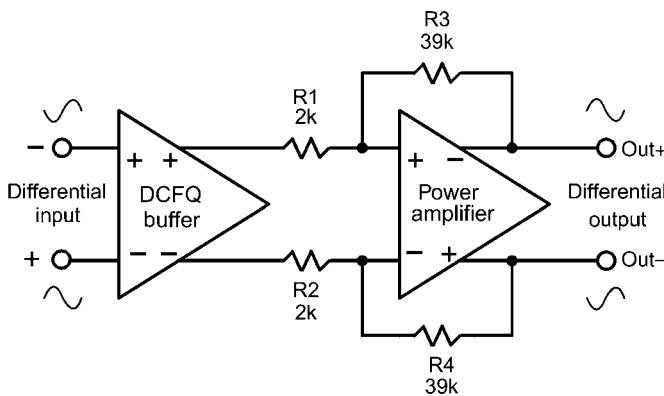
FIGURE 26.7   A true balanced amplifier with differential-mode feedback.

Differential-Mode DC Servo

The use of a DC servo is just as advantageous in a true-balanced amplifier as it is in a single-ended amplifier. As with the main feedback, the DC servo feedback must operate in the differential mode. It must be responsive to the DC difference of the two output terminals, and it must apply its correction in a differential fashion. The differential DC servo is easily implemented with a differential integrator, as shown in Figure 26.8. The output of the integrator is applied through R5 to one of the inputs of the open-loop amplifier while an inverted version of the DC correction signal is applied to the input of opposite polarity by R6.

Common-Mode DC Servo

In single-ended amplifiers the negative feedback establishes the output DC level and drives DC offset to zero. Differential-mode feedback is unaware of the common-mode output level of the amplifier and therefore cannot stabilize it to a value near zero. For this reason a second feedback loop called a *common-mode feedback loop* is needed in most true balanced amplifiers to sense the output common-mode level and drive it to zero. However, if the differential inputs of the open-loop amplifier have high common-mode rejection, as desired, they will not be responsive to common-mode error signals fed back by the common-mode feedback. The common-mode feedback typically must be applied somewhere within the forward path of the amplifier. This feedback loop must
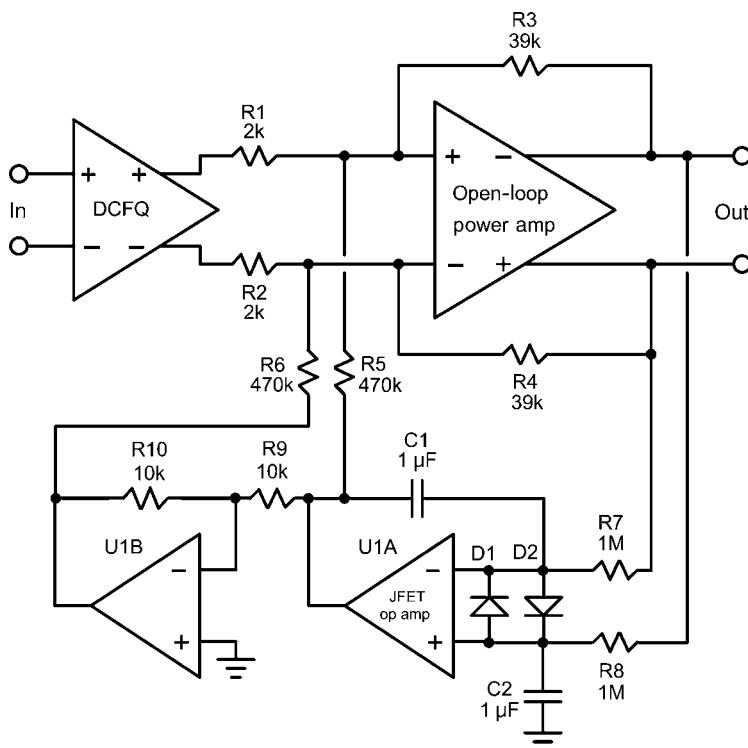
FIGURE 26.8   A balanced amplifier with differential-mode DC servo.
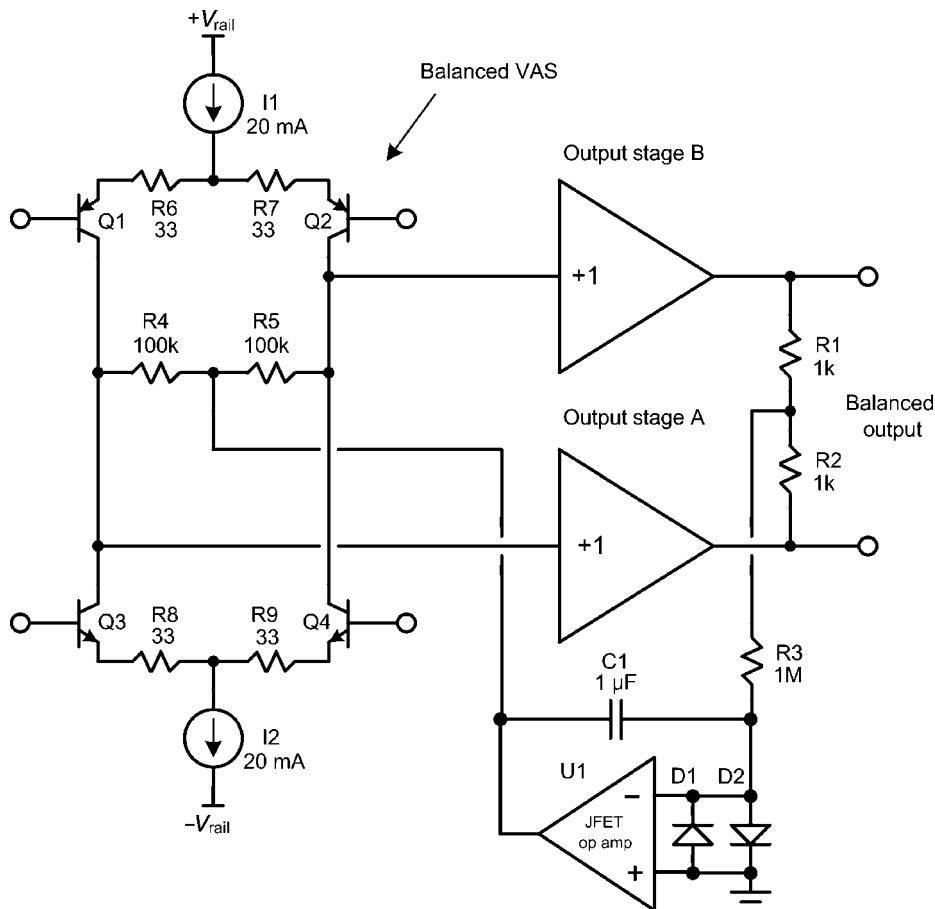
FIGURE 26.9   A common-mode DC servo arrangement.

also obey stability criteria. However, this loop need not have high closed-loop band-
width. In fact, this circuit can be just another DC servo.

Figure 26.9 shows a balanced amplifier with a common-mode DC servo. A simpli-
fied version of a differential VAS is shown, and the two output stages are merely
shown as gain blocks. The usual bias spreaders have been omitted for simplicity. The
common-mode component of the output signal is derived by summing resistors R1
and R2 and applied to the integrator of the common-mode DC servo. The DC error
signal from the servo is applied to VAS load resistors R4 and R5. If the common-mode
output voltage is too high, the integrator output will go negative and pull both VAS
output nodes in a negative direction to correct the error. Notice that the VAS load
resistors are not unlike the load resistors employed in low-feedback amplifiers, but in
this application they can have much higher values. Current sources I1 and I2 should
be well matched in this approach so that the common-mode servo has adequate cor-
rection range. In other IPS-VAS arrangements the common-mode correction signal
can be applied to the input stage.

This page intentionally left blank

Integrated Circuit Power Amplifiers and Drivers

I n this chapter we'll discuss power amplifiers that can be built from integrated circuits that are designed to function as complete power amplifiers on a chip. Power amplifier driver chips that can implement most of the complexity of a power amplifier on a single chip will also be discussed. Such chips typically need only a BJT or MOSFET output stage attached to them to form a complete power amplifier. Finally, an integrated circuit class AB bias controller IC will be discussed. This chip eliminates the need for the bias trim resistor and can reduce dynamic bias instability that results from output stage thermal swings.

27.1 IC Power Amplifiers

Integrated circuit power amplifiers have been around for quite some time and have been used extensively in high-volume consumer gear. Often, these have been of relatively low power capability and without a strong focus on true high-fidelity performance.

However, in recent years several companies have introduced IC power amplifiers that are capable of substantial power and high-fidelity performance. Power capabilities in the 25-W to 80-W range with very good distortion specifications are readily available. Although such amplifiers are not the primary focus of this book, an overview is presented here for completeness. Numerous companies produce such amplifiers, but perhaps the most well known is National Semiconductor. These products are the ones with which I have had direct experience.

Integrated circuit power amplifiers have made tremendous strides in the last ten years. In recent years the National Semiconductor LM3886 and its cousins have even been popularized for use in some audiophile power amplifiers [1, 2]. These applications are most often referred to as *Gain Clones*. The term arises from an early audiophile amplifier based on the LM3875 chip called the *Gaincard* [3, 4]. It was rated at 25 W per channel into 8 Ω. The design approach was then copied and modified by many, thus the name *Gain Clone*. In addition to its very good performance, the allure of the device is that it allows many more DIY audiophiles to get involved with building power amplifiers without getting deeply involved in the complexities and risks of discrete power amplifier design.

27.2 The Gain Clones

Quite some years ago a Japanese designer named Kimura-San of 47 Laboratory introduced an IC-based power amplifier to the serious audiophile community and called it the *Gaincard* [3]. It was based on the National Semiconductor LM3875 [4]. The amplifier was greeted with surprising enthusiasm and many variants on the basic approach emerged, especially in the DIY community. Such IC high fidelity power amplifier variants, usually employing one of several different National chips, have become known as *Gain Clones*. Most of the information needed to build a Gain Clone can be found in the National Semiconductor data sheets and application notes for these devices.

A Basic Gain Clone Design

The LM3886 is not unlike a power op-amp and can be used in a multitude of op-amp topologies. Figure 27.1 shows a typical LM3886-based Gain Clone similar to the design recommended by National in their data sheet [1]. This is a simplified diagram and does not show compensation details.

As with many power amplifiers, a large electrolytic capacitor is included in the return leg of the feedback network to reduce the closed loop gain to unity at DC and reduce offset voltage at the output. Unfortunately the presence of such electrolytic capacitors in the signal path can create distortion and otherwise impair sound quality. Shortly we'll see a couple of ways to eliminate this electrolytic capacitor.

A Gain Clone Using the Inverting Mode

Most operational amplifiers produce somewhat lower distortion when operated in the inverting mode, and the LM3886 is no exception. Operation in the inverting mode improves performance by eliminating common-mode distortion in the input stage of the LM3886. A disadvantage of the inverting mode is its relatively low input impedance. For this reason the amplifier should be preceded by an inverting buffer. This arrangement is shown in Figure 27.2. The inversion in U1B also restores the overall polarity of the signal path to noninverting. The inverter should be implemented with a high-quality audio-grade op-amp. Here the OPA2604 dual JFET op amp is used.
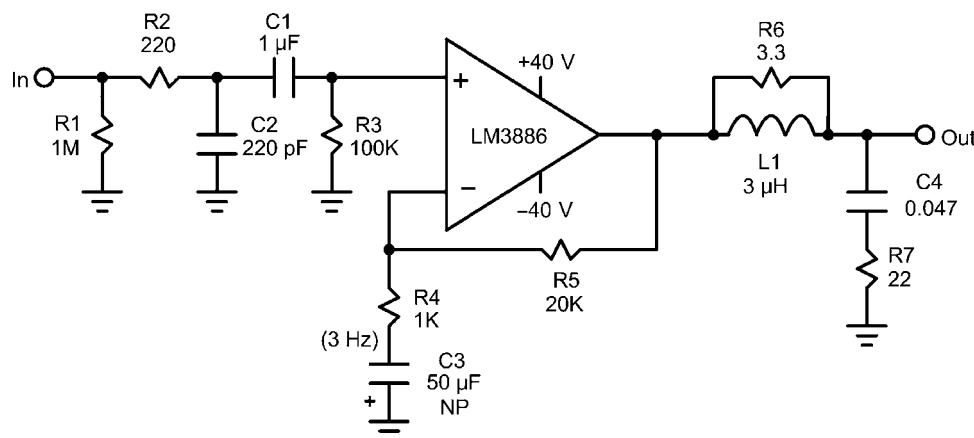
FIGURE 27.1   A 50-W Gain Clone amplifier based on the LM3886.
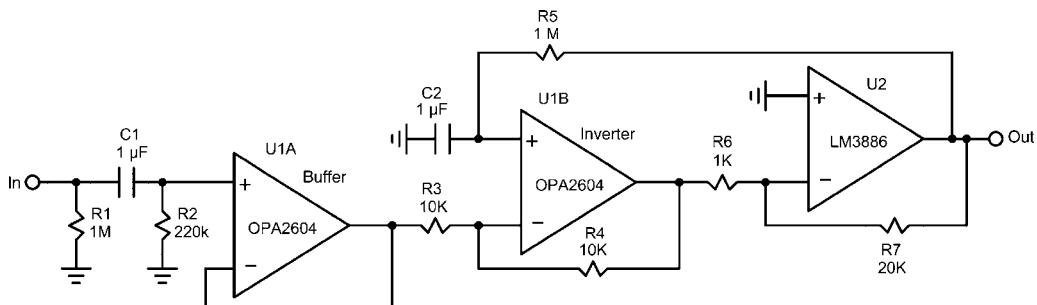
FIGURE 27.2 Gain Clone in inverting mode reduces input common-mode distortion and eliminates the electrolytic capacitor.

The inverter also has a moderate input impedance of only 10 kΩ. This would require a fairly large input coupling capacitor. For this reason, it is preceded by unity gain JFET input buffer U1A employing the other half of the JFET op amp. This provides very high input impedance, allowing the use of a high-quality film input capacitor of reasonable size and cost.

Avoiding Electrolytic Capacitors While Controlling Offset

The inverting stage preceding the LM3886 provides an opportunity to eliminate the electrolytic capacitor in the feedback network of the LM3886 in the form of its unused noninverting input. This input provides a noninverting gain of 2 to the output of the stage. As shown in Figure 27.2, DC feedback from the output of the LM3886 can be separately fed back to this input through a large resistance and then filtered with a film capacitor of modest value.

27.3 The Super Gain Clone

The *Super Gain Clone* is an inexpensive quality power amp block based on the popular National LM3886 IC power amplifier chip [5]**.** This circuit encapsulates the LM3886 IC and maximizes its achievable quality.

A DC servo is employed for offset control instead of the passive DC feedback circuit illustrated above. The availability of the extra inversion in the signal path makes it possible to employ a simple inverting integrator for the servo. The schematic of the Super Gain Clone amplifier is shown in Figure 27.3. It includes the compensation and filtering circuitry recommended by National Semiconductor. The Super Gain Clone includes an input buffer stage, an inverter, the LM3886 power amplifier operating in inverting mode, and an integrating DC servo for offset control.

Input Circuits

The amplifier begins with the usual 4.7-Ω resistor that isolates analog ground from circuit ground so as to prevent ground loops. A passive LPF input network provides two poles of roll-off and minimizes RFI ingress. U1A is a conventional noninverting unity gain buffer employing half of an OPA2604 dual FET op-amp. This is a good audio op-amp, especially for the price.
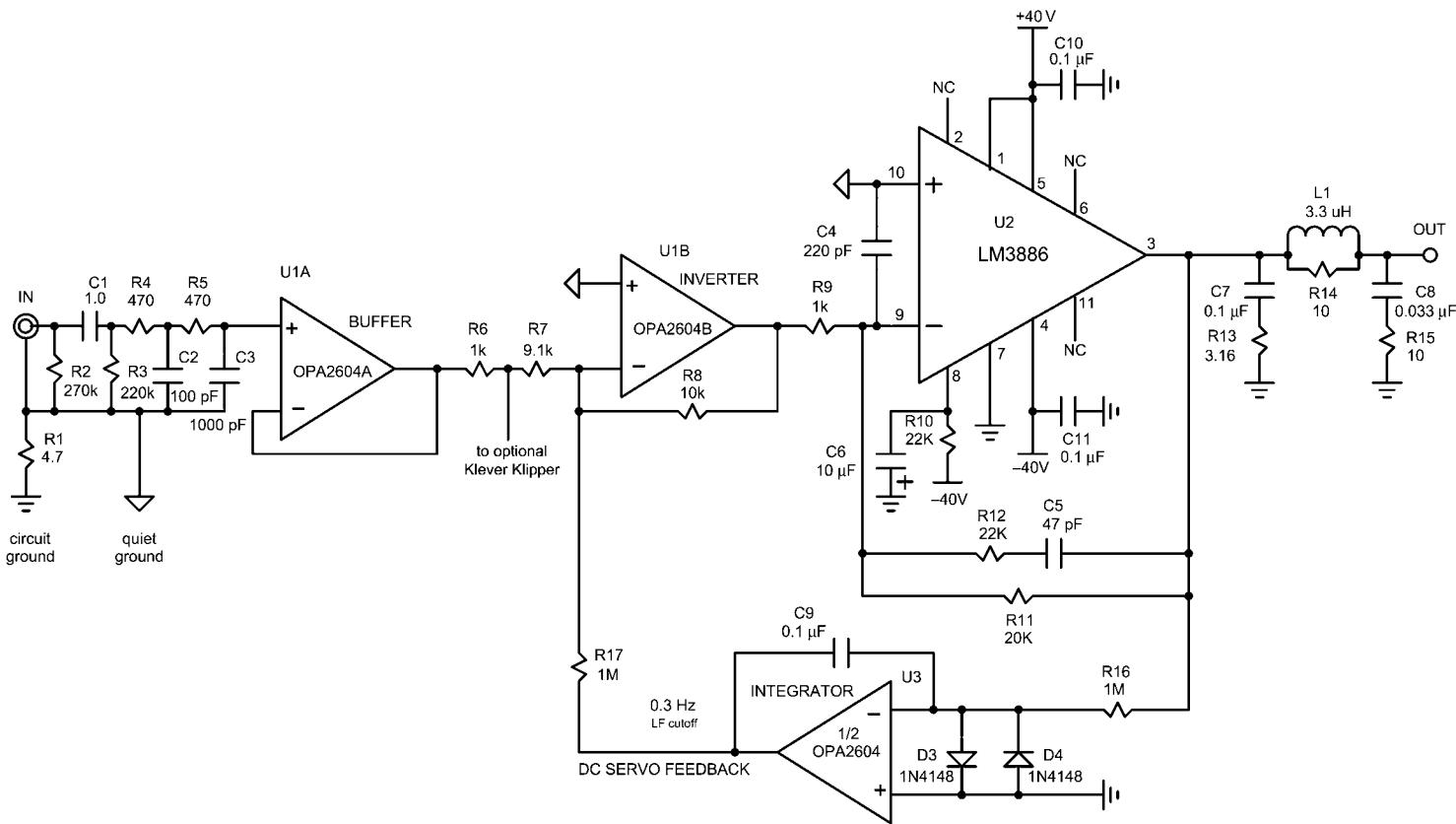
Figure 27.3 The Super Gain Clone employing a DC servo.

U1B just acts as the unity gain inverter. It cancels the inversion that results from using the LM3886 in its inverting mode. Note also that this inverter is also the point at which the offset control signal from the DC servo is injected via R17.

Power Amplifier

The inverter feeds the LM3886 power amplifier through R9 (1 kΩ) in the inverting mode. In combination with 20-kΩ feedback resistor R11, the power amplifier produces a gain of –20. Capacitors C4 and C5, in combination with R12, provide feedback compensation for the LM3886, as recommended in its data sheet [1].

Output Network

The output network is a pi-section arrangement with Zobel networks on both sides of the L-R network. This provides enhanced resistance to RFI ingress via the speaker cables. The inductor is optionally constructed as an air-core toroid to keep the magnetic field circulating largely inside the toroid, reducing possible magnetic coupling to other circuits. The first Zobel, comprising C7 and R13, is located close to the output of the LM3886. The L-R network and second Zobel are located close to the speaker output terminals, optionally on a small separate board. The output signal is carried from the main board to the output network board by about 6 in. of high-quality speaker cable.

DC Servo

Op-amp U3 forms an integrator that is used to provide the DC servo function. Values are set so that a 3-dB point of about 0.3 Hz is achieved for the overall amplifier. A full swing of the integrator output can accommodate over 100 mV of offset correction.

Performance

The Super Gain Clone delivers over 40 W into an 8-Ω load with ±35-V power supply rails (at full load). THD at full power is plotted as a function of frequency in Figure 27.4 with an 8-Ω load.
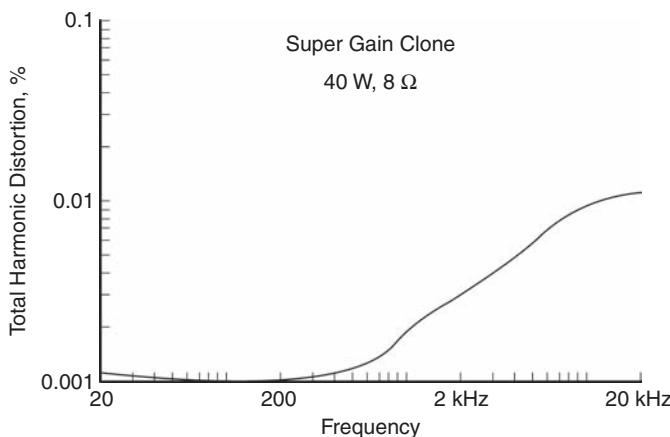
FIGURE 27.4   THD versus frequency at full power (40 W).

27.4 Integrated Circuit Drivers

In many cases a higher power capability is desired than can be accommodated by a fully integrated power amplifier IC. In other cases a higher level of quality is desired, while still being able to take advantage of the integration of most of the power amplifier circuitry. National Semiconductor has addressed this need with a line of audiophile power amplifier driver ICs [6–11]. In this case, the power transistors are discrete and are merely driven by the driver circuit. In some cases the output stage driver is also discrete.

The LME49810

The LME49810 is a complete power amplifier input/driver with which a power amplifier can be made by simply adding power transistors and a bias spreader [6]. The device can be operated with power supply rails up to ±100 V, making possible amplifiers rated in excess of 300 W into 8 Ω. The device includes emitter follower output driver transistors that can supply 50 mA to the external output stage. Separate pins are provided for connection of a bias spreader, such as a V_{be} multiplier. Figure 27.5 is a simplified schematic of a power amplifier built with the LME49810 and one pair of BJT output transistors. Input offset voltage is less than 3 mV, and input bias current is less than 200 nA. Input-referred noise is about 10 nV/√Hz. A bias current of 2.8 mA flows through the V_{be} multiplier.

Better performance and higher amplifier output current can be achieved by employing an output Triple as shown in Figure 27.5. The output emitter followers in the LME49810 serve as the predrivers while external discrete drivers are used to drive the output transistors.

The maximum bias-spreading voltage available from the LME49810 is only 10 V. For this reason the device may not be capable of properly driving some vertical power MOSFETs [8]. Vertical power MOSFETs with smaller turn-on voltages, such as the Toshiba 2SJ201/2SK1530 pair, are compatible with the LME49810. Lateral MOSFETs, with their still smaller turn-on voltages, can also be driven by the LME49810.

The output sense, mute, and clip flag pin connections are not shown for simplicity. A more complete amplifier is shown in Figure 27.6. This design also includes a bias
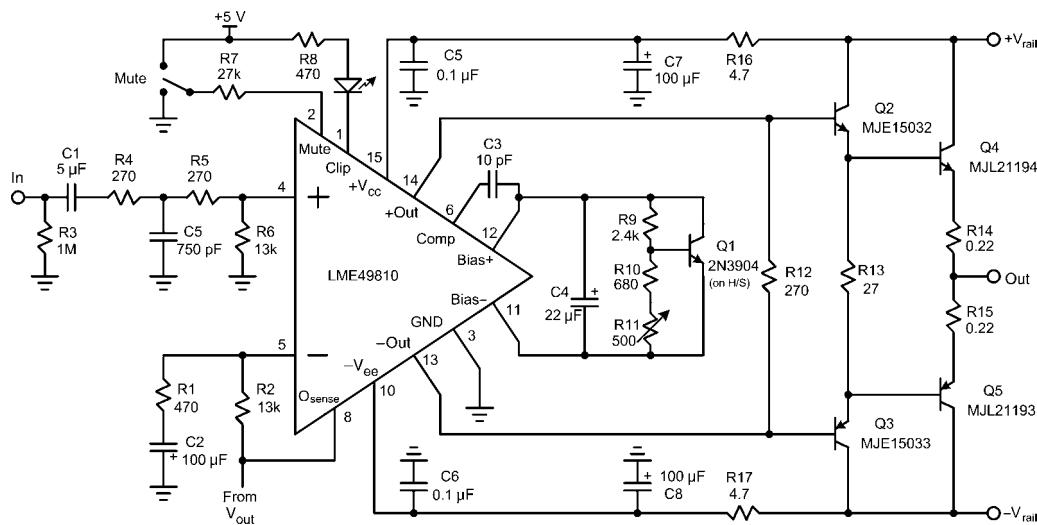
FIGURE 27.5 A simplified power amplifier based on the LME49810.
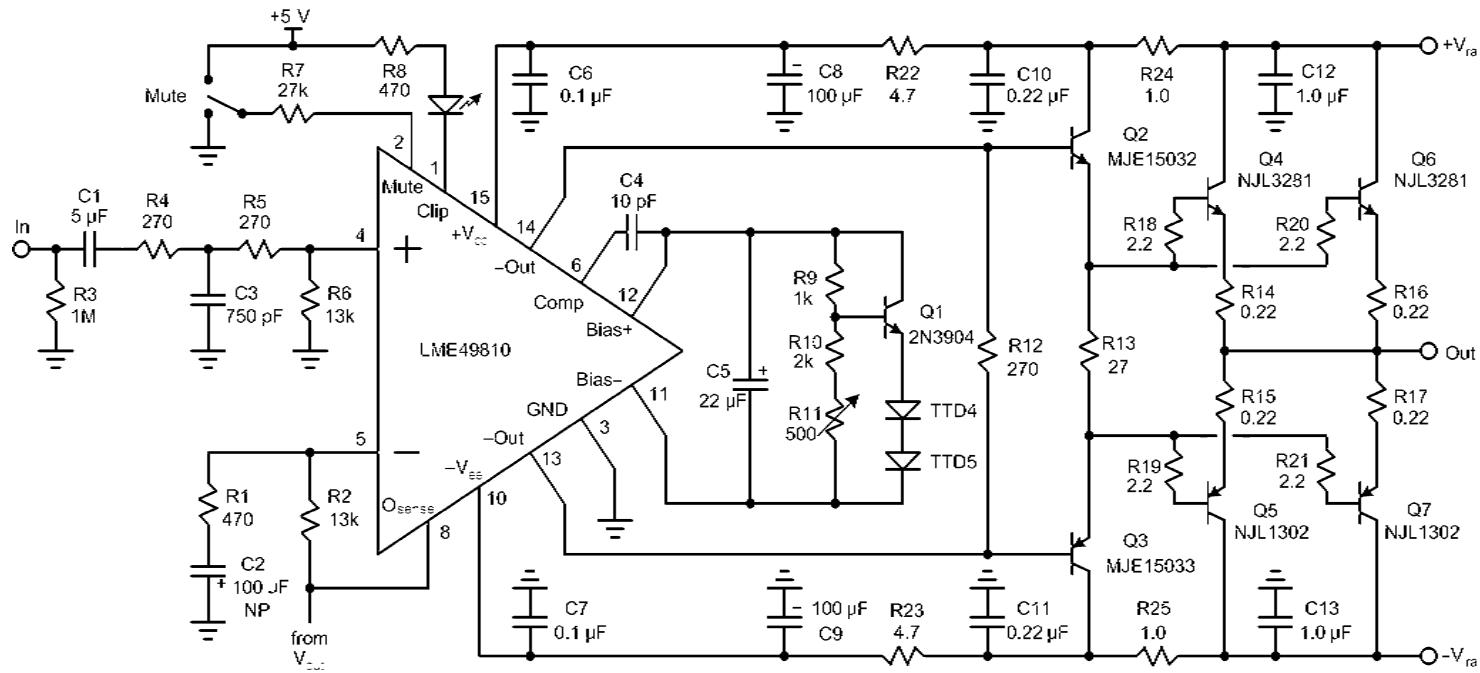
FIGURE 27.6 An amplifier employing the LME49810 with a Triple output stage. The predriver is inside the LME49810.

spreader that employs the tracking diodes in the ThermalTrak™ output transistors. Depending on the detailed thermal arrangement, other variations of the bias spreader may provide better thermal tracking. For example, the bias spreader of Figure 14.19a, where a resistor connected from base to emitter of Q1 is added, may be preferable. This amplifier employs two output pairs and ±55-V power supply rails (no load).

The amplifier delivers 125 W into an 8-Ω load when the rails have sagged to ±49 V. It will deliver 180 W into a 4-Ω load when the power supply rails have sagged to ±44 V.

All of the techniques employed in the Super Gain Clone can be applied to the amplifier of Figure 27.6. These include the DC servo and the approaches that allow the use of small film capacitors in place of electrolytic capacitors.

The LME49830

The LME49830 is similar to the LME49810, but it is optimized for use with power MOSFETs instead of bipolar output transistors [10, 11]. It is capable of supporting bias spread voltages as high as 16 V; this makes it fully capable of properly driving vertical power MOSFETs like the IRFP240/9240. The LME49830 lacks the Baker clamps and clipping indicator outputs of the LME49810. Its input circuits have similar characteristics to those of the LME49810. The device feeds 1.6 to 2.7 mA through the bias spreader. It would be nice if this number were a bit bigger. The outputs that drive the MOSFET gates are push-pull, so they can source or sink current. Figure 27.7 illustrates a power amplifier employing two pairs of the popular IRFP240/9240. Total bias current for the two pairs is set at 300 mA.

The bias spreader employs a transistor mounted on the circuit board and a diode-connected transistor mounted on the heat sink to achieve the proper degree of temperature compensation for the IRFP240/9240 MOSFET devices used.

27.5   An Integrated Circuit Bias Controller

The Linear Technology LT1166 integrated circuit class AB bias controller is a clever device that seeks to eliminate the conventional V_{be} multiplier bias spreader and its attendant dynamic thermal tracking limitations [12, 13]. The LT1166 uses feedback from the sources or emitters of the output transistors to sense real-time transistor current and adjust the bias-spreading voltage in such a way that both top and bottom transistors are always conducting to some extent and contributing to output stage transconductance. This means that the LT1166 actually modulates the bias spread in real time in accordance with output current. It is a dynamic bias spreader. The LT1166 also conveniently includes current-limiting circuitry for a degree of output stage protection. You are referred to the LT166 data sheet for a more detailed explanation of how the device operates.

The LT1166 greatly simplifies bias circuit electrical and physical design and also greatly reduces dynamic biasing errors that occur due to thermal mistracking. Most significantly, it eliminates the bias adjustment pot. A simplified MOSFET output stage employing the LT1166 is shown in Figure 27.8 [12]. The current sources shown can be fixed current sources if the signal is fed to the input pin of the LT1166. Alternatively, the current sources can be the collectors of a conventional VAS if the input pin is not used. I will be using the latter connection here. Source resistors R1 and R2 sense the currents in Q1 and Q2. The key functionality of the LT1166 is that it servos the bias spread so that
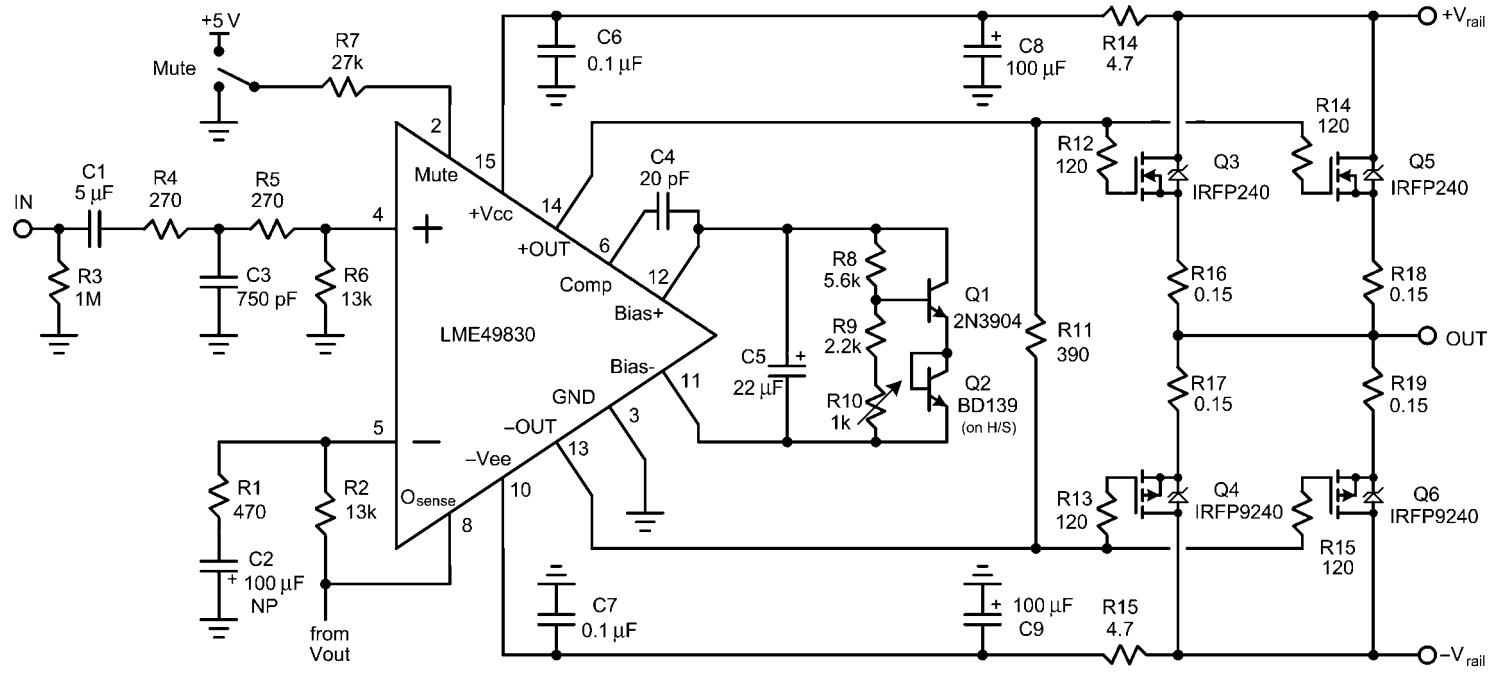
FIGURE 27.7 A MOSFET power amplifier based on the LME49830.
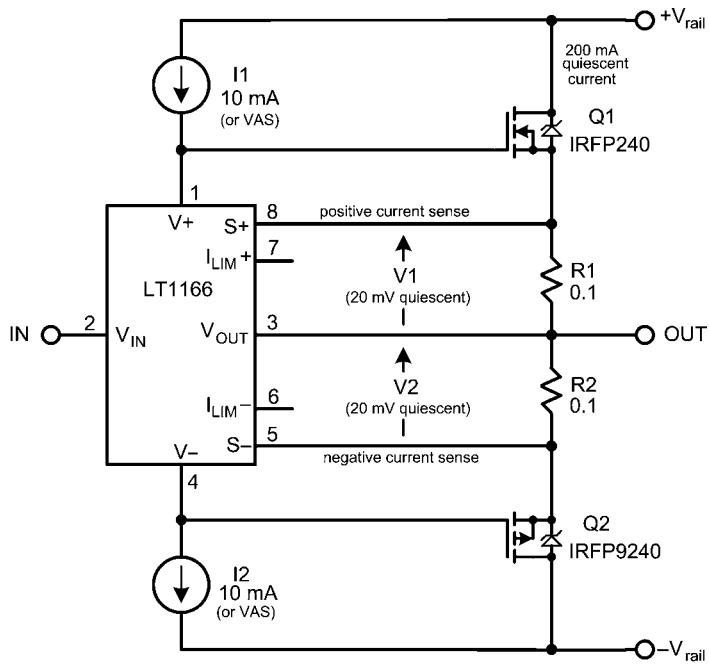
FIGURE 27.8 A simplified MOSFET output stage using the LT1166.

the product of V1 and V2 remains constant at 0.0004 V². This means that neither output transistor ever fully turns off. When no output current is flowing, V1 and V2 are each 20 mV. The product of these two 0.02-V numbers is 0.0004 V². If R1 and R2 are each set to 0.1 Ω, then the quiescent bias current I_q of the MOSFETs will be 200 mA.

It is easy to see how the servo action of the LT1166 sets the output stage bias current to a known stable value by this feedback process. It is important to understand that this process is achieved by dynamically modulating the bias spread voltage as a function of signal current. The bias spread voltage will increase as output current increases from zero in either direction. This in turn means that the signal across the bias spreader is quite distorted with third-order distortion products. This also means that the bias spreader formed by the LT1166 should not be bypassed (V_{be} multiplier bias spreaders usually are bypassed).

A simplified amplifier employing the LT1166 is shown in Figure 27.9. There are several ways in which the LT1166 can be used, but here we focus on its use as a shunt-regulating bias spreader, analogous to a V_{be} multiplier. In this arrangement the signal does not actually pass through the LT1166 on its way to the output stage. This arrangement provides a much lower distortion solution than a circuit that applies the input signal to the V_{in} pin. The V_{in} pin of the LT1166 is left floating.

The LT1166 floats with the signal at the VAS output and is powered by the VAS bias current. It requires a minimum bias-spreading voltage of 4 V and minimum bias current of 4 mA for proper operation. The LT1166 is especially well suited for use with power MOSFETs because of their higher gate-to-gate voltage spread, from which the LT1166 is powered. However, the device also works well with bipolar output stages if they are designed to require a sufficiently high bias spreader voltage. A Triple that is designed to
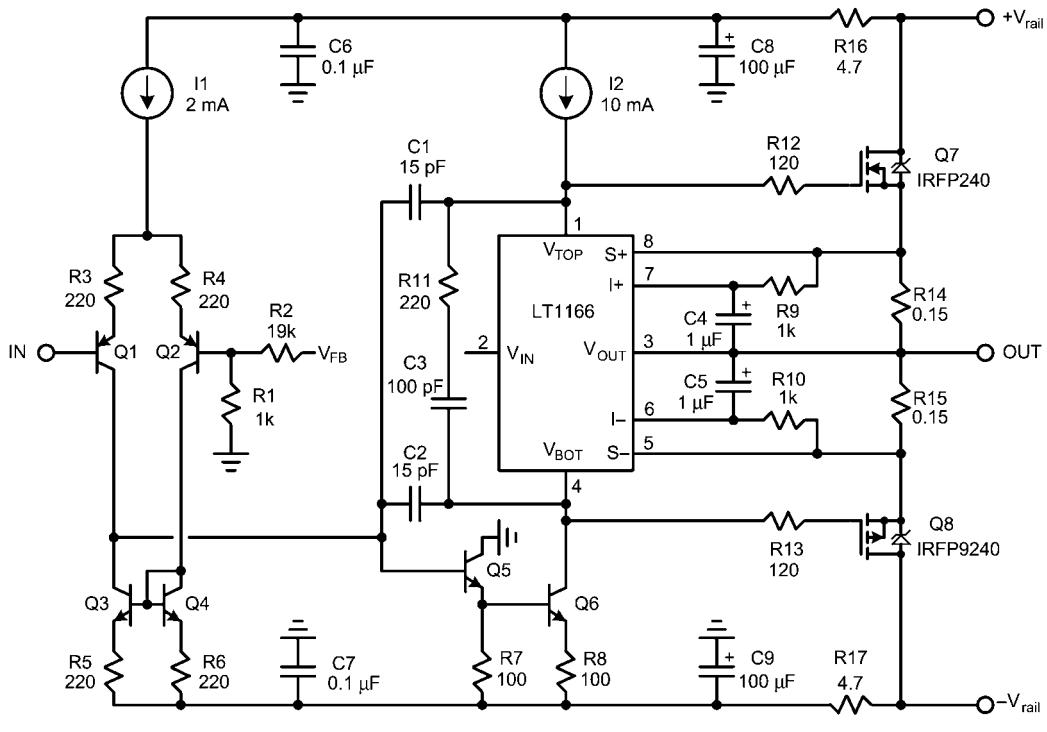
FIGURE 27.9 A simplified amplifier using the LT1166.

require sufficient bias spread at its predriver inputs under worst-case conditions (like high temperature) will work if a bit of extra DC drop is introduced into its forward path.

The IRFP240/9240 MOSFET output pair requires a total bias spread of about 8 V, so that voltage is what appears across the LT1166 between V_{top} and V_{bot}. Source resistors R14 and R15 are set to 0.15 Ω, resulting in $I_q = 133$ mA. R9, R10, C4, and C5 control the current-limiting process of the LT1166. Current limiting begins when the I_{LIM} pin voltage exceeds the output pin by 1.3 V. With the 0.15-Ω source resistors shown, the current limit will be about 8.7 A. V_{top} and V_{bot} are limited to no more than a 12-V difference with respect to the output node by internal clamps in the LT1166 to protect the device. This also limits gate drive to the MOSFETs in the event of a fault.

Compensation of the Amplifier

The voltage across the bias spreader varies with signal current in a nonlinear way; it increases when the signal goes positive, and it also increases when the signal goes negative. It is important that this nonlinear *common-mode* spreading voltage does not make its way into the signal path and introduce distortion. This is particularly important at high frequencies. To first order, changes in the bias spread will not cause distortion. For this reason, we want the center point of the bias spread to remain a linear representation of the signal.

This impacts the way in which Miller feedback compensation must be applied to the VAS. If the Miller capacitor is just connected to one end of the LT1166 dynamic bias

spreader, distortion will result because this node contains the signal plus half the non-linear spreading voltage. Instead, Miller capacitors of equal value (C1 and C2) should be connected from each end of the dynamic bias spreader back to the input of the VAS. This will force the virtual center tap of the bias spreader to be the desired linear representation of the signal.

Alternatively, a center tap can be formed with two precision resistors of equal value connected in series across the dynamic bias spreader. A single Miller capacitor can then be connected from this point back to the input of the VAS. This arrangement will introduce a zero into the Miller compensation roll-off, which may actually be helpful in some designs. In the design of Figure 27.9, a pair of 5-kΩ resistors will result in an effective source resistance of 2.5 kΩ, which in combination with the single 30-pF Miller capacitor will introduce a zero at about 2 MHz, two octaves above the specified gain crossover frequency of 500 kHz. The added resistors will consume about 0.8 mA of the spreading current available to the LT1166 if the bias spreading voltage is 8 V.

Compensation of the LT1166

The LT1166 common-mode dynamic bias-spreading feedback loop also needs compensation. Moreover, for very high frequencies, this loop can go essentially static and a properly biased (on average) class AB output stage will remain.

The stability of the common-mode feedback loop implemented by the LT1166 must be understood and maintained over all current swings and conditions of bias spread. The LT1166 contains an internal compensating capacitor for this. It appears that the LT1166 operates this common-mode feedback loop with a fairly high unity gain frequency, causing concerns about stability under some conditions. Compensation of the loop can be augmented with the addition of a series R-C network (R11 and C3) from V_{top} to V_{bot}. This reduces common-mode loop gain at high frequencies.

As a caution, the application notes do not discuss operation of the LT1166 with bipolar output stages, even apart from the issue of bias voltage needed to operate the LT1166. BJT output stages are slower and have higher transconductance, possibly leading to higher common mode loop gain with greater excess phase. So with BJT output stages in particular, more conservative compensation may be necessary with the LT1166 in such arrangements.

A Non-Switching Amplifier

By its very way of biasing the output stage, the LT1166 provides a non-switching amplifier, since neither output transistor ever turns off. There will be no abrupt hand off of signal handling from one transistor to the other. The transistor that would normally be off and reverse biased will always be conducting at least slightly, always at the ready to contribute transconductance to the output stage.

A MOSFET Power Amplifier Using the LT1166 and LME49830

Combining the LT1166 bias controller with the LME49830 driver can result in a compact amplifier that combines the benefits of integrated circuit technology with the high performance achievable with a discrete output stage.

Figure 27.10 illustrates how the LME49830 and the LT1166 can be combined. Current source I1 forces the VAS quiescent current in the LME 49830 to be increased by 10 mA so as to provide adequate bias spreading current for the LT1166. C4 and C5 provide
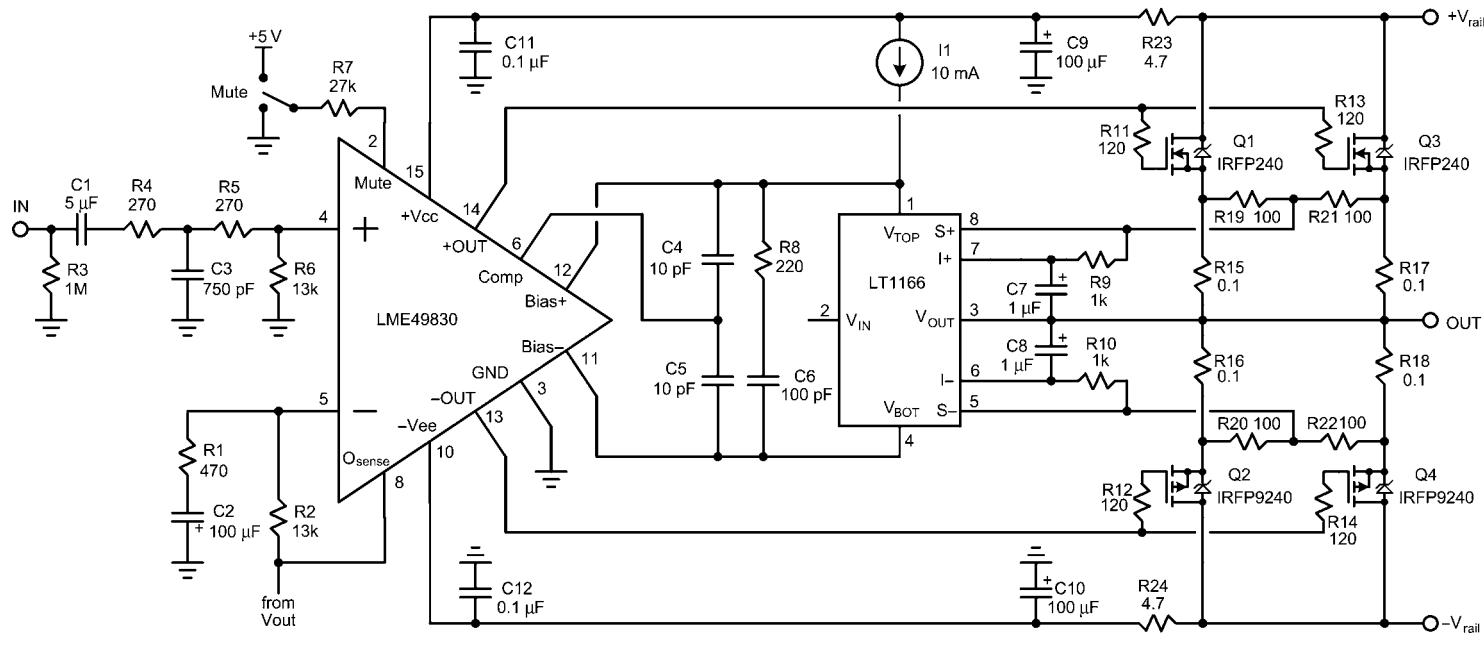
FIGURE 27.10 A MOSFET power amplifier based on the LT1166 and LME49830.

Miller compensation feedback whose source is the effective center-tap of the top and bottom terminals of the LT166 dynamic bias spreader. C6 and R8 augment the common-mode feedback compensation of the LT1166.

The beauty of the LT1166 is that it provides correct, accurate automatic bias without trimming and, moreover, eliminates the effects of thermal stability variation due to dynamic junction temperature changes.

Finally, there is reason to believe that the dynamic bias-spreading action tends to reduce MOSFET crossover distortion due to better control of the class AB transition and appropriate modulation of the bias. Notice that the bias current in the output stage is effectively increased as the signal output current departs from zero.

27.6 Summary

While integrated circuit audio power amplifiers and drivers may not meet the needs of all serious audiophiles, they do present a very convenient and valuable option for achieving surprisingly high performance at greatly reduced cost and complexity.

References

1. National Semiconductor data sheet "LM3886 Overture Audio Power Amplifier Series High-Performance 68W Audio Power Amplifier w/Mute," www.national.com.
2. National Semiconductor AN-1192 "Overture Series High Power Solutions," application note, www.national.com.
3. 47 Laboratory model 4706 Gaincard, Sakura Systems, www.sakurasystems.com.
4. National Semiconductor data sheet "LM3875 Overture Audio Power Amplifier Series High-Performance 56W Audio Power Amplifier," www.national.com.
5. "The Super Gain Clone"; available at www.cordellaudio.com.
6. National Semiconductor data sheet "LME49810 200V Audio Power Amplifier Driver with Baker Clamp," www.national.com.
7. National Semiconductor AN-1490 "LM4702 Power Amplifier," www.national.com.
8. National Semiconductor AN-1645 "LM4702 Driving a MOSFET Output Stage," www.national.com.
9. National Semiconductor data sheet "LME49811 Audio Power Amplifier Series High Fidelity 200 Volt Power Amplifier Input Stage with Shutdown," www.national.com.
10. National Semiconductor datasheet "LME49830 Mono High Fidelity 200 Volt MOSFET Power Amplifier Input Stage with Mute," www.national.com.
11. National Semiconductor AN-1850 "LME49830TB Ultra-High Fidelity High Power Amplifier Reference Design," www.national.com.
12. Linear Technology Corporation data sheet "LT1166 Power Output Stage Automatic Bias System," www.linear.com.
13. Linear Technology Corporation Design Note 126 "The LT1166: Power Output Stage Automatic Bias System Control IC," www.linear.com.

Class D Amplifiers

Traditional audio power amplifiers have served us well for many decades and will continue to do so. However, class D amplifiers are the wave of the future. They have already found their way into many consumer and professional audio products. The proliferation of multichannel receivers in the home theater market has created an increased need for amplifiers that require little space and generate a minimal amount of heat. At the same time, the quality achievable with class D amplification has improved dramatically. Although the *D* in class D does not stand for *digital*, digital signal-processing techniques are playing an increased role in some class D amplifier implementations.

Part 6 covers the class D amplifier technology. The design of class D amplifiers requires a somewhat different skill set that may be unfamiliar to designers of conventional power amplifiers. I have found that there is a great deal of information on class D amplifier design available, but it is scattered across many sources. I have tried to bring much of that together in Part 6 of this book in a way that is easily assimilated by those new to this exciting field of power amplifier design.

This page intentionally left blank

Class D Audio Amplifiers

Class D amplifiers operate on an entirely different principle from those discussed elsewhere in this book. The output stage in a class D amplifier comprises switches that are either *on* or *off*. The switches apply the positive supply to the output for one brief period and then connect the negative supply rail to the output for the next brief period. The process is then repeated indefinitely. This results in a square wave at the output. If these two intervals are the same, the net output is zero. If the first is longer than the second, the output has a net positive value. A low-pass filter extracts the average value to drive the loudspeaker. The cutoff of the LPF often lies in the 30- to 60-kHz range.

This process is referred to as *pulse width modulation (PWM)*. These switching intervals alternate at a high frequency, often in the range of 500 kHz. Thus, the average value of the square wave drives the load. Because the switches are either on or off, they dissipate little power. Virtually all of the input power from the power rails is transferred to the load, so efficiency is very high and power dissipation is very low. Efficiency of 85% to 95% is not uncommon. Small amplifiers that run cool are the result. A big challenge in class D amplifiers is the proper driving of the output stage switches so that the on and off timing intervals accurately reflect the input signal.

Class D amplifiers have long suffered from poor distortion performance. Matters have improved dramatically since the late 1990s. The need to squeeze more power capability into a smaller space while generating less heat has driven their development. This has been especially the case in portable battery-operated consumer devices, but also includes the following important areas in audio:

- Home theater receivers
- Subwoofers
- Pro sound
- Self-powered loudspeakers

As we'll see, the implementation of class D amplifiers is far more involved than the simple description above. Although the *D* in class D does not stand for digital, it is true that the implementations of class D amplifiers are moving more toward digital, and in fact there are approaches that involve direct digital conversion from PCM input streams to class D audio outputs.

There are numerous ways to build a class D power amplifier, but those based on PWM are the oldest and still very popular. This chapter will discuss PWM in depth; other approaches will be covered in Chapter 30.

The emphasis in these chapters will be on class D amplifiers designed for high sound quality, as opposed to smaller or more efficient amplifiers designed for more pedestrian applications like hand-held consumer electronics. Entire books can be devoted to the subject of class D amplifiers. The limited space here permits only the scratching of the surface as a primer on class D amplification.

28.1   How Class D Amplifiers Work

Figure 28.1 shows a simple arrangement that converts an analog input to a digital PWM signal [1–3]. This circuit is referred to as a PWM modulator. A triangle waveform at several hundred kilohertz is applied to one side of a comparator while the input signal is applied to the other side. Whenever the input signal is more positive than the reference triangle wave, a positive pulse is produced that lasts as long as the input signal is above the threshold set by the triangle wave. With a perfect triangle wave, it is easy to see that the pulse width is linearly proportional to the input amplitude. Conversely, when the input signal is below the time-varying threshold set by the triangle wave, the output of the comparator is negative.

The output of the comparator is thus a square wave whose duty cycle corresponds to the amplitude of the input-signal voltage. The frequency of the square wave is referred to as the carrier frequency. It is easy to see that the average value of the square wave is an accurate representation of the input signal. If the comparator output is used to drive power MOSFETs on and off, the average output will reflect the input signal value multiplied by the power supply rail voltage. The average output is extracted from the high-power pulse stream by a low-pass output filter, as shown in Figure 28.2. The technical term for this process of retrieving the analog signal from a pulse train is *reconstruction;* a discrete-time switched signal is converted to a continuous-time signal. The output filter also suppresses high-frequency EMI that is a part of the square wave.

The gain of this amplifier is equal to the ratio of the power supply rail voltage to the peak voltage of the triangle wave. If the peak value of the triangle wave is 2 V and the peak value of the input signal is just equal to 2 V, the output of the comparator will be
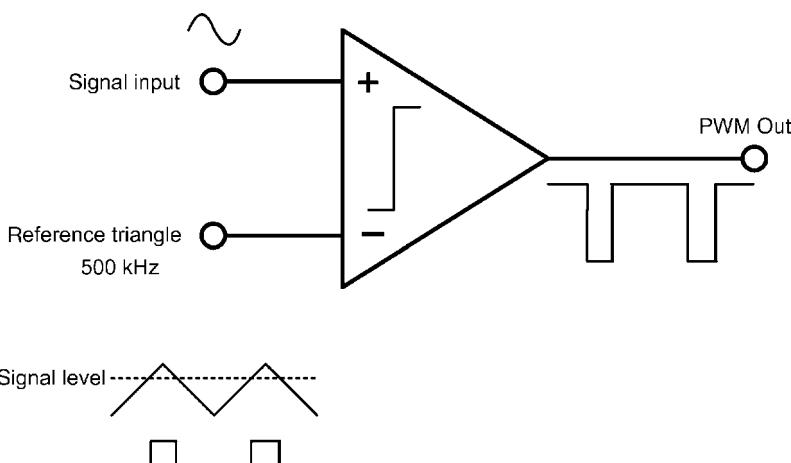
Figure 28.1   A simple PWM modulator.
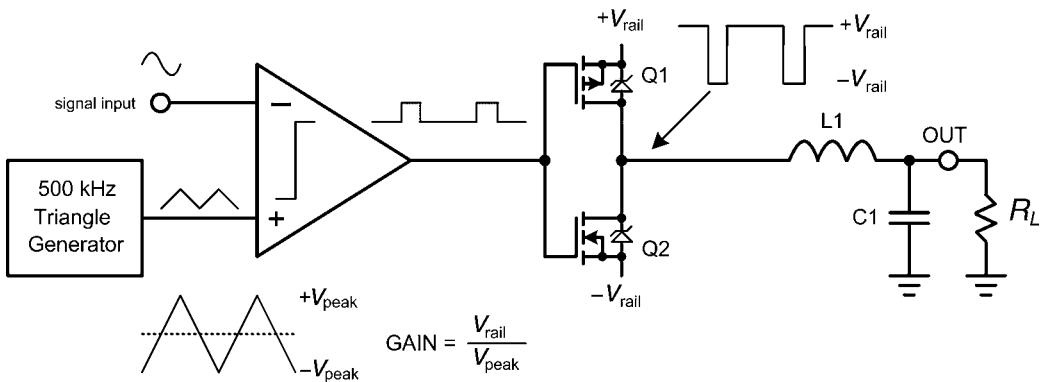
FIGURE 28.2 A simple PWM class D amplifier.

high all of the time and the positive rail will be connected to the load 100% of the time. If the rail voltage is 40 V, the peak output will be 40 V and the gain of the amplifier will be seen to be 20. The positive duty cycle of the square wave is reflective of modulation depth, which is the relative degree of departure from a 50% duty cycle in either direction.

Analog Class D and Digital Class D

The arrangement described above is described as analog class D because the pulse width modulator is implemented in the analog domain. There also exist various forms of digital class D in which digital techniques are employed to construct a PWM signal whose duty cycle is a faithful representation of the signal amplitude. Digital techniques can also be used to implement *pulse density modulation* (PDM) wherein the pulse density represents signal amplitude. The digitally generated signal is then used to drive the output switching devices. Finally, there is direct digital class D. In this case a PCM digital input signal is converted in the digital domain to the string of pulses required to drive the output MOSFET switches.

Synchronous and Asynchronous Class D

The fixed-frequency triangle wave PWM modulator described in Figure 28.1 is a synchronous modulator because the period of the output frequency is always the same; only the duty cycle changes. There also exist asynchronous modulators like the so-called self-oscillating modulators where the switching frequency is not determined by a fixed-frequency oscillator and may actually change as a function of the signal. There are also sigma-delta modulators where a fixed high-frequency clock is employed, but where the resulting pulse density stream does not reflect a particular carrier frequency.

28.2 Buck Converters

Those familiar with switching power supplies will recognize some similarities with class D amplification [2]. One good example is the Buck converter, which takes a DC input voltage and steps it down to a lower DC voltage. It operates with high efficiency
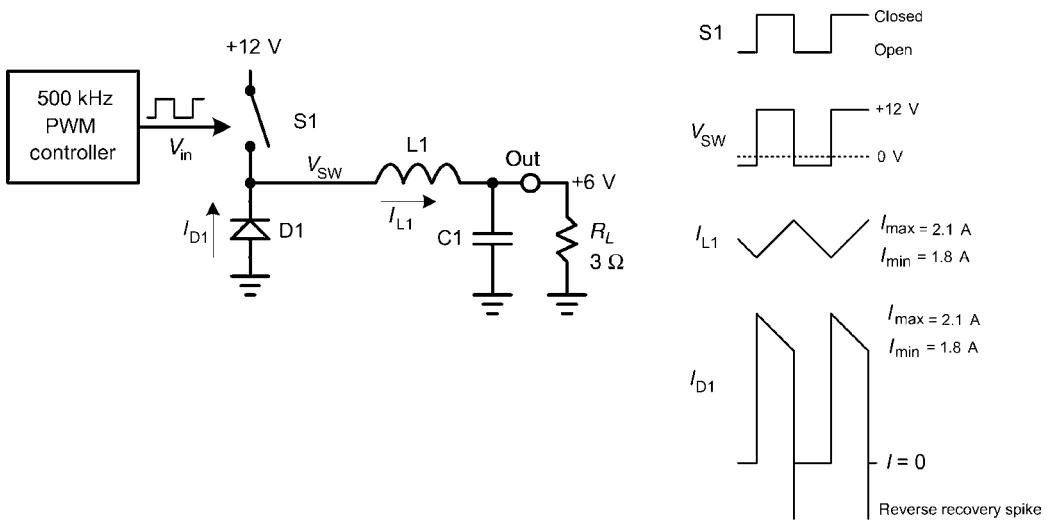
FIGURE 28.3   A Buck converter switching supply.

because its output devices switch on and off. The relative on time of these switches controls the amount of energy that is delivered to the load and thus the output voltage. It is basically a PWM arrangement. Having a basic understanding of the Buck converter is a very big step toward understanding a class D amplifier and some of its issues. For that reason we'll take a quick detour here and discuss Buck converters.

Figure 28.3 shows a very simple diagram of a Buck converter. It consists of a single switch that connects the supply rail to the output inductor for a variable amount of time. In this case the duty cycle is 50% and the output voltage will be half the supply voltage of 12 V. The converter also includes diode D1 and an output filter capacitor C1. A 3-Ω load is shown which will draw 2 A from the 6-V output of the converter. In a real circuit S1 will be implemented with a MOSFET. During the first half-cycle when S1 is closed, the rail voltage is applied to the inductor and the current will rise linearly with time in accordance with the voltage across the inductor and the inductance. It will reach a value I_{max}. This is also illustrated in Figure 28.3.

When S1 opens, the current in L1 will continue to flow due to its collapsing magnetic field. Inductors resist current change and try to keep current flowing. This current is usually referred to as the *flyback current* or the *commutation current*. During the second half-cycle the only place the current can flow from is through D1 from ground. The switched output voltage thus snaps from +12 V down to about –0.7 V, the forward drop of D1. It is very important in switching circuit design to recognize that the current continues to flow through the inductor during this second half-cycle. During the second half-cycle, the current in the inductor will fall linearly to I_{min}. Switching frequencies and inductor values are such that I_{min} is greater than zero at the end of the second half-cycle. The average of I_{max} and I_{min} is the output current into the load. The difference between I_{max} and I_{min} is called the *ripple current*.

Diode D1 is often called a *freewheeling*, *flyback*, or *commutating diode*. As shown in Figure 28.3, D1 is in a conducting state at the end of the second half-cycle when S1 again closes and raises the switched output from –0.7 V to +12 V. Diodes in a conducting state

cannot instantly stop conducting and become an open circuit when the current is reversed. Silicon diodes that have been conducting contain stored charge in the form of *minority carriers* that must be swept out before the diode can allow reverse voltage across its terminals. This process is called *reverse recovery*. As a result, a brief large current spike will occur when S1 closes. This is undesirable and represents lost energy and a source of EMI. Fast diodes with small reverse recovery times are thus desirable. Shottky diodes do not involve minority carriers and are largely free from the reverse recovery effect. They are also preferred because of their smaller forward voltage drop.

Synchronous Buck Converter

Figure 28.4 illustrates a synchronous Buck converter. Here D1 is replaced with a switch S2. This arrangement is more efficient because there is no junction drop when the inductor current is flowing from ground on the second half-cycle. That voltage drop represents lost power. S2 is sometimes referred to as a *synchronous rectifier*. It is a switch that is turned on when it is supposed to be conducting like a rectifier. In this arrangement, S2 is off when S1 is on and vice versa. For illustration, the duty cycle for S1 in the figure is set to 75%, resulting in a 9-V output and a 3-A current flow into the 3-Ω load resistor. Operation is largely identical to that of Figure 28.3 with the exception that the switched output voltage falls almost to zero during the second half-cycle instead of to –0.7 V.

There is one problem with the synchronous Buck converter. If both switches are on even briefly, the input power supply will be shorted to ground and a very large *shootthrough* current will flow. This must be avoided by adding *dead time* to the operation of the switches where both switches are off for a brief time.

If S1 opens and S2 has not yet closed, a very large negative flyback voltage will be created by the collapsing magnetic field of L1. The flyback voltage is clamped by adding D1. The switched output node will then be prevented from going more negative than –0.7 V. For this reason the negative portion of the switched output voltage will exhibit negative "ears" at the beginning and end of the second half-cycle when both switches are open.

Because the dead time is usually kept very small compared to the period, most of the improved efficiency contributed by S2 is preserved. Importantly, the R_{DSON} of the MOSFET used for S2 must be small enough so that the voltage drop across it when it is on is considerably smaller than the on voltage of D1. All MOSFETs designed for switching applications have D1 built into them in the form of the source-drain silicon body diode.
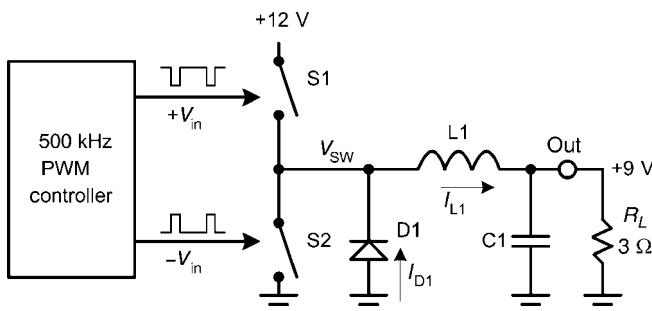
FIGURE 28.4 A synchronous Buck converter.

Unfortunately, this arrangement does not prevent the reverse recovery current spike when S1 closes. This is because D1 becomes conducting during the dead time just before the end of the second half-cycle. The reverse recovery shoot-through current can be reduced if a Shottky diode is connected in parallel with the MOSFET. It will prevent the slower silicon diode from ever turning on.

The switched output waveform depends only on the edge times of the high side switch S1. The on time of the low side switch S2 has no influence on the timing of the output edges as long as there is finite dead time. This is because a significant average current is being sourced to the load by the high side switch. The output goes low as soon as the high side switch turns off, before the low side switch turns on. This is due to the flyback behavior.

The output goes high only when the high side switch turns on, after the low side switch has turned off. The flyback current keeps the output low even after the low side switch has turned off. As long as current is being sourced to the load through the inductor, flyback current will be flowing through D1 until the end of the second half-cycle. This means that the timing of the low side switch will have no influence on the output edge times. This observation will be important when the influence of dead time on distortion in a class D amplifier is discussed.

The synchronous Buck converter looks very much like a class D amplifier, does it not?

Gate Drive Requirements and Power Dissipation

The gates of the switching MOSFETs must be driven on and off very quickly; this requires fast charge and discharge of the gate capacitance. This brings up the issue of gate charge. Consider an effective gate capacitance of 2000 pF and gate voltage drive amplitude of 10 V p–p. Assume that the gate drive voltage must transit through 10 V in 20 ns. The current required to accomplish this is

$$I = CV/T = (2 \text{ nF} * 10 \text{ V})/20 \text{ ns} = 1 \text{ A}$$

This means that the gate driver must be able to source or sink 1 A of gate current. This is quite a high current, even though its duration will be only 20 ns. This activity also consumes power.

Gate Charge

Gate charge is important in any switching application because it governs the amount of current required to charge the effective gate capacitance to turn the MOSFET on. This takes into account the change that is occurring in the drain voltage V_{ds} during turn-on. Gate charge is the effective charge contained in both the gate-source capacitance C_{gs} and the gate-drain capacitance C_{gd} when the device has turned on and V_{ds} is near zero. Gate charge also takes into account the strong nonlinearity of C_{gd} as a function of V_{ds}. Gate charge is defined in units of *coulombs*, where one *nanocoulomb* (nC) is the charge on a 1 nF capacitor with 1 V across it. The coulomb is also defined as a current flow over a period of time. One mA flowing for 1 µs corresponds to 1 nC.

Figure 28.5 illustrates how the MOSFET capacitances change as a function of V_{ds} for the IRFP240 [4]. C_{iss} is the total gate input capacitance and is the sum of the gate source capacitance C_{gs} and the gate drain capacitance C_{gd}. Capacitance C_{gd} is plotted separately, so C_{gs} can be inferred from the difference of the two plots. Notice that C_{gd} increases
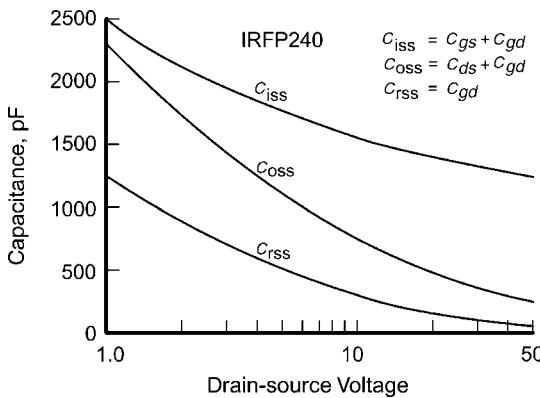
FIGURE 28.5   Capacitances for the IRFP240 N-channel MOSFET.

markedly as V_{ds} becomes small, rising from less than 50 pF at high voltages to more than 1200 pF at $V_{ds} = 1$ V. This accounts for most of the change in C_{iss} as a function of V_{ds} and implies that C_{gs} is fairly constant.

The output capacitance C_{oss} represents the sum of C_{gd} and the gate source body diode capacitance C_{ds}. Much of the increase in C_{oss} as V_{ds} decreases is a result of the increase in C_{gd} at low voltage. C_{ds} by itself increases from 200 pF to 1100 pF as V_{ds} decreases to 1 V.

A simplified gate charge diagram for the IRFP240 is shown in Figure 28.6a [4]. The gate charge diagram is sometimes difficult to understand at first glance. The diagram can be best understood by looking at the way gate charge is typically measured. Figure 28.6b shows a common test circuit for measuring gate charge. The MOSFET under test is connected in a common source arrangement and the drain is loaded with a current source that can pull the drain up to the specified test voltage. The current source at the drain sets the drain current test condition that is specified for the gate charge measurement. The gate is then forward-biased with a current source, starting from $V_{gs} = 0$. For the moment, think of the X axis of Figure 28.6a as time instead of charge. The gate voltage will initially rise to V_{gs_on}, where the device is able to conduct the test current. The rate of rise of V_{gs} during this time is reflective of C_{gs}.
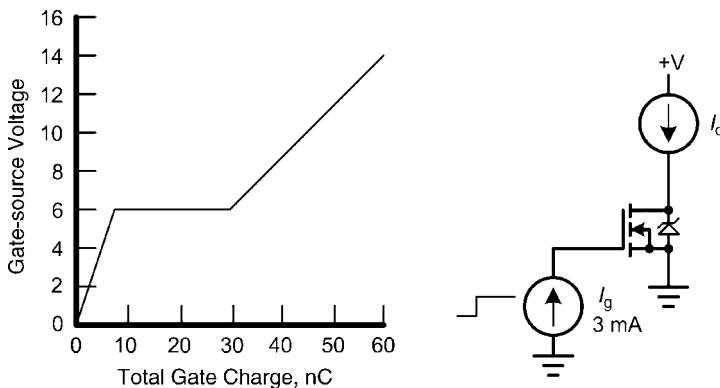
FIGURE 28.6   (a) Gate charge diagram. (b) Measurement setup.

The drain voltage will quickly fall once the gate voltage is sufficient to turn the device on and conduct the full amount of the test current. The voltage gain of the stage is very large at this point because of the current source load. During this time the gate voltage will hardly move because of the very large capacitance seen looking into the gate as a result of the Miller effect. The current being fed into the gate is charging the Miller capacitance.

After V_{ds} has fallen to zero, the gate voltage will again begin to rise. During this interval the rate at which the gate voltage rises is reflective of charging both the gate-source capacitance and the gate-drain capacitance. The gate-drain capacitance is not multiplied by the Miller effect during this interval, but is very large because V_{ds} is zero.

In the actual figure, the X axis is not time, but rather the amount of charge that was put into the gate as the process described above went forward. The initial turn-on slope reflects the rise of gate voltage with the constant gate current applied. Since charge is the product of current and time, and a constant current is applied to the gate, charge increases linearly with time so the X axis can represent time or charge. Since Q also represents the product of voltage and capacitance, the slope of the turn-on portion is reflective of C_{gs}. That slope is in nanocoulombs per volt, which has the units of capacitance. In the diagram the slope is 1.2 nC/V, which corresponds to 1.2 nF.

MOSFET Figure of Merit

The Figure of Merit (FOM) for MOSFETs in switching applications is the product of on resistance R_{DSON} and total gate charge Q_g [5]. Smaller FOM is better. R_{DSON} is important because it determines power losses when the device is turned on. Typical values lie in the range of 0.02 Ω to 0.2 Ω. The total gate charge is important because it determines how much power is expended in turning the transistor on and off. The power required to turn the gate on and off at a given frequency is simply $Q_g * V_g * f$. This is called *switching loss*.

Typical FOM for 200-V MOSFETs ranges between 5 Ω-nC and 25 Ω-nC. FOM tends to be larger for higher-voltage devices because they have higher R_{DSON} for a given amount of gate capacitance. The FOM is also larger for P-channel devices because they depend on hole conduction, which has a lower carrier mobility than electron conduction. As a result, P-channel device R_{DSON} is higher for a given amount of effective gate capacitance. For example, the 30-V, 7-A IRF9410 has FOM = 0.5 Ω-nC. By comparison the 30-V, 6-A P-channel IRF7406 has FOM = 1.62 Ω-nC.

The familiar IRFP240 has FOM = 12.6 Ω-nC, while the complement IRFP 9240 has FOM = 22 Ω-nC. These are conventional HEXFET-type devices. Some N-channel trench-type MOSFETs in this voltage range have FOM = 5 Ω-nC. Unfortunately, trench-type P-channel MOSFETs are much less common in this voltage range, especially with high current ratings. Indeed, it appears that 200-V P-channel trench type MOSFETs have little advantage in FOM over conventional devices. Table 28.1 shows the FOM for some representative MOSFETs.

Conduction Loss

Consider a MOSFET with $R_{DSON} = 0.2$ Ω that must operate at 10 A with a 50% duty cycle. Its average conduction power loss will be 10 W. This is plainly not insignificant. It represents a 5% efficiency loss in a 200-W amplifier, and that is for only one half of the output stage. A second transistor could be placed in parallel, but that would double the

Device	Type	V_{BR}	ID, A	R_{DSON}	Q_g, nC	FOM, Ω-nC
Si7431DP	P-trench	200	3.8	0.18	135	24.3
IRF9640	P-conv	200	11	0.5	44	24.2
IRFP9240	P-conv	200	12	0.5	44	22.0
27N20-78	N-trench	200	27	0.08	60	4.8
IRF640	N-trench	200	16	0.18	63	11.3
IRFP240	N-conv	200	20	0.18	70	12.6
IRFB23N15D	N-conv	150	23	0.09	56	5.0

TABLE 28.1   Figure of Merit (FOM) for Several Power MOSFETs

gate charge and the FOM of the pair would remain the same. Conduction loss would be cut in half, but switching loss would be doubled. A good design will strike a proper balance between conduction loss and switching loss. If switching loss is low, it makes sense to parallel devices.

Switching Loss

Whenever a capacitance is charged and discharged at a certain frequency, power is expended. Consider a 2000-pF capacitor that is charged to 10 V in 20 ns. This requires a charging current of 1 A for 20 ns from a 10-V source. The current source is thus consuming 10 W for 20 ns. If it does so at a 500-kHz frequency f_s, whose period is 2 μs, then the duty cycle of this 10-W dissipation is 1%, and the average power is 100 mW. The power expended in charging and discharging a capacitor at frequency f_s is simply P = CV^2f_s = 100 mW. The accumulated charge Q on the capacitor is the product of its voltage and capacitance expressed in nanocoulombs. Here the charge is 20 nC. The power dissipated can instead be expressed as $P = QVf_s$.

Consider a MOSFET with Q_g = 70 nC and operating at a switching frequency f_s of 500 kHz. Assume that the gate drive voltage is 10 V p–p. The power required to drive it will be $Q_gV_{gs}f_s$ = 70 nC $*$ 10 V $*$ 500 kHz = 0.35 W.

Reverse Recovery Loss

There is a second significant source of switching loss. This one results from the reverse recovery time t_{rr} of the MOSFET body diode. If the low side body diode is in conduction when the high side switch turns on, a very large current will flow from the positive rail into the diode to sweep out its minority carrier charge. This is a form of shoot-through current. Normally the low side switch will have been on during this time, shunting the body diode and preventing it from being in conduction. However, if inductor flyback current is flowing during the necessary dead time prior to the turn-on of the high side switch, the inductor current will flow through the body diode during the dead time, forward biasing it and allowing it to accumulate a minority carrier charge.

Body-diode conduction is another issue that underlines the importance of low R_{DSON} for the switching MOSFETs. If R_{DSON} is so large that the flyback current causes a voltage drop across the MOSFET equal to a one junction drop, the body diode will be on during a large portion of the half-cycle when the MOSFET should be shunting it and keeping

it off. This will add to distortion by allowing the peak value of V_s to be larger by one junction drop than the rail voltage. It may also exacerbate body diode reverse recovery current spikes, especially relative to what they might have been if dead time is kept very small.

28.3 Class D Output Stages

The output stage is where many of the challenges lie in class D amplifiers [2, 5]. This is where the power supply rail voltages are alternately switched onto the output bus at very high frequencies with very fast rise and fall times. Typical carrier frequencies are in the 500-kHz range while typical rise and fall times are in the 20-ns range. In an amplifier with ±50-V rails where the output transitions through 100V in 20 ns, the voltage rate-of-change at the output switching node is about 5000 V/µs. To put this in perspective, 2.5 A is required to drive a 500-pF capacitor at this voltage rate of change (slew rate).

Single-Ended and H-Bridge Output Stages

Figure 28.7 illustrates two common class D output stages [2]. The first is a single-ended version employing complementary MOSFETs. An N-channel MOSFET is used for the low side switch, and a P-channel MOSFET is used for the high side switch. Both of these devices are in a common-source configuration. A typical second-order output filter is shown. The second arrangement is what is called an *H-bridge*. This circuit is driven so that when one side is high the other side is low, doubling the output voltage available to the load. Interestingly, the H-bridge conveniently has an off position where no current flows in the load if both sides of the bridge are high or low. The single-ended output arrangement is commonly referred to as a *half bridge*, while the H-bridge arrangement is referred to as a *full bridge*.

The full bridge requires twice as many components, but only half the power supply voltage to realize a given output power capability. This is analogous to linear amplifiers that are bridged. The full bridge also has some technical advantages in regard to the class D amplification process that will be discussed later. MOSFETs with desirable switching characteristics are more readily available with lower voltage ratings (below about 150 V), so high-power class D amplifiers will often employ a full bridge.

N-Channel Output Stages

N-channel MOSFETs inevitably have better switching characteristics than P-channel devices. Their FOM is usually less than half that of corresponding P-channel devices. For this reason, output stages often employ N-channel devices for both the low side and
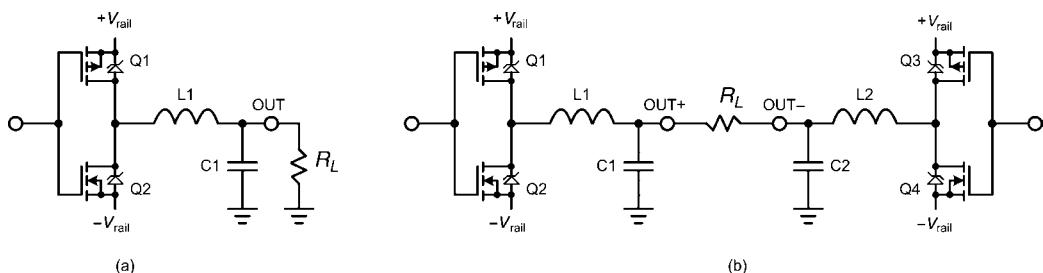
FIGURE 28.7 Half bridge and full bridge class D output stages.
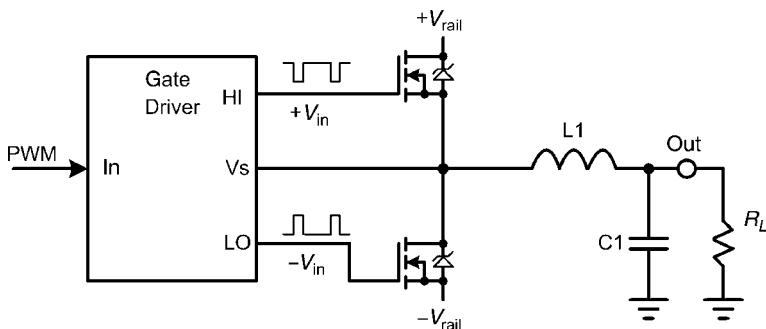
Figure 28.8 Half bridge output stage with N-channel high side and low side MOSFETs.

high side switches, as shown in Figure 28.8. These designs require more complex drivers that include level shifters and boost supplies [1, 5]. The gate drive for the high side N-channel MOSFET must float on top of the output signal, since it is referenced to the source of the device. The boost supply is required because the high side N-channel switch requires gate drive voltages above the positive rail in order to turn on. Fortunately, integrated circuit drivers are available that take care of most of the complexity. An example is the International Rectifier IR2011 [5].

The boost voltage is usually obtained by a bootstrap circuit consisting of a diode and a capacitor pumped from the square wave on the output node. The bootstrap supply can suffer performance problems when the PWM duty cycle approaches 0% or 100% as a result of the very narrow pulses that it has to work with under these conditions. For the highest sound quality and maximum achievable depth of modulation, a separate linear or switching supply can be used to provide the gate drive boost voltage. Such a supply will then not depend on the nature of the audio signal.

Gate Drive Control

The input impedance of a MOSFET gate is very high at low frequencies, but becomes quite low at high frequencies as a result of gate-source (C_{gs}) and gate-drain (C_{gd}) capacitances, which can be quite high. These gate capacitances must be charged and discharged at a very high speed in class D output stages. Further adding to the gate drive burden is the Miller effect involving the gate-drain capacitance. Peak gate drive currents can lie in the ampere range even in a 100-W class D amplifier. Further complicating this is the need to provide highly precise gate timing to minimize distortion.

Dead Time Control

When switches are connected from both the positive and negative rails to a single output node, there is always the possibility that both switches will briefly be on at the same time. This will cause shoot-through current to flow directly from the positive supply to the negative supply. At minimum, this will result in wasted power. In some cases it will result in the destruction of the output stage. For this reason there is a very small dead zone incorporated into the MOSFET drive circuit. This ensures that there is always a very small time when both devices are turned off. With slight variations in timing, there should never be a situation where both devices are on simultaneously. Unfortunately, the presence of this dead time is a cause of distortion [5]. This will be discussed in Chapter 29.

Adaptive Dead Time Control

Proper dead time is critical for most class D solutions to prevent shoot-through current and minimize distortion. The amount of dead time is measured in nanoseconds, yet it may vary from part to part and unit to unit and with temperature and operating conditions. If the presence and amount of shoot-through current can be measured, dead time for the high side and low side switches can be independently controlled. This can be done by a set-and-forget approach or by a control loop.

Dead time controllability can be implemented in analog PWM circuits by changing the bias and slicing point at key places in the driver chain. Digital modulators offer other means for adjustment of high side and low side dead time. A digital modulator operating with a 100-MHz clock can manipulate dead time in discrete increments of 10 ns.

Closed-loop control of dead time can be based on actual output stage behavior. If the presence of shoot-through current can be sensed, the feedback loop can adjust the dead time inserted to a small acceptable value. Such dead time control is not unlike the spark-timing control system in an automobile engine where a detector monitors the engine for evidence of pinging and backs off the timing just to the point where the pinging becomes small and inconsequential.

The presence of shoot-through current is detectable in a number of ways. The spikes are very narrow, and of high amplitude, so placing even a small amount of inductance in series with the power rail can make them easily detectable. A 0.05-Ω wire wound resistor will suffice. Shoot-through can be observed by measuring the impulse current at the leading edge (turn-on) of the driver with the smaller pulse width. The leading edge is not affected by body diode reverse recovery. If shoot-through is detected, turn-on of that device should be retarded. Dead time for the low side device is evaluated on positive half-cycles, while dead time for the high side device is evaluated on negative half-cycles.

28.4   Summary

While the operating principle for class D amplification is fairly simple, the devil is truly in the details. As we have already begun to see, there are many potential sources of imperfection and many design challenges associated with class D. Chapter 29 will delve more deeply into the challenges posed by simple PWM class D amplifiers.

References

1. Honda, Jun, and Adams, Jonathan, "Class D Audio Amplifier Basics," International Rectifier Application Note AN-1071, February 2005.
2. Neilsen, Karsten, "A Review and Comparison of Pulse-Width Modulation (PWM) Methods for Analog and Digital Input Switching Power Amplifiers," paper No, 4446, 102nd AES Convention, March 1997.
3. Gaalaas, Eric. "Class D Audio Amplifiers: What, Why, and How," *Analog Dialog,* pp. 40–06, June 2006.
4. Vishay-Siliconix IRFP240 data sheet.
5. High Power Class D Audio Power Amplifier using IR2011S, International Rectifier application note IRAUDAMP1, www.irf.com, 2005.

Class D Design Issues

T his chapter really gets into the nuts and bolts of class D amplifier design, focusing on the many challenges that must be overcome to achieve high sound quality from what is essentially a switching process that alternately applies the positive and negative power supply rails to the output to drive the loudspeaker. Imperfections in the high-speed switching process are a major contributor to distortion in class D amplifiers, and these are discussed in detail. This is an area that is somewhat foreign to many designers of conventional linear amplifiers.

Negative feedback must be applied to most class D amplifiers so that acceptable performance can be achieved, and yet the application of negative feedback to these amplifiers is not always straightforward. The necessary output low-pass filter in class D amplifiers will usually cause a significant increase in the output impedance of the amplifier and lead to frequency response aberrations and tonal coloration that depend on the frequency-dependent load impedance of the particular loudspeaker being driven. Some class D amplifiers enclose all or part of the output filter in the feedback loop, but this can make achieving stability quite difficult.

The high-speed switching in class D output stages can be a powerful source of EMI. This can result in unacceptable EMI emissions that may interfere with radio transmissions and associated audio equipment. Without adequate precautions, the loudspeaker cable can become an effective antenna for spreading these emissions.

29.1   The Output Filter and EMI

The raw output of the class D output stage is a sharp-edged rectangular waveform whose pulse width varies. Rise times of the switched output pulses are often between 5 ns and 40 ns. The output filter serves two very important purposes. First, the filter extracts the low-frequency average from the high-frequency rectangular waveform to provide the audio output signal. In this regard, it is a PWM-to-analog converter. Secondly, it must filter out the very high-frequency carrier and its harmonics to prevent EMI radiation from the amplifier. The filter must be designed to operate at high current with low distortion. The radiation of the filter itself within the amplifier must also be considered carefully as this could cause distortion in the analog circuits.

The simplest output filter is the second-order filter with a single inductor and capacitor. Its response will fall off at 12 dB per octave (40 dB/decade) above its cutoff frequency. It is not unusual to employ an output filter with a cutoff frequency that is about a decade below the PWM carrier frequency. This will provide about 40 dB of attenuation at the carrier frequency and about 60 dB of attenuation at the third harmonic of the carrier frequency.

It is important that the filter capacitor has low ESR and low ESL so that it maintains low impedance at high frequencies. For this reason it is unwise to employ only a film capacitor. A film capacitor should be bypassed with a large-capacitance ceramic NPO capacitor.

The stray capacitance in the filter inductor can cause EMI leak-through at high frequencies; above their self-resonant frequency, inductors look like capacitors. For this reason, inductor geometry can be important. Output inductors with very high self-resonant frequencies should be chosen, especially when output filters are of only second order.

Higher-order filters employing a multiplicity of inductors and capacitors can provide improved attenuation at the higher harmonic frequencies that are often more troublesome for EMI conformance. This does not necessarily mean that the filter has to grow a lot in size or total series inductance. In many cases it means a redistribution of the existing amount of inductance and capacitance into a multiplicity of smaller elements. It is worth noting that smaller shunt capacitors are usually better at suppressing high frequencies because of their lower ESL and ESR.

Example of second-order and fourth-order output filters are shown in Figure 29.1. The fourth-order filter is an example of a higher-order filter as discussed above. Half of the original 20-μH inductance of the second-order filter is placed in the first inductor and only 3 μH is placed in the second inductor, for a net reduction in total inductance. Most of the original capacitance is split to lie on either side of the second inductor. The second inductor can be made physically quite small. The third inductor is only 100 nH and comes from the wiring to the amplifier output terminals. A few inches will create this much inductance. A lesser distance will result in this amount of inductance if a small one-turn loop is put in the wire. The third capacitor, only 0.02 μF, is placed right across the output terminals. These last two components technically make the filter sixth order, but the last pair of poles is at a much higher frequency. This arrangement does not change the attenuation at 500 kHz (both 40 dB), but it greatly improves the attenuation at higher frequencies. It also greatly reduces high-frequency EMI *sneak-through* that may result from the real-world imperfections of simpler filter implementations. The output amplitude from this filter at the seventh harmonic of the carrier frequency (3.5 MHz) is over 35 dB lower than from the second-order filter.

Compared to the second-order filter, the higher-order filter has less variation in response at 20 kHz when the load impedance varies from 4 Ω to 8 Ω, and also has a higher 3-dB bandwidth (60 kHz with a 4-Ω load and 90 kHz with an 8-Ω load). The phase characteristic of the higher-order filter is also more linear than that of the second-order filter. These output filters work well with a 50 kHz single-pole filter at the input of the amplifier.
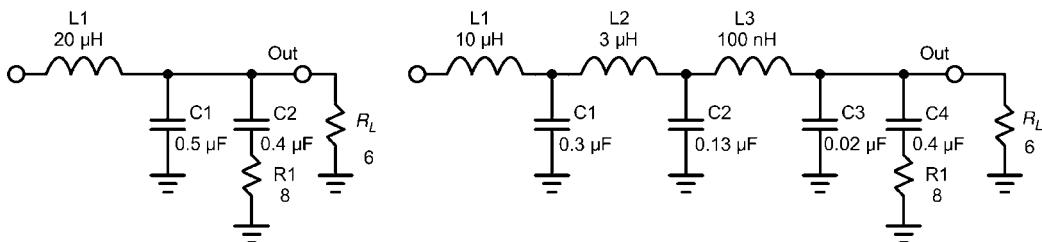
FIGURE 29.1 Example of second- and fourth-order output filters with Zobel networks.

The Zobel Network

Proper operation of the output filter depends on it being loaded with the correct impedance. Unfortunately, the impedance of loudspeakers is all over the map. This is of particular concern at high frequencies where the filter action is taking place. Loudspeakers can become inductive at high frequencies, as can the speaker cable driving them. For this reason a Zobel network is often placed at the output of the filter so that at high frequencies there appears a resistive load [2]. This network will usually comprise an 8-Ω resistor in series with a capacitor, much like the Zobel network used in linear amplifiers. The corner frequency of the Zobel network impedance will often be set to be in the vicinity of the cutoff frequency of the filter. For a Zobel impedance corner of 50 kHz with 8 Ω the capacitance will be about 0.4 μF. Such a Zobel network is illustrated in the filter of Figure 29.1. As with linear amplifiers, some dissipation will occur in the Zobel network and the resistor must be sized accordingly. It is especially desirable that the Zobel resistor in a class D amplifier be noninductive.

Differing Loudspeaker Impedance

While the Zobel network can at least keep the load impedance fairly resistive at high frequencies, the need for a class D amplifier to drive loudspeakers of differing nominal impedances can create even more problems for filter design. Indeed, even resistive loads ranging from 2 to 8 Ω can play havoc with filter frequency response and force serious compromises. Worse yet, the filter characteristic driving a very high impedance or no-load condition can develop serious peaking. This is not something we are used to with conventional amplifiers.

Linear Phase Approximation

Because the filter cutoff frequency is less than a decade above the audio band it becomes important to do the best job possible with its phase response and group delay. This means attempting to approximate a linear phase response that corresponds to a constant time delay. This means that maximally flat filters like the Butterworth may not always be the best choice. The overall linear phase characteristic of the amplifier can also be achieved in part by designing the amplifier input filter to work with the output filter. A fourth-order output filter that has a shallow initial roll-off will provide a better approximation to a linear phase characteristic than a second-order filter. The objective is to have a phase characteristic that approaches a straight line when phase is plotted with an X axis that is linear in frequency. The need to drive speaker loads of differing nominal impedances makes the goal of achieving a linear phase filter characteristic for all conditions elusive.

Reducing Output Filter Size

There is a strong incentive to reduce the physical size and series inductance of the output filter. This will reduce cost, improve damping factor, and reduce distortion. These objectives are usually met by increasing the filter's cutoff frequency. Anything in the class D amplifier design that allows a higher filter cutoff frequency helps in this regard. Doubling the PWM carrier frequency will permit doubling the filter cutoff frequency; this in turn will allow the inductance to be reduced by a factor of 4 if the capacitance in the filter is held constant.

The PWM carrier frequency is the highest-amplitude EMI frequency and lies at the point of lowest output filter EMI attenuation. If carrier frequency EMI is a problem,

sometimes a filter with a notch at the carrier frequency (or an elliptic filter) will be used to enhance carrier rejection.

Input Filter and Aliasing

While on the subject of filters it is worth mentioning the importance of the amplifier input filter. All class D amplifiers involve a sampling process of one kind or another applied to the analog input signal. This means that aliasing is always possible. For this reason the input filter that is commonly found on linear power amplifiers takes on even greater importance. The input filter need not necessarily have a low cutoff frequency, but it must have good attenuation at frequencies approaching half the PWM carrier frequency and above.

The different frequencies that can be produced when the triangle wave and the audio signal are together passed through the odd-order nonlinearity of the comparator are discussed in Ref. 2. This process can produce lower frequencies that must be kept above the audio band. If f_c is the PWM carrier frequency and f_s is the signal frequency, then aliases will be produced at numerous frequencies including the following:

$$f_c, f_c \pm 2f_s, 2f_c \pm f_s, 2f_c \pm 3f_s, \dots$$

The lowest of these cited by Leach is $f_c - 2f_s$. If f_c is 500 kHz and f_s is 20 kHz, then the alias frequency will be 460 kHz. However, there is not a brick wall filter at 20 kHz. The output of an SACD player often has significant high-frequency content, sometimes including some sampling tones at ultrasonic frequencies. One SACD player that was measured produced about 50 mV RMS at its output at 80 kHz. A tone at 80 kHz will produce an alias at 340 kHz. Fortunately, this is still well above the audio band. It is also important to recognize that noise from the signal source in the upper ultrasonic band can be aliased down into the audio band.

Other EMI Issues

There are many sources of EMI in a switching amplifier by the very nature of the fast, sharp-edged signals transitioning at high frequencies within the circuit. In many cases these exist as high that can create high-frequency magnetic fields, especially if the loops through which these currents circulate are not kept very small. If the body diode of the output MOSFET is allowed to conduct, its reverse recovery time will lead to brief high currents when the diode is quickly changed from a forward-biased condition to a reverse-biased one. The brief high-current flow required to sweep out the minority carrier charge in the diode will be a source of EMI. The use of Shottky commutating diodes from drain to source on output transistors can help here.

Output Filter Distortion

The components employed in the output filter must pass high currents. This is a problem for the output inductor, which almost always includes a magnetic core of some kind to keep the size reasonable. The core is subject to nonlinearity and ultimately saturation [3]. Indeed, the value of the inductance is current-dependent, so that the tuning of the output filter may actually change as a function of load current. This can cause decreased effectiveness of tuned notch filters and can certainly cause PIM. Any degree of core saturation will also introduce switching losses, which will decrease the efficiency of the amplifier. Powder core toroidal inductors are most often employed for the output coils.

In applications for highest sound quality, air-core toroids can be considered, especially if space permits and the value of inductance can be kept below about 4 μH. A non-ferrous plastic toroidal former can be employed.

29.2   Sources of Distortion

As suggested in Chapter 28, there are numerous sources of distortion in class D amplifiers. A few of these are listed below and each is discussed briefly [4]**.**

Triangle Reference Linearity and Bandwidth

Any departure from linearity in the reference triangle waveform in a class D PWM modulator will translate directly to distortion in the audio output [1, 4]. While the production of a very linear ramp is not difficult at low frequencies, it becomes progressively more difficult at higher frequencies. Limited bandwidth in the generation or processing of the triangle wave will result in rounded edges rather than straight and pointed edges. This corresponds to nonlinearity as well, and therefore causes distortion.

Pulse Width Quantization

Simple digital approaches to the production of a PWM signal rely on functions like counters and timers to determine the width of the modulator output pulses. This leads to quantization in the time domain. Consider a simple digital modulator that employs a 100-MHz clock. This will result in pulses that are quantized to 10 ns. Now assume that the PWM switching frequency is 500 kHz, with alternating 1-μs positive and negative pulses at idle. This means that the width of each pulse has a resolution of only 1%. This corresponds to a factor of 100, which in turn corresponds to a granularity of only about 7 bits. This is not very good. Analog PWM solutions do not suffer this limitation.

Dead Time

The necessary dead time in the PWM output stage causes distortion [4]. For this reason dead time must be minimized. However, if nominal dead time is made small, there is a greater risk of shoot-through current unless very precise timing in the output stage can be maintained. There is thus a delicate trade-off between distortion and design margin. Dead time subtracts from effective pulse width and causes the relationship between modulator pulse width and output pulse width to become nonlinear and so results in distortion.

Low distortion in the output stage depends on the areas of the positive and negative pulses at the switching output being in the same proportion as the corresponding pulse areas in the waveform driving the output stage from the PWM modulator. If the positive and negative supply voltages are the same, this translates to faithful reproduction of the duty cycle ratio from the PWM modulator output to the switching output. Within the output stage, the positive and negative pulses are each shortened on their leading edges to create necessary dead time. However, the actual switching output pulse waveform V_s is different from the gate drive waveforms. The V_s waveform has no dead time. Understanding which edges of the switch driver waveforms control the switched output waveform transitions is key to understanding the dead time distortion mechanism. This time relationship was touched on briefly in the discussion of the synchronous Buck converter in Chapter 28.
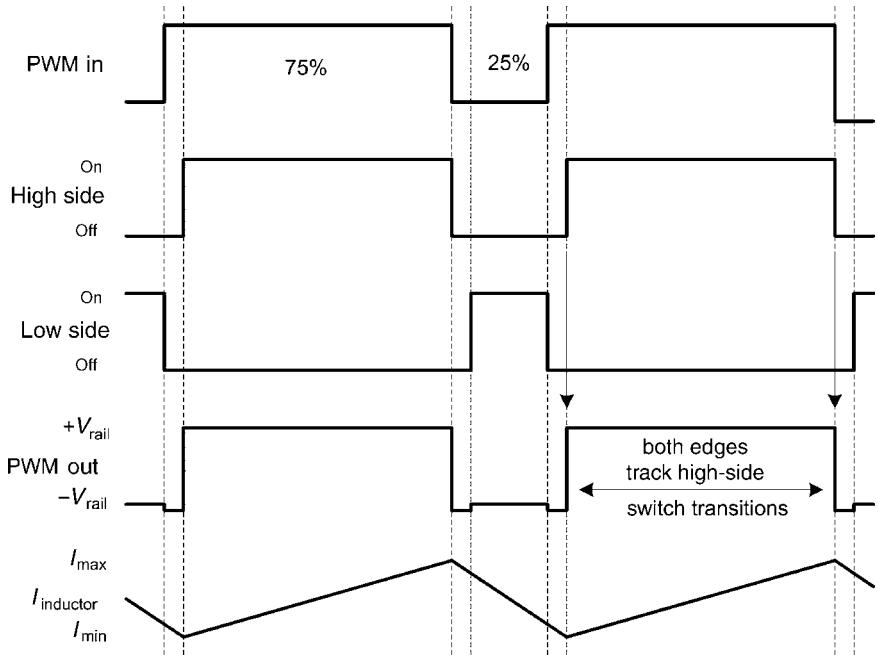
FIGURE 29.2   PWM waveforms when duty cycle is 75%.

Consider a 500-kHz PWM square wave with 75% duty cycle from the modulator, as shown in Figure 29.2. It will be high for 1500 ns and low for 500 ns. Assume that a fairly large nominal dead time of 50 ns is introduced. After passing through dead time control, the high side drive pulse will be 1450 ns and the low side drive pulse will be 450 ns. Assume that $t = 0$ is defined at the turnoff of the low side switch. The high side switch will be activated at $t = 50$ ns and will turn off at $t = 1500$ ns. The low side switch will be turned on at $t = 1550$ ns and will be turned off at 2000 ns. We assume no delay in the switches.

The switched output V_s will go high at 50 ns when the high side switch turns on. It will go low at 1500 ns, when the high side switch opens and the flyback process begins. Notice that the output goes low before the low side switch has turned on. The flyback process made it go low, not the turning on of the low side switch. The output will stay low until the high side turns on at 2050 ns. The output will not rise at 2000 ns when the low side switch turns off because the flyback current is still reversing the low side switch. Flyback current is still flowing at the end of the second half-cycle because a large net current is being sourced to the load.

The key observation here is that the switched output waveform V_s follows both rising and falling edges of the high side switch [4]. Detailed timing of the low side switch has nothing to do with the output edge times under these conditions. This is because the high side is sourcing significant net current to the load and the inductor current remains positive throughout the entire cycle. The positive output pulse width will be 1450 ns, representing a duty cycle of only 72.5%. Some attenuation has thus occurred as a result of dead time.

The situation will be analogous in the case where the PWM duty cycle is small and the low side switch is on most of the time. In this case, both edges of the low side switch will govern the edges of V_s. It is clear that if the dead times for the high side and low side are not identical, the incremental gain of the output stage will be different for positive and negative signals, and distortion will result.

This is not the end of the story. Even if the two dead times are identical, distortion will still result. Recall that there is ripple current in the inductor. When the amplifier is sourcing current to the load the inductor current is at I_{max} at the end of the high side switch time and decreases linearly to I_{min} at the end of the second half-cycle. The difference between I_{max} and I_{min} is the ripple current and the average of I_{max} and I_{min} (I_{avg}) is the net current sourced to the load. As long as I_{max} is at least twice I_{avg}, I_{min} will not go negative and flyback current will persist in the low side switch circuit until the end of the cycle. The situation will be as discussed above.

Notice the small negative-going "ears" on V_s in Figure 29.2. Flyback current is being sourced to the load during the time when the high side switch is off. When the low side switch is also off during the dead times, the flyback current is sourced through the commutating diode, causing V_s to go negative by the amount of the forward drop of the commutating diode. This phenomenon also affects net output pulse area and can contribute to distortion.

Whenever flyback current is flowing during a dead time, it will flow through a commutating diode and will cause V_s to go slightly beyond the rail voltage. This effect can be reduced by employing Shottky diodes because their forward voltage drop is smaller than that of the silicon diodes incorporated in the MOSFETs.

If I_{max} is less than twice I_{avg}, I_{min} will go negative, as illustrated in Figure 29.3. Put another way, if the average load current is less than half the peak-to-peak ripple current, the condition will be satisfied. Under this condition the direction of the inductor current will reverse before the end of the cycle. This further means that flyback current through the low side switch will cease before the end of the cycle. With the low side switch still on, the low side switch will begin to conduct forward current before the end of the cycle, sinking current from the load. In this case, the turnoff of the low side switch will create a flyback of V_s to the positive rail, even before the high side switch has turned on. In this scenario the time when the low side switch turns off controls the positive edge of V_s. This is very different from the scenario discussed earlier where both edges of the high side switch controlled the edges of V_s. The edges of V_s are now controlled by the falling edges of the gate drives of the high and low side switches [4].

PWM Crossover Distortion

If the turn-off edges of both switches control their respective edges of V_s, then the signal attenuation due to dead time pulse narrowing described earlier no longer exists. The duty cycle of V_s is a more faithful replica of the duty cycle created by the PWM modulator. The incremental gain of the output stage is thus higher when the current delivered to the load is smaller than half the peak-to-peak inductor ripple current. We will refer to this as the *central region* of operation.

In the region of 50% modulator duty cycle, the duty cycle of V_s is a faithful replica of the incoming PWM duty cycle, independent of dead time. This region of operation is not unlike the class A region of a linear class AB amplifier where both top and bottom transistors are contributing to the output. When larger signal currents cause the class D output stage behavior to exit this region, crossover distortion occurs because the incremental
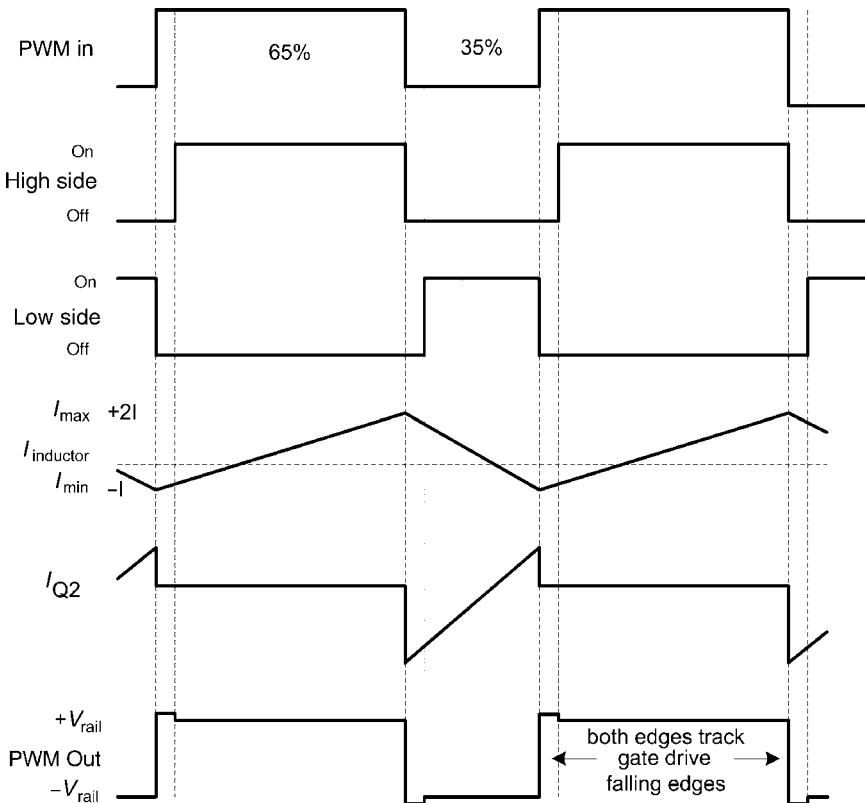
FIGURE 29.3   Current waveform of low side transistor Q2 when duty cycle is 65%.

gain of the output stage decreases. This is akin to *gm* doubling in a linear class AB output stage where output stage gain decreases at currents outside the class A region.

The PWM Central Region

The central region of PWM operation extends to peak signal output currents that are half the peak-to-peak inductor ripple current. The peak-to-peak inductor ripple current at idle is related to the rail voltage V_{rail}, the output inductance, and the duration of one-half cycle of the PWM switching period T. During the half-cycle, the current in the inductor increases linearly in accordance with the voltage across it and its inductance.

$$I_{ripple} = V_{rail}(T/2)/L \tag{27.1}$$

With 50-V rails, a 20-μH inductor and a 2-μs period, the peak-to-peak ripple current will be 2.5 A p–p when the filtered output voltage is 0 V. This means that the central region will extend to a peak output current of 1.25 A. This corresponds to 6.25 W into 8 Ω. This in turn corresponds to a PWM duty cycle of 60%.

When the amplifier output voltage is non-zero due to signal swing, the peak ripple current will change because the difference between the rail voltage and the output voltage will be larger or smaller. However, the smaller calculation of ripple current on one

half-cycle will be offset by the larger value of ripple current on the other half-cycle, keeping the net peak-to-peak ripple current essentially the same over signal swing excursions.

Notice that, all else remaining equal, an amplifier with higher rail voltages will have a correspondingly larger central region of operation due to larger ripple current. It is also of interest to note that in the PWM central region there is no body diode reverse recovery spike. This is because the diode current will have gone to zero before the associated MOSFET turns off for its dead time. There is thus no minority carrier charge in the diode when the opposite-side switch turns on.

Extending the PWM Central Region

The central region can be extended if the ripple current is increased. This can be accomplished by decreasing the size of the output inductor. If the output inductor value is cut in half, the ripple current will be doubled and the extent of the central region of PWM operation will be doubled (quadrupled in power). In this respect, the amount of ripple current is akin to the amount of quiescent bias current in a linear class AB output stage.

If the inductance is cut in half and the size of the capacitor in the filter is left unchanged, the cutoff frequency of the filter will be increased by 1/2 octave and EMI will be increased. It may be possible to employ a fourth-order filter to restore the high-frequency attenuation, however.

Asymmetrical Rise/Fall Times

If a switch is conducting forward current when it turns off, the switched output node will *fly back* to the opposite rail voltage in a *freewheeling* fashion; rise time will be controlled by the inductor and capacitances at the switching node. On the other hand, if a switch is off before the end of its half-cycle period, commutation current will be flowing in the reverse direction and the rise time will be governed by the turn-on current of the opposite switch when it turns on. The resulting rise time at the switching node may be much faster in that case. Asymmetry in switching node rise and fall time will thus result. This phenomenon will generally occur when the signal current is large enough to be outside the central operating region.

Body Diode Conduction Time

Another small error is introduced into the pulse areas by the additional voltage dropped across the body diode during the time it is conducting the flyback current instead of the associated switch. This occurs during the dead time on the switching side whose pulses are narrower when the output stage is operating outside the central region. The effective rail voltage during this time is larger by the junction drop of the conducting body diode. As a result, the area of the smaller pulse is increased slightly. This is evidenced by the "ears" on the low side pulse in Figure 29.2.

Sliver Pulses

At very high modulation levels the pulses on one switch side become very narrow. Consider a PWM modulator operating at 500 kHz with an output stage that has 20-ns dead times and 20-ns rise and fall times on the switched output. Let the PWM duty cycle be 99%. This means that the idealized on time of the low side switch will be 1 % of

the period of 2000 ns, or 20 ns. It is immediately apparent that the low side switch will never turn on because its dead time equals the PWM modulator off time. Bear in mind that under these conditions high current is being delivered to the load and the timing of V_s will be entirely governed by the leading and trailing edges of the high side switch. The modulator on time is 1980 ns and the high side switch on time is 1960 ns.

When the high side switch opens V_s will transition to the negative rail, taking 20 ns to do so. It will remain there for 20 ns until the high side switch closes. V_s will then rise to the positive rail, taking 20 ns to do so. The effective duration of the low pulse is 40 ns. The effective duration of the high pulse is 2000 − 40 = 1960 ns. This is fortunately the same as the high side switch on time. Even at 99% duty cycle the output stage works largely as expected. This is a bit nonintuitive.

29.3   Bus Pumping

Bus pumping represents the transfer of energy from one power supply to the opposite power supply when a half bridge output stage is employed [4]. Assume that the low side has been on and sinking current from the load through the inductor. The magnetic field in the inductor represents stored energy. When the low side turns off, the output voltage will quickly transition from the negative rail to the positive rail as the magnetic field collapses. Commutation current will continue to flow in the same direction through the inductor for some time because inductors seek to keep current flowing in the same direction.

The commutation current flowing into the inductor now must come from the positive supply, but it is in a direction that actually seeks to make the positive supply more positive. The commutation current pumps up the positive rail through the high side commutation diode. The process represents an almost lossless transfer of energy from the negative supply to the positive supply. If the duty cycle of the square wave is less than 50% over a long period of time (as with a negative DC output condition or a negative low-frequency half-cycle), more energy will be transferred from the negative supply to the positive supply during this period, representing an average transfer of energy from the negative supply to the positive supply. If the positive supply cannot absorb this energy, its voltage will rise as a result of the pumping.

The pumping occurs even with a resistive load; it does not depend on the reactive nature of a loudspeaker. Bus pumping depends on the reactive behavior of the output inductor. The reactive nature of the loudspeaker can exacerbate pumping, however. The effects of bus pumping are worse at low frequencies because the reservoir capacitors can change their voltage over the signal cycle if the power supply cannot absorb the pump current. If there is another source of heavy current drawn from the supply in excess of the commutation current that is pumping the supply, then there will be no problem.

Figure 29.4 shows the amount of current flowing back into the positive supply as a function of PWM duty cycle. The pump current is greatest at a duty cycle of about 25%, representing a fairly strong negative output current. The positive supply must be able to sink this current or its voltage will rise. Negative values on the Y axis indicate current that the positive supply must source when the load is being driven positive. These values are shown for context. The values shown are for a half bridge output stage with ±50-V rails driving a 4-Ω load.

The full bridge is largely immune to the bus pumping effect because the long-term current of the low side from the negative rail is matched by a similar long-term current
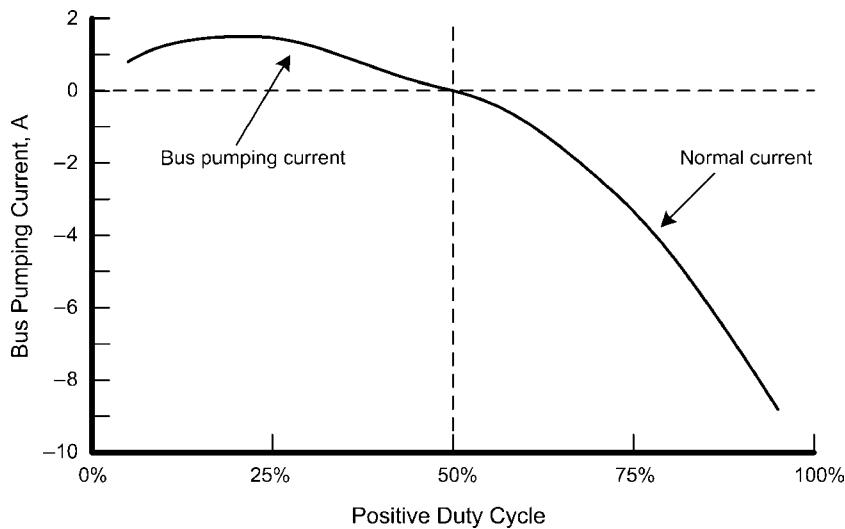
FIGURE 29.4 Bus pumping current as a function of PWM duty cycle. Negative values show normal bus sourcing current.

of the high side from the positive rail that flows on the other side of the bridge. The commutation current is thus returned to the other rail. In effect, the commutation current flows through a closed loop [4].

Power supply variation due to bus pumping must be avoided because any variation will influence the audio signal as a result of the 0 dB PSRR of the PWM class D amplifier. Bus pumping is mainly a problem at low frequencies where the rail capacitance may not be large enough to suppress rail voltage increases. Large reservoir capacitors help to mitigate these effects.

Some switching power supply architectures are able to absorb the pump current with very little loss and return it to the opposite supply or to a common supply source. Indeed, the same phenomenon that causes supply pumping can be used in reverse by a dedicated switch mode circuit to return the pump current to the opposite supply. This is not unlike the pump current circulation that occurs naturally in full bridge architectures.

29.4 Power Supply Rejection

Most class D amplifiers suffer from poor power supply rejection (PSRR); in some cases PSRR is literally 0 dB [1, 4].

When either output switch is on, one of the power supply rails is connected directly to the output of the amplifier. This means that there is virtually no power supply rejection inherent to the class D output stage. Indeed, power supply ripple and noise is sampled by the class D process and applied to the output. Recall that the gain of the simple class D amplifier is also defined in terms of the ratio of the power supply rail voltage to the peak voltage of the triangle reference wave. Changes in power supply voltage thus modulate the gain of the output stage.

All of this means that the power supply for the class D output stage must be very quiet and well regulated. Any variation in the power supply voltage caused by the signal will result in gain variations and thus intermodulation distortion. We will see later that several techniques are available to improve power supply rejection. Most of these involve negative feedback in one form or another.

Poor PSRR is the Achilles heel of most class D amplifier designs. PSRR in conventional linear class AB amplifiers is reflective of how much power supply ripple and noise gets added to the program signal. It is very important to understand that PSRR in a class D amplifier is reflective of more than just the addition of noise to the program signal. Because the power supply voltage directly influences the gain of the class D amplifier, lack of PSRR also causes intermodulation distortion in class D amplifiers. This is something that is definitely not mitigated by the use of a full bridge output stage.

Loop Gain Modulation

The fact that power supply fluctuation, ripple and noise can modulate the gain of the PWM amplifier can be problematic for PWM amplifiers that employ negative feedback. If the open-loop gain of the PWM amplifier is modulated, the unity-gain frequency of the negative feedback loop will also be modulated. This is not unlike the role that amplitude intermodulation distortion plays in modulating the closed-loop bandwidth in linear feedback amplifiers. When the closed-loop pole frequency is modulated, the in-band phase shift is modulated; this gives rise to *phase intermodulation distortion (PIM)*.

Power Supply Feedback to the Triangle Generator

The gain of the PWM amplifier is proportional to the power supply rail voltage and is inversely proportional to the amplitude of the triangle reference voltage. If the same variation that is present on the power supply rails is used to control the amplitude of the reference generator, some of the power supply modulation of the PWM amplifier gain will be canceled out. A key detail here is that the variations on the positive and negative rails may not be the same.

29.5   Power Supplies for Class D Amplifiers

The poor power supply rejection of class D amplifiers can place greater performance requirements on the power supply design than in linear amplifiers. Although the use of negative feedback in PWM amplifiers is a powerful tool for lessening the power supply effects, it is always important to strive for the best open-loop linearity before the application of negative feedback. This is no different than the objective in linear amplifier design. Class D amplifiers that do not employ some kind of negative feedback require especially quiet power supplies.

Linear Power Supplies

Conventional class AB power amplifiers employ linear power supplies that are made up of a transformer, rectifier, and reservoir capacitor. There is no reason why such power supplies cannot also be used for class D amplifiers if they can be made sufficiently quiet and free of voltage variations as a function of signal.

It is usually not practical to regulate the main rails of a power amplifier, but for audiophile class D amplifiers it may be wise to employ soft rail regulation that quiets

the rails and tracks the available supply voltage. Such regulators are also known as *capacitance multipliers*. Because the output voltage tracks the available input voltage, the average voltage drop across these regulators is small and dissipation is fairly low. Such regulators also present an opportunity for electronic rail fusing.

Switching Power Supplies

Since class D amplifiers are themselves switching devices it is only natural that modern switching power supplies be used with class D power amplifiers. They have the advantage of operating at high switching frequencies that reduce ripple and create it at much higher frequencies where it can be more easily filtered. However, if they are not implemented with the usual hefty reservoir capacitors used with linear power supplies, there may not be adequate current reserves to supply the needs of the output stage during high-amplitude bass notes. The need for large reservoir capacitors also derives from the power supply pumping phenomena when half bridge output stages are employed.

Switching power supplies are inherently regulated with high efficiency because the output power equals the input power to within better than 90%. The regulation can be made soft or stiff. As long as good reservoir capacitors are used with effective high-frequency bypassing, the ripple and noise at the output of switching supplies can be made very small and the current reserve can be made as large as that of a linear power supply with the same size reservoir capacitors. The switching supplies can be made stiff and quiet. Unfortunately, sometimes the switching supply invites the use of undersized reservoir capacitors.

If synchronous PWM modulators are used, it is desirable that the switching power supply clock synchronized with the PWM carrier so that beat frequencies will not be created that might fall into the audio band.

Switching power supplies that employ isolated synchronous Buck converters with high side and low side switches also enjoy the property that power can flow in both directions at their output terminals. This means that half bridge class D amplifiers that create bus pumping may not suffer from power supply rail fluctuations or overvoltage conditions. If isolated synchronous buck converters are employed, two separate converters may have to be used for implementation of the positive and negative power supply rails. Another approach is to employ a linear supply with a mains frequency power transformer to generate raw positive and negative rails. Each of these rails is then passed through a nonisolated buck converter that provides the main operating rails.

29.6 Negative Feedback

While traditional class AB power amplifiers profit from negative feedback, closing a feedback loop around a class D power amplifier can be challenging [2, 3]. The feedback can be taken from before or after the output filter. The use of negative feedback is especially important for improving the very poor PSRR of many class D amplifier architectures. Many class D amplifiers that run open loop also suffer high distortion.

If the negative feedback is taken from before the filter, the signal has not yet been reconstructed. Even at this point there is some effective phase delay due to the sampled data nature of the forward path. Some low-pass filtering or integration must be placed somewhere in the loop for purposes of reconstructing the feedback signal. The signal

must be converted from a discrete-time representation to a continuous-time representation (analog). Feedback taken from the near side of the filter (pre-filter) will not reduce output filter distortion or improve the high-frequency damping factor.

If the feedback signal is taken from the output of the amplifier at the far side of the filter (post-filter), quite a bit of excess phase will be introduced into the feedback loop by the output filter and it will be difficult to achieve loop stability. If the closed-loop bandwidth of the feedback loop is restricted to achieve adequate stability, then there may not be enough loop gain at the higher audio frequencies to make much of an improvement.

The ability to operate at higher PWM carrier frequencies pays many dividends when applying negative feedback.

Closing the Loop Before the Output Filter

One approach to implementing negative feedback from the near side of the filter is shown in Figure 29.5 [2]. An inverting Miller integrator is placed in front of the class D amplifier. The analog input is applied through R1 while the switched PWM feedback is applied through R2. The forward path integrator serves the need for reconstruction of the raw switched output that is fed back. The closed loop gain is simply the ratio of R2 to R1. The feedback gain crossover frequency is at $\omega_0 = k/(R1 * C_M)$ where k is the forward gain of the class D amplifier. This is a fairly conventional dominant pole approach to compensation of the feedback.

There is inevitable delay between the input signal and the output signal in a PWM amplifier, even without considering the effects of a reconstruction filter. The delay is a result of the sampling process that is fundamental to analog-to-PWM conversion. The analog input signal is sampled twice per period of the PWM carrier, once when it slices the positive slope of the triangle reference and once when it slices the negative slope of the triangle. A change in the analog signal will not result in a change in the PWM pulse ratio until an average of 1/4 of a sample period has elapsed. In this case, the sample period is the period of the PWM carrier frequency. If the carrier frequency is 500 kHz, the period is 2 µs and the effective signal delay is 0.5 µs.

A single pole introduces 45° of phase shift at its pole frequency. A 1-MHz pole introduces a phase delay of 0.125 µs (1/8 cycle where one cycle is 1 µs). Therefore, a 250-kHz

$$A_{cl} = R2/R1 \qquad \omega_o = k/(R1 * C_M)$$
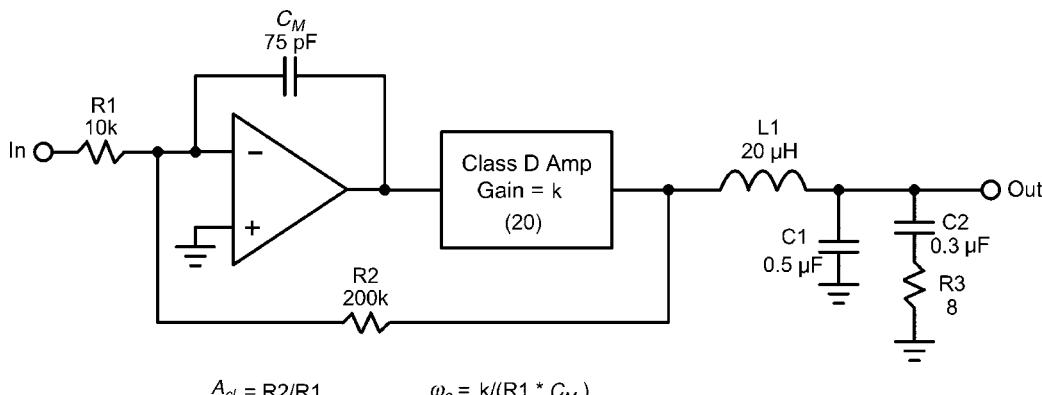
FIGURE 29.5 PWM amplifier with negative feedback taken before the filter.

pole introduces 0.5 µs of phase delay. If the phase lag created by sampling delay is approximated as a single pole, then the pole frequency is at 250 kHz. This happens to be the Nyquist frequency for a 500-kHz sample rate. This sampling pole places a serious constraint on the unity-gain frequency of negative feedback placed around a PWM amplifier. This suggests that the gain crossover frequency should be less than 250 kHz to ensure reasonable phase margin. This will provide about 22 dB of negative feedback at 20 kHz in the simple arrangement shown in Figure 29.5.

Many more sophisticated approaches to pre-filter feedback are applied in practice [5, 6]. The big disadvantage of pre-filter feedback pickoff is that it does nothing about filter distortion or filter degradation of damping factor.

Closing the Loop Around the Output Filter

Output filters introduce distortion and reduce damping factor. For this reason, it is desirable to close the negative feedback loop around the output filter, but this raises potentially serious stability problems [1].

Taking the negative feedback from the far side of the filter incurs the phase lag of the filter and the consequent danger to stability. The allowable gain crossover frequency in such an arrangement may be fairly low, so the feedback may be of limited help in reducing high-frequency distortion and in maintaining an adequate damping factor at 20 kHz. Moreover, some of the distortion-reducing ability of pre-filter feedback with a higher gain crossover frequency may be sacrificed. Phase lag introduced by the output filter is also influenced by load impedance. Some caution is required and some margin must be built in. It is especially important in this case to employ a Zobel network that will keep the net load impedance low at the higher frequencies where the filter is active. A lightly loaded second-order filter will have significant amplitude peaking. Moreover, its phase lag will increase very rapidly beyond its cutoff frequency.

To make the best use of post-filter feedback the PWM carrier frequency and the filter cutoff frequency should be made as high as possible. The fact that the output filter has already reconstructed the feedback signal is helpful. This can reduce or eliminate the role of the forward path integrator.

The output filter response falls at 12 dB/octave beyond its cutoff frequency if it is of second order. At its cutoff frequency it will typically introduce 90° of phase lag that will climb to 135° about an octave above the cutoff frequency. This would normally be the highest feedback gain crossover frequency allowed, providing about 45° of phase margin (if phase lag due to sampling delay is ignored). If a zero is introduced into the loop at this high frequency, it will contribute 45° of leading phase shift, bringing the phase margin back to 90°. This will extend the permissible gain crossover frequency.

Figure 29.6 shows one possible arrangement for an amplifier where the negative feedback is taken from the far side of the output filter. The forward path integrator is retained, but it includes a resistor in series with C_M for insertion of a zero. The feedback path also includes capacitor C_L that can insert another zero. The insertion of zeros in the feedback path must normally be done with caution because it allows the introduction of EMI from the speaker cables to the input circuitry.

The filter in Figure 29.6 is a fourth-order filter. This permits the use of higher filter pole frequencies while retaining adequate attenuation at the PWM carrier frequency. This filter is not a Butterworth filter, and it is assumed that the poles of the first section of the filter are at a lower frequency than those of the second section.
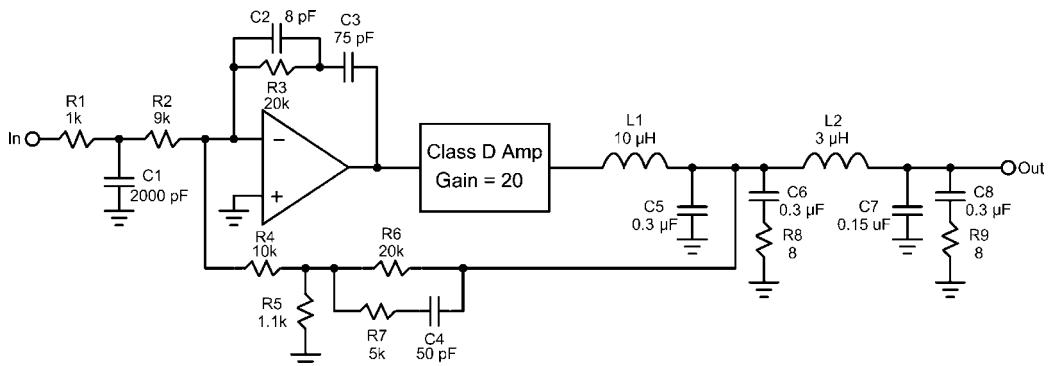
FIGURE 29.6   An arrangement where negative feedback is taken after the primary part of the output filter.

The feedback is tapped after the first section of the filter so that the added phase lag of the second section is not introduced into the feedback loop. The reasoning here is that the second section of the filter can be made small enough and of sufficient quality that it will not introduce much distortion or damping factor degradation. The second section of the filter also blocks EMI from the speaker cable. If the inductor in the second section of the filter is 3 µH, it will add only 0.4 Ω to the output impedance of the amplifier at 20 kHz.

The loop gain in this arrangement can be rolled off at an average rate of about 9 dB per octave. This is analogous to the increased slopes attainable with two-pole compensation in linear amplifiers. If a gain crossover frequency of 100 kHz can be achieved, about 20 dB of feedback will be available at 20 kHz. Other feedback arrangements are possible where a combination of pre-filter and post-filter feedback is employed [3, 5].

29.7   Damping Factor and Load Invariance

Damping factor is the effective output impedance of an amplifier divided into 8 Ω. Damping factor is not just important for accurate bass response. Amplifiers with low damping factor will have their frequency response affected by the variations in loudspeaker load impedance with frequency. They will have poor load invariance. Class D amplifiers that do not employ negative feedback tend to suffer from a poor damping factor because they are operating open loop.

The damping factor of a class D amplifier can be degraded by the impedance in the output filter or by the effective impedance of the power supply; this is an indirect consequence of the lack of power supply rejection. Load invariance is a problem for any class D amplifier that does not incorporate negative feedback around the output filter. However, in-band load dependence will be reduced in amplifiers that incorporate filters with higher cutoff frequencies.

As a point of reference, the impedance of a 20-µH filter inductor at 20 kHz is about 2.4 Ω. This corresponds to a damping factor of only 3.3 at 20 kHz. Define load variance as the change in response at 20 kHz when the load resistance decreases from 8 Ω to 4 Ω. Consider a second-order filter with 20 µH and 0.5 µF. The frequency response at 20 kHz decreases by 1.4 dB when the load resistance decreases from 8 Ω

to 4 Ω. The load variance is thus 1.4 dB. This filter also exhibits a +2.8 dB peak in response at 42 kHz when driving the lighter 8-Ω load.

If the filter is designed to be maximally flat when loaded with 8 Ω by employing a 0.16-µF capacitor, then response at 20 kHz decreases by 1.2 dB when the load impedance drops from 8 Ω to 4 Ω. The two filters have very similar load variance at 20 kHz.

29.8   Summary

The conventional PWM class D amplifier has numerous shortcomings that can be difficult to overcome. For this reason other approaches to class D modulators have been pursued and implemented. Some of these will be discussed in Chapter 30. Many of these are responsible for the significant improvements in performance and sound quality that have been made in class D amplifiers in recent years.

References

1. High Power Class D Audio Power Amplifier using IR2011S, International Rectifier application note IRAUDAMP1, www.irf.com, 2005.
2. Leach, W. Marshall, Jr., *Introduction to Electroacoustics and Audio Amplifier Design,* 2nd ed., Kendall/Hunt, 2001.
3. Gaalaas, Eric, "Class D Audio Amplifiers: What, Why, and How," *Analog Dialog,* 40-06, June 2006.
4. Honda, Jun, and Adams, Jonathan, "Class D Audio Amplifier Basics." International Rectifier application note AN-1071, February 2005.
5. Cox, Stephen, and Candy, Bruce, "Class-D Audio Amplifiers with Negative Feedback," *117th Audio Engineering Society Convention,* San Francisco, October 2004.
6. U.S. Patent #6,297,692, "Pulse Modulation Power Amplifier with Enhanced Cascade Control Method," October 2, 2001.

This page intentionally left blank

CHAPTER 30

Alternative Class D Modulators

There are numerous ways to build a class D power amplifier, but those based on *pulse width modulation* (PWM) are the oldest and still very popular. This chapter will discuss alternatives to traditional PWM modulators. Some are variants of PWM modulators that produce a PWM stream by different means. These include so-called self-oscillating loops that do not require a triangle-wave reference generator and actually rely on oscillation that results from a negative feedback process. These schemes reap the benefits of negative feedback without the struggle to keep it stable. Other approaches to PWM generation depend on high-speed digital logic and/or digital signal processing.

An entirely different group of class D modulators is based on so-called sigma-delta modulators (SDM or $\Sigma\Delta$). These produce a high-speed bitstream whose bits are of uniform duration, but whose density reflects the amplitude of the audio signal. This is a form of *pulse density modulation (PDM)*. Sigma-delta modulators can be implemented in the analog domain or in the digital domain. They depend on a process called *noise shaping* that works in conjunction with oversampling. This technique, used in most audio A/D and D/A converters, shifts most of the inevitable quantization noise out of the audio band to parts of the frequency spectrum above the audio band.

Some class D modulators operate entirely in the digital domain, taking as their input a PCM digital audio signal and converting it to a PWM or $\Sigma\Delta$ output stream. This is attractive in many applications where the signal is already available in digital form.

30.1   Self-Oscillating Loops

Using a triangle reference generator and a comparator is not the only way to generate a PWM stream. There is another type of analog PWM class D amplifier design that comprises a so-called self-oscillating loop [1–4]**.** These are sometimes referred to as a *controlled oscillation modulator* (*COM*). In this approach there is no carrier frequency triangle reference source. These designs are asynchronous. While they produce a PWM stream, the frequency of that stream is not fixed. Instead, the loop oscillates on its own as a result of feedback around the loop. Some designs take the feedback from the near side of the filter (pre-filter feedback) while other designs take the feedback from the far side of the filter (post-filter feedback). A number of commercial class D amplifiers use the self-oscillating loop principle.
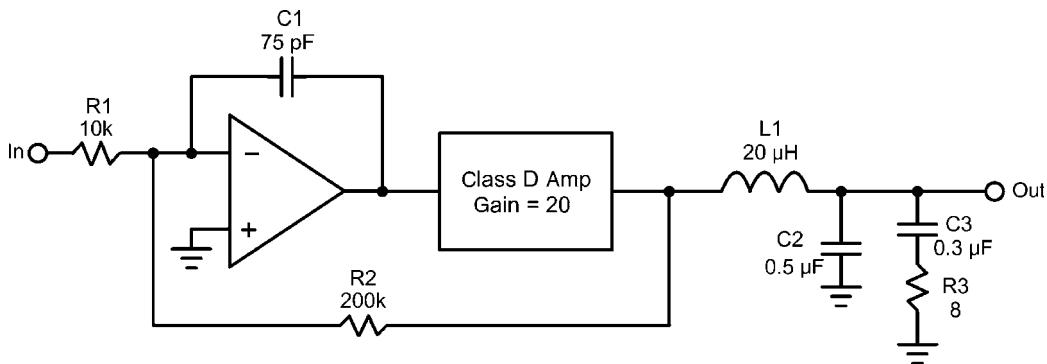
FIGURE 30.1　PWM amplifier with prefilter feedback.

　　The self-oscillating loop PWM amplifier often enjoys improved performance over conventional fixed-frequency triangle-based PWM amplifiers because the bandwidth of the feedback loop can be higher than that of a conventional feedback loop that must obey conservative stability criteria.

Self-Oscillation with Pre-filter Feedback

Consider the PWM amplifier arrangement of Figure 30.1 where pre-filter feedback encloses a class D amplifier whose gain is 20. If additional phase lag is added to the feedback loop, the circuit will become unstable and oscillate. Oscillation will occur even without the triangle reference signal. When the input signal is added to the oscillating loop, the output will be pulse width modulated, as desired.

　　Figure 30.2 illustrates a conceptual arrangement of a self-oscillating PWM modulator and amplifier. There are numerous ways to arrange the loop and add additional low-pass filtering to the loop to obtain controlled oscillation [1]. The arrangement here illustrates a somewhat general case where two summers in the forward path are separated by low-pass filters. Feedback is applied to both summers. A low-pass filter can also be placed in the main feedback path to provide some signal reconstruction prior to injection at the summers.
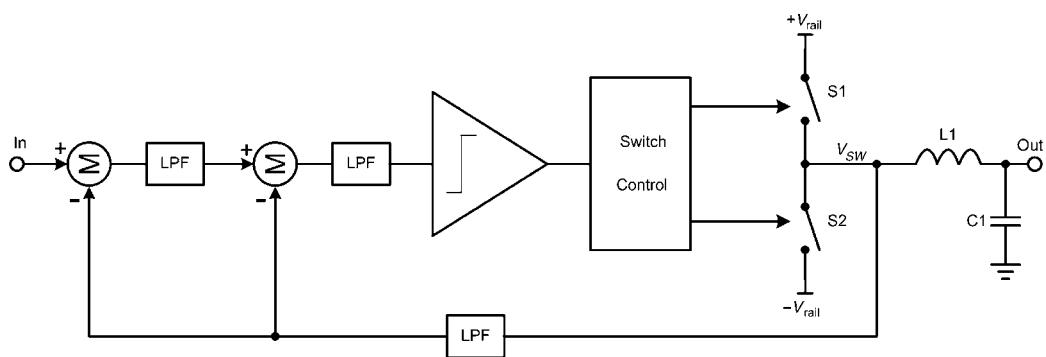
FIGURE 30.2　Self-oscillating PWM class D amplifier.
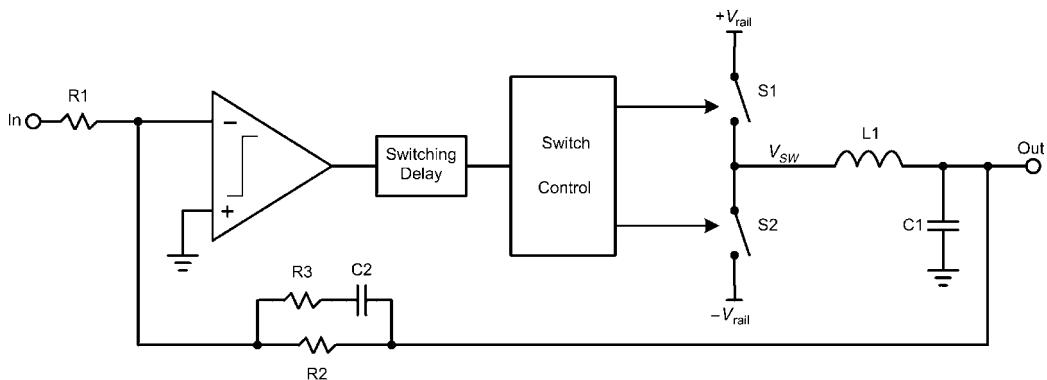
Figure 30.3 Simplified illustration of a self-oscillating PWM modulator with post-filter feedback.

Self-Oscillation with the Output Filter

In Section 29.6 the struggle to close the feedback loop around the output filter was discussed. Adequate feedback stability can be difficult to achieve in light of the phase shift introduced by the output filter.

The PWM approach in Ref. 1 instead takes advantage of this "problem" by allowing the loop to oscillate in a controlled fashion. It is a self-oscillating design wherein the instability resulting from post-filter feedback is put to good use [1, 2]. The simplified amplifier illustrated in Figure 30.3 oscillates at about 400 kHz, over 10 times the corner frequency of the second-order output filter. At this frequency the phase shift of the filter is nearly 180°, so it does not take much additional phase shift to push the loop into oscillation. This additional phase shift is provided by the switching delay in the forward path. A phase-lead network is placed in the feedback path to control the frequency of oscillation.

The stroke of genius here is that applying an input signal to an otherwise-oscillating class D amplifier will result in the appropriate PWM duty cycle signal corresponding to the audio waveform.

The filter frequency is about 35 kHz and the oscillation frequency is about 400 kHz. The loop gain is almost independent of power supply voltage and depends almost solely on the frequency response of the output filter. Loop gain is about 30 dB, flat across the audio band out to about 35 kHz. The gain crossover frequency is at about 200 kHz, while the closed loop frequency response is down 3 dB at about 40 kHz. This design obviously profits from postfilter feedback, reducing filter distortion and providing good load invariance.

A discussion of the circuit details can be found in Ref. 2. The self-oscillating design is simple and provides high performance, but it is not clear that, with its nonfixed frequency, it can be mated with a direct-digital input.

Self-Oscillation Using a One-Shot

Other self-oscillating loop PWM designs use pre-filter feedback and employ other means to cause the loop to oscillate. One such approach is illustrated in Figure 30.4 [3, 4].

A one-shot multivibrator is central to the operation of this PWM modulator. The cycle begins when the one-shot is triggered and turns on the high side switch for a fixed
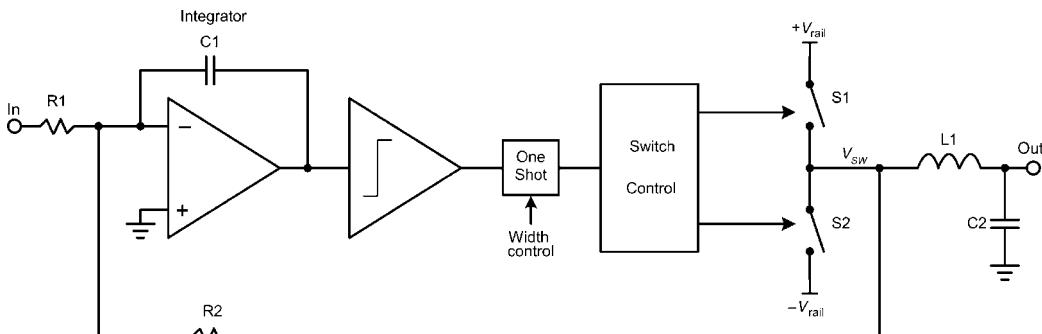
FIGURE 30.4   A self-oscillating PWM modulator employing a one-shot.

period. During this period the error between the switched output signal and the input signal is integrated for the duration of the one-shot pulse. The error grows during this period. The high side switch turns off at the end of the one-shot period and the error integrates negatively. The circuit ends a switching cycle when the difference between the audio signal and the PWM waveform is zero. The one-shot will be triggered and the process repeated when the error gets back to zero.

This process seeks to drive the error between the input signal and the integrated output signal to zero (on each cycle). In some respects, this is not radically different from a triangle PWM modulator preceded by an integrated feedback approach where the input signal and feedback are compared by an integrator in the forward path. The technique described here is said to remove switching error faster than any other class D approach [3, 4]. This approach compensates for errors introduced by dead time and nonideal switching edges because it is responsive to net pulse area. As a result, it also tends to reject power supply deviations and noise.

If a fixed-width one-shot is used, the frequency of the design described will vary widely with signal, since half the period is fixed and the other half of the period must change to accommodate the needs of the input signal amplitude. For this reason, a control circuit is added to constantly adjust the pulse width of the one-shot.

Synchronized Self-Oscillating Loops

One disadvantage of most conventional self-oscillating class D amplifiers is that the PWM carrier frequency is poorly defined and may vary with the signal conditions. This can lead to beat frequency phenomena when multiple channels of class D amplification are in close proximity. For this reason there have been self-oscillating loop designs where some means of frequency synchronization has been incorporated [5, 6]. In some cases synchronization is achieved by employing a form of injection locking.

It is also possible to use more explicit locking techniques such as a *phase-locked loop (PLL)*. If the self-oscillating loop has some means to control its frequency, it can be viewed as a VCO and can be locked to a common frequency source if the overall design has sufficient lock range in the presence of the audio signal. The frequency of a self-oscillating loop based on feedback from the near side or far side of the output filter can be controlled by including voltage-dependent phase shift in the loop or by including voltage-dependent feedback coefficients in the loop. The frequency of a multivibrator-based

self-oscillating loop can be controlled with a one-shot whose delay is voltage-dependent. A significant design issue in a PLL-based approach is the choice of loop bandwidth and loop order.

30.2 Sigma-Delta Modulators

The PWM class D amplifier is essentially an open-loop device around which negative feedback may be placed. The sigma-delta modulator is an alternative means of generating a bitstream whose average value corresponds to the signal amplitude [7]. Negative feedback is intrinsic to its operation. These modulators are also referred to as delta-sigma modulators. The basis of a commercial implementation of a sigma-delta class D amplifier is described in Ref. 8.

Figure 30.5 illustrates a simple first-order sigma-delta modulator (SDM or ΣΔ). As in a conventional PWM modulator, it is operated at a fixed frequency. However, instead of producing pulses at a carrier frequency whose width is continuously variable, it produces pulses whose width is in discrete increments of the clock period. This is a form of pulse density modulation. Because the pulses are in increments of the clock period, this signal is quantized in time. As a result, quantization noise is introduced. This is a problem that must be addressed. The simple answer is that the clock for the sigma-delta modulator is at a much higher frequency than the PWM carrier frequency. The ΣΔ modulator fundamentally depends on oversampling where the sampling frequency is larger than twice the maximum frequency of the signal being sampled.

The ΣΔ modulator comprises a summing circuit, an integrator, a comparator, and a D-type flip flop. The output of the flip-flop is the bitstream. As with PWM, the average value of the switched output signal represents the analog output. The switched output signal is fed back to the summer, where the input signal is compared to the average value of the feedback signal. If the input signal is larger than the average value of the feedback signal, the integrator output will move in a positive direction, eventually crossing the threshold of the comparator and causing its output to go high.

On the next positive clock edge the D-type flip-flop will be clocked high and the output will go high for this bit period. On subsequent positive clock edges, the output will continue to be clocked high until the fed-back output catches up with the more
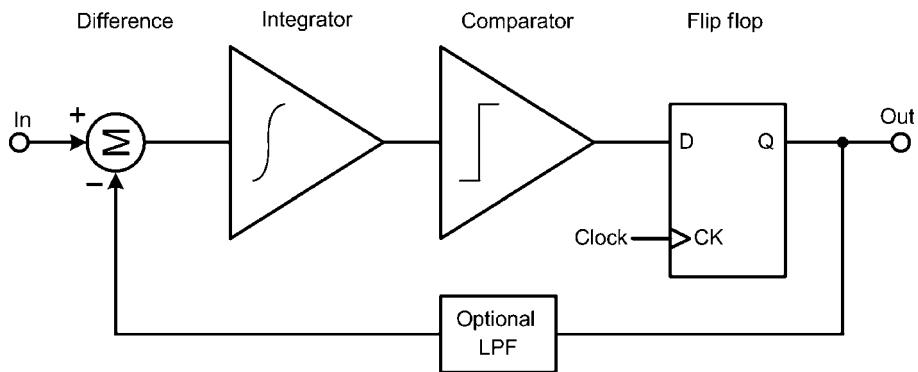
FIGURE 30.5 A simple analog sigma-delta modulator.

positive input and actually passes it. At that point, the integrator output will fall a sufficient amount to go below the comparator threshold and cause the flip flop to be clocked low on the next positive clock edge. This whole process repeats indefinitely, with the ΣΔ loop always seeking to keep the difference between the input and the reconstructed output small. If the input signal is at zero, the output of the modulator will toggle between high and low levels at the clock rate.

Because the average value of the output bitstream is driven to equal the input signal by feedback, the pulse density in the bitstream will be a faithful representation of the input signal amplitude. In a conventional ΣΔ class D amplifier, the bitstream that is fed back is the bitstream that exists at the output of the amplifier prior to the filter.

It is important to recognize that the feedback signal to the analog summer in Figure 30.5 is not reconstructed if the optional LPF is not in place; it is either a positive or negative reference voltage in discrete time. Reconstruction of the feedback signal into a continuous time representation takes place in the integrator. In most class D amplifiers the switched signal fed back is not a fixed reference signal (1-bit A/D), but rather an attenuated version of the actual switched output signal. In this way the pulses fed back are a more faithful representation of the areas of the actual output pulses of the amplifier. If the power supply rail increases, for example, that will be appropriately reflected in the area of the pulse that is fed back. This improves PSRR. In some designs the feedback signal is low-pass filtered before application to the summer.

Notice that when a pulse occurs, it will never have a width less than one clock period. This is in contrast to the output of a PWM modulator, where very small pulse slivers can be created when the signal is near its maximum magnitude. Conversely, there is no limit to the width of a pulse in a sigma-delta bitstream. Moreover, there is no periodic regularity to the time when pulses go from positive to negative or vice versa. There is no carrier frequency.

The negative feedback process that is intrinsic to the operation of the ΣΔ modulator significantly improves PSRR, since the input is being compared to the actual average value of the digital output, regardless of the amplitude (and area) of the pulses that create that average value. In fairness to PWM, this is not unlike the benefit of pre-filter feedback in a PWM amplifier that was illustrated in Figure 30.1.

Oversampling

Because sigma-delta modulators create quantization noise in the time domain, it is important that they run at significantly higher clock frequencies than PWM modulators. This allows for finer granularity of the pulse time intervals. The high rate at which the ΣΔ modulator is clocked is referred to as oversampling. The ratio of the ΣΔ clock rate to the required Nyquist sampling rate is referred to as the *oversampling ratio (OSR)*. The Nyquist sampling rate for a 20-kHz analog signal is 40 kHz. A ΣΔ modulator operating at 4 MHz will have an OSR of 100.

Oversampling reduces in-band noise by spreading the total sampling noise power over a much larger range of frequencies [9]. An OSR of 2 will spread the noise over twice the frequency spectrum, cutting the in-band noise power in half and improving SNR by 3 dB.

Increasing the clock rate of a first-order ΣΔ modulator reduces noise by 9 dB per octave of OSR. This larger decrease than 3 dB per octave results from a process called noise shaping that will be discussed later. Increasing the clock rate from 5 MHz to 20 MHz thus reduces the quantization noise by 18 dB. Employing a higher-frequency

clock also allows the use of a physically smaller output filter with a higher 3-dB frequency.

There is a limit to the smallest pulse that can be handled by a class D amplifier output stage, especially when necessary dead time margins are considered. This was discussed earlier in connection with sliver pulses produced by PWM modulators at very high or very low duty cycles. The switching rate of the class D output stage also has an upper limit (apart from minimum pulse width) because its power loss increases with the average switching rate. Each time the output state is switched, power is dissipated. The product of the clock frequency and the transition density of the bit stream is what influences heat generation from switching losses.

High-Speed Class D Sigma-Delta Amplifiers

A PWM modulator operating at 500 kHz has pulses that are on average 1 μs in duration with a 2-μs period. At 95% modulation, the minimum pulse width is 100 ns. If this same minimum pulse width is employed for the ΣΔ modulator, then the clock rate will be 10 MHz. Unfortunately, this also means that a zero-output (first-order) ΣΔ "idle pattern" will consist of alternating 100-ns one and zero pulses, corresponding to a 5-MHz square wave. This is 10 times the frequency of the quiescent output frequency of the 500-kHz PWM modulator and may result in excessive switching losses.

It is possible with a simple digital algorithm to keep the average switching frequency (transition density) low enough to avoid overheating. A simple coding scheme to reduce transition density would be to convert any 1010 sequence into the 1100 sequence or a 0011 sequence. The same operation can be performed on the result to further reduce the permissible peak transition density by another factor of 2. In that case groups of four like bits will be produced. Yet another stage of this coding process can be used to reduce the transition density by another factor of 2. At each stage the choice of whether the result has leading 1s or leading 0s can be randomly controlled to minimize artifacts. This process need not interfere with the fundamental fineness of quantization of the final pulse permitted by the clock frequency.

Another approach is to force the avoidance of an alternating idle pattern by deliberately adding out-of-band noise (dither) to the signal. Such an approach mitigates EMI concerns because it will not create discrete tones, but rather a signal having a spread spectrum nature. The key is to introduce some deliberate random quantization noise into the ΣΔ loop and then have the loop shape it out of band. Alternatively, one can introduce noise that does not have any in-band spectral component in the first place.

If the ΣΔ loop can be operated at a higher clock rate while guarding against an excessive average switching frequency, the modulator can achieve much finer pulse granularity, more closely approaching that of analog PWM. This allows the use of an output stage with the same speed capability and amount of switching loss per transition.

The switching losses due to a high-frequency ΣΔ idle pattern also must be put into perspective, especially for an audiophile application. While it is true that increased switching losses decrease efficiency, idle patterns are of concern primarily under the condition when output power is near zero. This condition is an otherwise low-dissipation situation for the class D output stage; conduction losses are low and reverse recovery diode shoot-through current is low. This means that from a total power dissipation point of view, some additional power dissipation at idle due to a high switching density idle pattern can be accommodated.

High Sigma-Delta Modulator Clock Frequencies

Modern digital circuitry is easily capable of operation at clock rates well in excess of 100 MHz, even if a class D amplifier output stage is not. This is especially true internal to a chip. Even FPGAs are available that can operate at internal clock frequencies of 500 MHz or more. If proper transition density control is in place, there is no reason why the $\Sigma\Delta$ clock rate cannot be made 100 MHz, fully 10 times higher than in the example above. This results in much finer time quantization of 10 ns. Recall that in the pulse sliver example a 500-kHz PWM modulator at 99% duty cycle produced 20-ns pulses and that the output stage was shown to be able to handle those pulses with reasonable fidelity.

If 100-MHz $\Sigma\Delta$ modulation is used, it is also desirable to employ pulse width constraints so that no pulse is narrower than some fixed amount like 20–50 ns. In such a case, the 10-ns granularity can be enjoyed while avoiding the production of any pulses narrower than would be encountered in PWM at high modulation depth. This allows the intrinsic quantization of the digital process to more nearly approximate the continuous-time behavior of an analog PWM solution.

One approach to limiting pulses to a 50-ns minimum is as follows: If the modulator produces a single positive 10-ns pulse, it is replaced with a 50-ns pulse and a subsequent negative pulse is extended by 40 ns. Alternatively, the preceding and following negative pulses can be extended by 20 ns each.

Adaptive Transition Density Limiting

The concern about high idle-state transition density with high frequency $\Sigma\Delta$ modulation is mostly one of heat generation in the output stage. This means that short periods of high transition density can be tolerated until temperatures build up. There are a number of ways that transition density limiting schemes can be implemented. Indeed, under many signal conditions they can be turned off so that any small degradation of the sound or signal-to-noise ratio due to the scheme is eliminated entirely.

One approach is to provide closed-loop control of the average transition density. The transition density is monitored and averaged. The result is used to control the aggressiveness of the scheme that limits average transition density. With such a scheme the control loop is closed within the digital processor domain and operating temperature of the output stage is not directly controlled (open loop).

A second scheme controls the transition density by monitoring the temperature of the output stage. If the output stage gets too hot, more aggressive transition density limiting is employed. This scheme presumes that the high output stage temperature is due to transition density instead of operation at high power. This may not be the case, so additional monitoring and control means need to be put in place. Direct transition density feedback can be combined with temperature feedback. For example, the maximum allowed average transition density can be controlled by the heat sink temperature. If the processor is aware that the average output power is high, a detected high temperature will not be attributed to excessive transition density and other means may be invoked to reduce temperatures.

Noise Shaping

Noise shaping is a technique whereby the noise power, which is normally flat with frequency, is pushed out of the audio band up to higher frequencies [9]. This is how

A/D and D/A converters with a small bit resolution achieve much higher effective resolution in the audio band. The ultimate example of this is the 1-bit converter. Noise shaping is different than the simple reduction of in-band noise achieved by oversampling. With oversampling, the quantization noise power is spread over a wider frequency band that extends beyond the audio band. This dilutes the amount of noise power that lies in the audio band. In general, in-band noise goes down only with the square root of the OSR.

Noise shaping employs the principles of negative feedback to reduce the in-band noise power at the expense of increased out-of-band noise power. In other words, the noise power is spread nonuniformly over the available bandwidth.

The sigma-delta modulator in Figure 30.5 is said to be a first-order modulator because it incorporates only one integrator in its forward path. The gain of the integrator increases at 6 dB per octave as frequency decreases. Modulator quantization noise is injected into the system after the integrator. Recall the input-referred noise analysis approach described for linear amplifiers. There the effective noise contribution of a noise source was decreased by the amount of open-loop gain lying ahead of it. The increased gain of the SDM integrator at low frequencies reduces input-referred quantization noise by 6 dB per octave as frequency decreases. The total noise power at the output of the sampling process is constant, so the noise taken away from the low-frequency end of the spectrum appears as increased noise in the high-frequency portion of the spectrum that lies above the audio band. Oversampling provides a larger amount of out-of-band spectrum in which to dump this noise that has been taken from the in-band portion of the spectrum.

Second-Order Sigma-Delta Modulators

If two integrators are placed in the forward path, the noise-shaping process will have a slope of 12 dB per octave. The input-referred noise will decrease at 12 dB per octave as frequency decreases. Correspondingly, the in-band sampling noise will be decreased by 12 dB for each doubling of the $\Sigma\Delta$ clock frequency. This in-band SNR improvement is on top of the 3 dB per octave reduction in noise that is simply attributable to the higher sampling frequency. The net reduction of in-band noise is then 15 dB for each doubling of the clock frequency. Increasing the clock frequency from 5 MHz to 20 MHz will yield an SNR improvement of 30 dB.

Figure 30.6 illustrates a second-order $\Sigma\Delta$ modulator [8]. It comprises essentially the same architecture as the first-order loop but with a second integrator added in the forward path. The reconstructed output is compared with the input signals of both integrators.
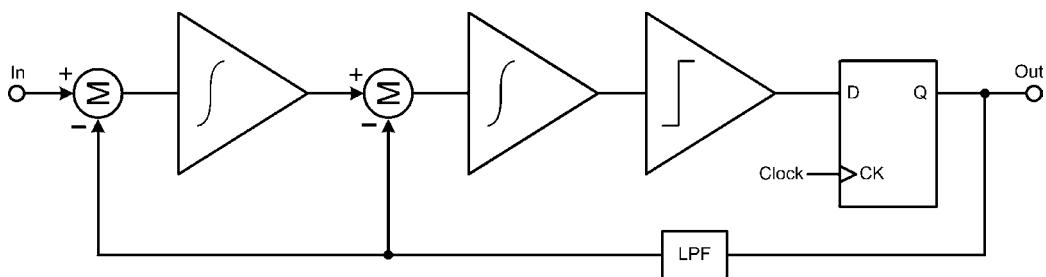
FIGURE 30.6 A second-order sigma-delta modulator.

Think of the second integrator as the one in Figure 30.5. The second-order ΣΔ modulator has thus had an additional difference circuit and integrator added in front of it. The first-order modulator part of the circuit is now trying to minimize the integrated difference of the input signal and the reconstructed output signal.

Higher-Order Sigma-Delta Modulators

The noise-shaping properties of ΣΔ modulators can be more aggressively exploited by employing high-order loops. These often fall in the range of third to fifth order. The order of the loop is generally the same as the number of integrators in the loop. Higher-order loops provide much more in-band SNR for a given clock frequency. One price paid for these modulators is stability, especially under overload conditions. Higher-order modulators are more often found in DSP implementations and are seen less frequently in the analog implementations used for class D ΣΔ amplifiers.

EMI of Sigma-Delta Class D Amplifiers

The pulse pattern generated by the ΣΔ modulator is much more irregular than that from a PWM modulator. This creates a frequency spectrum that is much more spread out and less concentrated at the clock frequency and its harmonics; this results in much less tendency to produce RF tones.

However, idle tone EMI can sometimes be a problem, especially for first-order ΣΔ modulators. When there is no audio signal, a ΣΔ modulator will tend to create an idle tone at half the clock frequency. The more concentrated spectrum of energy under these conditions can create increased EMI. This can be mitigated by measures that deliberately add randomness to the idle tone, creating noise at frequencies lying above the audio band. Second-order and higher-order ΣΔ modulators tend to produce more irregular idle tones, and so tend to create a bit less EMI under idle conditions.

The Output Filter

The clock frequency of a ΣΔ modulator is usually much higher than the carrier frequency of a PWM modulator. As a result, the EMI is spread out over a higher frequency band and the output filter can be designed with a higher cutoff frequency. This means that the output filter will be physically smaller and will have a frequency response in the audio band that is less dependent on the load impedance. It may also mean that the output filter will create less distortion as a result of the smaller inductances that can be employed. There is a caveat. Aggressive transition density control schemes may push some of the EMI energy to lower RF frequencies, so the output filter must be designed with this in mind.

Post-Filter Feedback

It is desirable to enclose the output filter within a negative feedback loop to improve the damping factor and make the behavior of the amplifier more load-invariant. As in PWM amplifiers, there are challenges in putting negative feedback around an output filter that contributes a large amount of lagging phase shift.

If the cutoff frequency of the ΣΔ output filter is high, it is possible to enclose the filter in the loop and achieve larger amounts of negative feedback in the audio band with less danger of instability. The governing consideration here is how high the output filter cutoff frequency can be set. Pre-filter feedback will still often be taken to form the

ΣΔ modulator itself. This provides a defined closed-loop gain around which additional feedback from the far side of the filter can be taken. Some examples of post-filter feedback with a ΣΔ modulator are described in Ref. 8.

30.3   Digital Modulators

In some ways the power amplifier is one of the last things to go digital in many areas of consumer electronics. For this reason, and given the tremendous processing capability made available at low cost by VLSI chips, it is only natural for class D modulators to be implemented in all-digital form.

Class D amplifiers using digital modulators are a natural fit to digital audio sources where the signal often originates in PCM format from an I²S bus. The I²S format (Inter-IC Sound) is a popular standard developed by Philips Semiconductor for transport of digital audio signals. Use of a digital modulator eliminates entirely the analog interface and potentially some other mixed-signal functions. This can be especially attractive in HT receiver applications where most of the audio signals are handled in digital fashion.

Digital PWM Modulators

The PWM waveform for driving the output stage can be generated digitally. This can be especially attractive when the source material is in digital PCM form. With appropriate processing, PCM can be converted to PWM entirely within the digital domain. PWM outputs can then be generated with great accuracy without reliance on an analog triangle reference generator. Dead time can also be implemented digitally, with separate outputs for the high side and low side switches provided by the digital device.

Unfortunately, the digital generation of PWM brings with it time quantization and associated noise. High clock frequencies must be used to minimize time quantization, but even a 100 MHz clock will result in quantization to 10 ns. This amount of quantization in a 2000-ns PWM carrier period represents a timing precision corresponding to only 6–8 bits. *Digital signal processing* (DSP) must be added to implement noise shaping to drive the resulting quantization noise to frequencies above the audio band. Noise shaping of the PWM signal is usually done with a subsequent ΣΔ modulator implemented with DSP, adding to complexity, but amenable to integration.

Digital Sigma-Delta Modulators

The differencing and integration functions that make up ΣΔ modulators are easily implemented entirely in the digital domain. Moreover, DSP offers great precision and consistency in filter coefficients, allowing the implementation of sophisticated higher-order loops. An example of a digital ΣΔ class D amplifier implementation can be found in Ref. 10.

Feedback and PSRR

The impairments introduced in a class D amplifier by the output stage are fundamentally analog in nature. For this reason some form of analog feedback must be introduced into the modulator chain if low distortion and good PSRR are to be achieved. This can be challenging in a digital modulator arrangement and usually requires some kind of mixed-signal circuitry, such as an A/D converter, in the feedback signal path. This offsets slightly

some of the advantages of the digital modulator approach. Some low-cost all-digital implementations omit the feedback and suffer the consequences.

References

1. U.S. Patent #7,113,038, "Power Amplifier" (Bruno Putzeys), September 26, 2006.
2. Putzeys, Bruno, "Simple Self-Oscillating Class D Amplifier with Full Output Filter Control," presented at the *118th AES Convention,* May 2005.
3. U.S. Patent #6,084,450, "PWM Controller with One Cycle Response," July 4, 2000.
4. "One-Cycle Sound™ Audio Amplifiers." PowerPhysics White Paper, www.powerphysics.com, 2002.
5. U.S. Patent #7,119,629, "Synchronized Controlled Oscillation Modulator," October 10, 2006.
6. U.S. Patent #6,297,693, "Techniques for Synchronizing a Self-oscillating Variable Frequency Modulator to an External Clock," October 2, 2001.
7. Schreier, R., and Temes, G., *Understanding Delta-Sigma Data Converters,* Wiley-IEEE Press, 2004.
8. U.S. Patent #5,777,512, "Method and Apparatus for Oversampled, Noise-Shaping, Mixed-Signal Processing," July 7, 1998.
9. Hawksford, M. J., "Oversampling and Noise Shaping for Digital to Analogue Conversion," *Reproduced Sound 3*, pp. 151–175, Institute of Acoustics, 1987.
10. U.S. Patent #6,943,717, "Sigma Delta Class D Architecture Which Corrects for Power Supply, Load and H-bridge Errors," September 30, 2005.

Class D Measurement, Performance, and Efficiency

Τhis chapter concludes the class D amplifier discussion by considering the amplifier as a whole, ignoring the highly technical implementation details. It is written more from a user perspective, with emphasis on applications that demand high sound quality. For those who demand the highest sound quality and who can compromise on efficiency, there is a middle ground available at the expense of greater complexity. This approach can be referred to as *hybrid class D*. In such a design a class D amplifier provides the lion's share of the power while the actual signal delivered to the loudspeaker comes from a low-power analog class AB amplifier.

Measurement of class D amplifiers requires a different approach in many cases. This is due in part to the fact that class D amplifiers usually have smaller bandwidth than traditional linear amplifiers. Distortion harmonics that lie above the audio band may be seriously attenuated. As a result, the measurement of high-frequency THD (like THD-20) is virtually useless and can be downright misleading. The presence of out-of-band noise at the output of most class D amplifiers further complicates many measurements. Measurement techniques for class D amplifiers are covered in Section 31.2.

31.1   Hybrid Class D

In some cases higher sonic performance can be achieved by combining class D amplifiers with analog power amplification. A simple example of this is to amplify the signal with both class D and class AB amplifiers to the same level. The class AB amplifier is a low-power, high-current amplifier that actually drives the load. Its output stage power supply is floating on the output signal of the class D amplifier. This is somewhat analogous to a linear power amplifier wherein a floating class A amplifier is driven by a class AB amplifier.

Figure 31.1 is a conceptual illustration of a hybrid class D amplifier. The most straightforward approach is to have the class D amplifier drive the entire power supply of the class AB amplifier. That power supply can be either a linear supply or a switcher.

The hybrid class D amplifier has several advantages. It isolates the class D output from the load, taking the output filter out of the signal path and greatly reducing EMI. It also preserves the damping factor that would be attained by a linear amplifier. Finally, it allows the negative feedback to be closed from the output terminals of the amplifier without suffering the consequences of phase shift introduced by the output filter.

Note also that only the output stage of the class AB amplifier needs to be run from the flying rails provided by the class D amplifier. All of the earlier stages can be run
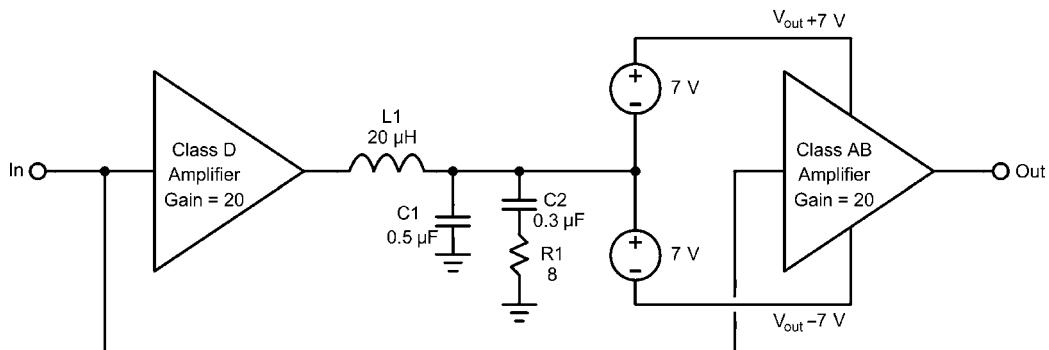
FIGURE 31.1   Conceptual diagram of a hybrid class D amplifier.

from a very clean linear supply because they require very little power. Then, decent PSRR of the linear output stage is all that is needed.

The hybrid class D amplifier is an intelligent trade-off, providing improved sound quality in exchange for a reduction in efficiency. The class AB amplifier can be run at low voltage, but it must still be designed to be able to deliver the full current produced by the amplifier. The use of small local rail voltages in the class AB amplifier section greatly eases safe area requirements for the output transistors.

Figure 31.2 shows estimated power dissipation as a function of output power for a conventional class AB amplifier, a hybrid class D amplifier, and a standard class D
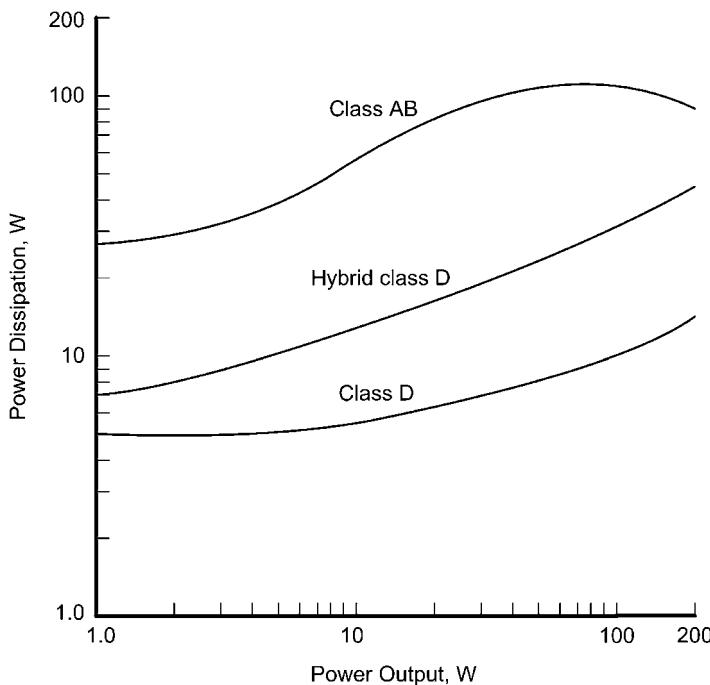
FIGURE 31.2   Estimated power dissipation of class AB, hybrid class D, and standard class D amplifiers.

amplifier, all rated at 200 W/8 Ω. The class AB amplifier within the hybrid class D amplifier is assumed to have ±7-V floating rails. Even with low-voltage rails, the floating class AB amplifier dominates the total power dissipation of the hybrid design. All of its input power is dissipated as heat because it really delivers no added power to the load. Unfortunately, given the need to deliver high current into low-impedance loads and the reality of implementation tolerances, it is very challenging to design a floating class AB amplifier with rail voltages less than about 7 V.

It is interesting to note that the hybrid class D amplifier does not exhibit increased power dissipation at less than full power, even though it includes a class AB amplifier as part of its implementation. The hybrid class D amplifier enjoys its greatest advantage over the class AB amplifier at power output levels between 5 and 50 W. In this region its power dissipation is smaller by a factor of about 4.

Audiophiles usually care most about maximum dissipation as opposed to overall efficiency. These are two very different things. Audiophiles don't care as much about power drawn from the outlet. They care about how big they must make their heat sinks in order to achieve a given output power and sound quality. This is why hybrid class D may be attractive for some audiophiles.

31.2   Measuring Class D Amplifiers

Class D amplifiers do not usually have as much bandwidth as analog amplifiers and so they present some measurement challenges. More importantly, the inevitable high-frequency noise and carrier leak-through at the output corrupts distortion and SNR readings. At times, high-frequency EMI at the output of a class D amplifier can actually disturb the functionality of sensitive test equipment connected to the amplifier.

The AES17 Filter

To deal with the spurious EMI that may be present at the output of class D amplifiers, the Audio Engineering Society published a filtering recommendation called AES17 [1]. The low-pass filter is placed between the amplifier output and measurement instruments like distortion analyzers. The filter is very sharp, flat to 20 kHz and then down by 60 dB at 24 kHz. This usually requires a seventh-order elliptic filter, most or all of which should be implemented with passive components so that sensitive active circuitry in test instruments is not disturbed by the EMI. Without the filter, measurements at low signal levels will be especially affected in an adverse way.

Total Harmonic Distortion

THD measurement of class D amplifiers is practical and relevant when conducted at low frequencies like 1 kHz. However, THD measurements are of very limited use when conducted at high frequencies like 20 kHz. This is because the class D amplifier's output filter will block many of the upper harmonics, rendering an optimistic result and low sensitivity to those higher harmonics considered most offensive. If the AES17 filter is in place, all harmonics of a 20-kHz test signal will be blocked. Indeed, only the second harmonic of a 10-kHz test signal will barely manage to get through. THD-1 is a satisfactory basic test, but it provides virtually no information about high-frequency nonlinearities.

SMPTE IM

The SMPTE IM test employs tones at 60 Hz and 7000 Hz in a 4:1 ratio. It tests intermodulation distortion inflicted on the smaller 7-kHz carrier by the larger 60-Hz aggressor signal. The SMPTE IM test provides a very good measurement of frequency-independent static nonlinearities. An example of such nonlinearity in class D amplifiers is nonlinearity in the triangle reference signal in a PWM modulator.

The test is especially valuable for class D amplifiers because it will show up problems related to PSRR. Recall that the open-loop gain of many class D amplifiers is proportional to power supply voltage. If the large 60-Hz component of the test signal causes variation in the supply voltage, intermodulation of the 7-kHz carrier will be the direct result. Bus-pumping intermodulation will also be revealed by the SMPTE IM test.

CCIF Tests

The 19 + 20-kHz CCIF two-tone test with spectral analysis is an excellent test for class D amplifiers because it stresses the amplifier at high frequencies while producing distortion components that are in-band. This is at least true of the lower IM sidebands. Spectral components at 18 kHz reflect third-order nonlinearities, components at 17 kHz reflect fifth-order nonlinearities, etc. Even-order nonlinearities show up starting at 1 kHz beginning with the second order.

Aliasing

It is very important to sound quality that out-of-band frequency components in the input signal not create aliasing in the class D amplifier, where these frequency components are folded back into the audio band as spectral lines or noise. Modern signal sources often contain energy above 20 kHz, whether it be program material or collateral energy, such as that often present at the output of SACD players.

One way to test for aliasing is to apply a moderately high-level sinusoid that is swept in frequency from 10 kHz to 100 kHz while observing the output of the class D amplifier on a spectrum analyzer. A baseline spectrum analysis should first be done to identify spectral lines and the noise floor present in the absence of the test signal. With the test signal applied, the output of the spectrum analyzer is then evaluated for the presence of new spectral lines or an increase in the noise floor. Input frequencies that cause such results should be noted. This can be a time-consuming test.

A different approach is to apply out-of-band white noise at a fairly high level. This noise should be prefiltered so that it contains very little energy in the audio band. Once again, the spectrum analyzer results are evaluated before and after application of the test signal.

PSRR

Power supply rejection ratio (PSRR) is not usually measured explicitly in a linear amplifier when the amplifier is measured as a block box. The effects of power supply noise are typically just lumped in with the SNR of the amplifier. The situation is not so simple with class D amplifiers if valid results are to be obtained. This is important because PSRR is often a bigger problem for class D amplifiers than for linear amplifiers.

There are two concerns with PSRR measurement in class D amplifiers. First, ripple and noise on the power supply rails create intermodulation distortion with the audio

signal in addition to adding noise. This effect will not be seen in a simple noise measurement when no signal is applied. The second concern is that full bridge class D amplifiers will not show much of the power supply noise when measured differentially across the speaker terminals because the same rail noise is present in both sides of the bridge [2, 3].

For these reasons PSRR should be measured or inferred from a test that shows up intermodulation distortion. As mentioned above, the SMPTE IM test can reveal PSRR issues if the low-frequency component of the test at 60 Hz causes significant amplitude deviations on the power supply. Measurement of PSRR is preferably carried out with a spectrum analyzer where IM sidebands can be seen. This approach is especially useful in an amplifier development environment where a PSRR test signal can be added to the amplifier's power supply rails for measurement purposes.

Conductive Emissions

As mentioned earlier, EMI can be a problem for class D amplifiers. EMI is categorized into *conductive emissions* and *radiated emissions*. Conductive emissions are those that can be measured electrically at one of the amplifier ports. For a class D amplifier, the most relevant is the output port. Radiated emissions travel through the air and are measured by radio receiver-like instruments. They will not be discussed further here. Conductive emissions are turned into radiated emissions by the antenna formed by the speaker cable and the loudspeaker.

On the assumption that conductive emissions below 500 kHz are relatively harmless, a reasonable test can be implemented with a sixth-order high-pass filter connected to the amplifier output and followed by a wideband (10 MHz) true RMS voltmeter like the HP 3400A. The conducted emissions voltage should be measured with the amplifier connected to a 4-Ω load at no power and 1 kHz full power. The measured voltage should be reported in dBV.

31.3 Achievable Performance

The stumbling block to adoption of class D amplifiers in the past has been sound quality. That has changed dramatically in recent years but still has a way to go for high-end audio.

Efficiency

The typical efficiency of a 100 W class D amplifier employing readily available components is on the order of 90%. A good example of putting this to good use is the widespread use of class D amplifiers in subwoofer plate amplifiers.

Distortion

Getting the distortion down is still a very big challenge for class D amplifier designers, but the ever-higher digital clock speeds available combined with increased DSP sophistication can be expected to yield significant improvements here.

A related issue concerns sound quality that is not addressed by lab measurements. This continues to be a nagging problem in conventional high-end audio and can be expected to be worse with class D if for no other reason than the far smaller amount of design, measurement, and listening experience with the class D technology.

References

1. AES17, "AES Standard Method for Digital Audio Engineering–Measurement of Digital Audio Equipment," Audio Engineering Society, 1998.
2. Firth, Michael, and Quek, Yang Boon, "The Real Story About Closed-loop, Open-loop Class D Amps," *EE Times-Asia*, no date available.
3. Madsen, Kim, and Soerensen, Tomas, "PSRR for PurePath™ Audio Amplifiers," TI Application Report SLEA049, June 2005.

Index